Simulation of plant growth and crop production

F.W.T. Penning de Vries and H.H. van Laar (Eds)

Simulation Monographs

Simulation Monographs is a series on
computer simulation in agriculture and
its supporting sciences

Simulation of plant growth and crop production

F.W.T. Penning de Vries and H.H. van Laar (Eds)

CONTENTS

PREFACE

This book is an introduction to dynamic simulation of plant growth and crop production. It summarizes a good deal of the experience in modelling an programming of this subject that has been accumulated in Wageningen, the Netherlands, in the last decade. It concerns in particular the disciplines of crop physiology, crop micrometeorology, soil physics and soil microbiology. The experience results from research done at the Department of Theoretical Production Ecology of the Agricultural University and its teaching programmes, from research at the Centre for Agrobiological Research and at other departments and institutes, and from the work of visiting scientists. Much of this technical experiences and know-how is presented in the Chapters 2 to 6 in this book. We have tried to make it accessible to readers by means of many exercises and examples.

The systems approach applied to a wide range of subjects has led to a particular view of simulation and modelling of plant growth and of crop production. This view has been translated into a practical approach. Both view and approach are the subject of the introductory contributions in Chapter 1 of this Monograph.

The motive to publish this Simulation Monograph was an advanced international course on the same topic, held in Wageningen in the spring of 1981. It was organized by Dr van der Kloes of the Foundation of Post Graduate courses of the Agricultural University in Wageningen. The 15 lectures of this course have been moulded into this book with the full cooperation of the authors.

During the editing of this Monograph, Ir Drees has been particularly helpful in developing exercises and formulating their answers. For the skillful typing of the manuscript and drawing of the figures Mr van Amersfoort and Mr Beekhof are kindly acknowledged.

F.W.T. Penning de Vries
H.H. van Laar

CONTRIBUTORS

Basstanie, L.J.M., Department of Theoretical Production Ecology, Agricultural University, P.O. Box 430, Wageningen, the Netherlands.

Drees, E.M., Department of Theoretical Production Ecology, Agricultural University, P.O. Box 430, Wageningen, the Netherlands.

Feddes, R.A., Institute for Land and Water Management Research, P.O. Box 35, Wageningen, the Netherlands.

Ferrari, Th.J., Institute for Soil Fertility, P.O. Box 30003, Haren (Gr.), the Netherlands.

Frissel, M.J., Institute for Atomic Sciences in Agriculture, P.O. Box 48, Wageningen, the Netherlands.

Goudriaan, J., Department of Theoretical Production Ecology, Agricultural University, P.O. Box 430, Wageningen, the Netherlands.

Keulen, H. van, Centre for Agrobiological Research, P.O. Box 14, Wageningen, the Netherlands.

Laar, H.H. van, Department of Theoretical Production Ecology, Agricultural University, P.O. Box 430, Wageningen, the Netherlands.

Penning de Vries, F.W.T., Centre for Agrobiological Research, P.O. Box 14, Wageningen, the Netherlands.

Rabbinge, R., Department of Theoretical Production Ecology, Agricultural University, P.O. Box 430, Wageningen, the Netherlands.

Spiertz, J.H.J., Centre for Agrobiological Research, P.O. Box 14, Wageningen, the Netherlands.

Stroosnijder, L., Department of Soil and Fertilizers, Agricultural University, Wageningen, the Netherlands.

Veen, J.A. van, Institute for Atomic Sciences in Agriculture, P.O. Box 48, Wageningen, the Netherlands.

Vos, J., Centre for Agrobiological Research, P.O. Box 14, Wageningen, the Netherlands.

Wit, C.T. de, Department of Theoretical Production Ecology, Agricultural University, P.O. Box 430, Wageningen, the Netherlands.

1 THEORY OF MODELLING

1.1 Simulation of living systems

C.T. de Wit

1.1.1 Systems, models and simulation

System analysis and simulation has been used by engineers for more than 30 years. Their successes inspired biologists and agronomists to apply similar techniques in their disciplines. The approach is characterized by the terms: systems, models and simulation. A system is a limited part of reality that contains interrelated elements, a model is a simplified representation of a system and simulation may be defined as the art of building mathematical models and the study of their properties in reference to those of the systems.

Although any model should have definite goals, be lucid and achieve its objective, in practice it seems that goals are too often described in such broad terms that sufficient lucidity is reached only for the initiated, and that the models achieve less than expected by the biologist. For these reasons the word 'art' rather than 'science' is used in the definition of simulation.

It follows from the definition that a model is a system, but the reverse may also be true. A work of art is a simplified representation or a model of the vision of the artist. A machine is a model of the conception of the engineer and it certainly performs worse than anticipated. And when an engineer applies simulation, he develops simulation models that lie in between his conception and reality. The ultimate machine is in fact a model of his simulation model, which in its turn is a simplified representation of his mental conception.

Although some wish it otherwise, biological systems are not simplified representations of the conception of the biologist, and the interchange of the terms models and systems does not make any sense. Therefore, it may be that the approach that has been so successful in engineering is not as useful in biology. Fools rush in where wise men fear to tread. Much of this rushing in simulation in biology is done by agronomists, perhaps because they are fools, but maybe because they deal with systems in which the technical aspects overrule more and more the biological aspects.

As has been said, a system is a limited part of reality, so that a border has to be chosen. It is wise to make this choice so that the system is isolated from its environment. This is almost always impossible, but then it should be attempted to choose a border so that the environment may influence the system, but the system affects the environment as little as possible. To achieve this, it may be necessary to choose a system that is larger than necessary for the original purpose.

In agricultural systems, for instance, the microclimate is often part of the system, but everybody happily neglects the influence of the agricultural system on the macroclimate, even though this is not correct. However, the assumption

that everything is related to everything is sure to kill all research.

1.1.2 Explanatory models

A file with data on an ecosystem may be called a model, but it is a model without purpose and lucidity. Potential uses of the data may be formulated and then lucidity may be introduced by a treatment of the data. This may result in maps that represent aspects of the ecosystem, or in statistical analyses, which summarize some of the interrelations. Dynamic models are obtained if the time dimension is introduced during the collection and treatment of the data. But those models remain descriptive, showing the existence of relations between elements without any explanation, but, of course, this was not their purpose to begin with.

However, models that have the purpose of explaining systems are possible in biology because various levels of organization are distinguished in this science, as many other natural sciences. These different levels of organization may be classified, according to the size of the system, as those of molecules, cell structures, cells, tissues, organs, individuals, populations and ecosystems. Models that are made with the objective of explaining are bridges between levels of organization; they allow the understanding of larger systems on the basis of the knowledge gained by experimentation on smaller systems. In this way the properties of membranes may be understood better by studying molecules and the properties of ecosystems by studying species.

If the knowledge on the level which is used for explanation is sufficiently detailed and complete, and on the basis of this a model of the system which behaviour has to be explained is designed, it may not be necessary to evaluate the model by comparing its results with those of the real system. For example, models for space travel are so good that the 'proof of the pudding' – the journey itself – is unnecessary. But explanatory models in biology are so rudimentary that proof of their usefulness is necessary. And even when there is good agreement, there is room for doubt. However, good agreement is still more the exception than the rule.

If there are discrepancies between model and real system, the model may be adjusted to obtain better agreement. Then, something that started as an explanatory model degenerates progressively into a descriptive model. The term 'degeneration' in this context does not mean that descriptive models are inferior to explanatory models. It is used here to emphasize that in this way inscrutable models are obtained with an unjustified pretention to explain something. It is for this reason that many models are still doing more harm than good.

The proper way of working is heuristic, by the road of gradual improvement. If unacceptable discrepancies between model and system are observed it may be possible to judge which aspects of the model should be treated with suspicion, by experimenting with both. These aspects are then studied on the level that is used for explanation. On basis of this renewed study, elements of the model

4

may be replaced by others and then a renewed confrontation between the results of the model and the real system may be again useful.

Explanatory models may be of the static or dynamic kind. An example of a static model is a model that contains all the necessary calculations to achieve the relation between respiration and growth on basis of the knowledge of the underlying biochemical processes. Another example is a model that is used to calculate the light distribution over leaves based on canopy architecture, leaf properties, solar position and so on. Such static models form often a part of dynamic models.

It is characteristic for all systems discussed in this book that major elements (like plant biomass) change only gradually in amount with time or in space in response to changing external factors such as weather or fertilization. Such systems are called 'continuous', in contrast to 'discrete' systems (cf. Brockington, 1979), which deal with numbers and discontinuities in time.

1.1.3 The state-variable approach

For dynamic models that claim to be of the explanatory type, the state-variable approach is gaining wide acceptance. These models are based on the assumption that the state of each system at any moment can be quantified, and that changes in the state can be described by mathematical equations. This leads to models in which state, rate, and driving variables are distinguished.

State variables are quantities like biomass, number for a species, the amount of nitrogen in soil, plant or animal, the water content of the soil. Roughly, those variables that can still be measured when time stands still as in the fairy world of the Sleeping Beauty, are state variables.

Driving variables, or forcing functions, characterize the effect of the environment on the system at its boundaries, and their value must be monitored continuously. Examples are macrometeorological variables like rain, wind, temperature and irradiation, but also the food supply or migration of animals over the boundaries of the system. It depends on the position of these boundaries whether the same variables are driving, state or rate variables. For instance, the heat stored within a vegetation canopy is a state variable when the system includes micrometeorological aspects, but a driving variable that has to be measured when the micrometeorological aspects are excluded from the system.

Each state variable is associated with rate variables that characterize their rate of change at a certain instant as a result of specific processes. These variables represent flows of material or energy between state variables, for example, between vegetative biomass and grazing animals. Their values depend on the state and driving variables according to rules that are based on knowledge of the physical, chemical and biological processes that take place, and not on a statistical analysis of the behaviour of the system that is being studied. This is the most important distinction between models that describe and models that attempt to explain.

After the calculation of the values of all rate variables, these are used to calculate the state variables according to the scheme: state variable at time $t + \Delta t$ equals state variable at time t plus the rate at time t multiplied by Δt. This procedure, called integration, gives the new values of the state variables, by means of which the calculation of rate variables is repeated. The time interval Δt has to be chosen so small that the rates do not change materially within this period. To avoid instabilities, the time interval of integration has also to be smaller than one-third of the time coefficient or response time. This characteristic time of a system is equal to the reverse of the fastest relative rate of change of one of its state variables. The smaller the time coefficient, the smaller the time interval of integration.

Rates are not dependent on each other in these state determined systems. Each rate depends at each moment on state and forcing variables only and is therefore computed independently of any other rate. Hence it is never necessary to solve n equations with n unknowns. An example may be needed. It is clear that the rate of growth of a plant, as measured by the increase in weight of its structural tissues, is closely related to the rate of photosynthesis of the leaves. In a state variable model, this dependency is a result of the simultaneous operation of two independent processes. Photosynthesis contributes to the amount of reserves and this amount is one of the states that determine the rate of growth. At the onset of darkness, photosynthesis stops immediately, but growth proceeds until the reserves are depleted, or even longer, but then at the expense of existing tissue.

Especially for the uninitiated, attempts are made to depict simulation models by relational diagrams, often according to a method that was developed by Forrester (1961) to represent models of industrial systems. Examples of such relational diagrams may be found throughout this book. The state variables are represented by rectangles and the flow of material (water, carbon, nutrients) by solid arrows. The rate control of these flows is presented by the valve symbol. Constants, driving variables or forcing functions are often placed between parentheses. The dotted lines indicate the flows of information that are considered. Relational diagrams do not contain any quantitative information. Such a diagram of the simplest dynamic system is given in Figure 1. If the rate is mathematically described as RATE = CONSTANT • STATE it depicts exponential growth. It is the most simple information feedback loop, which must always contain one state variable whose change is controlled by a rate and a flow of information from state to rate.
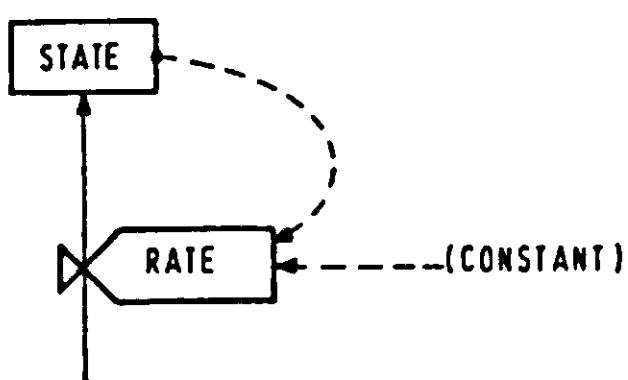
Figure 1. A relational diagram of exponential growth, drawn according to the conventions of Forrester (1961).

1.1.4 A practical problem

The number of state variables that may be distinguished in a living organism or in an ecosystem is depressingly large. They concern not only primary producers, consumers and decomposers, but also the various species, their number, size, age, sex, stage of development, etc. For plants, not only the weight and surface area of the leaves are of importance but also their nitrogen and mineral content, their enzymes and other biochemical characteristics. One can continue in this way and therefore a model that is based on full knowledge of all biological, physical and chemical phenomena that occur is never realised. Models are simplified representations of systems, and the simplification manifests itself by the limited number of state variables that are considered.

Analogous with other approaches, it is assumed that considerable reduction of the number of state variables may be obtained by limiting the boundaries of the model and by focussing on those aspects of interest for which understanding is most wanted. Then processes can be ordered by their importance and only processes within the limited focus need to be handled in detail.

The number of state variables that can be considered in any model is limited, not so much because of the size of the computer or the cost of computer time, but because the research effort that can be invested in any one problem is limited. Models that contain about a hundred state variables are for this reason already very large, but at the same time they may be small compared with the complexity of the systems that are considered.

For each purpose there is somewhere an optimum in the number of state variables that should be considered. At first the applicability of the model to the real world problem increases with increasing number of state variables, but then it decreases again as the addition of new state variables diverts attention from state variables introduced earlier because they were considered more important. The heuristic process of obtaining a set of state variables in order of their importance takes much time, and many modelling efforts in ecology are sometimes explicitly, but mostly implicitly, geared towards this goal.

1.1.5 A validation problem

Simulation may aid the understanding of important aspects of complex systems in such a way that their behaviour is visualized and a guide to their management is obtained. But solutions are only accepted as such if methods to falsify them are available or, to express it more positively, if they can be verified or their usefulness can be proven. Are there models that can be validated? Yes, but only models of systems that are repeatable or recur. Only then may the model be derived from the analyses of some systems and validated on others. Examples of repeatable systems are found in microbiology (manufacture of vinegar), agriculture (growth of maize) or industry (manufacture of cars). Examples of recurring systems are stars, individuals of a species and ecological systems with so

much resilience that after disturbance the original course of development is restored in due course (peat bogs). These recurring ecological systems appear to the observer at different places at the same time in different stages. The strength of the field ecologist lies in his ability to interpret as a time series in one place what is observed in different places at one moment. Repeatable systems can always be analysed by experimentation, but recurring systems sometimes only by observation. There is at present a strong emphasis on the experimental analysis of recurring ecological systems and this is justified because disturbances are damped and destruction of the system during experimentation may be acceptable because there are many of them.

But there are also unique ecological systems or ecological systems with unique aspects. These are systems in which development is not governed by negative feedback, so that their development is diverse, although the origin may be the same. Other systems are unique because of the geographical situation, like some estuaries, lakes, islands and of course the world as a whole. Models of unique systems are concepts that cannot be validated experimentally but only more or less verified by observation of the behaviour of the real system over time. They remain therefore speculative models. The faith in speculative models is strengthened if similar methods of systems analysis, applied to repeatable or recurring systems, lead to validated models that cannot be falsified. Such models of physical systems exist: speculative models that predict the chances of flooding on the basis of an analysis of the physical processes are trusted, although sufficient floods for verification never occur within a life span. But whatever the model predicts, the dykes are strengthened as soon as one flood takes place and this proves that trust in models of this kind has its limits. Speculative models of ecological systems cannot be trusted as yet, because few models that are properly validated exist and the principles of modelling in ecology are still being developed. This certainly holds for 'world models' unless their results are so obvious that the proper conclusion may be drawn without sophisticated techniques.

But if a speculative model of a unique system is sufficiently trusted, can it be used? For this purpose it is at least necessary to initialize the model so that the values of all the state variables have to be determined within such a short time span that they do not change materially. And this should be done without disturbing the unique system to such an extent that its course of development is affected. This is impossible. Therefore, in the final analysis it may appear that the ecologist is in the same position as the outmoded physicist, who claims that it is only necessary to determine at the same time the position, mass and velocity of all gas atoms in his room to predict their future. He may be in an even worse position because he has to live with or even within his unique system as one of its elements and cannot escape the problem by using the law of averages.

1.2 Systems analysis and models of crop growth

F.W.T. Penning de Vries

1.2.1 Systems of plant production

A way to consider the real world is to divide it into systems. A functional description of a system is 'a part of reality with strongly interacting elements, but little influence on its environment'. Ideally, boundaries are chosen such that the environment influences processes within the system, but that the system itself does not modify its environment (see also Section 1.1). What part of the real world is singled out as a system depends first of all upon objectives. A system may be defined with a plant, a crop or a farm in its focus, and with current weather conditions, insect pests or farm product prices as the environment for growth and production. A definition of a system can sometimes be given in a straightforward manner. But there may also be complications: some elements of a system, not directly related to the goals of the analysis, may still deserve special attention in the delimitation of a system because they interact strongly with the main elements. This is reflected by the term 'whole system approach'. Upon defining a system, one should thus account for objectives and for such natural contours, and consider all essential parts that co-determine the content of a system. An example may illustrate this point. Plant production in fields with fertile and irrigated soils may be visualized as a system in which processes like CO_2 assimilation, growth, maintenance and development interact intensively. The rates of these physiological processes depend strongly on weather conditions, but weather is not modified noticeably by plant growth. One can thus delimit this plant production system by drawing a line between physiological and meteorological processes. But in a greenhouse, air humidity, temperature and ambient CO_2 concentration are modified by crop growth, and the 'weather' has become part of the system. The boundaries of a system can thus move with changes that seem unrelated to the objective of the study. For concepts on models and modelling of systems see Section 1.1.

An elegant and practical delimitation of systems of growing vegetations and of crops was proposed by de Wit (de Wit & Penning de Vries, 1982). His approach to growth and production emphasizes dry matter production, and not so much morphogenetic development. He distinguishes four levels of plant production. The systems of plant growth and crop production at each of these levels can be considered as belonging to one broad class. Those levels in an order of descending productivity are:

– Production level 1
Growth occurs in conditions with ample plant nutrients and soil water all the time. The growth rate of the vegetation is determined by weather conditions and

9

in terms of dry matter amounts to 150-350 kg ha^{-1} d^{-1} when the canopy covers the soil fully. The absorbed radiation is often the factor limiting the growth rate during the growing season, but low temperatures may restrict growth earlier on. In fact, this is quite a common situation in cool climates. Major elements in this class of systems are the dry weights of leaves, stems, reproductive of storage organs and of roots, and the surfaces of photosynthesizing tissues; major processes are CO_2 assimilation, maintenance and growth, assimilate distribution and leaf area development. A situation with plant growth at this production level can be created in field and laboratory experiments, while it is approached in practice, for example, in glasshouses and in the very intensive production of sugar-beet, potato and wheat on some Dutch farms.

– Production level 2

Growth is limited by water shortage at least part of the time, but when sufficient water is available the growth rate increases up to the maximum rate set by the weather. Such situations can be created experimentally by fertilization in temperate climates and in semi-arid zones; it is approached in practice, for example in non-irrigated, but intensively fertilized, fields, such as many Dutch pastures. The extra elements of this class of systems are the water balances of the plant and soil; crucial processes are transpiration and its coupling to CO_2 assimilation, and all other processes of loss or gain of water by the soil, such as evaporation, drainage and run-off. The heat balance of the canopy needs consideration in detailed analyses at this production level because of its relation to the water balance.

– Production level 3

Growth is limited by shortage of nitrogen (N) at least part of the time, and by water or weather conditions for the remainder of the growth period. This is quite a common situation in agricultural systems using little fertilizer, and is also normal in nature. Even with ample fertilization, N shortage commonly develops in crops at the end of the growing season. Important elements of this class of systems are the various forms of N in the soil and in the plant; important processes are the transformations of nitrogenous compounds in the soil in forms less or more available to plants, leaching, denitrification, N absorption by roots, the response of growth to N availability and redistribution of N within the plant from old organs to growing ones.

– Production level 4

Growth is limited by the low availability of phosphorus (P), or by that of other minerals, like potassium (K) at least part of the time, and by N, water or weather for the remainder of the growth period. Lack of P is particularly interesting because of its relation to the metabolism of N. Growth rates in terms of dry matter are typically only 10-50 kg ha^{-1} d^{-1} during a growing season of 100 days or less. This situation occurs often in heavily exploited areas where no fertilizer is used, such as in the poorest parts of the world. Important elements of this class of systems are the P or mineral contents of the soils and of the plants; important processes are their transformations into organic and inorganic forms

of different availabilities, absorption of minerals by roots and the response of plant growth to their absolute availabilities. For P, the availability relative to that of N is also important.

It is rare to find cases that fit exactly into one of those four production levels, but it is a very practical simplification of a study to reduce specific cases to one of them. It focusses the attention on the dynamics of the principal environmental factor and on the response of the plants to it. Other environmental factors can then be neglected, because they do not determine the growth rate. It is rather the other way round: it is the growth rate that sets the rate of absorption or efficiency of utilization of this non-limiting factor. If, for example, plant growth is limited by the availability of N, there is little use in studying CO_2 assimilation or transpiration to understand the current growth rate. All emphasis should then be on N availability, the N balance and the response of the plants to N.

This textbook is organized according to those four production levels: after a general introduction into systems and modelling of plant growth and crop production (Sections 1.1-1.4) and in modelling techniques essential in this field (Sections 2.1-2.3), the Sections 3.1 to 3.4 deal with growth and light and energy utilization at Production level 1, the Sections 4.1 to 4.3 deal with growth and water use at Production level 2, the Sections 5.1 to 5.3 deal with growth and N use at the Production level 3. Simulation of growth at the lowest level of production will not be treated in this book, primarily because this subject is not sufficiently advanced. The Section 6.1 deals with simulation of effects of diseases and pests on growth of crops at Production level 1.

1.2.2   Simple systems of crop growth

Let us take this analysis one step further. The remarks about the primary environmental factor can be used to formulate very simple systems and models of the four levels of plant production and describe their basic forms. In other parts of this textbook, these models will be expanded.

At Production level 1 the intensity of the irradiation, the degree of interception and utilization of light and the efficiency of use of energy in the plant are key factors for the understanding of the growth rate. Irradiation is a driving variable, and its intensity is obviously not modified by the crop. The efficiency of utilization of light by a crop is a characteristic of the plant species and the canopy density. The assimilated carbohydrates, stored only temporarily in an easily accessible form like starch ('reserves'), are utilized for maintenance or growth. In growth processes, reserves are converted into 'structural biomass' with a certain efficiency. Structural biomass, in contrast with reserves, consists of those components that are not mobilized again for growth or maintenance processes elsewhere in the plant. The essence of models at this production level is presented in Figure 2.

At Production level 2, the degree of exploitation of soil water and the effi-
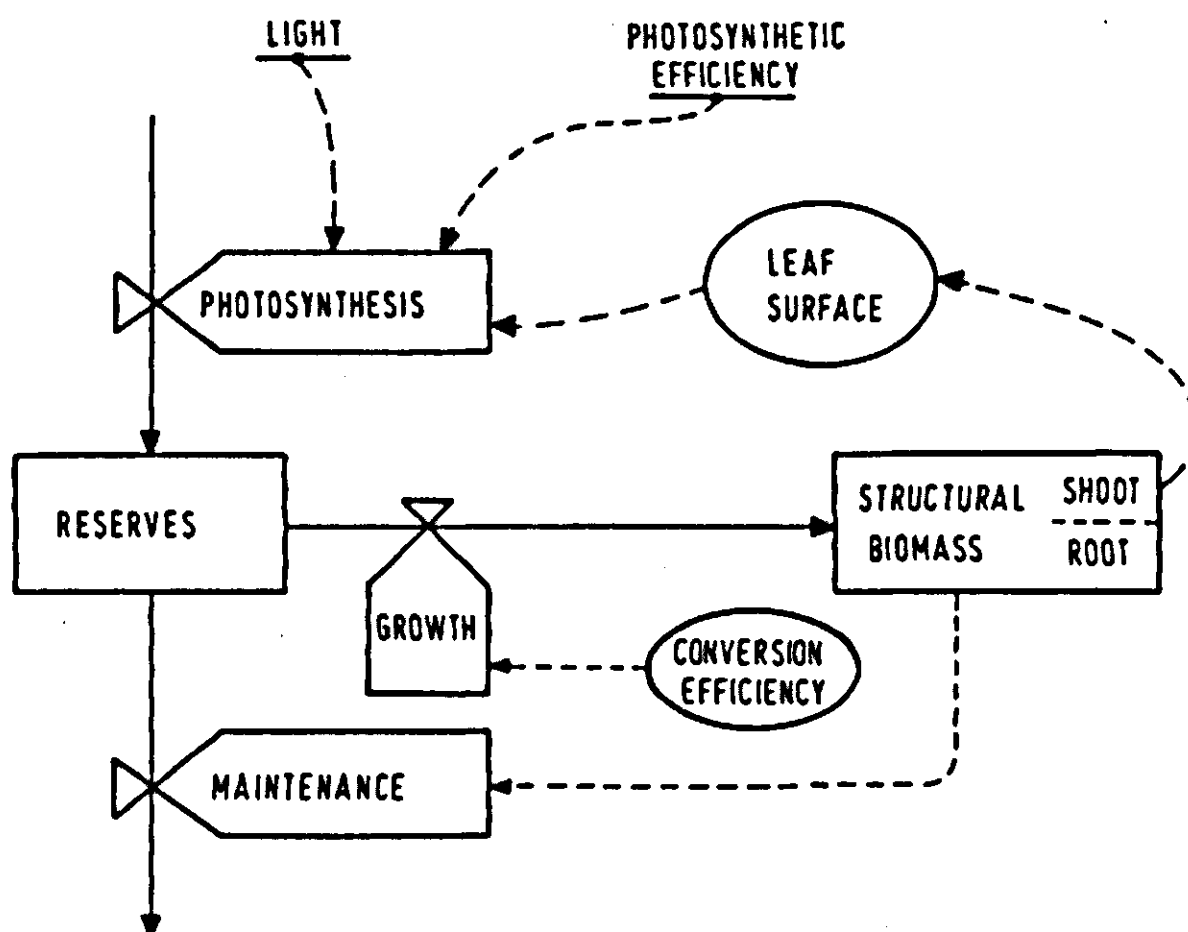
Figure 2. A relational diagram of the essence of a system at Production level 1 when light is the limiting factor. The diagram is drawn according to Forrester (1961): rectangles represent quantities, valve symbols represent flows, circles auxiliary variables and underlined variables external variables; drawn lines represent flows of material, broken lines flows of information (see also Figure 9).

ciency of its utilization by the crop are key factors. Water shortage leads to stomatal closure, and to simultaneous reduction of CO_2 assimilation and transpiration. The rates of both processes are therefore closely linked, and the calculation of canopy transpiration is a direct route to crop CO_2 assimilation. The amount of water stored in the soil is a buffer between rainfall and the processes by which water is lost. This buffering capacity of the soil and the simultaneous loss of water by transpiration and by non-productive processes cause the growth rate to depend only indirectly on the driving variable: rainfall. The relation of plant growth to the driving variable of this system is thus principally different from that at Production level 1. A relational diagram of this system is given in Figure 3.

At Production level 3, the nature of the availability of N to the plants from the soil is not much different from that of water: a pool of inorganic N exists in the soil, and most of it is available to the roots that are sufficiently close. Growth of the soil microflora may compete with the plants for N in this pool and other processes may interfere as well. Mineralization of organic N adds to the pool of inorganic N. But contrary to water in the plant at Production level 2, the N in plants must be distinguished in two fractions: a mobilizable and an immobilizable one. The amount of N that remains mobilizable from old tissues for the development of new organs is often considerable. This 'internal reserve of N' makes current increase in plant dry matter largely independent of the current absorption of N. The reason is that the concentration of N in the tissues can

12

Figure 3. A relational diagram of the essence of a system at Production level 2 where water shortage is the main limiting factor. For use of symbols see Figures 2 and 9.

often drop to half or a quarter of its original value (due to decomposition of proteins and export of amino acids) before the tissue stops functioning. Figure 4 illustrates this situation. New tissues can thus grow at the expense of old tissues. Only after exhaustion of the internal N reserve is growth directly related to the rate of absorption of N. The mobilizable fraction consists largely of enzymes, but all enzymes cannot be considered reserves because cells cannot function without them. (The 'internal N reserve' resembles money in a bank, and the plant resembles a *rentier* who lives from the interest: photosynthates, other metabolic products and cellular activities. In bad times, part of the capital is consumed and the *rentier* has to live with less interest.) The immobilizable frac-

Figure 4. A relational diagram of the essence of a system at Production level 3 where nitrogen shortage is the main limiting factor. For use of symbols see Figures 2 and 9.

13

tion of the N in tissues is tied up in stable proteins that are not decomposed and that are possibly a part of the cellular structures. When the growth rate is primarily determined by the availability of N from soil and internal reserve, the rate of CO_2 assimilation is a consequence of the growth rate and should no longer be considered as a driving variable of the system.

Production at level 4 (this discussion is limited to the element P) differs from that of Production level 3 in that a much higher root density is required for a good exploitation of the soil for P than for inorganic N, and that the quantity of the dissolved P in the soil is so small that its rate of replenishment controls the supply to the plant directly. Both organic and inorganic forms of P in the soil may provide and capture dissolved P. The concentration of P in old tissue may undergo a reduction as for N, so that one can also speak of an internal reserve of P in plants. Figure 5 presents a diagram of this situation.

This analysis of plant production systems thus allows a considerable narrowing of the subject of study and hence a more rapid progress in research. Diseases, insect pests and also competition with weeds may occur at each of these production levels, and give them, in a sense, an extra dimension. The fact that actual situations are often more complex does not contradict the general usefulness of this scheme of four production levels as a basis for distinction between causes and consequences of plant growth.

The definition of systems at different levels of production is rooted in the analysis of agricultural crops. But as this delimitation is based on the effect of external factors on physiological processes, it is not restricted to agronomic situations and applies to plant growth and production in general. Moreover, cultivation of crops has changed little or none in the basic physiology of species, and similarities in physiological and biochemical functioning of different species are often remarkably large. An example of this are the similarities between modern forms of wheat and their ancestors (Khan & Tsunoda, 1970). This analysis is
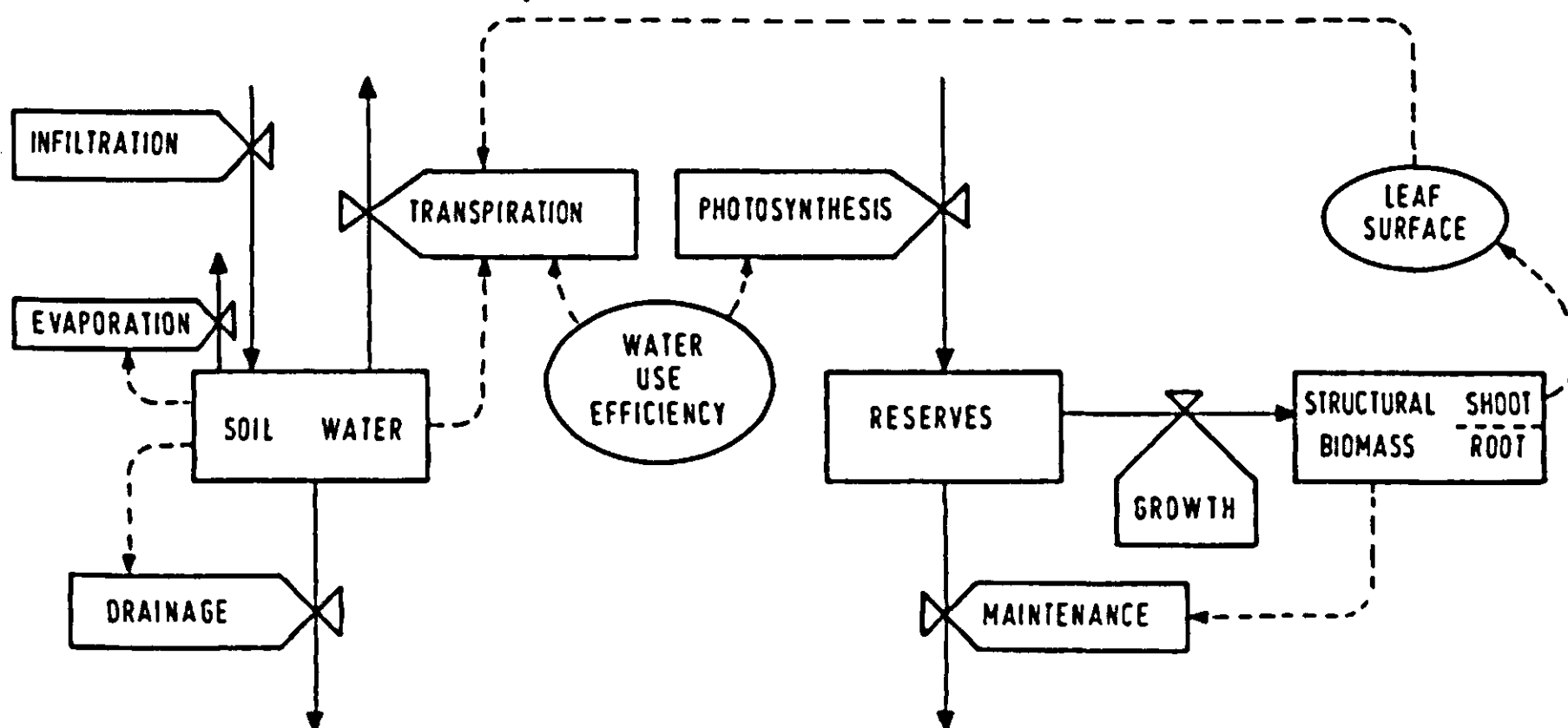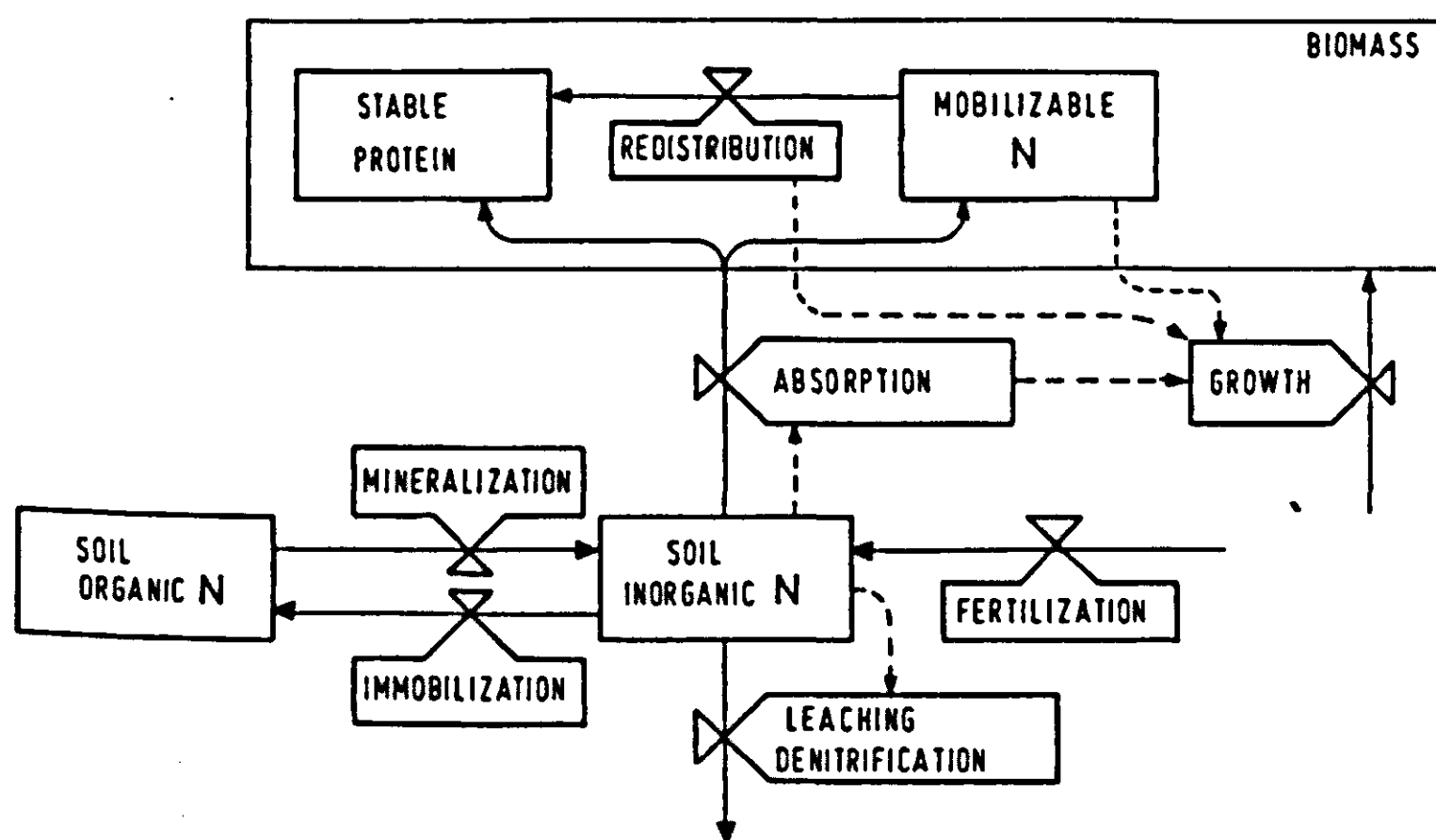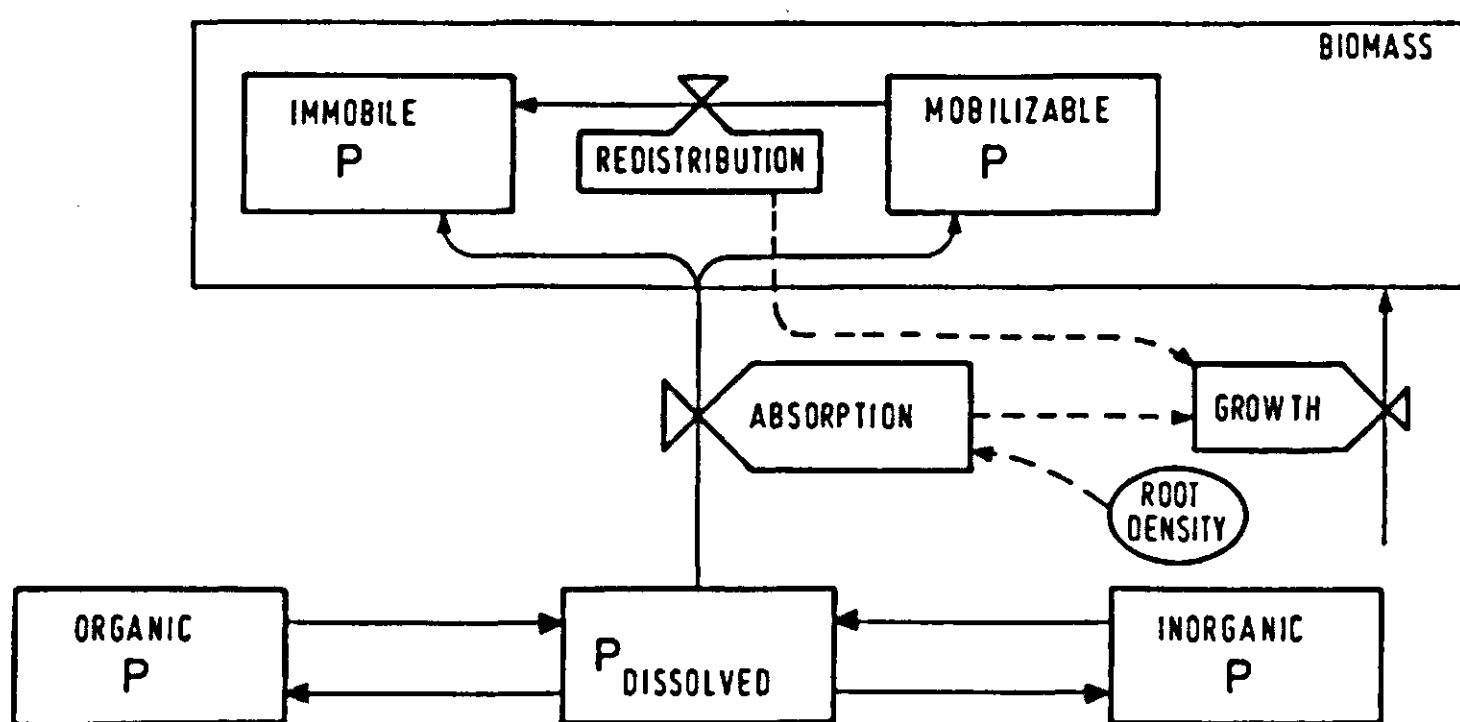
Figure 5. A relational diagram of the essence of a system at Production level 4 where phosphorus shortage is the main limiting factor. For use of symbols see Figures 2 and 9.

14

therefore applicable to all situations of plant growth in agricultural and in 'natural' environments. But the homogeneity of agricultural crops as compared to natural vegetations gives the modeller of agricultural systems an important advantage over his colleagues in plant ecology.

1.2.3 From one production level to the next

If shortage of water, or N or P is sufficiently severe, it is usually fairly easy to recognize the main growth limiting factor. In other cases, however, this is not quite clear because growth occurs in an intermediate situation where two environmental factors are almost equally important. This poses the question of how plant production between the production levels distinguished in the beginning can be approached. Figure 6 is a diagramatic representation of the way how the four levels of production can be related to each other, in particular for crop growth in arid and semi-arid zones. It is highly simplified, and has in fact too few dimensions for a fully appropriate connection of the four production levels. This diagram is based on the idea of successively diminishing levels of growth.

The main process determined at the Production level 1 (Figure 6, Quadrant a) is the growth rate: the slope of the line relates time of growth to production. In the example given, a typical growth rate in terms of dry matter of 200 kg ha^{-1} d^{-1} has been used; it corresponds roughly with a rate of CO_2 assimilation of 500 kg ha^{-1} d^{-1}. Irradiation is the single most important factor that determines this slope. The longer the growth period, the higher the final yield. The early exponential phase of growth has been included in the diagram to emphasize that the crop growth rate is only about 200 kg ha^{-1} d^{-1} when it covers the soil fully. In early phases, growth is more or less exponential. The duration of this exponential phase depends on weather and seed density in particular, and is not further . discussed here. In this example it is assumed that the biomass of the crop in terms of dry matter is 1000 kg ha^{-1} at the end of a 15 day exponential growth phase.

Going to the situation that applies to Production level 2, it is the availability of water that determines in particular the duration of the growth period, as indicated in the same quadrant. This is particularly true for dry zones where the growing season is short (see Section 4.2). At a certain regime of precipitation, the period of growth at a constant rate may be 45 days, the example chosen in Figure 6, so that a biomass of 10 000 kg ha^{-1} is attained at the end of the growing season. The more water available, the longer the growing season and the higher the production.

Biomass, formed in presence of sufficient plant nutrients, has an N content of about 2% of the dry matter in mature tissue in C_4 type crops. This corresponds to a seasonal N uptake by the crop of 200 kg ha^{-1}. If less N has been available for the crop, as is the case at Production level 3, the final yield falls below the 10 000 kg ha^{-1} level. The N concentration decreases initially faster than the biomass production (leaving it with a lower N concentration). At very

15
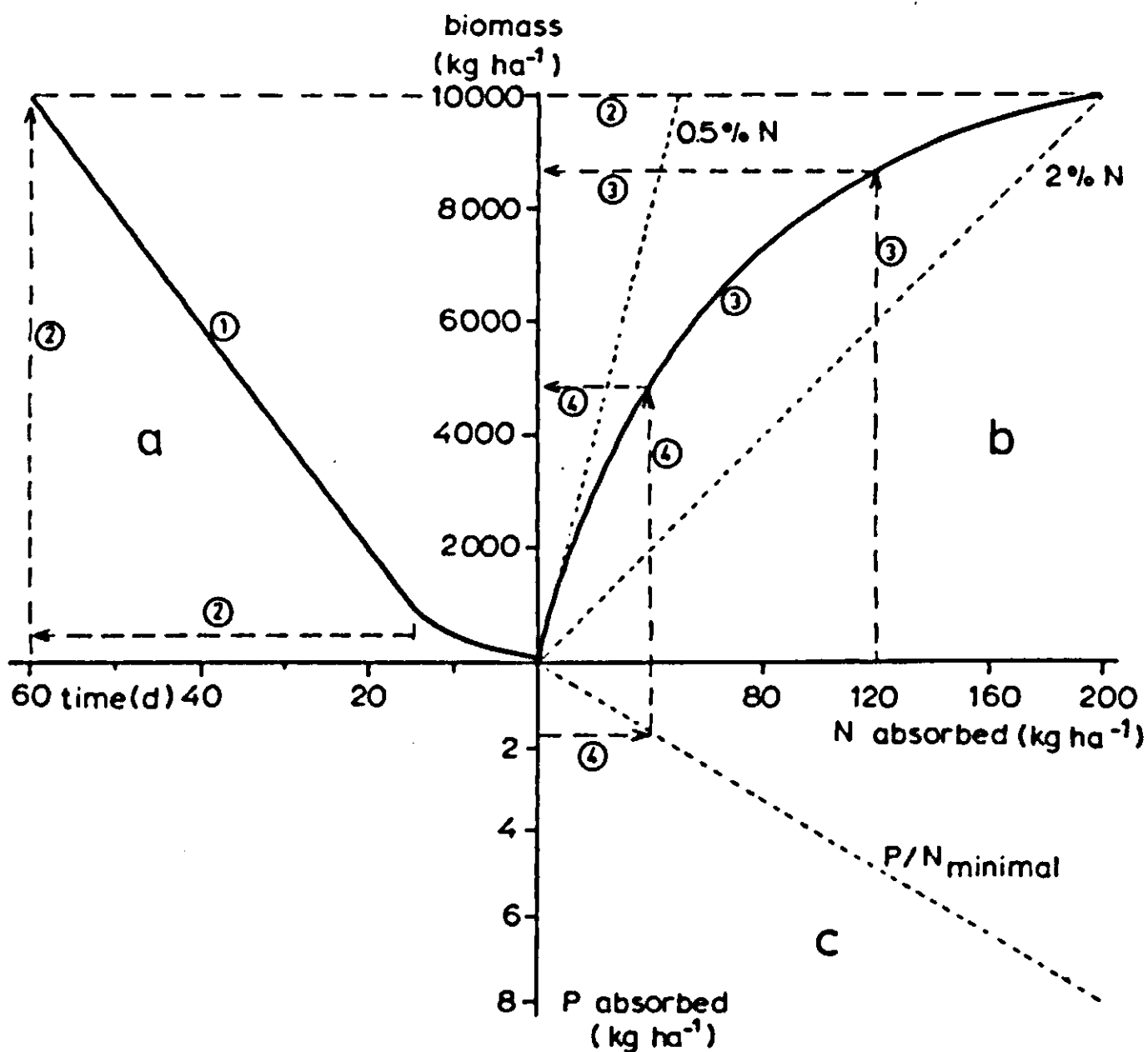
Figure 6. A diagram to show how crop production may be considered when moving from one production level to the next. Line ① refers to growth at Production level 1: the growth rate of an established crop is constant, assuming stable weather conditions. A restriction of the growing season to 60 d is a simple illustration of the effect of shortage of water (Production level 2, broken lines ②). The solid line ③ relates final yield to nitrogen absorbed (Production level 3): its maximum is that of Production level 2. The broken lines ③ illustrate the case that a nitrogen uptake of 120 kg ha^{-1} corresponds with a biomass yield of 8 600 kg ha^{-1}. At Production level 4, the small absorption of phosphorus restrains absorption of nitrogen, and hence productivity. The broken lines ④ show that with 1.6 kg ha^{-1} of phosphorus absorbed, no more than 40 kg ha^{-1} of nitrogen can be contained in plants so that biomass production is limited to 4 800 kg ha^{-1}.

low levels of availability of N is the amount of biomass almost proportional with the amount of N that it contains. The slope of the curved line in the origin is 0.5% for C_4 type crops , as in the example of Figure 6. This subject is discussed further in Section 5.1. The Quadrant b shows this curvilinear relationship between biomass and N absorbed up to the level dictated by water availability. This curve could thus represent the final yields of a series of fertilization experiments in a particular growing season. In Quadrant b is shown with a broken arrow line how much biomass will be formed when only 120 kg ha^{-1} of N can be absorbed.

Compared with P, N is often more readily available to the plant early in the growing season. Since plants cannot contain an amount of N that exceeds 25 times its P content (Section 5.1), N uptake can be limited by the P uptake in young plants. Later on, the N content in such plants is diluted by growth to its

16

minimum value, whereas the P uptake continues. This is the reason that P shortage often ultimately expresses itself as N shortage (de Wit & Krul, 1982). In Figure 6, Quadrant c, this is shown for the situation where only 1.6 kg ha^{-1} of P could be absorbed during the period that N was available, reducing the N absorption to 40 kg ha^{-1}, and hence the biomass produced to just below 5000 kg ha^{-1} (in this particular example for a 60-day growing season).

Less common is straight P shortage with sufficient N all the time. In such cases the response curve of biomass formed to P absorbed is similar in form to the response curve of yield to N absorbed with sufficient P. The slope of the curve in the origin is about 0.05% P on a dry weight basis for C_4 type crops.

As far as the relation between N absorbed and N supplied is concerned: this is approximately proportionally to the gift above a minimal value supplied by the soil without any fertilization. A maximum of uptake, corresponding to the maximum biomass with the highest N concentration, is not exceeded. This is further discussed in Section 5.1.

1.2.4 Analysis of more complex situations

One environmental factor may affect another environmental factor, which then affects plant growth indirectly. In this way a basically non-limiting factor may influence the availability of a limiting factor. Soil water, for example, is not of direct importance to plant growth at Production level 3, but if it runs low it may reduce the availability of N and P. Such interactions may be intricate, but as they are not principally different from the limiting factor approach, they may be unravelled by straightforward analysis. However, our knowledge of interactions between factors is still limited, and its modelling is not yet far advanced.

In more detailed studies, the complex situation earns consideration in which different growth limitations occur successively, or even intertwine, during the growing season. The factor that limits growth in the beginning of the season may improve relative to other factors, and can consequently be replaced by another as the limiting factor. In a typical situation of plant growth in temperate regions the growth-weather relation is of major importance in the beginning of the growing season, and nutrient shortages may reduce crop growth at a later stage. But at any time, a brief dry spell may cause a water shortage and reduce growth. A nice illustration of quite a different situation is described for the Sahel (Penning de Vries & van Keulen, 1982), where it is not uncommon that the initial growth of grass seedlings is restricted by a scarcity of water. A very low P status of the soil reduces the growth in a next phase. But because of an expanding root system, continuous uptake of P, and a diminishing demand for it, P does not remain the limiting factor: the plants are finally limited in their growth by the very small quantity of N that they have been able to absorb from the soil. Many of the annual grasses in the Sahel flower under photoperiodic control and ripen a few weeks later; an internal mechanism that overrides all environmental
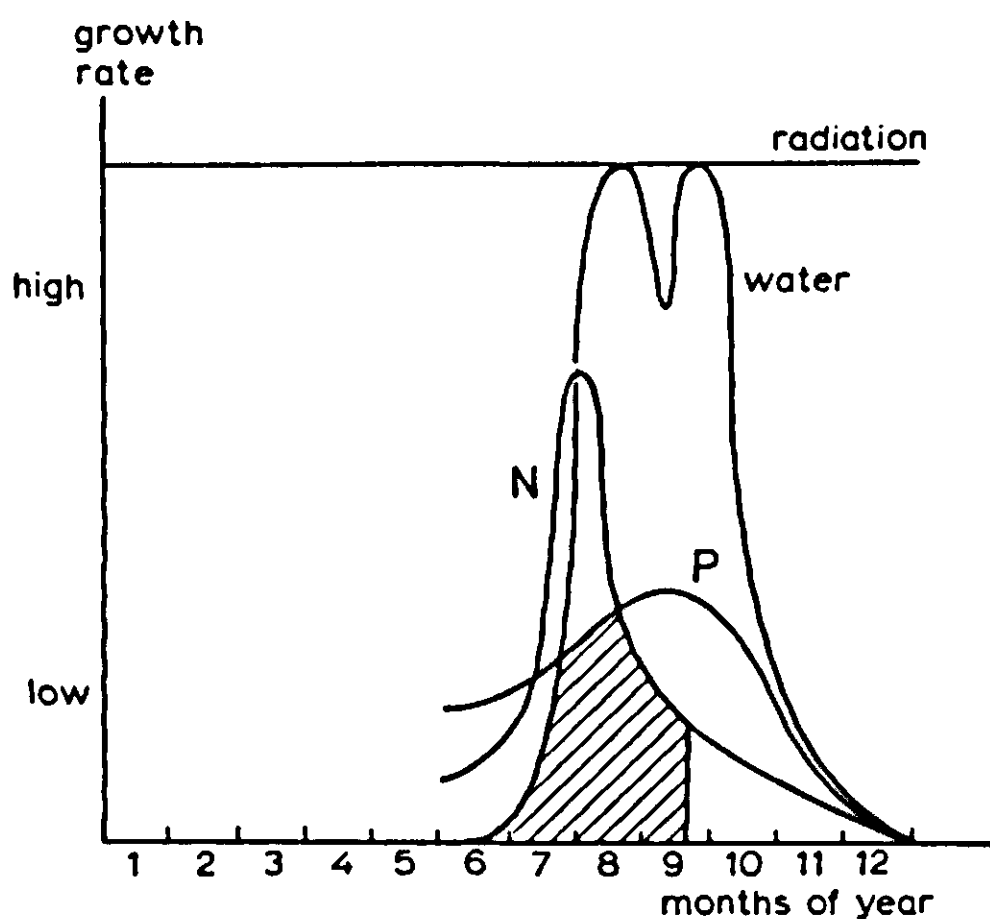
Figure 7. The effect of the relative availability of the four principle external factors — irradiation, water, N and P — on plant growth in the Sahel. The shaded area represents the zone of actual growth, the non-shaded area below the upper line represents the potential growth. Water poses a maximum to the growth rate after germination, the low availability of P for some time afterwards, while the availability of N limits growth at the end of the season. Annual grasses often mature photoperiodically before the soil dries out, as is shown here. The example is imaginary, but based on field observations.

factors. Figure 7 presents this sequence schematically. Thus this approach basically follows Liebig's law of the minimum to describe the effect of limiting factors on growth.

If one is interested in day-to-day growth, one has to follow each environmental factor on a day-to-day basis and the plant response on a day-to-day basis. But if productivity at the end of the season is the principal point of the exercise, one could ask the question: is it not sufficient to study the availability of the factor that limits growth last? For absorption of light and for P absorption this is quite clearly not so: they are absorbed from a source that provides them at an almost constant rate (per ha and per cm of root, respectively), and loss of time for absorption cannot be compensated for. But also at the levels 2 and 3, with stocks of water and N in the soil, the answer is still negative, because other processes are competing with the plant for them, and these are more successful when plant growth is more restrained. For example, transpiration 'competes' with evaporation, and if transpiration is suppressed by N shortage, water will be lost from the soil anyway and does not remain for 'better times'; absorption of N by roots 'competes' with immobilization, leaching and denitrification, so that the N not absorbed rapidly by roots may be lost in other ways.

As a result, in a more detailed study one should not only look to the factor that limits growth at the end of the growing season, but follow the dynamics of each of the factors water, N and P and determine which of them at any moment

is the crucial one to limit growth. Plant production can then be seen as one large system in which the processes occurring at two or even three of the four plant production levels are combined, and in which their relative importance changes. The four production levels distinguished are only focal points of a large continuous system. For production and growth models, it is practical to consider the structure of a system to be invariable during the time-span of interest, and to consider the parts of the model that are temporarily unimportant as harmless ballast. However one might also argue that the structure of the system changes in such a case, and that one ought to change during the simulation run, e.g. from a model structured like the one of Figure 3 into one in Figure 4. That conception may become effective in stages of model development still to come.

Another problem in considering plant growth systems in detail is that the efficiency of use of one factor can be modified by a previous shortage of another factor. For example, in conditions of bright weather and optimal water and nutrient supply, a maize crop had a very high rate of CO_2 assimilation of about 850 kg ha^{-1} d^{-1} (Penning de Vries, 1982a). A very high transpiration rate, exceeding 10 or even 15 mm d^{-1} was coupled to this. When stomatal control of transpiration by photosynthesis is effective (see Section 3.2), probably induced by a brief water stress, the effectivity of water use is increased (the transpiration rate is reduced to about half of the previous values), but this is coupled to an increase in stomatal resistance. This higher resistance sets a lower maximum rate of CO_2 assimilation of about 650 kg ha^{-1} d^{-1}, and this lower rate is maintained after relief of the stress. Although details of this switch are not yet known, this example makes it clear how strong the effect of previous stress can be. Another example of an after effect is the change in leaf morphology as an adaptation to drought that can modify CO_2 assimilation characteristics. If the induction period for such a change is short, it may well escape the modeller's notice if he uses a coarse simulation model. This is another reason for using a detailed, hour-to-hour simulation, and to discourage the too quick and easy use of daily or even weekly averages of environmental factors to simulate plant growth.

1.3 Phases of development of models

F.W.T. Penning de Vries

1.3.1 Phases of development

For more than a decade models have been used to simulate plant growth and crop productivity. The processes of the carbon balance and water balance have been strongly emphasized. As a result many aspects of models at the Production levels 1 and 2 are now well developed, as is demonstrated in the Sections 3.1-3.4 and 4.1-4.3. For a few years now, some simulation studies direct themselves towards relationships of plant growth and availability of nutrients from the soil. However, knowledge of the underlying processes is as yet little developed. As a consequence, their models are still less advanced (Sections 5.1-5.3; Penning de Vries, 1980).

Models of plant growth and production can be divided into classes: preliminary models, comprehensive models and summary models. Such phases of evolution of models are discussed here briefly, and more extensively in other literature (Penning de Vries, 1982b).

During development, a model moves gradually from one phase into the next. Preliminary models are defined as models with structure and data that reflect current scientific knowledge. They are considered simple because insight at the explanatory level is still vague and imprecise. A comprehensive model is a model of a system whose essential elements are thoroughly understood, and in which much of this knowledge is incorporated. Summary models are models of comprehensive models: in them essential aspects of the comprehensive models are formulated in less detail than is possible. This is done to simplify the model and to make it more accessible for users. Summary and comprehensive models are found at the levels of production where soil moisture or weather limits growth, whereas models for the production levels where nitrogen or phosphorus is the main limiting factor are predominantly of the preliminary type, or even basically a regression of yield to an environmental variable. The models of these three developmental stages differ considerably in their value for instruction, for prediction, for scientific progress and in simplicity (see Subsection 1.3.5). Table 1 rates them on an arbitrary scale.

The division of dynamic models into three classes is obviously an oversimplification. Particularly those models that have been developed over a long period and that are still being improved consist of submodels of which some are in fact summary models, others are comprehensive in nature, and still others are preliminary submodels. The characteristics given for the three phases of development of models apply then to the individual submodels. The coordination of submodels within the framework of a large model is discussed in Section 1.4.

20

1.3.2 Preliminary models

At the frontiers of knowledge, preliminary models are very common. They enable the quantification and evaluation of hypotheses and are useful as such, but they seldom survive a long time. The category of preliminary models shows the largest diversity of hypotheses on processes and their relationships on the explanatory level, making these models highly interesting for scientists and stimulative for experimental research. See for example Subsection 5.2.1. Their predictive value is generally fairly low. If preliminary crop growth models are presented unreservedly, one often finds that potential users are actually discouraged as a result.

A typical preliminary model is that of tulip growth by Rees & Thornley (1973). It is a very small model of growth of individual plants that describes in an unrefined way all essential processes. It consists of only 18 simple computer statements and describes the carbon flow from a mother bulb to the developing top and to the daughter bulb from top emergence until leaf death. The top is supposed to grow heterotropically, while the daughter bulb utilizes mother bulb reserves and monopolizes also all photosynthetic products. Net plant CO_2 assimilation equals top weight times the incident irradiation intensity times a constant. Emergence and death occur at fixed dates. This model is labelled preliminary because of the very simple description of the CO_2 assimilation, respiration and growth processes, and because of the absence of any consideration of environmental conditions on the date of emergence and the rate of plant development. Unfortunately, only very few preliminary models have the elegant simplicity of this tulip-growth model.

Most of the models on growth under nutrient stress fall in this group, as essential processes in plants and soils are still little understood, the physiological effects of extreme shortage of some microelements being an exception (cf. Wright, 1977). Models to simulate the morphological development of plants and of its organs are also still of a preliminary nature, or even purely descriptive. Section 3.4 discusses some of their features.

1.3.3 Comprehensive models

Comprehensive models are developed from preliminary models as a result of scientific progress: more knowledge and insight become available, so that the functioning of the real system becomes more lucid, and its simulation becomes more truthful. The expectation that such models may become finally predictive tools can provide a strong motivation for their construction. Comprehensive models are explanatory models par excellence: their behaviour can be explained fully from the well known underlying processes that are integrated in them. However, models of this group are often large, intricate and unwieldy, so that in practice they can only be used by those who participated in their development. Because large and complex models are almost impossible to communicate

in full to potential users, this phase of comprehensive models should not be considered as a final stage, but summarization should necessarily follow it. But though the summary model of a system may become the most utilized model of a system, in some cases it remains necessary to employ the full, complex model. This will be required when a high accuracy of results is needed, but also to check whether modifications of existing summary models are implemented correctly.

• The model BACROS is an example of a comprehensive model. It simulates vegetative growth of crops at non-limiting levels of soil water and soil nutrients on basis of standard meteorological observations and many physical, biochemical and physiological characteristics. In its current stage, neither germination nor the reproductive growth phase is considered. The model has been developed over more than a decade by de Wit and a team of co-workers (de Wit et al., 1978); it is described to a large extent in the Sections 3.2 and 3.3. Laboratory research, literature study and frequent evaluations led to a model that simulates growth, yield and water use quite reliably over a wide range of environmental conditions for annual crops of C_3 and C_4 type species. Its structure reflects cereal and grass crops, and small but specific sets of parameters and functional relationships specify the actual species under consideration. The model is adaptable to other types of species. Like all models in this group, BACROS is still particularly weak in the simulation of regulation of distribution of biomass, and in development of leaf surface area. The latter limitation is a handicap for the early stages of growth, and to its transferability to other geographic areas.

It is not by accident that the current comprehensive models are all at the Production levels 1 and 2. Processes of the carbon balance and water balance received much attention from crop physiologists and from soil physicists. However, as most farming is done under nutrient stress, the practical utility of the current comprehensive models is still largely restricted to setting maxima for yield potentials and establishment of the contribution of the individual processes and factors to it (de Wit & Penning de Vries, 1982).

1.3.4 Summary models

Summarizing a comprehensive model can and should be done to make it more accessible to others in an intellectual and a practical sense. The extent to which summarization is useful depends on many factors, among which future use of the model and its inherent complexity, but simplification should achieve a level at which the model becomes really accessible to non-specialists. In the process of summarization, it is essential to indicate specifically the limits within which the model is valid. Construction of summary models should be done by scientists who know the comprehensive model by heart, and who are in contact with potential users for suggestions in which direction and to what extent to summarize it. Unfortunately, modellers may not always be motivated to do so, as the process provides little scientific challenge. Summary models can be made by shedding all excessive detail, using sensitivity analysis and by regression of model results

22

to the main driving variable of the system. An example of the result of the first procedure to obtain a summery model is presented in Section 3.1, a result of the second procedure in Section 3.2. The latter case concerns a summary of a canopy CO_2 assimilation model. Without loosing much flexibility, a large model could be reduced enormously because there are few interactions of the CO_2-assimilation processes with the environment. See also Section 1.4 on coordination of models.

It will be obvious that THE summary model of any comprehensive model does not exist: different summaries can be made with different degrees of depths and for different purposes. The summary model in Section 3.1 of growth of a crop is a small simulation model, and it is meant for use on a computer system upon which the simulation language CSMP (see Section 2.2) is available. By specifying a few crop-specific parameters, different types of annual crops can be simulated. Considerably simpler than this summary model is an earlier model by van Keulen (1976) about the potential production of rice crops. Its size, and the amount of calculations required for the simulation are such that the complete model can be programmed on a pocket calculator. Its basis is an equation in which the growth rate (GTW, in $kg\ ha^{-1}\ d^{-1}$) can be given as:

$$GTW = (DTGA \cdot 0.68 - MC \cdot TWT) \cdot CVF$$

DTGA stands for gross CO_2 assimilation (in $kg\ ha^{-1}\ d^{-1}$; a factor of 0.68 converts it to glucose assimilation, in $kg\ ha^{-1}\ d^{-1}$), TWT for total dry weight (kg ha^{-1}), MC for the maintenance coefficient in glucose per dry matter ($kg\ kg^{-1}\ d^{-1}$) and CVF for the conversion efficiency of glucose for the growth process ($kg\ kg^{-1}$). Van Keulen distributes biomass formed in one time step over roots, leaves, stems and, after flowering, over inflorescences plus seeds in predetermined proportions related to the physiological age of the crop. DTGA is calculated from standardized data. The leaf surface area, required in the CO_2 assimilation calculation, is found by dividing the leaf weight by $1000\ kg\ ha^{-1}$. MC reflects the energy requirement to maintain living tissues in their current state, and has a value of 0.02-0.015; the effect of temperature on MC could be neglected as this model was applied in a fairly constant environment. CVF is only a function of the chemical composition of the biomass formed; a value of about 0.7 is common (Subsection 3.3.4). Final yield is calculated by proceeding with time steps of 10 days and adding the biomass increment to the biomass already present.

The interested reader is invited to compare both summary models for his own purpose on aspects such as simplicity in use, accuracy in results, flexibility for adaptations to specific conditions of crop parameters.

1.3.5 Uses of models

A model is a tool that can be useful for development of science, for prediction and for instruction, but not for each aspect to the same extent: scientifically in-

23

Table 1. The relative values of certain aspects of models in different stages of development (the more plusses, the higher the value).

	Predictive value	Scientific value	Instructive value	Simplicity
Preliminary model	+	+ + +	+ +	+ +
Comprehensive model	+ +	+ + +	+	+
Summary model	+ + +	+	+ + +	+ +

teresting models are often too detailed for those who want to apply them, while models used for predictive or management purposes are often too trivial or crude to challenge scientific interest. Table 1 characterizes models in different stages of development in this respect.

A scientifically interesting model contributes to our understanding of the real world because it helps to integrate the relevant processes of the system and to bridge areas and levels of knowledge. It helps also to test hypotheses, to generate alternative ones and to suggest experiments to falsify them. Subsection 3.3.8 provides an interesting illustration. A predictive model should simulate accurately the behaviour of a part of the real world. It is therefore a good instrument to apply scientific knowledge in practice. It should predict reasonably well over a range of boundary conditions to provide its users with alternative solutions of a problem. The less detailed the desired results are, the simpler the predictive model can be. The instructive value of a model is its use for propagation of knowledge.

The size of a model may increase because its objectives are broadened, or because it is elaborated. In the first case, the number of parameters usually increases and the sensitivity of the model behaviour to each parameter decreases. Elaborating the model of a system implies the formulation of more structure. A thorough knowledge of a complex real world system, and thus a large model of it, is always required before the model can be summarized reliably for use by others. The simpler a dynamic model that still accomplishes it purpose, the better it is for instruction and for those who want to apply it in other fields or higher up in the model hierarchy. Hence, the model attains its maximal scientific value while it is being elaborated, while its value for application increases during subsequent summarization.

1.3.6 Evaluation of models

The first thorough test of a model is often the comparison of its behaviour with that observed of the real system in an analogous situation. This behaviour includes, for instance, the general shape of the time course of variables, the presence of discontinuities and the qualitative sensitivity of output to parameter values. However one should be aware that aspects of model behaviour that seem

counter-intuitive at first sometimes turn out to be realistic. If the behaviour of the model matches qualitatively that of the real world system, a quantitative comparison and an evaluation of the predictive success of the model should be made. At this stage, statistical tools can be useful. But even when sufficient and accurate data are available, a model cannot be proven to be correct. Sometimes, model behaviour can be falsified, and thus one or more model components may be shown to be in error; a model cannot be proven to be incorrect as a whole. Calibration of a model, the adjustment of some parameters such that model behaviour matches one set of real world data, is a very restricted form of evaluation. Extensive calibration degrades simulation into curve fitting. Behavioural analysis is a useful form of sensitivity analysis. Innis (1978) presents some good examples. Sensitivity analysis is done by increasing or decreasing one parameter value over a broad range, and comparing direction and shape of the output with the known or expected direction.

Large-system simulation models have been developed by various groups. The evaluation of such models is difficult because many detailed observations are needed before a critical overall test can be made. It was found that if such observations are available before the final tests of a model are performed, some of the information is often, unintentionally, used for 'tuning' some parameter values. It is almost impossible to avoid this, particularly in early stages of the modelling effort, and it should therefore be realized that the inputs of the model are then not independent of the ones with which the model is compared. It is therefore useful, but often difficult, to obtain independent data for evaluation of models from literature. When observations of the behaviour of the whole system are not available, evaluation must take place at the level of sub-systems. Evaluation of models remains often superficial as a result of too small a data base. Quite some models are only 'evaluated' by establishing a good correspondence between 'predicted' and 'observed' results, while these same observed results were used to derive constants in the model. That this is a dangerous procedure needs no further emphasis. Strong experimentation is indispensable in parallel with modelling: experimentation at the explainable level for evaluation, and at the explanatory level for further improvement (See Subsection 1.1.5).

A source of increasing concern are errors in models and in their documentation. The fundamental and most difficult errors are conceptual mistakes. Apart from these, even carefully screened simulation programs often contain simple technical errors, such as key-punching errors, dimensionally incorrect parameters and deleted variables in expressions, or deleted equations. Some of these appear when the model is used to simulate new situations, or when someone else studies the simulation program. Through vigorous evaluation, modellers should eliminate as many errors as possible before releasing the model. No guarantee, however, can be given that a model is really free of errors.

Further information about sensitivity analysis, evaluation, validation and verification can be found in articles and books by Baker & Curry (1976), van Keulen (1976), Penning de Vries (1977) and Innis (1978).

1.4 Coordination of models

C.T. de Wit

1.4.1 Necessity of coordination

The main processes and phenomena that are considered in this textbook are schematically presented in Figure 8. They all centre around the plant, but they are nevertheless related to various fields of knowledge that have been developed rather independently of each other, for example plant physiology, biochemistry, meteorology, population dynamics, soil science and soil biology. Crop models that attempt to simulate crop growth under field conditions contain important elements of these fields of knowledge. These disciplines are thus interrelated in one way or another and they should be considered together at some stage of the modelling effort.

The existence of these interrelations poses problems of coordination between and within disciplines, certainly at the present stage of knowledge and modelling. Those coordination problems cannot be treated in any way exhaustively, so that a more pragmatic introduction must suffice here.

1.4.2 Linkage of submodels-

A model may be built out of submodels that originate in different disciplines. Each may describe different parts of the system, which are often connected on only a few characteristic points. The connections may often be severed without affecting the integrity of the submodels. Such models may be developed and used on their own. The only thing that has to be done is to replace the effect of the eliminated submodel by some forcing functions.

A model of an insect that feeds on plants, and makes in the process holes in the leaves, is an example. The insect and the plant model may be developed independently of each other by supplying the model-insect with varying amounts of food and damaging the leaves of the model-plant with varying numbers of holes. Linkage may then be achieved at any time by transposing the consumption rate of insects into a rate of increase of the number of holes in the leaves and equalizing the mass of food available for the insect to the leaf-mass of the plant. Section 6.1 provides an example. Models of the uptake of water by plants from soil are another example. The effect of the soil model on the plant model may be replaced by a forcing function of the soil water tension around the roots and the effect of the plant model on the soil model by a forcing function of the uptake of water.

Since submodels out of various disciplines operate to a large extent independently of each other there is no reason at all to elaborate them to what is con-

26
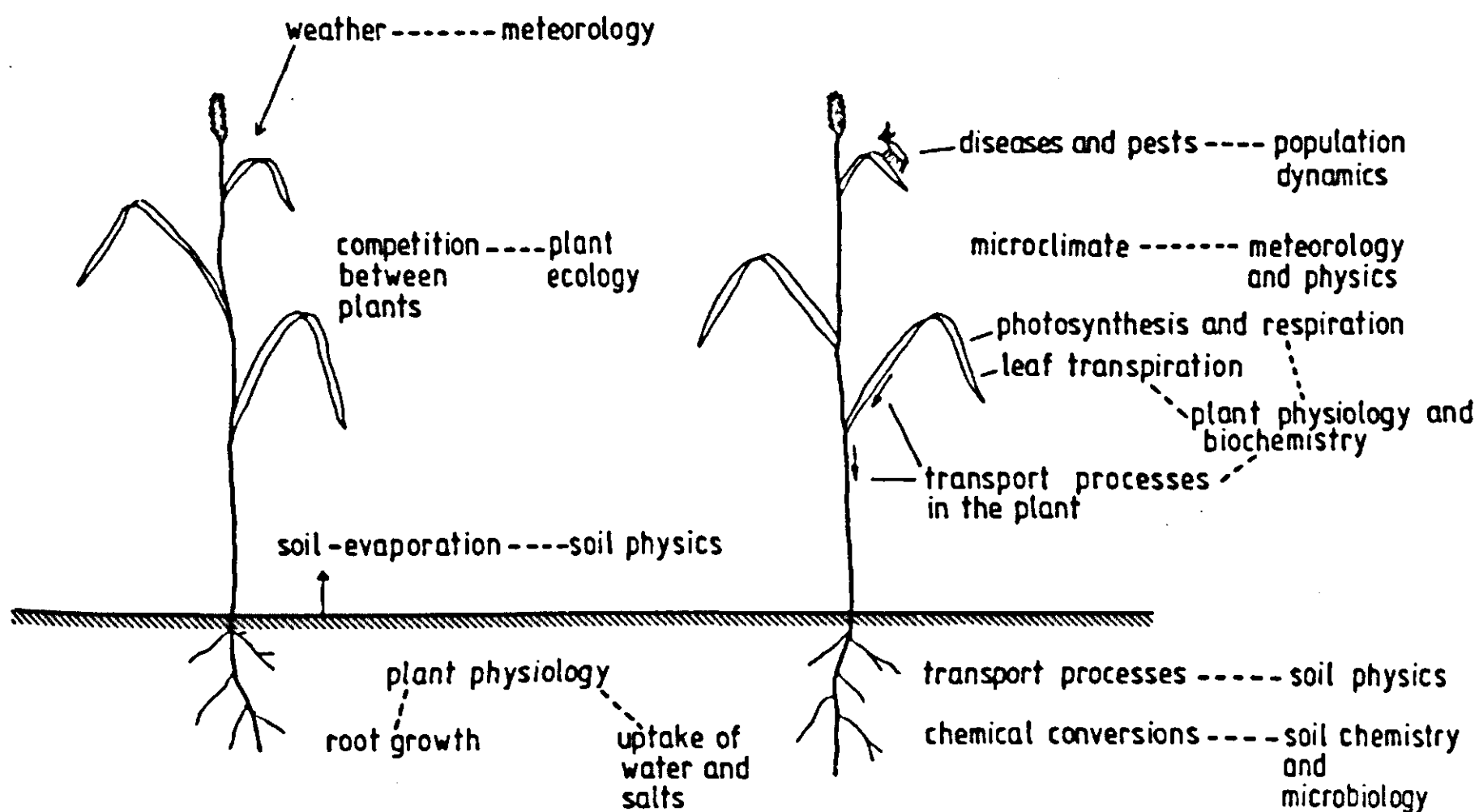
Figure 8. Fields of knowledge that need consideration in a study of plant growth.

sidered a comparative level of detail. Depending on the focus of interest, the insect model or the soil model may be worked out and the plant model may be treated elementary, or vica versa.

Preliminary, comprehensive and summary submodels may be intertwined. With respect to each other, submodels are ordered in a parallel or serial fashion. The main problem is often the maintenance of lucidity. This is facilitated by the use of higher order programming languages that allow a conceptual presentation of the model, since the language itself takes care of the construction of a proper algorithm. A well known example of such a language is Continuous Systems Modeling Program (CSMP), which will be discussed in Sections 2.2 and 2.3.

The simplest form of linkage occurs when one submodel provides an output that is used as input for another submodel, there being no effect of the latter on the former. The models can then be executed independently of each other, the first model generates data that are used as parameters or tabulated functions in the second model. The advantage is obvious. Once correct, the first model does not have to be executed again during simulation with the second model.

An example of such a uni-directional linkage between models was presented previously in Subsection 1.2.3. There the model for the first production level — optimal water and nutrients — provides the input data for the model of the second production level — optimal nutrients, but at times water shortage. Likewise, the results of a macrometeorological model may be used directly as an input for a micrometeorological model.

In the latter case there is obviously a weak feedback of the micrometeorological situation in the field under consideration to the macrometeorological

27

situation, but the complexity of the interrelations is greatly reduced by neglecting this. Such a neglect of weak feedbacks is especially justified in situations where there is a lack of knowledge or little interest in details. The ease of handling and operation of the whole then often outweighs whatever may be gained by purism. Unfortunately, rules of thumb for this type of simplification cannot be given — it is a question of common sense and experience.

1.4.3   Hierarchical nesting

As has been said in Subsection 1.1.2, an inherent feature of biological sciences is the conceptualization of complex systems in organizational levels: molecules, organellas, cells, organs, plants, populations and communities. This conceptualization is the starting point for the distinction of explanatory and descriptive models. In the explanatory approach, the processes that are recognized at the lower organizational level are incorporated in a model that aims at understanding the phenomena at a higher level. Here again submodels may be used, for instance to represent leaves, cells, stomatal behaviour or the photosynthesis process. These submodels are then, however, not so much ordered with respect to each other in parallel or serial fashion, but are what may be called hierarchically nested: models on the higher organizational level envelop those on the lower level, like a leaf envelops its cells.

The lower and the more hierarchically nested an organizational level is, the more numerous and smaller its elements are. A crop may consist out of a hundred thousand plants, which have together millions of leaves and billions of cells. This problem of excessive numbers may be overcome by lumping plants in size classes, leaves in position classes and cells according to their function. But this lumping does not overcome the problem of size: cells remain small and respond therefore rapidly to changing conditions.

As has been said in Section 1.1, small time coefficients or response times of processes lead to small time intervals of integration and these may lead to serious problems in growth models. For instance a growing plant may recover within a week or so from pruning part of the root system, whereas stomatal cells that govern the water loss of the leaves may open or close in minutes. Hence, a crop physiologist who develops a simulation program is likely to work with time intervals of integration in the order of days, whereas a stomatologist works with time intervals of less than a minute. As long as both work separately, there is no problem. The time interval of integration for the stomatologist is large enough to execute his program for an hour and the time interval of integration for the crop physiologist is large enough to execute his program for a month.

The problem starts when the crop physiologist discovers that the program of the stomatologist is useful to him and he incorporates it as a submodel in his simulation program. He creates then a situation where he has to integrate with time intervals of a minute over a period of a month. Hence all his rates, also those who change rather slowly, have to be calculated every minute or so and

this leads to excessive number crunching. A stomatologist trying to incorporate molecular submodels in his simulation program would meet the same difficulty and the crop physiologist who would then try to incorporate this stomatal model in his crop growth program would have to face the problem squared.

Any simulation program that spans response times that are orders of magnitude different contains this so-called stiff-equation problem. At least when it is executed on a digital computer. With analog computers the problem does not exist because in them all integrations are physically executed in truly parallel fashion, as in real life. Obviously the problem has to be avoided in simulation programs that are executed on digital computers by restricting the number of hierarchical levels that are incorporated into one simulation program or, what amounts to the same, by limiting the range of response times within the same simulation program.

1.4.4 The time interval of integration in crop growth models

One of the key variables in any crop model is the relative growth rate. This rate may amount to 0.25 kg kg^{-1} d^{-1} or to formulate it otherwise, the time coefficient of growth is about $1/0.25 = 4$ d. It appears in practice (see Section 2.1) that a time interval of integration of about 1/4 of the time coefficient, in this case 1 day, is often small enough to justify the assumption that the rate of growth does not change materially over this time interval. Hence in this case 150 integration steps would be sufficient to cover a crop growth period of 150 days.

Indeed, quite a number of crop simulators that emphasize growth use daily time intervals of integration. But one fundamental problem with all these is that the diurnal course of the meteorological forcing functions, especially irradiation and temperature cannot be handled satisfactorily. This course is, however, accounted for in sufficient detail with time intervals of an hour; their use leads to $24 \times 150 = 3600$ time intervals of integration. As will be shown later, computers are fast and their use is generally cheap enough to make this a manageable number. But is this time interval acceptable for the crop physiologist who aims at the construction of a process-oriented model that explains at least in part the phenomena at the crop level? This appears to depend to a large extent on the possibility to simulate the water status of the crop with this time interval of integration, because this status determines many important physiological processes of growth, transpiration and water-uptake.

The water content of a crop may be 5 kg m^{-2}; a 10 percent difference in relative water content being the difference between full turgidity and permanent wilting. The transpiration of this crop in the full sun may amount to 0.5 kg m^{-2} h^{-1} and this leads to a first estimate of the time coefficient of the process of dessication of (0.5 kg m^{-2})/(0.5 kg m^{-2} h^{-1}) = 1 h. A time interval of integration of this length could therefore violate severely the assumption of constancy of the relative water content over this period. In practice it appears that the time interval of integration should not exceed 0.1 h, because growth and stomatal

opening respond to difference in relative water content of a few percent. The resulting number of integration steps is then 240 per day. This appears acceptable for simulation programs that cover a few days and that are centered around the analyses of the diurnal course of growth. However the number appears to be prohibitive for simulation programs that cover the whole period of growth, especially when these are used for routine purposes.

Sacrificing the simulation of the relative water content in a reasonable way means sacrificing a process-oriented description of many of the growth processes and therefore it is worthwhile to investigate possibilities of tracking dynamically this water content, without using small time intervals of integration. One possibility is to compute the water content every hour in an interactive fashion. This is done by assuming that the relative water content is the same as in the previous hour and to calculate on the basis of this assumption the stomatal opening, the rate of transpiration by the leaves and the rate of water uptake by the roots. When these calculated rates differ the water content is adjusted by iteration until both are sufficiently equal. This equilibrium water content is then also used for all other rate calculations and serves again as the first estimate for the next interval of integration. Examples are given in the Subsections 2.3.4 and 3.3.7.

It may be feasable to handle a few other phenomena in similar fashion, but by and large it must be concluded that the inclusion of processes that require shorter time intervals of integration than considered here is practically impossible.

This holds also for such a central process as leaf CO_2 assimilation. Much is known about the biochemistry of the process, but incorporating this knowledge into crop simulation programs would require time intervals of integration that are an order of magnitude smaller than feasable because the concentration of intermediates and mediating enzymes may respond very rapidly to changing conditions. These small time intervals are then avoided by using strictly descriptive functions of the relation between CO_2 assimilation and light intensity on the leaf level. Of course it becomes then very difficult to incorporate adaptive phenomena into the simulation program, like for instance the transition of sun into shade leaves. These descriptive functions on the leaf level are either obtained by experiment or generated in their turn by a leaf CO_2-assimilation model on a biochemical basis. This model provides then basic parameters for the simulation program and in this respect the treatment does not distinguish itself from those other uni-directional linked submodels.

One other remark should be made. When a modeller reduces the time interval of integration of his model to improve on the simulation of a process, with a short time coefficient he should realize that this does not imply that the simulation of the time course of other processes improves automatically. For instance, by adding a submodel that simulates properly the behaviour of stomates with time intervals of minutes to a crop growth model, based on 1 h time steps, the simulation of growth and respiration processes has not been refined: although the

computation of such rates occurs then more frequently, the model still implies a direct link of the carbohydrate reserve level to the rate of growth (Subsection 3.3.4), whereas it is in fact an indirect link that takes some time to establish. Obviously the degree of accuracy of simulation of a process does not increase by decreasing the time interval of integration to below about one-quarter of the corresponding time coefficient.

31

2 BASIC TECHNIQUES OF DYNAMIC SIMULATION

2.1 Introduction to dynamic simulation

Th. J. Ferrari

2.1.1 Introduction

In the preceding chapter the definitions of concepts related to the state variable approach for simulation of living systems have been given. The method of construction of models according to this approach is introduced in this and the two following sections (Section 2.2 and 2.3). Particular attention is given in this section to the system dynamics of the most simple unit of a system. Such a unit consists of a number of elements and may contain a feedback loop. With a number of such units, larger systems with a closed structure can be described, with which the behaviour of the larger systems can be analyzed. In applying system dynamics for simulation of living systems, one does not need to have much knowledge of the mathematics of integration. In the computation of state variables, we use in fact often only the elementary arithmetical operations of adding, subtracting, multiplying and dividing.

How the knowledge of a system, i.e. of the factors on which the rates of a process depend and of the relationships between these factors, can be translated into a relational diagram of this system, according to certain conventions, will be shown in Subsection 2.1.2. Such relational diagrams are not necessary, but they do form an useful help to gain a better insight into the mutual relationships and enable surveying of the relevant factors. With these diagrams, the definition can be facilitated of the rate equations (the differential equations) to compute the rate variables and of the state equations (the integral equations) to compute the state variables (Subsections 2.1.3 and 2.1.4). Although integration in simple systems can often be done analytically, the numeric solution will be emphasized here (Subsection 2.1.5). This solution is based on a repetitive computation of changes occurring during successive, small time-steps. It will be shown that the analytical solution for models of systems of plant growth is impossible to use in practice, even for relatively simple systems. The differential equation is an important element of the description of the feedback phenomenon (Subsection 2.1.6). The time coefficient of a system or a process is the subject of Subsection 2.1.7; it can be used to characterize delays and mathematical, dispersion (Subsection 2.1.8), included in many models.

2.1.2 Relational diagrams

Relational diagrams are not necessary, but they have several advantages, so many people find them useful for building and elaborating more abstract models. At the start of research, a relational diagram summarizes the most important

elements and relationships and helps the researcher to maintain an overall picture
Especially when problems are complex, it simplifies the definition of rate and
state equations. It makes also the content and characteristics of a model easily
accessible to others. Finally, a relational diagram improves the comprehensibili-
ty of a model so that consequence of different concepts of the structure of a
system on its behaviour, and the significance of certain structures (loops) for the
behaviour stand out more clearly.

An example of a simple relational diagram is shown in Figure 2 of Section 1.2.
Its representation is based on a number of conventions summarized in Figure 9.

Figure 9. Basic elements of relational diagrams. Abbreviated names of variables repre-
sented by these elements are usually written in or next to them. Note that driving variable
are often underlined or placed between parentheses. Intermediate variables are often
characterized by a circle.

A state variable, or integral of the flow; final result of what has happened

Flow and direction of an action by which an amount, or state variable
is changed; if necessary, different sorts of lines can be used to distin
guish between various states but no broken lines.
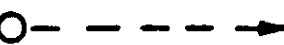
Flow and direction of information.
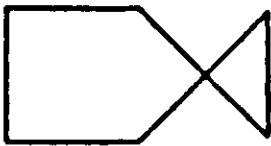
Valve in a flow, that indicates that a decision takes place here; the line
of incoming information indicate upon which factors the decision de
pends.

Source and sink of quantities in whose content one is not interested
This symbol is often omitted.

A constant or parameter.
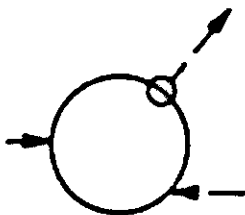
Auxiliary or intermediate variable in the flow of material or of informa
tion.

36

The relations between elements in a diagram are indicated in a qualitative way only. Quantification of relations occurs during the definition of rate and state equations, and this is to be discussed in the following subsection. Sometimes during the research it appears that a factor supposed to be constant is variable after all (see Subsection 1.4.3). Then it has to be replaced by something else, perhaps a table, an auxiliary equation or a connection with an integral. One sometimes indicates with a + or − sign whether a loop concerns a positive or negative feedback.

Special emphasis must be given to the flows. The flow of material or energy is presented by solid arrows and the flow of information by dotted arrows. The solid lines connect state variables. Information is only transmitted and usually not processed, thus information is given, directly or indirectly, only to the decision functions and never to state variables. The use of information does not affect the information source itself. The flow of information can be delayed, and as such be a part of a process itself.

2.1.3 Rate and integral

The rate by which the numerical value of a state variable changes is expressed in the dimension: amount per time. Depending on the nature of the state, this amount can relate to different quantities, such as weight, length, number and even rate. The rate itself may be constant for a certain period; it may also change without a clear pattern (at random) or according to certain rules. These so-called decision rules must then be converted into differential equations. Note that decision does not have a human connotation: the differential equation describing a chemical reaction can be considered as a decision rule. Neither does it yield only a 'yes' or 'no': it can have any value.

It has great advantages to illustrate with simple examples a discussion on nature and function of a differential equation and on the integration associated with this equation. The principles used hereby are essentially the same as for more complex phenomena. The simplest case is the solution of a differential equation to describe the constant speed or rate of change in position of a vehicle. Plotted against time in hours (h) on a graph, this speed (km h^{-1}) is shown as a straight line parallel to the time axis (Figure 10). What is the result of this speed after a certain period? In other words, what is the distance covered? This question can be answered easily. The speed is multiplied by the length of time or period concerned and the distance covered is obtained as a result. One has now integrated the differential equation $ds/dt = c$, in which s is the distance (km), t the time and c a constant with the dimension km h^{-1}. The differential quotient or derivative ds/dt is a notation for the rate during an infinitely small time interval dt; another notation is $\dot{s}$.

In a graph this integration is the same as the computation of the area delimited by the time axis, by the line parallel to this time axis at a value c of the rate ordinate and by the both lines, parallel to the vertical rate axis, at two
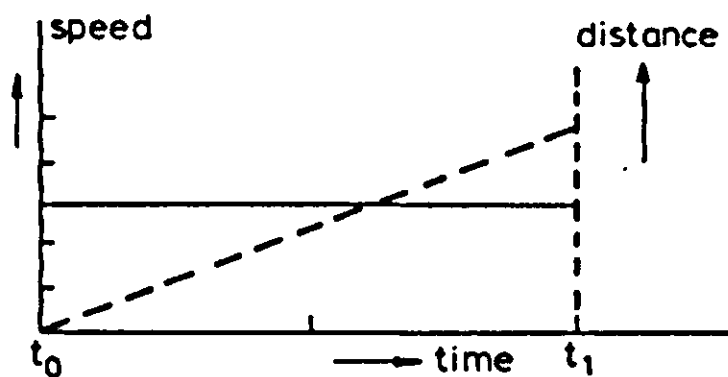
Figure 10. Speed in km h^{-1} (solid line) and distance covered in km (broken line) as function of time in h. The area delimited by the speed line, the two lines at the moments t_0 and t_1 and the time axis equals the distance covered after $t_1 - t_0$ time units.

points of time indicating the period. The result of the integration, s, is plotted as a function of time and given in Figure 10 by the dashed line through the origin with slope c. In this graph the slope of a straight line or the tangent to a curve represents the speed or rate at a certain moment.

Exercise 1
In a graph, the distance in meters on the y axis is plotted against the time in seconds on the x axis; the result is a straight line.
a. What does the slope of the line represent?
b. What is its dimension?
c. What can be said about it if the line is parallel to the x axis?

Such a procedure is always performed by integration. The right side of the differential equation is mostly more complex. The mathematician usually tries to integrate such differential equations mathematically by introducing boundary conditions or constraints in the model. This analytical, or mathematical, solution often gives a better understanding of the behaviour of the system than the numerical solution (computation of surfaces, for example) but can be applied less easily to practical situations. The necessary constraints can also be unacceptable in view of the purpose of the modelling effort.

2.1.4 Differential and finite difference equations

One starts mostly with simple differential equations. But with an increase in knowledge, there is the tendency to make the differential equations more complex so that they can no longer be integrated analytically. One might expect an equation that cannot be solved to be of little practical value. However, the numerical solution of such equations is often not very difficult (see Subsection 2.1.5).

Both methods can be illustrated with the help of some examples. Exercise 2

refers to the problem of filling a tank with water. The constructor has regulated the rate of filling by a valve with a time switch. From this one can derive that the rate as function of time is represented by the differential equation $dw/dt = -(1.2/30) \cdot t + 1.2$ up till time $t = 30$, in which w is the number of litres and t the time in seconds; dw/dt is the rate of change with which the water is flowing into the tank; the rate is zero after $t = 30$.

An analytical integration of this differential equation gives the amount of water w in the tank as a function of time according to $w = -1.2/60 \cdot t^2 + 1.2 \cdot t$. With this equation it is now possible to compute the inflow of water for each period between the points $t = 0$ and $t = 30$.

Exercise 2

Plot the rate of water flowing into a tank in litres per second on the y axis against the time in seconds on the x axis using the differential equation given above. The result is a straight line descending with a rate of 1.2 litres per second at point $t = 0$ and with a rate equal to zero after 30 seconds.

a. What is the amount of water in the tank after 30 seconds if there was no water in the tank at point $t = 0$?

b. Calculate the amount of water in the tank as a function of time between $t = 0$ and $t = 30$.

c. Check the results of the calculations based on the differential equation using the integral given.

We stress that the rate of inflow is not dependent on the amount of water already present in the tank in this example. However rates generally depend on states in the system (Subsection 1.1.3). For instance, an ecologist may think, on biological grounds, that the number of animals in an area increases by a certain percentage every year. Now the rate of increase, expressed in numbers of animals per year, would be determined by the number of animals already present and consequently would not be constant in successive years. Under such conditions, the following differential equation holds: $dy/dt = c \cdot y$, in which y is the number of animals at a certain moment and c the annual relative growth rate. The rate is a function of the number of animals y; in a graph this is represented by a straight line through the origin. This differential equation can be integrated analytically and produces the well-known exponential growth curve $y_t = y_0 \cdot e^{ct}$, in which t is the time in the chosen units and e the base of the natural or Napierian logarithms. The subscripts of y represent time; consequently, y_t and y_0 are the amounts of moment t and at the start of the calculation, respectively.

Exercise 3

Sketch the graph of the exponential growth curve with an annual relative growth rate of 0.03 over a period of 50 years, starting with a herd of 10^4 animals. Draw one graph on a linear scale and one with $\ln y$ instead of y on the ordinate.

2.1.5 Numerical integration

Until now we have investigated the influence of a certain rate equation on the state variable by analytically integrating this equation. The numeric value of a state variabale could be represented as a function of time by performing this integration for different time spans. In this way we can compute its behaviour. It is also possible to calculate the evolution of the value of the state variable by computing the changes during a number of successive short periods. The rate during such a short period can be supposed to be constant. One starts with a certain initial state y_0. By using the rate equation concerned, one can calculate the absolute rate during the next time interval or time step Δt and the subsequent change in state during this time interval. The new state again causes a new rate which holds for the next interval Δt, and so on.

The following example explains this procedure. Suppose that the rate at which an amount of water w is flowing into the tank through an adjustable valve, is given by the differential equation $dw/dt = 1/4 \cdot (16 - w)$. Suppose also that there is no water in the tank at $t = 0$; thus $w_0 = 0$. The rate by which water is flowing at that moment into the tank equals: $1/4 \cdot (16 - 0) = 4\,l\,s^{-1}$. If we take the length of the time interval Δt equal to 2 s, then 8 l water will have flowed into the tank after 2 s, and w becomes 8 l. During the following time interval of 2 s, the rate is than: $1/4 \cdot (16 - 8) = 2\,l\,s^{-1}$. Therefore, during this time step 4 l is flowing into the tank, so that the total quantity of water in the tank equals to $8 + 4 = 12$ l. The calculation proceeds as follows:

time (s)	inflow during the interval (l)	amount of water in tank (l)	difference from the maximum of 16 l (l)	rate of inflow (l s^{-1})
0 $\}\,\Delta t$		0	16	4
2 $^{\}\,\Delta t}$	8	8	8	2
4				
6				
8				
10				
12				

40

Exercise 4

Complete the calculation and plot the amounts of water in the tank against time.
a. What do you notice?
b. When is the rate of inflow zero?
c. What happens if 8 is substituted for 4 in the fraction 1/4?
d. Suggest a name for this fraction, and what is its dimension?

In filling out such a scheme one has performed a numerical integration. Analytical integration may also be applied here. Integrating the differential equation $dw/dt = 1/4 \cdot (16 - w)$ gives the equation $w_t = 16 - (16 - 0) \cdot e^{-t/4}$. Figure 11 shows the state variable w as a function of time.

Exercise 5

Plot the results of the calculation of Exercise 4 in Figure 11.
a. Are the results of this calculation of the amount of water in the tank under-estimated or overestimated compared with those of the analytical solution?
b. How do you explain this difference and in which way could it be corrected? (see also Subsection 1.1.3).
c. Repeat the calculations from t_0 onwards with $\Delta t = 1$ s.

With the calculation just discussed a numerical integration is performed in basically the same way as with a computer. The researcher converts continuous differential equations into finite difference equations, or rate equations, with a difference quotient $\Delta y/\Delta t$; with the aid of these finite-difference equations the new states or amounts are computed.
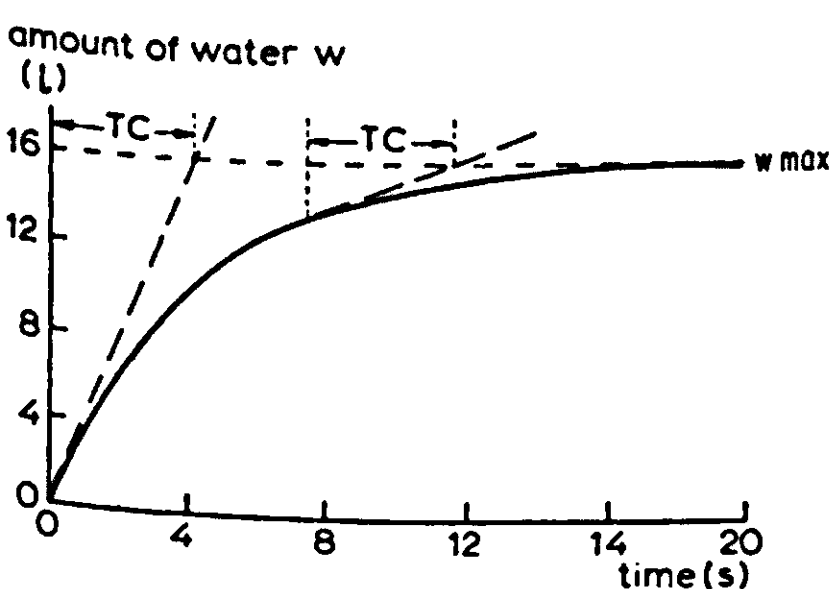

Figure 11. The amount of water w as function of time. The curve is the integral of the differential equation $dw/dt = 1/4 \cdot (16 - w)$ in which w is the amount of water at moment t. For explanation of TC, see Subsection 2.1.7.

—The state equations describe how the changes are effected and form the integral. Their basic form is always:

$$\text{state}_{t+\Delta t} = \text{state}_t + \Delta t \cdot \text{rate}_t$$

(see Subsection 1.1.3). This computation is repeated many times by resetting $t + \Delta t$ to t after integration. Initial values of the state variables, and not of rate variables, define the situation at the onset of simulation. The numerical integration method of Euler (the rectangular method, see Section 2.3) is the most straightforward and works mathematically just as given here. More sophisticated integration methods that compensate considerably for inaccuracies inherent to numeric integration also exist (Exercise 5, Section 2.2 and 2.3). The use of simulation languages facilitates the expression of rate and state equations in a form that can be processed by a computer. In the formulation of the ultimate program used by the computer, the time subscripts can usually be dropped.

It is worthwhile to consider the implications of this formulation of numerical integration. State variables are updated after each time interval: they obtain then a new value by adding to them the rate of change multiplied with the duration of the time interval. Numerical integration requires that changes in the state variables and in all other elements of a system are small during a time interval. If this is not the case, the duration of the integration time interval is too long and should be reduced. Obviously, the rates of change are unaffected by this adaptation: they may be quite large, but then the corresponding time interval should be very short.

Proper numerical integration requires the computation of all rates of change before the integration starts. Simulation languages may take care of this (see Subsection 2.2.4) so that the modeller is not bothered by it. When using other computer languages the programmer should take care that this requirement is met.

Rate equations and the state equations can be extended in various ways. Rates of different, parallel processes can be included in a state equation. A rate equation may contain every combination of state variables and constants required by the problem. Furthermore, the number of rate equations and state equations can be increased as specified by the content of the problem. When the equations are formulated, the following points have to be taken into account. The time interval Δt is only found in state equations. A rate does not depend directly on another rate (Section 1.1) and because in reality a rate can be determined only indirectly through changes of state variables, rate equations contain only states, other variables and constants. The states are altered only by rates. The dimension of an element in the equation does not determine by itself whether it is a rate variable or not.

2.1.6 Feedback loops

Study of the behaviour of man-made control and servo-mechanisms has

42

shown that the structure of a system may be more significant for its behaviour than the individual elements are. An important structure is the closed loop, or feedback loop, in which the state of an element or variable determines the degree of action or flow, which subsequently changes this state. This process takes place in a continuously circulating loop. There are two kinds of feedback loops.

In a positive feedback system, the action enhances the state, and vice versa, so that the action becomes greater and greater until a limitation within the system is encountered. An example is the exponential growth according to $y_t = y_0 \cdot e^{ct}$ with as underlying differential or growth-rate equation $dy/dt = c \cdot y$. This is the model of, for example, the growth of capital at a fixed interest per year, and of the growth of algae in a lake with a constant relative or intrinsic growth rate $(dy/dt)/y$. The absolute increase per time unit is determined by the amounts already present, so that the increase in amounts is enormous until it becomes restricted by internal limitations of the system. A positive feedback loop produces, as it were, a departure from some reference, neutral condition or goal, which is often that of zero activity. Such an equilibrium state in a positive feedback loop is often called an 'unstable' equilibrium.

Unlike the positive feedback, the negative feedback loop tends to return the system to an equilibrium situation; a departure from this equilibrium produces an action to return the value of the state variable to this equilibrium level. An example is a mechanism for the automatic filling of a tank with water up to a certain level. The tank may then be filled according to the equation $w_t = w_{max} - (w_{max} - w_0) \cdot e^{-ct}$, obtained by integration of the differential equation $dw/dt = c \cdot (w_{max} - w)$. The term w_0 is the amount of water in the tank at the beginning of the calcultation, w_{max} is the maximum level in the tank, which in this case is also the equilibrium value.

Exercise 6

a. Trace how the negative feedback loop in the last example works with the help of the differential equation.

b. In a certain crop, leaves are formed and die simultaneously. They are formed at a rate of 50 kg ha^{-1} d^{-1}. The rate of dying of the leaves is described by $dy/dt = -c \cdot y$, in which y is the amount of leaves and c the relative death rate, which equals 0.03 g g^{-1} d^{-1}. Does this system contain a positive or a negative feedback loop?

c. What is the rate equation and what is the equilibrium of the system?

Because a feedback system has a closed boundary, its behaviour must be accounted for by the structure only: it arises from the properties inside the system. Although factors outside the system do influence it, they are not essential for the pattern of behaviour. State variables and decision functions are parts of
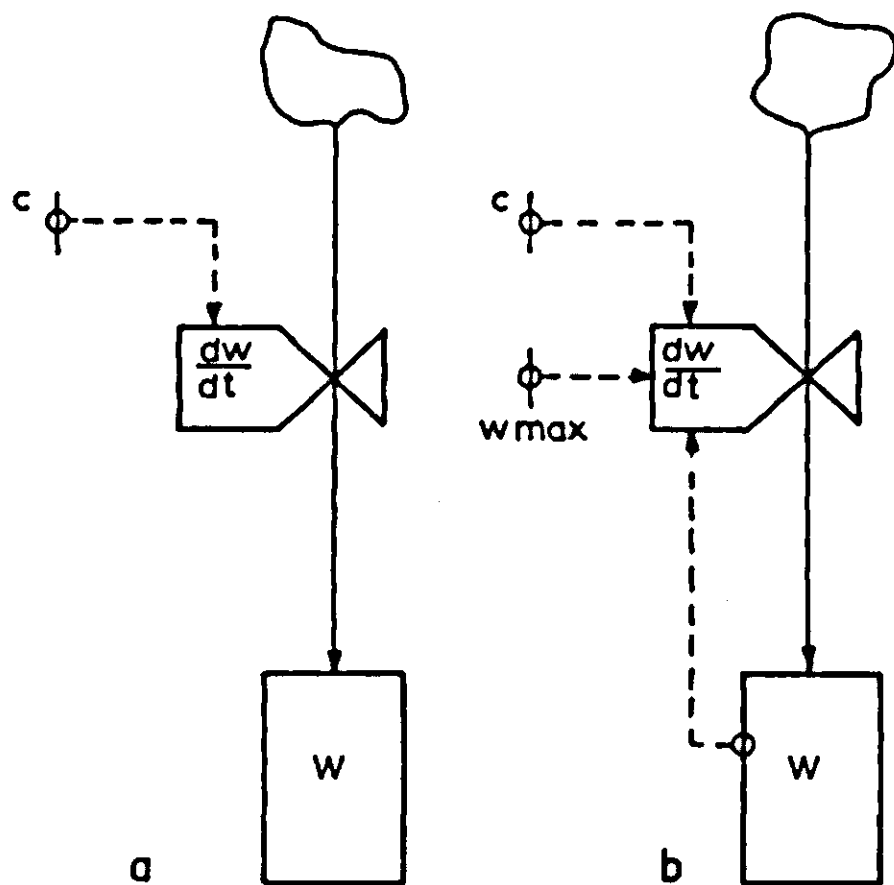
Figure 12. Relational diagram of systems of filling a tank with water. a. Without feedback loop and without maximum level. b. With feedback loop and a maximum level.

this feedback loop and are connected by an information chain or flow. The components of a decision function are the equilibrium situation, the state as observed by the decision function, the discrepancy between this state and the equilibrium and finally the necessary action resulting from this discrepancy.

The importance of the feedback structure and how it works can be illustrated best by two comparable examples, one with and one without a feedback structure. Both examples refer to the filling of a tank with water through an adjustable valve and are worked out in Figure 12 by relational diagrams. In Figure 12a there is no connection between the water-level in the tank and the aperture of the valve; the valve is not affected by the water-level: it has an aperture that does not change. In Figure 12b, however, the valve is affected by the water-level in the tank: through the float in the tank and the level between float and valve, the water-level determines the position of the valve and thus the aperture and the flow rate or decision. The builder of this system fitted a valve whose aperture closes increasingly with a rising level of water, until the flow is cut of when the water level in the tank has attained its maximum. The system reacts instantaneously to information; it is striving towards an equilibrium, namely the maximum level. Consequently, this system contains a negative feedback loop.

In the first example (Figure 12a) the rate of flow is constant and independent of the water-level, and the relevant differential equation is $dw/dt = c$. By integration, one can derive that the amount of water w at every moment can be calculated from $w_t = c \cdot t$. In the example with the feedback structure, the aperture of the valve on which the rate of flow depends, is a function of the amount of water and therefore not constant. How is this function derived? It is reasonable to suppose that the rate of flow is a constant fraction of the difference between the maximum amount w_{max} and the instantaneous level w. The lower the

44

water in the tank, the faster the flow. The differential equation now becomes $dw/dt = c \cdot (w_{max} - w)$, from which after integration the amount of water in the tank can be calculated as function of time according to $w_t = w_{max} - (w_{max} - w_0) \cdot e^{-ct}$; the parameter c is a constant and w_0 represents as usual the initial value. The rate of flow is zero at the moment that the water-level in the tank has reached the maximum. This situation is called a static equilibrium because the rate of flow at that level has become zero and will be zero again some time after disturbance of the water-level. (This state must be distinguished from a dynamic equilibrium, in which the total amount present does not change, but where the rates are not equal to zero).

2.1.7 Time coefficient

Many processes are described by characteristic rates. For the exponential growth, the relative growth rate *(rgr)*, is such a characteristic rate. In the equation in which the rate is given as a function of the amount, $dy/dt = rgr \cdot y$, the left side presents an amount per time unit, and the right side an amount and the relative growth rate. The dimensions on both sides of the equal sign should equal each other. This means that the *rgr* has the dimension T^{-1}. In comparing processes in systems it is customary, especially in the technical sciences, not to use this characteristic rate but its inverse: the time coefficient. This coefficient is important for the behaviour of the system and has often a characteristic name. It is discussed briefly in the Subsections 1.1.4 and 1.4.4, and we will return to it later on. In the equation of the exponential growth, the relative growth rate equals the inverse of the time coefficient (TC). The equations become then $dy/dt = (1/TC) \cdot y$ and $y_t = y_0 \cdot e^{t/TC}$, respectively.

Exercise 7

a. Calculate the time coefficients when annual relative growth rates are 1.50, 0.25, 0.05, 0.02 and 0.001.

b. What is the value of y_t after one year, starting with the initial value $y_0 = 100$?

c. Compare the percentage of the total increase with the relative growth rate.

A warning for mistakes may appropriate here. The time coefficient is calculated correctly in Exercise 7. But when the growth percentage, given to indicate the increase in amount after one year (e.g. an increase from 100 to 125 corresponds with a growth percentage of 25% per year) is used to calculate the TC, an incorrect result is obtained. In Exercise 7 it is shown that this growth percentage of 25% per year is not identical with a *rgr* of 0.25. The relative growth rate is in fact less: after one year, y_t becomes $y_t = 125 = 100 \cdot e^{rgr \cdot 1}$, hence $rgr = \ln 1.25 = 0.223 \text{ yr}^{-1}$; the TC equals 4.48 yr instead of $1./0.25 = 4$. Especially

with large relative growth rates this difference between the percentage of increase and the relative growth rate can be considerable. The cause of the difference is the feedback in the exponential increase or decrease. The relative growth rate is therefore smaller than the percentage of increase after a unit of time for an exponential increase, and the relative rate of decrease is larger than the percentage of decrease after a unit of time for an exponential decrease.

The time coefficient TC appears to be an important element to characterize the behaviour of a system. It determines mainly the reaction rate and indirectly the behaviour of the system. To demonstrate this we confine ourselves to its influence in the most simple feedback systems: the exponential growth curve and the system by which a tank is filled automatically with water. In such feedback systems with only one state variable, TC is the time needed to bring the system into equilibrium if the rate of change were constant. This applies to any point of the exponential growth curve, as is illustrated by the extension of the tangent until it intercepts the equilibrium line (Figure 11).

Exercise 8

a. Prove this statement by using the rate equation of the system for automatic filling of a tank with water. Verify that this holds indeed for every point of the integrated function!

b. This is also correct for a positive feedback system, but the formulation is different. Why?

The significance of the time coefficient is generally recognized, as is indicated by well known names of this coefficient and of related concepts in various sciences: the time constant, transmission time in control-system theory, the doubling time, the average total residence time, the delay time, the extinction time and the relaxation time. In population biology and in many crop growth models the inverse of the time coefficient, the relative growth rate $(dy/dt)/y$, is mostly used.

Exercise 9

For exponential growth the doubling time, defined as the time needed to double the amount, equals $0.7 \cdot TC$ and is therefore smaller than the time coefficient.

a. How can the factor 0.7 be derived?

b. What could be a definition of half-life or half-value time? The half-life period equals $0.7 \cdot TC$.

The relaxation time, often used in physics, is the time needed to decrease the tate to 1/e-th, or 0.37th, part of the original value. It is the time coefficient of he exponential return to the original state and can be used as a measure of the peed with which a system is absorbing disturbances. Suppose that a population if N animals decreases by death according to the exponential death curve $y_t = $ $y_0 \cdot e^{-t/TC}$, and that there is no increase by birth or by migration. In this case the ime coefficient equals the average residence time. The average residence time of inimals among other living beings is called the average life-time of the animals.

Finally, the time coefficient is important for the length of the time interval Δt or numerical integration. We have already seen that the drawbacks of numeri-al solutions can be overcome partly by using small time intervals (see Subsec-ion 2.3.6). However, smaller intervals require extra computer time and cost noney. Therefore, the tendency to increase the length of the time interval does aise the question how far this enlargement may proceed without invalidating he prediction. As a rule the length of the interval should not be greater than ine-fifth to one-quarter of the smallest time coefficient of the system (see Sub-ections 1.1.4 and 1.4.4). If the interval in the simulation procedure is too large, he behaviour of the simulation model will have nothing to do with reality. For nstance, if the time interval of integration of the simple system of the automatic illing of a tank is taken to be $2 \cdot TC$, oscillations will occur.

1.8 Exponential delays and dispersion

Closely related to the concept of the average residence time is that of delay ime. This concept involves a change of place, amount or form that is not realized mmediately. A transformation of raw material into a product requires time for nanufacture, just as the transfer of oil from the mining area through the pipe-ine to the client takes time. The transmission of information takes time, ex-iressed as an information delay.

Oil pumped into a pipe takes some time to arrive at its destination, but once here, it is all there. This type of delay is called a pipeline delay. Exponential de-ays are another type of delay: not all material arrives at the same time, but ome early, some late and most in between.

Suppose for instance that a group of seeds have been wetted at the same mo-nent. They do not germinate immediately, but after a delay. The average ger-nination time (or residence time or delay time) may be 10 days. Only a few eeds will take exactly 10 days to germinate because there are differences in the ate of germination between individual seeds. Hence the germination dates how a dispersion according to a certain frequency-distribution curve. These lispersions are met in all kinds of problems. Some examples are: the difference n biological-response time to signals or to manipulation, and the difference in ihysiological development of biological subjects; responses to changes of rates lso show similar patterns.

The phenomena delay and dispersion as they occur in reality can be described
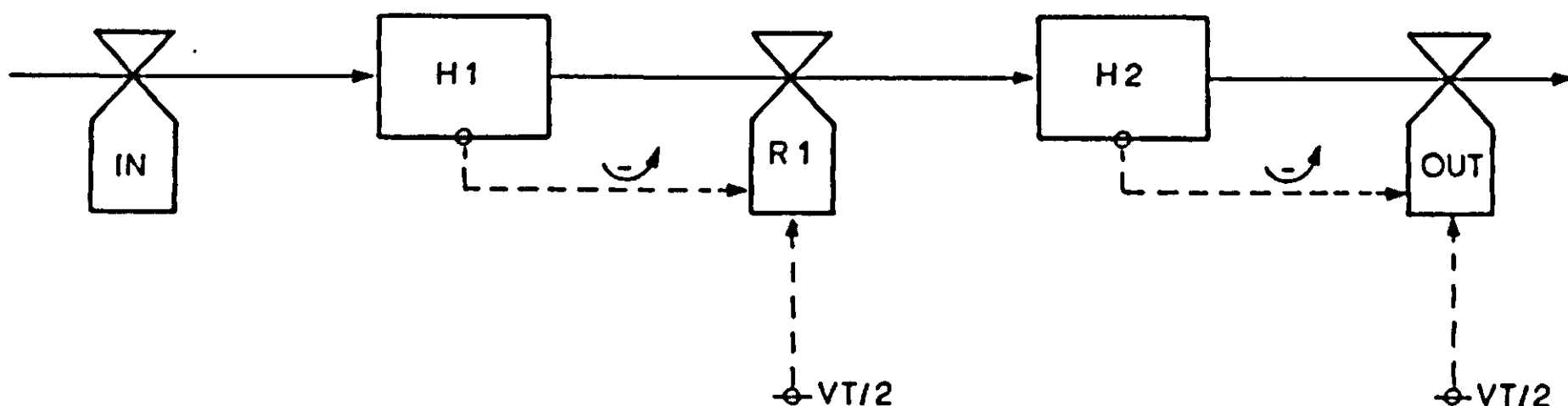
Figure 13. Relational diagram of an exponential delay of the second order of a rate. The input IN is changed; this change is effectuated in the output in a delayed and transformed way.

well with help of certain structures of system dynamics. It appears that distribution curves, representing the dispersion, can be obtained by using a cascade of successive integrations. An example is the relational diagram Figure 13, which represents a second order exponential delay of a rate (two integrals H1 and H2, between the rates IN and OUT) with a total delay time of VT. The corresponding state and rate equations are:

$$H1_t = H1_{t-1} + \Delta t \cdot (IN_{t-1} - R1_{t-1}) \text{ and } R1_t = H1_t/(VT/2),$$
$$H2_t = H2_{t-1} + \Delta t \cdot (R1_{t-1} - OUT_{t-1}) \text{ and } OUT_t = H2_t/(VT/2).$$

Figure 14 presents the rates R1 and OUT that result from a stepwise INput. The response of R1 to IN represents a first order exponential delay. The average delay time of a first order exponential delay equals the time coefficient of the filling process of H1 by IN.

Exercise 10

a. Why has VT/2 been taken as time coefficient in both rate equations?

b. What are the values of H1 and H2, assuming that the steady state is reached for a constant inflow rate IN?

c. In a lake district, water flows from one reservoir to the other. The outflow from each reservoir is proportional with the content. We consider two similar lakes in succession. In a steady state the rate of inflow (IN) is 100 m³ per week; the total delay time (VT) is 8 weeks. Outflow from the last lake can be represented by the second order exponential delay.

Assume that the inflow rate (IN) in the first reservoir (H1) is doubled suddenly. Calculate the time course of R1 and OUT (in m³ per week) at intervals of 2 weeks, for a period of 3 months. Draw a figure of R1 and OUT against time and compare with Figure 14.

d. What equilibrium state is reached at the end?
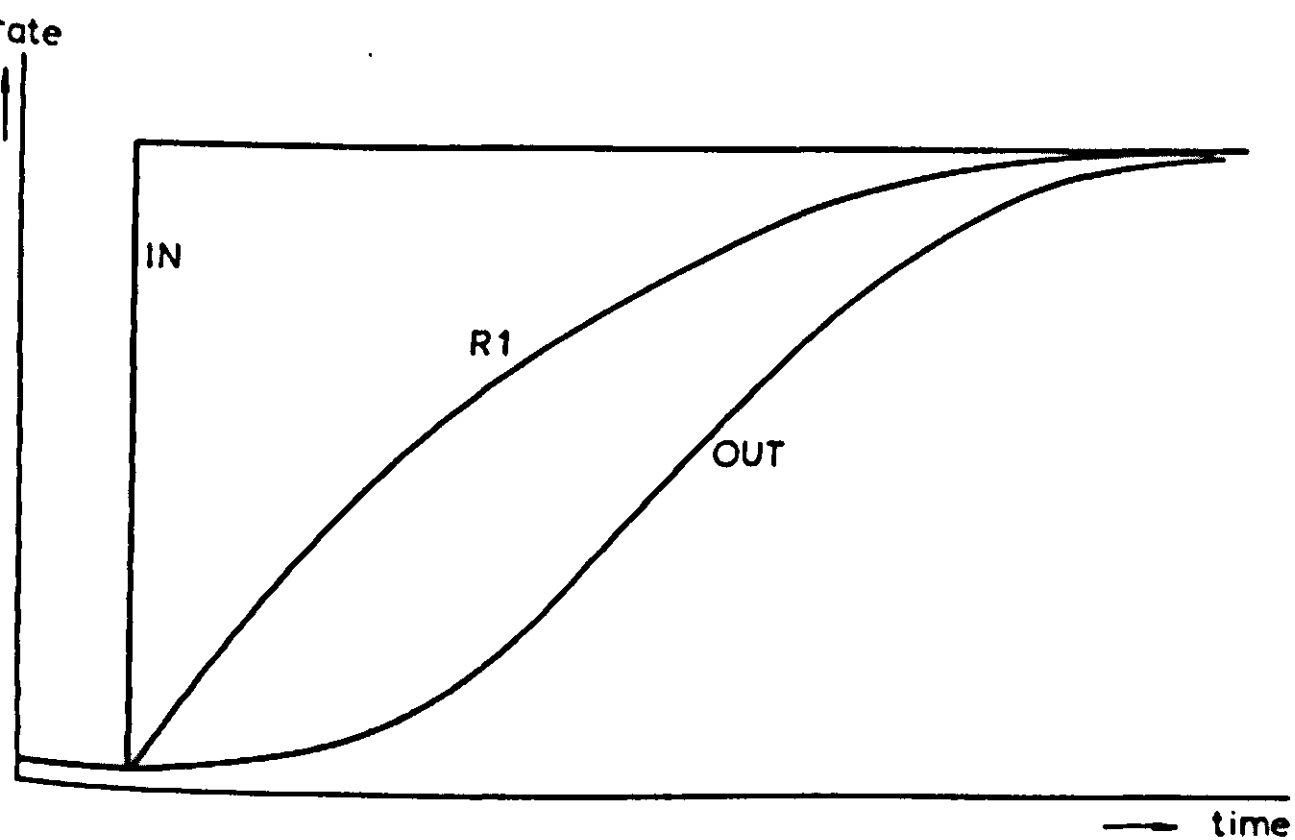
Figure 14. The responses of the rates R1 and OUT to a stepwise changing input (IN) for the model shown in Figure 13.

Delays of higher order than the second order can be formulated in a similar way. It appears that cascades of successive first-order delays yield dispersion curves that are distinct from those of Figure 14. Some of these curves are brought together into Figure 15 where the simulated output, resulting from a sudden and permanent change in the input, is given. The greater the order of the delay, the steeper the distribution curve and the narrower the distribution. The relationship between order and standard deviation is formulated by the expression $N = (VT/s)^2$, in which N represents the order or the number of integrations, VT total delay time and s the standard deviation in time units. With a delay of infinite order the deviation disappears and a 'pipeline' effect is obtained. This computed dispersion can be used in model studies to simulate the dispersion found in nature. This technique can be applied in many fields.
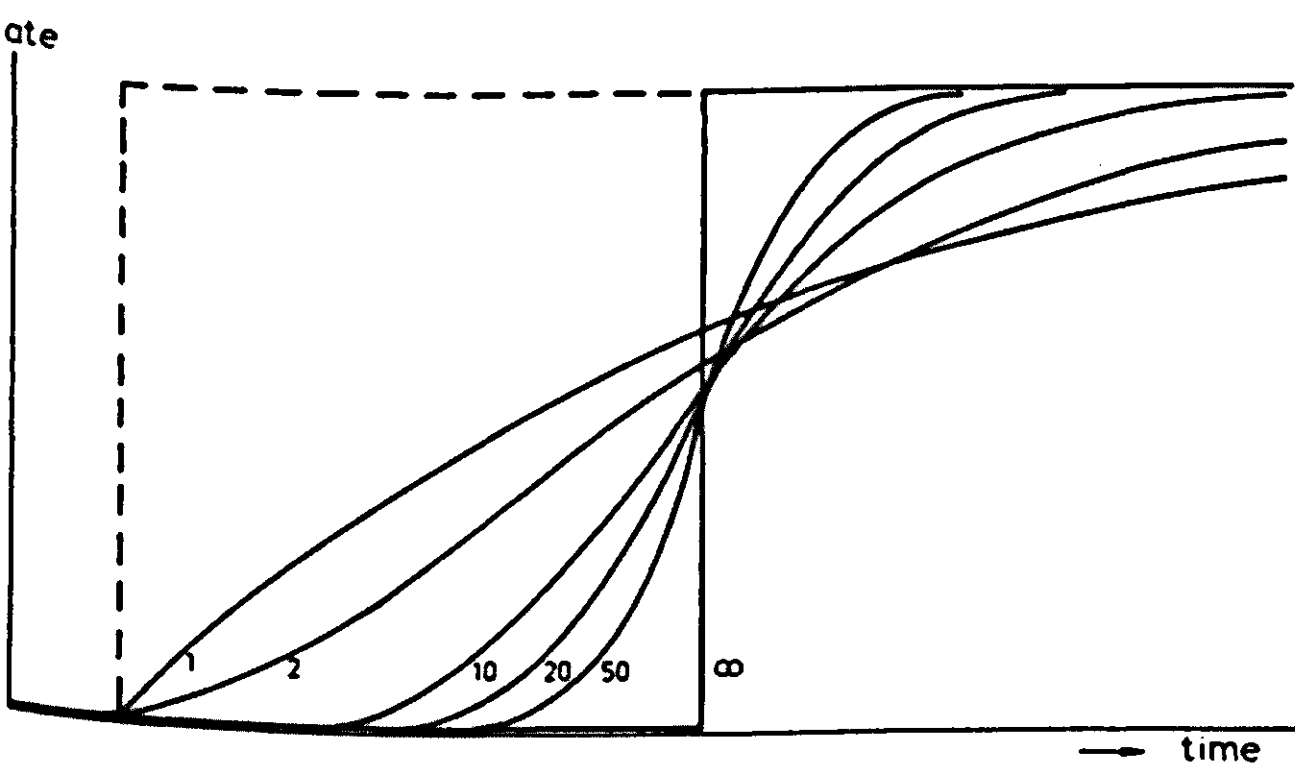
Figure 15. Some characteristic patterns of responses of the output rates on sudden and permanent changes in the input rate (-----). Delays of the 1st, 2nd, 10th, 20th, 50th and finite order are shown.

2.2 Introduction of CSMP by an elementary simulation program

L.J.M. Basstanie and H.H. van Laar

2.2.1 Introduction

The scientific approach toward studying ecological and physiological phenomena often results in their being described by mathematical expressions. A great deal of these phenomena behave in a 'dynamic' fashion which means the 'state' of the ecological system changes with time. With knowlegde of the processes within the system one can develop a mathematical model to study the dynamic behaviour of the system.

De Wit & Goudriaan (1978), Ferrari (1978) and Brockington (1979) have written introductory textbooks on simulation of ecological processes. Although the main topic of this book is modelling of growth processes and related phenomena, those textbooks are useful for their complementary explanations and illustrations.

In this section we introduce the simulation language CSMP (Continuous Simulation Modeling Program) (IBM, 1975), which is used throughout this book. Basic principles of its use are demonstrated by construction of a simple program for the simulation of crop dry-matter production (Subsection 2.2.2). In its first form the program calculates photosynthesis, respiration, dry-matter distribution, and leaf area index during a growth season, assuming a constant environment. Subsequently the program is modified to account for a varying environment and its effect on some of the processes (Subsection 2.2.3). Starting from this basic level has the advantage that the reader who is not familiar with growth modelling and programming in CSMP can find handholds in such a simple program. Gradually, as processes are treated in more detail in the following sections, more elaborate modelling techniques and their programming in CSMP will be discussed.

Subject of this section is also the internal structure of a CSMP program with special attention to the sorting mechanism (Subsection 2.2.4). Finally some basic CSMP programming knowledge is summarized (Subsection 2.2.5) to provide sufficient information for a good comprehension of the following sections. In Section 2.3 some of these aspects will be elaborated. The CSMP manual (IBM, 1975) may be useful for those with some programming experience.

2.2.2 An elementary simulation program for dry-matter production

In a first approximation dry-matter production of a crop can be simulated based on the simple model depicted in Figure 16. Gross CO_2 assimilation feeds a pool of carbohydrates that supplies material for growth and respiration. Part of

50
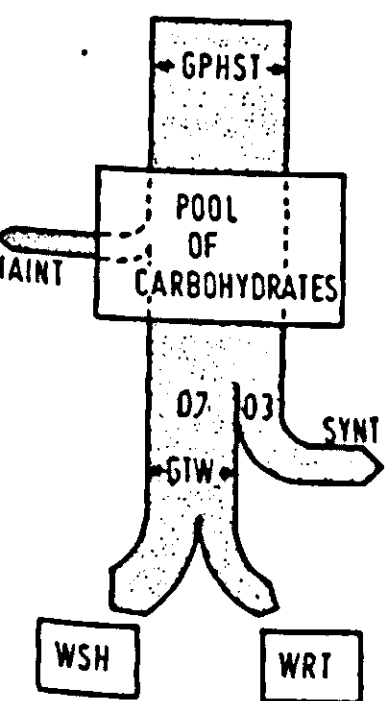
Figure 16. Flow of carbohydrates in a simple crop-production model.

his pool is needed for maintenance of the crop, a process usually defined as maintenance respiration. The substrate for growth is also taken from this pool, and the conversion into shoot and root biomass involves a loss of carbohydrates, defined as synthesis respiration. The relational diagram of such a system has been presented in Figure 2, Section 1.2.

Because we would like to describe this model and use it for simulation of growth on a day-to-day basis, one simplification of the relational diagram has to be made: we will assume that all carbohydrates from photosynthesis are consumed by growth and maintenance processes within one day. As a result, we can omit the pool of carbohydrates as a separate variable from the model. In Section 3.3 this simplification will be explained more extensively.

The relational diagram reveals the kind of quantitative information that should be available. A standard value for the gross photosynthetic rate (GPHST) of a green and completely closed canopy, well supplied with water and nutrients is in terms of glucose production on the order of 400 kg $ha^{-1}d^{-1}$ on clear summer days. When the canopy is not fully closed the actual value of the gross photosynthetic rate (GPHOT) is a fraction of GPHST. This fraction corresponds with the fraction of absorbed visible radiation, calculated with an exponential extinction of radiation as function of the leaf area index (LAI, an area fraction of leaves to ground surface, in m^2m^{-2}). A value of 0.7 for the extinction coefficient results in a fraction $(1. - EXP(-0.7 * LAI))$ of absorbed visible light.

Maintenance respiration (MAINT), expressed in glucose, is related to the total dry matter weight (TWT), a proportionality factor of 0.015 kg $kg^{-1} d^{-1}$ is a fair estimation. As for growth, a conversion factor (CVF, in kilogram of dry matter per kilogram of glucose) of 0.7 quantifies reasonably well the efficiency of synthesis of structural material from the carbohydrates, the remainder being lost as respiration. Dry matter is distributed between shoot (WSH) and root (WRT), both in kg ha^{-1}; fixed fractions of respectively 0.7 and 0.3 have been chosen for the purpose of this example.

With this information the equations characterizing the model can be written.

51

By using a simulation language, such as CSMP, these equations can be easily coded into a small set of statements comprehensible to reader and computer. Figure 17 represents the actual computer program of the simple model that is developed above. A computer program is normally the last stage in the construction of a 'working version' of a simulation model. When the program is submitted to a computer, the output gives a picture of the behaviour of the model. Numerical values of state variables are computed starting from their initial value at simulation time zero until the end of the simulation period. For defined time intervals, a list of calculated values of variables in which one is interested can be printed.

We will discuss the program of Figure 17 line by line. It is useful to start by identifying the program with a TITLE statement:

TITLE DRY MATTER PRODUCTION

Subsequently the structure of the model is defined. The goal of the simulation is the total dry matter weight (TWT), which is the sum of the dry matter weight of the shoots (WSH) and the roots (WRT):

TWT = WSH + WRT

WSH and WRT are state variables in the model that change according to their characteristic growth rates GSH and GRT. Integration of these growth rates gives the actual values of WSH and WRT at any moment. CSMP provides the INTGRL function (Table 2) as a means to integrate numerically a specified rate in time:

WSH = INTGRL (WSHI, GSH)
WRT = INTGRL (WRTI, GRT)

Initial conditions (WSHI, WRTI) and relevant rates (GSH, GRT) have to be specified as arguments of the INTGRL function and are placed between brackets. At time zero, WSH equals WSHI and the current value of WSH at any time is found by integrating GSH. A similar reasoning is valid for WRT. At the beginning of the growth season, shoot and root dry weight can be estimated at 50 kg ha^{-1}. In an INCON statement we can assign numerical values to these INitial CONditions:

INCON WSHI = 50., WRTI = 50.

The growth rates GSH and GRT are calculated as

GSH = 0.7 * GTW
GRT = 0.3 * GTW

in which GTW is the net rate of total dry matter increase (kg ha^{-1} d^{-1}). As illustrated in Figure 16, we can express GTW as
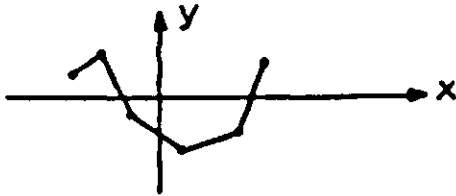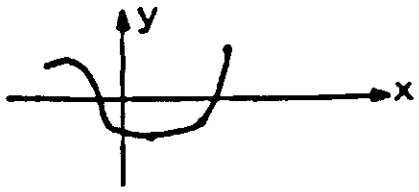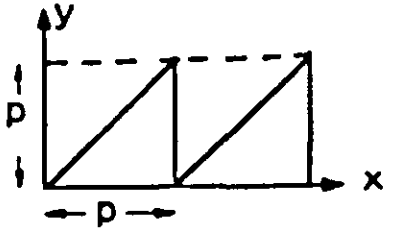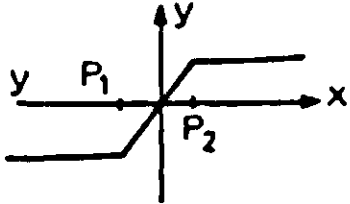
GTW = (GPHOT − MAINT) * CVF

Figure 17. Listing of the simulation program for calculation of 'dry matter production' and its output.

```
TITLE DRY MATTER PRODUCTION
       TWT   =WSH+WRT
       WSH   =INTGRL(WSHI,GSH)
       WRT   =INTGRL(WRTI,GRT)
INCON WSHI=50., WRTI=50.
       GSH   =0.7*GTW
       GRT   =0.3*GTW
       GTW   =(GPHOT-MAINT)*CVF
       MAINT =(WSH+WRT)*0.015
       GPHOT =GPHST*(1.-EXP(-.7*LAI))
       LAI   =AMIN1(WSH/500.,5.)
PARAM CVF=.7, GPHST=400.
TIMER FINTIM=100., DELT=1., PRDEL=5., OUTDEL=5.
METHOD RECT
PRINT TWT,WSH,WRT,GTW
OUTPUT TWT
END
STOP
ENDJOB
```

```
1   DRY MATTER PRODUCTION
0   TIME          TWT           WSH           WRT           GTW
    0.000000D+00  100.00        50.000        50.000        17.880
    5.000000D+00  243.08        150.16        92.924        50.534
    1.000000D+01  614.06        409.84        204.22        115.80
    1.500000D+01  1347.1        922.94        424.12        188.94
    2.000000D+01  2384.7        1649.3        735.40        227.14
    2.500000D+01  3542.1        2459.5        1082.6        233.86
    3.000000D+01  4689.0        3262.3        1426.7        222.31
    3.500000D+01  5777.5        4024.2        1753.2        210.88
    4.000000D+01  6810.0        4747.0        2063.0        200.04
    4.500000D+01  7789.4        5432.6        2356.8        189.76
    5.000000D+01  8718.4        6082.9        2635.5        180.00
    5.500000D+01  9599.7        6699.8        2899.9        170.75
    6.000000D+01  10436.        7285.0        3150.7        161.97
    6.500000D+01  11229.        7840.1        3388.6        153.64
    7.000000D+01  11981.        8366.7        3614.3        145.74
    7.500000D+01  12695.        8866.2        3828.4        138.25
    8.000000D+01  13371.        9340.0        4031.4        131.14
    8.500000D+01  14014.        9789.5        4224.1        124.40
    9.000000D+01  14623.        10216.        4406.8        118.01
    9.500000D+01  15200.        10620.        4580.1        111.94
    1.000000D+02  15749.        11004.        4744.6        106.19
1$$$ SIMULATION HALTED FOR FINISH CONDITION  TIME      100.00
     TIME          TWT
     0.00000E+00   100.00       +             I             I             I             I
     5.0000        243.08       +             I             I             I             I
     10.000        614.06       I+            I             I             I             I
     15.000        1347.1       I---+         I             I             I             I
     20.000        2384.7       I------+      I             I             I             I
     25.000        3542.1       I---------+   I             I             I             I
     30.000        4689.0       I-----------I-+           I             I             I
     35.000        5777.5       I-----------I----+        I             I             I
     40.000        6810.0       I-----------I--------+    I             I             I
     45.000        7789.4       I-----------I-----------+I             I             I
     50.000        8718.4       I-----------I------------I-+           I             I
     55.000        9599.7       I-----------I------------I----+        I             I
     60.000        10436.       I-----------I------------I------+      I             I
     65.000        11229.       I-----------I------------I---------+   I             I
     70.000        11981.       I-----------I------------I-----------+             I
     75.000        12695.       I-----------I------------I-----------I-+           I
     80.000        13371.       I-----------I------------I-----------I---+         I
     85.000        14014.       I-----------I------------I-----------I-----+       I
     90.000        14623.       I-----------I------------I-----------I-------+     I
     95.000        15200.       I-----------I------------I-----------I---------+  I
     100.00        15749.       I-----------I------------I-----------I-----------+
1$$$ CONTINUOUS SYSTEM MODELING PROGRAM III   V1M3     EXECUTION OUTPUT $$$
```

53

Table 2. Some CSMP III functions. From: IBM (1975).

CSMP III Functions	Equivalent Mathematical Expression
Integrator Y = INTGRL(IC, X) where: IC = y_{t_o}	$$y(t) = \int_{t_o}^{t} x\,dt + y(t_o)$$ where: t_o = start time t = time
Arbitrary function generator (linear interpolation) Y = AFGEN(FUNCT,X)	 y = f(x)
Arbitrary function generator (quadratic interpolation) Y = NLFGEN (FUNCT,X)	 y = f(x)
Modulo function Y = AMOD (X,P)	$y = x - nP$ n is an integer value such that $0 \leqslant y < P$
Limiter Y = LIMIT(P1,P2,X)	$y = P_1 \;;\; x < P_1$ $y = P_2 \;;\; x > P_2$ $y = x \;;\; P_1 \leqslant x \leqslant P_2$
Not Y = NOT (X)	$y = 1$ if $x < 0$ $y = 0$ if $x > 0$
Input Switch Relay Y = INSW(X1,X2,X3)	$y = x_2$ if $x_1 < 0$ $y = x_3$ if $x_1 \geqslant 0$

The maintenance respiration is supposed to be 1.5 percent of the total dry matter per day:

MAINT = (WSH + WRT) * 0.015

The equation respresenting the relation of the gross photosynthetic rate and green surface has an exponential form:

GPHOT = GPHST * (1. − EXP (−0.7 * LAI))

The leaf area index (LAI) is here assumed to be proportional to the shoot dry matter (WSH) to a maximum of 5 ha ha^{-1}. The AMIN1 function (Table 3) can be used to achieve this:

LAI = AMIN1 (WSH/500., 5.)

The AMIN1 function takes the minimum value of its arguments separated by comma's.

Dead time (DELAY)	
Y=DELAY(N,P,X)	$y = x(t-p) \; ; \; t > p$
where: P=delay time N=number of points sampled in interval p · (integer constant) and must be $\geqslant 3$, and $< 16{,}378$	$y = 0 \quad ; \; t < p$ Equivalent Laplace Transfer Function: $\dfrac{Y(s)}{X(s)} = e^{-ps}$
Implicit function Y=IMPL(IC,P,FOFY) where: IC=first guess P = error bound FOFY=output name from final statement in algebraic loop definition	$y = f(y)$ $\lvert y - f(y)\rvert \leqslant p\,\lvert y\rvert$
Impulse generator Y=IMPULS(P1,P2) where: P1=time of first pulse P2=interval between pulses	$y = 0 \quad ; \; t < p_1$ $y = 1 \quad ; (t-p_1) = kp_2$ $y = 0 \quad ; (t-p_1) \neq kp_2$ $k = 0, 1, 2, 3, \cdots$

The parameters CVF and GPHST have to be specified to complete the numerical information for the program. The PARAMeter statement is used to assign values to variables used as parameters:

PARAM CVF = 0.7, GPHST = 400.

So far the structure of the model has been transformed into a simulation program that can be executed. Only timing, output format and an appropriate integration method must still be specified. A TIMER statement gives the time of finishing the simulation (FINTIM), the printed output interval (PRDEL) and plotted output interval (OUTDEL), and the size of the time step for integration (DELT):

TIMER FINTIM = 100., DELT = 1., PRDEL = 5., OUTDEL = 5.

All TIMER variables are expressed in days, as this is the basic unit of time in this program. A numerical integration method is selected from a set of available

55

Table 3. Some FORTRAN functions, which can be used in CSMP III statements. From: IBM (1975).

FORTRAN Functions	Equivalent Mathematical Expression
Exponential Y = EXP (X)	$y = e^x$
Trigonometric sine Y = SIN (X)	$y = \sin (x)$
Trigonometric cosine Y = COS (X)	$y = \cos (x)$
Square root Y = SQRT (X)	$y = \sqrt{x}$
Largest value (Real arguments and output) Y = AMAX1(X1, X2)	$y = \max (x_1, x_2)$
Smallest value (Real arguments and output) Y = AMIN1 (X1, X2)	$y = \min (x_1, x_2)$

routines in CSMP (Subsection 2.3.7). For instance, to perform the simulation using the rectangular method after Euler, the next statement has to be used:

METHOD RECT

Printed output of the variables is obtained by means of:

PRINT TWT, WSH, WRT, GTW

Plotted out can be obtained by:

OUTPUT TWT

The END statement defines the end of the simulation model and the STOP statement the end of the simulation program.

END
STOP
ENDJOB

The ENDJOB statement finishes the computer job. Figure 17 shows a complete listing of the example model and the output after execution.

Exercise 11

Run the program. (Subsection 2.2.5 may be helpful when you are editing your program).

During a simulation run all statements defining the structure of the model are executed several times, the number of which equals FINTIM divided by DELT, when using the rectangular method. DELT, equivalent to Δt in Section 2.1, plays a critical role since it indicates the size of the time interval for integration. For a CSMP statement with an integral function like:

WSH = INTGRL (WSHI, GSH)

the equivalent numerical expression when using a rectangular integration method, as in Subsections 1.1.3 and 2.1.5, is:

$WSH_{now} = WSH_{previous} + GSH \cdot DELT$

From this equation it is clear that the rectangular integration method implicates a constant growth rate during the whole time step DELT. Taking appropriate time steps, such that the rate of change can be regarded as effectively constant, will give good approximations of the value of the state variable (cf. Subsection 2.3.6).

Exercise 12

a. Simplify the program for the case that you are only interested in the total dry matter increase (do not consider biomass distribution into shoots and roots). Assume that the crop is completely covering the soil (GPHOT = GPHST). Run this program.

b. Explain why the results of this simple model are qualitatively similar to the filling of a water tank as discussed in Subsection 2.1.4. Write the governing differential equation for this system and derive from this the time coefficient and equilibrium level.

c. What is the implication of the introduction of the relationships in which gross photosynthesis depends on LAI, and LAI depends on WSH in the form discussed above? What happens with the time coefficient?

2.2.3 Program modifications with forcing functions

Until now we assumed that all external conditions, or driving variables (Subsection 1.1.2), are constant. However, CO_2 assimilation rates are strongly

dependent on irradiation and irradiation itself can vary from day to day over a relatively wide range. If we want to make the model realistic, we should introduce the actual irradiation level instead of a fixed rate of gross CO_2 assimilation. Irradiation will drive CO_2 assimilation in the model and is not affected by the state of the system. Therefore we call it a driving or forcing function. More generally, forcing functions are defined as those variables that are not affected by processes within the system, but characterize the influence from outside (Subsection 1.1.3). They are an input to the model. In very simplified models, forcing functions can be introduced in the program as parameters:

PARAM GPHST = 400.

Very often forcing functions show a characteristic pattern over a certain time period (day or year). An equation describing such regular fluctuations in time may provide approximate values for the use in a general program. For example, the yearly course of daily incoming short-wave irradiation is reasonably well represented by a sinusoidal curve, just like daily gross photosynthesis. For the daily gross photosynthesis (GPHST, expressed as glucose) the equation is

GPHST = 300. + 200.*SIN(2*PI*(DAY-(365./4.)+10.)/365.)
PARAM PI = 3.141592

DAY stands for the number of a day in the year; counting starts from 1 January. GPHST reaches a minimum value of 100.0 (kg ha^{-1} d^{-1}) on 21 December (DAY = 355) and a maximum value of 500.0 on 21 June (DAY = 172). DAY can be calculated by:

DAY = STDAY + TIME
PARAM STDAY = 60.

In this way simulation starts on 1 March (STDAY = 60.). TIME is a variable generated by CSMP which expresses the current time during simulation. At the start of simulation TIME = 0., and its value is augmented by DELT when the integration of all state variables is accomplished. (The symbolic name TIME is reserved by CSMP to keep track of time, and cannot be used for other purposes). A second way of keeping track of the number of the day is to give the variable TIME an initial value. This can be done in the TIMER statement:

TIMER TIME = 60., FINTIM = 210., DELT = 1., PRDEL = 5.

When the time course of a driving variable has been measured, direct use of these values is another option for formulating a forcing function. Measured values, with the corresponding dates can be introduced by a FUNCTION statement:

FUNCTION GPHSTB = (60., 300.), (100., 400.), (150., 450.), (210., 500.)

In this statement, an ordered set of pairs defines the content of a table, named GPHSTB. The first value in each pair of numbers between parentheses stands

58

for the independent variable (TIME, d), the second expresses the dependent variable (GPHST, kg ha^{-1} d^{-1}). The distance between the coordinates of two pairs does not have to be equal in size; the value of the independent variable should always increase, but the dependent variable can vary in an arbitrary way. The current value of the dependent variable is calculated by means of an AFGEN function (Arbitrary Function GENerator), which performs a linear interpolation in the function table. Function name and independent variable should be specified as arguments of the AFGEN function:

GPHST = AFGEN(GPHSTB, TIME)

Exercise 13

The gross photosynthetic rate, expressed as CO_2 assimilated, is proportional to the absorbed short-wave radiation with a proportionality factor of 4.35 10^{-9} kg Joule^{-1}; the conversion factor from CO_2 to CH_2O (glucose) is 30.0/44.0. Use following values for daily totals of incoming visible (400-700 nm) irradiation (DTR) in 10^6 Joule m^{-2} d^{-1} on a standard clear day for a latitude of 50° N (Goudriaan & van Laar, 1978):

FUNCTION RADTB = (15., 2.61), (46., 4.80), (74., 8.07), . . .
(105., 12.20), (135., 15.44), (166., 17.01), . . .
(196., 16.41), (227., 13.75), (258., 9,80), . . .
(288., 5.96), (319., 3.19), (349., 2.11)
DTR = AFGEN (RADTB, TIME) * 1.E6 * 1.E4

Assume that 10% of the irradiation is reflected. Formulate the new equations and replace the former equations of the model of Figure 17. Use the program to calculate the dry matter production from Day 60 until Day 210.

Another example of a forcing function that plays a critical role in growth models is temperature. The next exercise illustrates how maintenance respiration can be modelled more realistically by taking the effect of temperature into account.

Exercise 14

Extend the program of Exercise 13 so that maintenance respiration becomes dependent on temperature. Assume a linear temperature course for the simulation period between 10 °C on the first day and 20 °C on the last day. Use the following table:

TEMPERATURE	10.	20.	30.
MAINTENANCE COEFFICIENT	0.008	0.015	0.030

Repeat the simulation for a more realistic course of the temperature.

AFGEN provides a simple linear interpolation between 2 points (x_1, y_1) and (x_2, y_2). The function value y for a certain x is expressed as:

$$y = y_1 + (y_2 - y_1) \cdot (x - x_1)/(x_2 - x_1)$$

In a sense, a broken line is generated by connecting subsequent points. If we want to employ a higher order interpolation we need more than two points: three points for a parabolic and four points for a cubic relation. Generally, through n points fits a curve of order $n - 1$. The CSMP function NLFGEN (Non Linear Function GENerator) does this job with $n = 3$. Although theoretically NLFGEN is applicable in many cases, caution should be exercised in its use. For an AFGEN function it is not so difficult to imagine what happens: straight lines connect two points. The situation is much more complicated for a NLFGEN function which fits a parabolic interpolation function to three neighbouring points. For this reason application of NLFGEN is less self-evident as it might be for the AFGEN function. In particular, if the data points imply an abrupt discontinuity, we should take into account large distortion there if using NLFGEN. For such situations it may be preferable to use AFGEN. Exercise 15 illustrates this hidden danger of using NLFGEN.

Exercise 15
Consider the next program:

```
FUNCTION XTB = (0., 1.), (1., 1.), (2., 0.), (3., 0.)
X1 = AFGEN (XTB, TIME)
X2 = NLFGEN (XTB, TIME)
TIMER FINTIM = 3.0, OUTDEL = 0.1, DELT = 0.1
OUTPUT X1, X2
```

Compare the output of the AFGEN and NLFGEN function.

2.2.4 The structure of the CSMP language

CSMP is a problem-oriented language designed to facilitate the digital simulation of continuous processes on large-scale digital computers. The advantage of using such a language is that it simplifies the programming. The user is not concerned with the rather difficult programming of numerical integration and interpolation methods, and he need not to worry about the computational order of the statements. (We will return to this important point). A convenient output form is provided by the program itself. The programmer is only responsible for writing the statements that define the model and supplying it with a proper data set. An additional advantage specific for CSMP is that the full capability of the widely used FORTRAN language is available. In addition to FORTRAN facilities, CSMP includes a set of functions that are particularly suited to working with a continuous system (e.g. INTGRL and AFGEN functions).

Every simulation run essentially starts from a well defined initial condition. When needed, one can separate this part from the description of the structure of the model itself. The determination of the final situation of a simulation run and decision for a possible new run can be separated as well in a program. To do so, a CSMP model can be divided into three segments — INITIAL, DYNA-MIC and TERMINAL — that describe the computations to be performed before, during and after each simulation run. The TERMINAL segment will not be discussed here.

The INITIAL segment is exclusively used for initialization of variables and computations of variables to be expressed in more basic parameters. Statements in the INITIAL segment are executed only once per simulation run. Assume for example the initial weights of shoot and root depend on the weight of the seed sown, then the simulation model can be modified as:

```
TITLE DRY MATTER PRODUCTION
INITIAL
INCON SEED = 150.
WSHI = SEED * 0.6 * 0.5
WRTI = SEED * 0.6 * 0.5
```

The factor 0.6 is a reasonable value for conversion of seed into plant material; a shoot:root ratio of 1. is used here.

The DYNAMIC segment contains the complete description of the system dynamics, together with any other computations and decisions to be performed for successful simulation. For most simple models, the DYNAMIC segment consists of one section:

```
DYNAMIC
TWT = WSH + WRT
WSH = INTGRL (WSHI, GSH)
.          and so on, as in Figure 17 until:
.
.
END
```

In more complicated systems, the DYNAMIC segment can be divided in several sections, each section dealing with a separate submodel (Subsection 2.3.2).

Specification of an INITIAL segment is optional and is often omitted for small models. In that case the DYNAMIC segment has not to be declared explicitly by the DYNAMIC label.

One of the main advantages of CSMP is its sorting routine. It enables the user to write a simulation program with its statements in the same order as he thinks about the process or system and in which he considers it most lucid and readable. Such an order of statements, however, is often the reverse of what the computational order must be. The CSMP sorting routine finds the proper order from any sequence of statements presented. Sorting of statements is necessary

because computations have to be performed in a correct order: calculation of rate variables must always preceed the updating of state variables. This is a consequence of the concept of dynamic simulation (Section 1.1). Also all variables, used to compute rate variables at time t, must have the appropriate value, and not one corresponding with one time interval DELT earlier or later. Sequencing statements in an appropriate computational order is also required if one programs in FORTRAN, but with FORTRAN the sequencing must be done by the programmer (and one is usually not warned when it is done incorrectly).

The FORTRAN program that results from the sorting and some other conversions by the CSMP compiler is called UPDATE. It is accessible like other computer generated files.

Exercise 16
Put the statements of the model of Subsection 2.2.2 in a computational order, and notice the difference with the order presented. Request the translation of the program into FORTRAN (the UPDATE-version) by submitting the program. Compare the results with your own sorting. Spell a name incorrectly, and see what happens. What can occur if a statement is incorrect. For example try

MAINT = (GSH + GRT) * 0.015

The CSMP programming system sorts the statements in the INITIAL and DYNAMIC segments automatically, independently of each other.

2.2.5 Some basic CSMP programming rules

To write a correct CSMP program, a minimum knowledge of the common expressions of this language is necessary. The intention of this part is to provide a summary of frequently used CSMP statements. Readers who want to know more are referred to a CSMP manual (IBM, 1975).

Data statements

Data statements are used to assign numeric values to parameters, constants and initial conditions. For instance:

```
PARAM P1 = ...., P2 = ....
CONSTANT C1 = ...., C2 = ....
INCON I1 = ...., I2 = ....
```

Parameters specified in a PARAM statement are constant during the simulation run. Variables can be introduced by means of a FUNCTION label (see Subsection 2.2.3).

Structure statements

Structure statements describe the functional relationships between the variables of the model. FORTRAN statements can be used within a CSMP program, and all FORTRAN functions are valid (Table 3). Some examples of structure statements:

```
Y = (A + B) * C
ROOT = SQRT (X ** 2 + Y ** 2)
A = INTGRL (2., X ** 2 + R/D)
```

For more information about available CSMP and FORTRAN functions see Tables 2 and 3 and particularly the Program Reference Manual (IBM, 1975).

Expressions should be written at the right hand side of the equal sign and their numeric value is assigned to the variable at the left. The calculation of an expression is performed according to the standard hierarchy:
- evaluation of brackets (in combination with FORTRAN or CSMP functions)
- exponentiation (* *)
- multiplication and division (*, /)
- addition and subtraction (+, -)

Operators of the same hierarchy are performed from left to right.

Output control statements

The TITLE statement allows the user to specify the program and it appears at the top of each page of the output listing. A PRINT statement is used to specify variables whose values will be printed at each PRDEL interval. For output of some variables in printed graph form the OUTPUT statement is used. For examples see Subsection 2.2.2, and Table 9 and Figure 24 of Section 3.1.

Execution control statements

In a TIMER statement we specify the values of certain system variables.
FINTIM : finish time for terminating a simulation
OUTDEL: time interval for print-plot output
PRDEL : time interval for printing the values of requested variables
DELT : integration interval (see also Subsection 2.3.5)
TIME : initial value of time, to be specified only if not zero.

A condition to terminate the simulation, e.g. when TWT exceeds 20 000 kg ha^{-1}, can be introduced by a FINISH label:

FINISH TWT = 20000.

Also the integration method is specified in an execution control statement, for instance:

METHOD RECT

If METHOD RECT is not specified, the RKS method is used by default (see Section 2.3).

The statement

END	: completes the specifications of the model.
STOP	: terminates the simulation run(s)
ENDJOB	: terminates the job.

Reruns

If the simulation is to be repeated with new data and/or output and execution control statements, these statements are to be placed between two END-statements:

```
. . . . .
END
PARAM . . .
TIMER . . .
END
STOP
ENDJOB
```

Only data statements with labels such as PARAM, CONST, INCON and FUNCTION can be used to specify reruns, not equations. Running a program a number of times for multiple values of a parameter is induced by writing their values between parentheses. For example:

PARAM GPHST = (300., 400., 500.)

This feature can be used for only one variable in each rerun.

Exercise 17
Use these features to study in only one program the total dry matter production for all combinations of the values 300., 400., 500. for GPHST and values 400., 500., 600. for the ratio kg (shoot dry matter) ha^{-1} (leaf surface) in the calculation of LAI. Start from the program described in Subsection 2.2.2.

Syntax

Some syntactic rules may be helpful when editing a program.
- maximum 6 characters for names of variables
- each statement on one line
- a statement followed by three dots (...) means that statement will be continued on the next line; this is not allowed within a MACRO! (Subsection 4.2.3)

- spaces between variable names and operators are allowed
- columns 1 to 72 can be used for the program, columns 73-80 are for identification
- statements can begin in any column, except for ENDJOB, which must begin in the first column
- * in the first column stands for comment.

Tracing errors

If the proper Job Control Language is used, the computer will give an answer to your problem. If the program is not free of errors, the computer will give one or more error messages. Sometimes these messages are self-explanatory, otherwise you should consult the CSMP reference manual (IBM, 1975).

If the computer is generating no diagnostics and the results seem to be correct, you still cannot be sure whether your program is free of errors, especially when the program is large and has a complex structure. Some ways of checking are:
- make sure the dimensions are correct. Check them. This can also be quite instructive as one can learn more about the significance of the various coefficients and parameters
- run your program for extreme conditions
- make use of the DEBUG feature. For example, write just before the END statement:

      NOSORT
            CALL DEBUG (2, 10.)

All variables, not only those specified in the output list, are printed twice, first at time 10 and then after one integration step. This allows you to check all computations.

2.3 Some techniques in dynamic simulation

J. Goudriaan

2.3.1 Introduction

Good quality dynamic simulation can only be attained if a few basic techniques are mastered. CSMP, introduced in Section 2.2, provides the model builder with a package of convenient features. Some of these features, their principles and pitfalls will now be explained so that they can be used more efficiently and lead to more reliable results. For further studies of numerical techniques, good handbooks are available, for example that of Scheid (1968). Sequencing of program statements, how sorting can be suppressed, and how sortable blocks can be constructed that are internally sequential, is discussed in Subsection 2.3.2.

The MACRO feature of CSMP can be used when a piece of program is repeated several times in the same model with different names. Defined once in the beginning, this piece of program is written by the CSMP translator in all places where a MACRO is invoked. This is explained in Subsection 2.3.3. Solution of implicit equations is possible with iteration techniques. The CSMP provided IMPLicit loop will be discussed as well as a self-written method (Subsection 2.3.4). Next, numerical integration is discussed (Subsections 2.3.5, 2.3.6 and 2.3.7). Characteristics of the modelled system, such as occurrence of feedback and discontinuities and the time coefficient determine which integration method should be used, and also the time interval of integration.

2.3.2 Sorting

The basic rule for sorting program statements in a computational order is that any variable used on the right-hand side of the equal sign in a statement should have been defined in an earlier stage of the program. This simple rule is incorporated in the CSMP translator that prepares the source program for proper handling by the FORTRAN compiler (Subsection 2.2.4).

However, situations exist where the programmer would like to cancel this rule. For example, during the night there is no point in performing laborious calculations of light extinction, so one would rather skip this part of a model. That means that a conditional jump must be inserted: an instruction to jump over a number of statements if the irradiation level is zero. Once the programmer has determined which statements must be skipped, he would not like to see the CSMP translator disturbing the well-balanced sorting effort, and so he inserts a command that the translator should not touch these statements. There are two such commands: NOSORT and PROCEDURE.

The label NOSORT is valid until it is cancelled by the label SORT; so a non-sorted block of statements between the labels NOSORT . . . SORT is created. Statements outside this block can be freely sorted by the CSMP translator, except that they cannot be moved across the NOSORT block: NOSORT cuts the program into sections.

If complete sortability is desired, the PROCEDURE label must be used. The translator will consider the group of statements between this label and the label ENDPRO as one big sortable statement. Consequently the translator demands a specification of input and output variables of this block, so that it can properly locate it between the other program statements: a PROCEDURE does not cut a program into sections. For example, suppose we need the sum of the integer numbers between N1 and N2, which are calculated somewhere else in the program. The result S is used somewhere else. Then we can make a program with a PROCEDURE:

```
FIXED    I, N1, N2
PARAM    N1 = 0
         N2 = TIME
PRINT    S
TIMER FINTIM = 10., PRDEL = 3.3
PROCEDURE S = SUM(N1, N2)
         S = 0.
         IF(N2.LT.N1)GOTO 10
         I = N1
    11   S = S + I
         I = I + 1
         IF(I.GT.N2)GOTO 10
         GOTO 11
    10   CONTINUE
ENDPRO
END
STOP
ENDJOB
```

In the PROCEDURE for summing, a few new statements are used. The variables I, N1 and N2 are declared integer by the label FIXED. In an IF statement the values of two variables are compared with each other to see, for instance, whether the left one is greater than (GT) or less than (LT) the right one. If this is true the computer follows the GOTO command and jumps to the line starting with that number. If it is not true the computer continues with the next line. The unconditional GOTO 11 command will make the computer return to previous lines to repeat a block of statements. In the paragraph about iteration techniques, we shall see an application of a PROCEDURE.

2.3.3 Programming with CSMP MACRO's

In a MACRO the structure of a process is described that different species or different model components have in common. In this sense it resembles a FORTRAN subroutine, but the difference is that it is not invoked in the execution phase, but in the translation phase. Every time a MACRO is invoked, the CSMP translator will expand it to the full text with the appropriate symbols. After this has been completed, the CSMP sorting routine will become operative so that inside the definition of a MACRO, the statements need not be in computational order.

As an example, the simple crop growth model (Subsection 2.2.2) is extended to deal with competition. In a mixture, light absorption will supposedly be proportional to the leaf area of each species. First the MACRO definition:

```
MACRO TWT, LAI = GROWTH(TWTI,MC,CVF,ALU,LAR)
       TWT = INTGRL(TWTI,GTW)
       GTW = (GPHOT  −  MC*TWT)*CVF
       GPHOT = ALU*AVIS
       AVIS = IVIS*(1.−  EXP(−0.7*LAIT))*0.9*LAI/LAIT
       LAI = TWT*LAR
ENDMACRO
```

In this MACRO the following new variables and coefficients occur:

ALU	average light use efficiency, expressed as glucose formed per amount of light absorbed	4.E-5	kg m^2 ha^{-1} J^{-1}
AVIS	absorbed visible radiation		J m^{-2} d^{-1}
CVF	conversion factor of glucose into biomass	0.7	kg kg^{-1}
IVIS	incoming visible radiation	10.E6	J m^{-2} d^{-1}
LAR	leaf area ratio	1.E-3	ha kg^{-1}
MC	maintenance coefficient, expressed in glucose per dry weight	0.015	kg kg^{-1} d^{-1}

These numerical values only give an indication of a reasonable number, and are by no means natural constants.

A MACRO definition must be placed before the label INITIAL. It is clear that the sequence of the statements is not computational here. (If desired, the PROCEDURE feature can be included in a MACRO definition). The structure that is given in the MACRO definition will be written in the main program each time the CSMP translator encounters a call to it. Two such calls (for two plant species) are:

```
TWT1,LAI1 = GROWTH(TWTI1,MC1,CVF1,ALU1,LAR1)
TWT2,LAI2 = GROWTH(TWTI2,MC2,CVF2,ALU2,LAR2)
```

It is good practice to put the input variables of the MACRO in the right hand list. In the main program these variables should either be calculated or be given as parameters and initial constants. In this example TWTI1 and TWTI2 must be

given separately on an INCON line, and likewise MC1, MC2, CVF1, CVF2, ALU1, ALU2, LAR1 and LAR2 on PARAM lines. There may also be variables that are common to both species, here for example LAIT. Therefore this variable does not occur in the argument list and is defined in the main program:

LAIT = LAI1 + LAI2

Obviously the TIMER and output control statements must be specified in the normal way.

A variable like GTW, which is used only inside the MACRO, is not known in the main program, because its name was not listed as an argument. It can be made common to the main program by including it in the argument list.

Exercise 18
Complete the program that was started here, run it and study the UPDATE, as well as the output.

2.3.4   Iterative techniques

An iterative procedure in a simulation model can be used to calculate the value of a state variable, when its time coefficient (Subsection 2.1.7) is small in comparison with the integration interval. This technique can be useful in complex models that span three hierarchical levels (Subsection 1.4.4). Then we may assume that this state variable is in equilibrium with its environment after each time step. This steady state can be found by an iterative technique that searches the point where the rate of change of the integral is zero. Of course, the sign of the feedback that controls the rate of change must be negative. As an example we shall treat the simulation of production and consumption of assimilates that flow through a reserve pool. The time coefficient of such a reserve pool is in the order of half a day, so that every day must take care of its own demand. When a diurnal course is simulated and the integration step is on the order of minutes, the reserve pool can be treated as a state variable (Subsection 3.3.3). For simulation of the growth throughout a season, a convenient time step is one day and the equilibrium level of reserves must be found by iteration. For comparison, we shall first consider the state variable formulation:

```
TITLE    RESERVES AS A STATE VARIABLE
INCON    RESLI = 0.1
         RESI = RESLI * TWT
DYNAMIC
         RESL = RES/TWT
         RES = INTGRL(RESI,GPHRED - MAINT - CGR)
```

```
                MAINT = 0.015 * TWT
                CGR = 0.1 * RES/(RESL + KRESL)
      PARAM  KRESL = 0.1,TWT = (2000.,10000.)
                GPHRED = GPHOT * REDF
                GPHOT = GPHST * (1. − EXP(−0.7 * LAI))
                REDF = AFGEN(REDFT,RESL)
                LAI = AMIN1(WSH/500.,5.)
                WSH = 0.7 * TWT
      FUNCTION REDFT = 0.,1.,0.2,1.,0.25,0.,0.5,0.
      PARAM  GPHST = 400.
      TIMER  FINTIM = 20.,PRDEL = 1.
      PRINT  RES,RESL,GPHRED
      END
      STOP
      ENDJOB
```

In the INITIAL the reserve level is set to 0.1 of the total plant weight TWT, and then the initial amount of reserves RESI is calculated. In the DYNAMIC the amount of reserves RES is integrated with a rate calculated as gross photosynthesis GPHRED, minus maintenance respiration MAINT, minus consumption rate for growth CGR; all rates being expressed in glucose and in kg ha^{-1} d^{-1}. The rate of maintenance respiration is 1.5% of the total dry weight per day and independent of the reserve level. The consumption rate for growth CGR shows a saturation type curve response to the reserve level (Moldau & Sôber, 1981). In this example a hyperbolic relation is used with a Michaelis-Menten constant (KRESL) of 0.1. The maximum rate of consumption is taken as 0.1 of the total dry weight per day.

Exercise 19
What do these numbers mean for the time coefficient of the reserve level?

The rate of gross photosynthesis GPHRED is reduced by some hypothesized inhibiting factor when the reserve level rises above 20%. This reduction is obtained by multiplication with the reduction factor REDF, which drops to zero at and above 25%. The combined action of these processes on the rate of reserve accumulation is given in Figure 18, where GPHRED,MAINT and CGR have been drawn. At the point of equilibrium GPHRED is equal to MAINT + CGR.

In view of the comparison with an iterative solution of the reserve level the total weight of the crop has been fixed during the simulation. The output (Table 4) shows the equilibrium values with TWT = 2000. as 0.22548 for RESL and 168.55 for GPHRED, almost reached in about 2 days. With TWT = 10000. they are 0.0312 and 387.92.
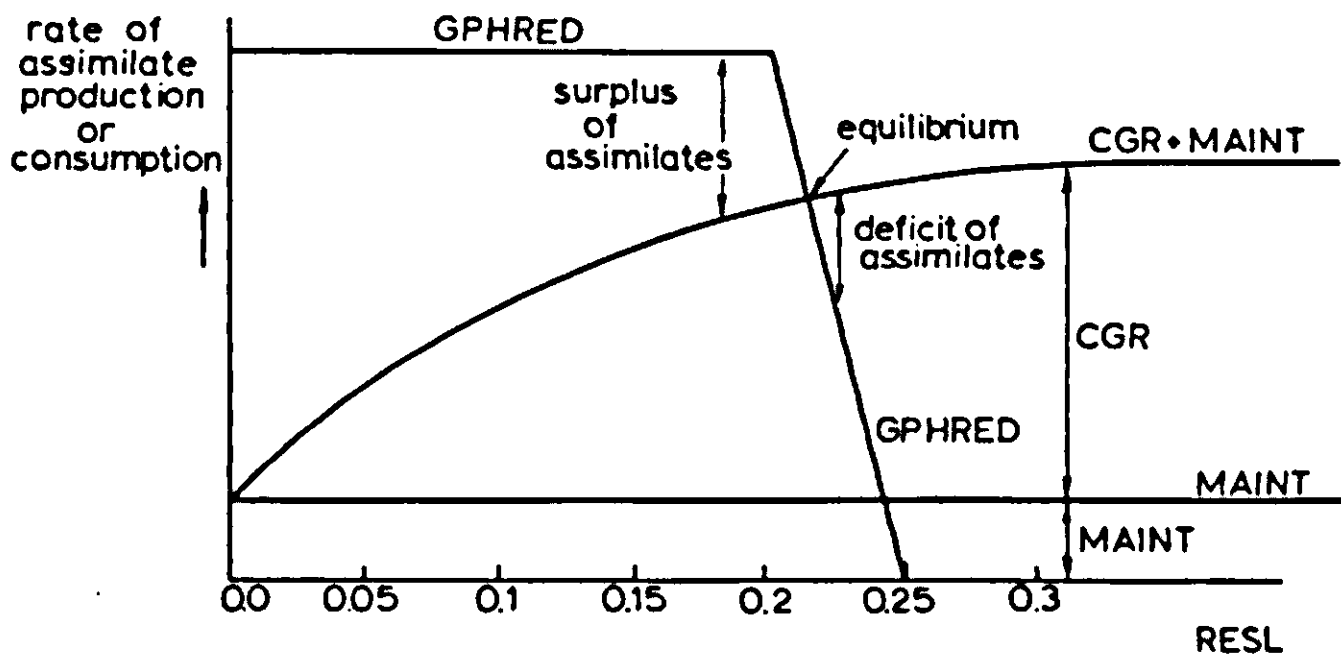
Figure 18. Production and consumption of assimilates as a function of reserve level (RESL).

There are several iterative methods available, of which only two will be discussed. More elaborate methods can be found in handbooks for numerical analysis. All iteration methods have in common that a value for an unknown variable (here RESL) must be found for which two rates are equal. It is then implicitly assumed that sufficient time has passed within the time interval for integration to establish an equilibrium. Here the production rate GPHRED must be equal to the total consumption rate CGR + MAINT. Often this problem is graphically represented as the problem to find the intersect of two lines (Figure 18).

In CSMP, the IMPLicit loop is available as a method to solve this problem. Essentially the method is based on repeated substitution. First a value for RESL is guessed, the corresponding rate of photosynthesis is calculated, then the reserve level is calculated at which the total consumption rate is equal to the previously calculated photosynthesis rate and the procedure is repeated until sufficient convergence is reached. The first drawback of this method is that one of the relations between rate and unknown variable must be inverted: RESL must be written either as a function of total consumption rate or as a function of photosynthesis. When AFGEN functions have been used such an inversion is not possible. Therefore RESL cannot be written as a function of photosynthe-

Table 4. Simulated time course of amount of reserves (RES), the reserve level (RESL) and gross CO_2 assimilation (GPHRED) with the state variable approach.

TIME	RES	RESL	GPHRED
0.	200.00	0.10000	343.66
1.	394.69	0.19735	343.66
2.	449.30	0.22465	174.24
3.	450.90	0.22545	168.72
4.	450.95	0.22547	168.57
5.	450.95	0.22548	168.55

sis, but must be written as a function of CGR by making RESL explicit in the hyperbolic equation. The resulting IMPLicit loop is given in the following simulation program:

```
TITLE    RESERVE LEVEL WITH IMPLICIT LOOP
INCON    RESLI = 0.23
         MAINT = 0.015 * TWT
         GPHOT = GPHST * (1. – EXP( – 0.7 * LAI))
         LAI = AMIN1(WSH/500.,5.)
         WSH = 0.7 * TWT

         RESL = IMPL(RESLI,0.0001,RESL1)
         REDF = AFGEN(REDFT,RESL)
         GPHRED = GPHOT * REDF                    implicit loop
         CGR = GPHRED – MAINT
         RESL1 = CGR * KRESL/(0.1 * TWT – CGR)

PARAM  GPHST = 400.
PARAM  KRESL = 0.1,TWT = (2000., 10000.)
FUNCTION  REDFT = 0.,1.,0.2,1.,0.25,0.,0.5,0.
TIMER    FINTIM = 1., PRDEL = 1.
METHOD RECT
PRINT    RESL,GPHRED
END
STOP
ENDJOB
```

In this program there is no integral RES. Instead, RESL is calculated as the result of the implicit loop that starts with

RESL = IMPL(RESLI,0.0001,RESL1)

Here RESLI is the initial guess, 0.0001 is the convergence criterion and RESL1 is the name of the variable that closes the implicit loop. This closing statement is in fact the hyperbolic equation for the dependence of CGR on RESL in which RESL has been made explicit. The three statements in between replace the state variable formulation.

With TWT = 10000., the results of this program correspond with those of the state variable approach.

Exercise 20
Check this by comparing the results of the two methods. Repeat the calculation with both programs for TWT = 2000.

72

production and consumption
of reserves (g g⁻¹h⁻¹)

mathematical
equilibrium

GPHRED

CGR·MAINT

third guess
in negative region

asymptote of CGR·MAINT

CGR·MAINT

physical equilibrium

GPHRED

third
guess

0.0

second
guess

first
guess

0.25
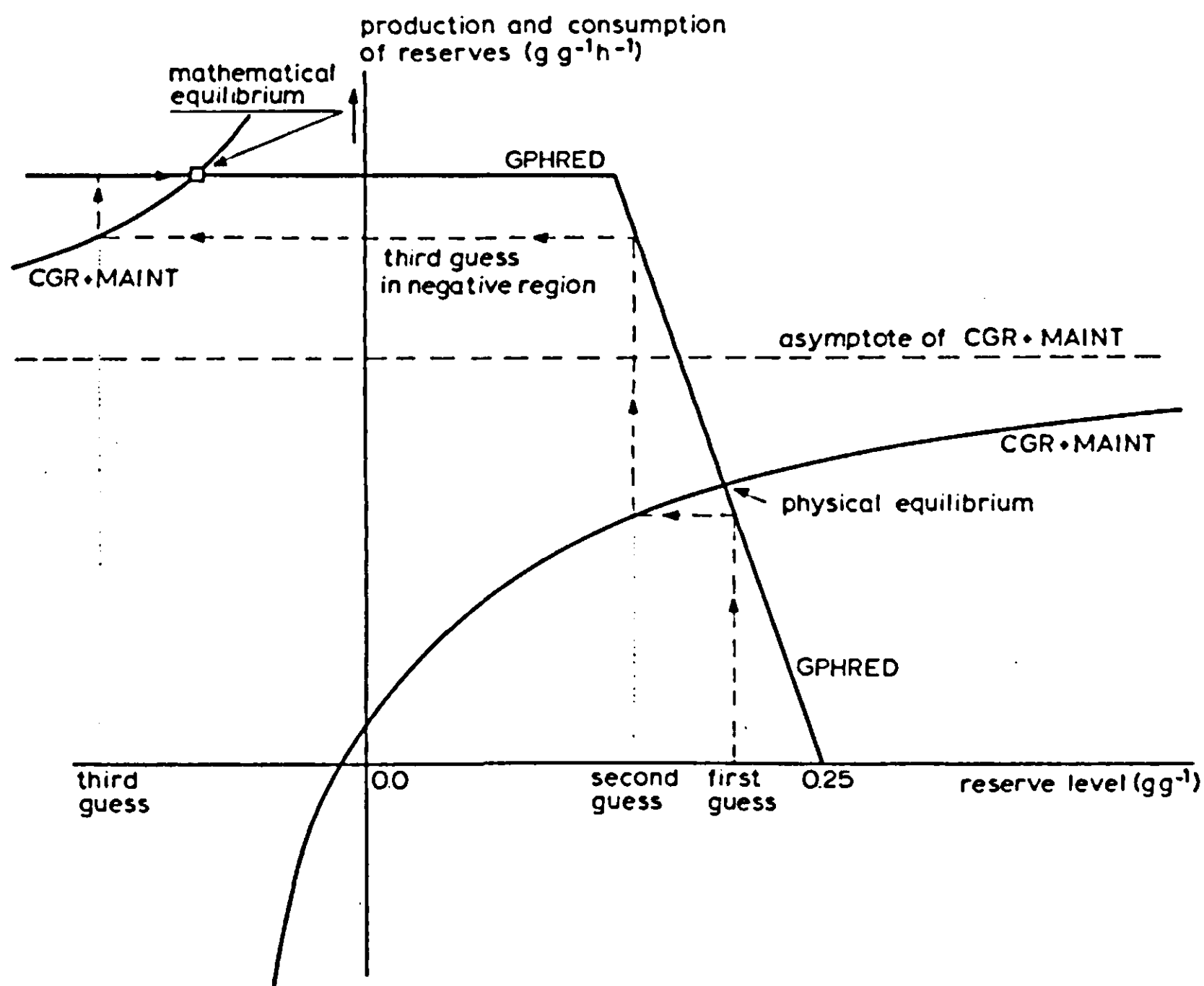
reserve level (gg⁻¹)

Figure 19. Course of the iteration process followed by the IMPLicit loop to find equilibrium between production and consumption of assimilates.

For TWT = 2000., the results of the implicit loop are disappointing. The calculated reserve level is negative! The reason for this bad behaviour is shown graphically in Figure 19. It is related to divergence of the repeated substitution method. This danger is always present in the CSMP-provided IMPLicit loop and when it strikes it can be resolved by rearrangement of the statements within the implicit loop. However, then the other equation with the unknown variable has to be inverted, which is not always possible. In this example it is hard to write RESL as a function of photosynthesis.

To summarize, the implicit loop may or may not work, dependent on the sequence of the statements. Of course, this is an uncomfortable feature of the implicit loop. In contrast, the halving/doubling method also known as bisection method is absolutely reliable, but its programming requires more work. This method is based on very simple reasoning. First a lower and an upper value are guessed, which certainly comprise the range of the unknown variable. In this example one might choose the values 0. and 0.25. For each of the two guesses the rates of production and consumption are calculated, and, of course, the signs of their differences are opposite. That means that the point where production and consumption match, must lie somewhere in between. Therefore the value halfway is tried and its accompanying production and consumption values.

Figure 20. Listing of CSMP program that employs the halving-doubling iteration method, and its output.

```
TITLE RESERVELEVEL WITH HALVING/DOUBLING ITERATION METHOD
INITIAL
INCON RESL1=0.,RESL2=.25
* LOWER VALUE OF RESL IS ZERO, AND UPPER VALUE IS 25 PERCENT

DYNAMIC
* FOR DEMONSTRATION PURPOSES, TWT IS MADE A FUNCTION OF TIME:
        TWT=20.*TIME

        MAINT=0.015*TWT
        LHI=AMIN1(WSH/500.,5.)
        WSH=0.7*TWT
        GPHOT=GPHST*(1.-EXP(-0.7*LHI))
        GPHFED=GPHOT*AFGEN(REDFT,RESL)


PROCEDURE RESL=ITERA(RESL1,RESL2,GPHOT)
        COUNT=0.
  130   CGR1=0.1*TWT*RESL1/(RESL1+KRESL)
        CGR2=0.1*TWT*RESL2/(RESL2+KRESL)
        AVAIL1=GPHOT*AFGEN(REDFT,RESL1)-MAINT
        AVAIL2=GPHOT*AFGEN(REDFT,RESL2)-MAINT
        COUNT=COUNT+1.
        IF(COUNT.GT.100.)GOTO 150

        IF((CGR1-AVAIL1)*(CGR2-AVAIL2).LT.0.) GOTO 110
* IF THE SOLUTION IS WITHIN THE CHOSEN RANGE GOTO 110

* ELSE DOUBLE THE RANGE INTO THE CORRECT DIRECTION:
        IF(CGR1.GT.AVAIL1) RESL1=2.*RESL1-RESL2
        IF(CGR2.LT.AVAIL2) RESL2=2.*RESL2-RESL1
* AND TRY AGAIN:
        GOTO 130

* RESL3 LIES HALFWAY THE LOWER AND THE UPPER VALUE
  110   RESL3=(RESL1+RESL2)*0.5
        CGR3=0.1*TWT*RESL3/(RESL3+KRESL)
        AVAIL3=GPHOT*AFGEN(REDFT,RESL3)-MAINT
* TEST FOR THE PRESET CONVERGENCE CRITERION:
        IF(ABS(CGR3-AVAIL3).LT.ERROR) GOTO 200

* CRITERION NOT SATISFIED,SO INCREMENT THE COUNT AND HALVE THE RANGE
        COUNT=COUNT+1.
        IF(COUNT.GT.100.) GOTO 150
        IF((CGR3-AVAIL3)*(CGR1-AVAIL1).GT.0.) GOTO 100
* UPPER BOUNDARY IS REPLACED BY THE HALFWAY VALUE:
        RESL2=RESL3
        GOTO 110

* LOWER BOUNDARY IS REPLACED BY THE HALFWAY VALUE:
  100   RESL1=RESL3
        GOTO 110

  150   WRITE(6,800)
  800   FORMAT(' TOO MANY ITERATIONS')
  200   RESL=RESL3

* THE RANGE FOR THE NEXT TIME INTERVAL IS CHOSEN:
        RESL1=RESL3
        RESL2=RESL3+0.001
ENDPRO


PARAM ERROR=0.001
PARAM KRESL=0.1
PARAM GPHST=400.
FUNCTION REDFT=0.,1.,0.2,1.,0.25,0.
TIMER FINTIM=500.,PRDEL=20.,DELT=20.
METHOD RECT
PRINT TWT,RESL,GPHFED
END
STOP
ENDJOB
```

74

```
1  RESERVELEVEL  WITH  HALVING/DOUBLING  ITERATION  METHOD
0  TIME          TWT           PESL            GPHRED
   0.0000000+00  0.00000E+00   0.00000E+00     0.00000E+00
   2.0000000+01  400.00        0.23685         34.125
   4.0000000+01  800.00        0.23434         68.072
   6.0000000+01  1200.0        0.23160         101.81
   8.0000000+01  1600.0        0.22863         135.31
   1.0000000+02  2000.0        0.22548         168.55
   4.0000000+02  8000.0        5.03535E-02     387.92
   4.2000000+02  8400.0        4.53091E-02     387.92
   4.4000000+02  8800.0        4.10078E-02     387.92
   4.6000000+02  9200.0        3.72974E-02     387.92
   4.8000000+02  9600.0        3.40635E-02     387.92
   5.0000000+02  10000.        3.12200E-02     387.92
1$$$ SIMULATION HALTED FOR FINISH CONDITION  TIME      500.00
1$$$ CONTINUOUS SYSTEM MODELING PROGRAM III   V1M3   EXECUTION OUTPUT $$$
```

The sign of their difference is compared with that of the lower value. If it is the same, the halfway value replaces the old lower value in its function as lower value and the procedure is repeated. If the sign is opposite the halfway value becomes the new upper value, and the procedure is repeated. This iteration is continued until the difference between the upper and lower value is reduced to a preset convergence criterion. Every iteration cycle the possible range is halved, so that 10 iterations are required to obtain an accuracy of 1/1000 of the initial range ($2^{10} = 1024$), and by 20 we have a reduction by a factor of 10^6. This method never fails provided there is only one possible solution between the two starting positions.

When we use this method in simulation, most likely the current situation does not differ considerably from that at the previous time interval. It could then be advantageous to use the last solution as one of the starting points, and accept the possibility that the solution is outside the chosen range. We then have to make a provision for being able to double the range in the correct direction until it contains the solution, after which we apply the halving method again. In Figure 20, a self-explanatory listing is given of a CSMP program for the calculation of crop photosynthesis where the halving/doubling iteration method is used. From the output we see that at time 100 when the assumed crop weight is 2000, the result is equal to that of the state variable method. At time 0, when crop weight is assumed zero, of course no result can be obtained. The sturdiness of the method is shown by the absence of zero divisions or overflows for this situation, and resumption of its usual performance at time 20.

A special use of an implicit loop for a crop-water-balance simulation, using one hour time steps, is explained in Subsection 3.3.7.

2.3.5 Some numerical integration methods

Popular numerical integration methods, all available in CSMP, are the rectangular method (METHOD RECT), the trapezoidal method (METHOD TRAPZ), the Runge-Kutta method with fixed integration interval (METHOD RKSFX), and the Runge-Kutta method with a self-adapting integration interval (METHOD RKS). The latter is used by default in CSMP, in the situation that the model builder did not specify a method. To make a proper choice of integration method

for a model, it is worthwhile to consider them a bit further.

The simplest method, the rectangular one, will be discussed first. In this method a rate calculation is followed by an integration step, then time is incremented by the time interval DELT, and the procedure is repeated for the next time interval. Graphically, it is convenient to represent the integral as an area under a curve, where the rate of change corresponds to the function value of the curve. In Figure 21 an example is given. The 'true' area is the area under the continuous curve, and the result of the rectangular method is given by the area of the vertical bars. In this case, where a rising curve is integrated the numerical result is less than the true area; with a decreasing function it would be the opposite. Even if we do not know the exact value of the difference between the numerical result and the 'true' area it is possible to estimate it. In this case the error of the numerical integration is approximately equal to the sum of the areas of the triangles above the vertical bars, formed by connecting their corners.

As a standard example we shall study the integration of the exponential function of time:

$$R = R_0 \cdot EXP(RGR \cdot T) \tag{1}$$

where R is the rate to be integrated, RGR the relative growth rate, T time and R_0 the rate at time zero. Formulated in this way, R is a driving force, that means a function of time only and not dependent on the result of the integration. The dimension of the relative growth rate RGR is T^{-1}, so that the product $RGR \cdot T$ is dimensionless. (It is good practice to verify that arguments of exponentials, logarithms, etc., are dimensionless.) Because the expression for the rate R (Equation 1) can be integrated analytically (which we will consider as the 'true' result), it is possible to find the errors caused by different numerical integration methods. Assuming the value of R_0 is unity, the analytical solution of the integral (A) of R between time T_0 and time T_1 is:

$$A = (EXP(RGR \cdot T_1) - EXP(RGR \cdot T_0))/RGR \tag{2}$$

Using the values RGR = 1, T_0 = 0 and T_1 = 4 we find A = 53.598150.

Figure 21. Graphical representation of numerical integration. The rate of change (R) is on the vertical axis, so that areas represent values integrated over time intervals Δt. Exponential function of time (solid line), rectangular integration (▨▨), trapezoidal integration (▨▨+▧▧); Δt is time interval of integration.

Exercise 21

Write a CSMP program to find the numerical integral of R with time intervals (DELT) of 1, 0.1 and 0.01. Calculate the error as the difference between the analytical and numerical result. Use the methods RECT, TRAPZ and RKSFX.

2.3.6 Error analysis

Integration of a driving force (no feedback)

Obviously the results are better using TRAPZ, and still more so with RKSFX. The errors of these methods are explained graphically in Figures 21 and 22. By using TRAPZ the triangles above the vertical bars have been included in the integral value, because this method averages the rate at the beginning and at the end of the time interval. Graphically, such averaging can be represented by connecting the corners of the vertical bars by straight lines. We have seen that the error of RECT was just about equal to the area of the triangles formed.

Now we shall try to make a quantitative estimate of the error and how it is related to the time interval of integration. The conclusions of the paragraphs below are summarized in Table 6.

To derive these conclusions, a thorough analysis of the integration procedure is required. For the sake of simplicity this is not done here in full detail. Additional information can be found in Scheid (1968) and Lanczos (1967).

Life is made simple, because R, the rate of change of the integral A of Equation 2, grows exponentially, so that each time interval the same fraction is added to its value and the same relative error is made over and over again. In fact, for RECT the relative error is equal to the ratio of the area of the triangle to that of the vertical bar. This ratio is:

$$E_{rel} = RGR \cdot DELT/2 \tag{3}$$

Since this ratio does not change, the absolute error at the end is

$$E_{abs} = RGR \cdot DELT \cdot A/2 \tag{4}$$

Table 5. Numerical integration results (A) and their errors for three values of integration steps with the integration methods RECT, TRAPZ and RKSFX.

DELT	RECT		TRAPZ		RKSFX	
	A	ERROR	A	ERROR	A	ERROR
1	31.193	22.405	57.992	−4.3938	53.616	−0.01807
0.1	50.963	2.6353	53.643	−0.04466	53.598	−0.0000014
0.01	53.331	0.26754	53.599	−0.000446	53.598	−0.0000005

Table 6. Relative errors of the numerical integration results

	With feedback	Without feedback
RECT	$2 \cdot (DELT/TAU) \cdot (TIME/TAU)$	$(DELT/TAU)/2$
TRAPZ	$(DELT/TAU)^2 \cdot (TIME/TAU)/6$	$-(DELT/TAU)^2/12$
RKSFX	$(DELT/TAU)^4 \cdot (TIME/TAU)/120$	$-(DELT/TAU)^4/2880$

We can check with Table 5 that this estimate is quite good, except for DELT = 1, in which case the result is just too far off. Note that A in Equation 4 is numerically not identical to A in Equation 2, as its value depends on method and DELT chosen.

In the trapezoidal method the triangles have been taken into account, so that the error is much smaller. The remaining error is given in Figure 22 as the area between the straight line and the curved solid line. The best estimate of this area is obtained when a parabola is constructed through the function values at time T, T + DELT/2 and T + DELT and the area between the parabola and the straight line is taken. Some algebraic work shows that the remaining relative error is now:

$$E_{rel} = -(RGR \cdot DELT)^2/12 \qquad (5)$$

In Table 5 this result can be checked. Similarly it was derived that for METHOD RKSFX, the relative error is given by

$$E_{rel} = -(RGR \cdot DELT)^4/2880 \qquad (6)$$

Figure 22. Geometrical representation of the trapezoidal (below straight line) and Runge-Kutta (below curved dashed line) integration methods. The curved solid line is the exponential which has to be integrated. The rate of change (R) is on the vertical axis, so that areas represent integrated values.

For DELT = 0.01 the resulting relative error is drowned in the truncation errors that always occur. The exponent of the dimensionless product (RGR · DELT) that occurs in the expression for the relative errors, reflects that the method RECT, TRAPZ and RKSFX are of the first, second and fourth order, respectively. This result has wider applicability than just this example of integration of the exponential function. However, there are exceptions where with some luck a lower-order integration method does just as well as a higher-order one.

Exercise 22
Repeat Exercise 21 for the integration of
 a. R = TIME
 b. R = TIME * *2
 c. R = SIN(2 * PI * TIME)

between TIME 0. and TIME 0.5, and with PI = 3.141592

Integration with feedback

Influence of feedback on development of errors is considerable. With feedback (Subsection 2.1.6), either positive or negative, the situation is worse than discussed before, because errors will propagate. In exponential growth of a single plant, an underestimation of leaf area will cause an underestimation of photosynthesis, and hence growth, and hence leaf area. With numerical integration the same thing happens, and moreover a new error will be added every time interval. Therefore, in contrast to integration of a driving force, relative errors tend to grow during simulation time, although negative feedback may sometimes help us. The error analysis is slightly different from that for a driving force, because the relative error will refer to the total integral value, which consists of integrated amount and initial value together.

As an example we shall study the integration of the rate R = RGR · A. Ideally the result of this integration is the same as integration of the exponential function EXP(RGR · T), but by linking the rate to the integral value A itself, feedback is introduced. In the rectangular method the value of the integral A after one integration step will equal:

$$A_{T+DELT} = A_T \cdot (1 + RGR \cdot DELT) \qquad (7)$$

so that the rate at time T + DELT is given by

$$R_{T+DELT} = RGR \cdot A_T \cdot (1 + RGR \cdot DELT) \qquad (8)$$

In the trapezoidal method this rate and the one at time T are averaged and used to find a better estimate of A_{T+DELT}. The corrected estimate can be written as:

$$A_{T+DELT} = A_T \cdot (1 + RGR \cdot DELT + (RGR * DELT)^2/2) \qquad (9)$$

79

As before, we assume that the difference between the result for TRAPZ and RECT is a good estimate for the error involved in RECT. By comparing Equation 7 and Equation 9 we find that for one integration interval the relative error in RECT can be estimated as:

$$E_{rel} = (RGR \cdot DELT)^2/2 \tag{10}$$

In contrast to Equation 3, $RGR \cdot DELT$ occurs here in an quadratic form. This is so because in Equation 3 the error is related to the integral, not considering its initial value. In Equation 10, the initial value is included because with feedback one is interested in the total result. This relative error occurs each integration step, and in contrast to the situation without feedback, these errors accumulate. At time T, when T/DELT integration steps have been performed, the resulting relative error is

$$E_{rel} = RGR^2 \cdot T \cdot DELT/2 \tag{11}$$

Interestingly, the relative error is again proportional with DELT, both with and without feedback. A similar procedure for evaluation of the errors involved in TRAPZ and in RKSFX yields the result presented in Table 6. In this table RGR has been replaced by 1/TAU, where TAU stands for time coefficient. Time coefficient has a more general meaning than relative growth rate and it can be loosely defined as the shortest duration of time in which at least one of the integrals or driving forces of the model system can change considerably (cf. Subsections 1.4.4 and 2.1.7).

In principle the results of Table 6 are also valid when the feedback is negative, but it should be remembered that they refer to the difference between the integral and the equilibrium level. Since that difference decreases in time, the absolute error decreases as well. The relative error of the difference between equilibrium and integral increases all the time, but in most applications that is not disturbing. If we define relative error as absolute error divided by integral itself, negative feedback will help to dissipate old errors. Only in the extreme situation that the time interval exceeds the time coefficient is the dampening effect of the negative feedback insufficient to constrain the growth of the integration errors.

Integration with discontinuities

Discontinuities in forcing functions also need to be considered. The error analysis discussed before is not possible when a discontinuity occurs, because the derivatives do not exist at the breaking point. When an integration interval overlaps a discontinuity, the error in any integration method will be large. To estimate how large, we must first find out what type of discontinuity we are dealing with. In Figure 23 different types of discontinuities have been illustrated. The time course has been given of the content of an integral (state) and its corresponding rate of change is above it. The first discontinuity in this graph is characterized by a jump in the integral content (point t_0). Such a jump can only be realized if the rate gets an infinitely high value at this moment during an
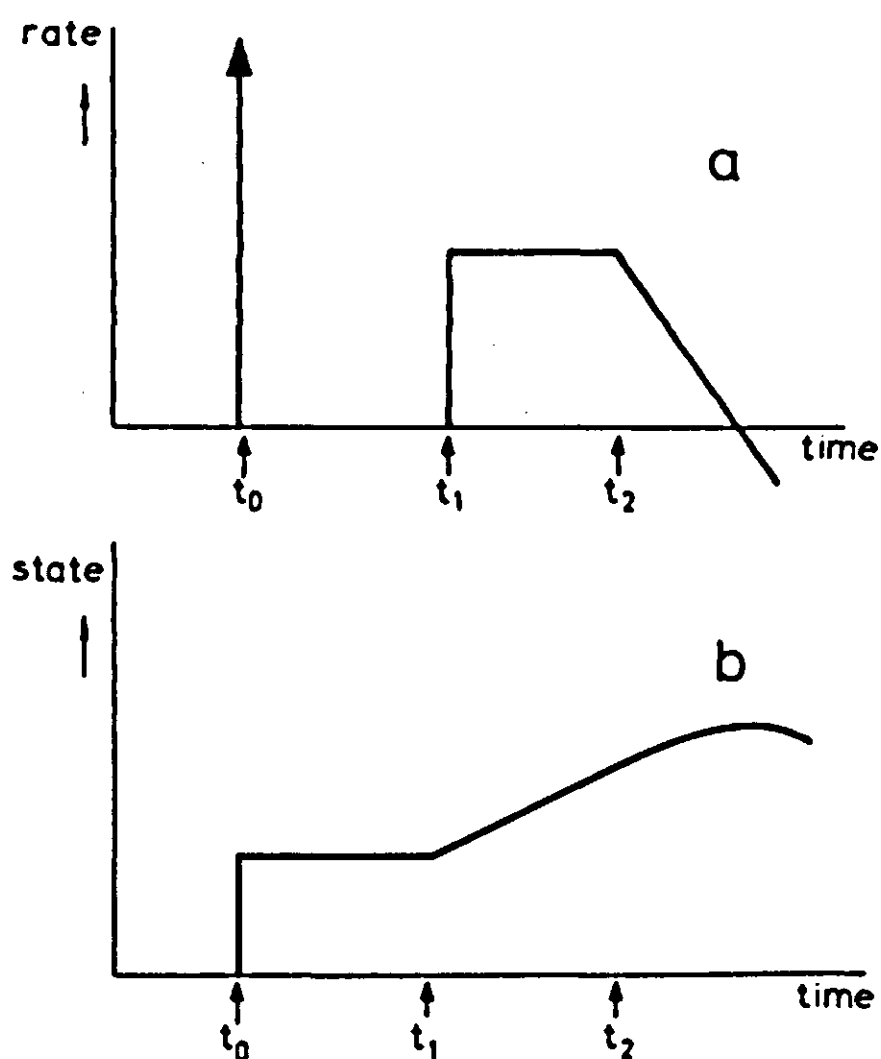
Figure 23. Discontinuities of zero-th, first and second order in a rate variable and their consequences for the state variable.

infinitely short duration of time, in such a way that the area of this pulse is equal to the jump of the integral. In physics such a pulse is called a Dirac pulse and often denoted by $\delta(t_0)$. Let us call this phenomenon a discontinuity of the zero-th order. In the second example, at time t_1 the rate shows a jump, resulting in a change of slope in the state. This is a discontinuity of the first order. The last example shows a discontinuity of the second order at time t_2; it is hardly noticeable in the graph of the state.

It is clear that these discontinuities have a decreasing order of difficulty for simulation. The most serious one, the discontinuity of the zero-th order, occurs when the content of an integral has to be changed instantaneously, e.g. when a crop is harvested. Then the only permissable integration method is METHOD RECT. The Dirac pulse of the rate is approximated by a pulse with width DELT and a height equal to the amount of change divided by the time interval. For instance, if an integral must be emptied we get

$$A_{T+DELT} = A_T - DELT \cdot (A_T/DELT) \tag{12}$$

It is characteristic for these constructions that a division by DELT occurs somewhere in the program. It ensures that the numerical error because of the discontinuity itself has been corrected, and that the remaining errors can be analyzed in the traditional way.

Discontinuities of the first and second order may occur when weather data are available as daily totals or as daily averages. For instance, the average temperature may jump at midnight. Usually these discontinuities can be handled by a self-adapting method like RKS. Whatever method is used, the error will be proportional to the time interval around the discontinuity; and so it can be made as small as one wishes. In Table 7 a summary is given of the line of reasoning

Table 7. Decision table for integration method and time interval.

Do discontinuities of the zero-th order occur?

    Yes: Choose METHOD RECT
        Synchronize DELT with the discontinuities if they appear at regular intervals.
        Choose DELT smaller than the smallest time coefficient, usually about 1/10 of it.

    No: Is the time coefficient stable and known?
    Yes: Choose METHOD RKSFX
        Choose DELT about ½ of the time coefficient.
    No: Specify neither METHOD (RKS is default)
        nor DELT (is automatically adapted)

---

that must be followed to arrive at the proper integration method.

2.3.7 Computation schemes of the integration methods

From the scheme in Table 8 it is possible to find how many times the UPDATE is executed for each integration interval DELT. The calculation of the rate(s) R is represented by a call of the UPDATE (see Subsection 2.2.4): R = UPDATE (A_n, T_n) in which A represents the state variable and T time. In RECT this call is done once, in TRAPZ twice and in RKSFX four times. This larger expenditure is more than compensated by the much larger size of time intervals that can be taken to reach the same accuracy. For instance, with a required accuracy of 0.1% for each simulation period of one time coefficient we need 500 computations with RECT, 25 with TRAPZ and only seven with RKSFX. When we know the time coefficient, we can make an estimate of the needed time step beforehand. In complicated systems with many simultaneous processes such an estimate is difficult. It is possible to use an empirical method like running the model twice with different time steps. It is also possible to use the CSMP-provided integration method RKS that chooses the time step itself. In this method two integration routines are executed simultaneously, their results are compared, and when they differ too much the time step is halved. If the deviation is much smaller than required, DELT will be doubled for the next step.

Sometimes the preset error criterion is not met, and DELT is decreased below the minimum value DELMIN. Then the error message 'DELT IS LESS THAN DELMIN' is given, and the simulation is automatically terminated. Such an event usually means a programming or conceptual error, or at least an awkward model structure. Because of the feature of automatic adaption of the time-interval of integration, the method RKS is recommended as a standard method.

In the RKS method, the statements of the computer programs are executed many times, only to obtain a preliminary estimation of the rates. How many

Table 8. Summary of the integration methods RECT, TRAPZ, RKSFX. T stands for TIME.

RECTANGULAR

$R = UPDATE(A_n, T_n)$
$A_{n+1} = A_n + DELT \cdot R$
$T_{n+1} = T_n + DELT$

TRAPZ

$R1 = UPDATE(A_n, T_n)$
$A1 = A_n + DELT \cdot R1$
$T_{n+1} = T_n + DELT$
$R2 = UPDATE(A1, T_{n+1})$
$A_{n+1} = A_n + DELT \cdot (R1 + R2)/2$

RKSFX

$R1 = UPDATE(A_n, T_n)$
$A1 = A_n + DELT \cdot R1 \cdot 0.5$
$T_{n+\frac{1}{2}} = T_n + DELT \cdot 0.5$
$R2 = UPDATE(A1, T_{n+\frac{1}{2}})$
$A2 = A_n + DELT \cdot R2 \cdot 0.5$
$R3 = UPDATE(A2, T_{n+\frac{1}{2}})$
$A3 = A_n + DELT \cdot R3$
$T_{n+1} = T_n + DELT$
$R4 = UPDATE(A3, T_{n+1})$
$A_{n+1} = A_n + DELT \cdot (R1 + 2 \cdot R2 + 2 \cdot R3 + R4)/6$

---

times this execution is done can be checked by introduction of some counters into the program. To this end, an initial segment is introduced, in which the counters COUNT1 and COUNT2 are set to zero. At the very end of the DYNAMIC segment, that is evaluated each time interval, a section is introduced with the card NOSORT to indicate that the statements after this card cannot be sorted.

```
NOSORT
COUNT1 = COUNT1 + 1
COUNT2 = COUNT2 + KEEP
END
```

These statements cannot be sorted because the same variables occur to the left and to the right of the equal sign (see Subsection 2.3.2). Each time this statement is executed, COUNT1 is incremented by 1, and COUNT2 by KEEP. The variable KEEP is an internal CSMP variable and has the value 1 if the integration step is actually executed, and a value 0 if the statements are only executed for a preliminary evaluation. In this way both the number of time intervals and the number of calculations of the whole program can be kept track of.

Exercise 23
Use this NOSORT block with the program introduced in Exercise 21; change the NOSORT block into a PROCEDURE and repeat the calculations.

3 CROP PRODUCTION AND PLANT GROWTH IN OPTIMAL CONDITIONS

3.1 A summary model for crop growth

H. van Keulen, F.W.T. Penning de Vries and E.M. Drees

3.1.1 Introduction

As outlined in Section 1.3, different models of the same system may exist, all equally valid but differing in the purpose for which they were developed. One of the types of models discussed is the 'summary model', which in itself is relatively simple, but relies heavily for its functional relationships on more detailed process models.

In this section such a simple model is presented for the calculation of potential crop production at Production level 1 (Section 1.2), where water or plant nutrients are not limiting factors. It may be applied to different crops or plant species by introducing in the model the appropriate parameters and functions for each of these. It is to a large extent based on sections of the comprehensive model BACROS. In a sense, this section can also be seen as an introduction to that model. The summary model is fully explained here, but in a superficial way. More detail is given in the three following sections.

3.1.2 Description of the model

The model simulates the time course of dry matter production of a crop, from emergence till maturity, in dependence of daily total irradiation and air temperature. The dry matter produced is divided into roots (WRT), leaves (WLV), stems (WST) and storage organs (WSO). Partitioning factors are introduced as a function of the phenological state of the crop.

A complete listing of the program is given in Table 9. Parameter values for a wheat crop growing in Zambia are used. The abbreviations in the text refer to names used in the program and a complete list of them is given in Table 10. The program is structured in a logical way, which means a calculation of the principal variables is given first, followed by calculation of those variables that are required for the quantification of the principal ones.

This simple and universal crop growth model, named SUCROS, is written in CSMP (see Section 2.2); it can be easily translated into other computer languages.

CO_2 assimilation

The basis for the calculation of dry matter production is the rate of gross CO_2 assimilation of the canopy. This rate is obtained from the CO_2 assimilation-light response curve of individual leaves of the species, the total green (leaf) area of the canopy, the spatial arrangement of the leaves and on the one hand their op-

Table 9. A listing of the program of the model SUCROS.

```
TITLE SUCROS - A SIMPLE AND UNIVERSAL CROP GROWTH SIMULATOR
***   DRY WEIGHT OF PLANT ORGANS, GROWTH RATES AND PARTITIONING

      WLV = INTGRL(WLVI,GLV-DLV)                                          101
      WST = INTGRL(0.,GST)                                               102
      WSO = INTGRL(0.,GSO)                                               103
      WRT = INTGRL(WRTI,GRT)                                            104
*  WEIGHTS OF LEAF BLADES, STEMS (TRUE STEMS AND LEAF SHEATHS), STORAGE
*  ORGANS AND ROOTS RESP., IN KG/HA
INCON WLVI=25., WRTI=25.                                                 105
*  WEIGHT OF LEAVES AND ROOTS AT EMERGENCE


      GTW=(GPHOT-MAINT)*CVF                                              106
*  GROWTH RATE OF ALL ORGANS COMBINED, IN KG/HA/DAY
      GRT=GTW*(1.-FSH)                                                   107
      GSH=GTW*FSH                                                        108
      GLV=GSH*FLV                                                        109
      GST=GSH*FST                                                        110
      GSO=GSH*FSO                                                        111
*  GROWTH RATES OF ROOTS AND SHOOTS (LEAVES,STEMS, STORAGE ORGANS) IN KG/HA/DAY
      DLV = WLV*RDR                                                      112
*  DEATH RATE OF LEAVES, IN KG/HA/DAY
      RDR = AFGEN(RDRTB,DVS)                                             113
FUNCTION RDRTB = 0.,0., 1.,0.. 1.01,0.03. 2.,0.03                        114
      WLVD = INTGRL(0.,DLV)                                              115
*  DEAD MATERIAL (LEAVES) AT THE FIELD IN KG/HA


      FSH = AFGEN(FSHTB,DVS)                                             116
FUNCTION FSHTB=0.,0.5,   0.3,0.5. 0.45,0.775, 0.7,0.825, 1.,1., 2.,1.    117
*   FRACTION OF GROWTH OCCURING IN SHOOTS AS FUNCTION OF DEVELOPMENT STAGE
      FLV = AFGEN(FLVTB,DVS)                                             118
      FST = AFGEN(FSTTB,DVS)                                             119
      FSO = 1.-FLV-FST                                                   120
FUNCTION FLVTB = 0.,1., 0.45,1.. 0.85,0..             2.,0.              121
FUNCTION FSTTB = 0.,0., 0.45,0., 0.85,1..1.,1., 1.01,0., 2.,0.           122


***  CARBON BALANCE PROCESSES

      LAI = WLV*SLFA                                                     201
PARAM SLFA = 0.0020                                                      202
*  LEAF AREA INDEX IN HA/HA AND SPECIFIC LEAF AREA IN HA LEAF/KG LEAF WEIGHT


      GPHOT=DTGA*30./44.                                                 203
      DTGA = FOV*DGAO+(1.-FOV)*DGAC                                      204
*  GROSS PHOTOSYNTHESIS IN KG (CH2O AND CO2 RESP.) PER HA PER DAY, CALCULATED
*  FROM LEAF CHARACTERISTICS (AMAX, EFF). LAI AND ACTUAL DAILY RADIATION
*  (AVRAD). AND CORRECTED FOR DAYLENGTH (DL AND DLE):
      DGAC=INSW(LAI-5.,PHCL,PHCH)                                        205
      DGAO=INSW(LAI-5.,PHOL,PHOH)                                        206
      PHCH=0.95*(PHCH1+PHCH2)+20.5                                       207
      PHCH1=SSLAE*AMAX*DLE*X/(1.+X)                                      208
      X=ALOG(1.+0.45*DPC/(DLE*3600.)*EFFE/(SSLAE*AMAX))                  209
      PHCH2=(5.-SSLAE)*AMAX*DLE*Y/(1.+Y)                                 210
      Y=ALOG(1.+0.55*DPC/(DLE*3600.)*EFFE/((5.-SSLAE)*AMAX))             211
      SSLAE=SIN((9U.+DEC-LAT)*PI/180.)                                   212
      PHCL=AMIN1(PHC3,PHC4)*(1.-EXP(-(AMAX1(PHC3,PHC4)/AMIN1(PHC3,PHC4))))  213
      PHC3=PHCH*(1.-EXP(-0.8*LAI))                                       214
      PHC4=DL*LAI*AMHX                                                   215
      PHOH=0.9935*PHOH1+1.1                                             *216
      PHOH1=5.*AMAX*DLE*Z/(1.+Z)                                         217
      Z=DPO/(DLE*3600.)*EFFE/(5.*AMAX)                                   218
      PHOL=AMIN1(PHO3,PHC4)*(1.-EXP(-(AMAX1(PHO3,PHC4)/AMIN1(PHO3,PHC4))))  219
      PHO3=PHOH*(1.-EXP(-0.8*LAI))                                       220
      EFFE=(1.-REFLC)*EFF                                                221
PARAM EFF= 0.5, AMAX = 30., REFLC=.08                                    221
*  INITIAL LIGHT USE EFFICIENCY AND LIGHT SATURATED CO2 ASSIMILATION RATE
*  OF INDIVIDUAL LEAVES. UNITS: KG CO2/HA/HR /(J/M2/S) AND KG CO2/HA LEAF/HR
```

```
        FOV = (DRC-AVRAD)/(0.8*DRC)                                      222
*   AVERAGE FRACTION OF PERIOD OVERCAST DURING A DAY.
*   CALCULATION OF DAILY RADIATION OF A CLEAR AND AN OVERCAST SKY (DRC
*   AND DRO. P.A.R., IN J/M2) AND OF DAYLENGTH (IN HR) AS A FUNCTION OF
*   LATITUDE (LAT. IN DEGREE), DECLINATION (DEC, IN DEGREE) AND DATE:
        DRC=0.5*1300.*RDN*EXP(-0.1/(RDN/(DL*3600.)))                     223
        DRO=0.2*DRC                                                      224
        RDN=3600.*(SINLD*DL+24./PI*COSLD*SQRT(1.-(SINLD/COSLD)**2))      225
        SINLD=SIN(DEC*PI/180.)*SIN(LAT*PI/180.)                         226
        COSLD=COS(DEC*PI/180.)*COS(LAT*PI/180.)                         227
        DEC=-23.4*COS(2.*PI*(DAY+10.)/365.)                            228
        DL=12.*(PI+2.*ASIN(SINLD/COSLD))/PI                             229
        DLE=12.*(PI+2.*ASIN((-SIN(8.*PI/180.)+SINLD)/COSLD))/PI         230
        DLP=12.*(PI+2.*ASIN((-SIN(-4.*PI/180.)+SINLD)/COSLD))/PI        231
CONSTANT PI = 3.1416                                                    232
PARAM LAT = -15.                                                        233


*   MAINTENANCE RESPIRATION
        MAINT =AMIN1(GPHOT,MAINTS*TEFF)                                  234
        MAINTS=WLV*0.03+WST*0.015+WSO*0.01+WRT*0.01                      235
        TEFF  =Q10**((0.1*TMPA-2.5)                                      236
PARAM Q10 = 2.                                                          237


*   GROWTH EFFICIENCY
        CVF= (FLV*0.72+FST*0.69+FSO*CVFSO)*FSH+(1.-FSH)*0.72            238
PARAM CVFSO=0.73                                                        239


*** DEVELOPMENT OF THE VEGETATION

        DVS = INTGRL(0.,INSW(DVS-1.,DVRV,DVRR))                         301
FINISH DVS = 2.                                                         302
        DVRV= 0.0252 * AFGEN(DVRTTB,TMPA) * AFGEN(DVRDTB,DLP)           303
        DVRR= 0.0477 * AFGEN(DVRPTB,TMPA)                               304
FUNCTION DVRTTB =10.,.63, 15.,.83, 20.,.92, 25.,.96, 30.,.98, 35.,.99  305
FUNCTION DVRRTB= 10.,.08, 15.,.38, 20.,.575, 25.,.71,30.,.80, 35.,.865 306
FUNCTION DVRDTB= 10.,0.223, 11.,0.425, 12.,0.575, 13.,0.685, ...       307
        14.,0.767, 15.,0.828, 16.,0.872, 17.,0.906                     307


*** WEATHER DATA
        DAY   = AMOD(TIME,365.)                                         401
        AVRAD = 0.5*41820.*AFGEN(AVRADT,DAY)                            402
FUNCTION AVRADT = 1.,523., 15.,526., 46.,532., 74.,575., 105.,557.,... 403
        135.,509., 166.,466.,196.,482.,227.,545.,258.,611.,288.,644.,...403
        319.,556.,349.,521.,365.,523.                                  403


        TMPA = 0.5*(AFGEN(TMAXT,DAY)+AFGEN(TMINT,DAY))                  404
FUNCTION TMAXT = 1.,28.6, 15.,28.3, 46.,28.1, 74.,28.7,105.,28.9,...   405
                135.,27.2,166.,24.9,196.,24.7,227.,27.4,258.,29.9,...  405
                288.,33.6,319.,31.3,349.,28.9,365.,28.6                405
FUNCTION TMINT = 1.,18.2, 15.,18.2, 46.,18.2, 74.,16.3,105.,13.9,...   406
                135.,10.1,166., 8.5,196., 7.4,227., 9.7,258.,13.4,...  406
                288.,16.6,319.,18.2,349.,18.2,365.,18.2                406


*** SIMULATION RUN SPECIFICATIONS
TIMER FINTIM = 1000.,DELT = 2.,PRDEL=2., OUTDEL= 2., TIME=300.         501
*    INITIAL VALUE OF TIME INDICATES STARTING DAY OF SIMULATION
METHOD RKSFX                                                           502
PRINT WLV,WLVD,WST,WSO,WRT,LAI,DVS,MAINT,DTGA,CVF                      503
        NWRT =-WRT                                                     504
        WLVT =WLV+WLVD                                                 505
        WVEG =WLVT+WST                                                 506
        TADRW=WVEG+WSO                                                 507
FRTPLOT NWRT,WLV,WLVT,WVEG,TADRW                                       508
PAGE GROUP, NPLOT=5                                                    509
END
STOP
ENDJOB
```

Table 10. An explanation of the abbreviations used in the model SUCROS as listed in Table 9.

NAME	DESCRIPTION	UNIT
AMAX	CO2 ASSIMILATION RATE OF A LEAF AT LIGHT SATURATION	KG(CO2)/HA(LEAF)/H
AVRAD	ACTUAL DAILY RADIATION (400-700 NM)	J/M2/D
AVRADT	TABLE MEASURED GLOBAL RADIATION (CAL/CM2/D) VS DAYNUMBER	-
CVF	CONVERSION EFFICIENCY FOR GROWTH OF PLANT DRY MATTER	KG(DM)/KG(CH2O)
CVFSO	CONVERSION EFFICIENCY FOR FORMATION OF STORAGE ORGANS	KG(DM)/KG(CH2O)
DAY	NUMBER OF DAY IN THE YEAR FROM 1ST OF JANUARY	DAY
DEC	DECLINATION OF SUN WITH RESPECT TO THE EQUATOR	DEGREE
DGAC	DAILY GROSS CO2 ASSIMILATION -CLEAR SKY-	KG(CO2)/HA/D
DGAO	DAILY GROSS CO2 ASSIMILATION -OVERCAST SKY-	KG(CO2)/HA/D
DL	ASTRONOMICAL DAYLENGTH	H
DLE	EFFECTIVE DAYLENGTH	H
DLP	PHOTOPERIODIC DAYLENGTH	H
DLV	DEATH RATE OF THE LEAVES	KG/HA/D
DRC	PHOTOSYNTHETICALLY ACTIVE RADIATION -STANDARD CLEAR SKY-	J/M2/D
DRO	PHOTOSYNTHETICALLY ACTIVE RADIATION -STANDARD OVERCAST SKY-	J/M2/D
DTGA	ACTUAL DAILY GROSS CO2 ASSIMILATION	KG(CO2)/HA/D
DVRDTB	RELATION BETWEEN RATE OF DEVELOPMENT AND DAYLENGTH	-
DVRR	RATE OF DEVELOPMENT IN REPRODUCTIVE PHASE IN RELATION TO TEMPERATURE	1/D
DVRRTB	TABLE OF DVRR AS FUNCTION OF TEMPERATURE	-
DVRTTB	RELATION BETWEEN RATE OF DEVELOPMENT AND TEMPERATURE	-
DVRV	RATE OF DEVELOPMENT IN VEGETATIVE PHASE IN RELATION TO TEMPERATURE AND DAYLENGTH	1/D
DVS	DEVELOPMENT STAGE OF THE CROP	FRACTION
EFF	EFFICIENCY OF USE OF ABSORBED VISIBLE RADIATION FOR CO2 ASSIMILATION AT LOW LIGHT LEVELS	KG(CO2)/J/HA/H M2S
EFFE	EFF BASED ON INCIDENT RADIATION	KG(CO2)/J/HA/H M2S
FLV	FRACTION OF LEAVES IN SHOOT BIOMASS	-
FLVTB	TABLE FLV VS DEVELOPMENT STAGE	-
FOV	FRACTION OF TIME THAT SKY IS OVERCAST	-
FSH	FRACTION OF SHOOT IN TOTAL PLANT BIOMASS	-
FSHTB	TABLE FSH VS DEVELOPMENT STAGE	-
FSO	FRACTION OF STORAGE ORGANS IN SHOOT BIOMASS	-
FSOTB	TABLE FSO VS DEVELOPMENT STAGE	-
FST	FRACTION OF STEMS IN SHOOT BIOMASS	-
FSTTB	TABLE FST VS DEVELOPMENT STAGE	-
GLV	GROWTH RATE OF THE LEAVES	KG(DM)/HA/D
GPHOT	DAILY GROSS CO2 ASSIMILATION	KG(CH2O)/HA/D
GRT	GROWTH RATE OF THE ROOTS	KG(DM)/HA/D
GSH	GROWTH RATE OF THE SHOOT	KG(DM)/HA/D
GSO	GROWTH RATE OF THE STORAGE ORGANS	KG(DM)/HA/D
GST	GROWTH RATE OF THE STEMS	KG(DM)/HA/D
GTW	GROWTH RATE OF TOTAL PLANT BIOMASS	KG(DM)/HA/D
LAI	LEAF AREA INDEX	M2/M2
LAT	LATITUDE	DEGREE
MAINT	MAINTENANCE RESPIRATION OF THE VEGETATION	KG(CH2O)/HA/D
MAINTS	MAINTENANCE RESPIRATION AT STANDARD TEMPERATURE (25 C)	KG(CH2O)/HA/D
NWRT	NEGATIVE WEIGHT OF ROOTS (OUTPUT VARIABLE)	KG(DM)/HA
PI	CIRCUMFERENCE OF A CIRCLE, DIVIDED BY ITS DIAMETER	-
Q10	INCREASE IN RATE OF MAINTENANCE PROCESSES PER 10 DEGR. C	-
RDN	AVERAGE LEVEL INCOMING PHOTOSYNTHETIC ACTIVE RADIATION	J/M2/S
RDR	RELATIVE DEATH RATE OF THE LEAVES	1/D
RDRTB	TABLE RDR VS DEVELOPMENT STAGE	-
REFLC	REFLECTION COEFFICIENT OF THE CANOPY	(FRACTION)
SLFA	SPECIFIC LEAF AREA	HA(LEAF)/KG(LEAF)
TADRW	TOTAL ABOVE-GROUND BIOMASS	KG/HA
TEFF	EFFECT OF TEMPERATURE ON RATE OF MAINTENANCE RESPIRATION	-
TIME	SIMULATED TIME	DAY
TMAXT	TABLE MAXIMUM TEMPERATURE VS DAYNUMBER	-
TMINT	TABLE MINIMUM TEMPERATURE VS DAYNUMBER	-
TMPA	AVERAGE AIR TEMPERATURE	DEGREE C
WLV	WEIGHT OF THE GREEN LEAVES	KG/HA
WLVD	WEIGHT OF THE DEAD LEAVES	KG/HA
WLVI	INITIAL WEIGHT OF THE LEAVES	KG/HA
WLVT	WEIGHT OF THE GREEN PLUS DEAD LEAVES (OUPUT VARIABLE)	KG/HA
WRT	WEIGHT OF THE ROOTS	KG/HA
WRTI	INITIAL WEIGHT OF THE ROOTS	KG/HA
WSO	WEIGHT OF THE STORAGE ORGANS	KG/HA
WST	WEIGHT OF THE STEMS	KG/HA
WVEG	WEIGHT OF THE VEGETATIVE PARTS (OUTPUT VARIABLE)	KG/HA

tical properties, and from the incident irradiation, on the other. A method to calculate daily values of gross CO_2 assimilation for any day as a function of daily total irradiation and geographical latitude was worked out by de Wit (1965) and amended and summarized by Goudriaan & van Laar (1978). In the model presented here, the Goudriaan & van Laar procedure is imitated very accurately with a small group of statements (Lines 203-221). It is described further in Subsections 3.2.3 and 3.2.4. For wheat, a value of the light saturated assimilation rate of individual leaves in terms of mass of CO_2 per leaf area (AMAX) of 30 kg $ha^{-1} h^{-1}$ is introduced, in combination with an initial light use efficiency (EFF) of 0.5 kg $ha^{-1} h^{-1}$ per Joule per square metre per second of absorbed visible irradiation. When based on incident irradiation, this efficiency is somewhat lower due to reflection. (Note that the variable named AMAX is completely different from the CSMP function AMAX1 (see Section 2.2, Table 3)). Such values are normal for C_3 type cereals. The rates of CO_2 assimilation of the canopy under completely clear and completely overcast conditions (DGAC and DGAO, respectively) that are computed with this group of equations reproduce accurately data that were established with a large computer model (Goudriaan & van Laar, 1978). The actual rate of CO_2 assimilation of the canopy (DTGA) is an average of both assimilation rates, weighted according to the actual fraction of the specific day that happened to be 'overcast'. The procedure also takes into consideration the reduced light interception and reduced CO_2 assimilation at incomplete soil cover. After multiplication of the rate of CO_2 assimilation by 30./44., (Line 203), gross photosynthesis (GPHOT) is expressed in glucose (CH_2O).

The fraction of the day that the sky is overcast (FOV) is calculated by comparing the measured level of incoming photosynthetically active radiation (AVRAD) to that on a completely clear and on a fully overcast day. The level of irradiance on completely clear days is computed from equations that integrate solar height as a measure of irradiation, multiplied with a solar constant, and corrected for day length (Lines 223-233, Goudriaan, personal communication). Photosynthetically active irradiation on overcast days is assumed to be 20% of that value.

The combination of both procedures for obtaining standardized daily totals for photosynthetically active irradiation and CO_2 assimilation are quite flexible, and they can be used with a high degree of accuracy in both hemispheres between 70°N and 70°S for crops with an LAI between 0.1 and 10.

Exercise 24
Use these procedures to compute the daily total of photosynthetically active irradiation and the daily gross CO_2 assimilation at your latitude today, assuming that the sky is fully clear.

Respiration and growth

Part of the carbon fixed by the assimilation process is respired to provide energy for biological functioning of the organism. The remainder is the carbon incorporated in structural dry matter. Maintenance respiration is considered explicitly, growth respiration only implicitly.

Maintenance respiration provides energy to maintain cells and their biostructure and ionic gradients. Although accurate data on maintenance requirements are scarce, reasonable estimates can be made on the basis of the composition of the biomass present. In the present model, the maintenance requirements for leaf, stem and root tissue are expressed in mass of glucose and are set at 0.03, 0.015 and 0.01 $kg\,kg^{-1}\,d^{-1}$, respectively (Line 235). These values hold at 25 °C; the effect of other temperatures is taken into account with a Q_{10} value of 2 (Lines 236, 237). For all types of storage organs, a value of 0.01 at 25 °C is adopted. For further detail, see Subsection 3.3.5.

Growth implies the conversion of primary photosynthates into structural plant material. The efficiency of the conversion depends on the chemical composition of the dry matter formed. In the model, average conversion factors of 0.72, 0.69 and 0.72 $kg\,kg^{-1}$ are used for leaf, stem and root biomass, respectively, and 0.73 $kg\,kg^{-1}$ for grains of wheat. The latter value depends on the nature of the storage organ, and its value is specific for each type of crop. In this model, a weighted average (CVF) of these organ specific conversion factors is calculated (Line 238) by multiplying the organ specific values with the fractions that these organs obtain from total weight increment. Multiplication of the amount of carbohydrates available for growth with this CVF value yields the total increase in dry matter of the crop per day (GTW, Line 106). All carbohydrates formed during that day and not consumed in maintenance processes are available for growth.

The amount of CO_2 lost as a result of growth processes (the growth respiration) also depends on the composition of the biomass formed (Subsection 3.3.4). The complement of CVF represents – roughly – the extent of growth respiration, but this is not modelled explicitly here.

Partitioning of dry matter

The increase in total dry weight (GTW), in $kg\,ha^{-1}\,d^{-1}$, of the crop is partitioned over the plant organs: roots, leaf blades, stems and leaf sheaths and the storage organ (grains, beets, pods, etc.). This is correct simulation of what occurs during the vegetative phase. Storage organs, however, may not only be formed from current photosynthates but also from carbohydrates and proteins that have been stored temporarily in vegetative parts and are redistributed during the reproductive stage. In this model, the latter process is not yet incorporated: the total growth of the crop is partitioned among the plant organs according to partitioning factors that are introduced as forcing functions; their values change with the development stage of the crop.

In allocating the biomass formed, first assimilates are diverted to the roots

(Lines 116 and 117). In general, it is difficult to obtain reliable data for assimilate supply to below ground organs, the more so since the processes of growth and decay may proceed concurrently, so that weights determined at any particular point may not be indicative for the amount of material invested in the roots. The function specified in this model is based on data supplied by Jonker (1958) for wheat. This description, in which biomass is first partitioned between shoot and root, is chosen to provide the option of modification of the biomass distribution values when stress conditions develop (Section 4.1; see Figure 33a, Section 3.3).

To obtain the increase in dry weight of leaves, stems and storage organs, the total shoot growth is multiplied by the appropriate factors. The partitioning between leaf blades and other vegetative structures (sheaths, true stems) is strongly schematized. For wheat, for example, it is assumed that only leaf blades are being formed until the development stage reaches 0.45, after which stem elongation starts and more of the assimilates are invested in these structures (Lines 121 and 122, cf. Rawson & Hofstra, 1969; Spiertz, 1977). After flowering, all available carbohydrates are used for grain formation (Line 120; see Figure 33a, Section 3.3).

As already stated, any contribution of pre-anthesis carbohydrates to grain yield is disregarded in this approach, which certainly is an oversimplification (Stoy, 1965; de Vos, 1975; Vos, 1981). We have not included even a simple description of this process, to avoid compromising the nature of the model: a summary of well known processes. As a result the prediction of economic yield can be up to 10-20% too low, depending upon crop type and growth conditions. Users are invited to improve on this (Subsection 3.4.9 provides an example). The model in its present form is essentially a source-oriented model in which dry matter accumulation is governed by the availability of assimilates. However, in reality, situations may occur for which the size of the sink, characterized in wheat by the number of grains present and the potential growth rate per individual grain, limits the rate of accumulation of dry matter in the grain (Section 3.4). Since actual grain numbers are not simulated in the model such a phenomenon cannot properly be taken into account. For application in particular situations adaptation of the model may then be necessary.

Leaf area growth

The increase in photosynthesizing surface, i.e. green area of the canopy (Line 201), follows directly from the growth rate of the leaf blades, by assuming a constant specific leaf area (SLFA) to mass of dry matter of 0.002 ha kg^{-1} (leaf dry matter) (Aase, 1978). In this description the area of green sheaths and stems is not taken into account separately, but it is generally a negligible fraction of the total green surface during the vegetative phase (Fisher, 1982).

93

Exercise 25

Why are results of simulation with this model sensitive to changes in the value of SLFA? Is there positive or negative feedback?

Leaves only have a limited life-span, and some of the earlier formed leaves will die even during the vegetative stage of the canopy. In the model, senescence is taken into account only after flowering, when the sink action of the developing grain accelerates leaf deterioration. Leaf death is effectuated by assuming a relative death rate of the green area as a function of crop development stage (Lines 112-115). The values introduced here lead to reasonably realistic simulations of decline in green area, such that sometimes physiological maturity is reached before all assimilating tissue has stopped functioning, whereas in other cases the reverse is happening. In this schematized description, the contribution to the assimilation process of green tissue other than leaf blades, which may be important after flowering, is also included. Note that this formulation of senescence has no fundamental basis, and is therefore descriptive rather than explanatory.

Crop phenology

The development pattern of a growing plant is characterized by the rate and order of appearance of vegetative and reproductive plant organs. The rate of development, that is the inverse of the duration of a particular growth stage, is determined by genetic properties as well as by environmental conditions. Genetic properties account for differences in growth duration among cultivars growing at a given time at a certain location (short vs. long duration cultivars), whereas environmental conditions, notably temperature and day length, cause variations in growth duration for one cultivar at different locations and/or seasons. In the model, the phenological state of the canopy is characterized by its development stage (DVS), a variable having the value 0. at emergence and 1. at flowering. Intermediate values are obtained by integration of the rate of development (DVR), which depends on the average daily temperature and day length in the vegetative phase, and on temperature only afterwards (Lines 301-307). Differences in temperature sensitivity between species and cultivars may exist, associated with photoperiodic influences (Angus et al., 1981). This is discussed further in Subsection 3.3.2.

After flowering, the crop is allowed to proceed until the development stage (DVS) of maturity is reached, which is introduced as a cultivar specific value (Line 302).

3.1.3 Application of the model

The model can be executed with time steps of one day with the simple recti-

linear method of integration (RECT), or time steps of 10 days with the integration method RKSFX (Section 2.3). The latter method is used here (Line 502), but to obtain more detailed output, a time step of two days (Line 501) is specified in Table 9. End of execution is achieved via a FINISH statement, which is operative when the crop reaches maturity.

When appropriate parameters and functions are available, the model may be used to predict potential productivity of different crops under varying conditions and at different locations. It should be kept in mind that its applicability is restricted by the assumptions underlying the present description, i.e. no constraining factors are present other than the level of irradiance. To achieve the productions as predicted by the model in the real situation for validation purposes, growing conditions should be optimal in terms of supply with water and plant nutrients, weeds should not seriously interfere with crop production and the crop should be free of pests and diseases. It may be problematic, even under experimental conditions, to create such an ideal situation, but then the model may indicate the scope for improvement that is still possible.

The model is thought to be valid universally where potential growth conditions can exist, including climate rooms, but with exception of extremely high and low temperatures, or very low light levels and with exception of situations where considerable relocation from vegetative to reproductive organs occurs. The user is advised not to modify structure or data, with the exception of those indicated in the next paragraph, unless he is very familiar with the subject. In some of the following sections, examples will be given how this simple model can be expanded by adding more detail to the description of certain processes, and by including other aspects of crop growth and other growth limiting factors.

Input data requirements

Specific for each situation are the latitude (LAT, negative values for the Southern Hemisphere) and the date at which the crop emerges. The latter can be defined by giving the variable TIME (Line 501) an initial value equal to the day number of the Julian calender. DAY equals TIME up to Day 365, after which DAY equals TIME $-$ 365. This is achieved by means of the AMOD function (Table 2 of Section 2.2). The example chosen refers to wheat growth in Zambia (LAT $= -15$ °) starting on October 27 (Day 300).

The next group of data concern the initial conditions. For this purpose, 'initial' is defined as the moment at which the contribution of seed reserves to the young plants becomes negligible, which for wheat is about 10 days after sowing. In the example of Table 9, 50 kg of plant material is present per hectare, of which half is root (WRTI) and half leaf (WLVI, Line 105). This corresponds roughly to 85 kg of seed. These figures are of course specific for the particular plant type and seed rate used.

The next group of data required are physiological characteristics: CO_2 assimilation, respiration and partitioning. CO_2 assimilation is characterized only with a constant initial light use efficiency for all species and the maximum rate of

CO_2 assimilation per unit leaf area at light saturation. This value is about 30 kg $ha^{-1} h^{-1}$ for many C_3 plants. It is an important parameter, and considerable attention should be given to its quantification. The formulation of respiration processes in the model is sufficiently general to require little attention from the user. Only the conversion factor to form the reproductive organs from photosynthates is specific for each crop. Such data, for 23 different crops, have been reported by Penning de Vries et al. (1982). Since the partitioning of biomass over plant organs with respect to development stage is specific for species and cultivars, such data need to be specified. Three examples (wheat, potato and soybean) are given in Figure 33 of Section 3.3. The rate of development of the crop, including the effects of temperature and day length is also specific and not predictable from basic data, and need thus to be specified. In many cases, this will require at least one good field experiment with the very crop plant or a similar one in the very environment or something that resembles it closely.

The specific leaf weight is an important parameter. Its value varies little between species, but as this factor is an important one in the model, attention should be paid to it. The decline in green leaf area at the end of the crop growth cycle has to be defined, but there are many similarities between groups of species, and users are not encouraged to use other data unless specific information is available.

The environmental conditions of the crop are specified by daily irradiation, and daily minimum and maximum temperatures, or average daily temperatures. All environmental conditions may be specified per day or as monthly means; in the first case the time step of the model should be reduced so that it equals or is smaller than the input data interval.
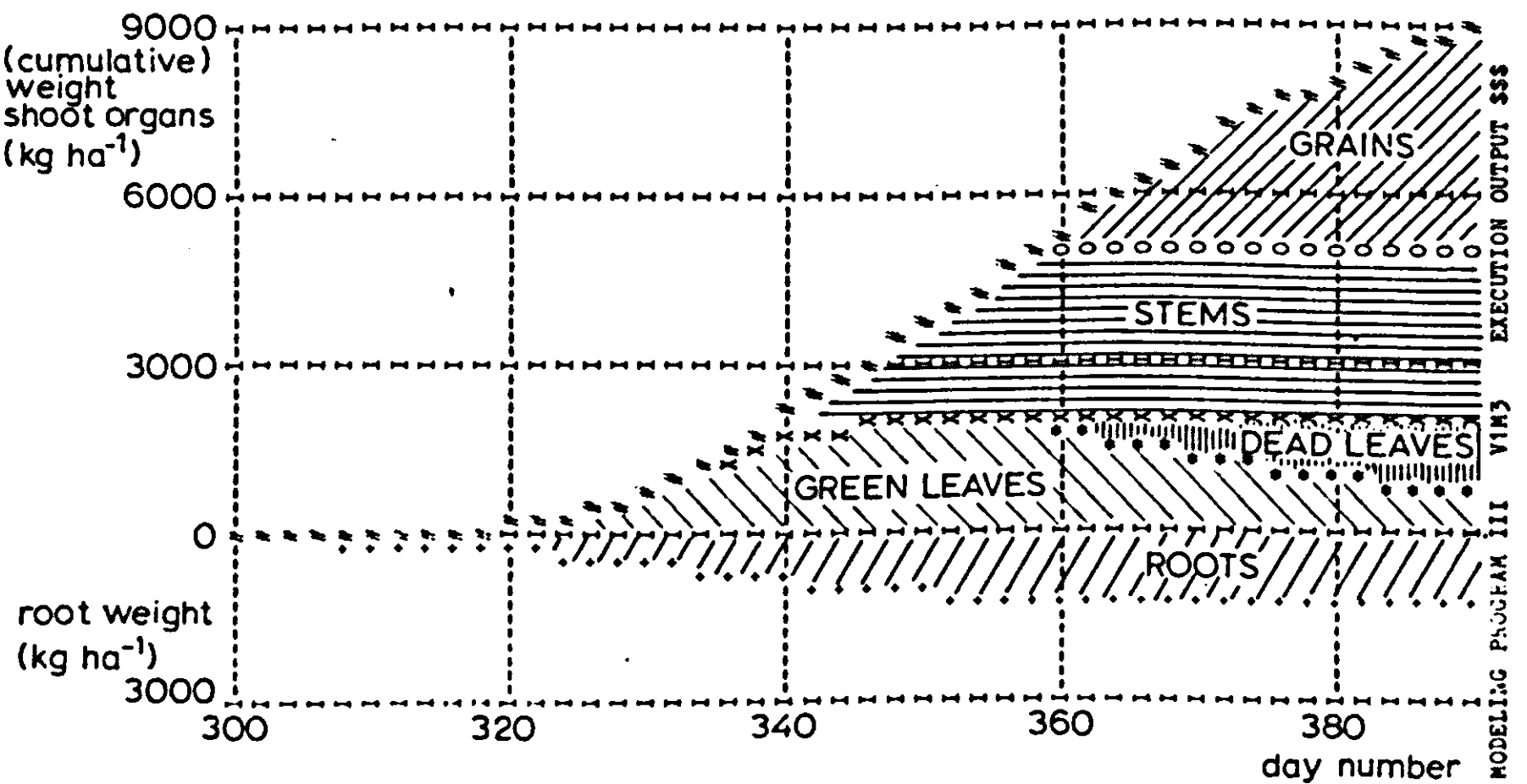
Figure 24. An adapted reproduction of the CSMP PRinTPLOT of the cumulative weight of the shoot organs and of the roots, as these develop during a growing season. The results were obtained with the SUCROS model as listed in Table 9.

An example of the use of SUCROS with the data as given in the program of Table 9 is given in Figure 24. It is basically the output generated by CSMP by the Lines 503-508.

Exercise 26

a. Run the model SUCROS, and check that your results are identical to those of Figure 24.

b. Simulate wheat production for your own latitude.

c. Run the model for another crop with other characteristics for partitioning of assimilates, for instance those of Figure 33b or 33c, Section 3.3.

d. It is not realistic to run SUCROS for other crops by changing only assimilate partitioning. Suggest reasonable values for other important parameters of these crops.

3.2 Potential production processes

J. Goudriaan

3.2.1 Introduction

The potential production rate of a crop is defined as the growth rate of a closed, green crop surface, optimally supplied with water and nutrients, in a disease and weed-free environment under the prevailing weather conditions (see Subsection 1.2.2).

Growth will be used in the meaning of accumulation of dry matter, which mainly consists of carbohydrates. Since carbohydrate accumulation is a result of the combined effort of the leaves of a crop canopy it is logical to calculate crop production as the sum of the contributions of the individual leaves. Simulation of photosynthesis and photorespiration of leaves of C_3 and C_4 type plants is presented in the Subsection 3.2.2. With the information about the calculation of radiation levels and of penetration of light into a canopy (Subsection 3.2.3), this gives a basis for computation of canopy photosynthesis (Subsection 3.2.4). Many exercises are provided to facilitate the reader to become acquainted with simulation of photosynthetic processes. The energy balance of leaves and canopies is presented in Subsection 3.2.5. The simulation of the physiological link between the rates of CO_2 assimilation and transpiration is presented in Subsection 3.2.6.

3.2.2 Leaf photosynthesis

The major portion of the photosynthetic energy is used for the production of glucose from water and carbon dioxide. Therefore photosynthesis is loosely identified and measured as the rate of CO_2 uptake. In Figure 25 the dependence of leaf CO_2 assimilation on absorbed photosynthetically active radiation (PAR)
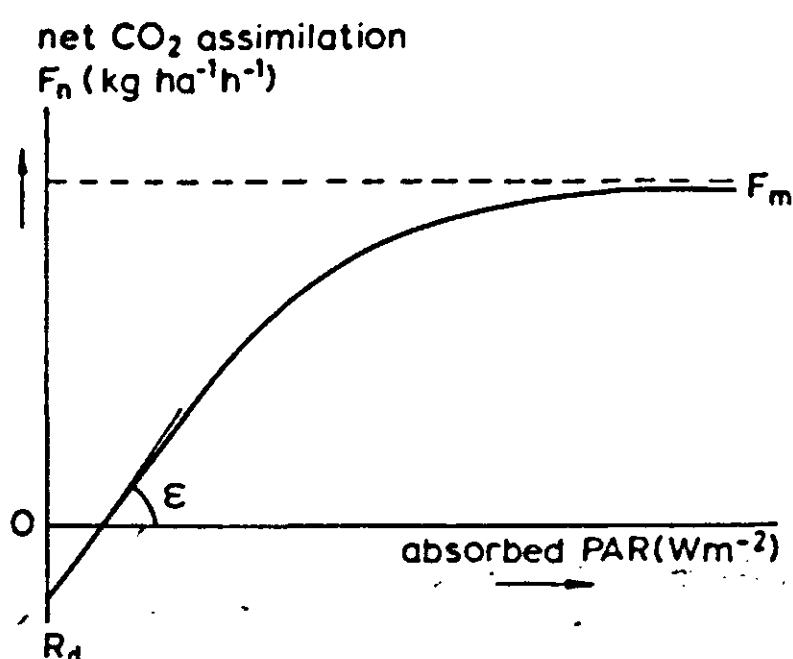
Figure 25. A typical light response curve of the assimilation of CO_2 for an individual leaf. R_d stands for the dark respiration, ε for the slope (or efficiency) at a low light level and F_m for the net assimilation rate at light saturation.

98

Table 11. Some C_3 and C_4 type species.

C_3	C_4
Small grains (wheat, barley, oats, rye, rice). Temperate grasses. Sugar-beet, potato, sunflower, cotton. All leguminous species with nitrogen fixation. Almost all trees (except Mangrove).	Tropical grasses as maize, sorghum, millet, *Cenchrus biflorus,* sugar-cane, Rhodes grass. Some halophytes as *Spartina townsendii. Salsola kali, Atriplex rosea,* Mangrove.

is given. At high light the assimilation rate is saturated with light and approaches a maximum value F_m. Other parameters that characterize the curve are the respiration rate in the dark R_d and the initial slope or light-use efficiency ε. The largest variation is in the maximum rate F_m; it ranges between 30-90 kg ha^{-1} h^{-1} for C_4 plants and between 15-50 kg ha^{-1} h^{-1} for C_3 plants. In Table 11 a concise list of some important C_3 and C_4 species is given. More extensive lists can be found in Downton (1975) and in Raghavendra & Das (1978). In C_4 species the main acceptor of CO_2 is phospho-enolpyruvate (PEP), yielding malate or oxalate with 4 C atoms. In C_3 plants Ribulose-Biphosphate (RuBP) acts as the acceptor yielding two 3 C atom components. The affinity of PEP for CO_2 is much higher than that of RuBP, which is part of the reason why C_4 plants have a higher maximum assimilation rate than C_3 plants. The temperature dependence of F_m is also different for C_3 and C_4 species: C_4 species have a higher optimal temperature.

The light-use efficiency for fixing CO_2 is about $14 \cdot 10^{-9}$ kg J^{-1} (absorbed PAR) in C_4 plants and about $11 \cdot 10^{-9}$ kg J^{-1} in C_3 plants. Its variation is much less than of F_m; it does however increase a little in C_3 plants with increasing CO_2 concentration. For the time being we will consider it as constant. The dark respiration rate R_d reflects the activity of the leaf and is therefore correlated with the maximum rate F_m. Usually it is less than 0.1 of F_m at 20 °C, but this fraction rises with increasing temperature. Experimental evidence indicates that a linear rise with temperature is more common than an exponential increase. There are two equations that are often used to describe the photosynthesis light-response curve:

$$F_n = (F_m + R_d)\,(1 - \exp(-H\varepsilon/(F_m + R_d))) - R_d \quad \text{(asymptotic exponential)} \quad (13)$$

and:

$$F_n = (F_m + R_d)\varepsilon H/(\varepsilon H + F_m + R_d) - R_d \qquad \text{(rectangular hyperbola)} \quad (14)$$

in which:

F_n is net CO_2 assimilation for leaves in kg ha^{-1} h^{-1}

F_m is the maximum rate of net CO_2 assimilation for leaves at high light intensities in kg ha^{-1} h^{-1}

R_d is dark respiration in kg ha^{-1} h^{-1}

H is the absorbed radiant flux in the 400-700 nm range in J m^{-2} (leaf) s^{-1}
   (= W m^{-2})

$\mathcal{E}$ is the initial light use efficiency for fixing CO_2 in leaves in kg J^{-1} (14.10^{-9}
   kg J^{-1}, which equals 0.5 kg ha^{-1} h^{-1} J^{-1} m^2 s)

Exercise 27
Check the units in these equations. Analyse and compare their results, graphically and numerically. Assume that $F_m = 60$ and $R_d = 4$ kg ha^{-1} h^{-1}.

Although experimental evidence indicates that the asymptotic exponential gives a better fit for leaf photosynthesis (Peat, 1970; English, 1976), the hyperbolic equation has the appeal of its relatively simple structure. Essentially it is a Michaelis-Menten response to absorbed light, which enables the introduction of CO_2 concentration as a factor influencing assimilation. This is particularly important in C_3 plants, where the CO_2 dependent photorespiration reduces the net assimilation. Therefore a simple carboxylation model will be constructed to better understand the relation between net CO_2 assimilation, light intensity, CO_2 concentration and some leaf properties. First we shall assume that the gross assimilation F_g follows a hyperbolic response to the CO_2 concentration (C) at the carboxylation site and also to absorbed light H:

$$F_g = \frac{F_{mm}\mathcal{E}HC}{F_{mm}\mathcal{E}Hr_x + \mathcal{E}HC + CF_{mm}} \tag{15}$$

or:

$$F_g = \frac{F_{mm}\mathcal{E}H}{F_{mm}\mathcal{E}Hr_x/C + \mathcal{E}H + F_{mm}} \tag{16}$$

In this equation F_{mm} is the absolute maximum assimilation rate, which is approached when both light and the CO_2 concentration are very high. In that situation the processing of photosynthetic products and regeneration of RuBP becomes rate limiting, and not the external supply.

When the CO_2 concentration is low enough this equation can be simplified to:

$$F_g = C/r_x \tag{17}$$

where r_x has the dimension of a resistance. Since C is the CO_2 concentration at the site of carboxylation, r_x is called the carboxylation resistance.

100

Exercise 28

Construct a consistent dimensional set of units for all variables of Equation 16.

Exercise 29

Which equation arises from Equation 16 at both low light and low CO_2? What is then the Michaelis-Menten constant for CO_2?

The dark respiration R_d can be subtracted from the gross assimilation as given by Equation 16, which then results in the expression for the net assimilation in C_4 plants:

$$F_n = \frac{F_{mm}\mathcal{E}H}{F_{mm} + (F_{mm}r_x/C + 1)\mathcal{E}H} - R_d \tag{18}$$

Exercise 30

Reduce Equation 18 to Equation 14 and express F_m in F_{mm}, r_x, C and R_d.

When the net assimilation rate is zero, the compensation point is reached. From Equation 18 one can see that there is not just one compensation point, but a continuous range of H and C values, which may be called the compensation line. When the light intensity is high enough, the corresponding CO_2 concentration of the compensation line approaches a stable value, which is usually called the CO_2 compensation point.

Exercise 31

Derive the expression for the compensation line, and also for the light and CO_2 compensation points. What are the numerical values of the CO_2 and light compensation points when $R_d = 4 \text{ kg ha}^{-1} \text{ h}^{-1}$, $r_x = 80 \text{ s m}^{-1}$, $F_{mm} = 200 \text{ kg ha}^{-1} \text{ h}^{-1}$.

In C_3 plants, photorespiration occurs besides the dark respiration, so that the net assimilation rate is lower than in C_4 plants. The photorespiration takes place during the CO_2 assimilation process only, and it does not use sugars from the

reserve pool. Normally its magnitude is about 0.2-0.3 of the gross assimilation rate, and because it follows gross assimilation with a delay of less than a minute its effect is normally included when net CO_2 assimilation is measured. Therefore, F_g and F_n in the Equations 15, 16 and 18 contain the effect of photorespiration. Still, it must be considered separately, because photorespiration is reduced when the CO_2 concentration rises, and also when the O_2 concentration is lowered. Oxygen interferes because it competes with CO_2 in reacting with RuBP (oxygenation instead of carboxylation). Photorespiration occurs later in the reaction cycle to recover RuBP from its oxygenation. According to Laing et al. (1974) the ratio of photorespiration R_f and gross assimilation F_g is

$$\frac{R_f}{F_g} = \frac{t \, V_o O \, r_x}{K_o C} \tag{19}$$

where t is the fraction of glycolate carbon released (0.25), V_o the maximum rate of oxygenation, K_o the Michaelis-Menten constant for the O_2 concentration O. The gross rate F_g itself is also reduced by the competing effect of O_2, which is reflected in an extended Michaelis-Menten equation:

$$F_g = \frac{\varepsilon H C}{\varepsilon H r_x (1 + O/K_o) + C} \tag{20}$$

This expression shows that the carboxylation resistance r_x has been multiplied by a factor $1 + O/K_o$ (about 1.7).

At high light F_g approaches $C/(r_x(1 + O/K_o))$. The net assimilation rate F_n is given by $F_g - R_f - R_d$, or (Equation 19):

$$F_n = F_g(1 - \frac{t V_o O r_x}{K_o C}) - R_d \tag{21}$$

The CO_2 compensation point Γ at high light can be found as the CO_2 concentration at which Equation 21 gives $F_n = 0$:

$$\Gamma = t V_o O r_x / K_o + R_d r_x (1 + O/K_o) \tag{22}$$

At low light the expression for F_n approaches:

$$F_n = \varepsilon H(1 - \frac{t V_o O r_x}{K_o C}) - R_d \tag{23}$$

so that the apparent light-use efficiency is reduced. Because the second term in Equation 22 is relatively small in C_3 plants the multiplication factor for ε is practically equal to $1 - \Gamma/C$.

Experimental results with C_3 plants show that Γ is of the order of 50-70 cm^3 m^{-3} and C of 200-250 cm^3 m^{-3}, so that the light-use efficiency is lowered by about 25%. When the CO_2 concentration is increased, the light-use efficiency will also go up, and gradually approach the value of C_4 plants.

In a simulation model the light-use efficiency of C_3 and C_4 type plants can be found as the product of a common value (14.10^{-9} kg J^{-1}) multiplied by the factor $(1 - \Gamma/C)$. The compensation point Γ should then be given as an input parameter, or perhaps be made dependent on temperature and water stress (Lawlor & Pearlman, 1981; Bykov et al., 1981).

3.2.3 Radiation

Radiation drives both photosynthesis and transpiration, so that it must be included in models for plant growth and water use. All radiation, as a source of thermal energy, is important for transpiration, but only the photosynthetically active radiation (PAR) keeps photosynthesis going. For all practical purposes PAR can be identified with visible radiation (400-700 nm) and is about 50% of the global irradiation (as measured with a Kipp radiometer) under a clear sky and about 60% under an overcast sky. Irradiation under an overcast sky is extremely variable, but as a rule of thumb we adopt that it is one fifth of what would have been measured under a very clear sky (de Wit et al., 1978). The dependence of incoming PAR (in W m^{-2}) under a clear sky on solar height β can be expressed as follows:

$$S_v = 640 \cdot \sin\beta \cdot \exp(-K_{atm}/\sin\beta) \tag{24}$$

where K_{atm} ranges between 0.1 for a very clear atmosphere, and 0.18 for a rather humid and dusty one. More details can be found in Ross (1981).

The extinction of radiation in a canopy is approximately exponential with leaf area index (LAI) reckoned from the top. In a simple model situation one can visualize the leaves as arranged in layers below each other. If the leaves are horizontal and black, each layer will intercept a fraction equal to its own leaf area index. In this situation there is no mutual shading within such a layer. As a result the downward flux decreases in a geometric series, which can also be represented as:

$$S(\text{LAI}') = S_0 \exp(-K \cdot \text{LAI}') \tag{25}$$

where LAI' is the leaf area index reckoned from the top, K is the extinction coefficient and S is the downward flux. Above the canopy S equals S_0.

Exercise 32
Calculate the effective K and the fraction of light absorbed in the described situation for LAI = 3 and for black model layers of leaf area index 0.5, 0.1 and 0.01, respectively.

If the leaves scatter light, the radiation will penetrate deeper than with black

leaves, so that the extinction coefficient is smaller. If the leaf transmission coefficient and reflection coefficient are each equal to half the scattering coefficient σ, if the sublayers are infinitesimally small and if the leaves are horizontal, the extinction coefficient equals (Goudriaan, 1977):

$$K = (1 - \sigma)^{0.5} \tag{26}$$

The reflection coefficient ϱ_c of the canopy (if LAI is large enough) is then:

$$\varrho_c = (1 - K)/(1 + K) \tag{27}$$

Exercise 33

Why must the LAI be large enough? Make a graph of ϱ_c as a function of σ. How large is crop reflection as compared to individual leaf reflection for low σ?

Green leaves absorb less green light (550 nm) than red (680 nm) or blue (450 nm) light. A dramatic increase in scattering occurs at the transition from visible to near infrared light (700 nm). This phenomenon justifies the rough distinction between these two wavelength bands. Averaged over the wavelength bands the scattering coefficient of green leaves is about 0.2 for visible radiation and about 0.8 for near-infrared radiation. Reflection and transmission share their portion rather equally.

The leaf angle influences the extinction coefficient. Model computations indicate that for an isotropic or spherical leaf angle distribution the extinction coefficient is approximately equal to:

$$K = 0.5(1 - \sigma)^{0.5}/\sin \beta \qquad \text{for direct light} \tag{28}$$

and:

$$K = 0.8(1 - \sigma)^{0.5} \qquad \text{for diffuse light} \tag{29}$$

The radiation absorbed per leaf area can be calculated by using the exponential extinction. The difference of the net radiation flux between two levels is divided by the leaf area between them.

Exercise 34

Assume a solar height of 60 degrees, overcast sky, $K_{atm} = 0.15$, LAI $= 5.$, horizontal leaves. Calculate absorbed visible radiation per leaf area in five subsequent layers of leaf area of unity. Choose the values 30 kg ha^{-1} h^{-1} for F_m, 3 for R_d and 0.4 kg ha^{-1} h^{-1} m^2 s J^{-1} for ε, and calculate the net CO_2 assimilation rates of the five layers using Equation 13.

When the sun shines, sunlit leaf area must be separately considered from shaded area within the same layer. Also the sunlit leaf area must be classified according to the angle of incidence of the direct light on the leaf. Most of the sunlit leaf area will be light-saturated. If the leaf area index is sufficiently high the sunlit leaf area can be simply calculated as the inverse of the extinction coefficient for direct irradiation and black leaves.

Exercise 35
Why the inverse of the extinction coefficient? What is the value of the sunlit leaf area index for a horizontal and for a spherical leaf angle distribution?

Solar height depends on latitude, day of the year and time of the day as follows:

$$\sin \beta = \sin \lambda \sin \delta + \cos \lambda \cos \delta \cos (2\pi (t_h + 12)/24) \tag{30}$$

where λ is latitude, δ declination of the sun and t_h hour of the day (be sure to use local solar time). Declination varies with the day of the year as follows:

$$\delta = -23.4 \cos (2\pi (t_d + 10)/365) \tag{31}$$

where t_d is the number of day since 1 January, and δ is expressed in degrees.

Exercise 36
Make a CSMP program that calculates daily total irradiation on clear days (DRAD) and day length (DLENG) for different latitudes and seasons.

To calculate crop photosynthesis we need to know the fractions of diffuse and direct irradiation under a clear sky. When no measurements are available, the following equation can be used as an estimate of the fraction direct irradiation out of the total:

$$\frac{S_{dir}}{S_{tot}} = \exp(-0.15/\sin \beta) \tag{32}$$

In fact this ratio is higher for near infrared (NIR) than for PAR. A differentiated partitioning can be obtained by using an extinction coefficient of 0.1 for NIR and 0.2 for PAR, to replace 0.15 in Equation 32.

We have seen in Exercise 34 how extinction and absorption of diffuse radiation is treated. Now attention will be focussed on direct radiation, and on the diffuse scattered radiation caused by it. The direct incoming component S_1 (Fig-
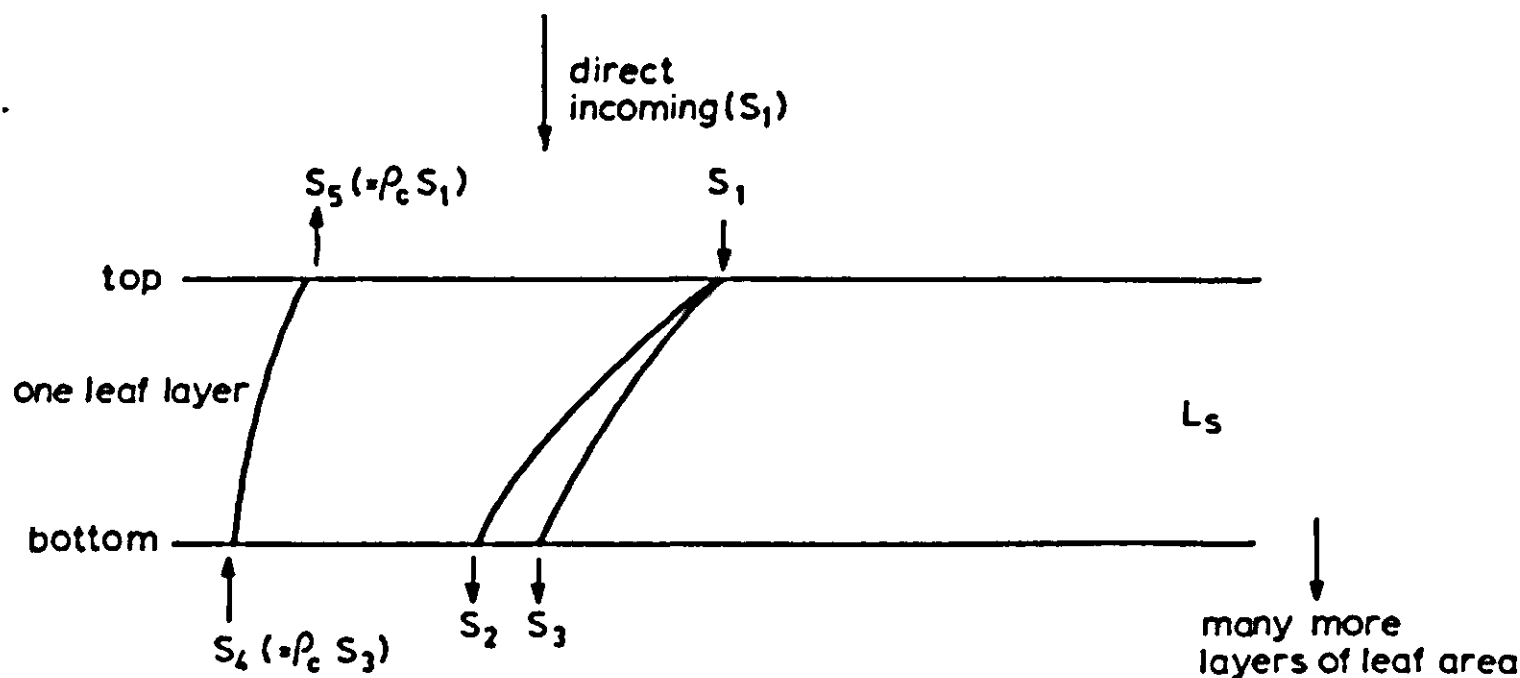
Figure 26. A scheme of the different fluxes of the direct incoming irradiation (S_1) in a leaf layer.

ure 26) causes a reflected flux $S_5 = \varrho_c S_1$. After passing the first layer with leaf area index L_s, the direct flux S_2 has been more reduced than the total downward flux S_3, because of the addition of scattered radiation.

The equations for S_2 and S_3 are:

$$S_2 = S_1 \cdot \exp\left(-K_{dir} \cdot L_s\right) \tag{33}$$

$$S_3 = S_1 \cdot \exp\left(-K_{dir} \cdot \sqrt{(1 - \sigma)} \cdot L_s\right) \tag{34}$$

Because there are many more layers of leaves underneath there is also a reflected flux entering the first layer from below:

$$S_4 = \varrho_c S_3 \tag{35}$$

By taking the balance of the incoming and outgoing fluxes we find that the flux absorbed in this layer is given by

$$S_1 + S_4 - S_3 - S_5 = (1 - \varrho_c) \cdot S_1 \cdot (1 - \exp\left(-K_{dir} \cdot \sqrt{(1 - \sigma)} \cdot L_s\right)) \tag{36}$$

The intercepted part of the direct flux is given by $S_1 - S_2$, but must be multiplied by $1 - \sigma$ to find the absorbed portion of it. In the model BACROS (Subsection 3.3.8) the absorbed direct and diffused fluxes together (Equation 36) are called VIST (for PAR) or NIRT (for NIR) and the absorbed direct fluxes only are called VISD and NIRD, respectively. The difference VIST − VISD gives the diffuse background absorption, which is common for sunlit and shaded leaves. These numbers are still expressed per ground area, and to find them on a leaf area basis they must be divided by the leaf area index of that layer, L_s.

3.2.4 Canopy photosynthesis

With Equation 13 on leaf photosynthesis and the radiation levels described above, a sufficient number of elements are presented to simulate canopy CO_2 assimilation on an instantaneous and on a daily basis.

Exercise 37

With this knowledge it is possible to construct a simulation model for net leaf photosynthesis of a crop canopy with horizontal leaves and a LAI of 5, under a clear sky. Try to formulate the most important equations yourself and study the listing.

A result of this simulation is presented in Figure 27. It is obvious that these results grossly overestimate the real respiration of the canopy. In this simple model all leaves, the heavily shaded ones too, respire at the same rate. As a result the lowest layers operate below compensation point, which would presumably lead to abscission of these leaves. Moreover, the horizontal leaf angle distribution causes a strong levelling of photosynthesis around noon.

To simulate canopy photosynthesis the sunlit leaf area in each canopy layer (see Exercise 35) must be calculated. In horizontal leaves there is only one angle of incidence of direct irradiation on individual leaves. In a spherical leaf angle distribution, the density distribution of leaf area with sine of incidence is uniform. Therefore the fraction of leaf area receiving direct irradiation between two sines of incidence is equal to their difference.

Now that we have developed the models for the instantaneous rates of radiation flux and assimilation it is only one step further to integrate the rates and
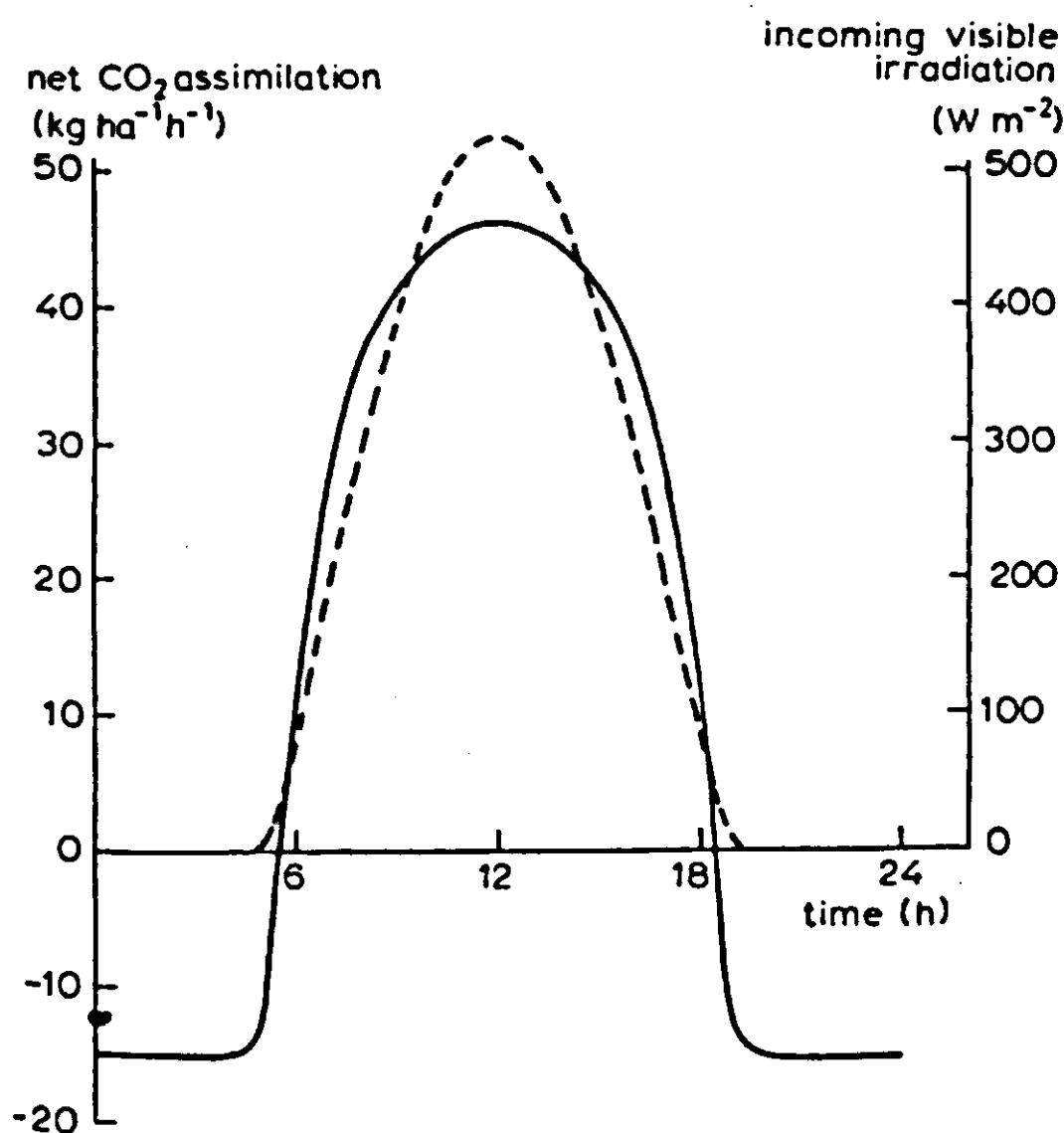
Figure 27. The simulated daily course of visible irradiation and of net CO_2 assimilation of a crop canopy with horizontal leaves and an LAI of 5, under a clear sky as simulated with a simplified example.
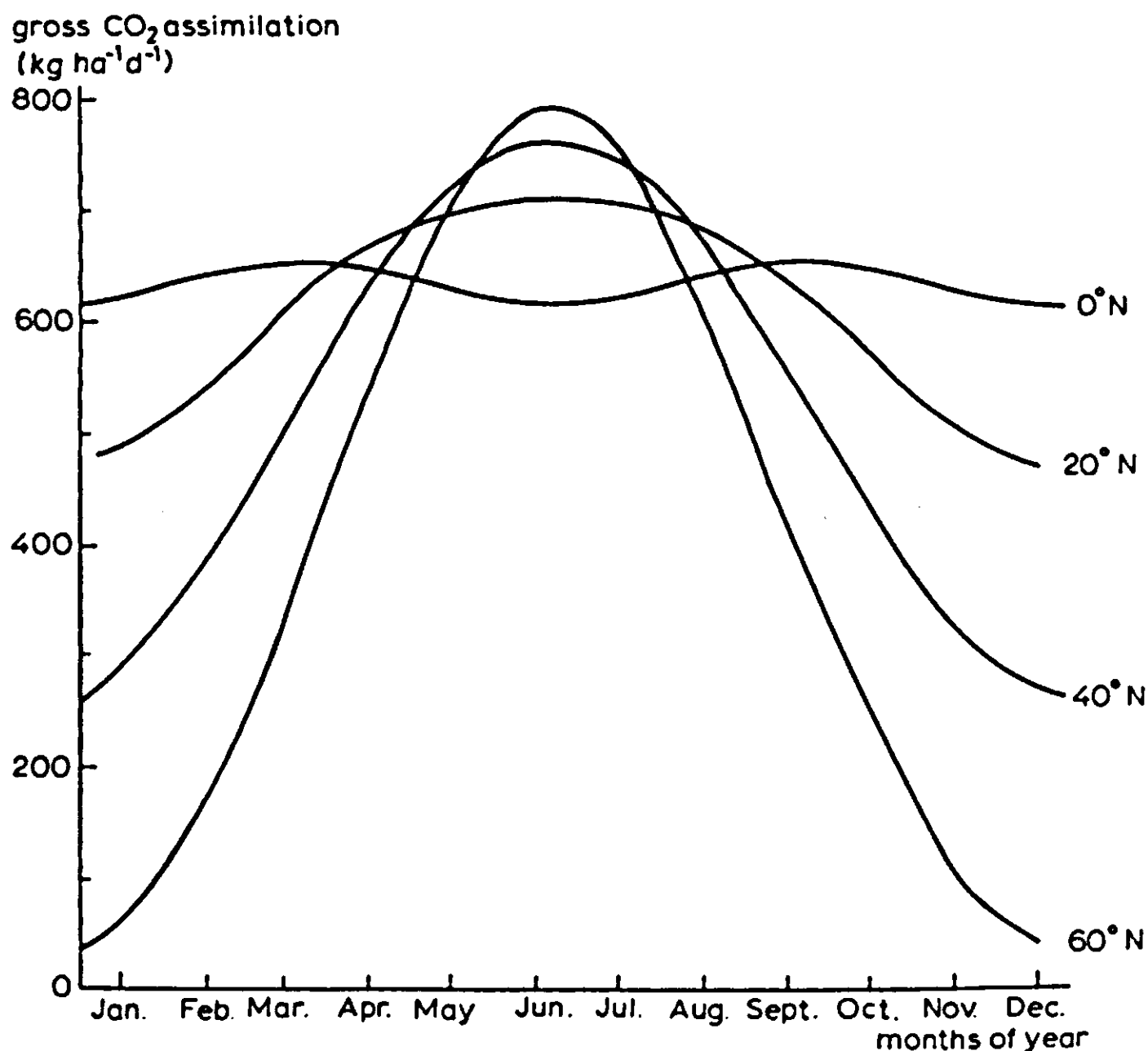
Figure 28. The simulated annual course of daily gross CO_2 assimilation on clear days for a closed green canopy at latitudes ranging from the equator to $60°$ N (F_m = 30 kg ha^{-1} h^{-1}; ε = 14.10^{-9} kg J^{-1}).

find the daily totals. In Figure 28 the simulated annual course of daily gross CO_2 assimilation on very clear days for a closed green canopy with F_m = 30 kg ha^{-1} h^{-1} and ε = 14.10^{-9} kg J^{-1} has been plotted for four different latitudes on earth. The major component of variation is related to daily total of irradiation as appears from Figure 29. In midsummer the same daily total of irradiation is used more efficiently, because of the longer day length. Also on overcast days the light-use efficiency is much higher at all latitudes (dashed line in Figure 29). These graphs may be used for a quick estimate of daily gross assimilation on basis of a measured daily total irradiation. In a computer model with time steps of one day it may be convenient to use a summary model in a tabular form, or in a CSMP procedure (Goudriaan & van Laar, 1978), or as a small group of sortable statements (Subsection 3.1.2).

3.2.5 Leaf energy balance and transpiration

The rate of transpiration E of a canopy can be simulated on basis of its energy balance. This can be done because of the strict coupling of the amounts of water and energy involved in the process: the heat of vapourization of water, λ, is 2390 J g^{-1}. The energy flux (or latent heat loss, in W m^{-2}), used for transpira-

108
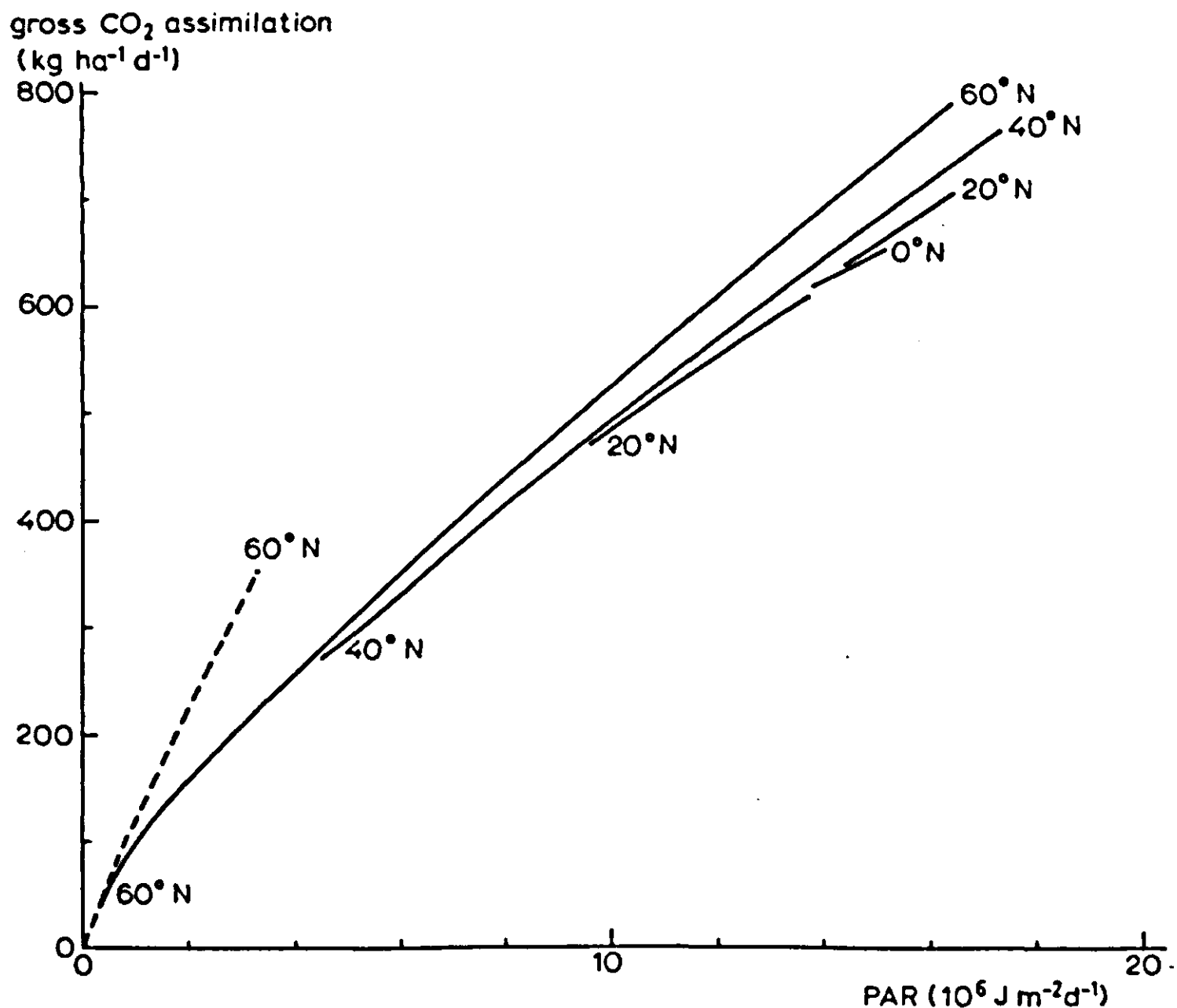
Figure 29. The relation of daily gross CO_2 assimilation on clear days with the daily total of irradiation at latitudes ranging from the equator to 60° N (solid lines) and on overcast days (broken line).

tion, is given by:

$$\lambda E = \frac{sR + \delta}{s + \gamma*} \tag{37}$$

In this equation s is the slope of the saturated vapour pressure curve at air temperature in mbar K^{-1}, R is the absorbed radiation per leaf area (all wavelengths), δ the drying power of the air (given below), and $\gamma*$ the apparent psychrometer constant. The drying power of the air is defined by:

$$\delta = \frac{(e_s - e_a)\varrho c_p}{r_b} \tag{38}$$

where e_s is the saturated vapour pressure at air temperature and e_a is the actual vapour pressure, ϱc_p is the volumetric heat capacity of the air (about 1200 J m^{-3} K^{-1}), r_b is the boundary layer resistance. The apparent psychrometer constant is defined by:

$$\gamma* = \gamma \cdot \frac{(r_b + r_l)}{r_b} \tag{39}$$

109

where γ is 0.63 mbar K^{-1} and r_l is the leaf resistance to water vapour. By the energy balance equation, the heat flux to the air or sensible heat loss W (in W m^{-2}), can be found:

$$W = R - \lambda E \tag{40}$$

Note that this equation neglects the small amount of energy incorporated in photosynthetic products. These equations describe the partitioning of the net absorbed radiant energy among transpiration and heat loss to the air. The equation for the temperature of the leaf (T_l) is simply:

$$T_l = T_a + W\left(\frac{r_b}{\varrho c_p}\right) \tag{41}$$

where T_a is the air temperature in °C.

The derivation of Equation 37 is based on combination of the following four equations. Since this was first done by Penman (1948), Equation 37 is often called the Penman equation.

$$R - W - \lambda E = 0 \qquad \text{(energy balance)} \tag{42}$$

$$W = \frac{(T_l - T_a)\,\varrho c_p}{r_b} \tag{43}$$

$$\lambda E = \frac{(e_s(T_l) - e_a)\,\varrho c_p}{\gamma(r_l + r_b)} \tag{44}$$

$$e_s(T_l) = e_s(T_a) + s(T_l - T_a) \tag{45}$$

The last equation is an approximation, but a good one if the leaf and air temperature are not too different. This can be checked in Table 12 where e_s and s are tabulated against temperature. In the simulation program e_s is approximated by

$$e_s = 6.11 \cdot \exp(17.4T/(T + 239)) \tag{46}$$

In Equation 42 there is no term for storage of heat in the leaf, so that equilibrium of leaf temperature is assumed.

Exercise 38
Write a simulation program to calculate leaf temperature, latent heat loss and sensible heat loss. Assume $R = 200$ W m^{-2}, $r_b = 20$ s m^{-1}, $T_a = 20$ °C, $e_a = 15$ mbar, areal heat capacity of the leaf $= 10^3$ J m^{-2} °C^{-1} and volumetric heat capacity ϱc_p of the air 1200 J m^{-3} °C^{-1}. Make reruns for $r_l = 0, 10, 100, 1000$ and 10^4 s m^{-1}, respectively. Compare a dynamic simulation where heat content of the leaf is a state variable, with a static solution according to the Penman approach.

110

Table 12. The saturated water vapour pressure e_s, as a function of temperature. The results of an analytical expression to approximate e_s are also given. The last column gives the derivate of e_s with respect to temperature.

T (°C)	e_s (mbar)	$6.11 \cdot \exp(17.47T/(T + 239))$	s (mbar K^{-1})
0	6.11	6.11	0.445
5	8.72	8.73	0.609
10	12.27	12.29	0.823
15	17.04	17.07	1.10
20	23.37	23.42	1.45
25	31.67	31.74	1.89
30	42.43	42.54	2.44
35	56.24	56.40	3.12
40	73.78	74.04	3.94

It is also possible to use an iterative technique to solve the simultaneous Equations 42-46. In Section 2.3 some iteration methods have been discussed that can be applied here.

Exercise 39
Try the IMPLicit loop of CSMP and the halving/doubling method for the situation as described in Exercise 38.

3.2.6 Leaf conductance and CO_2 assimilation

Because water vapour and CO_2 pass through the same stomatal pores, transpiration and assimilation are tied together. The direction of the causal relationship (of the information flow) depends on the circumstances. The situation is obvious for high light and low CO_2 conditions, when we may safely assume that diffusion of CO_2 is a limiting factor for the net assimilation rate. In a simple resistance scheme leaf resistance and mesophyll resistance (which consists of a small transport component and a dominating carboxylation component) are series-circuited between the external (C_e) and internal CO_2 concentration (C_i). Then a hyperbolic relation between net assimilation and leaf conductance should be expected. Experimentally such a result is hard to obtain, because almost every action to change leaf conductance will also independently change net assimilation, and vice versa. Only when stomatal oscillations occur in a constant environment can a hyperbolic relation be observed (Farquhar et al., 1980).

When assimilation and conductance are simultaneously affected by the envi-

ronmental conditions often a linear relation exists between them (Goudriaan & van Laar, 1978; Wong et al., 1979; Louwerse, 1980). Since the drop in CO_2 concentration across the leaf resistance is proportional to the ratio of assimilation to conductance, the slope of the line indicates an asymptotic value of the drop. Typically this drop is about twice as high in C_4 plants as in C_3 plants. In maize and some other C_4 plants, the internal CO_2 concentration in full light is about 0.4 of the external value, whereas in C_3 plants it is at least 0.7 of the external concentration. Whenever this relation exists it offers an easy way of modelling stomatal behaviour. The method consists of first calculating the net assimilation rate of the leaf, and then deriving the leaf resistance required to obtain a preset value of the internal CO_2 concentration. This resistance is then used in the calculation of the leaf transpiration rate after division by a factor of 1.6 to allow for the faster diffusion of H_2O compared to CO_2. The role of the cuticle is not quite clear. Here the cuticular conductance of CO_2 is assumed to be the same as for water vapour divided by 1.6. Therefore its treatment is the same as stomatal conductance, and together they give rise to the leaf conductance. The factor to account for the difference in the rate of diffusion in the boundary layer resistance is 1.3 (Monteith, 1973). The resulting equation for r_l (water vapour) is:

$$r_l = ((C_e - C_i)/F_n - 1.3 \cdot r_b)/1.6 \tag{47}$$

Equation 47 links the rate of net CO_2 assimilation of individual leaves to their conductance, and hence to their rate of transpiration (Equations 37 and 39). However, as a result of the regulating mechanism that maintains a more or less constant concentration of CO_2 in the stomatal cavity under most light levels, the equations are also approximately valid when applied to a whole canopy. The leaf resistance r_l becomes then the canopy resistance r_c, and C_e the average concentration of CO_2 in the air within the canopy. When C_e is measured above the canopy, where it is more constant, an additional resistance for transport of water and CO_2 must accounted for: the so-called turbulence resistance (r_t). Its value is in the order of 50 s m^{-1}, and is equal for water vapour and CO_2. In this case, $r_t + 1.3 \cdot r_b$ replaces $1.3 \cdot r_b$ in Equation 47. A detailed discussion of the computation of r_t is presented elsewhere (van Laar et al., 1983; Goudriaan, 1977).

This regulation mechanism accounts for opening of stomata with increasing light, and also with a decreasing external CO_2 concentration. A complication occurs when the stomatal resistance required for photosynthesis is smaller than is permitted by the actual water status of the plant. Under water stress mesophyll resistance also increases, so that a further drop in internal CO_2 concentration is not likely to occur. The best modelling procedure is therefore to invert the used relationship and to recalculate net assimilation as:

$$F_n = (C_e - C_i)/(1.6 \cdot r_l + 1.3 \cdot r_b) \tag{48}$$

In this equation r_b and r_l are resistances to water vapour, and r_l is the lowest value permitted by the water status of the plant. In BACROS this value (called SRW) is a function of the relative water content of the crop (see Subsection

3.3.7).

Exercise 40

Make a graph of computed r_l versus absorbed PAR by using the Equations 13 and 47. Do it for a C_3 plant and also for a C_4 plant, assuming a value of C_i at 210 and 120 cm^3 m^{-3}, respectively.

Average values for the variables in the equations are:

	F_m	R_d	ε	C_i	C_e	r_b
C_3	30	4	0.4	210	330	10
C_4	60	4	0.5	120	330	10

The observed PAR may range from 0 to 300 W m^{-1}.

Exercise 41

Calculate the transpiration-assimilation ratio of a leaf, expressed in weight H_2O/weight CO_2 when $T_a = T_l = 20\,°C$, $e_a = 15$ mbar, the external CO_2 concentration is 600 mg m^{-3} and the internal 400 mg m^{-3} (how much are these concentrations in cm^3 m^{-3}?). Convert the vapour pressure to weight per m^3 by using the density of air at 1 bar and 20 °C (1200 g m^{-3}) and the molecular weights of water (18) and air (average 29).

3.3 Simulation of growth processes and the model BACROS

F.W.T. Penning de Vries and H.H. van Laar

3.3.1 Introduction

This section complements the previous section, which dealt with crop photosynthesis and transpiration. The modelling of development in plants is discussed first (Subsection 3.3.2). The simulation of rates of growth (Subsection 3.3.3) and of efficiency of growth processes (Subsection 3.3.4) including growth respiration, are discussed next. Computation of maintenance respiration is the subject of Subsection 3.3.5. Modelling dry-matter partitioning (Subsection 3.3.6) and a discussion of the crop water balance in relation to regulation of partitioning (Subsection 3.3.7) concludes this part of the section.

The comprehensive simulation model BACROS is presented in Subsection 3.3.8 and its use is demonstrated briefly. It contains many of the elements discussed in this and the preceding section. The model, which has been developed in over a decade by a team of scientists, simulates growth and transpiration of field crops in optimal conditions. A detailed description of BACROS has been given by de Wit et al. (1978). The model has been evaluated extensively. Since its publication in 1978, the model found to contain some minor errors, and some new developments have taken place. These developments are published elsewhere (van Laar et al., 1983, see also Subsection 3.3.8), including an up-to-date listing of the model. The publication, which will be updated periodically, is available upon request.

3.3.2 Plant development

Plant development is different from plant growth: 'development' relates to the physiological age of the plant and to its morphological appearance, whereas 'growth' relates to biomass increase in particular. It is often necessary to simulate plant development, as it is a key to the partitioning of assimilates to different organs. Development of plants cannot be expressed simply as ageing, because temperature and other environmental factors can speed up or reduce the rate of development considerably. The approaches given below are highly descriptive, but often function satisfactorily.

The modelling of the development of plants is relatively easy for determinate species, i.e. plants with a terminal florescence. Such plants have a fixed pattern of development: a fairly constant number of leaves is formed before flowering starts and seed filling is initiated. The development stage can conveniently be defined to have the value 1.00 (dimensionless) at flowering and 0.00 at germination. It can be regarded as a state variable, DVS, whose value increases with the

rate of development, DVR. In CSMP one can write:

DVS = INTGRL(0.,DVR)

If it takes 70 days, for example, from germination to flowering, DVR equals 0.0143 d^{-1}.

Exercise 42
DVR may be 0.0143, 0.02 and 0.0286 d^{-1} at 15, 20 and 25 °C, respectively. Explain why a plant at a constant temperature of 20 °C flowers later than one in an environment in which the temperature is 20 °C on average, but fluctuates between 15 and 25 °C.

This description of the development process closely resembles the degree-days concept that is widely used by crop physiologists (cf. Hesketh et al., 1980; Subsection 3.4.7). However, temperature is not the only environmental factor that influences the rate of development. Day length can also strongly modify the rate of development in the vegetative phase. Angus et al. (1981) demonstrate this with an analysis of an extensive set of experiments with wheat; Breman et al. (1979) show the effect of day length on the duration of the vegetative period in some annual grasses in the Sahel. In general, temperature increase speeds up plant development, while long days speed up the development rate in long-day plants, but reduce it in short-day plants. The model of Section 3.1 contains such a description of the development process (Lines 301-307); the numerical data are those for wheat, cultivar UQ189 from Angus et al. (1981). Following their conclusion, the effect of temperature on the rate of development is programmed to change after anthesis. Sensitivity to day length lasts, of course, only up to anthesis. The model BACROS does not contain a simulation of plant development stage.

The relation of DVR to temperature and the effect of day length on DVR are specific for species and variety, and need thus to be established experimentally. This is unfortunate, as in many cases new observations on each new type of plant one is interested in are required. Effects of water stress and of nutrient shortage on the rate of development are usually small.

Day length, for the simulation of photoperiodism, can be computed as in Subsection 3.2.4, or as in SUCROS (Subsection 3.1.2). The photoperiodic reaction is already sensitive to dim light, and the corresponding day length (DLP) must be counted from just before sunrise to just after sunset. This is attained by specifying in the equation for DLP that the effect should be counted for all inclinations of the sun larger than −4 degrees (Line 231).

Exercise 43
a. What change in yield results from the selection of a day length-insensitive wheat cultivar in the conditions specified in SUCROS (Subsection 3.1.2) if the crop is sown on 27 May or on 27 October? Choose the effect of day length on the rate of development to be a constant 0.575.
b. What yield change occurs if a new cultivar is introduced that behaves at any temperature the same as the old cultivar does for a temperature of 1 °C higher?

Though this model of the development process functions well in many cases, other descriptions can be more appropriate for other species. From the review paper of Hodges & Doraiswany (1979), a model can be derived in which the sensitivity for day length is not constant, but small or absent in a juvenile phase and strong thereafter up until flowering. Van der Sar et al. (1983) suggest that drought stress can prolong the juvenile phase. They suggest also that the actual sensitivity to day length may be very short, at least in some grass species. This note makes clear that a general, explanatory model of photoperiodism has not yet been developed in spite of the large amount of physiological knowledge accumulated about this phenomenon.

The development of indeterminate plants can be regarded in the same way (i.e. DVS = 1. at flowering). Growth of vegetative organs will continue parallel with formation of fruits for a period, the duration of which is not genetically programmed, but depends on environmental conditions. Meyer et al. (1979) modelled development of indetermined soybean similar to what is described above, with only an effect of temperature. After flowering, one node with a leaf, a stem segment and a flower is formed per development stage interval of 0.08.

For a continuously vegetative crop, like sugar-beet, there is a problem in defining the development stage, as it does not flower normally. The time-span between formation of leaves in standard conditions, a plastochron, defines then the unit of DVS. This is done, for example, in SUBGOL, a sugar-beet simulator developed by Loomis and collegues (Loomis et al., 1979).

In some cases it is useful to know the distribution of biomass with age or development stage, for instance when the potentials for growth of new organs or for regrowth after cutting are considered. These potentials are much higher in young, meristematic tissue than in old tissue. To make this distinction in the model, total biomass (BM) may be divided, for example into five age classes. The state variables BM1 through BM5 can be defined, where BM1 + BM2 + ... + BM5 = BM. Their growth rates GR1 through GR5 are equal to 0., except for a certain time span: GR1 equals the growth rate GR in the first period and is 0. otherwise, GR2 equals GR in the second period, and so on. BM1 will then be the biomass formed in the first period, BM2 in the second, and so on.

116

By means of the CSMP INSW function (Table 2, Section 2.2), this can be programmed easily.

Exercise 44
Program this for WLV in the model of Section 3.1 for age classes of 10 days. What are the weights at flowering? What is computed if one uses only one INSW function in each equation?

Instead of having an INSW function responding to TIME, the switch can also be activated and deactivated at certain values of DVS. A potential difficulty is then that the integration step may not quite coincide with the threshold value of DVS for the change to the next biomass class. But this problem is small when relatively short time steps are taken.

A disadvantage of this manner of programming an array of biomass classes is that it requires a large number of state variables (INTeGRaLs). In large models, such arrays may occupy too much computer memory. The 'boxcar train method' may then be a useful alternative. De Wit et al. (1970) developed it to simulate the potential growth capacities of shoots and roots of whole plants; Goudriaan (1973) described the method more extensively. Of a number of 'cars', only the first boxcar is filled. Then, at a certain moment, its content is transferred into the second boxcar, and the filling of the first starts again. At the next shift signal (PUSH = 1.), the content of the second car is transferred into the third, that of the first into the second, and the first is filled again. Programmed in FORTRAN style within a CSMP program, the size of the boxcar train is virtually limitless. Use of fixed time-step integration method RECT is required. Time steps must be many times shorter than the boxcar shift period. Its programming can be done as shown in Table 13.

PUSH can be defined as a function of TIME with the CSMP IMPULS function, or be set equal to 1.0 after each increment DVSI of DVS, as in Table 13, using an INSW function. DVSI is the development stage interval. The distribution of total leaf weight over 25 classes of development at some time after anthesis (DVS = 1.25), simulated in this way with SUCROS, is presented in Figure 30.

Exercise 45
Use the BOXCAR of Table 13 to keep track of the development of leaf weight in SUCROS, and try to obtain the same results as those of Figure 30. Use as an alternative to the assumption that leaves die at a rate of 3% of the weight of dry matter per day after flowering (Lines 112-114), the supposition that leaves function for 1.00 unit of DVS.

Table 13. A BOXCAR function, programmed in CSMP, to distinguish 25 development classes of leaves. GLV is growth rate of leaves, WLV is total weight of live leaves, WLVD that of dead leaves. DVR is rate of development, DVS is development stage.

```
* BOXCAR TRAIN METHOD (SIZE:  26 CARS)
* IN INITIAL:
STORAGE BOX(26)
TABLE BOX(1-26)=26*0.
FIXED I
* I IS USED AS A NUMBER OF A BOXCAR,
* AND IS DECLARED INTEGER IN THIS WAY
* IN DYNAMIC:
BOX1=INTGRL(WLVI,GLV-BOX1/DELT*PUSH)
PROCEDURE WLV,WLVD=BOXCAR(PUSH,BOX1)
    BOX(1)=BOX1
* NEXT 7 LINES ARE ONLY EXECUTED IF PUSH EQUALS 1.
    IF (PUSH.LT. 1.) GO TO 2
    BOXT=0.
    BOX(26)=BOX(26) + BOX(25)
    BOX(25)=0.
    DO 1 I=25,2,-1
* NEXT 3 LINES ARE REPEATED FOR DIFFERENT VALUES OF I,
* STARTING WITH 25, AND COUNTING BACKWARDS TO 2
    BOX(I)=BOX(I-1)
    BOX(I-1)=0.
  1 BOXT=BOXT+BOX(I)
  2 CONTINUE
    WLV =BOXT + BOX(1)
    WLVD=BOX(26)
ENDPROCEDURE
PUSH=INSW(DVS1-DVSI,0.,1.)
DVS1=INTGRL(0.,DVR-DVSI/DELT*PUSH)
* DIVISION BY DELT TO SUBTRACT DVSI IN ONE TIME STEP.
* SEE ALSO SUBSECTION 2.3.6
PARAMETER DVSI=0.04, DVR=0.025
METHOD RECT
TIMER DELT=0.2
```

Related to this approach to development, but conceptually different, is the simulation of transfer of biomass from one state into the next by means of a time coefficient description. This simulation of 'development' states that each amount of biomass of one class has, at any moment, a certain chance to go into the next class. This may be an expression of a strong external influence on this 'development' or of a considerable heterogeneity within each class. The rate of suberization (named SYR) of roots from the class 'young' (named WYR) to 'old', suberized roots (WOR) with a time coefficient (SUBC) of 5 days is programmed in this way in BACROS, because of its convenience:

SYR = WYR/SUBC
WYR = INTGRL(IWYR,GYR − SYR)
WOR = INTGRL(IWOR,SYR)

(some minor details are omitted, and the rate of growth of young roots, GYR, is not discussed here).

Other examples of this kind of development are presented in Subsection 2.1.8 under the name of first order exponential delay, and some implications of this formulation are discussed there.

If many states of development are to be distinguished instead of only young
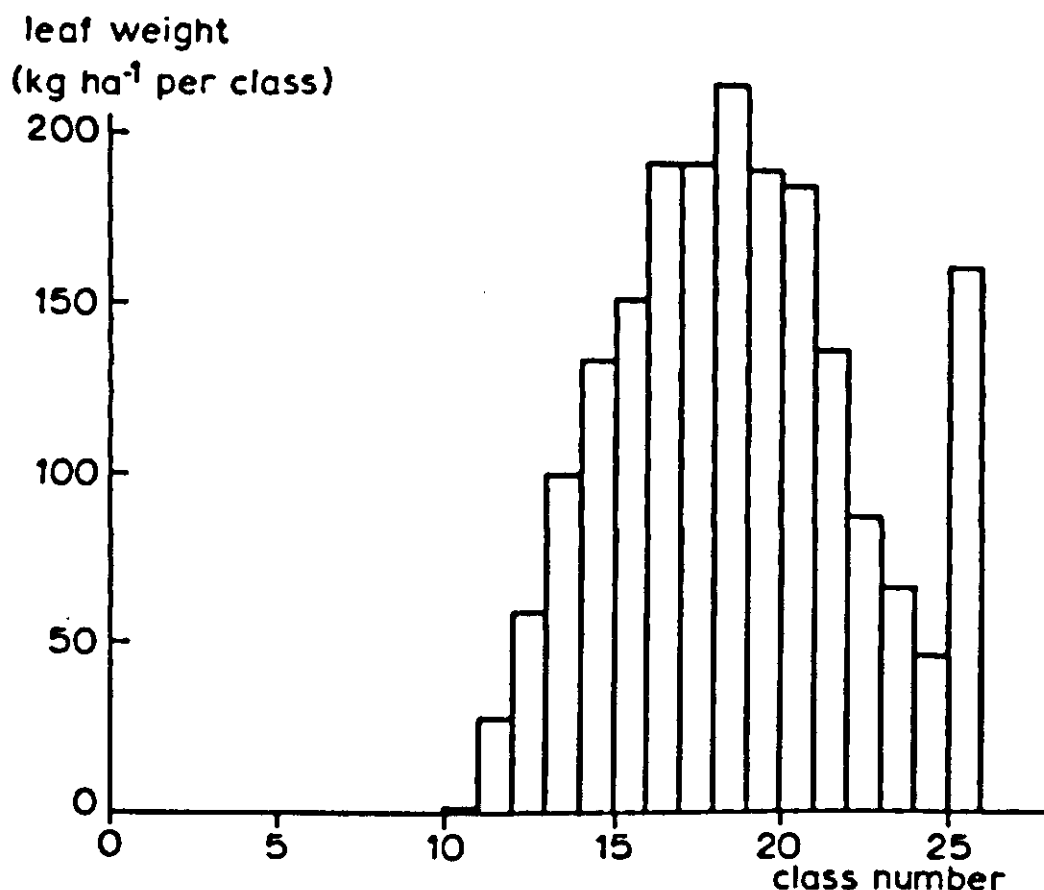
Figure 30. Distribution of the total weight of live leaves (WLV) over 25 classes at DVS = 1.25 (TIME = 366.2) for a standard run of SUCROS. Each class represents the leaves formed during one development stage interval. Class 26 represents the total of dead leaves.

and old, the programming with the time coefficient approach looks like the boxcar train approach. However, it remains in principle different. This will become clear if one compares the results of Figure 30 with those of Figure 15, Section 2.1, for the second till nth order exponential delays. By programming development using time coefficients, the dispersion phenomenon can be simulated elegantly (Subsection 2.1.8). This has been programmed by Janssen (1974) to simulate the germination process of winter annuals. Dispersion phenomena, however, are rarely encountered in plant growth models; they are not further discussed here.

3.3.3 Rate of growth

For models in which growth is simulated with time steps of one day or more this subsection is of no interest because all carbohydrates formed during the day are then supposed to be consumed for growth and maintenance within 24 h. Daily growth rate of the total biomass GTW is then sufficiently defined by:

$$GTW = (GPHOT - MAINT) * CVF$$

GPHOT and MAINT stand for daily photosynthesis and maintenance respiration, respectively (see Section 2.2). The value of the conversion factor (CVF) is often about 0.7; it is explained below.

If the dynamics of growth during the day are important, one recognizes quickly that GTW is only indirectly a function of GPHOT and MAINT. Growth is a physiological process whose rate depends on internal conditions and environmental factors. 'Growth' is defined as the formation of structural material from

119

reserves. 'Structural material' consists of cell walls, some enzymes and membranes. Once formed, it is never again substrate for growth or maintenance. The total dry biomass of plants consists of structural material plus 'reserves'. Reserves are largely made up of carbohydrates, in particular starch and glucose, though some protein is present as well. However not all starch and soluble sugars are necessarily reserves. In sugar-beet, for example, the stored sucrose is not withdrawn from the beet, even when the leaves are starving. For practical purposes, however, 'reserves' is identical to the soluble sugars plus starch in vegetative organs (cf. Subsection 3.4.7).

The amount of reserves (RES, expressed as glucose, in kg ha^{-1}) can be simulated by:

$$RES = INTGRL(0., GPHOT - MAINT - CGR)$$

in which CGR represents the rate of consumption of reserves in growth processes (this equation is identical to the one in Subsection 2.3.4). The reserve level is the fraction that reserves form of the total plant dry structural weight. An illustration of the fluctuation of the reserve level during the day, as a result of photosynthesis and of growth in particular, can be found in the work of Challa (1976) with cucumber plants (Figure 31).

What is of interest is in the first place the growth of the whole plant, rather than growth of individual organs. The rate of plant growth is determined by internal and external factors. Of the internal conditions, the amount of reserves and the maximum capacity to grow are the most important ones; among the external factors temperatures and water stress are most important.
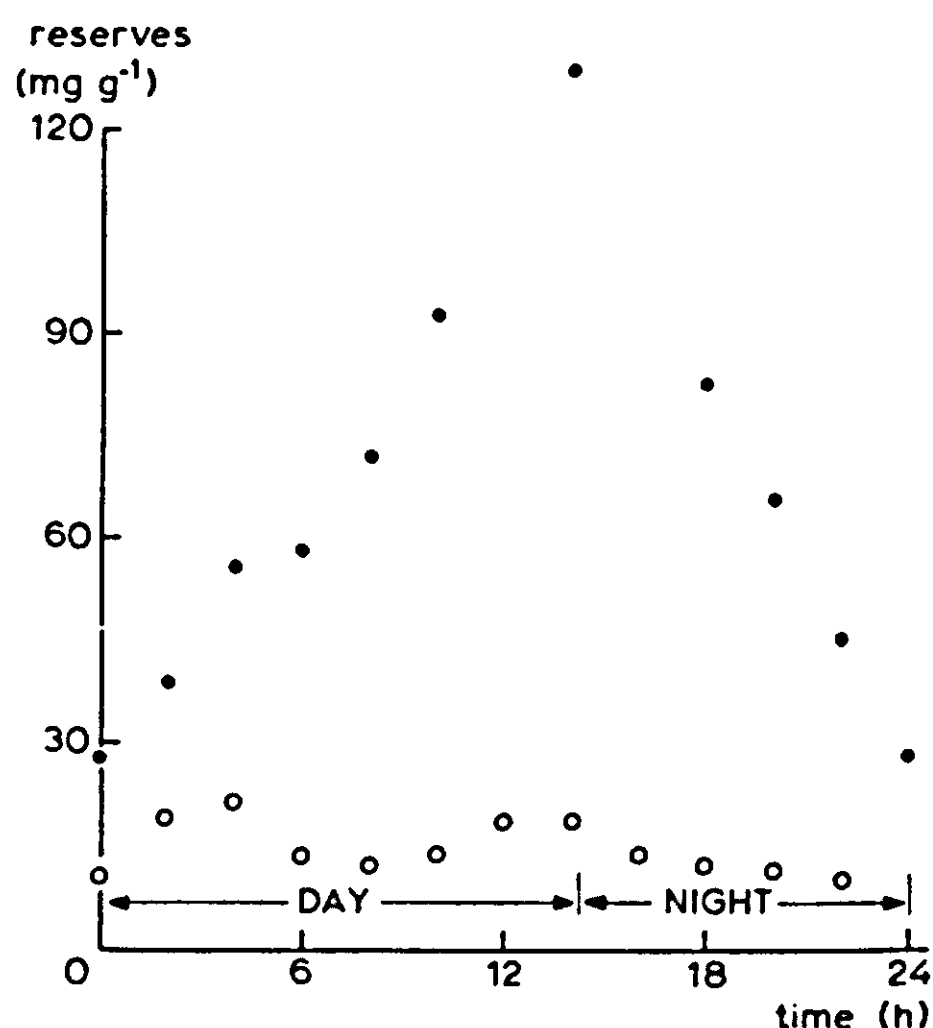
Figure 31. The course of the reserve level during 24 h in cucumber plants (Challa, 1976). Open circles indicate the glucose level, closed circles the level of glucose + starch. Plants were grown in climate chambers.

How the growth rate of wheat plants is related to the reserve level, to temperature and to the water potential is depicted in Figure 32. These results were obtained from laboratory experiments and were more or less similar for rye grass and maize plants (Penning de Vries et al., 1979). Results of Moldau & Sôber (1981), shown in Figure 18 of Section 2.3, show a similar relationship of growth rate and reserve level. In the field, however, such effects are conceivably more smoothed out, as a result of adaptation processes, than in the short duration laboratory study. No observations of that kind are known as yet (Patterson, 1980). However, in the long run, the exact shape of the response curves are not very important, because they are part of a negative feedback loop.

Exercise 46
Of which negative feedback loop are they a part?

And the end result of a simulation over a full day is still that of the one day growth equation. Moreover, the relations may be specific for each species or
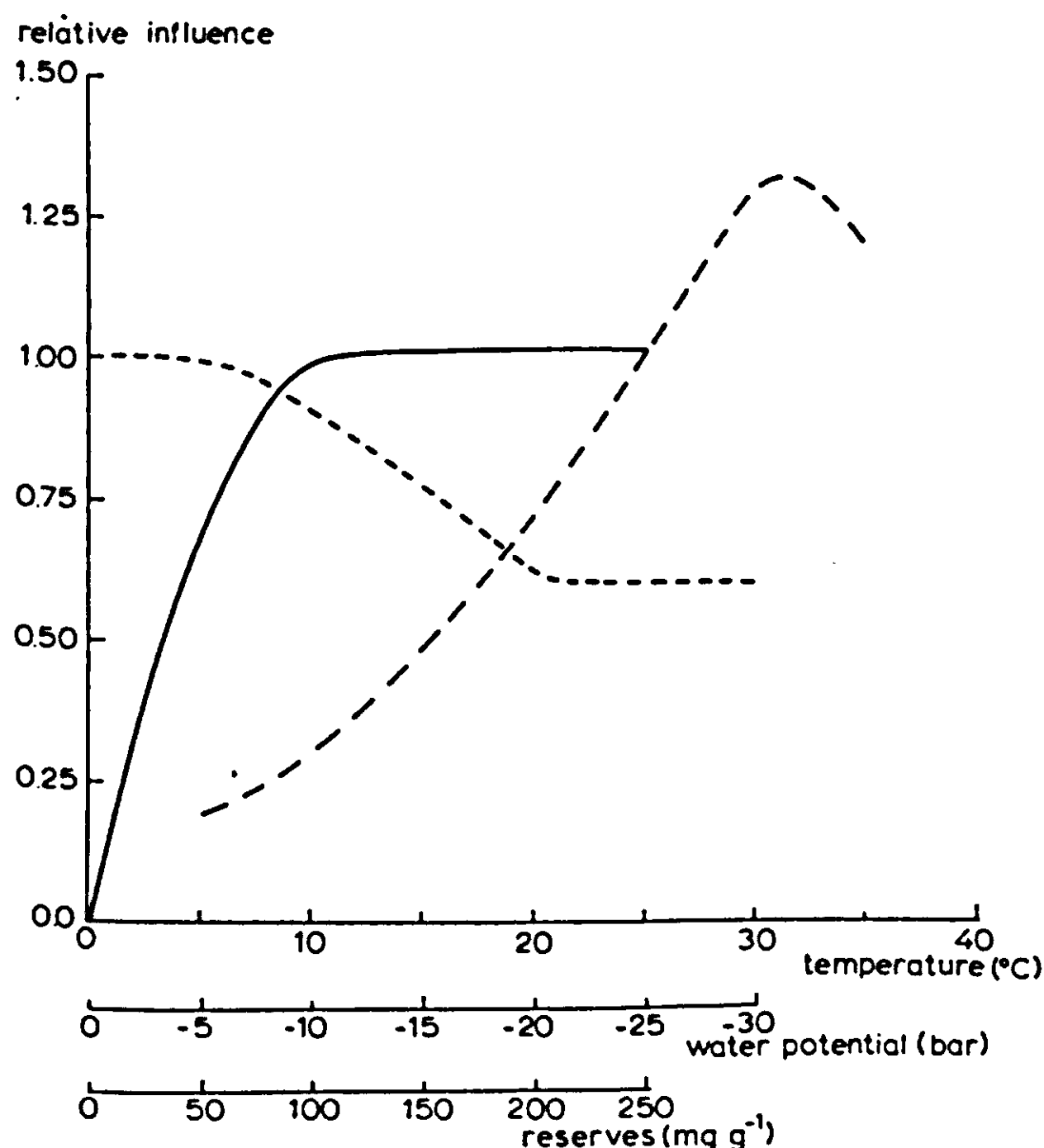
Figure 32. The relative response of the growth rate of young wheat plants to the reserve level (————), temperature (— — —) and water stress (----) (Penning de Vries et al., 1979).

cultivar, so it would be cumbersome to obtain them experimentally. It is thus not worthwhile to spend much effort in improving these relationships.

The cumulative effect of the internal conditions and these external factors is generally simulated by multiplying the relative effects of temperature (ET), water stress (EW) and reserve level (ER) (cf. Loomis et al., 1979):

GTW = BM * RGRS * ET * EW * ER

Exercise 47
As an alternative, the smallest of the individual factors might be chosen. What are the physiological implications of both assumptions? Devise an experiment to distinguish between these possibilities.

The constant before the multiplication factors in the above equation is the relative growth rate in standard conditions for whole plants (RGRS); the current biomass is represented by BM. The constant to be used with the data of Figure 32 is $0.3 \text{ g g}^{-1} \text{ d}^{-1}$. Its value depends on the age of the tissue: young tissues have much higher values than old ones. In fact, the RGRS of the tissue that actually grew in maize plants in the same set of experiments was $1.3 - 1.7 \text{ g g}^{-1} \text{ d}^{-1}$.

The highest values reported of RGRS for whole, autotrophic plants are about $0.5 \text{ g g}^{-1} \text{ d}^{-1}$ (Björkman et al., 1975). RGRS . BM is the maximum plant growth rate at standard temperature. This maximum rate of growth requires special attention in a model when the internal conditions for growth are such that this maximum is attained for some time. In other words, when sink size is limiting the rate of formation of structural dry matter. This occurs often at the level of individual organs during their initiation; it may occur during the filling of the storage organ; and it occurs frequently during regrowth after cutting. This subject is discussed in more detail in Section 3.4, with wheat grain as an example.

The question of whether it is really important to quantify RGRS (and the growth capacity) accurately, depends on feedback: if an intermediate pool of reserves builds up temporarily without modifying the rate of CO_2 assimilation, an improper choise of RGRS will only yield a delayed or advanced reaction of growth to assimilation. However, if the rate of assimilation becomes impaired, for example when the reserve level builds up too high (Moldau & Karolin, 1977), the effect should be clearly considered. But in our opinion plant growth in the vegetative phase and for optimal growth conditions almost never encounters this situation.

BACROS simulates vegetative growth only. It contains a still simpler approach to quantifying the crop growth rate: it is assumed that there is continuously sufficient biomass with the capacity to grow and to consume all reserves in about one day. This is programmed as a relative rate of consumption of reserves of about $1 \text{ kg kg}^{-1} \text{ d}^{-1}$. But this works well only in a fairly smooth

growth situation, where no limitiation due to lack of growing points occurs.

The translocation process of reserves from source to sink need not be discussed here: its rate is well adjusted to the growth rate (although it is possible that some of the responses of growth to environmental factors are in fact responses of the translocation system rather than of the growing cells). Note that this discussion of growth rates does not include hormones or growth substances explicitly. These substances may be transmitters of information about levels of reserves or of potentialities of growth, but need not to be made explicit as such. Hormones seem to be related to development processes and assimilate distribution, possibly by affecting phloem unloading directly, rather than to growth as such (H. Veen, personal communication).

3.3.4 Efficiency of growth processes

The six chemical components to be distinguished in plants are: carbohydrates (structural), proteins, lipids (including oils and fats), lignin, organic acids and minerals. Other types of molecules are rarely important quantitatively. Different biochemical pathways are employed for conversion of reserves into each of these components, and differences in efficiencies (on a weight basis) are its result. These efficiencies are characterized as 'conversion efficiencies'. Their values for these five organic fractions are presented in the equation below in an inverse way, which shows how much glucose is required for synthesis of one gram of the components. These values were determined in a series of theoretical analyses, and account for changes in atomic composition and for energy requirement in biosynthesis. The cost of transportation of molecules is relatively low, and was included in the conversion equation. The value of the conversion factor for growth of biomass, weighted according to its composition, can be computed in a simple way from the fraction of carbohydrates, proteins, fats, lignin, organic acids and minerals (FC, FP, FF, FL, FO, FM, respectively) in the current dry matter increase:

$$CVF = 1./(FC*1.242 + FP*1.704 + FF*3.106 + FL*2.174 \ldots$$
$$+ FO*0.929 + FM*0.050)$$
$$CPF = FC*0.170 + FP*0.462 + FF*1.720 + FL*0.659 \ldots$$
$$- FO*0.011 + FM*0.073$$

CVF is expressed as the ratio of structural biomass formed over glucose consumed ($kg \, kg^{-1}$). CPF stands for the carbon dioxide production factor and is the ratio of CO_2 evolved per amount of component formed ($kg \, kg^{-1}$) and can be used to calculate the growth respiration. There are good reasons to suppose that those equations and constants apply to all species at all non-extreme temperatures (Penning de Vries et al., 1974).

In SUCROS it is assumed that leaves, stems and roots of annual crop species, growing in optimal conditions, have a more or less typical biochemical composition, which leads to a more or less typical value for CVF for each of these

organs independent of species (Line 238, Table 9, Section 3.1). The storage organs of different crops are too variable in their composition to generalize on the efficiency of their formation. Values for 23 important crop species are reported by Penning de Vries et al. (1982).

A slightly different procedure to calculate the efficiency of growth is followed in BACROS: growth of individual biochemical fractions and the corresponding starch consumptions are computed; the computation of a CVF value for biomass as a whole has been skipped. The values in the above equations are also not completely identical to those in the BACROS program (see de Wit et al., 1978), because of simplifications introduced here. Moreover, reserves in BACROS are expressed as starch; for conversion of glucose into starch equivalents multiply them by 0.900.

Exercise 48
Structural dry matter consists of carbohydrate, protein, fat, lignin, organic acid and minerals. Of those components, 1 g of dry leaves may contain 520 mg, 250 mg, 50 mg, 50 mg, 50 mg and 80 mg respectively, 1 g of dry stems may contain 620 mg, 100 mg, 20 mg, 200 mg, 20 mg and 40 mg respectively, while 1 g of dry roots may contain 560 mg, 100 mg, 20 mg, 200 mg, 20 mg and 100 mg respectively; 1 g of dry wheat grain contains 760 mg, 120 mg, 20 mg, 60 mg, 20 mg and 20 mg, respectively. Calculate the corresponding CVF and CPF values. Show that the sum of the fractions always equals 1000 mg g^{-1}.

In somewhat approximate simulations of growth of vegetative biomass, the value of CVF of 0.7 will often do fairly well. If a higher degree of precision is required, not only is the computation of CVF to be repeated more often, but also the chemical composition of the biomass increment must be specified. Such information can be given directly, as in SUCROS, or computed in the simulation program from observed field data. The latter route is taken in BACROS. A prediction of what biochemical composition will be in a given species and under certain conditions has not yet been tried.

A feature recently added to BACROS is that of legume crops. The most obvious change is the cost of nitrogen (N) fixation in root nodules, which replaces the cost of nitrate reduction, a process that usually occurs in leaves. According to Minchin et al. (1981) the lowest cost of fixation, expressed as a C/N ratio, is 2 g g^{-1}, but values of 6 - 15 g g^{-1} have been established for field plants. Apparently the fixation cost varies with species, and possibly with growth conditions. Faba bean *(Vivia faba)* tends to be a very efficient N fixer, and hence the cost in this model has been set to the minimum value (see Subsection 3.3.8). Another change is that amino-acid synthesis in legumes occurs in roots, whereas most of the synthesis in non-leguminous crops under optimal conditions occurs in leaves. These aspects change some of the equations in the program a little. The option to use

BACROS to simulate a leguminous or non-leguminous crop type is effectuated by setting a parameter LEG to a value of 1. or −1., respectively, which changes all necessary constants in equations accordingly with an INSW function.

There is a large variation in the rate of growth of individual plant organs in time. Their biochemical composition changes also: less protein and more carbohydrates are usually formed when the organ gets older. This makes the growth respiration change. The intensity of the maintenance processes is also not constant (see below). Each of these aspects contributes to a continuous drift in the rates of respiration of the organs and of the whole plant. Not only is this a complex phenomenon to register, it is also tricky to simulate correctly because of the complexity of the process. It is therefore wise to include a carbon (C) balance in a comprehensive model, and to check continuously its completeness. The amount of C in plants can be found in two ways: from the total net CO_2 assimilation of the whole crop during the whole growing season (in kg ha^{-1}) after multiplying it by 12/44 to obtain the weight of the C; and as the sum of the fraction C in each of the biochemical components grown, plus the change in the amount of reserves in the plant. The C content of structural carbohydrates is on average 0.4504 g g^{-1}, 0.4444 for reserves, 0.5556 for proteins, 0.7733 for fats and oils, 0.6899 for lignin, 0.3746 for organic acids and 0.0 for minerals. Both ways of computing the C content should give identical results. Rounding-off errors of up to 1% can be permitted, but larger differences must result from incorrect changes in the program or improper data of the biochemical composition. In BACROS the simulation is then halted by a FINISH condition.

Exercise 49
Is a C balance in equilibrium proof of a correct simulation, or only proof of consistency of the assumptions about growth and CO_2 exchange? Add a C balance to SUCROS and program two types of error to illustrate your answer.

3.3.5 Maintenance respiration processes

Maintenance processes in plants consist of resynthesis of degraded proteins (protein turnover) and maintenance of ion gradients across cell membranes. Both processes require a constant supply of energy, delivered by the maintenance respiration process: the mitochondrial combustion of glucose. The efficiency of energy production of this process is about as high as is biochemically possible, but the intensity of the process is still insufficiently quantified. As a result the quality of simulation of maintenance respiration is less than that of growth respiration. Effects of environment on the intensity of the process are also not well established. Temperature, the most important factor, usually stimulates the maintenance processes by a factor of 2.0 per 10 °C temperature increase, and this Q_{10} of 2.0 is commonly used. However, both lower and higher

Q_{10} values have been reported (cf. Subsection 3.4.7). A light water stress does probably not affect the intensity of maintenance processes.

The description of the effect (TEFF) of the actual temperature (ATEMP) on maintenance respiration with a Q_{10} concept can be programmed easily with the Q_{10} value (Q10) and the reference temperature (RTEMP) as follows:

TEFF = Q10* *((ATEMP – RTEMP)/10.)
PARAMETER Q10 = 2., RTEMP = 25.

Note that in this equation it is not expressed that the range of validity is only 10-20 °C.

For the calculation of the rate of maintenance respiration of a crop at standard temperature, three different procedures can be followed (indicating that its modelling is still in a preliminary phase; see Subsection 1.3.2). The simplest is to state that maintenance requires daily 0.015 g reserves (glucose) per gram biomass. It is used for example in the model of Section 2.2. This is roughly correct at the temperature to which the crop is adapted and grows very well, which may be 20-25 °C for temperate crops, and 30-35 °C for tropical crops (McCree, 1974). It is slightly more sophisticated to indicate that the processes are related to protein content, in part, and hence to base its calculation on protein content of the tissue. This was done, for example in ELCROS (de Wit et al., 1970) a predecessor of BACROS. This requires, however, additional information: the protein content of the crop. The information can also be given indirectly, by stating that leaves, the organ with the highest protein content, have the highest rate of maintenance respiration: about 0.03 g g^{-1} d^{-1} for field grown plants; stems have much lower rates – about half of that of leaves – and roots lower still. Storage organs may be high or low in protein, but most of their protein is inactive, so that their maintenance requirement is low (cf. Penning de Vries et al., 1982). The assumption that the rate of maintenance respiration of organs differs, but is more or less specific per type of organ at the reference temperature, was the basis for the formulation in SUCROS (Section 3.1):

MAINTS = WLV*0.03 + WST*0.015 + WRT*0.01 + WSO*0.01

The third approach to the quantification of maintenance processes was followed in BACROS: it is computed from protein and mineral content and in addition from the average metabolic activity of the crop. This is based on.the observation (Penning de Vries, 1975) that more active tissues have higher rates of maintenance respiration than less active ones. Its explanation is that probably more enzymes are turned over and maintained at high than at low activity. Leaves, which are more biochemically active than stems or roots, have the highest rates of maintenance respiration per unit of tissue. The rate of CO_2 production related to maintenance respiration is 44/30 times the rate of glucose consumption.

Exercise 50
Add an INTGRL of glucose consumed for maintenance to SUCROS, and test the sensitivity of the model to the coefficients used for different values for various organs, and for the Q_{10} value.

3.3.6 Assimilate distribution

The usual way to describe the distribution of current assimilates over plant organs, often called dry-matter distribution, is by employing a certain key. This key changes with the development stage of the plants. Figure 33 presents typical keys of the distribution of dry matter over the principal organs of wheat, potato and soybean plants (van Heemst, personal communication). These keys are characteristic for each crop, and its course with DVS may even be different for cultivars of one species. The effects of environmental conditions on the pattern of assimilate distribution are often fairly small at the level of potential productivity. (For lower levels of production, see Section 4.1 and 5.3).

About the internal control of distribution of assimilates in plants, still little is known. This implies that data about dry-matter distribution are to be collected experimentally, and also that all simulation models are fairly weak in their application to conditions where morphology may be expected to be different than in the area where the data were obtained.

However, in addition to the static description of dry-matter distribution, some inroads into its dynamic simulation have been, or are being, developed. Among them are the simulation of grain production in wheat crops as a function of C and N reserves and of current CO_2 assimilation and N uptake, as is presented in the Subsections 3.4.5 and 3.4.7, and in the simulation of tiller dynamics and grain initiation (Subsection 3.4.10). Another inroad is the analysis by Horie et al. (1979) of leaf size and leaf number in developing plants in an attempt to characterize morphology with a minimum of parameters.

One assimilate distribution mechanism that merits special attention is the interaction between shoot growth and root growth. According to the functional balance concept of Brouwer (Brouwer & de Wit, 1968), the shoot needs a certain amount of roots to provide it with water, while the roots cannot do without assimilates from the shoot. As a consequence, growth of the shoot becomes reduced when there are too few roots for a sufficiently high water uptake (as a result of root damage, an increased transpirational load or a drier root environment). Roots, closer to the source of water, supposedly suffer less. As a result of a decrease in shoot growth and in utilization of reserves, the reserve level builds up, and root growth becomes stimulated to a higher level. This continues until the equilibrium is restored. Due to this balance, most of the growth of roots occurs during the day and most of the growth of shoots during the night.

The functional balance in ELCROS (de Wit et al., 1970) was simulated by different responses of shoots and roots to water stress and reserve level. SUBGOL (Loomis et al., 1979) does likewise. The current version of BACROS simulates it by considering the water status only, stating that a low relative water content of the crop stimulates root growth but reduces shoot growth, and vice versa.

In spite of the existence of the functional balance, many models, including SUCROS, simulate crop growth using a predetermined distribution of biomass between shoot and root (excluding tubers and beets), as shown in Figure 33. The reason for following this procedure, rather than the dynamic concept, is that it is simpler and also often satisfactory at the highest production level if one is not
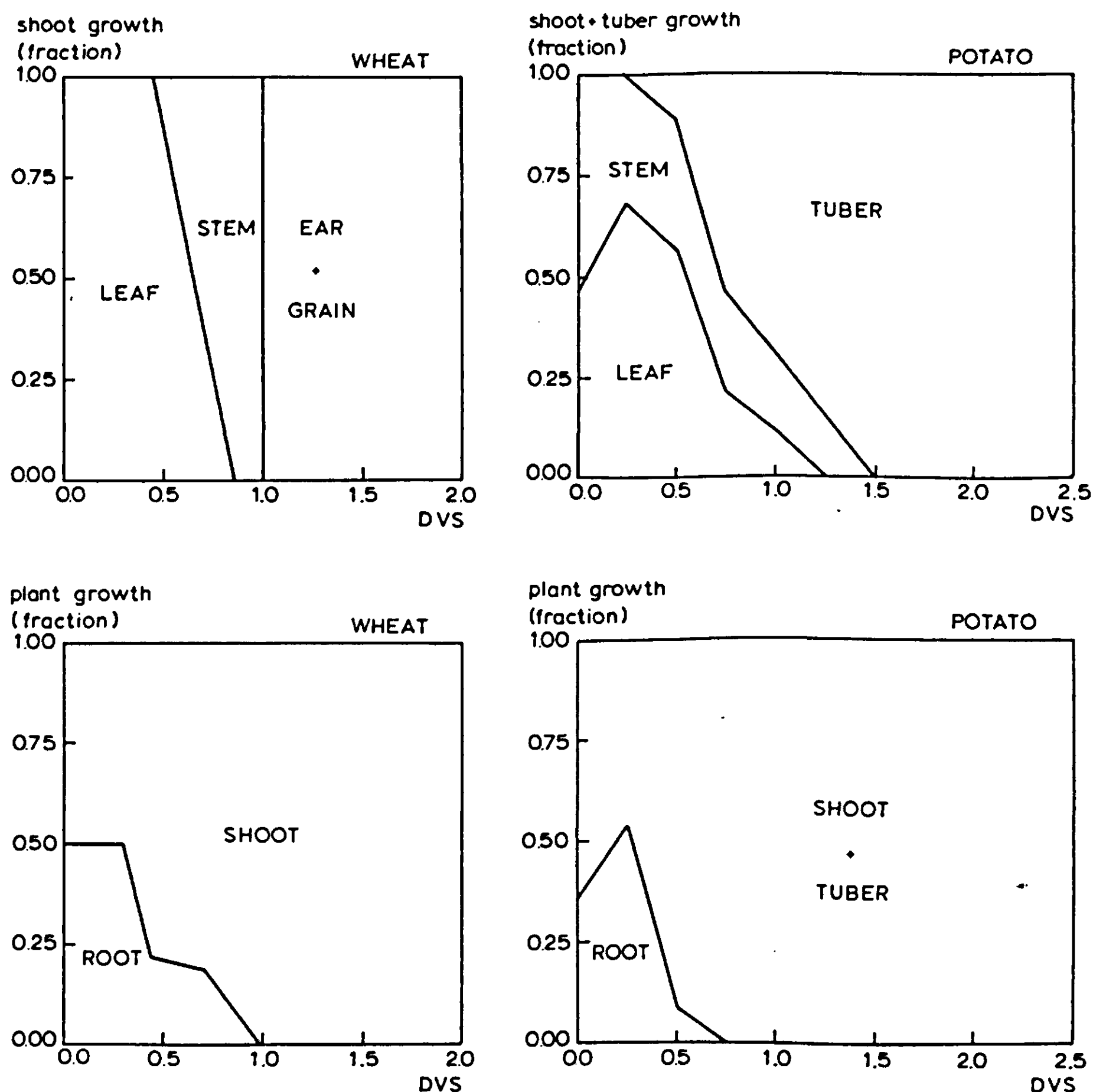
Figure 33. The partitioning of dry matter increments over shoot and root (lower graphs) and among shoot organs (upper graphs) during development of three crop species: wheat (a), potato (b) and soybean (c) (van Heemst, personal communication). The fractions are presented in a cumulative fashion.

interested in the daily course of processes. At the level of production where water or nutrients are limiting growth, the shoot-root distribution pattern changes towards roots. This change can also be programmed fairly easily in this way (Subsection 4.1.4 and 5.3.2) by increasing the fraction going towards roots to an extent that is related to the degree of water shortage.

3.3.7 Crop water balance

To simulate the dynamics of shoot growth during a day in the field at the highest level of production, the degree of water shortage in the crop has to be

shoot growth
(fraction)
SOYBEAN
1.00
STEM
0.75
POD
0.50
SEED
LEAF
0.25
0.00
0.0   0.5   1.0   1.5   2.0
DVS

plant growth
(fraction)
SOYBEAN
1.00
0.75
SHOOT
0.50
0.25
ROOT
0.00
0.0   0.5   1.0   1.5   2.0
DVS
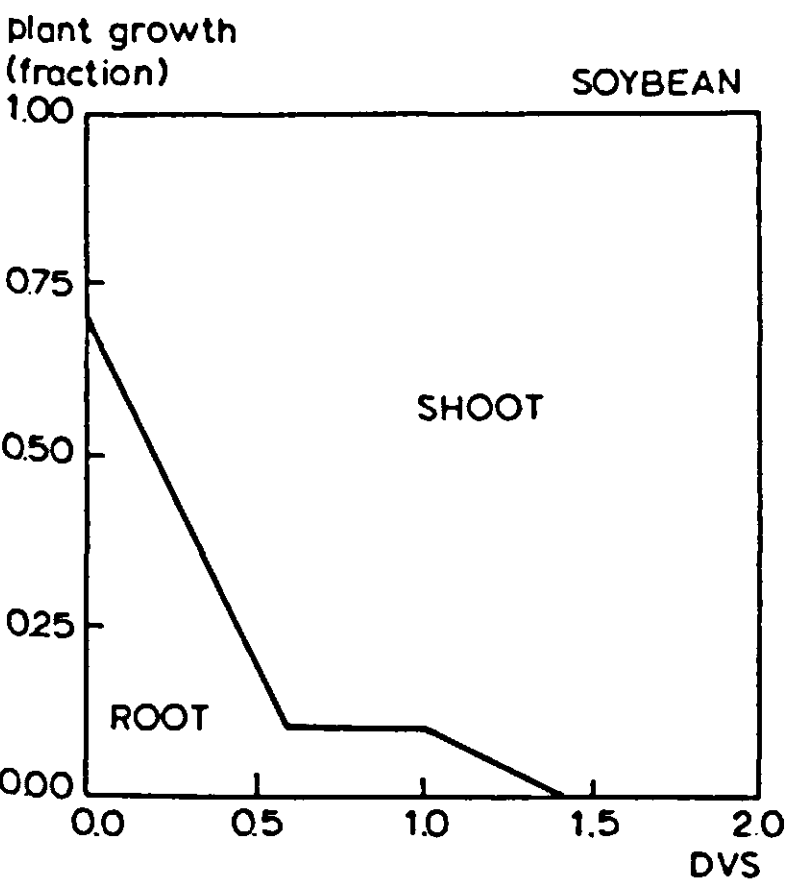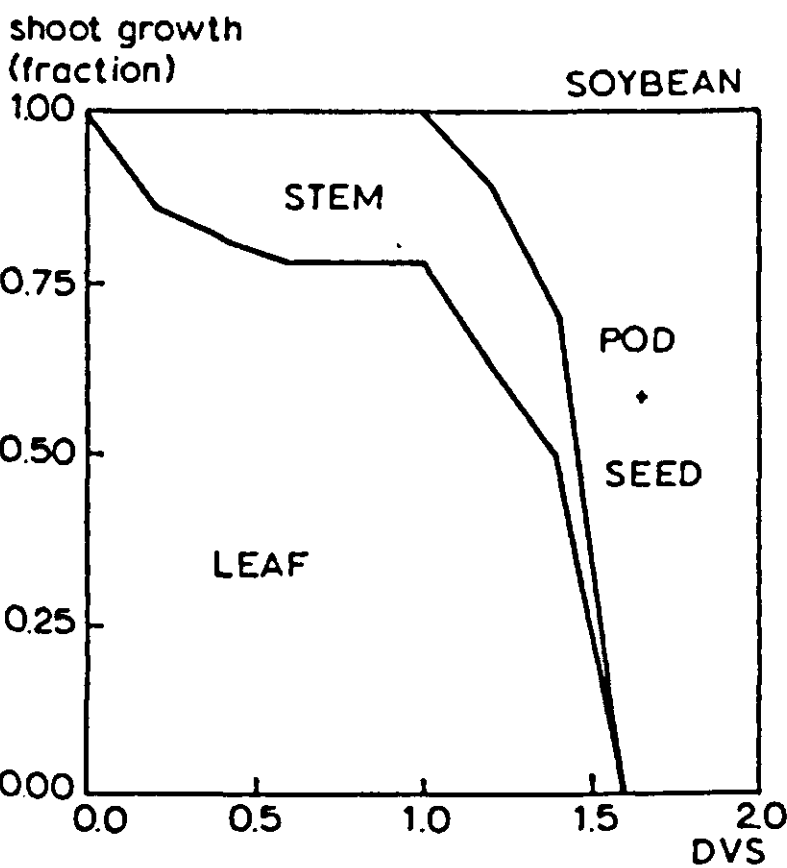
tracked. A water balance of the canopy must thus be included in the model. The balance can be simple, as the conductivity for water in the tissues is high and important differences in potential between plant parts usually do not develop at this level of production. The only resistance to water entering the plant is the root resistance, the only one to water leaving the plant the stomatal resistance plus air-layer resistance. Moreover, the availability of soil water is supposed to be continuously optimal (by definition). Another reason for simulating the crop water balance is the computation of transpiration. This might be useful in itself, for example to establish the water requirement of the crop for irrigation purposes and provide another possibility to evaluate model behaviour.

The water balance consists basically of the rate of transpiration, discussed in Subsection 3.2.5, the rate of water uptake by the root system and a buffering volume of water in the plants. As the relative water content (grams water per gram fresh weight over grams water per gram fresh weight of fully saturated tissue) decreases and the water potential in the plant becomes more negative, stomata start to close and transpiration becomes reduced; a higher water potential difference across the roots, on the other hand, increases water uptake. It is not very important to know the absolute position of the relations between the relative water content and the degree of stomatal closure and between the relative water content and the water potential, again because of negative feedback (cf. Exercise 46). This also makes modelling of the water balance relatively simple. An example of a simple water balance can be found in the model PHOTON (de Wit et al., 1978), a special form of BACROS that is described below.

However, a time-step size problem may arise (see also Subsections 1.4.4 and 2.3.5): the margin in water content of a fully watered crop and a wilted one is often in the order of $1000 \, l \, ha^{-1}$. The plant regulates turgidity by modifying its stomatal resistance on a much finer level. The rate of transpiration of a closed canopy can reach $0.5 \, mm \, h^{-1}$, or $5000 \, l \, ha^{-1} \, h^{-1}$. Hence, a 1 h time step will be too large, and probably cause an unrealistic oscillation in the simulation of the plant water content. The 1 h time step, on the other hand, may be very suitable for the simulation of the C balance processes. There are three solutions to this problem: make more computations of these C balance processes than necessary, make the water balance calculations as often as required and the others less frequently, or make all computations less frequently and adapt the program. The first solution is the easiest. But it is the most expensive, and it also gives the false impression of a higher degree of precision in time of the C balance simulation then is actually the case. The second requires some skillful programming, using the so-called bypass method (Goudriaan, 1977), and is not advised for novices. The third is used in BACROS: it simulates the canopy water content only once per hour, and assumes that transpiration and water uptake are continuously equal, although their values may be different each time step. This is another way of saying that the conditions for the water balance change slowly during the day. This method does not provide a fully dynamic simulation of the water balance, but a realistic simulation of equilibrium situations. By using an implicit

130

loop (see Subsection 2.3.4), the equilibrium water content at each hour is found. (A disadvantage of the CSMP IMPLicit loop is that its equations need to be grouped, reducing the readability of the program. Therefore, a self-constructing implicit loop has been programmed in BACROS by means of two sortable procedures called BSCIL and ESCIL. A dummy variable SELECT was defined exclusively to optimize the result of the sorting procedure.)

Water uptake can be simulated using an equivalent to Ohm's law, with the water potential difference between plants and soil as driving force, and root conductivity as the only limitation to it. The conductivity of the root system in BACROS is modelled in a rudimentary way by distinguishing two categories of roots (Subsection 3.3.2) with different conductivities: old ones, suberized, are three times less permeable than young ones. Young roots become old roots with a time coefficient of 5 d. These values are not critical, and received little attention in evaluation studies.

3.3.8   Results of the models BACROS and PHOTON

Elements of the model BACROS have been presented in this section and in Section 3.2. There are many more elements, particularly in details and in crop micro-meteorology. For those elements and arguments about their background, see de Wit et al. (1978) and van Laar et al. (1983). The model BACROS simulates plant growth during a growing season with time steps of 1 h. The principal data to be specified for its use are given in Table 14.

To evaluate its behaviour, field experiments with periodic harvests have been performed. They provide useful background data for evaluations, but yield few suggestions of explanations if differences are encountered. Moreover, a day by day comparison is practically impossible, given the unavoidable sampling errors, and field heterogeneity. Crucial aspects of the gas exchange processes could therefore not be evaluated profoundly. To overcome this handicap, two things were done. The first and simplest step was to develop the model PHOTON, that is identical to BACROS except that it uses much smaller time steps (in the order of a few minutes, as determined by the integration method RKS) and requires therefore a somewhat different elaboration of some processes, such as the water balance. To avoid excessive computation costs, it is only used for periods of a few days. The second step was to start to measure continuously crop gas exchange processes (CO_2 and H_2O) in a crop enclosure in the field using mobile equipment (Louwerse & Eikhoudt, 1975). Evaluation runs of the models BACROS and PHOTON have been published (de Wit et al., 1978).

Another example of such a two-level evaluation is provided here to give an impression of the 'state of the art' of modelling at the level of potential crop production. A Faba bean experiment was followed throughout the 1979 season with periodic harvests to establish overall crop growth rates. The Faba beans grew very well in conditions that must have approached closely optimal growth conditions (Subsection 1.2.1). Nodulation of roots was excellent. A few times

Table 14. List of input variables that must be specified to use the model BACROS. Variables of Category 1 must be given in all cases; those of Category 2 must be given for simulation of specific experiments; those of Category 3 can be specified for maximum accuracy. If a variable is not specified, a default value is used.

Category	Data on crop	Weather data	Other
1	C_3 or C_4 maximum rate of leaf photosynthesis leguminous or non-leguminous crop stomatal regulation effective or not	daily total global radiation daily maximum and minimum temperature and humidity	latitude start and duration of the vegetative growth period
2	width of leaves leaf area development in a similar experiment	windspeed	
3	temperature effect on photosynthesis plant height development development of biochemical composition of biomass	constants in long-wave radiation equation	
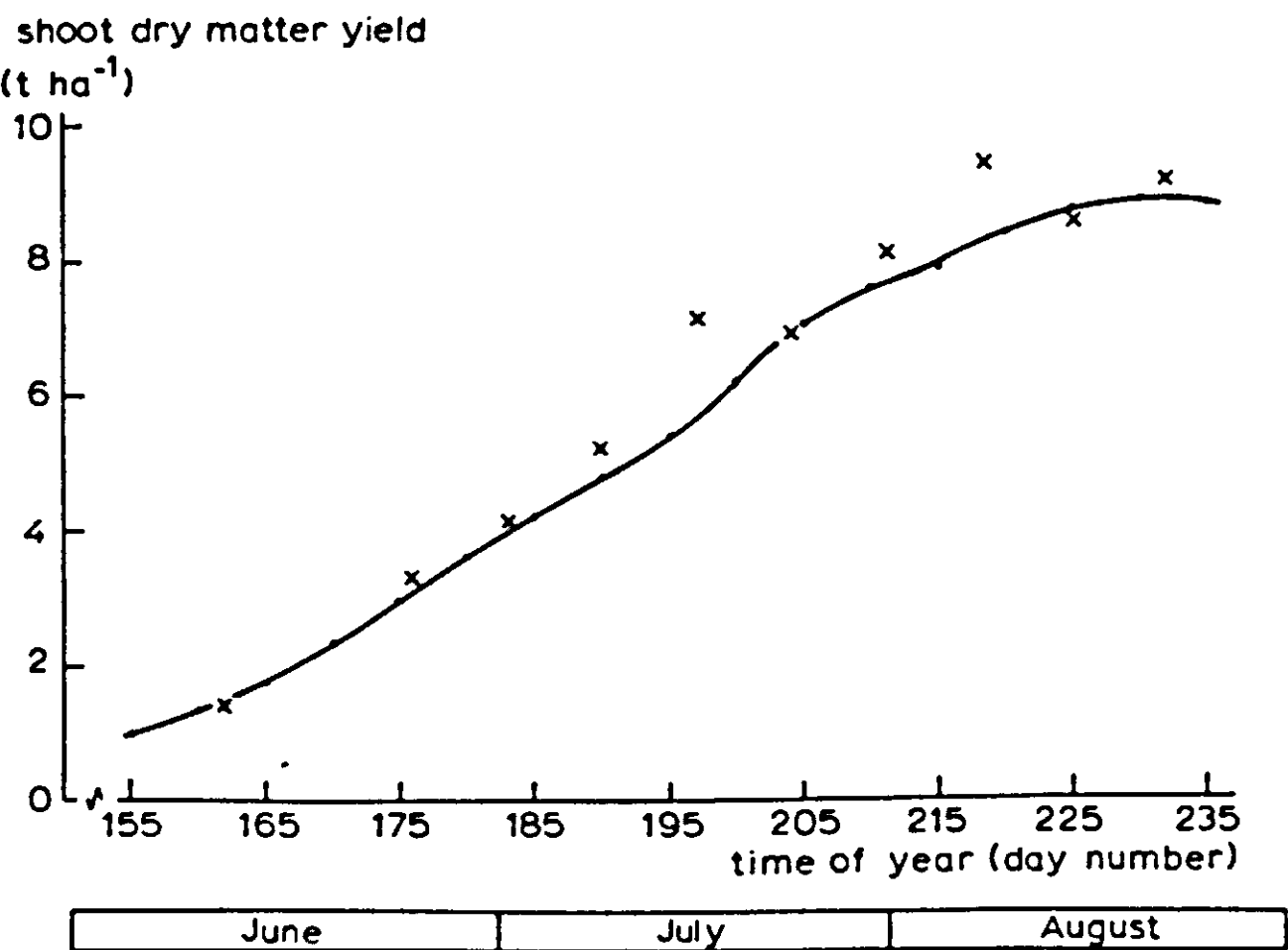
Figure 34. The measured (x) and simulated (—) above-ground biomass of a Faba bean crop in Wageningen, 1979.
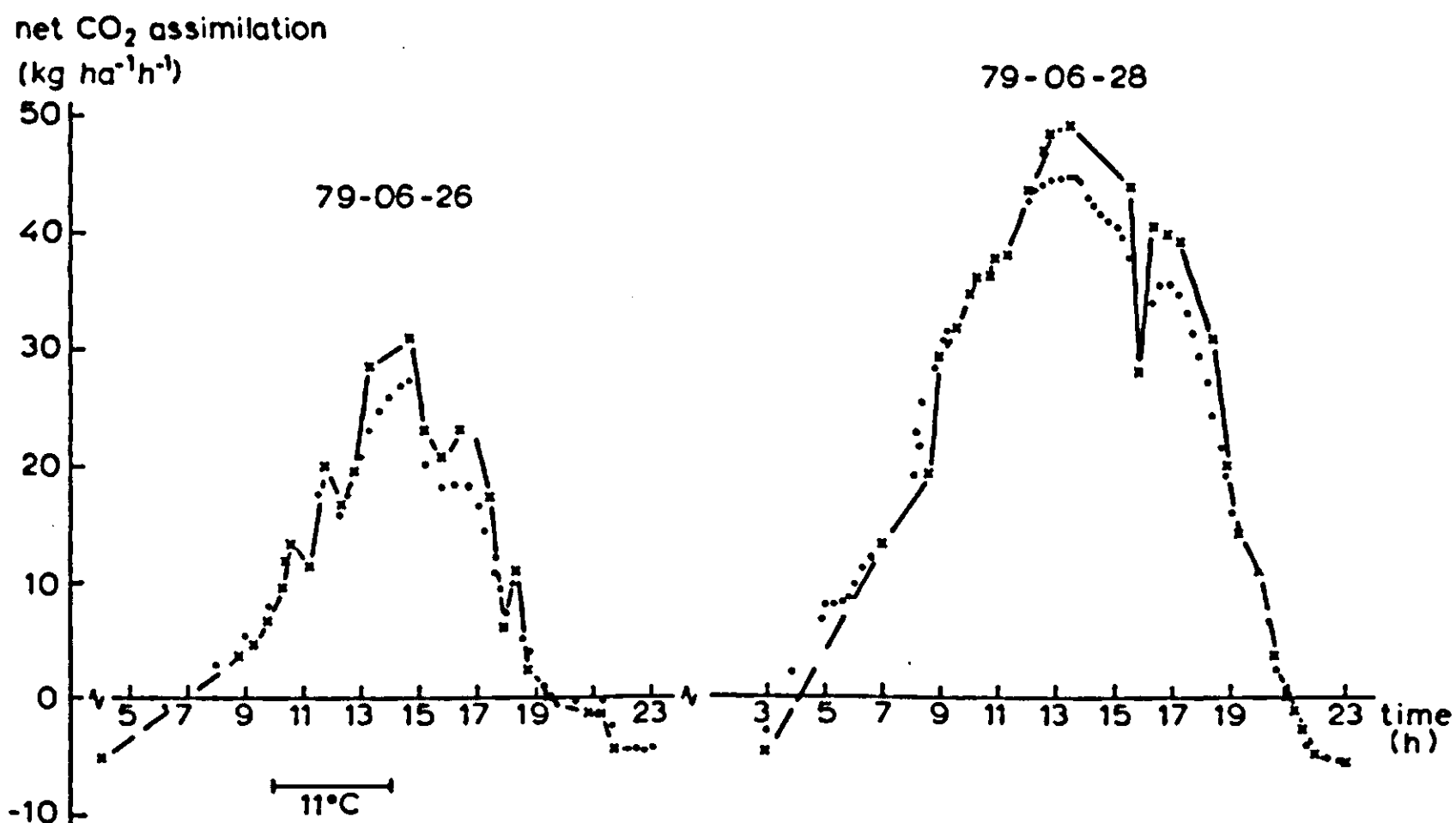
Figure 35. The measured (x) and simulated (•) rates of net CO_2 exchange of the Faba bean crop on 26 and 28 June 1979; temperature was set at 20 °C, except for an induced 9 °C temperature drop. Both days had plenty of bright sunlight. Daily total global irradiation was 0.9 10^7 J m^{-2} on the first day, and 2.4 10^7 J m^{-2} on the second.

during the season, the mobile equipment was used on the same field to measure gas exchange. Simulation was done with a program identical to that of van Laar et al. (1983), with account being taken for the fact that the crop was grown under a plastic cover (that reduced light intensity by 20%, and net long wave radiation by 100%). Unfortunately a direct measurement of the maximum rate of leaf photosynthesis of these field-grown Faba beans was not available, so that an estimated value had to be used. Results of this experiment and its simulation are provided in Figures 34, 35, 36a and 36b.

Figure 34 shows the evolution of the total above-ground biomass of the crop; leaves, stems and pods are not distinguished. Agreement between observed and simulated growth rates is good, although there are a few deviations and the simulation tends to underestimate the real growth rate slightly. Additional measurements with the mobile equipment in June and simulation of the same situation (initializing PHOTON with values simulated with BACROS for those days), confirmed that the model describes this fast-growing, almost completely vegetative, canopy reasonably well on a day to day and an hour to hour basis. Also the simulated rate of transpiration agreed very well with observed values. The reduction of the gas exchange rate that resulted from an induced 9 °C temperature drop was also simulated properly (Figure 35).

Later in the season, in August, the simulated growth rate exceeds the observed growth rate. But the behaviour of PHOTON was qualitatively still appropriate, as Figures 36a and 36b show: the simulated directions of change of net CO_2 assimilation and of transpiration as a result of an experimentally in-
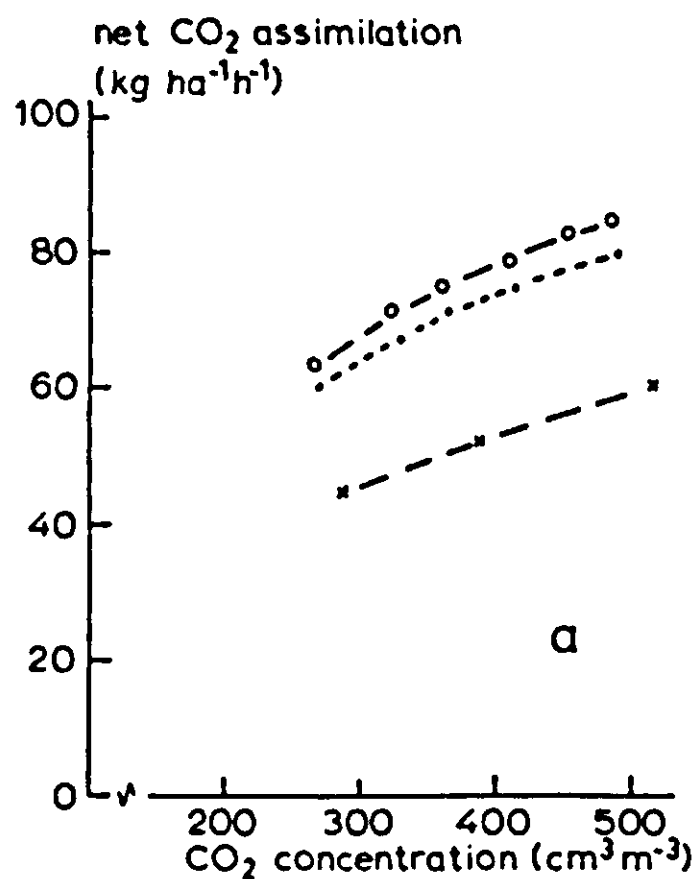
Figure 36a. The measured (x) and simulated (• : with regulating stomata; o : non-regulating stomata) response of the net CO_2 assimilation rate to the ambient CO_2 level at a constant light intensity ($330 \text{ J m}^{-2}\text{s}^{-1}$ artificial light) and temperature ($20\ ^{\circ}\text{C}$) on 2 August 1979.

duced increase of the ambient CO_2 level are similar to what has been measured. This indicates that stomata in the field plot plants, with old leaves by that time, were still regulating their stomatal conductance (Subsection 3.2.6). If not, the response curves would have had quite a different shape.

It is not surprising that differences develop between the simulated and the observed growth rate in a crop approaching maturity. By that time the redistribution of proteins and possibly of carbohydrates from vegetative parts towards pods is intensive. Those processes require quite some energy, but are not yet included in BACROS. In addition, senescence of leaves may have started, as a result of which leaf photosynthesis may decrease, which is another phenomenon that is not yet included. (We will come back to this in the Subsections 3.4.5 and 3.4.7). In fact, those two processes should decrease the growth rate even further
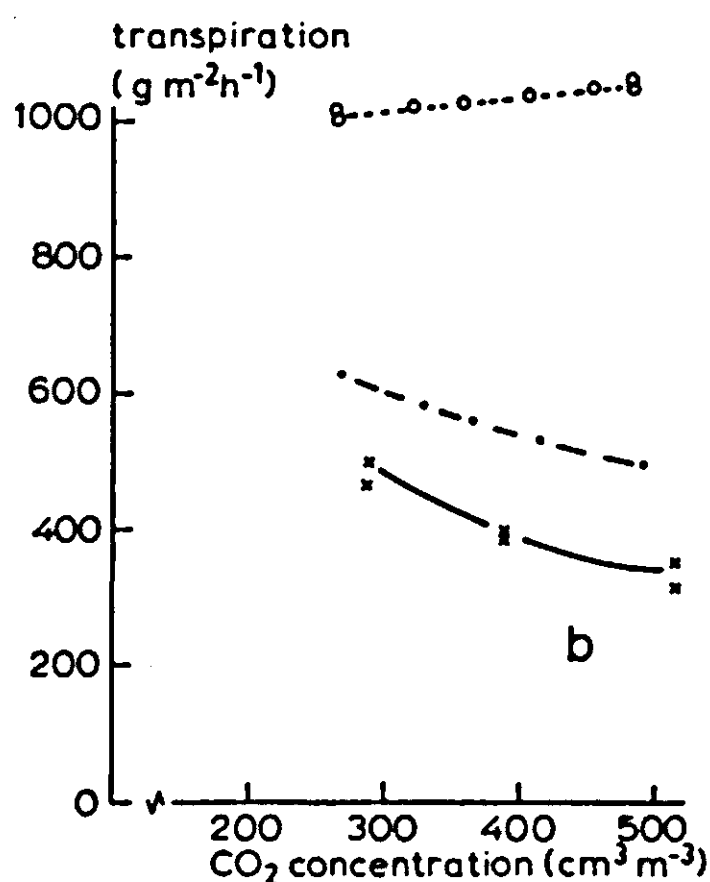
Figure 36b. The measured (x) and simulated (• :with regulating stomata; o : non-regulating stomata) response of the canopy transpiration rate in the experiment of Figure 36a.

than what is observed in Figure 34. The fact that the growth rate is still simulated fairly well may even be caused by a compensating underestimation of the rate of photosynthesis. Although further analysis of experimental and literature data is still required, it seems that at least one oversimplification leads to an underestimation of canopy photosynthesis: the CO_2 assimilation submodel in BACROS (Subsection 3.2.4) is based on the assumption of an instantaneous adaptation of the rate of leaf CO_2 assimilation to the incident light intensity. This may not be quite correct (Sager & Giger, 1980), and it could cause an underestimation by 20-30% of the rate of CO_2 assimilation of a canopy with fluttering leaves in bright, direct light; at lower light levels the underestimation would be less. The simulated maximum rate of canopy CO_2 assimilation in Figure 35 stays below the measured rate, which is an argument that supports this hypothesis.

3.4 Grain formation and assimilate partitioning in wheat

3.4.1 Introduction

Rather then presenting a straightforward analysis of processes and of assimilate partitioning and their simulation, it will be demonstrated that the subject of regulation of distribution of assimilates and of redistribution of carbohydrate and protein reserves is not as thoroughly understood as processes discussed in earlier sections. This contribution consists particularly of a discussion and the development of hypotheses for these phenomena, and of a presentation of models on partitioning of substrates among plant organs. These models are still in a preliminary stage of development (cf. Subsection 1.3.2).

This section contains three parts, which are all focussed on growth of wheat. The first part (Subsections 3.4.2 − 3.4.6) describes the physiological basis of regulation of assimilate partitioning and arrives at a static, descriptive model of grain production. The second part (Section 3.4.7 − 3.4.9) presents a simulation model of CO_2 assimilation and N redistribution in plants during the reproductive phase. The third part (Subsection 3.4.10) demonstrates how assimilate distribution over competitive plant organs, like tillers and grains, can be viewed and simulated.

Part I. Ear development, assimilate supply and grain growth of wheat

J.H.J. Spiertz

3.4.2 Sources and sinks

In cereals, grain yield is the ultimate goal and therefore the partitioning of dry matter between grains and vegetative parts is of great importance. The partitioning of dry matter depends on the relative sink strength of roots, leaves, stems and ears. After anthesis, the relocation of reserves from vegetative organs (e.g. stems) to the grains also plays an important role in assimilate distribution. Discussions on whether assimilate supply (= source) or storage capacity (= sink) limits yield refer mostly to the grain-filling stage, since most grain growth is supported by concurrent CO_2 assimilation rather than by stored reserves of carbohydrates. However, the sink or storage capacity for assimilates at the grain-filling stage is to a large degree determined by the extent of carbon (C) assimilation, nitrogen (N) assimilation and assimilate distribution before anthe-

WHEAT PLANT

genotype ——— WHEAT PLANT ——— environment

TILLERING

LEAF GROWTH / ROOT GROWTH — VEGETATIVE TILLERS — EAR INITIATION / EAR FORMATION — EARS

LIGHT + TEMP. TEMPERATURE

CROP CANOPY ROOT SYSTEM

CO₂ ASSIMILATION / RESPIRATION — POOL OF CARBOHYDRATES

NITROGEN-ASSIMILATION — POOL OF NITROGEN COMPOUNDS

NITROGEN SUPPLY

GRAIN GROWTH

FLOWERING / FERTILIZATION

GRAIN WEIGHT   GRAIN NUMBER

GRAIN YIELD

Figure 37. A scheme of factors and processes related to grain growth of wheat. Note that this scheme is not presented as a relational diagram (cf. Subsection 2.1.2).

sis, especially from ear initiation onwards. Thus, whether source or sink limits grain production depends on the balance between growth and development of the crop during the various stages of its life cycle.

A scheme of factors and processes related to grain growth of wheat is presented in Figure 37. Generally, crop physiology and simulation deal mostly with source-related processes (e.g. CO_2 exchange, light interception, transpiration); sink-related processes (e.g. formation and activity of structural or storage organs) are relatively neglected in experimental and simulation studies.

3.4.3 Crop development and ear formation

The development of a wheat crop is characterized by the succession of various phases with a specific pattern of crop growth. The three main phases are:
— germination and juvenile growth
— vegetative growth
— reproductive growth.

After emergence the seedling becomes dependent on its own C and N assimilation. The growth of the plant will initially be restricted by the size of the photosynthetically active organs and by the ability to absorb nutrients. Leaf growth is then essential for improving the light interception. Initially in most crops, leaf

137

area increases exponentially, because the expansion of the number of leaves and of leaf size occurs simultaneously.

A central problem in integration at the whole plant level is to establish what consequences the metabolic activities in one organ have on the balance of the system. For example, growth of roots into new volumes of soil may increase nutrient supply but it requires assimilates that might have been used in shoot growth. Brouwer (1963) developed the idea of a functional balance between the activities of shoots and roots in which each organ is dependent on certain unique functions of the other: leaves supply carbohydrates and lose water while roots supply the water and nutrients (cf. Subsection 3.3.6). The balance operates to restrict root or shoot growth depending upon whether root or shoot factors are limiting. There is evidence in literature that supports a role of N in such relationships. However, there is no obvious reason why comparable effects should not be caused by other nutrients; e.g. in the case of legumes by phosphate. Generally, N supply increases the shoot/root ratio of grasses (Ennik et al., 1980), with a clear tendency for the root mass to decrease with increasing N supply. During the early vegetative stage the roots and leaves are the dominant sinks, but from the onset of growth of storage organs these organs become the major sink.

In cereals and grasses the increase of leaf area is promoted supplementary by
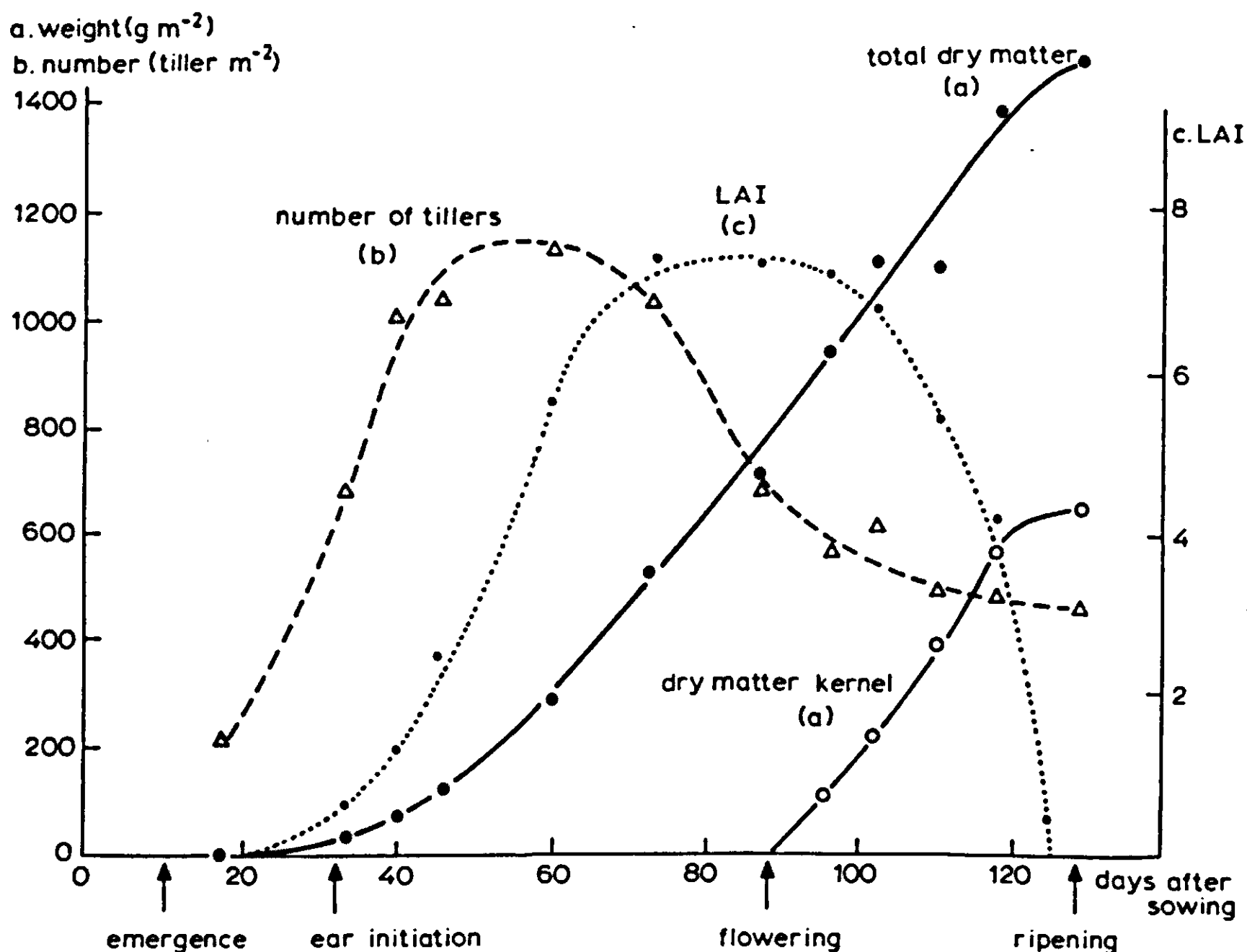
Figure 38. Course of shoot number, leaf area and dry matter production during the life cycle of spring wheat.

tillering (Figure 38; see also Subsection 3.4.10); in other crops a comparable effect is caused by branching of the main shoot. The maximum leaf area is attained at the moment that senescence of leaves offsets the increase in leaf area by formation of new leaves. Most crops can maintain a 'closed' canopy for two months or more. Reproductive crops with a determinate growing point, like cereals and maize, stop leaf growth before anthesis. After that stage, leaf area and photosynthetic activity are gradually declining due to ageing and subsequent senescence of the various leaf layers in an acropetal direction. The rate of leaf senescence depends on environmental conditions (temperature, water availability, nutrient supply, etc.) and on the occurrence of pests and diseases. An approach for modelling leaf growth is shown by Jones & Hesketh (1980).

The total sink strength and storage capacity is strongly associated in many crops with the number of storage cells in grains, seeds, tubers or roots. The morphogenesis of storage organs like grains is very important when considering the interdependence between growth and development and the relocation of assimilates to the various organs. The initiation of storage organs already takes place during the period of active vegetative growth. This very complex process is mainly under hormonal control but the development of storage organs is also strongly affected by environmental conditions that affect the availability of assimilates. The dynamic pattern of ear formation of cereals is shown in Figure 39. On average, ear initiation occurs in the four-leaf stage of a shoot, which coincides with tillering for the main shoot and the first tillers. Thus, even in the beginning a competition exists between the development of 'reproductive' shoots and the formation of new tillers. Late tillers suffer most from competi-
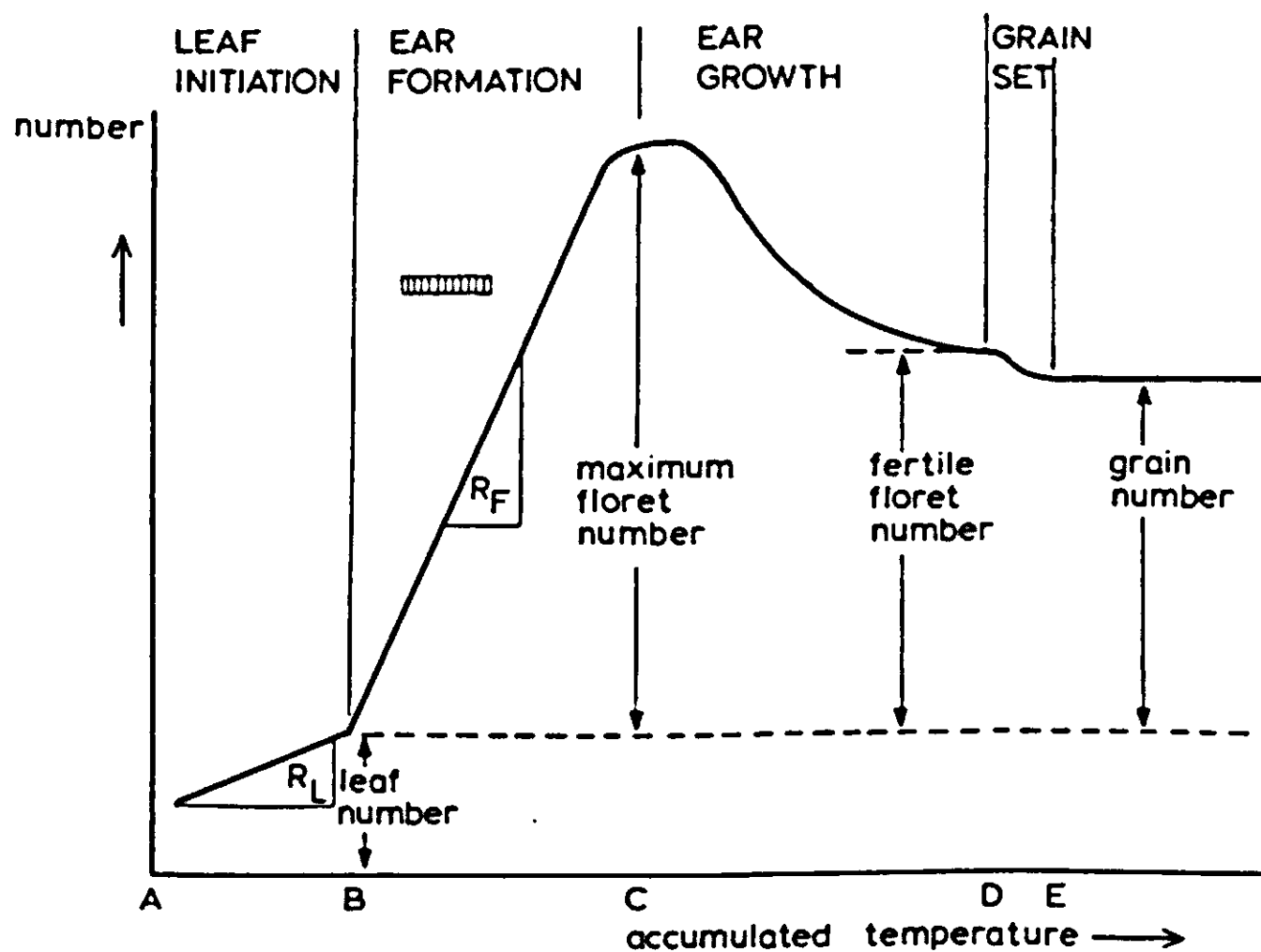
Figure 39. A general scheme for grain formation in cereals. R_L and R_F are the average rates of leaves and floret initiation, respectively; ▦▦▦ represents the period during which double ridges first become visible (after Gallagher, 1979).

139

tion and do not become fertile in a dense stand. The formation of spikelets and florets in a fertile shoot shows a great plasticity. Out of nine floret primordia in a spikelet on a central position of the spike, only 2-4 florets develop a grain. This plasticity in sink formation acts as a mechanism for adaptation to constraints in the growth conditions, but also for compensating a low number of fertile tillers.

Most of the endosperm is formed during the cell division phase following anthesis and fertilization of the florets; cell division ceases approximately two weeks after anthesis. Differences in cell number in the wheat endosperm due to a variety of causes (irradiation levels, water supply, intergrain competition) have been shown to result from variation in the rate of production of cells with the duration of the cell division phase being unaltered (Brocklehurst, 1979). These results suggest that the rate of production of endosperm cells is associated with the level of carbohydrate available to the grain, but it is not clear whether this is a causal relationship.

The levels of one or more phytohormones may regulate, as intermediates, the rate of cell division; a possible group of regulatory compounds are the cytokinins (see Figure 40). During grain development in wheat, the maximum level of each phytohormone varies with the maturity stage. The sequence is cytokinin, gibberellin, auxin and abscisic acid. The validity of the conclusions drawn from determination of endogenous hormones is limited due to the complexity of the hormonal relationships.

3.4.4 Assimilate supply and grain number

The maximum weight of individual kernels is under genetic control, and is relatively stable under disease- and pest-free conditions. Under conditions when
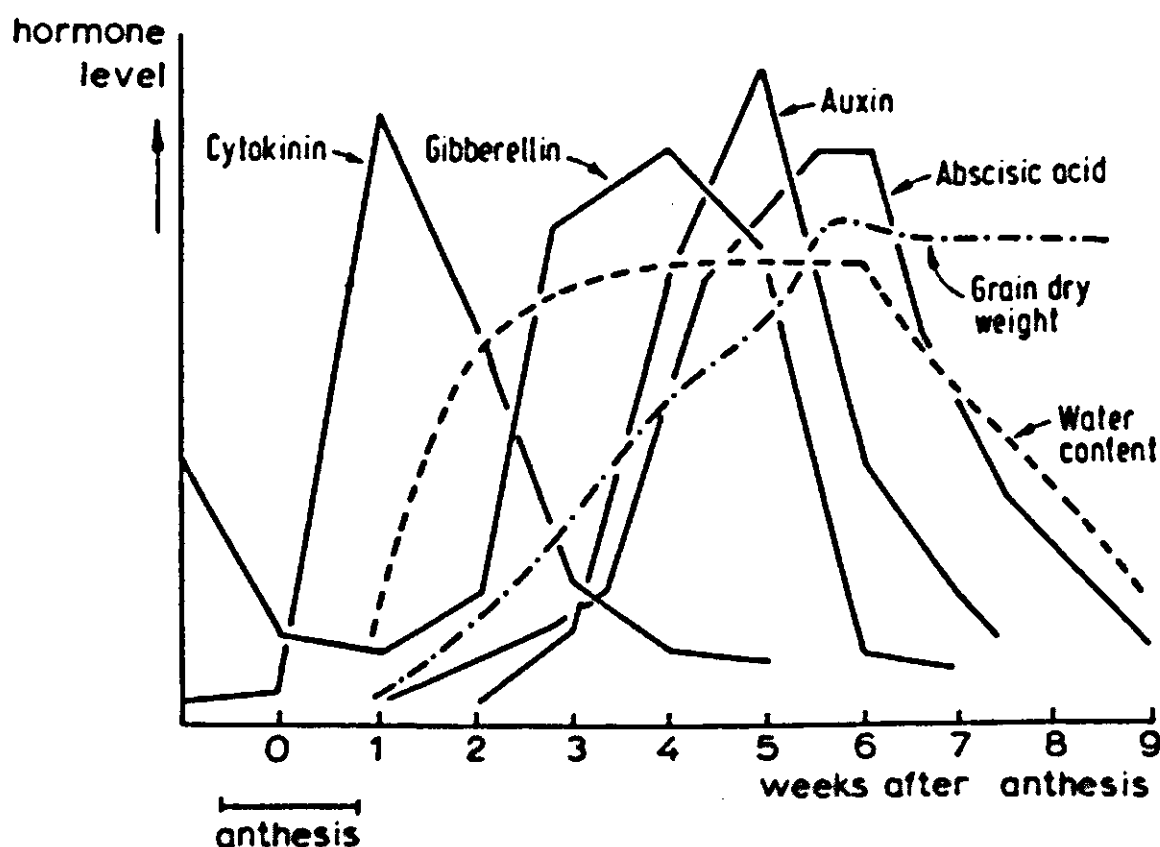
Figure 40. Endogenous levels of plant hormones in the developing wheat ear (after Gale, 1979).

140

this maximum weight is reached, the grain yield is directly related to the number of kernels. Hence, for temperate climate and optimal water and nutrient supply, the grain yield appears to depend more on the storage capacity than on assimilate supply. The number of grains, however, shows a strong response to environmental conditions. Therefore grain yield is quite often more strongly related to grain number than to grain size. Under temperate growing conditions at least 18-20 000 grains per square metre are required to achieve maximum grain yields. Clearly, actual grain yield might be below the potential level due to a low number of grains as well as to a low degree of grain filling. Grain weight often decreases with a rise in grain number due to mutual competition between grains for assimilates.

A close association between number of grains (N_g) per square metre and total above-ground dry matter yield at final harvest (DW_h) in g m^{-2} could be derived from data of a field experiment with winter wheat (Spiertz, 1980). This association can be represented by the following equation:

$$N_g = 12.4\,DW_h + 270 \qquad R^2 = 0.88 \qquad (49)$$

Assuming that dry matter yield at anthesis is reflected by the straw yield at final harvest, the ratio between grain number and dry matter yield at anthesis amounts to about 20 kernels per gram dry weight. Rawson & Bagga (1979) found a good correlation between the number of grains per main ear and the ratio total visible radiation:accumulated degree-days between sowing and anthesis. Differences in the ratio between grain number and dry weight at anthesis might be explained by the rate of net CO_2 assimilation per unit degree-day. This parameter can be used to compare the relative availability of assimilates for growth in plants with a different rate of development. CO_2 assimilation is only slightly influenced by temperature in contrast to the rate of development, which is strongly affected. High temperatures shorten the period from ear initiation to anthesis, thus reducing supply of assimilates to the ear relative to the rate of development.

3.4.5 Assimilate supply and grain growth

Genetic differences between cultivars in dry matter distribution during ear formation may also play an important role. Generally, modern semi-dwarf cultivars produce more grains per unit dry weight than older long strawed cultivars, which is associated with a more favourable dry matter distribution to the ear before and after anthesis. The harvest index of modern cultivars, the weight of the grain relative to the total final shoot weight, ranges from 0.45-0.55. The major processes involved in grain filling are carbohydrate and protein conversion and accumulation. Carbohydrates may be derived from current CO_2 assimilation and from stem reserves (Figure 41). The carbohydrates are translocated as sucrose and in the grain endosperm converted into starch. Nitrogenous compounds for grain growth are mainly supplied by the vegetative parts and only to a smaller extent derived from post-anthesis uptake. Generally, the following
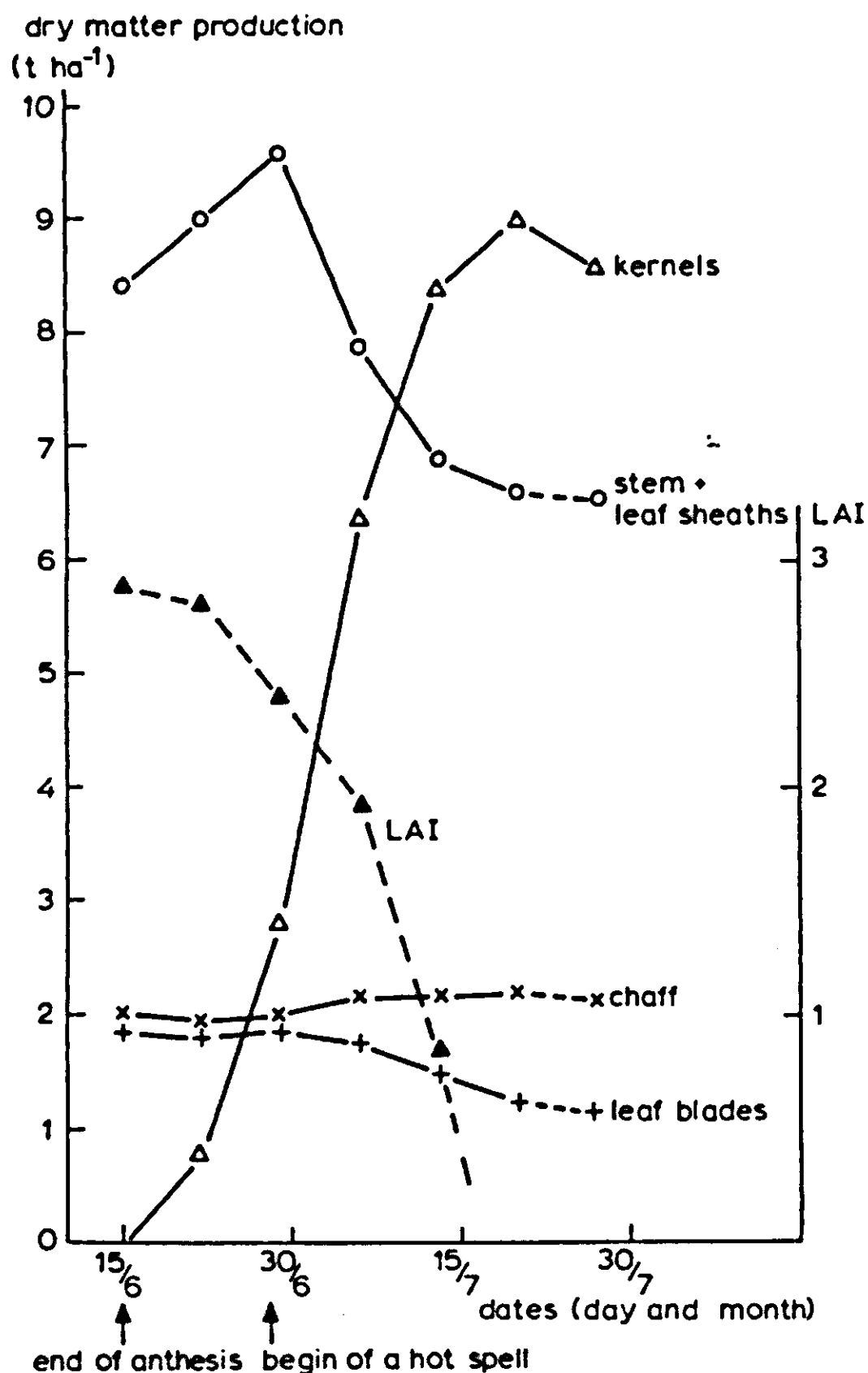
Figure 41. Dry matter distribution in wheat after anthesis (cv. Lely, fertilization with N at 200 kg ha^{-1}; 1976).

equation represents the post-floral balance of assimilates:

$$\text{STORAGE IN GRAINS} = \text{ASSIMILATION} + \text{MOBILIZATION OF RESERVES} \tag{50}$$

The rate of assimilate accumulation by grains is strongly governed by temperature; a rise in temperature enhances carbohydrate as well as N accumulation. N relocation and protein accumulation show a stronger response to temperature than carbohydrate accumulation. A high rate of grain growth can only be maintained with an ample assimilate supply. Because of the high rate of grain growth and a reduction of current net CO_2 assimilation, stem reserves may deplete very fast under warm growing conditions. It was found that the contribution to grain yield of assimilates stored prior to grain filling varies from 500 to 1500 kg ha^{-1}. However, the amount of mobile carbohydrates present at the end of anthesis ranges from 1500 to 3000 kg ha^{-1}. A large part of these reserves is apparently used in respiration processes or transported to the roots.

142

Adverse conditions during the grain filling period accelerate the depletion of N reserves in the vegetative parts of the wheat plant. This N depletion, especially of the leaves, might accelerate leaf senescence and thus reduce CO_2 assimilation towards the end of the growing season. It has been shown that late top dressings of N with control of pests and diseases increase the N content of the leaves and can delay their senescence. Under optimal conditions of water and nutrient supply the rate of crop CO_2 assimilation has been shown to remain at a constant level for about 3-4 weeks after flowering, after which there was a linear decline over the next 2-3 weeks.

The duration of maximum grain growth (D, in days) may be derived from the following equation:

$$D = R/(R_g - R_a) \tag{51}$$

in which R is the amount of crop reserves in kg ha^{-1}, R_g the rate of grain growth in kg ha^{-1} d^{-1} and R_a the rate of current assimilation or supply in kg ha^{-1} d^{-1}. For instance, for optimal supply of carbohydrates, Equation 51 becomes:

$$D = \frac{\text{Available carbohydrate reserves}}{\text{Rate of carbohydrate accumulation} - \text{Rate of net } CO_2 \text{ assimilation}}$$

$$= \frac{1500 \text{ kg ha}^{-1}}{(200 - 150) \text{ kg ha}^{-1} \text{ d}^{-1}} = 30 \text{ d}$$

and for optimal nitrogen supply:

$$D = \frac{\text{Available N reserves}}{\text{Rate of N accumulation} - \text{Rate of post-floral N uptake}}$$

$$= \frac{81 \text{ kg ha}^{-1}}{(4 - 1) \text{ kg ha}^{-1} \text{ d}^{-1}} = 27 \text{ d}$$

This concept is included in a dynamic simulation model in Subsections 3.4.7 and 3.4.9.

3.4.6 Nitrogen use, growth and grain yield

The uptake of N by a wheat crop depends on the amount of available soil N and the recovery of fertilizer N. The amount of N uptake without N dressing is associated with the nitrate made available from soil organic matter and with rooting characteristics (root length and activity). The efficiency of utilization of N by the wheat crop, defined as the amount of grain produced per unit N absorbed, is determined on the one hand by the N harvest index and on the other hand by the N concentration in the grain. The N harvest index (NHI), the proportion of the total amount of N in the plants that is present in the grains at the harvest, usually ranges between 0.74 and 0.82. If, however, during the grain-filling stage a water shortage develops, translocation of N from the vegetative

tissue to the growing grains may be hampered, resulting in a lower N harvest index, thus decreasing the N use efficiency. This effect may become even stronger, when the moisture stress leads to accelerated senescence of the photosynthetic tissue. The developing grain cannot be properly filled so that at harvest kernels have a high protein content and a low dry weight, in extreme situations leading to shriveled grains.

With regular N supply to the plants, on average about 65% to 80% of the grain N was derived from the vegetative parts, the remainder originating from uptake by the roots after anthesis. Available N for relocation to the grains can be derived from N content of the crop at anthesis minus N residues in straw and chaff. The former amounts to about 150 kg ha^{-1} and the latter to about 60 kg ha^{-1} for an average wheat crop in the Netherlands. Mobile N for relocation to the grains is contributed by the leaves (40%), the stem and leaf sheaths (40%), and chaff (20%).

The rate of N accumulation in the grains is determined by dry matter growth rate and the N concentration of the grain. A growth rate of 200 kg ha^{-1} d^{-1} and a N concentration of 20 g kg^{-1} results in a N accumulation rate of 4 kg ha^{-1} d^{-1}. At low N levels the relation between grain yield and total N uptake in the grain is linear with a slope of about 60 kg kg^{-1}. At higher N supply levels the yield response curve deviates from the straight curve, reflecting an increase in the N content of the grains. The level of the plateau where increased N uptake does not result in higher grain yields is determined by other limiting factors (e.g. water shortage, diseases and pests) (cf. Subsection 1.2.3).

Increase in supply of N to grains cannot be obtained by further increasing the concentration of N in vegetative tissue, because this is strongly associated with the adverse effects of a too leafy wheat crop (risk of lodging and increased susceptibility to diseases). A substantial post-anthesis N uptake is therefore a prerequisite for achieving high grain yields.

Part II. Modelling of post-floral growth of wheat

J. Vos, E.M. Drees and F.W.T. Penning de Vries

3.4.7 Description of the model

This section deals with aspects of modelling post-floral growth of wheat. A detailed treatment of such a model is described by Vos (1981). The model describes and interrelates gross CO$_2$ assimilation, respiration, accumulation of carbohydrates (starch) and proteins in the grains, redistribution and additional uptake of N and leaf senescence. Structural growth of all organs except grains is assumed to have ceased at anthesis. Grain dry matter is assumed to consist of carbohydrates and protein only. The model is designed to run with time steps of one day. Besides crop characteristics at anthesis, daily records of irradiation and

mean temperature have to be given as input. Effects of pests, diseases and water stress are not accounted for.

Daily gross CO_2 assimilation is computed by a set of equations described by Goudriaan & van Laar (1978); these are also described in Subsection 3.2.4. Here it is relevant to note that a reduction of AMAX (photosynthetic capacity at saturating irradiation per unit green area) of remaining green area as a result of senescence appeared to be necessary. Based on only limited experimental evidence, AMAX is assumed to decline in proportion to the decline of the green area.

Due to senescence, the area of green photosynthesizing tissue decreases in the grain-filling period. In this model, the reduction is related almost proportionally to the fraction of N in the leaves at anthesis that is exported to the grains. To account for the contribution of stems and ears to canopy CO_2 assimilation, the total green area is assumed to be 2.2 times that of the leaf blades at any time. Growth respiration of grains is computed using the CO_2 production factors for synthesis of carbohydrates from glucose and proteins from amino acids, given by Penning de Vries (1975) (cf. Subsection 3.3.4). The application of constant factors for maintenance and transport processes (Penning de Vries, 1975; de Wit et al., 1978) appeared to lead to an unacceptable underestimation of measured respiration rates. Respiration of non-grain organs is therefore computed with empirical coefficients (decreasing the explanatory nature of this model). These coefficients are temperature dependent with a Q_{10} of 2.0.

The grain-filling period (Figure 42) can be subdivided into three consecutive stages. During the first 10 days, the grain growth rate is generally small (endosperm cell formation); this is called the lag period. During the second stage the grain growth rate is almost constant; it extends over most of the grain-filling period and it is often called the linear stage of grain filling. During the third or maturation stage the rate of dry matter accumulation can be small. At any day the accumulation rate of grain constituents ($g\ m^{-2}$) is given by the product of the number of kernels per square metre (NOKER) and the growth rate per kernel. The number of kernels is fixed at the beginning of grain filling: NOKER is estimated very satisfactorily by the equation:

$$NOKER = 3500.0 + 14.0 * CRDWAN \qquad (52)$$

where CRDWAN stands for the dry weight of the crop at anthesis ($g\ m^{-2}$).

Exponential growth is assumed during the lag period. The relative growth rate is 0.3 $g\ g^{-1}\ d^{-1}$ at 16 °C, with a Q_{10} of 2.0. During the lag period the protein accumulation rate is fixed at 0.17 times the carbohydrate accumulation rate.

Exercise 51
Write statements describing the exponential growth during the lag period and account for the temperature dependency.
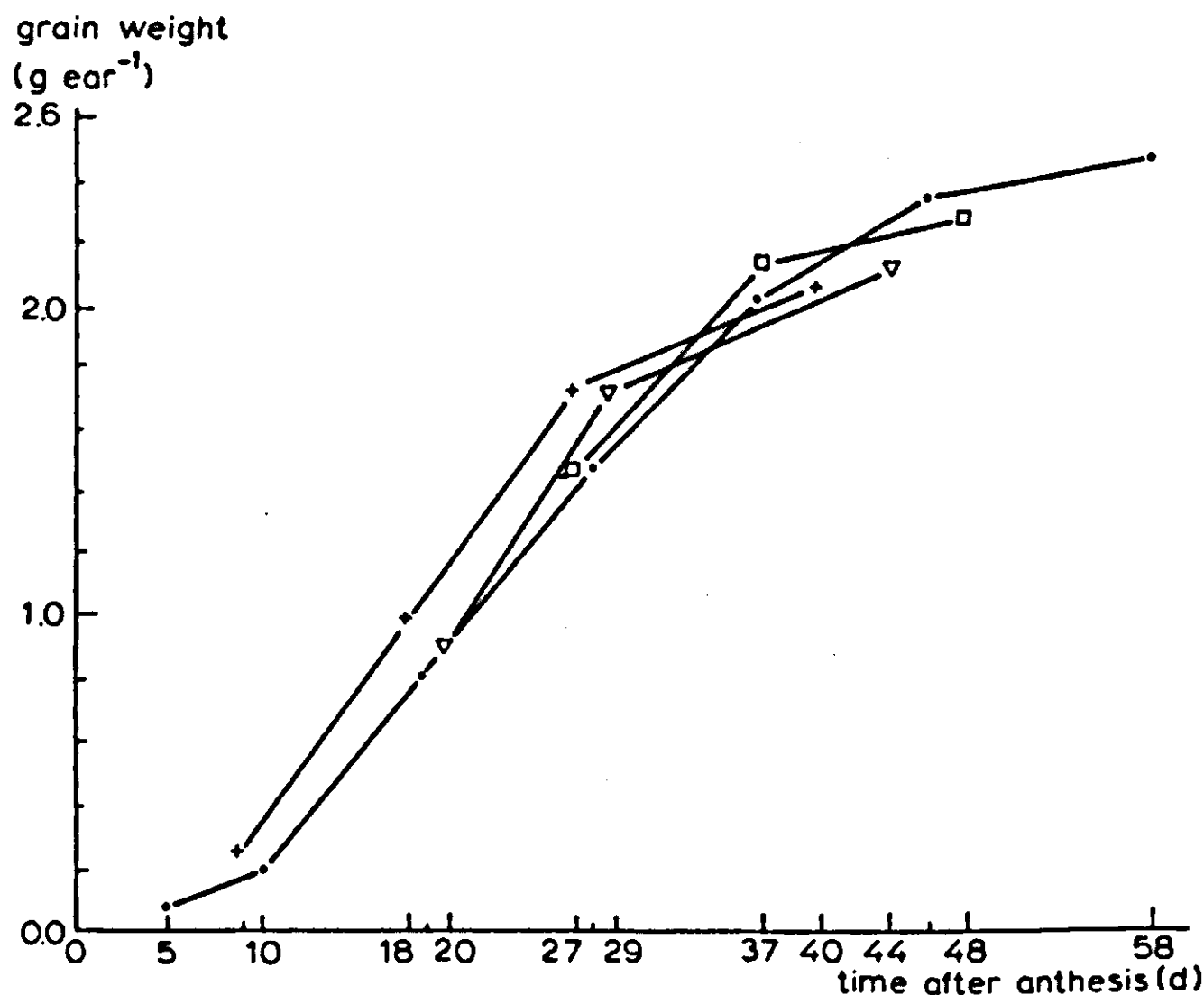
Figure 42. Change with time in grain dry weight as affected by air temperature. Data from Vos (1981). Treatments: • air temperature constant 16 °C; +, ∇ and □ transferred from 16 to 22 °C air temperature at 6, 17 and 24 days after anthesis, respectively. Root temperature 16 °C in all treatments.

Grain growth can be programmed to switch from exponential growth to linear growth when the exponential growth rate becomes equal to or larger than the (potential) growth rate during the linear stage. This last growth rate can be in the order of 25 g m^{-2} d^{-1} at 16 °C, with a Q_{10} of 1.5. The virtue of this approach is that it predicts an earlier transition from the lag period to the linear stage the higher the temperature (Figure 42).

Exercise 52
Which CSMP statements can be used for such transitions? Try this approach by simulation of the grain growth during the lag and linear period at high and low temperatures. Initial grain weight at 7.5 g m^{-2}.

The potential rates of accumulation of carbohydrates and proteins per grain (PRCHA and PRPRA, respectively) are taken to be constant during the linear stage and the maturation period at a reference temperature. As indicated before (Subsection 3.4.4) protein deposition in grains responds more to temperature (Q_{10} = 2.) than carbohydrate accumulation (Q_{10} = 1.5).
Gross CO_2 assimilation provides carbohydrates to the reserve pool (cf. Sub-

146

section 3.3.3), which is supposed to be situated in the stems only. Carbohydrates of this pool are consumed by accumulation of carbohydrates (starch) in the grain plus the associated growth respiration, growth respiration associated with protein deposition in grains, and respiration of non-grain organs. When daily gross carbohydrate production decreases and the supply of carbohydrate from the pool of reserves becomes smaller than the daily demand, carbohydrate accumulation in grains is the first process which is slowed down.

Daily 'demand' for protein by the grains is given by the product of the number of grains per square metre and the potential accumulation rate per grain. Sources of N for protein synthesis are additional uptake from the soil and removal from non-grain parts. Analyses of several experiments revealed a relationship between the contribution to final grain N yield by additional N uptake plus N removal from roots (treated as one variable, called MXRCRS: maximum relative contribution by roots and soil) and the initial N concentration in shoot dry matter at anthesis (Figure 43). This figure shows that the contribution to final N yield by uptake and removal from roots (calculated as the N content of grains that did not result from removal from aerial organs) decreases at higher initial shoot N concentrations. Furthermore, approximately similar relative distributions of shoot N (over ear structures, leaf blades and stems plus sheaths) were observed at the beginning and the end of the grain-filling period.

These feature allow modelling of the N regime of the reproductive wheat crop. The proportion of the daily N demand of grains to be supplied by additional uptake plus removal from roots (MXRCRS) is determined as displayed by Figure 43. The complementary fraction of the daily demand ($=$ 1. $-$ MXRCRS) is supplied by non-grain aerial parts, whilst the proportion of this fraction that is contributed by each of the various organs is equal to the proportion of shoot N initially present in these organs. (Note that this description is empirical, and may not apply in other situations of, for example, soil fertility.)

Export of N from non-grain shoot organs becomes reduced when the N concentration in the dry matter of these organs decreases below about 4 mg g^{-1}. When the minimum N concentration in the shoot (3.5 mg g^{-1}) is reached, protein accumulation in grains stops. The reduction of N supply from the roots is supposed to occur parallel to reduction from vegetative shoot organs.
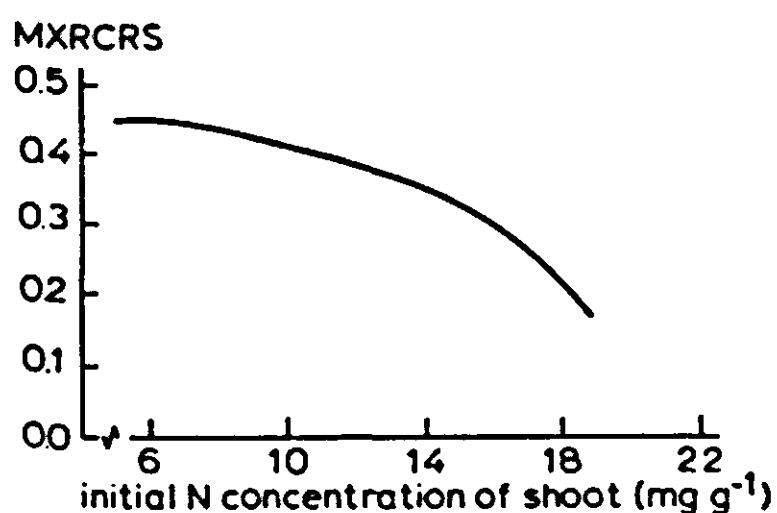
Figure 43. The relation between the relative contribution to final grain N yield by N uptake from the soil plus N removal from roots ($=$ MXRCRS) and the initial concentration of N in shoot dry matter at anthesis.

147

The duration of the grain-filling phase can be limited by the availability of either carbohydrates or N, but there is also a physiological maximum to this phase. This maximum duration can be described reasonably well by the simple degree-day concept (cf. Subsection 3.3.2): the period between anthesis and maximum grain dry weight can be approximated by a heat sum (HSUM) above a minimum temperature (TMIN). The rate of development (DVR) during this phase was calculated from the mean daily temperature (TEMP) as follows:

$$DVR = (TEMP - TMIN)/HSUM$$

Appropriate values for TMIN and HSUM are 6 °C and about 500 degree-days, respectively. The stage of development, DVS, is assigned an initial value of 0. and is augmented daily by DVR. When DVS reaches the value 1.0 the grain-filling period is complete.

3.4.8 Validations and extrapolations

The model was cross-checked with results of several field experiments. In general good agreement between measured and simulated courses of grain growth and N (re)distribution could be obtained by adjustment of three parameters, viz. AMAXI (the initial value of the photosynthetic capacity per unit green area), and the potential accumulation rates of grain constituents, PRCHA and PRPRA. The range in grain yields of those crops was between 400 and 850 g m^{-2}. However, the range in values for AMAXI required to reach agreement between measured and simulated results seems too wide to be biologically realistic, viz. from 1.5 to more than 3.0 g m^{-2} h^{-1}. The reasons for this are not clear.

Ranges in required values for PRCHA and PRPRA were comparatively smaller. These rates are partly specific for each genotype. The ratio between PRCHA and PRPRA varies between about 7 and 9 at moderate temperatures.

With respect to carbohydrate consuming processes the following comments can be made. There are enough indications pointing at the validity of Penning de Vries' (1975) coefficients for growth respiration. However, growth respiration of grains constitutes at its maximum 30% of total plant respiration only. Respiration of non-grain organs was computed by empirical coefficients. This treatment gave rise to total plant respiration rates, which were likely to be in the correct order of magnitude, but erratic predictions of the rate of this major respiratory component might occur when the model is applied in a wider range of conditions. Furthermore, there might be another drain of assimilates which was not and cannot be treated in sufficient detail yet, viz. the flux of assimilates to the root or root medium. This aspect seems to require more study.

Assimilate partitioning is comparatively simple as there is only one site for growth, viz. the grains. Potential accumulation rates per unit land area for carbohydrates and proteins in grains cannot be derived accurately enough from the state of the crop at anthesis. Usually there is a direct relation between the number of grains per square metre and the shoot vegetative biomass, but the

148

parameters of the regression vary considerably between experiments (Equations 49 and 52) and genotypes (Vos, 1981). Potential accumulation rates per grain differ between cultivars and are possibly affected by environmental factors until the number of endosperm cells is fixed. In conclusion it can be stated that modelling of grain growth (at a reference temperature) per unit area (as composed of rate per grain times number of grains) requires further analysis. Subsection 3.4.10 shows an attempt to do so. So far, the description of the difference in temperature sensitivity between carbohydrate and protein accumulation in grains proved to be satisfactory.

The treatment of the N regime, which turned out to be fairly useful, is in fact based on a generalized observed pattern of redistribution, without giving much explanation. Adaptations will be required when other factors, like water stress and diseases, are introduced into the model.

Under otherwise similar conditions grain dry matter yield in the field was predicted (Vos, 1981) to be smaller by 30 to 40 g m^{-2} per 1 °C rise in temperature throughout the grain-filling period (Dutch climate and crop management). A concomitant increase in visible radiation by 130 to 180 J cm^{-2} d^{-1} could offset the adverse effect of such a rise of temperature. Model calculations showed little effects of temperature and irradiation on grain N yields. Saturation type of response curves were predicted for grain dry matter yield and final grain N concentration versus initial shoot N concentration (at a fixed crop dry weight at anthesis). Yield increases of about 15 to 20% were predicted when the initial N concentration of the shoot is increased from low (8 mg g^{-1}) to high values (about 16 mg g^{-1}); final N concentration in grain dry matter would increase from about 15 to more than 20 mg g^{-1}.

3.4.9 A simple model of the carbohydrate-nitrogen interaction

The modelling of the economy of carbohydrates and nitrogenous compounds has been described separately. In whole plants, however, both processes interact. To demonstrate this with a small program, a simplified though basically realistic approach to C and N availability during grain growth, is described. This simple model is somewhat different from the model described before. In addition the effect of temperature has been omitted, and the example is based on values for 16 °C.

The dry weight of the grains (GDW, g m^{-2}) is calculated from the actual growth rate of the grains (GGR, g m^{-2} d^{-1}). The potential growth rate (PGR) depends on the number of kernels and the potential rate of carbohydrate (as grain) accumulation (PRCHA, g grain^{-1} d^{-1}). It is assumed that grains consist of 12.5% proteins in a standard situation, the rest of the biomass being carbohydrates. The actual growth rate is the minimum value of the potential growth rate and the growth rates determined by the availability of C (GRC) or of N (GRN) (for all abbreviations and constructions not explained here, one is referred to previous sections):

149

```
GDW      = INTGRL(0., GGR)
GGR      = AMIN1(PGR, GRC, GRN)
PGR      = NOKER*PRCHA/0.875
PARAM PRCHA = 0.00090
GRC      = PGR*RED1
RED1     = AFGEN(REDTB1, ACH/WVEG)
FUNCTION REDTB1 = 0., 0., 0.01, 0.0, 0.05, 1., 1., 1.
```

ACH is the available carbohydrates (g m^{-2}); WVEG is the dry weight of the vegetative mass (g m^{-2});

```
GRN      = PGR*RED2
RED2     = AFGEN(REDTB2, AN/WVEG)
FUNCTION REDTB2 = 0., 0., 0.0001, 0., 0.0005, 1., 0.1, 1.
```

AN is the available nitrogen (g m^{-2});

```
ACH      = INTGRL(ACHI, GPHOT-RNGO-CAG-MRG)
```

ACHI represents the available carbohydrates at flowering, GPHOT the actual photosynthesis (g m^{-2} d^{-1}), RNGO the respiration of non-grain organs (g m^{-2} d^{-1}), MRG the maintenance respiration of the grains (g m^{-2} d^{-1}) and CAG the carbohydrate accumulation in the grains (g m^{-2} d^{-1}).

```
CAG      = GGR/CVF
PARAM CVF = 0.73
MRG      = 0.005*GDW
RNGO     = WVEG*0.01
PARAM WVEG = 800., NOKER = 15000., ACHI = 160., GPHOTS = 30.
GPHOT = GPHOTS*AFGEN(REDTB3, ACH/WVEG)*...
          AFGEN (REDTB4, AN/WVEG)
```

GPHOTS is the standard rate of photosynthesis (g m^{-2} d^{-1}), RED3 is the reduction factor for photosynthesis as a consequence of too much available carbohydrates and RED4 represents senescence: it is the reduction factor of photosynthesis as a consequence of too little available N.

```
FUNCTION REDTB3 = 0., 1., 0.20, 1., 0.25, 0., 0.30, 0.
FUNCTION REDTB4 = 0., 0., 0.0001, 0., 0.001, 1., 0.01, 1.
```

```
AN        = INTGRL (ANI,UPTAKE-NAG)
```

The available N is the amount of N that can be translocated to the grains. The minimum level in the vegetative shoot, below which N is no more available, is 0.0035 g g^{-1}. FNS is the initial fraction of N in the shoot and determines the initial amount of N (ANI). ANI should be calculated in the intitial section.

```
ANI      = WVEG*(FNS-0.0035)
```

The uptake of N (g m^{-2} d^{-1}) in dependence of FNS is given in Figure 43.

```
UPTAKE  = DEMAND * MXRCRS
DEMAND  = NOKER * PRPRA * 1./5.95
PARAM  PRPRA = 0.00013, FNS = 0.010
MXRCRS  = AFGEN(MXTB, FNS)
FUNCTION MXTB = 0.0035, 0.45, 0.006, 0.45, 0.01, 0.4, 0.014, 0.35, ...
                0.08, 0.225
NG      = INTGRL(0., NAG)
```

NG is the amount of N in the grains (g m^{-2}). NAG is the rate of N accumulation in the grains (g m^{-2} d^{-1}), which is a fraction (PRPRA/(PRCHA*5.95)) of the actual growth rate of the grains. This fraction can be altered by the ratio of available N and available C: the reduction factor RED. Proteins are 5.95 times heavier than the N that they contain.

```
NAG     = GGR * 0.875 * PRPRA/(PRCHA * 5.95) * RED
RED     = RED2/AMAX1(0.5, RED1)
```

When the temperature is 16 °C the period between anthesis and maximum grain dry weight is 50 days.

Exercise 53

a. Run the program (with RKSFX and DELT=1.) and study the results, in particular of the course of the factors that limit grain growth. What happens when the initial N concentration of the shoot is higher (0.015) or what if the standard rate of CO$_2$ assimilation is lower (25.)? Check the harvest index for dry matter (DHI) and for N (NHI) with those of Subsections 3.4.5 and 3.4.6.

b. What range of concentrations of N in the daily weight increment of grain is implied in this formulation of grain growth?

Part III.   A deterministic approach to modelling of organogenesis in wheat

H. van Keulen

3.4.10   A preliminary model of organogenesis

The descriptive Equations 49 and 52 to calculate the number of grains per square metre are based on the weight of the crop at harvest and at anthesis, respectively. As a result of environmental conditions, among others, the constants in the equations are different for each new growing season. Although knowledge of the factors that govern kernel formation is still little developed, the pre-

liminary model on organogenesis presented below may clarify why a crop ends up in many cases with a number of kernels that matches more or less the carbohydrate supply in the post-anthesis phase. In the previous subsections attention is drawn to the fact that initiation and development of plant organs is governed by the interactive effects of genetic properties and environmental conditions. The necessary information is probably transmitted in the plant through hormonal levels. However, quantitative information on production and breakdown of plant hormones as affected by external and internal conditions, as well as on the influence of certain levels of these substances on relevant processes, is insufficient at the moment to keep track of such state variables in crop growth models. An alternative approach, which takes into account concepts outlined in foregoing subsections, was illustrated for tiller formation in Rhodes grass by Dayan et al. (1981). In this description the formation of new plant organs depends on the current supply of carbohydrates and the number of organs already present to utilize these assimilates, mimicking apical dominance. In basically the same way, this description is applied here to a wheat crop. The influence of a low availability of N is not considered, which implies that this preliminary model of organogenesis does not apply at levels of production where nutrient shortage is predominant.

First the number of tillers per ha is defined in an integral:

ANT = INTGRL (TLNI, RTF)

in which TLNI is the initial number of tillers per ha. The rate of tiller formation is described by:

RTF = (MXNT − ANT)/TCTF

in which TCTF is a time coefficient for tiller formation (d). MXNT, the maximum number of tillers per ha that could be supported at a particular moment, is obtained from:

MXNT = CHAVG/CHMPT

in which CHAVG is the carbohydrate supply for vegetative growth in kg ha^{-1} d^{-1} and CHMPT the flux of carbohydrates that can be monopolized by one tiller in kilogram per tiller per day. The value of the latter variable is supposed to be related to the rate of development (DVR, defined as in Subsections 3.1.2 and 3.3.2) as follows:

CHMPT = CHMPTB/(DVR ∗ 1.43)

in which CHMPTB is the 'basic' flux of carbohydrates that can be monopolized per tiller. CHMPTB is introduced in the model as a parameter and is cultivar specific, there being distinctions between prolific tillering varieties and those producing only limited numbers of tillers. It is as yet not possible to determine its value from independent measurements and it has to be derived from com-

parison between cultivars. This formulation ensures that final tiller number is mainly determined by assimilate supply and not by the length of the vegetative period for a given variety in accordance with experimental evidence.

In the present version of the model no distinction is yet made between tillers of different age in terms of assimilate supply or physiological characteristics.

During the period of ear initiation, which coincides partly with that for tiller formation, the rate at which ears are initiated is given by:

$$REARI = (ANT - EARN)/TCEI * AFGEN(CHPTT, CHPT)$$

with EARN as the number of already initiated ears per ha, CHPT = CHAVG/ANT as the available carbohydrates per tiller per day and TCEI as time coefficient for ear initiation (d). The value of CHPTT varies between 1. and 0.

After anthesis, those tillers that fail to become reproductive gradually die off. Especially translocation of N to the remaining tissue may take place and this is taken into account. Redistribution of C compounds is not considered.

The rate of spikelet differentiation per ear in the next stage is described by:

$$RSPLF = MXRSF * AFGEN(CHFPET, CHFPE)$$

in which MXRSF is the maximum rate of spikelet differentiation (number ear^{-1} d^{-1}) and CHFPE = CHAVG/EARN, the value of CHFPET again varying between 1. and 0.

$$SP = INTGRL(0., RSPLF)$$
$$SPNR = SP * EARN$$

in which SP is the number of spikelets per ear and SPNR the number of spikelets per hectare. The final spikelet number is thus affected both by the time available for initiation (high temperatures will shorten the development period available for spikelet formation) and by conditions governing assimilate supply (leaf area index, level of irradiance).

Spikelets may also be aborted — or cease further development — when the assimilate supply reaches very low levels. The carbohydrate 'maintenance' level for spikelets is set rather arbitrarily at one tenth of the value necessary for maximum development.

Finally the number of grains developing per spikelet (GN) is determined in dependence on the assimilate supply per spikelet (CHFPSP) during the appropriate development stage:

$$GNPSP = GNMIN + (GNMAX - GNMIN) * AFGEN(CHFPST, \ldots$$
$$CHFPSP)$$
$$RFGF = (SPNR * GNPSP - FGNR)/TCT$$
$$FGNR = INTGRL(0., RFGF)$$
$$GN = FGNR/SPNR$$

in which RFGF is the rate of grain formation (number ha^{-1} d^{-1}), GNPSP the maximum possible number of grains per spikelet determined by the supply of

assimilates per spikelet, GNMAX and GNMIN the maximum and minimum number of grains per spikelet, respectively, FGNR the total number of grains per hectare, and TCT the time coefficient for grain formation (d). CHFPSP = CHAGG/SPNR, CHFPST assumes a value between 1. and 0., CHAGG is the flux of carbohydrates available for grain growth, the flux of nitrogenous compounds is ignored for the time being. FGNR corresponds with N_g in Equation 49 and NOKER in the Subsections 3.4.7 and 3.4.9. The grain yield follows from the integrated value of CHAGG, and the weight per individual kernel can easily be calculated.

In this preliminary model the number of kernels per square metre is directly dependent on the carbohydrate supply during the last part of the vegetative phase. In many climates, the season proceeds in such a way that there is a good correlation between the carbohydrate supply in this period and that in the post-anthesis phase. This is why the number of kernels per square metre and the carbohydrate supply in the post-anthesis phase are often related, and how the crop ensures the formation of the number of kernels that it deserves. However, when there is a cool, overcast period during the end of the vegetative phase, or a dry spell followed by a bright period without water shortage, the number of kernels may be too low. Then, they reach their maximum individual weight before the vegetative parts are exhausted. When a bright period is followed by an overcast period, it may be the other way around, so that the weight of individual kernels is well below the maximum value. As stated earlier, this formulation is rather descriptive, but it accounts for the interaction between genetic properties and environmental conditions, while simulated results are in reasonable agreement with experimental data.

Exercise 54

a. Combine this modelling of the organogenesis in wheat with the model SUCROS and calculate ANT, EARN, SP, GN and FGNR. You need the following information:

INCON TLNI = 2.E6
PARAM TCTF = 2., TCEI = 2., TCT = 2.
PARAM GNMAX = 4., GNMIN = 1.
PARAM MXRSF = 0.3, CHMPTB = 2.E-7
FUNCTION CHPTT = (0., 0.), (1.E-5, 0.5), (2.5E-5,.8), ...
                 (3.E-5,.95), (3.5E-5,1.), (3.5E-4,1.)
FUNCTION CHFPET = (0., 0.),(1.E-6,.25), (2.5E-6, .5), (5.E-6,.9), ...
                  (1.E-5,1.), (1.E-4,1.)
FUNCTION CHFPST = (0.,0.), (1.0E-4, 1.), (1.0E-3,1.)

The tillers are initiated between DVS = 0. and DVS = 0.425, the ears and spikelets between 0.35 and 0.425 and the grains between 1.00 and 1.05.

b. Simulate a growing season with a constant high light level and one with a

constant low light level (fixed FOV at 0.2 and 0.8, respectively), one with a bright period followed by an overcast period (FOV = 0.2 until anthesis, and FOV = 0.8 afterwards), and one with an overcast period followed by a bright period (FOV = 0.8 and 0.2, respectively). What about yield and kernel number?

c. Combine the statements of the Exercises 52, 53 and 54a and repeat the simulation. Omit the influence of temperature on the growth rates.

4 CROP PRODUCTION AS DETERMINED BY AVAILABILITY OF WATER

4.1 Crop production under semi-arid conditions, as determined by moisture availability

H. van Keulen

4.1.1 Introduction

In the Sections 3.2. and 3.3 a detailed, physiologically based process model of plant growth has been described. An essential prerequisite for application of that model is that the supply of water and nutrients to the crop is not a limiting factor for production. Such a favourable situation is, however, an exception rather than the rule in the various agricultural production systems around the world. Adverse weather conditions, soils low in natural fertility and lack of capital means required for improvements, lead to systems where the low supply of water or plant nutrients to the crop during its growth cycle is the major determinant for its production potential. To simulate the productivity in such situations, it is necessary also to pay attention to the below-ground plant parts and to the processes taking place in the soil that determine the availability of water and nutrients to the roots. In principle, these elements could be added to the comprehensive model indicated above, but that would increase the size of that model substantially, and bring it to a level that is hardly manageable. Moreover, some of the processes that are treated in detail in that model lose much of their relevance when the supply of water or nutrients is the major constraint for production (see Subsection 1.2.2).

Here a model is treated, dealing with simulation of crop production under conditions where moisture is the main limiting factor. The model, named ARID CROP, was developed to simulate growth and water use of fertilized natural pastures in the Mediterranean region. Following the principle of the hierarchical approach, results of BACROS and other detailed models are incorporated in a simplified fashion in the present model. Since it is impossible to treat the complete model within the scope of this contribution, only a number of features will be highlighted. For further information reference is made to detailed descriptions by van Keulen and coworkers (van Keulen et al., 1981; van Keulen, 1975). The meteorological and physiological aspects of the relationship between plant production and water use are discussed in Subsection 4.1.2, followed by an example in which these principles are applied (Subsection 4.1.3). The way in which growth of the vegetation is simulated in ARID CROP is explained in Subsection 4.1.4, emphasizing the differences with descriptions discussed earlier, in Subsections 3.3.3 and 3.3.6. In the Subsections 4.1.5 and 4.1.6, the results obtained with this model are discussed, and possibilities for applying the model in other regions are indicated (Subsections 4.1.7 and 4.1.8).

A FORTRAN version of ARID CROP, programmed by Ungar & van Keulen (1982), is available.

4.1.2 Water use and plant production

Since water is the major production factor considered in the present model, we will first examine the relation between water use by plants and the associated dry matter production. This relation has been subject of extensive experimentation, ever since the work by Briggs & Shantz (1913). De Wit's (1958) analysis of the subject, based on a description of the physical and physiological processes governing transpiration and photosynthesis in plants, indicated that the relation between dry matter production and water use depends on the prevailing level of irradiance during the growing period. The nature of this relation will be considered below.

The rate of water loss from a crop surface (E) (and that from a free water surface as well) is practically proportional to the level of irradiance. The rate of photosynthesis (A) is, however, proportional to irradiance only at low levels, since eventually the rate of CO_2 diffusion towards the active sites becomes the rate limiting factor (Section 3.2). These dependencies and their ratio are shown schematically in Figure 44. The values at very low levels of irradiance are not of practical importance, since under such conditions low temperatures will prevent any crop growth. At intermediate levels, which are characteristic for the larger part of the temperate zone, the ratio E/A remains constant and is independent of the radiation level. At the right-hand side of Figure 44, where conditions are represented that prevail in arid and semi-arid regions situated around the equa-
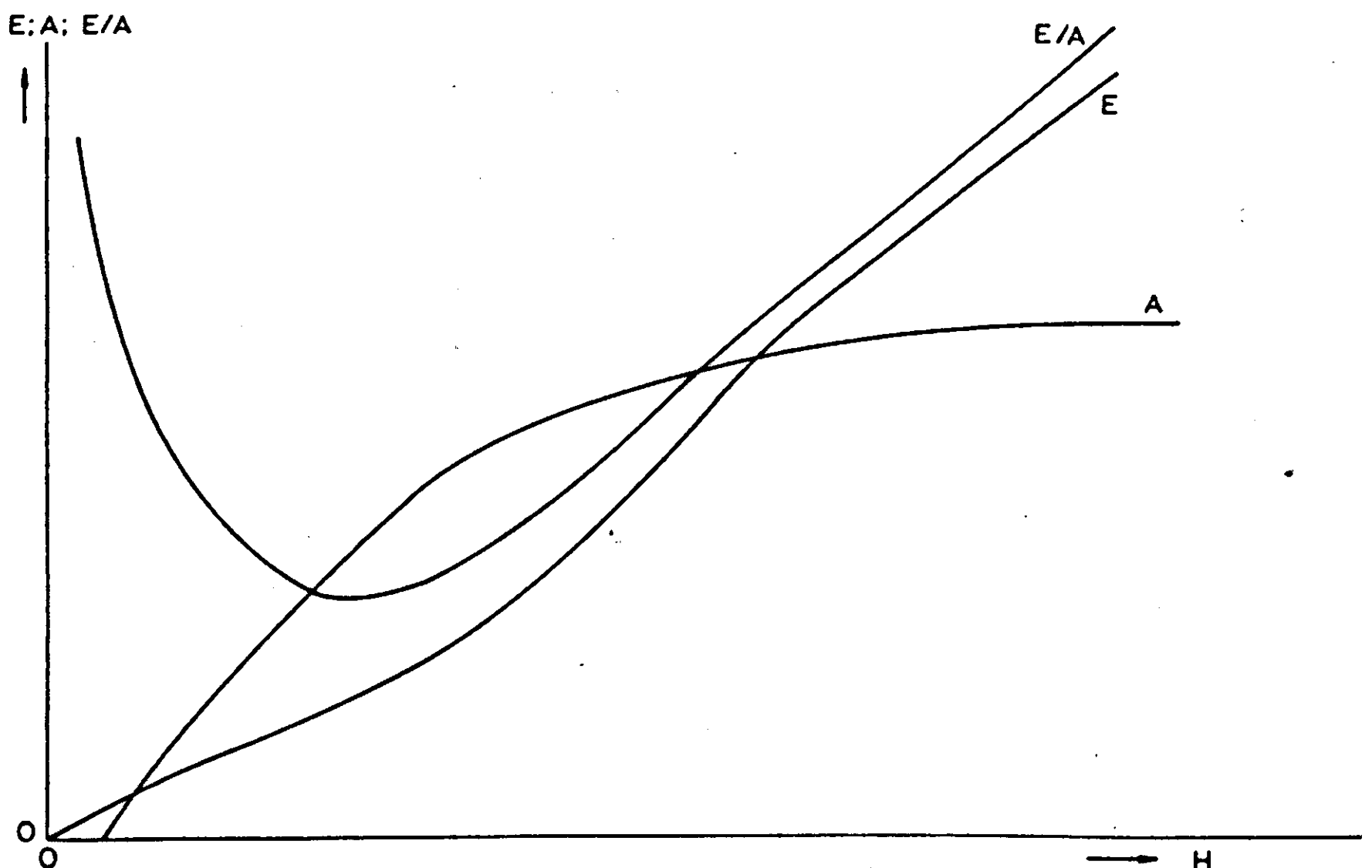
Figure 44. The relation between transpiration (E), assimilation (A) and their ratio (E/A) on the one hand and radiation intensity (H) on the other.

torial deserts, the ratio E/A is approximately proportional to the level of irradiance or the free-water evaporation. On the basis of these considerations, de Wit derived the relation:

$$P = M \cdot W \cdot E_0^{-x} \tag{53}$$

where P is the total dry matter production in kilograms, in most cases referring to above ground material only, W is the total water loss by the plants in kg, E_0 the average daily free water evaporation in kg ha^{-1} d^{-1} and M a proportionality factor, representing water use efficiency. M depends on plant species only, and has as dimension kg ha^{-1} d^{-1}. The value of x appeared to be 1 for conditions characterized by high levels of irradiance, and 0 for those where low levels prevail (Figure 44). This relation described satisfactorily the results of a variety of experiments on water use efficiency carried out in containers as well as under field conditions, some of which are summarized in Table 15.

There is a remarkable difference in the value of M between wheat and alfalfa

Table 15. Summary of measured M values for a number of crops.

Crop	Site	Condition*	M (kg ha^{-1} d^{-1})	Reference
Wheat	Great Plains	C	115	de Wit, 1958
	Turkey	F	106	Janssen, 1972
	Central Great Plains	F	125	Hanks et al., 1969b
	Central Negev	C	102-140	van Keulen, 1975
	Central Israel	C	88	Meyer (unpublished)
Sorghum	Great Plains	C	207	de Wit, 1958
	Great Plains	F	210	Doss et al., 1964
	Central Great Plains	F	140	Hanks et al., 1969b
Alfalfa	Great Plains	C	55	de Wit, 1958
	Central Negev	F	105	Tadmor et al., 1972
	Central Negev	C	108	van Keulen, 1975
	Central Negev	C	53	Meyer (unpublished)
	Wisconsin	F	214	Tanner & Sinclair, 1982
Maize	Great Plains	C	213	Briggs & Shantz, 1913
	Logan	F	215	Stewart et al., 1977
	Fort Collins	F	258	Stewart et al., 1977
	Yuma	F	262	Stewart et al., 1977
	Davis	F	314	Stewart et al., 1977
	Central Israel	F	290	Yanuka et al., 1981

* C = container; F = field experiment.

on the one hand, and sorghum and maize on the other hand. This contrast reflects the different photosynthetic pathways for the species: wheat and alfalfa are C_3 plants, sorghum and maize are C_4 plants. The main carboxylating enzyme in C_4 plants has an affinity to CO_2 that is about twice as great as that of the carboxylating enzyme in C_3 plants. Moreover the photorespiratory process is absent in C_4 plants. As a consequence the light saturated rate of CO_2 assimilation in C_4 plants is about twice as high as that in C_3 plants (Subsection 3.2.2).

Under some conditions, the assimilation process is controlled in such a way that the CO_2 concentration in the intercellular spaces of the leaves is regulated over a wide range of light intensities and external CO_2 concentrations through adaptation of the stomatal opening (Subsection 3.2.6). The level at which the concentration is maintained is about 210 cm^3 m^{-3} for C_3 plants and 120 cm^3 m^{-3} for C_4 plants. The consequence of this difference is that at low levels of irradiance and at normal external CO_2 concentrations of about 330 cm^3 m^{-3}, net CO_2 assimilation is about the same for both plant types but stomatal conductivity and hence the rate of transpiration is about half as great in C_4 plants as in C_3 plants. At high levels of irradiance, the net CO_2 assimilation of C_4 plants is twice that of C_3 plants at comparable values for stomatal conductivity, thus at approximately the same transpiration rate. Assimilation rate and transpiration rate are the main determinants for the M value which is consequently roughly twice as great for C_4 as for C_3 plants, irrespective of the level of irradiance.

Regulation of internal CO_2 concentration does not always occur, however. Some of the differences in the data of Table 15, especially those for alfalfa, can be understood if regulation was present in some cases and in others absent.

The M value is a useful parameter to describe the relation between production and water use, integrated over a reasonable period of time. It is especially suitable to compare different locations, different growing periods or different species. However, its application in the prediction of the growth pattern is much more limited. For regions with high levels of irradiance, to which most of the arid zone belongs, this is clear already from its numerical value: this value represents in fact the maximum attainable growth rate in situations where transpiration is equal to the free-water evaporation. Of course, the growth pattern of crops is such that the potential growth rate in mass of dry matter is low in the beginning of the growth period with incomplete light interception, whereas it increases to values of 200 (for C_3 plants) to 350 (for C_4 plants) kg ha^{-1} d^{-1} when complete cover is reached. The latter values could never be realized by using M values as tabulated in Table 15. Moreover, there are considerable fluctuations in M values when they are calculated over short periods of time, as is illustrated in Figure 45. These fluctuations are caused by different influences of the vapour pressure deficit of the air on crop transpiration and free-water evaporation. For a crop canopy the transpiring surface − the leaf area − may be a multiple of the surface area. Each of the leaf layers reacts practically independently to the vapour pressure deficit in the atmosphere and the transpiration increases virtually proportionally with increasing leaf area index. Thus, when the vapour pres-
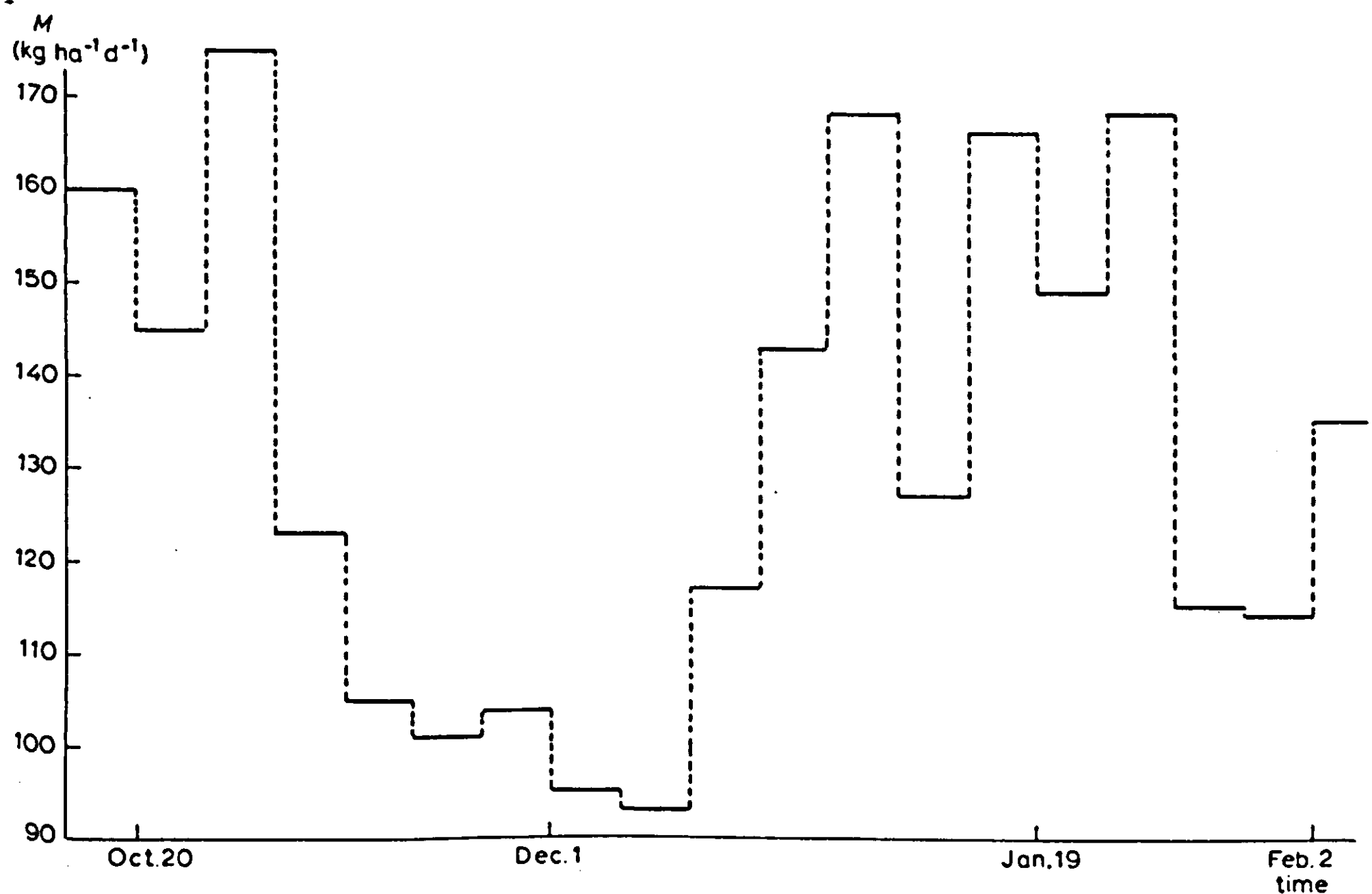
Figure 45. The variation in the calculated proportionality factor M for weekly periods in Avdat (Israel) 1972/1973.

sure deficit increases, crop transpiration increases relatively more than free-water evaporation, consequently the ratio W/E will increase, leading to lower values for M.

To avoid these difficulties the actual value of the transpiration coefficient ((W/P) from Equation 53) may be calculated in a simulation model for each individual time interval. The transpiration coefficient of the crop at a certain moment is equal to the ratio of potential crop transpiration rate, and potential dry matter production rate, both of which are obtained independently from the meteorological data of the current day.

4.1.3 Application in the simple crop growth model

The water use efficiency concept, worked out in Subsection 4.1.2 can be applied in a simplified way to obtain an indication of the water requirement of a crop growing at its potential rate in a high irradiation environment.

When for a C_3 plant an average M value of 125 kg ha^{-1} d^{-1} is assumed (Table 15), the ratio between dry matter production and transpiration can be estimated when E_0, the average rate of free-water evaporation (or the evaporation from an evaporation pan) is known. As an example a value of 4 mm d^{-1} is

163

taken, which is equivalent to 40 000 kg ha^{-1} d^{-1} of water. The production of 1 kg of dry matter is then coupled with a transpiration loss of (Equation 53) 40 000/125 = 320 kg of water, thus giving a transpiration coefficient of 320.

In the model presented in Section 3.1 the rate of increase in dry matter (GTW) is simulated. Multiplying that with the transpiration coefficient (TRPCF) yields the crop water requirement WREQ (kg ha^{-1} d^{-1}), which can be integrated to obtain total water requirement (TWREQ):

```
PARAM   TRPCF  = 320.
WREQ   = GTW * TRPCF
TWREQ  = INTGRL (0., WREQ)
```

To illustrate the influence of water shortage on crop production in an example, a very simple soil water balance can be added to the model (the next section treats this subject extensively). The amount of water available in the profile may be tracked in an integral (SWAT), initialized with pre-emergence soil water storage (ISWAT), and with effective rainfall (RAIN) and transpiration (TRANS) as rate variables. The rate of transpiration equals the actual growth rate (AGTW) times the transpiration coefficient. AGTW equals GTW when sufficient water is available, but becomes lower when moisture shortage occurs:

```
AGTW = GTW * RED
RED   = AFGEN (REDTB, SWAT/SWATM)
FUNCTION REDTB = (0., 0.), (0.04, 0.), (0.06,1.), (1.,1.)
PARAM SWATM = 150.E4
```

The degree of reduction in growth (RED) is related to the relative content of available water in the soil, which equals the actual amount in the soil (SWAT) divided by its maximum value (SWATM). Both quantities have the units kg ha^{-1}.

```
SWAT  = INTGRL (ISWAT, RAIN - TRANS)
INCON ISWAT = 150.E4
TRANS = AGTW * TRPCF
```

For simplicity, soil evaporation is neglected in this model. In this very schematized way some indications may be obtained about total water requirement for crops growing under different conditions, as well as about the necessity for supplemental irrigation.

Exercise 55

Add this water balance to the model SUCROS (Table 9, Section 3.1); replace GTW by AGTW in the Lines 107 and 108. Assume a rainfall of 15 mm each 14th day. Reduce the integration interval to 1 d.

Because of the considerable discontinuity introduced by the sudden rainfall expressed on a daily basis, simulation must proceed with time steps of 1 d (Section 2.3). Usually this will not cause any inconvenience. However, if the supply of water is as regular as in Exercise 55, as for an irrigation scheme, one might want to use time steps of 7 d to reduce computer costs. Particularly with the integration method RECT, a high rate of transpiration at the beginning of a time step may be extrapolated for too long, which leads to a negative soil water content and other nonsensical results. A way around such a problem is to compare SWAT plus the RAIN during a period with a duration of DELT with the amount of water potentially transpired in the period (WREQ*DELT), and to set the actual amount of water transpired equal to the lowest of these. The actual rate of transpiration in kg ha^{-1} d^{-1} is then equal to

TRANS = AMIN1(WREQ*DELT, SWAT + RAIN*DELT)/DELT

The potential growth in such a period is not computed from the relative soil water content, which changes too much in this period, but directly from the amount of water transpired:

AGTW = GTW*(TRANS*DELT)/(WREQ*DELT)

Exercise 56
Make these changes in the program of Exercise 55. Assume a soil with initially 50 mm water in the profile, irrigation of 25 mm every 14 days and DELT = 7.

4.1.4 Crop growth in the simulation model ARID CROP

In this subsection a brief overview will be given of the growth part of the comprehensive model ARID CROP. The soil section is treated in more detail in Section 4.2.

At the onset of the growing season seeds start to germinate after the first rains. Germination is assumed to be completed when the seeds, present in the upper 10 cm of the profile, are in a moist environment long enough to accumulate a heat sum of 150 degree-days (temperature above 0 °C). When the top soil compartments dry out before that moment, the seedlings die and a new wave of germination starts after rewetting only. When the required heat sum is accumulated, above ground and below ground dry matter is initialized with a predetermined initial biomass.

After initialization, the growth rate of the canopy, that is the rate of increase in dry weight of structural plant material, is obtained from the actual rate of transpiration and the value of the transpiration coefficient (Subsection 4.1.2). The latter is calculated as the ratio between the potential growth rate of the

canopy and the potential rate of transpiration ('potential' is defined here with respect to the actual state of the vegetation, but disregarding effects of water shortage). The potential growth rate follows from the rate of gross CO_2 assimilation, calculated from the leaf area index, the level of irradiance and the photosynthesis light-response curve of individual leaves (Subsection 3.2.4). Respiratory losses include maintenance respiration as a function of total amount of material present and temperature, and growth respiration, expressed as a weight conversion efficiency (Subsection 3.3.4). The potential rate of transpiration of the canopy is determined by the evaporative demand of the atmosphere (Subsection 3.2.5) and the leaf area index of the vegetation. The value of the transpiration coefficient is assumed to be independent of phenological stage of the canopy or moisture conditions in the soil. The latter assumption is an oversimplification, but one that has only a small effect on the ultimate dry matter production, since the amount of water transpired during drought periods is small. The actual rate of transpiration follows from the potential rate taking into account the interactive effects of rooting depth and soil moisture status.

During continuous testing of the model, using an increasing number of available data sets, it became clear that prolonged water stress influences some of the basic plant properties. The relative transpiration deficit (RTRDEF) is therefore included as a measure of the degree of moisture stress that the plant experiences. It is defined as the difference between potential (PTRAN) and actual (ATRAN) transpiration, as a fraction of the former:

RTRDEF = (PTRAN − ATRAN)/PTRAN

Its value divided by a time coefficient (in this case 10 days) is integrated to yield the cumulative relative transpiration deficit (CTRDEF). The assumption that a mild water stress will not have any lasting effect on plant performance, has resulted in a formulation that accumulates the relative transpiration deficit only when it exceeds the, rather arbitrarily chosen, value of 0.4:

CTRDEF = INTGRL (0., RARDEF − RDRDEF)
RARDEF = INSW (RTRDEF − 0.4, 0., RTRDEF/10.)∗(1. − CTRDEF)

The value of the cumulative transpiration deficit is constrained between 0. and 1. by multiplying its rate of accumulation by 1. minus its own value.

Exercise 57
What other formulation could have been chosen to limit the range of CTRDEF? What are the implications for the hypothesis on which these formulations are based?

When after a drought moisture becomes available again, the effect of the previous period of water shortage gradually disappears. This is described by an exponential extinction of the cumulative transpiration deficit (RDRDEF) at a relative rate of 0.1 d^{-1}, when the value of the relative transpiration deficit is below 0.4.

RDRDEF = INSW (RTRDEF − 0.4, CTRDEF/10., 0.)

Qualitatively this approximation provides a satisfactory description of the processes involved.

The light-use efficiency at low levels of irradiance and the CO_2 diffusion limited maximum value at light saturation of the photosynthesis light-response curve for individual leaves are both defined as state variables in ARID CROP. Both are initialized with the value valid for leaves grown under optimum conditions. There are indications that the CO_2 assimilation capacity of leaves, subjected to a prolonged period of water stress is impaired. This is taken into account by assuming that both the initial efficiency and the maximum level of CO_2 assimilation decrease when the cumulative relative transpiration deficit (CTRDEF) exceeds 0.5. The relative rate of decline of both state variables increases linearly from 0. when CTRDEF is below or equal to 0.5 to a maximum value of 0.05 d^{-1} when the latter reaches 1. When the cause of the stress is removed, i.e. when the relative transpiration deficit drops below 0.4, the photosynthetic capacity recovers at a rate proportional to the relative growth rate of the vegetation. Sufficiently prolonged favourable conditions may lead to complete restoration of the photosynthetic capacity of all remaining leaves. Such behaviour seems reasonable considering the fact that the newly formed leaves will have the maximum photosynthetic capacity and that in the surviving old leaves, impaired enzymes and membranes may be rebuilt.

The total amount of structural plant material produced each day is partitioned between roots, leaf blades, non-leaf vegetative material (stems and leaf sheaths) and seeds. As explained in Subsection 3.4.2, the physiological principles governing the morphogenetic characteristics of plants are only partially understood and it is difficult therefore to include morphogenesis in models at this stage. However for the type of models discussed here it is of prime importance to take the distribution pattern into account because it determines the division between below ground and above ground material, the latter being amenable to validation. Moreover the dry matter produced is in most cases exploited by grazing. To take that into account, the possibility of selective removal of certain plant organs (leaves) must be present.

The partitioning of dry matter between shoot and root is governed by a phenology-dependent distribution factor (Subsection 3.3.6) and is furthermore influenced by the moisture status of the vegetation. The functional balance between shoot and root (Subsections 3.3.6 and 3.4.3) implies that moisture stress in the plant leads to sub-optimal growth rates for the above-ground plant parts, which results in increased growth of the roots and hence in a shift in the shoot/root
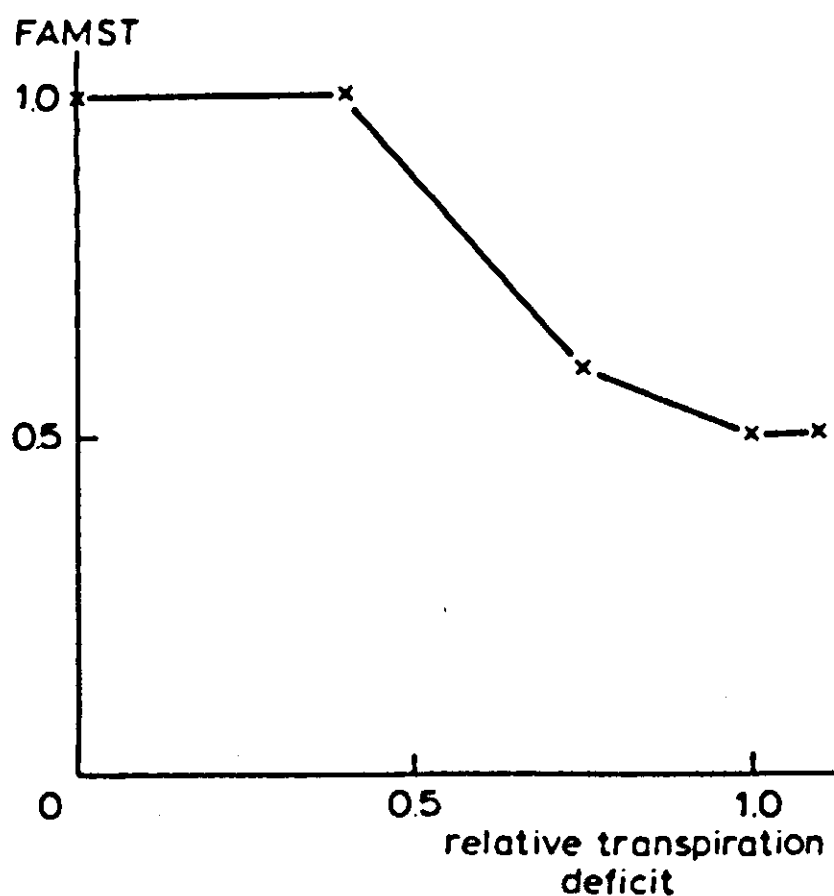
Figure 46. The relation between the reduction factor for shoot growth (FAMST) and the relative transpiration deficit.

ratio. The function presently applied in the model to restrict the share of the shoot in favour of the root in relation to the value of the relative transpiration deficit, is presented in Figure 46.

The material available for growth of the above-ground plant parts is partitioned into seeds, leaves and non-leaf material. Growth of the seeds starts at flowering and a constant fraction of the available dry matter is henceforth allocated to the seeds. (Both the development stage at flowering and the fraction allotted to the seeds are estimates based on field observations, which is a simplification especially when applied to a mixed sward. The differences in development pattern between species are often considerable, e.g. legumes and many other dicotyledons with indeterminate flowering as compared to grasses with determinate flowering.) The material remaining after the seeds have had their share is divided between leaf blades and other structures. The applied distribution factor is again a function of the development stage of the vegetation. The general shape is such that progressively less of the available dry matter is invested in the formation of new leaves (cf. Figure 33 of Section 3.3). The actual values used in ARID CROP are at the moment subject of renewed investigations.

Once plant tissue has been formed, it can lose its viability and die. In the model, two causes of death are considered. Upon completion of the plant's life cycle its vegetative structures stop functioning and dry up, either because of physiologically determined processes or due to translocation of vital elements from these structures to the developing seeds. Dying because of senescence also occurs at earlier stages of plant development, since the leaves have a limited lifespan and the first leaves will disappear at an early stage. This phenomenon could be taken into account if the developing leaves were kept in age classes. Where that is not the case, as in the present model, application of a relative death rate to the actual leaf mass present at any moment will overestimate senescence in the early stages. It has been assumed therefore that until the onset of

seed-fill leaf death from senescence is negligible. From then on, leaves die at a relative rate of 0.005 d^{-1} initially, a value that increases to a maximum of 0.1 d^{-1}, attained at maturity (cf. Subsection 3.1.2). These values describe fairly realistically the situation in the field, where towards maturity the vegetation dries up in about a fortnight, even when soil moisture is still available.

A second cause of death, especially important in the present context, is insufficient moisture in the soil. In the present formulation of the model, death under the influence of moisture stress is governed by the combined effect of the moisture status in the soil and the evaporative demand of the atmosphere. Especially during periods, characterized by high temperatures and low humidity (referred to in Israel as 'chamsin') the vegetation visibly deteriorates, even when soil moisture is well above wilting point. Evidently a situation develops, where even complete closure of the stomata does not prevent dehydration of plant tissue and subsequent death. It is assumed now that the rate of dying due to water shortage is proportional to the difference between the actual daily transpiration rate and the potential water loss through cuticular transpiration. The time coefficient for dying is set at 5 days, reflecting the considerable buffering capacity of the plant and the heterogeneity of the soil. The relative death rate is applied to both the leaf blades and to the non-leaf material, of which, in reality, the leaf sheaths will be much sooner affected than the stem proper. The result of this description is that appreciable death of leaves only takes place when the soil has dried out till permanent wilting point, except in situations where actual transpiration rates fall far short of the evaporative demand.

4.1.5 Evaluation of ARID CROP

Since the proof of the pudding is in the eating, the degree to which the model represents reality must be judged by comparison of its behaviour against that of the real world system. For this purpose it is of prime importance to have at one's disposal a number of data sets collected completely independently from the development of the model. In practice, however, the situation is often such that data collection and model development proceed in parallel, done by the same person or group. That fact introduces the danger of strong interactions between data collection and model development, and consequently the use of the model as a sophisticated curve-fitting method (cf. Subsection 1.3.6). Such behaviour is especially obvious when only one data set is available. In our situation we have at least the advantage that a relatively large number of years, each one with its own specific environmental conditions, is available to test the model. These data sets were collected in the northern Negev desert of Israel, a semi-arid environment with an average annual rainfall of 250 mm. The vegetation consists of a mixture of annual species, typical of abandoned crop land (van Keulen, 1975).

The results of two reasonably representative years are presented here in Figures 47 and 48, a more complete validation has been described by van Keulen et

al. (1981). The 1972/1973 growing season was a 'wet' year with high rainfall, favourably distributed over the growing season, whereas 1975/1976 was a year of prolonged drought, sufficiently severe to create stress conditions for the vegetation.

The measured and simulated growth curves for 1972/1973 (Figure 47a) are in excellent agreement for most of the growing season, except for a burst of growth towards the end of the growing period. The simulated and measured values of soil moisture in the rooting zone (Figure 47b) are also in close agreement.

In Figure 48a the measured and simulated course of dry matter production is given for the 1975/1976 growing season. Also for this season, the results of the model are in close agreement with the measured values. The present description of the influence of moisture stress on growth and development seems to be satisfactory, but needs further confirmation. Data on the moisture balance are given in Figure 48b. Only small changes occur over the growing season and there is a tendency for the simulated values to be lower than the measured ones, but the deviations are within the error bound set by the accuracy of the moisture sampling technique used.

The results presented here indicate that the model performs reasonably well in two growing seasons with strongly contrasting environmental conditions.
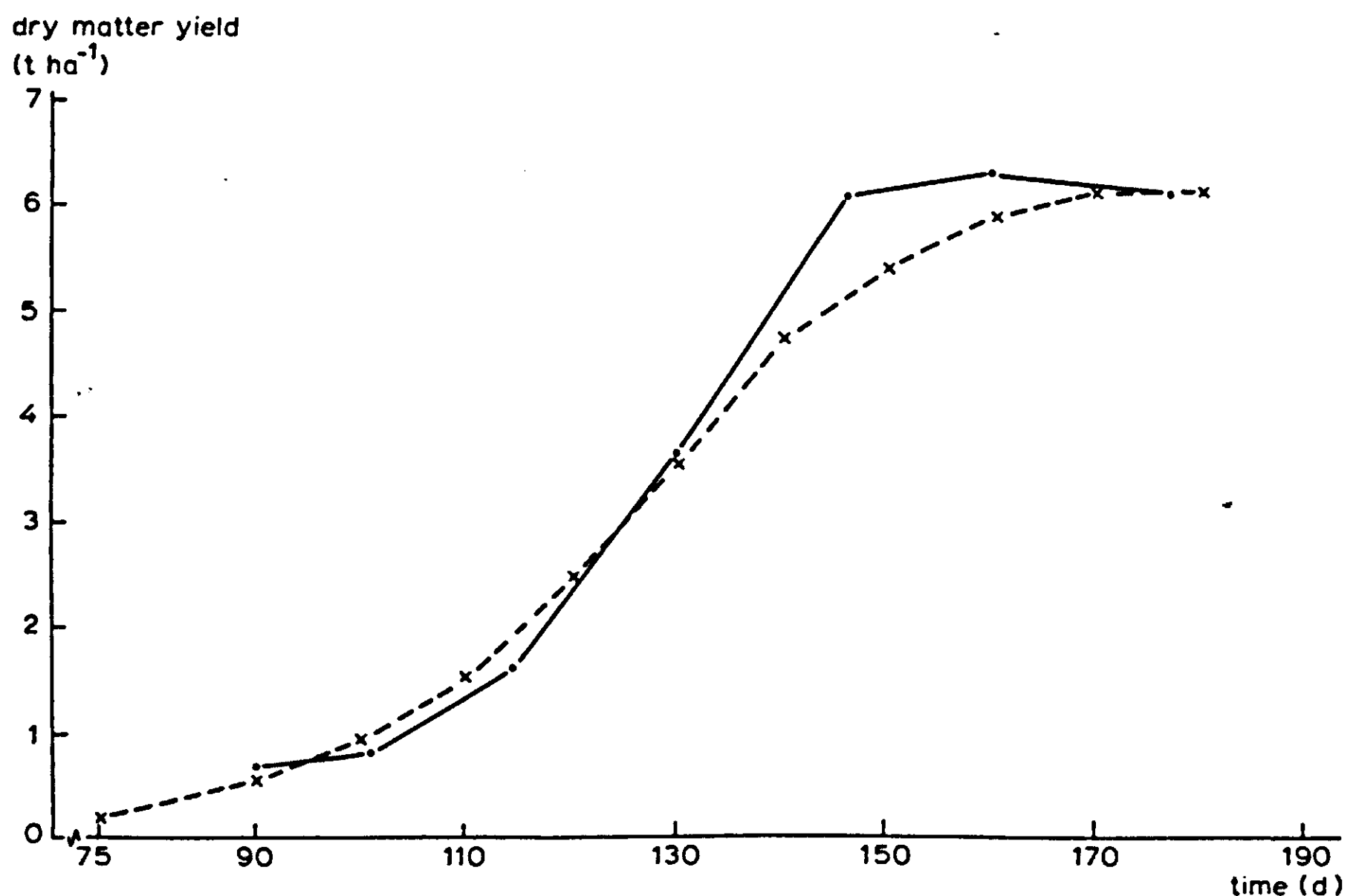
Figure 47a. Comparison between measured (•) and simulated (x) dry matter accumulation of natural pasture in Migda (Israel) 1972/1973.

170
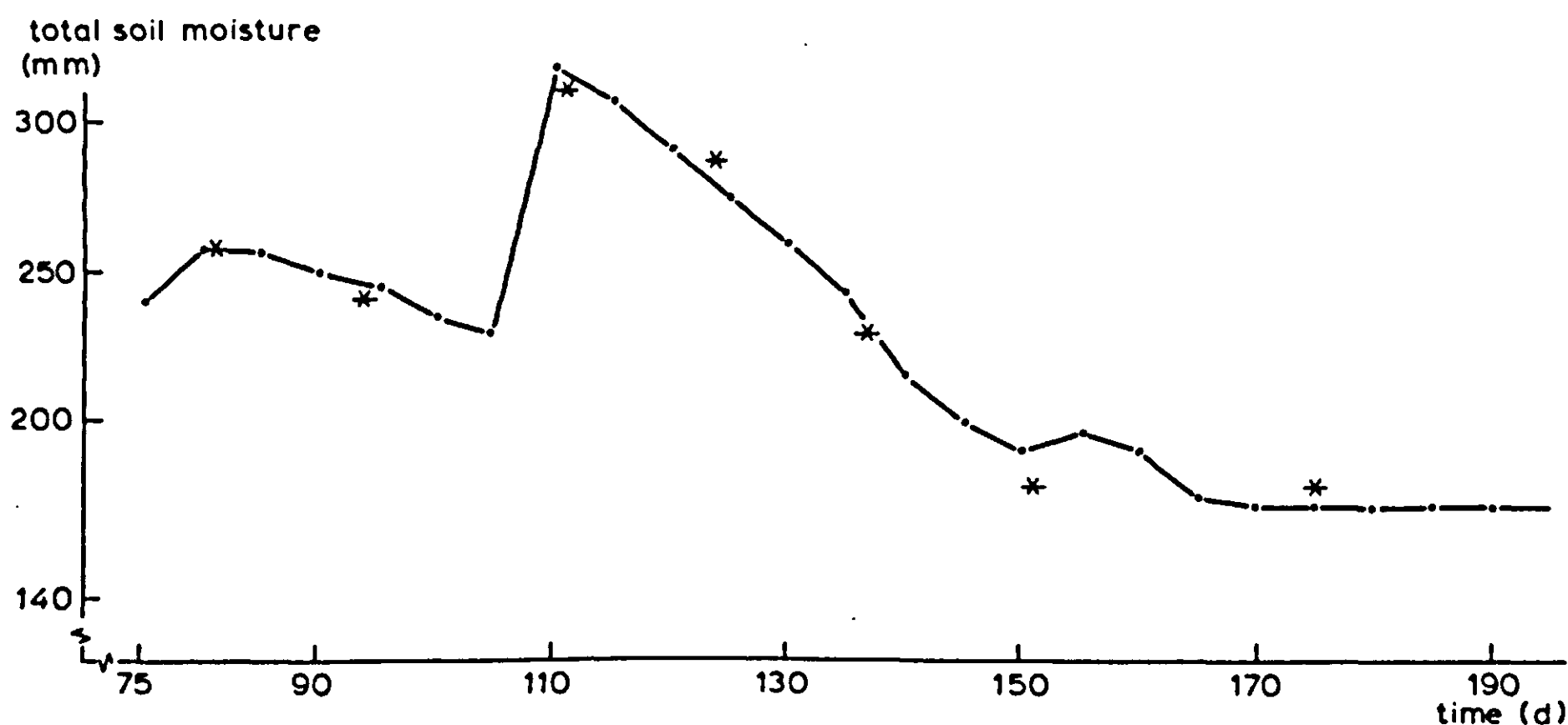
Figure 47b. Comparison between measured (*) and simulated (•) total soil moisture under natural pasture in Migda (Israel) 1972/1973.
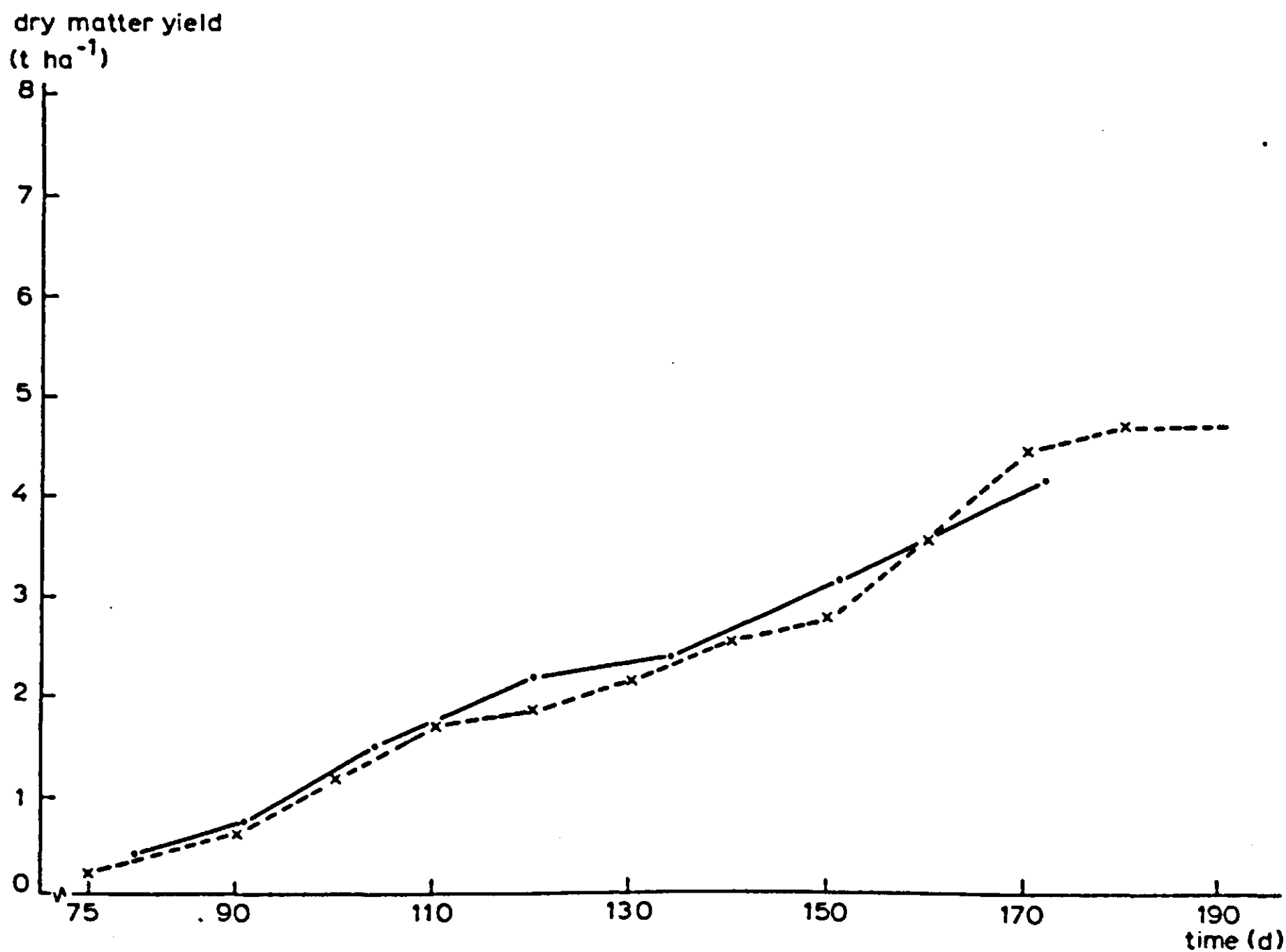
Figure 48a. Comparison between measured (•) and simulated (x) dry matter accumulation of natural pasture in Migda (Israel) 1975/1976.

171
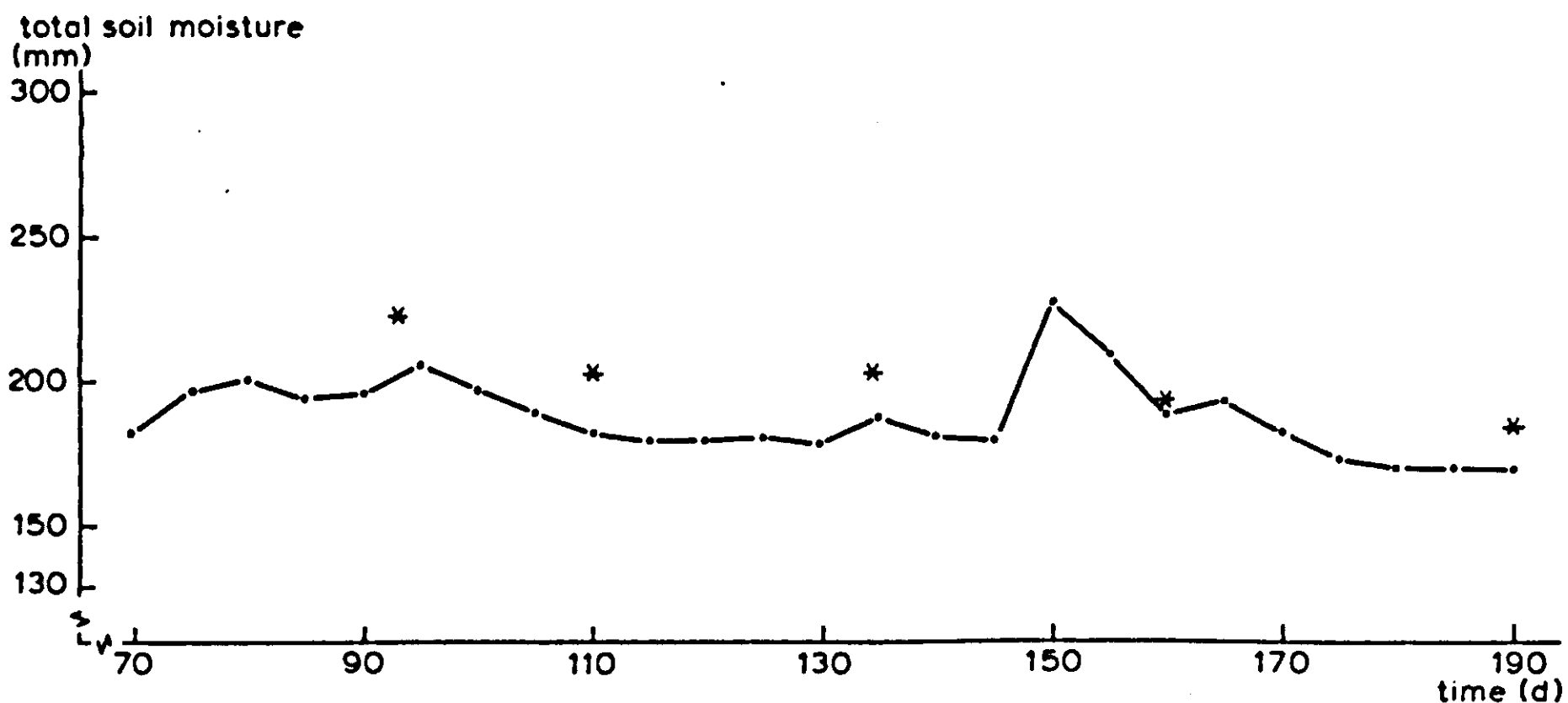
Figure 48b. Comparison between measured (*) and simulated (•) total soil moisture under natural pasture in Migda (Israel) 1975/1976.

4.1.6 Major problem areas in the model

Although the performance of the model is often realistic when compared to real-world behaviour, a number of weak points are known to exist. Most of these points are related to plant physiological questions. Some of them are briefly discussed here:

– The amount of dry matter present at the completion of the germination stage depends on the number of seedlings of the various species that can establish themselves. That number not only depends on the conditions during the germination process, such as the length of the wet period, temperature, etc., but is co-determined by the composition and the quality of the seed stock present in the soil. It is, at the moment, virtually impossible to determine the quantity of seeds present and it is even less clear how their viability should be appraised. The process of germination itself is complex, and although our insight into the various parameters influencing it is increasing, it is not yet possible to include that knowledge in a model as the one presented here. Prediction of the initial biomass therefore remains a major difficulty that needs attention. The best alternative at the moment is to measure biomass early in the growing season and adjust the initial value accordingly.

– The influence of prolonged moisture shortage on assimilation, partitioning of dry matter and dying of the tissue in ARID CROP is based on intelligent guesses. Much more experimental work is needed, both to determine these relations under controlled conditions and to collect data in the field that can serve for validation of the model results.

– Although the influence of moisture shortage on production is fairly well described, its effect on plant survival is largely unknown. What happens in the transition zone between the end of a positive carbon balance and the complete

172

disappearance of the vegetation has not been investigated in enough detail.

– Crop morphogenesis is by no means understood and the functions now governing the distribution of dry matter among the various plant organs are speculative. More research into quantitative aspects of leaf formation and the effects of environmental factors on the process are needed.

– Phenological development of the vegetation is also incompletely understood. In most cases the present description, in which the development rate is governed by temperature, satisfactorily predicts the behaviour of the canopy. However, in a subsequent season, where germination was very late – towards the end of December – temperature only proved to be inadequate to predict development. Apparently day length also plays a role then (cf. Subsection 3.3.2), as in many species found in the Sahelian region. Due to lack of observations these effects are still difficult to quantify.

– A point which needs attention is the fate of the root system under conditions where above ground material dies of water shortage. It seems reasonable to assume that the plants will hang on to the roots as long as possible, when water becomes scarce. However, when whole tops die, so will their roots. Since this process is not taken into account in the model, a situation may develop where, under severe stress, virtually all the above ground material is dead, yet a substantial root system is maintained.

4.1.7   Application of the model ARID CROP in a summer rainfall region

The model ARID CROP, developed for the conditions prevailing in the northern Negev desert, was subsequently applied in the Sahel (Penning de Vries & Djiteye, 1982). Apart from the introduction of the appropriate parameter values and driving variables for climate and soil conditions, a few modifications of the model were necessary to obtain a realistic behaviour. For changes in the soil water balance, see Subsection 4.2.3.

Description of the germination process along the lines applied for the winter annuals in the Northern Negev was not applicable to the conditions in the Sahel, where it rains in the summer. Therefore the start of the growing season is empirically defined as the moment that a certain amount of biomass is present in the field.

A summary submodel in ARID CROP accounts for the reduction of canopy transpiration as a result of stomatal closure of leaves at low light levels down in the canopy. This summary model in the form of a set of tables in ARID CROP is computed with BACROS (Subsection 3.3.8) for the appropriate conditions (van Keulen, 1975). It turned out that these values are much more invariable in the warm Sahel area than in the cool Mediterranean region of the Negev, and they could be replaced by the constant of 0.7 for the whole growing season.

Small changes are also introduced with respect to the quantification of the respiratory processes described by van Keulen (1975): the conversion efficiency is changed to 0.70, whereas a maintenance respiration requirement of 0.015 kg

$kg^{-1} d^{-1}$ is applied, since the high levels of irradiance permit a greater contribution directly from assimilatory processes.

The Sahelian species are in general quite sensitive to day length. Phenological development is therefore governed by both temperature and day length (see also Subsection 3.3.2). Semi-empirical formulations, based on extensive experimentation (de Ridder, 1979) are introduced in the model.

Some of the results obtained for the Sahelian region are presented in Section 4.2.

4.1.8 Concluding remarks

The results presented in this paper and elsewhere (van Keulen et al., 1981) show that ARID CROP performs well in relatively wet years, but most problems arise in the relatively dry growing seasons, thus the model does not quite live up to its name. This points to the fact that the survival and recovery response of annual plants subjected to moisture stress for a prolonged period cannot be explained without reference to the effects of that stress on morphological development, photosynthetic performance and phenology of the species involved. That in itself is, however, in a way a major justification for the development of the model, since it clearly points to the limits of the concepts underlying the model, in explaining the behaviour of arid production systems.

The model in its general outline seems applicable for different ecological conditions, provided that water is the major production determining factor. However, certain adaptations, related to specific plant properties, either physiological or phenological may be necessary. Lack of sufficient understanding of some of the basic principles, which leads to the application of partly descriptive rather than explanatory formulations, is the major reason for this requirement.

4.2 Simulation of the soil water balance

L. Stroosnijder

4.2.1 Introduction

As stated in the previous contribution (Section 4.1) the soil-water status influences crop growth in several ways, i.e. '... that prolonged water stress influences some of the basic plant properties', 'the functional balance between shoot and root implies that moisture stress in the plant leads to sub-optimal growth rates for the above ground plant parts, which results in increased growth of the roots and hence in a shift in the shoot-root ratio' and, finally, 'a second cause of death, especially important in the present context, is that of insufficient moisture in the soil'. Thus knowledge about the stock of moisture in the root zone is needed to be able to calculate crop growth. This includes knowledge about the spatial (in the vertical direction) distribution and availability of moisture to simulate root behaviour correctly.

The main source for the soil-water stock is rainfall (Figure 49). However part of the rain is lost due to interception by the plant cover and run-off. The remaining rain penetrates the soil by a process called infiltration and is distributed over different soil layers. The soil-water stock can also be replenished by water that flows upward from a water-table, i.e. by capillary action. Main sources of
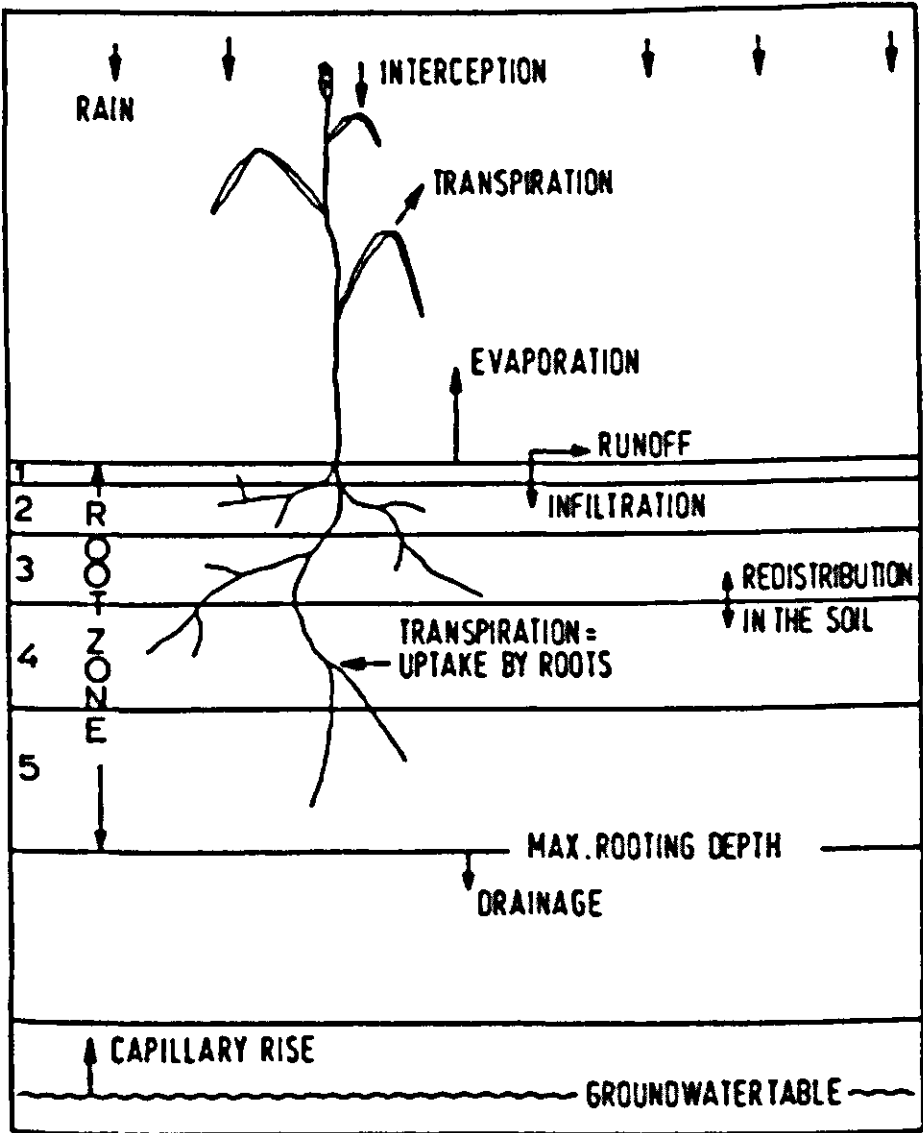
Figure 49. Schematic view of different elements and processes of the soil water balance.

175

depletion of the soil-water stock are uptake by plant roots (= transpiration), evaporation of soil water to the atmosphere, and drainage below the maximum rooting depth. To know how much and where water is available for plant growth, all sources of soil water must be considered, so that the soil-water balance can be quantitatively understood and simulated. As shown in Figure 49, the soil may be thought to be divided up into horizontal layers. Water is not static in the soil, but can be redistributed by flowing from one layer to another. A simple approach to the soil-water balance is to consider the water content of each layer as a separate state variable, and to describe the flow into and out of each compartment separately. This rate of flow depends on the driving force on the water, which is the sum of the gradient of the potential with which water is held by the soil and gravitational force, and on the hydraulic conductivity of the soil. If this force was proportional to the soil water content and if the conductivity was constant, the simulation model would be really simple. However, the relation of the potential of the soil water to the water content of the soil is quite non-linear, and the conductivity for water also depends very much on the water content, as illustrated in Figure 50. Because in reality there is a continuous gradient of the water content in the soil profile, the concept of a soil divided into layers makes it necessary to average water content, potentials and conductivities. Without going into detail, it will be clear that this aspect makes simulation of the soil water balance not a trivial problem. There are two approaches to its simulation. The first, described in this section, is to redefine from classical soil physics, concepts and parameters needed in the approximation of the water balance with a simple model as indicated. This may be called parametric modelling. The second is to follow the classical approach more closely and to develop the simulation program accordingly. This may be called deterministic modelling. This approach is emphasized in Section 4.3.

Subsection 4.2.3 describes a program to simulate the soil water balance as incorporated in the model ARID CROP and SAHEL GRASS NPK by the para-
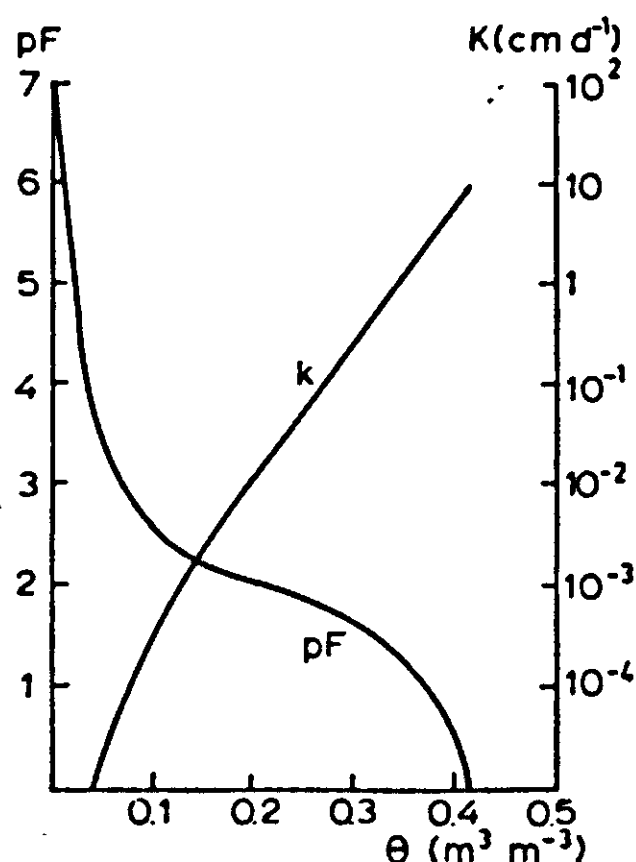
Figure 50. The relation of the soil water potential, expressed as pF (i.e. $-\lg$ (soil water potential in mbar)), and the conductivity, K, to the soil water content, θ, of loamy soil from the Sahel.

metric approach. Examples are given that are oriented towards semi-arid zones like the West African Sahel zone (Subsection 4.2.3). But first the link between parametric and deterministic modelling is discussed (Subsection 4.2.2).

4.2.2 Deterministic modelling of the flow of water in soils

The flow of water in a soil can be described mathematically with a partial non-linear differential equation − partial in time and space. This general flow equation is based on two basic (soil) physical principles (laws). For one-dimensional flow these are the (empirical) law of Darcy (Equations 54 and 55) and the mass continuity Equation 56:

$$q = -K(h) \frac{\delta H}{\delta z} \tag{54}$$

in which q is the soil water flux ($m^3 \ m^{-2} \ s^{-1}$); $K(h)$ the hydraulic conductivity ($m \ s^{-1}$), as a function of the soil water pressure head, h; z the vertical coordinate (m), with origin at the soil surface and for which upwards is taken as positive; and H the hydraulic head (m), which is the sum of the soil water pressure head, h, and the gravitational head, z. Thus Equation 54 can also be written as:

$$q = -K(h) \left(\frac{\delta h}{\delta z} + 1 \right) \tag{55}$$

$$\frac{\delta \theta}{\delta t} = - \frac{\delta q}{\delta z} - S \tag{56}$$

where θ is the volumetric moisture content ($m^3 \ m^{-3}$), t the time (s) and S the volume of water taken up by the roots per unit bulk volume of soil in unit time ($m^3 \ m^{-3} \ s^{-1}$). Equation 56 states simply that in one soil element, the rate of change of the water content with time equals the flow out of the element through its boundaries plus its flow out through the roots that it contains. Darcy's law as well as the continuity principle are in Figure 51.

To simulate the soil water balance, the soil is considered to exist of horizontal layers, usually 3-10. Equation 54 is used to calculate the rate of flow of water between the centres of two adjacent homogeneous soil compartments in dependence on the value of the state variables. After having calculated all rates of flow, the state variables in each compartment are updated by an integration with respect to time (equivalent to Equation 56), after which new flow rates can be calculated for the following time step. Within a time step, water flow is by definition stationary (Subsection 1.1.3). Clearly, the rates used in a certain time step are calculated parallel and not mutually dependent, so that the order in which they are calculated does not matter. In essence this solution method is a matter of accurate bookkeeping.

Combination of Equations 54 and 56 leads to a non-linear partial differential equation of first order in t and second order in z (Equation 57) with two inde-
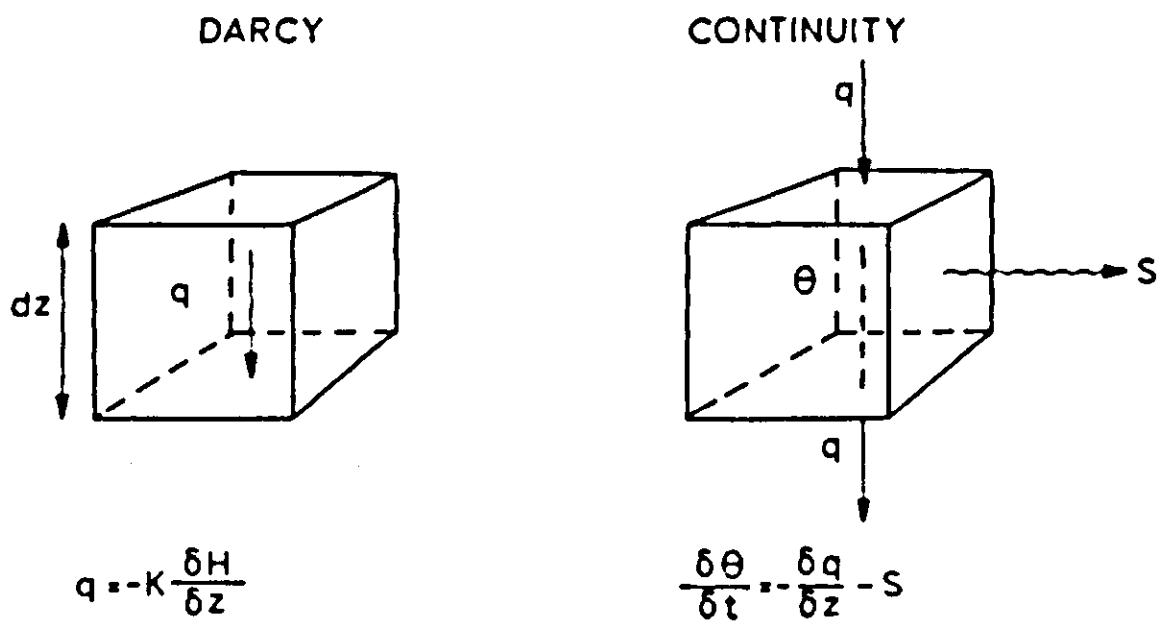
Figure 51. Schematic representation of the principle of flow and mass continuity including a sink term for water uptake by plant roots (Feddes et al., 1978).

pendent variables, z and t and two dependent variables, θ and h. The dependence between these last two variables is known as the soil-moisture characteristic or retention curve of the soil (Figure 50). Using this $h(\theta)$ relation, one may generate a general flow equation with one dependent variable only, either in θ or in h:

$$C(h) \; \frac{\delta h}{\delta t} = \frac{\delta}{\delta z} \; [K(h) \; (\frac{\delta h}{\delta z} + 1)] - S \tag{57}$$

with $C(h) = d\theta/dh$, the differential moisture capacity of the soil, which is a function of θ or of h. This form is more widely applicable, for positive (saturated soil) as well as for negative (unsaturated soil) values of h and in heterogeneous soils, than the θ form (Stroosnijder, 1976).

With a computer available, this Equation 57 can be solved by the finite difference approach (Subsection 2.1.4); the variables place and time, which in reality are continuous, are divided into small intervals so that the situation approaches continuity. Space in the soil is divided in a number of gridpoints, while time is divided in time steps. Equation 57 can be expressed in finite difference form in many ways. There are elaborate implicit approximations (or schemes) where a whole matrix of equations must be solved for each time step (e.g. Section 4.3). There are also the more simple explicit approximations where an unknown value of the state variable is calculated from a number of known values of the same state variable (see Figure 52). An excellent review of the most commonly used approximations and related computer solution schemes has been published by Vauclin et al. (1979).

An example of a finite difference form of Equation 57 is:

$$C_i^j \frac{h_i^{j+1} - h_i^j}{\Delta t} = \frac{1}{\Delta z} \; [K_{i+\frac{1}{2}}^j \; (\frac{h_i^j - h_{i+1}^j}{\Delta z} + 1) -$$

$$K_{i-\frac{1}{2}}^j \; (\frac{h_{i-1}^j - h_i^j}{\Delta z} + 1)] - S_i^j \tag{58}$$

which can be visualized with help of a gridpoint scheme as shown in Figure 52.

Emphasis is given here only to the above explicit approximation of Equation 57, since such an approximation is automatically used if the state variable approach is chosen. The latter is most commonly used in dynamic simulation models of the explanatory type (Section 1.1). Such models clearly distinguish state, rate and driving forces. As a consequence, the combined Equation 57 is not used in those models, but the more basic Equations 54 and 56.

Obviously, this simulation approach must be considered as an explicit solution for which stability and convergence determine rather stringently time step and compartment size. It was shown by van Keulen & van Beek (1971) that the time step taken must be small enough to avoid oscillation. The smallest time step is caused by the infiltration process, when water flows from a very wet compartment into a very dry one. The condition for the time step is then

$$\Delta t < (\Delta z)^2/D(\theta), \text{ with } D(\theta) = K(\theta)/C(\theta) \tag{59}$$

$D(\theta)$ is the soil water diffusivity $(m^2 \ s^{-1})$. According to Stroosnijder (1976) values for $D(\theta)$ in wet soil vary between $10^{-2} \ m^2 \ s^{-1}$ for sand to $10^{-4} \ m^2 \ s^{-1}$ for clay. Thus for a layer near the soil surface of 2 cm thickness, the time step to be used in the simulation of infiltration of water in dry sand equals:

$$\Delta t \leq 0.04 \ s \tag{60}$$

Equation 59 implies that the execution time of a simulation run may be reduced by increasing layer thickness and adjusting the time step as a function of the soil water diffusivity, $D(\theta)$. Obviously, the choice of layer thickness is related to the problem and to the accuracy desired. If one's problem deals with very steep moisture gradients, as in evaporation, one is forced to use rather small layers (e.g. 2 cm) to solve the problem not only in a deterministic way but also in a physically realistic way. On the other hand, the above example of a time step indicates a kind of minimum; for other soil water flow processes, like evaporation, much smaller values of $D(\theta)$ are involved and hence much larger time steps can be used. For a discussion of time step size and integration method, see Subsections 2.3.5, 2.3.6 and 2.3.7.

As can be seen from Figure 52 and Equation 58, one has to choose some
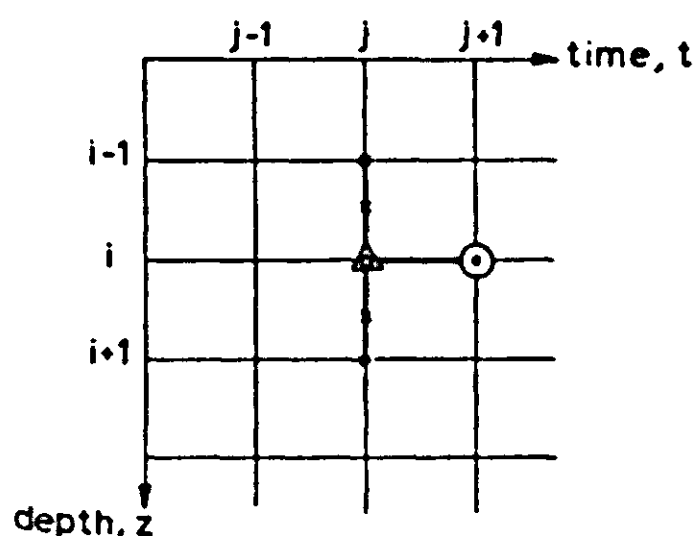
Figure 52. Illustration of Equation 58: the three known values of the state variable h at known time level j and gridpoints $i-1$, i and $i+1$ (•) are used to calculate one new value of h at time $j+1$ and place i (○). Soil parameters are used at gridpoint i (△) and in between the gridpoints $i-1$ and i and $i+1$ (x).

method for obtaining the value of the soil parameter $K(\theta)$ between two adjacent compartments. Several averaging methods seem possible:
- averaging of the conductivities, as is done in electricity for series resistance;
- average first the moisture contents of the two adjacent compartments and determine the corresponding conductivity;
- average the conductivities according to different weighting procedures.

The averaging can either be done taking account of the compartment size or not. The latter procedure, combined with simple arithmetic averaging of conductivities often give the best results when compared to analytical solutions (Rietveld, 1978). It can also be seen from the Figure 52 that (since an explicit approximation is used) only one known value of the soil water capacity, $C(\theta)$, is used and no linearization (Vauclin et al., 1979) with respect to time.

In spite of the above difficulties, a variety of useful deterministic models were developed (van Keulen & van Beek, 1971; de Wit & van Keulen, 1972; Stroosnijder, 1976; Hillel, 1977; Shaykewich & Stroosnijder, 1977; Rietveld, 1978; van Loon & Wösten, 1979). Using the terminology of the Subsections 1.1.2 and 1.3.1, these are explanatory, comprehensive models.

The discussion above, in particular on the integration time step, makes it clear that only relatively short simulation runs can be made at relatively high computer costs. It appears that the time step necessary for a deterministic simulation of soil-water flow is several orders of magnitude smaller than necessary for other elements in simulation models for crop growth. Such models, like ARID CROP (Section 4.1, van Keulen, 1975; van Keulen et al., 1981) and SAHEL GRASS NPK (a model used for grass growth under tropical semi-arid conditions with optimal supply of nutrients and natural rain) use a time step of one day. Thus in these models soil-water flow cannot be simulated in a deterministic way but must be done in a parametric way, i.e. simplified submodels must be developed that simulate the various aspects of the soil-water balance as well as possible with a time step of one day. The term parametric model is used to indicate that if deterministic models cannot be used, alternative models have to be developed, but also those models need not be black-box models. Parametric models, discussed in the next subsection, describe processes in a distinctly physical way, but that way is a simplification of the fully physical understanding. Often use is made of overall parameters to describe physical processes on a large time scale that in reality take place on a small time scale. This explains the name parametric model. The necessity of development of parametric models from deterministic models when soil physical and crop physiological processes are combined in one model is a good illustration of the problems of coordination between models of different hierarchical levels (Subsection 1.4.3). The validation ('the best possible') of these simplified models is done with help of detailed deterministic submodels (i.e. following the hierarchical approach) and with experimental data. In some cases, simplification of different deterministic elements of the soil-water balance can be combined into one parametric element. So, infiltration of the water in the soil and the subsequent redistribution of this water

over different soil layers were combined. This is due to the fact that redistribution is most important in the range of water contents between saturation and field capacity and is, by definition, very slow at lower moisture contents. This enables one to combine infiltration and redistribution in such a way that the water that enters the soil is directly distributed (in a parametric way) over different soil layers so that no layer becomes wetter than field capacity. This almost completely eliminates the need for a further computation of moisture redistribution. This has been proven for the prevailing choice of layer thickness and time step of integration as used for the description of crop growth processes, with refined deterministic models.

4.2.3 Parametric modelling of the soil water balance

The following elements of the soil-water balance, as used in the whole crop models ARID CROP and SAHEL GRASS NPK will be briefly discussed under the headings *Rain, Interception, Runoff, Infiltration, Evaporation* and *Transpiration*. In this discussion the original CSMP statements, as used in the SAHEL GRASS NPK model (August 1980 version) will be used. Since both models were developed for use in semi-arid regions, where often a perma-dry subsoil exists, the following elements (which are necessary in the simulation of the water balance under more humid conditions; see Section 4.3) are omitted from discussion: drainage, water-table and capillary rise.

Rain
Rain (RAIN (in mm d^{-1})) is an input to the model in the form of a table (RAINTB) of daily total rainfall; each day with its own number (DAYY).

$$RAIN = AFGEN (RAINTB, DAYY)$$

Interception
Not all rain reaches the soil surface due to interception (INTC) by the plant canopy. The amount of interception (in mm d^{-1}) is calculated according to Makkink & van Heemst (1975) as

$$INTC = AMIN1(RAIN, INTCAP/DELT)$$

where INTC is interception (mm d^{-1})
INTCAP is interception capacity (mm)

$$INTCAP = (1. - FRLT) * FAC * FREWT$$

where FRLT is fraction of radiation reaching the soil (−)
FAC is the mass fraction interception capacity of fresh weight (kg water kg^{-1} biomass)
FREWT is fresh weight of crop (kg m^{-2})

$$PARAMETER \ FAC = 0.2$$

181

EFRAIN = RAIN − INTC

where EFRAIN is the effective amount of rain reaching the soil surface (mm d^{-1})

Runoff

The procedure for calculating runoff is based on experimental data (Stroosnijder & Koné, 1982). The main input parameter is an average yearly runoff fraction of the rainfall. An additional table, which relates total daily rainfall to degree of runoff, enables the calculation of the amount of runoff on each individual day. Use of this table in combination with an estimated long-term average annual runoff factor enables automatic adaptation to individual years with more or less big rainstorms. This procedure is simulated with the following CSMP statements:

RRNOFF = EFRAIN * R * AFGEN(ROFINT, EFRAIN)

where RRNOFF is runoff (mm d^{-1})
R is long-term average fraction of rain that runs off (−)
ROFINT is factor to adjust R (in dependence of the total amount of a rainstorm) in order to calculate runoff from an individual storm (−)
To cite an example for a fine sandy soil in Mali we used

FUNCTION ROFINT = 0., 0., 5., 0.2, 10., 0.5, 20., 1.2, 30., 1.55, 70., 1.7
PARAMETER R = 0.24

Exercise 58
a. Calculate the cumulative amount of runoff (in mm) of the following rainshowers if the long-term average yearly runoff is 30% (assume interception = 0); precipitation = 12,21,8,53 and 18 mm respectively and the above-mentioned table for ROFINT.
b. What is the average runoff percentage of these five showers?
c. How can this average differ from the R value?

Infiltration

The infiltration rate (INFR) in mm d^{-1} is written as

INFR = EFRAIN − RRNOFF

In the above-mentioned crop models, one does not calculate the flow of water between soil layers. But the soil is divided into a number of layers of unequal thickness and moisture content, and one must specify which layers are wetted by the infiltration and also up to which moisture content they are allowed to be wetted. We use a procedure of van Keulen (1975), which fills up the compartments successively from the soil surface further downwards and replenish the

moisture content up to field capacity only. Simple but satisfactory, the model starts this procedure by taking the rate of water flow into the first (top) compartment to be equal to INFR and calculates what can be retained in this layer. The excess is the influx into the second compartment, and so on. To repeat these computations for all layers the statements are written in the following MACRO (for explanation of MACRO see Subsection 2.3.3.):

$$\text{MACRO WATER, MWATER, RWFB} = \text{COMP(RWFT, THCKN, } \ldots$$
$$\text{TRR, ER, DRF)}$$
$$\text{WATER} = 1000. * \text{DRF} * \text{WLTPT} * \text{THCKN} +$$
$$\text{INTGRL(0., RWFT} - \text{RWFB} - \text{TRR} - \text{ER)}$$

where WATER is the actual amount of soil moisture in a compartment (mm)
DRF is initial dryness factor as a fraction of moisture content at wilting point $(-)$
WLTPT is wilting point of soil (m^3 m^{-3})
THCKN is thickness of compartment (m)
RWFT is rate of water flow at the top of the compartment (mm d^{-1})
RWFB is rate of water flow at the bottom of the compartment (mm d^{-1})
TRR is rate of water uptake by plant roots (transpiration) from the compartment (mm d^{-1})
ER is rate of evaporation from the compartment (mm d^{-1})

$$\text{MWATER} = \text{FLDCP} * \text{THCKN} * 1000.$$

where MWATER is maximum tolerated amount of soil moisture in a compartment (mm)
FLDCP is field capacity of soil (m^3 m^{-3})

$$\text{RWFB} = \text{AMAX1(0., RWFT} - (\text{MWATER} - \text{WATER})/\text{DELT)}$$
$$\text{ENDMAC}$$

Note that in the above and following MACROs often the same variable is used either with a subscript T (at the top of a soil layer) or a subscript B (at the bottom of a soil layer). Furthermore the variable at the bottom of a layer has the same value as the one at the top of the layer below, e.g. RWFT2 = RWFB1.

Example 1: *Infiltration*
Thickness layer 1 = 0.02 m, $\theta 1$ = 0.10
Thickness layer 2 = 0.03 m, $\theta 2$ = 0.18
Thickness layer 3 = 0.04 m, $\theta 3$ = 0.12
Thickness layer 4 = 0.05 m, $\theta 4$ = 0.24
WLTPT = 0.04, FLDCP = 0.25
INFR = 5.0 mm d^{-1}

The calculation of the amount of water necessary to wet the first layer to field capacity is $(0.25 - 0.10) \cdot 20 = 3$ mm. The calculation for the second layer is $(0.25 - 0.18) \cdot 30 = 2.1$. With 5 mm of infiltration the soil will not be wetted for more than 2 layers (= 5 cm)(see also Figure 53).
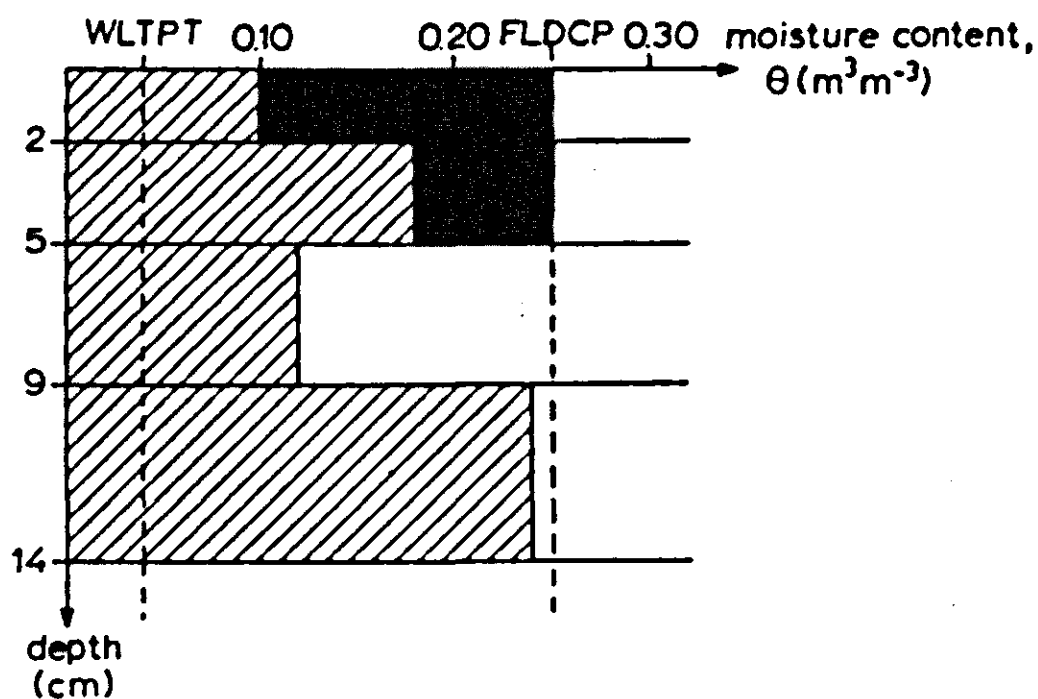
Figure 53. Example of the simulation of infiltration according to Example 1. WLTPT = permanent wilting point and FLDCP = field capacity (all variables in $m^3 m^{-3}$).

Exercise 59

Calculate the amount of infiltration necessary to wet all four layers of Example 1.

Evaporation

Potential soil evaporation depends on how much energy for evaporation (one may distinguish a 'irradiation' and a 'drying power' term) passes through the leaf canopy and reaches the soil surface. Actual evaporation is a fraction of the potential evaporation and this fraction depends on the dryness of the soil surface and the soil's capability to transport water from deeper layers towards its evaporation surface. In ARID CROP this fraction was determined (deterministic) by the soil-water potential of the first soil layer, but wetting of this layer from below was not taken into account. This incomplete deterministic approach was replaced in SAHEL GRASS by a completely parametric approach based on experimental data from the Sahel (Stroosnijder, 1978) and a fully deterministic submodel for evaporation (van Loon & Wösten, 1979). One now assumes that actual evaporation equals potential evaporation during the day of the rainfall and that during the next days the cumulative actual evaporation is proportional to the square root of time. This goes on until the next rainfall. The following CSMP statements (including the calculation of potential evapotranspiration according to Penman, cf. Subsection 3.2.5) achieve such a computation:

AEVAP   = INSW(INFR − 0.01, AEVAP2, AEVAP1)

where AEVAP is actual rate of evaporation (mm d^{-1})
INFR is rate of infiltration (mm d^{-1})
AEVAP2 is actual evaporation rate on rain-free days (mm d^{-1})
AEVAP1 is actual evaporation rate on the day of the rainfall (mm d^{-1})

AEVAP1 = AMIN1(PEVAP, INFR)

where PEVAP is potential evaporation rate as a function of soil cover and of

radiation reaching the soil surface (mm d^{-1})

```
AEVAP2 = AMIN1(PEVAP, EVAPC*(SQRT(DSLR))-...
         SQRT(DSLR-1.)))
PARAMETER EVAPC = 3.3
```

where EVAPC is evaporation constant, experimentally determined for Sahel conditions (mm d^{-1})

DSLR is number of days plus 1. since the last rainfall

```
DSLR    = INTGRL(1.001, 1.-INSW(AFGEN(RAINTB,...
          DAYY+1.)-0.01, 0.,DSLR-0.001))
```

DAYY is number of days (Julian calender); the small value 0.001 was added to avoid division by zero. This statement requires the use of METHOD RECT.

```
PEVAP  = EVAPR*FRLT + EVAPD*FRDP
```

where EVAPR is potential evapotranspiration due to radiation only (mm d^{-1})
EVAPD is potential evapotranspiration due to drying power air only (mm d^{-1})
FRLT is fraction of radiation reaching the soil (−)
FRDP is fraction of drying power reaching the soil (−)

```
EVAPR  = ((DTR*(1.-REFCF)-LWR)*DELTA/GAMMA)/...
         (1.+DELTA/GAMMA)*1./LHVAP
PARAMETER GAMMA = 0.49
PARAMETER LHVAP = 262.E4
```

where DTR is daily total irradiation (J m^{-2} d^{-1})
REFCF is reflection coefficient for short-wave radiation (−)
LWR is outgoing long-wave radiation (J m^{-2} d^{-1})
DELTA is slope of saturated vapour pressure curve at air temperature (mm Hg °C^{-1})
GAMMA is psychrometer constant (mm Hg °C^{-1})
LHVAP is heat of vaporization of water (J kg^{-1})

```
DTR     =AFGEN(DTRT, DAYY)
PARAMETER REFCF = 0.05
LWR     = 4.2E4*1.17E-7*(TMPA+273.)**4*(0.38-0.035*...
          SQRT(VPA))*(1.-0.9*FOV)
```

where TMPA is average daily air temperature (°C)
VPA is average vapour pressure in the air (mm Hg)
FOV is fraction of the day that is overcast (−)

```
DELTA  = 17.4*SVPA*(1.-TMPA/(TMPA+239.))/(TMPA+239.)
```

where SVPA is average saturated vapour pressure in the air (mm Hg)

```
EVAPD  = EA/(1.+DELTA/GAMMA)*1./LHVAP
```

where EA is contribution of drying power of the atmosphere to evaporative demand ($J\,m^{-2}\,d^{-1}$)

$$EA = 0.35*(SVPA-VPA)*(0.5+(WSR/1.6)/100.)*LHVAP$$

where WSR is measured windspeed ($km\,d^{-1}$)

$$FRLT = EXP(-0.5*LAI)$$

where LAI is leaf area index ($-$)

$$FRDP = EXP(-0.5*SQRT (0.2*CROPHT*LAI/(2.*0.5*\ldots$$
$$SQRT(4.*WDL*CROPHT/PI/LAI))))$$

where CROPHT is crop height (m)
WDL is width of the leaves (m)
FRDP according to Goudriaan (1977) p. 109-110.

Example 2: *Evaporation*
Calculate the cumulative evaporation and the average daily evaporation from DAYY = 180 to DAYY = 188 with the following information:
- There is rain at DAYY = 180 (29 June) that results in 12 mm of infiltration into the soil. The Penman potential evaporation (EVAP = EVAPD + EVAPR) equals 6.0 mm d^{-1}. From DAYY = 180 to DAYY = 184 the plants are so small that one may take LAI = 0.0.
- There is more rainfall 4 days later, at DAYY = 184, that results in 8 mm of infiltration. The Penman potential evaporation has decreased to 5.0 mm d^{-1} and from DAYY = 184 on plants are such that LAI = 0.5.
- Take (for simplicity) FRDP = FRLT.

DAYY = 180: INFR > 0, thus AEVAP = AEVAP1
LAI = 0, thus FRLT = 1.0
PEVAP = FRLT · (EVAPD + EVAPR) = 1 · 6 = 6.00 mm d^{-1}
AEVAP1 = PEVAP
DAYY = 181: INFR = 0, thus AEVAP = AEVAP2
DSLR = 2, thus AEVAP2 = 3.3 · ($\sqrt{2}$ − $\sqrt{1}$) = 1.37 mm d^{-1}
DAYY = 182: DSLR = 3, thus AEVAP2 = 3.3 · ($\sqrt{3}$ − $\sqrt{2}$) = 1.05 mm d^{-1}
DAYY = 183: DSLR = 4, thus AEVAP2 = 3.3 · ($\sqrt{4}$ − $\sqrt{3}$) = 0.88 mm d^{-1}
DAYY = 184: INFR > 0, thus AEVAP = AEVAP1
LAI = 0.5, thus FRLT = 0.78
PEVAP = FRLT · (EVAPD + EVAPR) = 0.78 · 5 = 3.89 mm d^{-1}
AEVAP1 = PEVAP
DAYY = 185: DSLR = 2, AEVAP2 = 1.37 mm d^{-1}
DAYY = 186: DSLR = 3, AEVAP2 = 1.05 mm d^{-1}
DAYY = 187: DSLR = 4, AEVAP2 = 0.88 mm d^{-1}

Total evaporation in 8 days equals 16.49 mm, equivalent to 2.06 mm d^{-1}.

All evaporation takes place at or near the soil surface, and this water is (partially) replaced by water flowing upward from deeper layers. However, since no flow between compartments is incorporated in the crop growth models considered, a method had to be found to extract the amount of evaporation from the successive soil compartments. Van Keulen (1975) developed a 'mimick procedure' with a moisture weighted exponential extinction with depth withdrawal function. Since this calculation must be repeated for all soil compartments, as for the computation of the infiltration, we must again use a MACRO:

MACRO TDB, EB, SUMB, ER = SOIL(TDT, ET, SUMT, THCKN,...
                                                        WATER)

ER = F*AEVAP

where ER is rate of moisture withdrawal from compartment (mm d^{-1}) and F is fraction of total actual evaporation withdrawn from compartment (−)

F = THCKN*VAR/(SUM10+NOT(SUM10))

where VAR is moisture weighted extinction (with depth) factor (−)
SUM10 is layer thickness weighted sum of VAR factors (m). The term NOT (SUM10) is introduced to avoid a possible division by zero.

VAR = AMAX1(0.001*WATER/THCKN−WCLIM, 0.)*
          EXP(−PROP*(TDT + 0.5*THCKN))

where WCLIM is volumetric moisture content at air dryness (m^3 m^{-3})
PROP is extinction factor for moisture withdrawal (to be determined by validation with a deterministic simulation model)
TDT is depth of the top of the compartment below the soil surface (m)

SUMB   = SUMT+VAR*THCKN
EB   = ET+ER
TDB   = TDT + THCKN
ENDMAC
PARAMETER PROP = 50.0

Example 3: *Mimic extraction*
The situation in Example 1 will be used with WCLIM = 0.02, PROP = 15.0 and AEVAP = 6.0. The mimic extraction procedure proceeds as follows:

VAR1 = (0.10−0.02) . exp(−15.0 . 0.010) = 0.069
VAR2 = (0.18−0.02) . exp(−15.0 . 0.035) = 0.095
VAR3 = (0.12−0.02) . exp(−15.0 . 0.070) = 0.035
VAR4 = (0.24−0.02) . exp(−15.0 . 0.115) = 0.039
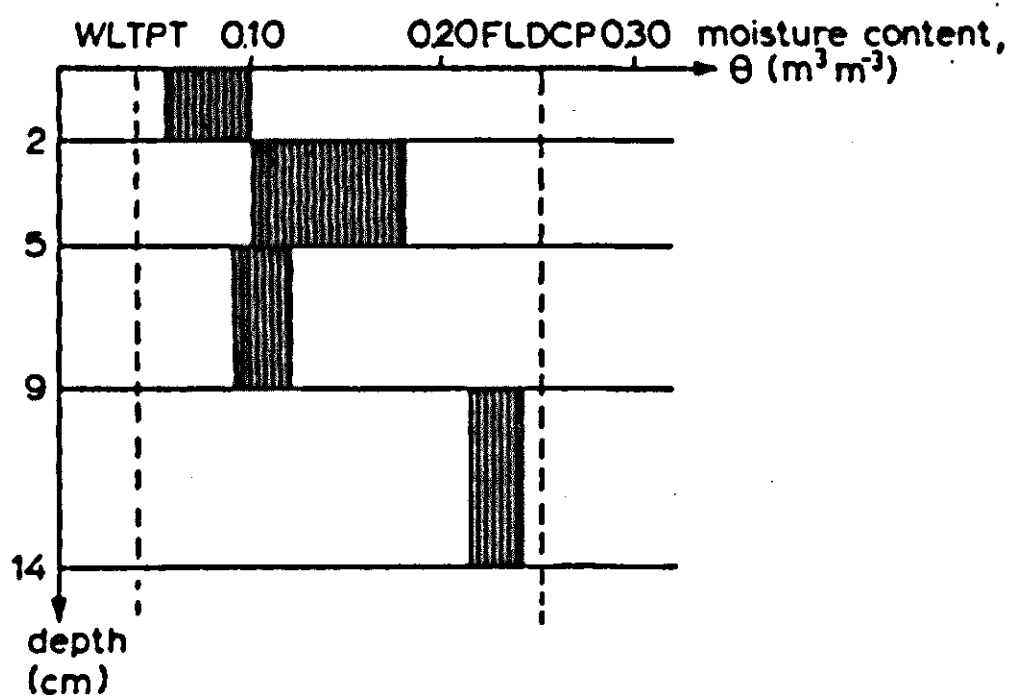
Figure 54. Example of the simulation of evaporation extraction from different soil layers (mimic extraction).

$$SUM1 = 0.069 \cdot 0.02 = 0.00138$$
$$SUM2 = 0.00138 + 0.095 \cdot 0.03 = 0.00423$$
$$SUM3 = 0.00423 + 0.035 \cdot 0.04 = 0.00563$$
$$SUM4 = 0.00563 + 0.039 \cdot 0.05 = 0.00758$$

$$F1 = 0.02 \cdot 0.069/0.00758 = 0.182$$
$$F2 = 0.03 \cdot 0.095/0.00758 = 0.376$$
$$F3 = 0.04 \cdot 0.035/0.00758 = 0.185$$
$$F4 = 0.05 \cdot 0.039/0.00758 = 0.257$$

$$
\begin{array}{lll}
ER1 = 0.182 \cdot 6.0 = 1.1 \text{ mm d}^{-1} & (\Delta\theta = -0.05) \\
ER2 = 0.376 \cdot 6.0 = 2.3 \text{ mm d}^{-1} & (\Delta\theta = -0.08) \\
ER3 = 0.185 \cdot 6.0 = 1.1 \text{ mm d}^{-1} & (\Delta\theta = -0.03) \\
ER4 = 0.257 \cdot 6.0 = \underline{1.5 \text{ mm d}^{-1}} & (\Delta\theta = -0.03) \\
 6.0 \text{ mm}
\end{array}
$$

$$\Delta\theta = 0.001 \cdot ER/THCKN$$

This extraction is shown in Figure 54 as the shaded areas in the different soil layers.

Exercise 60

Calculate the mimic extraction from the situation in Example 3 with four different layers for a case where AEVAP = 4 mm d^{-1}. Take for the initial moisture contents the final situation of Example 3.

Transpiration

Only the soil's influence on transpiration and its reverse will be discussed. In the plant part of the program SAHEL GRASS NPK are calculated:

— the total rooting depth (and no rooting density)
— the potential transpiration

The soil's section of the program checks first how active the roots in the various layers within the rooting depth are and calculates a total effective rooting depth (for example, if there are 10 layers, this is ERLB10). The main program divides the potential transpiration, PTRANS, by this value to obtain the potential transpiration per metre of active root depth (TRPMM). Then the soil's section calculates per layer the actual transpiration as a function of potential transpiration in that layer (TRPMM * RTL), the effectiveness of the roots as a function of moisture content (EDPTF), the temperature of the soil (TEC) and the reduction effect of dryness of the soil on water uptake by the roots (WRED). All computations are again programmed in a MACRO:

$$MACRO\ TRR,\ ERLB,\ TDB,\ TRB\ =\ LAYER(ERLT,\ TDT,\ TRT, \ldots$$
$$THCKN,\ WATER,\ TS,\ MWATER)$$
$$TRR\ =\ TRPMM * RTL * EDPTF * TEC * WRED$$

where TRR is transpiration rate of the soil layer (mm d^{-1})
TRPMM is potential transpiration rate per metre rooting depth in wet soil (mm m^{-1} d^{-1})
RTL is rooting depth in a compartment (m)
EDPTF is reduction factor for root effectiveness as a function of soil moisture content (−)
TEC is reduction factor for root conductivity as a function of soil temperature (−)
WRED is reduction factor for water uptake as a function of soil moisture content (−)

$$RTL\ =\ LIMIT(0.,\ THCKN,\ RTD-TDT)$$

where RTD is total rooting depth (m)
TDT is depth of the top of the compartment below the soil surface (m)

$$EDPTF\ =\ AFGEN(EDPTFT,\ AWATER/(MWATER-1000. * THCKN * WLTPT))$$

where EDPTFT is table of EDPTF versus reduced soil moisture content, $\bar{\theta}$ (see main program)

$$AWATER\ =\ AMAX1(0.,\ WATER-1000. * THCKN * WLTPT)$$

where AWATER is available amount of soil moisture in a compartment (mm)

$$TEC\ =\ AFGEN(TECT,\ TS)$$

where TECT is table of TEC versus soil temperature (TS) (see main program)

$$WRED\ =\ AFGEN(WREDT,\ AWATER/(MWATER-1000. * THCKN * WLTPT))$$

where WREDT is table of WRED versus reduced soil moisture content, $\bar{\theta}$ (see main program)

$$ERLB = ERLT + RTL * EDPTF$$

where ERLB is effective rooting depth at bottom of the compartment (m)

$$TRB = TRT + TRR$$
$$TDB = TDT + THCKN$$

where TRB is cumulative sum of TRR

ENDMAC

Since the program SAHEL GRASS NPK simulates 10 soil layers (August 1980 version) the total actual rate of transpiration (TRAN in mm d^{-1}) is

$$TRAN = TRB10$$

In the above example not all the relations between soil wetness and growth are discussed. In the original MACRO of SAHEL GRASS NPK we used another two sets of statements which also refer to relations between growth and soil moisture. The statements SWP and SWPB check whether there are still soil layers wet enough for the roots to grow deeper. The statements RAWR and RAWRB check whether there is still enough available water for growth or whether plants will suffer from drought. The final statement in this MACRO refers to drainage below the maximum rooting depth. This element of the water balance is not discussed here.

Example 4: *Actual transpiration*
Calculation of the actual transpiration for the example with four layers given earlier and with the following data:
- rooting depth 0.09 m. Hence only the first three layers have roots.
- T1, T2, T3 and T4 all 20 °C

- FUNCTION EDPTFT = 0., .15, .15, .6, .3, .8, .5, 1., 1.1, 1.
- FUNCTION TECT   = 0., 0.06, 3., 0.29, 10., 0.85, 16., 0.94, 20., ...
                 1., 31., 0.87, 40., 0.6, 50., 0.3
- FUNCTION WREDT = 0., 0., .1, .30, .15, .45, .3, .7, .5, .975, .75, ...
                 1., 1.1, 1.

- PTRANS = 2 mm d^{-1}
$\bar{\theta}$ is the reduced soil moisture content:
$\bar{\theta}_1 = (0.10 - 0.04)/(0.25 - 0.04) = 0.29$
$\bar{\theta}_2 = (0.18 - 0.04)/(0.25 - 0.04) = 0.67$
$\bar{\theta}_3 = (0.12 - 0.04)/(0.25 - 0.04) = 0.38$

EDPTF1 = 0.80	EDPTF2 = 1.00	EDPTF3 = 0.90
TEC1 = 1.00	TEC2 = 1.00	TEC3 = 1.00
WRED1 = 0.70	WRED2 = 1.00	WRED3 = 0.85

ERLB1 = 0.02 · 0.80 = 0.016
ERLB2 = 0.016 + (0.03 · 1.00) = 0.046
ERLB3 = 0.046 + (0.04 · 0.90) = 0.082

TRPMM = PTRANS/ERLB3 = 2.0/0.082 = 24.4 mm m^{-1} d^{-1}

TRR1 = 24.4 · 0.02 · 0.80 · 1.0 · 0.70 = 0.27 mm d^{-1} ($\Delta\theta_1$ = 0.01)
TRR2 = 24.4 · 0.03 · 1.00 · 1.0 · 1.00 = 0.73 mm d^{-1} ($\Delta\theta_2$ = 0.02)
TRR3 = 24.4 · 0.04 · 0.90 · 1.0 · 0.85 = $\underline{0.75\ \text{mm d}^{-1}}$ ($\Delta\theta_3$ = 0.02)

$$1.75 \text{ mm d}^{-1}$$

TRAN = TRB3 = 1.75 mm d^{-1}; the extraction over different layers is shown in Figure 55 as the black areas.

Exercise 61

Calculate the actual transpiration for Example 4 and with the following data:
— rooting depth = 14 cm
— T1 = 50 °C, T2 = 35 °C, T3 = 25 °C, T4 = 20 °C
— potential transpiration = 2.5 mm d^{-1}

As already mentioned, the above discussed parametric elements were used to calculate the water balance of the semi-arid Sahel. One of the results is shown in Figure 56. As can be seen the above-ground dry matter can be adequately simulated till the period of flowering; measured and calculated cumulative evapotranspiration also correlate reasonably well over this period. During and after flowering, part of the biomass dies. During this reproductive phase not all the processes are understood well enough to permit their proper simulation.
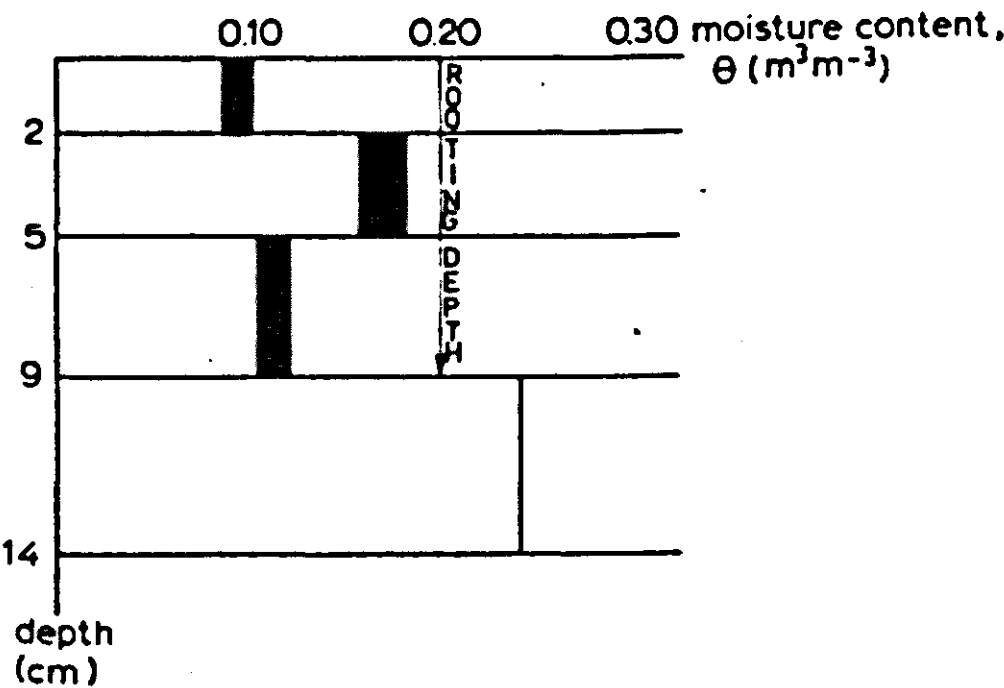
Figure 55. Example of the simulation of actual transpiration from different layers within the rooting depth.

191
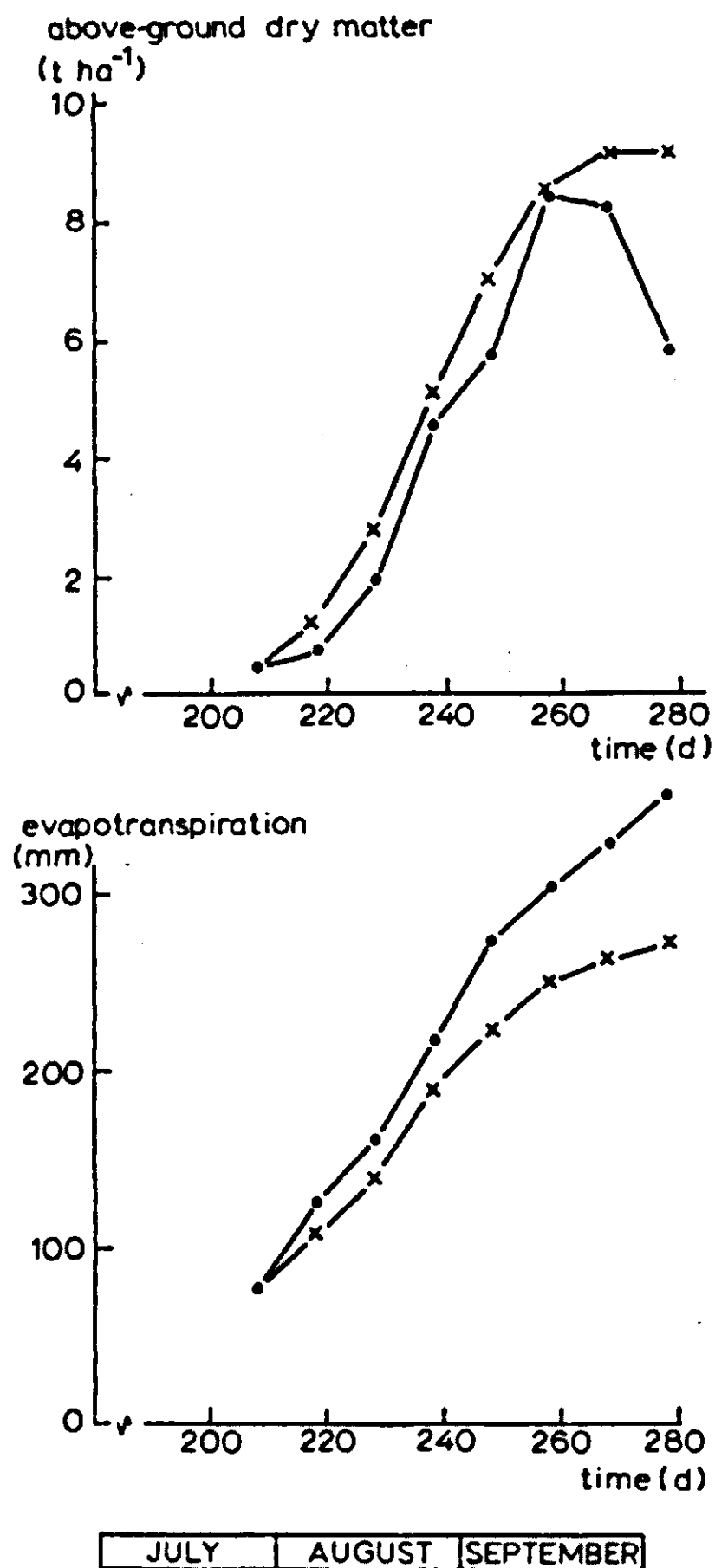
Figure 56. Calculated (x) and measured (•) above-ground dry matter and evapotranspiration of a natural Sahel vegetation with NPK fertilizer, on a clay soil, Niono, Mali, 1978; the program was initialized at Day 208.

4.2.4 Conclusions

Perhaps it is disappointing to hear that a fully deterministic approach to modelling of the important soil-water section of current whole-crop models is not possible because of the great difference in time coefficients of the various parts of such models. One reason for this is certainly the wish to use the state variable approach in combination with specially developed simulation languages like CSMP, which automatically leads to an explicit approximation of all differential equations. Good reasons for having a preference for the state variable approach and CSMP are its easy programming and the advantage that CSMP contains many preprogrammed routines, including those for data entry and output. Another reason is that one wishes to keep the soil divided into a number of layers of relatively small thickness. If one should change this attitude and

192

consider only two layers (e.g. a rootzone and a subzone) this would omit a number (but not all) of problems with the soil-water section. However, reasons for keeping this number of layers are: the wish to include the phenology of roots and to be able to simulate nutrient uptake by roots from various depths (see Subsection 5.3.2).

Our experience with the various parametric soil-water submodels (of which some results are also presented in Section 4.1) is that they can be fruitfully used as long as enough attention is given to a really hierarchical approach to derive and to validate them. The latter shows the need for a stock of deterministic (soil physical) submodels that are already validated and a stock of useful experimental data, both of which have to be updated regularly. This makes clear the role of soil (physical) science in the multidisciplinary effort to understand and simulate crop growth.

4.3 Simulation of field water use and crop yield

R.A. Feddes

4.3.1 Introduction

This contribution differs in two respects from the preceding sections on the simulation model ARID CROP. The model ARID CROP, written in CSMP, simulates transpiration and dry matter production of vegetations growing on homogeneous soil profiles and in absence of a soil water table. As a result of the long integration interval of one day, the description of the soil physical processes had to be simplified and treated somewhat differently than is usual in soil physics. The approach to simulation of the soil water balance presented in this section describes a field situation in a temperate climate with a heterogeneous soil profile and a high groundwater table. The program of the water balance section in this model is executed with fairly small time steps, so that the description of its processes can follow more closely the classical soil physics approach to water in soils.

Figure 57 depicts a typical situation that can be simulated with the model described below. It shows how flow takes place under cropped field conditions in a layered soil, the boundaries of which include two ditches on the side and a pumped aquifer at the bottom. In addition to the effect of these boundaries, fluctuations of the water-table are caused by water uptake by the crop (the roots
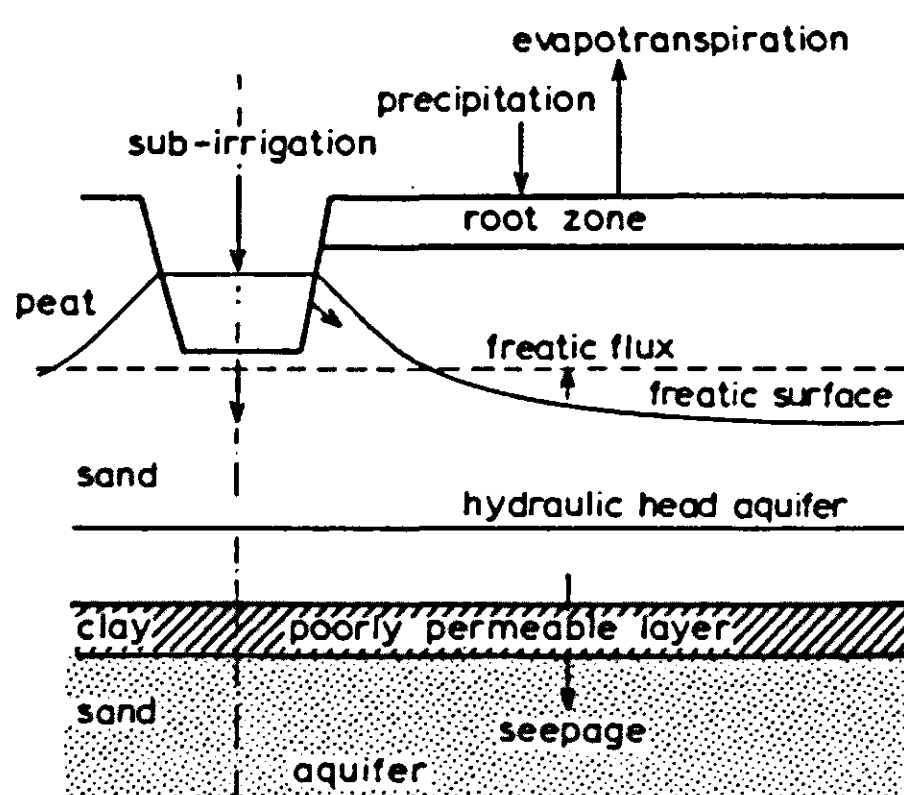
Figure 57. Scheme of the water balance for the case of sub-irrigation from open water courses, upward flow from the water-table to the root zone, and leakage into a pumped aquifer. Because of the symmetry, only half of the vertical cross-section between two ditches is given.

of which grow with time) and evaporation at the soil surface. The total of influences constitutes the so-called water balance. To be able to handle such a system, a rather detailed knowledge of the factors concerned is needed.

Originally, effects of water management, of groundwater recharge, of soil improvement and of other measures were often measured by establishing representative experimental fields, collecting as much data as possible, making various changes in the prevailing circumstances and analyzing the results. With the introduction of the computer it became possible to simulate the effects with the aid of physical-mathematical models, which ideally should react in the same manner to any changes made as the actual system. In the following, two models of Feddes, Kowalik & Zaradny (1978) will be presented that can be used either separately or conjointly. The first model, program SWATR, calculates the actual transpiration of a crop (Subsection 4.3.2). The second model, program CROPR, calculates the actual growth rate of a crop (Subsection 4.3.3). Finally, a discussion of strong and weak points of these models is presented (Subsection 4.3.4).

A diagram illustrating the approach is given in Figure 58. It shows the flow patterns and the action of various factors in the soil − plant − atmosphere system. The water balance of the soil − root system is shown on the left hand side of Figure 58. Irrigation or rain water that is not intercepted by the crop will
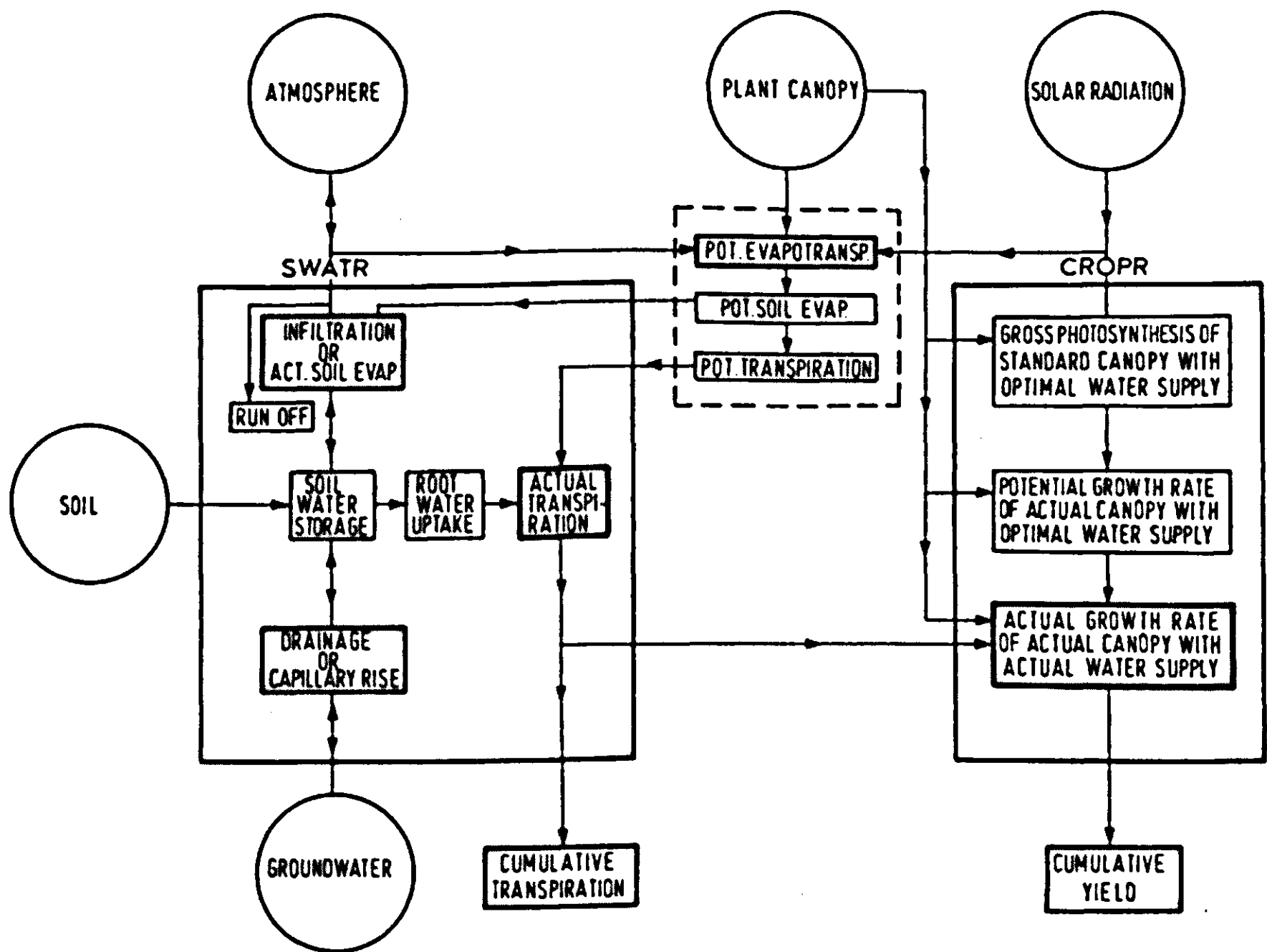
Figure 58. Flow chart of the integrated model approach to assess effects of changes of environmental conditions upon crop water use and crop yield (Feddes et al., 1978).

195

reach the soil. Part of it will become soil moisture, only to be lost by soil evaporation or transpiration. The part of rainfall that does not infiltrate will be lost as surface runoff. The excess of soil moisture will percolate downward to the groundwater table and recharge the groundwater storage.

The transformation of solar radiation into actual crop yield is schematically shown in the right hand side of Figure 58. Gross potential photosynthesis of a 'standard crop canopy' can be calculated according to a model of de Wit (1965) taking into account the height of the sun, the condition of the sky, the canopy architecture and the photosynthesis function of the individual leaves (cf. Subsection 3.2.4). A 'standard canopy' is defined as a canopy with a leaf area index 5 (5 m^2 of leaves per square metre of soil surface) that is fully supplied with nutrients and water. Under actual field conditions these maximum photosynthesis rates will never be reached and corrections have to be made for actual conditions of light energy flux, for air temperature, for fraction of soil covered and for amounts of roots. Moreover, the growth rate is lower than the rate of photosynthesis as a result of respiration losses and investment of dry matter in roots. Accounting for these effects yields the potential growth rate of an actual canopy with optimal water supply. Finally, the actual dry matter yield can be calculated by introducing the actual water uptake of the root system.

4.3.2 The model for field water use, SWATR

To describe one-dimensional water flow in a heterogeneous soil-root system we start with the continuity equation (see also Section 4.2):

$$\frac{\delta\theta}{\delta t} = - \frac{\delta q}{\delta z} - S \tag{61}$$

where θ is the volumetric water content (cm^3 cm^{-3}), t the time (d), S the volume of water taken up by the roots per unit bulk volume of soil in unit time (cm^3 cm^{-3} d^{-1}) and z the vertical coordinate (cm), with origin at the soil surface and directed positive upwards.

The integral of the sink term over the rooting depth z_r (cm, using positive values) yields the actual rate of transpiration T (cm d^{-1}):

$$T = \int_0^{z_r} S \, dz \tag{62}$$

A major difficulty in solving Equation 61 stems from S being unknown. In the field the root system will vary with the type of soil and usually changes with depth and time. Thus root properties, such as root density, root distribution, root length, etc., will also change with depth and time. Experimental and accurate evaluation of such root functions is both time consuming and costly. For these reasons Feddes et al. (1978) propose to use a root extraction term, S, that only depends on the soil-moisture pressure head, h, and the maximum extraction rate, S_{max}, as:

$$S = \alpha(h)S_{max} \qquad (63)$$

with:

$$S_{max} = \frac{T_m}{z_r} \qquad (64)$$

where T_m is the maximum possible, i.e. the potential transpiration rate (cm d^{-1}).

It is assumed (see Figure 59) that under conditions wetter than a certain 'anaerobiosis point' (h_1) water uptake by roots is zero. Under conditions drier than wilting point (h_4) water uptake by roots is also zero. Water uptake by the roots is assumed to be maximal when the pressure head in the soil is between h_2 and h_3. When h is below h_3 but larger than h_4, it is assumed that the water uptake decreases linearly with h to zero. Although it is recognized that h_3 depends on the transpiration demand of the atmosphere (reduction in water uptake occurs at higher (wetter) h_3-values under conditions of higher demand), the limiting point is taken to be a constant.

Equations 63 and 64 can be combined to:

$$S = \alpha(h)\ \frac{T_m}{z_r} \qquad (65)$$

which means that potential transpiration rate, T_m, is distributed equally over the rooting depth, z_r, and reduced for prevailing water shortages by the factor $\alpha(h)$. It is emphasized that Equation 65 is also a drastic simplification, made in the interest of practicality. One of the advantages of this model is that the root system is characterized by the rooting depth, z_r, only (as in ARID CROP, Subsection 4.2.3). In practice this parameter is easily measured. Also the proportionality factor α is a simple function of soil-water pressure head h.

An alternative formulation for S_{max} has recently been made by Hoogland et al. (1981). To account for effects of soil temperature, soil aeration, rooting intensity and xylem resistance upon S_{max}, these authors assumed a linear reduction of S_{max} with soil depth according to:
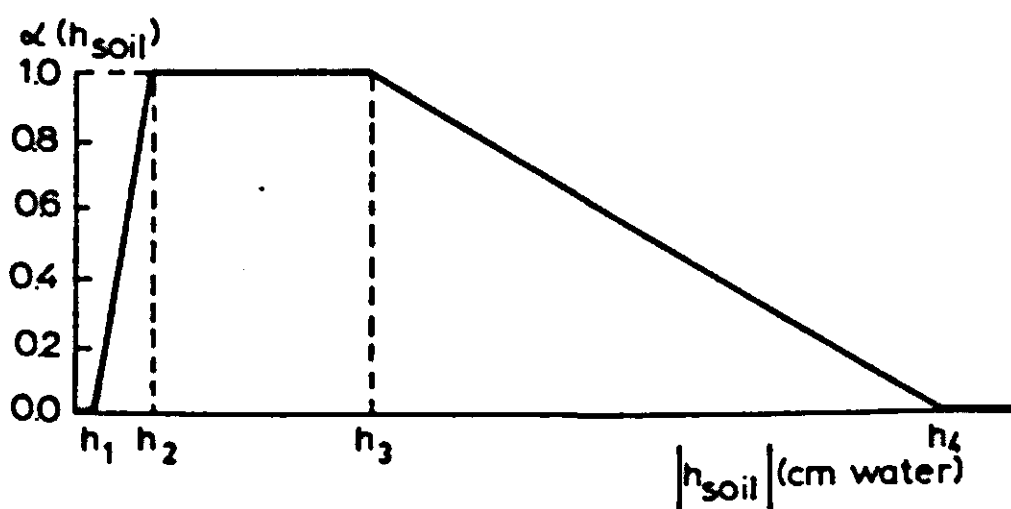
Figure 59. General shape of the dimensionless sink term variable, $\alpha(h)$, as a function of the absolute soil water pressure head, h (Feddes et al., 1978).

$$S_{max} = a - b|z| \quad \text{for} \quad |z| \leq z_r \tag{66}$$

where a and b are constants, in principle to be determined from measured root water uptake data. As a first estimation we assume that $0.01 \leq a \leq 0.03$ cm^3 cm^{-3} d^{-1}, with a mean value of about 0.02, as often found in the literature. The value of b is even more difficult to assess. (If no information about b is available, one may as a first approximation set b equal to zero, giving S_{max} a constant value.) The formulation for the modified sink term now becomes:

$$S = \alpha(h) \cdot S_{max}(z) \tag{67}$$

The water uptake summed over all layers cannot exceed the potential transpiration rate, thus:

$$\int_z^0 S \, dz \leq T_m \quad \text{for} \quad |z| \leq z_r \tag{68}$$

And because water extraction is calculated in the program from the top layer downwards, this formulation permits the simulation that water is extracted preferentially from the upper, relatively wet soil layers. The potential transpiration demand can be met as long as the plant does not extract water from all soil layers of the root zone.

By combination of Equations 61, Darcy's law and 63 and introduction of the differential moisture capacity $C = d\theta/dh$, one arrives at the partial differential flow equation that describes flow of water in the soil − root system as:

$$\frac{\delta h}{\delta t} = \frac{1}{C(h)} \frac{\delta}{\delta z} [K(h)(\frac{\delta h}{\delta z} + 1)] - \frac{S(h)}{C(h)} \tag{69}$$

with $S(h)$ defined according to Equation 65. To obtain a solution, Equation 69 must be supplemented by appropriate initial and boundary conditions. As initial conditions (at $t = 0$) the pressure head is specified as function of z:

$$h(z,t = 0) = h_0(z) \tag{70}$$

At the lower boundary ($-L$) the pressure head is specified as:

$$h(z = -L, t) = h_{-L}(t) \tag{71}$$

The soil-water (Darcian) flux, q, at the upper boundary is governed by the meteorological conditions. The soil can lose water to the atmosphere by evaporation or gain water by infiltration. While the maximum possible (potential) rate of evaporation from a given soil depends only on atmospheric conditions, the actual flux across the soil surface is limited by the ability of the porous medium to transmit water from below. Similarly if the potential rate of infiltration (e.g. the rain or irrigation intensity) exceeds the absorption capacity of the soil, part of the water will be lost by surface runoff. Here, again, the potential rate of infiltration is controlled by atmospheric (or other) external conditions, whereas the actual infiltration depends on antecedent moisture conditions in the soil.

198

Thus, the exact boundary condition to be assigned at the soil surface is not known *a priori*, but a solution must be sought by maximizing the absolute value of the evaporation flux (Hanks et al., 1969a).

If one takes $q^*(z = 0,t)$ as the maximum possible rate of evaporation from the surface, the following expressions must always be satisfied:

$$|q^*(z = 0,t)| \geq |q(z = 0,t)| = |-K(h)(\frac{\delta h}{\delta z} + 1)|$$ (72)

with $h_l \leq h \leq 0$ (73)

where h_l is the minimum pressure head to be allowed under air-dry conditions. Assuming that the pressure head at the soil surface is at equilibrium with the atmosphere, then h_l can be derived from the well-known relationship:

$$h_l = \frac{RT}{Mg} \ln(F)$$ (74)

where R is the universal gas constant (J mole^{-1} K^{-1}), T is the absolute temperature (K), g is acceleration due to gravity (m s^{-2}), M is the molecular weight of water (kg mole^{-1}) and F is the relative humidity of the air (fraction). T and F can be taken from the Stevenson screen.

The maximum possible soil evaporation flux (q^*, Equation 72) as well as the maximum possible transpiration rate (T_m, which determines the maximum possible water uptake by roots per unit area of soil, see Equation 65) can be determined in a number of alternative ways. Potential evapotranspiration ET^* is the sum of potential transpiration T_m and potential soil evaporation E^*:

$$ET^* = T_m + E^*$$ (75)

The value of ET^* can be calculated for example from the combination-energy balance equation of Monteith-Rijtema, from the Priestley and Taylor equation or as a multiplication of the Penman open water evaporation with a crop coefficient. The values of E^* can be computed from a simplified combination-energy balance equation by neglecting the aerodynamic term and taking into account only that fraction of R_n that reaches the surface (Ritchie-approach). Hence, T_m can be determined as the remaining unknown in Equation 75. For full details, see Feddes et al. (1978).

Knowing now the initial and other boundary conditions, Equation 69 could be solved by approximating it by an implicit finite difference scheme, laying a grid over the depth-time region as occupied by the independent variables z and t, respectively. The program SWATR (written in FORTRAN IV) has been designed for a two-layered soil profile and is able to handle maximally 25 nodal points, with constant depth increments. The time step Δt is variable and calculated according to:

$$\Delta t^{i+1} < \frac{\zeta \Delta z}{|q|^i}$$ (76)

where q is the actual flux at the top or bottom boundary of the system for the previous stage of computation and ζ is a factor where $0.015 < \zeta < 0.035$.

Input data in model SWATR are: $h(\theta)$ and $K(h)$ relationships for upper and lower soil layer, depth of the root zone z_r, critical values of the sink term as denoted in Figure 59, initial condition $h(z,t = 0)$, boundary conditions at the soil surface of $T_m(t)$ and of the maximum possible evaporation or infiltration flux through the soil surface $(q^*(0,t))$, boundary condition at the bottom of a water table with $h(z,t) = 0$. Values of $T_m(t)$ and $q^*(0,t)$ can be determined from meteorological and crop data.

Output data of the model include cumulative values of $T(t)$, of integrated water content over the soil profile, of upward/downward flows, of runoff, of $\theta(z,t)$, and $S(z,t)$.

The SWATR model was subjected to field tests. It was found that although computed soil water content profiles did not agree completely with measured profiles, cumulative (evapo)transpiration was simulated fairly well. One example of the results is shown in Figure 60, where curves of cumulative flow are
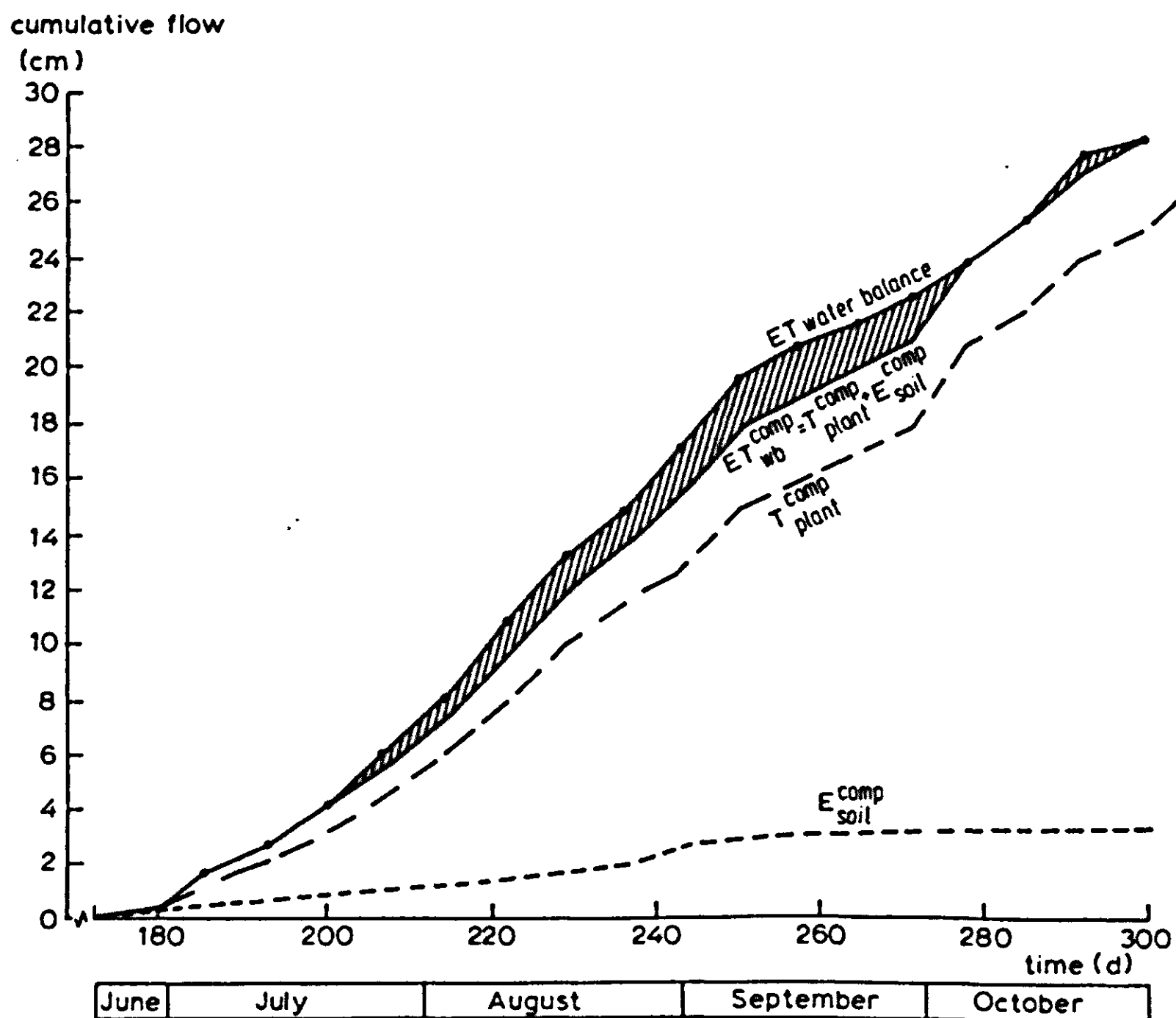
Figure 60. Comparison of the sum of cumulative transpiration and soil evaporation as simulated with model SWATR with lysimetrically measured data for a red cabbage crop, growing on clay in the presence of a watertable (Feddes et al., 1978).

given for a red cabbage crop growing on a clay soil: first the measured cumulative evapotranspiration ($ET_{\text{water balance}}$) as obtained from a lysimeter; secondly the cumulative transpiration $T_{\text{plant}}^{\text{comp}}$ as computed with the model by integration of the sink term over depth; thirdly the cumulative computed soil evaporation $E_{\text{soil}}^{\text{comp}}$; fourthly the sum of $T_{\text{plant}}^{\text{comp}}$ and $E_{\text{soil}}^{\text{comp}}$. From Figure 60 it is seen that there is rather good agreement between computed and measured evapotranspiration, especially at the beginning and end of the period considered.

It is to be noted that a proper estimation of potential transpiration, T_m, is necessary to obtain proper values of actual transpiration. Too high values of T_m will result in a too fast drying-out of the soil. However, there is some feedback in the model as a too-dry water content in one time step will result in a stronger reduction in transpiration during the next time step. Thus, although the distribution of cumulative transpiration with time may not be simulated well, final computed cumulative transpiration may still be quite good.

To extend the flexability of this model and approach, some modifications were introduced recently. Belmans et al. (1981) have developed a new version of SWATR, named SWATRE(extended). As compared with the previous program, the following modifications were made:

- application of another finite difference scheme, chosen according to Haverkamp et al. (1977) and Vauclin et al. (1979), that allows for lower computing cost and that still yields an acceptable accuracy of the soil water balance;
- extension to maximally five soil layers having different properties;
- maximally 40 compartments of equal size in which the entire soil profile is divided;
- the possibility of using the alternative sink term model, Equation 67;
- extension to the use of different types of boundary conditions. Options now include the use of one of the following boundary conditions at the bottom layer: a groundwater level; a flux from the saturated zone (prescribed) while the groundwater level is computed; a flux from the saturated zone (calculated as the sum of the flux towards ditches and the flux of deep percolation) and the groundwater level is computed; a flux from the saturated zone (calculated with a flux – groundwater level relationship) and the groundwater level is computed; a pressure head of the bottom compartment; zero flux at the bottom (of an unsaturated soil profile), i.e. when an impermeable layer is present; free drainage at the bottom (unit hydraulic gradient, unsaturated soil profile)

4.3.3 The model for crop production CROPR

The growth rate of a crop $\dot{q}$ (kg ha^{-1} d^{-1}) is influenced by such growth factors as solar radiation, temperature, water, nutrients and carbon dioxide. Only when all these factors are adequately available, both growth rate and yield will be potential ($\dot{q}_{pot}$ and Q_{pot}). Then potential growth depends on the biological growth capacity of the plant. When one of the growth factors is limiting, growth
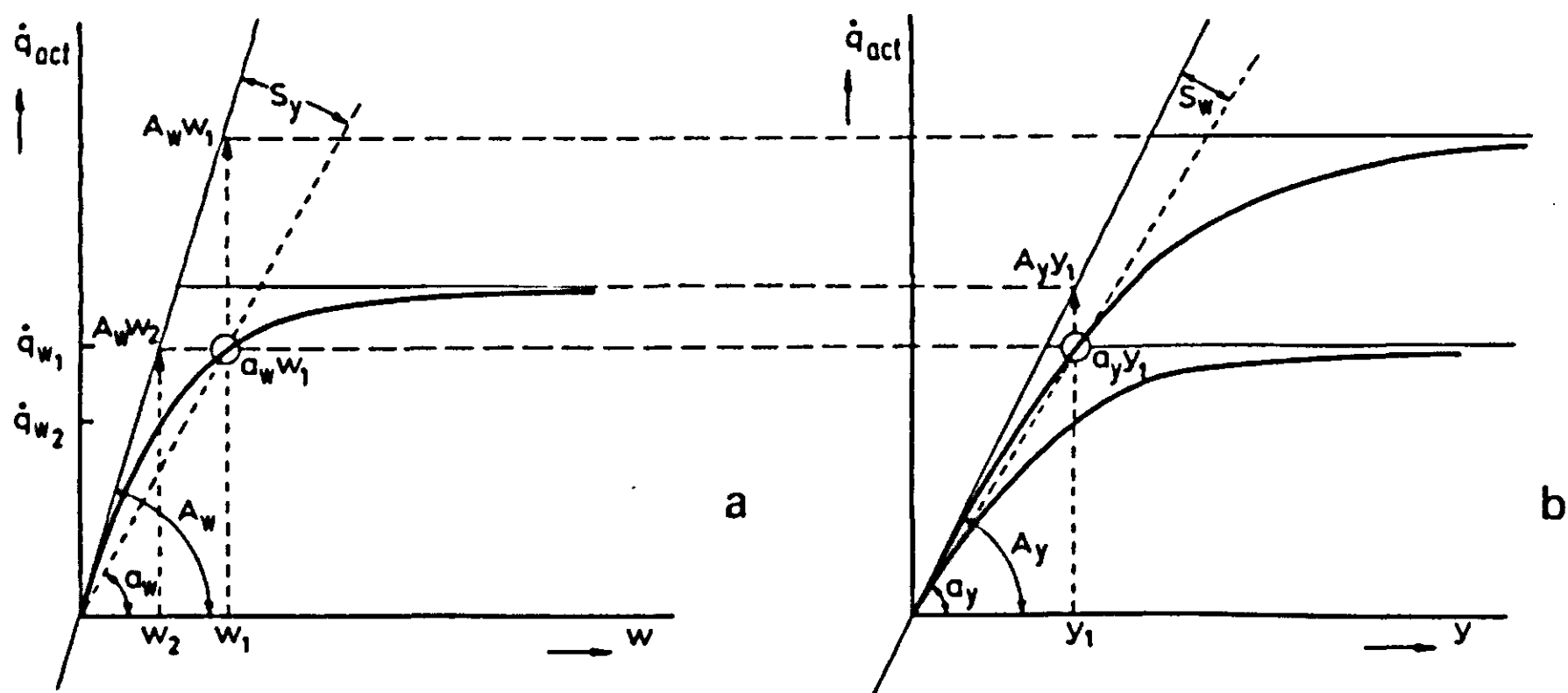
Figure 61a. The response curve of the actual rate of growth ($\dot{q}_{act}$) to the growth factor w at the value y_1 of the growth factor y. The growth rates $\dot{q}_{w_1}$ and $\dot{q}_{w_2}$ at the values w_1 and w_2 of w are shown. The upper asymptotes $A_w w_1$ and $A_w w_2$ of Figure 61b are determined in this graph (dotted lines). The slopes A_w, a_w and their difference S_y are discussed in the text.

Figure 61b. The response curves of the actual rate of growth to the growth factor y at the values w_1 and w_2 of the growth factor w. The upper asymptote $A_y y_1$ of Figure 61a is determined with this graph.

rate and yield are limited ($\dot{q}_{act}$ and Q_{act}). Although other growth factors may still be optimal, potential growth cannot be reached.

The growth rate of a crop as a function of a single growth factor may be represented by a hyperbolic function, with the potential growth rate as the upper limit and the efficiency of utilization of this factor as initial slope of the hyperbola. This is analogous to Figure 25 in Section 3.2 for leaf photosynthesis. Figure 61a shows such a relationship for the growth factor water, represented by the symbol w. A similar function may be drawn for other growth factors. In this section we consider a crop well supplied with nutrients, so that weather conditions, in particular the growth factor solar radiation, determine the potential growth rate. This growth factor is represented by the symbol y.

The question arises how to weight the combined effect of the growth factors water and radiation if both are below their optimum level. The approach of multiplication of relative effects of internal and environmental factors has been shown (Subsection 3.3.3), and the minimum value concept has been discussed briefly (Subsection 1.2.3). An alternative approach was adopted in CROPR, and is explained here in principle. More detail can be found in Feddes et al. (1978), where slightly different symbols are used.

Figure 61a presents a response of the growth rate, $\dot{q}$ (kg ha^{-1} d^{-1}) to the growth factor water (w), defined (Bierhuizen & Slatyer, 1965) as the rate of transpiration of the canopy (T, mm d^{-1}) divided by the water vapour deficit of

the air (Δe, mbar):

$$w = \frac{T}{\Delta e} \qquad (77)$$

T is obtained from SWATR or otherwise. The initial slope of the response curve (A_w, kg mbar mm^{-1} ha^{-1}) is a water-use efficiency factor. The upper level of the response curve is the potential growth rate $\dot{q}_{pot}$ (kg ha^{-1} d^{-1}).

With a high level of radiation (i.e.: a high level of $\dot{q}_{pot}$) and a relatively low value of w, the growth rate $\dot{q}$ is almost proportional to w. When w increases, the increase in $\dot{q}$ becomes smaller because its maximum value is approached. The slope of the line connecting a point from the hyperbola (encircled in Figures 61a and 61b) and the origin, may be called a_w. The difference between the slope A_w and a_w is small when w is small and large when w is large. This is an indication of the degree of insufficiency (S) of the other growth factor: radiation. Thus:

$$S_y = A_w - a_w \qquad (78)$$

The response curve of growth rate $\dot{q}$ versus radiation y can be described similarly (Figure 61b), where the variables A_y, a_y and S_w have corresponding meanings. Hence:

$$S_w = A_y - a_y \qquad (79)$$

(Please note that the measuring of the symbol S in the model SWATR is completely different.)

The upper asymptotes in both graphs are different from day to day, reflecting changes in crop and environmental conditions. Both response curves are mutually dependent. The upper asymptote of the response curve of growth to radiation y (Figure 61b) is the one under the actual availability of water: at the value w_1, this asymptote is $A_w w_1$. The asymptote for the response curve to water is the one determined by the radiation regime: $A_y y_1$. When the value of the growth factor w decreases from w_1 to w_2 (Figure 61a), the upper asymptote of the response curve to radiation decreases from $A_w w_1$ to $A_w w_2$ (Figure 61b). One observes that the result of such a decrease in transpiration is that, following the hyperbolic curve of Figure 61a, the actual rate of growth decreases from $\dot{q}_{w_1}$ to $\dot{q}_{w_2}$, S_y decreases as a consequence. Simultaneously, S_w in the new response curve to radiation will increase. This interdependence is precipitated in the following central supposition of this approach to crop growth rates: the decrease in insufficiency of one growth factor is accompanied by an increase in insufficiency of the other growth factor to such an extent that the product of both remains constant:

$$S_y \cdot S_w = C \qquad (80)$$

(for the mathematical derivation of this supposition: see Feddes et al. (1978)). This supposition implies that a dynamic equilibrium exists of the degree in which the plant experiences the sum of the stresses imposed by insufficiences of

the various growth factors, and that the resulting total stress is as small as possible.

The next question is a mathematical one: how to compute the actual growth rate $\dot{q}_{act}$ from this network of interrelated variables. In Equation 78, a_w can be replaced by $\dot{q}_{act}/w$, and in Equation 79 a_y can be replaced by $\dot{q}_{act}/y$ (Figure 61). Substitutions of Equations 78 and 79 into 80 yields:

$$(A_w - \dot{q}_{act}/w)(A_y - \dot{q}_{act}/y) = C \qquad (81)$$

Dividing the terms of Equation 81 by $A_w A_y$, and replacing $C/A_w A_y$ by the mathematical parameter ζ, gives:

$$(1 - \frac{\dot{q}_{act}}{A_w\,w})(1 - \frac{\dot{q}_{act}}{A_y\,y}) = \zeta \qquad (82)$$

Multiplication of both terms results in a quadratic expression of the actual growth rate:

$$\dot{q}^2_{act} - \dot{q}_{act}(A_w w + A_y y) + A_w w A_y y (1 - \zeta) = 0 \qquad (83)$$

Only the smallest of the two mathematical roots of this expression has a real meaning, so that the final expression of the growth rate becomes:

$$\dot{q}_{act} = \tfrac{1}{2}(A_w w + A_y y) - \tfrac{1}{2}[(A_y y + A_w w)^2 - 4A_y y A_w w(1 - \zeta)]^{0.5} \qquad (84)$$

The product $A_y y$ represents the potential rate of growth of the crop, $\dot{q}_{pot}$. This product might give the impression that the potential growth rate increases proportionally with the level of radiation without any maximum set to it. Obviously, this is not correct. Therefore, $\dot{q}_{pot}$ is not computed in CROPR as a simple product, but according to:

$$\dot{q}_{pot} = P_{st} \cdot \phi_r \cdot \alpha_T \cdot S_c \cdot \beta_h \qquad (85)$$

where P_{st} is gross photosynthesis rate of a 'standard canopy' according to de Wit (1965), ϕ_r is a factor to account for the total respiration of the crop, α_T is a parameter accounting for effect of temperature on growth, S_c is fraction of soil covered and β_h is ratio of harvested part to total plant. The values of ϕ_r, α_T, β_h and the development of crop cover with time S_c are inputs into the model. So there is not yet a feedback with computed actual production rates.

Having calculated actual growth rates, $\dot{q}^i_{act}$ day by day, final yield Q_{act} is calculated as the sum of the daily growth over the growing period:

$$Q_{act} = \sum_{i=1}^{n} \dot{q}^i_{act} \Delta t \qquad (86)$$

In a similar way one can calculate the potential yield:

$$Q_{pot} = \sum_{i=1}^{n} \dot{q}^i_{pot} \Delta t \qquad (87)$$

where Δt in both equations represents a period of one day.

204

Equation 82 is the expression of a non-rectangular hyperbola of the form presented in Figure 61a. To present the completely correct interpretation of Equation 82, Figure 62 is given. It shows that the response curve is bounded by the asymptotes:

$$\dot{q}_{act} = A_w w + \dot{q}_{pot}\, \zeta \tag{88}$$

and:

$$\dot{q}_{act} = \dot{q}_{pot}(1 - \zeta) \tag{89}$$

where $\dot{q}_{pot}$ represents $A_y y$. That its asymptotes are not exactly identical to $A_y y$ and $A_w w$, as was suggested in the beginning of this subsection and in the Figures 61a and 61b, is the result of the assumption (Equation 80) that the product of the insufficiencies in growth factors is a constant: the degree of insufficiency of any growth factor can never be completely zero, but always keeps a small value. This small value is represented by the constant ζ, to which the value of 0.01 has usually been attributed. It makes that both the initial slope and the maximum value of $\dot{q}_{act}$ of the response curves are 1% smaller than the values $A_w w$ and $A_y y$, and A_w and A_y, respectively. In principle ζ should be calculated from experimentally determined response curves.

The parameter ζ has an important effect on the shape of the response curves: it reflects their degree of curvature. A very small value of ζ results in hyperbolas close to their asymptotes (the hyperbolas transform into their asymptotes when ζ approaches zero).
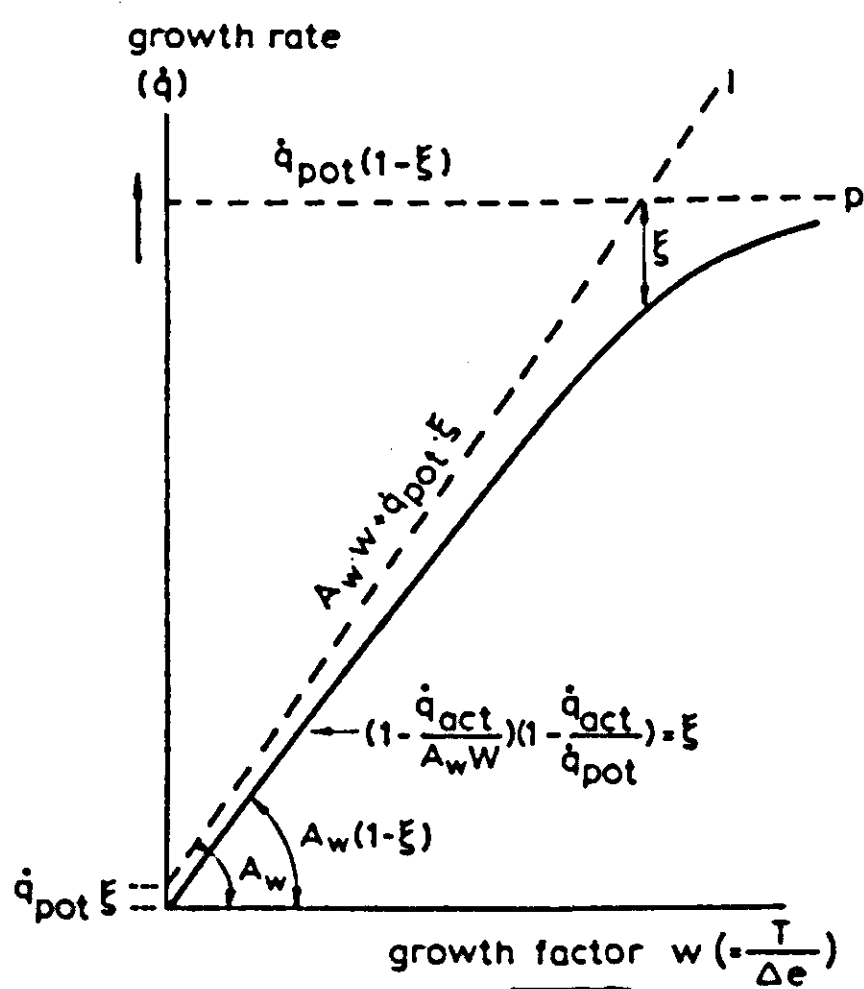
Figure 62. Actual growth rate $\dot{q}$ versus the growth factor water w described as a non rectangular hyperbola, Equation 81, bounded by the asymptotes l and p. Line l indicates the productivity of the crop for growth factor w. Line p represents the production level under conditions of adequate supply of growth factor w and limited supply of some other growth factor y (Feddes et al., 1978).
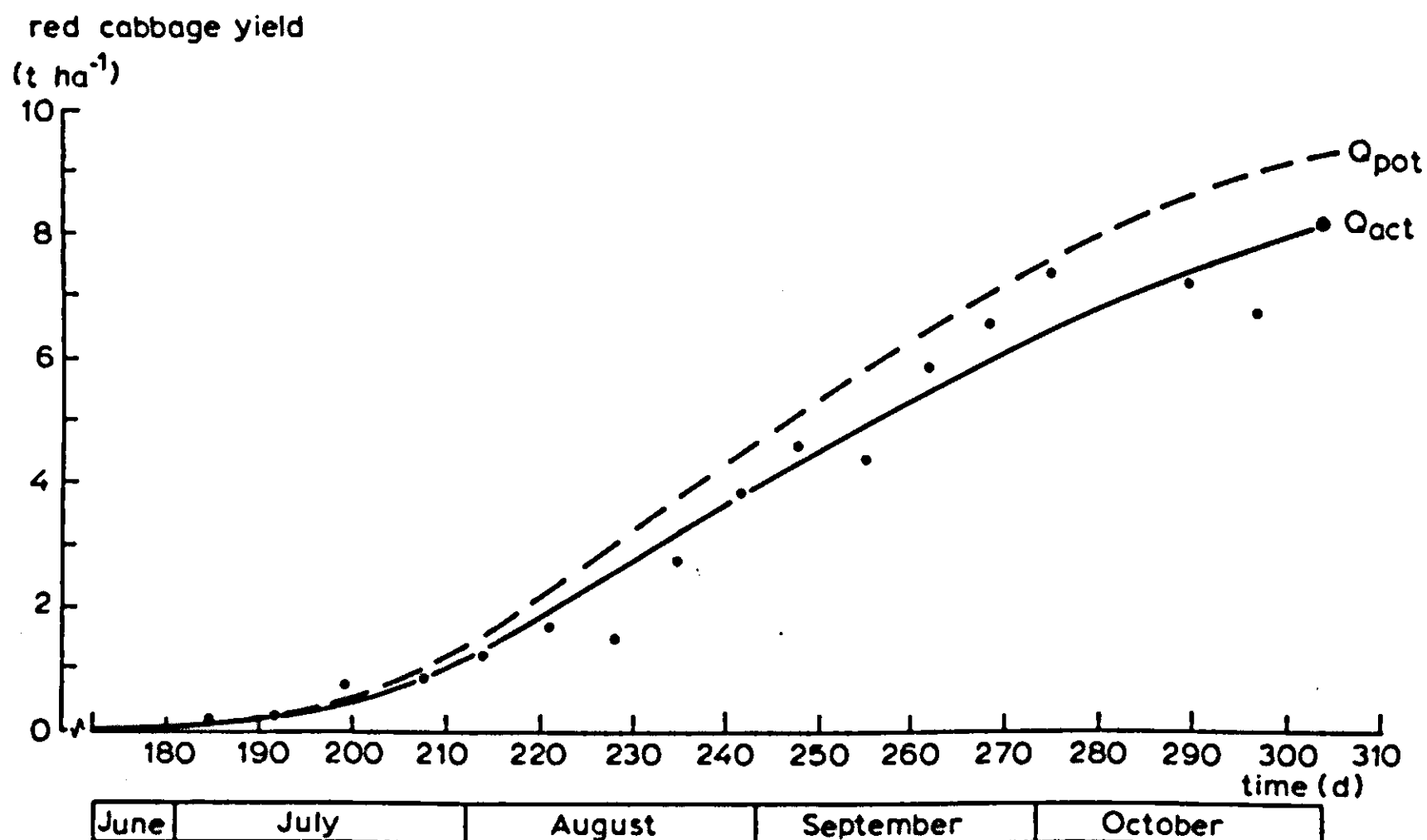
Figure 63. Comparison of measured yield data with computed actual (Q_{act}) and potential (Q_{pot}) cumulative dry matter yields of red cabbage crop derived with the production model CROPR, using as input the simulated transpiration data of Figure 60 (Feddes et al., 1978). Measured growth rates of individual plots (•); the result of the final harvest (●).

Using the transpiration data of Figure 60 as an input for CROPR, computed actual dry matter yields can be compared with measured data. Figure 63 shows that the calculations compare well with the measurements. The measured data represent weekly harvests of one plant. With a heterogeneous crop like cabbage, a relatively large variation in dry matter production then is to be expected. The points show a random scatter around the calculated curve, but the final yield was predicted quite well. The difference between actual yield and computed potential (maximum) yields appeared to be 12%.

The model CROPR was also used for calculating crop yields of grassland. Figure 64 presents computed growth rates and cumulative yields of grassland on two soil profiles in 1972. Measured cumulative yields also are given. The computed cumulative yields agree fairly well with the measured ones.

4.3.4 Discussion

About the approach to the effect of water shortage on the growth rate of the crop, some additional remarks can be made:

– the shape of the response curve of growth to water, as presented in Figure 61a, is not in agreement with the concept of a constant water-use efficiency, as discussed in Subsection 4.1.2. In practice, however, this difference might be small as the maximum value of transpiration is never such, that values of w at the far right hand side of the curve of Figure 61a are used;

206
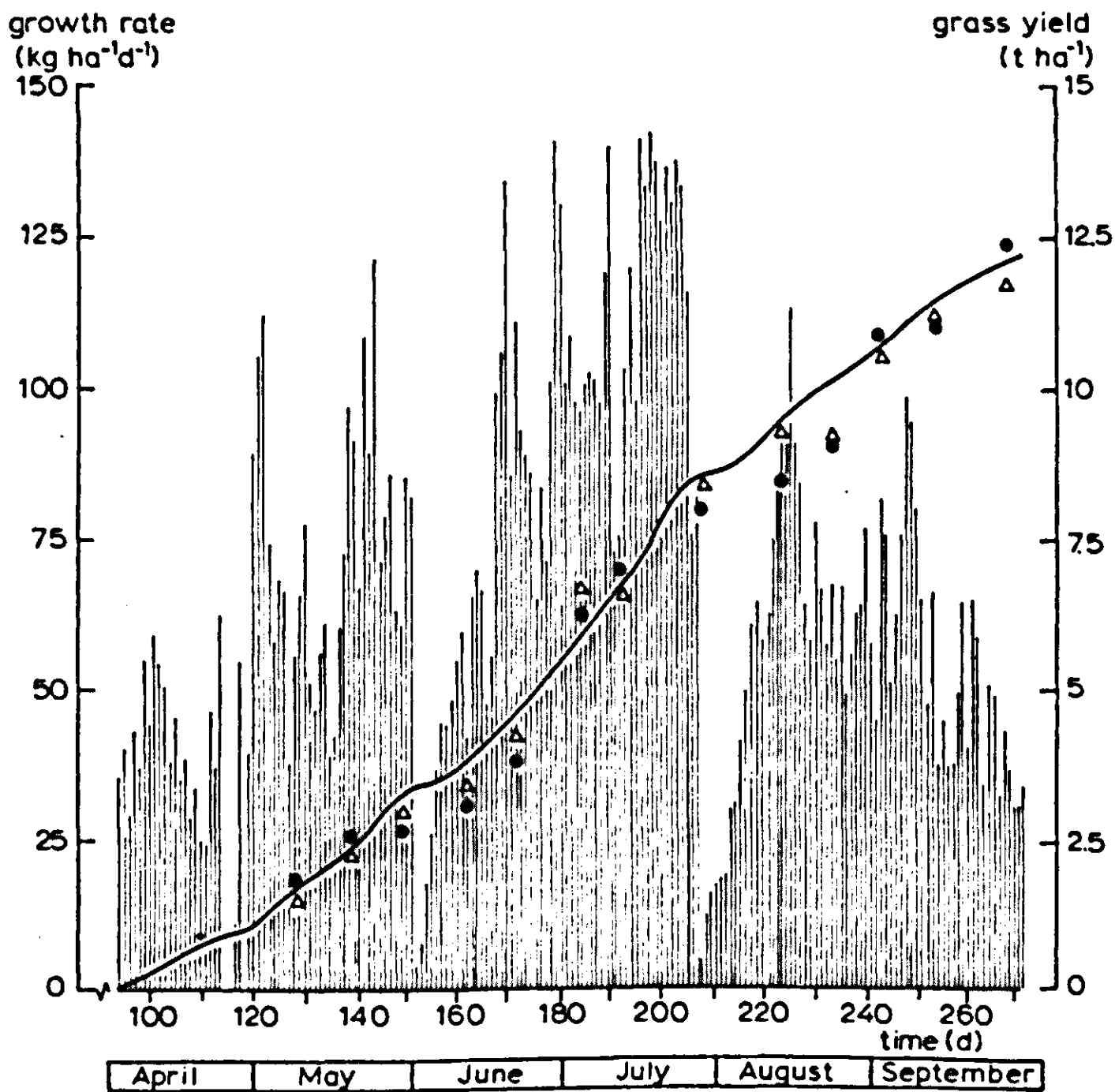
Figure 64. Comparison of computed actual growth rate ($\dot{q}_{act}$) and yield (Q_{act}) with measured maximum yield data on a silty clay over sand (●) and on a silty clay (Δ) of a grass crop in a wet year (Feddes et al., 1978).

- the parameter ζ usually has a value of 0.01. Sensitivity analysis showed that when changing ζ from 0.01 to 0.04 substantial reductions in final yield may occur. It seems therefore worthwhile to give proper attention to the estimation of ζ based on experimental data. The same holds for the value A_w.

- Feddes et al. (1978) present a generalized formulation of crop production that describes the combined effect of n different growth factors w, y, z, etc., as:

$$(1 - \frac{\dot{q}_{act}}{A_w\, w})(1 - \frac{\dot{q}_{act}}{A_y\, y})(1 - \frac{\dot{q}_{act}}{A_z\, z}) \ldots = \zeta \tag{90}$$

An advantage of this method is the relatively low number of parameters that are required to describe the effect of different growth factors: per factor, only the initial efficiencies A_w, A_y, A_z, ... have to be specified, plus the parameter ζ for all curves together, ζ having a relatively low value. This implies that the effect of shortage of a growth factor is generally proportional to the use of this factor up to the potential growth rate (for those conditions) and that luxury consumption of this factor may occur at still higher utilization rates. A disadvantage is that different kinds of responses cannot be distinguished. This might be a handi-

cap at the level of production where nitrogen availability limits growth, because there is no direct relation between the rate of uptake of nitrogen and the rate of growth of the crop (Subsection 5.1.2). However, for all other factors for which a response curve might be drawn as indicated in Figure 62, the approach of Feddes et al. (1978) can be followed.

Figure 60 showed that the model SWATR simulates water use quite well in a temperate and humid climate, as in the Netherlands, and the Figures 63 and 64 show that the model CROPR, using output of a corresponding simulation run of SWATR, simulates crop growth in these conditions fairly well. To improve further on the quality of the model, both models will be integrated more intensively some time in the near future. This is possible as more and more information becomes available about partitioning of dry matter production over leaf and non-leaf material as a function of the development stage of the crop and of moisture stress (e.g. Subsections 3.3.6 and 4.1.4), hence the actual development of soil cover or leaf area with time can be predicted more accurately. The submodel SWATR will then continue to be used with small time steps, and the submodel CROPR with one day time steps. The interaction between both submodels will occur at the frequency of the one day time step.

I will close with a few remarks about some other models on crop growth and water use that have been published. Compared to these models, in the combination of SWATR and CROPR more emphasis is given to soil physical as well as to soil hydrological aspects, i.e. different boundary conditions at the bottom of the soil system are considered. Furthermore, there is a different approach to handle the boundary conditions at the soil surface, while micrometeorological data are considered on a daily basis. It is recalled that the model is designed to simulate for conditions where moisture stress (shortage or excess) occurs, but where nutrients are sufficiently available and pests do not interfere.

The SWATR model requires a very limited amount of information about roots. Most water uptake models need detailed information about root distribution, root densities, conductivities of the soil-root system, soil and plant resistances. Often these parameters vary with soil type and, also, with depth and time. Their experimental evaluation is sometimes impossible, and always time consuming and costly. Moreover, investigations have shown that the parameters mentioned do not always adequately describe the complex root water uptake processes. Therefore, less detailed models have been proposed that are easier to handle and, despite the rough approximation of the problem, might serve the practical needs of the agronomist and engineer. The decision of which root water uptake model to use will largely depend on the amount and extent of input data available and on the specific goal.

Effects of soil aeration, soil temperature and soil fertility upon root growth and water uptake by roots have been dealt with in many separate laboratory and field experiments. Although some relationships have been found, the understanding of the entire complex system is still rather poor. Therefore in root growth and water uptake models corrections for temperature and aeration are

made according to very simple relationships. Generally one speaks in terms of 'minimum', 'optimum' and 'maximum' conditions for growth and uptake, with linear effects assumed between these points.

Root water uptake models can only be used if we are well informed about the physical properties of the soil. It is emphasized that the soil moisture retention and hydraulic conductivity curve should be determined from undisturbed soil samples. This is usually done for measurements in the relatively wet range. For the dry range however, one often uses disturbed samples. The application of the so-called hot-air method for determination of the hydraulic conductivity curve from undisturbed samples is recommended. This method was developed by Arya (1973) in the USA and it is now used in Europe. The method is simple, fast and covers a large soil moisture range. The use of undisturbed samples is important, because small differences in the soil profile may have large influences on both water flow in the soil and water uptake by the roots. Even when taking undisturbed samples, the variation of soil properties within a small 'homogeneous' region may be such that interpretation of the data becomes difficult. This problem of spatial variability has been addressed by e.g. Warrick et al. (1977).

For the reasons mentioned above one has to consider present root water uptake models as primitive tools in predicting water use of a crop. Strict meteorological methods to estimate (evapo)transpiration such as the energy balance approach, the aerodynamic or profile method, or the so-called combination method, however, seem no more accurate or useful.

Crop production models are often relatively simple and generally apply to crops without water sensitive growth stages, i.e. the effects of water stress on growth during all growth stages are similar. For crops showing different effects of water stress during various physiological stages of growth, rather complicated expressions have been developed. However, those models often do not show better results than the simple models (e.g. Stewart et al., 1977). For a literature review of existing simulation models of various crops, the reader is referred to e.g. Arkin et al. (1979). The adaptation of plants to water and temperature stress usually is not included in crop production models (cf. Subsection 4.1.6). For more information about morphological and physiological adaptations of plants to these types of stresses, and their influence on crop production, see, for example Turner & Kramer (1980).

5 CROP PRODUCTION AS DETERMINED BY AVAILABILITY OF NITROGEN

5.1 Crop production in relation to availability of nitrogen

F.W.T. Penning de Vries

5.1.1 Introduction

This section has a character that is different from the others in this book: the text is largely reflective in nature, and it describes the difficulties in developing simulation models on the level of production where nitrogen (N) limits productivity. It neither considers dynamic models, nor the modelling of processes. This is because there are still too many unanswered questions to permit the construction of dynamic simulation models of the depth and quality described in preceding sections. The underlying concepts at this level of production are often not clear, and the existing simulation models are still of a preliminary type (Subsection 1.3.2), i.e. very interesting for specialized scientists, but of little predictive value. Two attempts will be presented to show how far one can go currently with modelling in this field (Sections 5.2 and 5.3).

In the Subsections 5.1.2 and 5.1.3, some of our knowledge of the plant-soil system at this production level will be presented, but it is our approach that will be underlined. Some of the unresolved questions are posed in Subsection 5.1.4. Shortage of phosphorus can have a direct effect on the N uptake of plants, as discussed in Subsection 5.1.5.

5.1.2 Crop yield responses to nitrogen

In a situation in which shortage of N limits the productivity of the crop, there is a clear response within a set of experiments of crop yield to fertilization (e.g. Quadrant a of Figure 65). But if one compares results of fertilization experiments at different sites or in different years, the responses are often less clear. The observations are easier to interpret if data are plotted as in Figure 65, with N absorbed by the crop as an intermediate variable: yield versus N absorbed (Quadrant b), and N absorbed versus intensity of fertilization (Quadrant c). The response curve of yield to N absorbed goes through the origin, and has a horizontal asymptote. The recovery of fertilizer N is a constant fraction (r) of the dose applied, which is represented by a straight line with a positive intercept (Nu) with the horizontal axis, the N absorbed from the unfertilized soil. By introducing this type of analysis, van Keulen (1975) found that he could eliminate much of the variability of the dose-yield response curve of different experiments, and explain it in terms of varying values of the N absorbed from the unfertilized soil and of different values of the recovery fraction of fertilizer N. N absorbed refers to the N contained in the above-ground biomass at flowering or at maturity (the highest of both).

The upper limit of the yield response for any particular case is, of course, equal to the potential production in that situation (Subsection 1.2.1), and can be simulated with models described in the preceding sections. It equals 8500 kg ha^{-1} in this example (Quadrants a and b), that was taken from experiments reported elsewhere (Penning de Vries & van Keulen, 1982). The slopes of two important lines in this figure are also known: those representing minimum and maximum N concentration in the dry biomass at maturity: 5 and 20 g kg^{-1}. Those lines indicate, respectively, the initial slope of the yield response curve and the amount of N absorbed at the potential production level. Together, these three lines describe the response curve of total production to N absorbed already fairly well. Of those lines, only the position of the maximum yield level depends on the actual growth conditions, in particular on the duration of the growing season. The degree of curvature of the response curve is not quite predictable. It may depend on conditions during the growing season, and it may also be that some species are more inclined to dilute their N to the minimum levels than other species are.

The value of the N absorbed from the unfertilized soil is highly variable from one place to another: from as low as 10 kg ha^{-1} yr^{-1} or less on very poor soils and in natural grasslands in semi-arid regions, to values above 300 kg ha^{-1} yr^{-1} on freshly reclaimed soils, rich in organic matter. Its basis is usually the mineralization in the soil. The recovery of fertilizer N is generally between 0.3 and 0.7 g of nitrogen absorbed in above-ground parts plus, eventually, the N in below-ground storage organs, per gram of N applied. Recovery values of about 0.1 have been established in very unfavourable conditions, but also values as high as 0.8 or more have been reported. These values depend on conditions in the soil, on its aeration in particular, on the timing and method of fertilization, and also on the crop or vegetation type.

It is remarkable, but confirmed for many cases, that the value of the recovery fraction at a certain site is usually a constant and does not depend on the level of fertilization. It strongly suggests that all physical, chemical, plant physiological and microbiological processes that remove or utilize N from the soil depend in the same way on the soil nitrogen concentration.

The analysis of response curves according to Figure 65 has been quite useful in temperate and in semi-arid grassland systems (van Keulen & van Heemst, 1982; Penning de Vries & van Keulen, 1982; van der Meer, personal communication), and its generality points towards a common underlying basis of physiological, soil physical and soil chemical processes.

About this basis, there are two groups of questions: those concerning the soil as the source of N, and those concerning the response of the crop to a certain availability of N. Questions about the soil are in particular those about the amount of N provided by the unfertilized soil, the degree of recovery of fertilizer N, and also about the dynamics of the N balance in the soil: rates of mineralization, of immobilization, of nitrification, of denitrification, of leaching, of absorption of N by plants, etc. Section 5.2 will discuss them (except absorption)

214
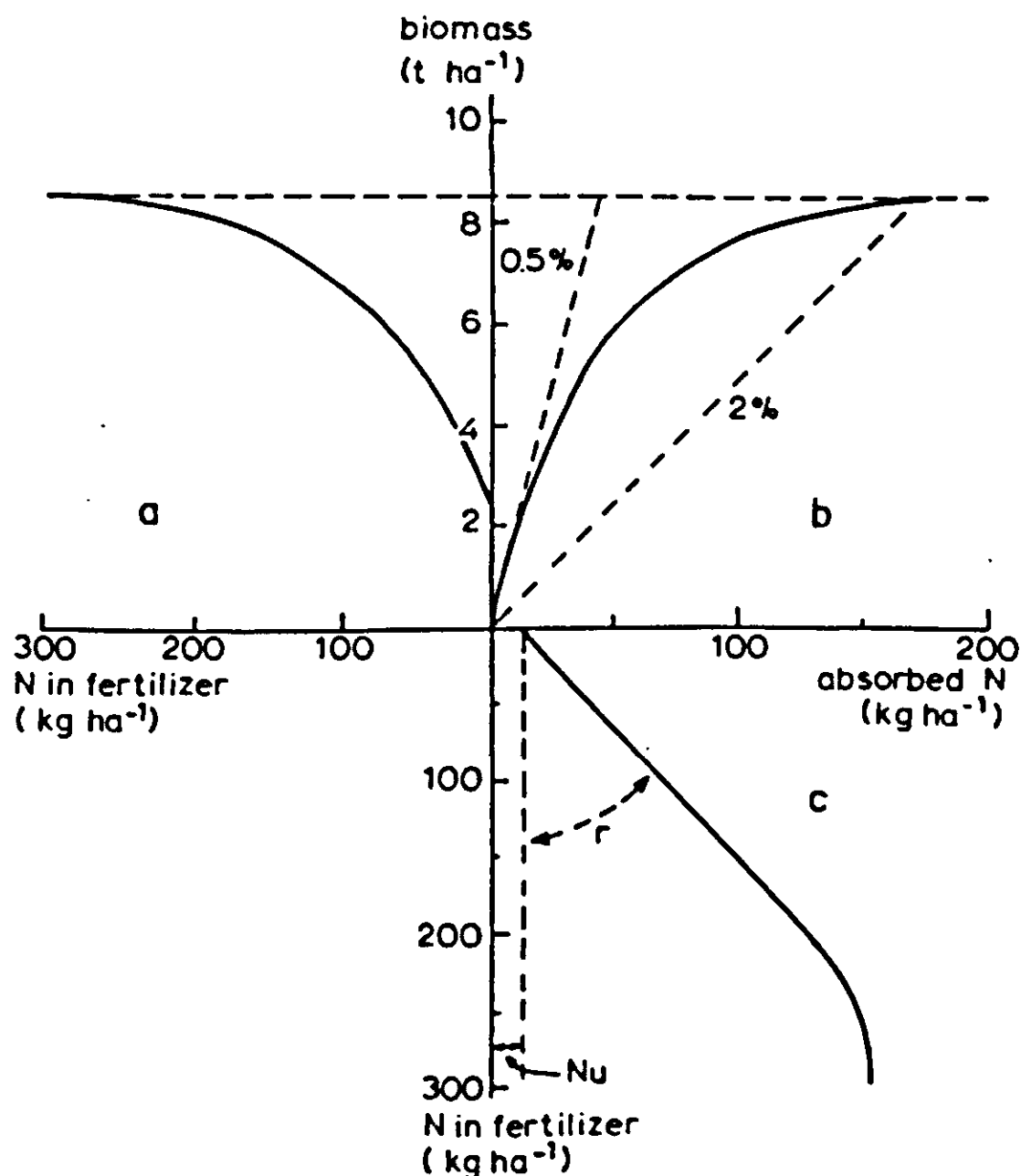
Figure 65. The relations of N absorbed, N applied and biomass yield in one set of experiments with a vegetation consisting of C_4 grasses (Penning de Vries & van Keulen, 1982). Nu is the N absorbed from the unfertilized soil and r is the recovery fraction of fertilizer N.

and show some of our difficulties in their modelling. The remainder of this section concentrates on the response of the crop to N shortage. Questions to be asked are: what is the quantitative response to N shortage, how does it vary between types of organs (in order to predict economic yields), and does it change during physiological development? Section 5.3 presents a preliminary dynamic simulation model that includes many elements of this section and of the next.

5.1.3 Maximum and minimum N concentrations

The supply of N to the plants is often relatively high in the beginning of the growing season, and lower later on. This means that growth of new tissue later in the season must take place with less N than earlier, and one finds that the concentration of N is lower in vegetative tissues that are formed later. This new biomass contains less proteins and more N-free or N-poor material, such as cellulose and lignin. But not only in new tissue does the concentration of N decrease, it commonly drops in old tissues too. A fine example is the work by van Egmond (1975), who studied in detail the concentrations of plant nutrients in

C-A(meq) and
N content (mmol) of
leaf number 10
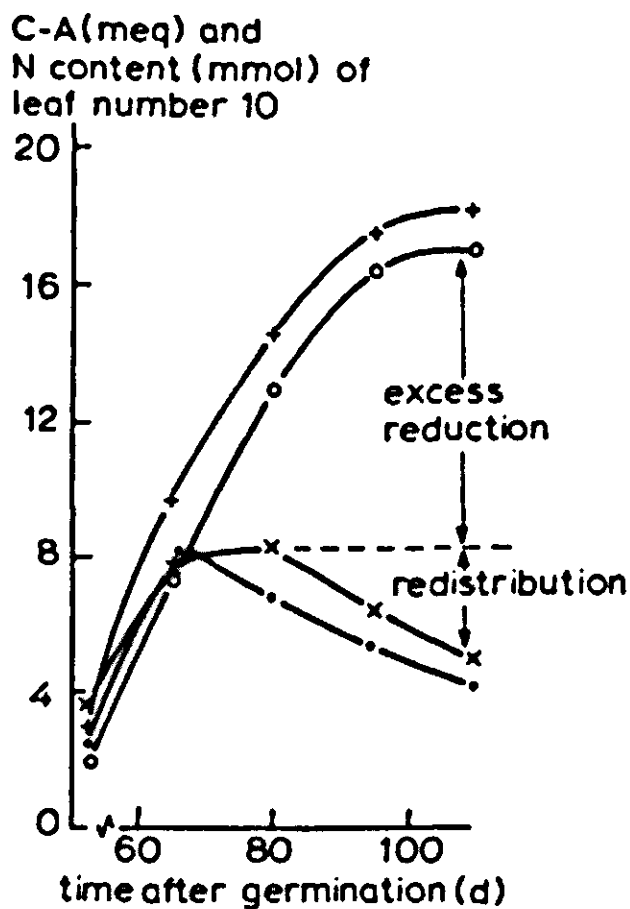
Figure 66. The course of N formed (C-A, upper lines) and N contained (N organic, lower lines) in some sugar-beet leaves (van Egmond, 1975). Of each set of lines, the upper ones correspond with a high intensity of fertilization, the lower ones with a low dose.

organs of developing sugar-beet plants (Figure 66). He concluded that 'leaves with numbers up to about 20 exported a great deal of the organic N they produced, e.g. leaf 10 about 70% at 109 days', and 'leaves with numbers over 25... have imported much of their organic N from the old leaves, e.g. leaf 40 about 30-50% at 109 days'. That import into young leaves concerns not only export of current products of old leaves, but includes also much of what was structural protein before, can be seen in Figure 66: the fraction 'C-A' in the figure represents all nitrate that has been reduced in this leaf and 'N organic' represents the N that is still in the leaf. The C-A fraction consists of organic acids, and is in a sense an immobile slag of nitrate reduced in this species (see van Egmond, 1975). The difference between C-A and N organic is the amount of organic N exported from this leaf. Much of it was N in nitrate form that was reduced in excess of the needs of the leaf, particularly in the young but fully extended leaf (see Figure 66).

Particularly because of synthesis of N-poor components, the concentration of N in the total above-ground biomass decreases in time, even in constant growth conditions. If the source of N becomes exhausted the decrease is even more important because of intensive redistribution. It is therefore of interest to know the range of N concentrations that can be encountered in plants. From a large number of analyses made of the above-ground parts of annual C_4 grasses, C_3 herbs and legumes, Figure 67 has been constructed (Penning de Vries & van Keulen, 1982). It depicts the highest and lowest concentrations of N in the total above-ground dry matter of plants of different development stages, observed in the field and in laboratory conditions. For reasons stated below, it is supposed that the three groups distinguished in this figure apply to the groups of annual C_4 plants (including C_4 dicotelydons), C_3 plants (including C_3 grasses) and legumes in general, rather than just to the smaller groups of species in which the observations are made. The individual species within the three groups distin-

216
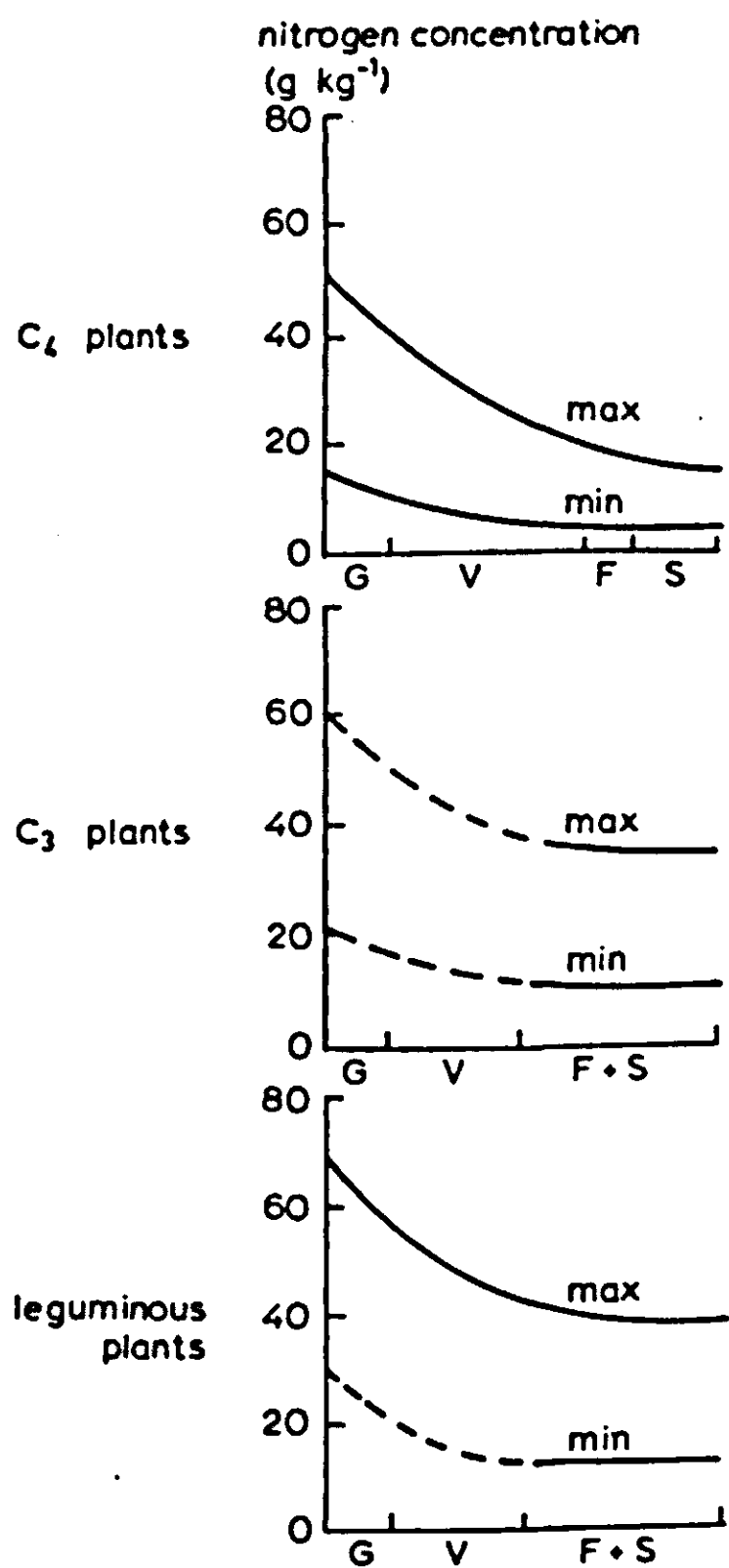
Figure 67. The course of the maximum and the minimum concentration of N in whole plants at different development stages: G stands for germination and early growth, V for vegetative phase, F for flowering and S for seed filling. Broken parts of the lines are based on a few observations only.

guished behaved similarly, but considerable differences occur between the groups.

Figure 67 is only a rough graph because it lumps all organs and many species. Yet one recognizes that there is a level of N in the dry matter below which the plant does not function, the minimum level. This level is about 20 g kg^{-1} in young C_3 plants and the minimum level drops to about 10 g kg^{-1} in mature C_3 plants. The maximum level seems to be about four times the minimum level at any moment in C_3 species. Leguminous species, all of the C_3 type, may form an exception and have still higher minimum values (but these are possibly not really minimum values, because those plants supply themselves with N). Both the maximum level and minimum level in C_4 plants appear often to be about half that of C_3 plants. The practical implication of this aspect of efficiency of N utilization is considerable: C_4 plants function well at much lower levels of N than C_3 plants do. Biomass production on poor soils can therefore be considerably higher with C_4 species than with C_3 species. (However, this may be a disadvantage, as biomass with a N concentration below 9 g kg^{-1} dry matter has lost much of its value as fodder for cattle.) In suitable conditions, it is recalled,

C$_4$ plants are also more efficient utilizers of solar energy and of water (Sections 3.2 and 4.1).

The major reason for the difference between the minimum concentration of N in C$_3$ and C$_4$ plants may be found at the biochemical level. A considerable fraction of N in crop plants is contained in enzymes. The C$_4$ plants contain small amounts of the enzyme Phospho-Enol-Pyruvate-Carboxylase (PEPC-ase), which increases the efficiency of Ribulose-Bi-Phosphate-Carboxylase (RuBPC-ase) to such an extent that photosynthesis can be intensive with much smaller amounts of the latter enzyme than in C$_3$ plants that lack PEPC-ase. This remark becomes more significant if one realizes that the enzyme RuBPC-ase alone makes up 25-60% of the total leaf proteins in C$_3$ plants, and 8-23% in leaves of C$_4$ plants (Ku et al., 1979, Pheloung & Brady, 1979). There is no reason to expect that C$_4$ plants need much more enzyme of another kind for other processes than C$_3$ plants do, so that the difference in photosynthesis system can express itself clearly in the minimum and maximum N concentration of photosynthesizing organs.

The decrease of the amount of organic N after it has attained a maximum in the leaf represents export of protein. This phenomenon of redistribution has been observed often in many crops. This is why in Figure 4 of Section 1.2 the total N in the plant has been divided into a part that remains in old leaves (N stable), while another part can be remobilized for growth (N mobilizable). Because of the redistribution phenomenon, plants can continue for some time to grow new tissue without uptake of N. This is clearly an advantage for plants growing on poor soils, but it provides a considerable handicap for research workers in the interpretation of growth curves in fertilization experiments.

Redistribution of N and other nutrients is closely linked with the process of senescence of organs. A decrease of the rate of photosynthesis in relation to a decrease in protein level in leaves has often be reported (e.g. Lugg & Sinclair, 1981). Section 3.4 discusses the relation of redistribution of N from vegetative parts towards the grains in wheat, and the causal relation of N export to plant senescence. Another good example on the relation between redistribution and senescence is provided by soybean plants, according to an analysis by Sinclair & de Wit (1976). They called the fast redistribution during pod filling 'self destruction' of the plant. If too few proteins remain in the cells, these cells will become unable to maintain themselves and deteriorate. A little before this level is reached, they will stop functioning properly.

From the observation that the amount of proteins in cells can drop, one must either conclude that this was storage protein, or that functional protein has been degraded and exported. The latter is most likely. The definition of reserves of carbohydrates (Section 3.3) as components different from structural material, is thus not applicable to protein. Proteins are like a capital that provides interest, but that also can be consumed if the need arises.

218

5.1.4 Principal questions that remain

To improve our capability of dynamic simulation of growth in N limiting conditions, there are some important questions to be answered by experimental and theoretical research:

— How variable are maximum and minimum concentration of N in tissues of different organs? To what extent is it a function of growth conditions? In what biochemical sense does remobilizable N distinguish itself from non-remobilizable N? The answer to this question is essential in the determination of how much N is remobilizable at each moment for growth elsewhere in the plant.

— The minimum level is defined as that concentration at which the plant stops growing. How far above this minimum level does the plant begin to function normally? How much 'luxury consumption' of N takes place?

— How low must the rate of N supply be before redistribution starts? Is there a minimum rate of supply related to the current growth rate? Or is there always a redistribution of N, even in well supplied tissues, but difficult to detect because protein resynthesis is continuously in equilibrium with degradation and export?

— What is, quantitatively, the relation between protein turnover processes as a result of maintenance processes in the cell (Subsection 3.3.5), redistribution and senescence?

— What does Figure 67 look like for individual organs? Or even better: what is the range of N concentrations for individual processes, like growth, photosynthesis (C_3 and C_4 type) and development. They are definitely different: stems function at very low N contents (and xylem vessels even lower), but growing cells need much N and P for proteins and nucleic acids. Van Keulen (Section 5.3) presents a suggestion for the reducing effect of low N levels on the intensity of processes.

— The uptake of N by the crop after flowering is often small. This is in many cases because the soil is exhausted, in particular at the production level where low N availability limits productivity. But also when there is plenty of nitrate in the soil, the crop does not take up much after flowering (cf. Subsection 3.4.7). It may be presumed that this results from a decreased root activity, possibly as a consequence of the strong demand of the reproductive organs for carbohydrates. A thorough analysis has still to be made.

— What about losses of N from the vegetation and from the soil? As for the vegetation, Wetselaar & Farquhar (1980) made a review and found inexplainable losses of N from growing plants. There are many questions as to when, where and by what process the N gets lost. But there is little doubt that losses of 10-30% of the plant N content can occur in a period of a few weeks at the end of the growing season. Volatilization of NH_3, leaching and insect damage are among the suggested explanations. NH_3 can also be absorbed from the air. The concentrations of NH_3 in the air is one aspect of absorption or loss, the concentrations of NH_3 and NH_4^+ in the plant is another. Of the first value few measurements exist, of the second hardly any. The NH_3 exchange processes with am-

bient air have not yet received much attention. Difficulties in measuring it are certainly an important cause of this. However, a better quantification and understanding of such loss and absorption processes is needed for the simulation on the crop N balance.

— What is the water use efficiency in case of N limitation? As large as when water limits growth (in other words: is the transpiration coefficient a constant?), or does it decrease because water is not limiting anyway. There is some experimental evidence to suggest that the water-use efficiency decreases to some extent in the field (Penning de Vries & van Keulen, 1982), though an indication from a laboratory study points to the constancy of this efficiency (Goudriaan & van Keulen, 1979). Further research is required.

5.1.5 Complications with phosphorus

Much of the considerations for N availability and growth could be repeated for phosphorus (P), only the absolute values are generally about 10-times lower than those for N (Figure 68). P is a constituent of nucleic acids and nucleotides, and it functions as such in energy transfer processes (ATP is a nucleotide). P is also mobile in the plants: van Egmond notes that 55% of the P in a mature sugar-beet has been redistributed. Much less research has been done on P and the effect of P shortage on growth than for N. But there seem to be many similarities between the approach to the effect of P shortage on growth, to that for N (see e.g. Figure 5, Section 1.2). The dynamics of P in the soil, however, are still more difficult than that of N and are not discussed here at all. Readers are referred to Beek (1979), Cole et al. (1977) and Krul et al. (1982).

There is, however, one important phenomenon that should not be overlooked: the concentrations of N and of P in plants are interdependent. From the Figures 67 and 68 it might be concluded that at any development stage, the ratio of P to N could vary about 20-fold: the concentration of N is always between its minimum and its maximum value, the latter being four to five times larger than the first at any moment; the same observation holds for the concentration of P. However, these values were measured in different plants. If a single plant is analyzed, one never finds a ratio of P to N lower than about 0.04 g g^{-1}, and rarely one higher than 0.15 g g^{-1}. This is a much narrower range, which indicates that the concentrations of N and of P are coupled to a certain extent. This reflects a biological feature: both elements play a role in active processes, so that their concentrations cannot be completely independent. From laboratory experiments, Dijkshoorn & Lampe (1980) conclude that the ratio of organic P to N in proteins and nucleic acids together equals 0.055 g g^{-1}. In addition, there is inorganic P in the plants, among others as a result of the splitting up of ATP into ADP and inorganic P during energy transfer. This inorganic P amounts to almost as much as the organic fraction. They conclude therefore that a plant must contain at least a ratio of P to N (total organic N) of 0.10 g g^{-1} for healthy growth.

220

phosphorus concentration

(g kg⁻¹)

C₄ plants

C₃ plants

leguminous plants
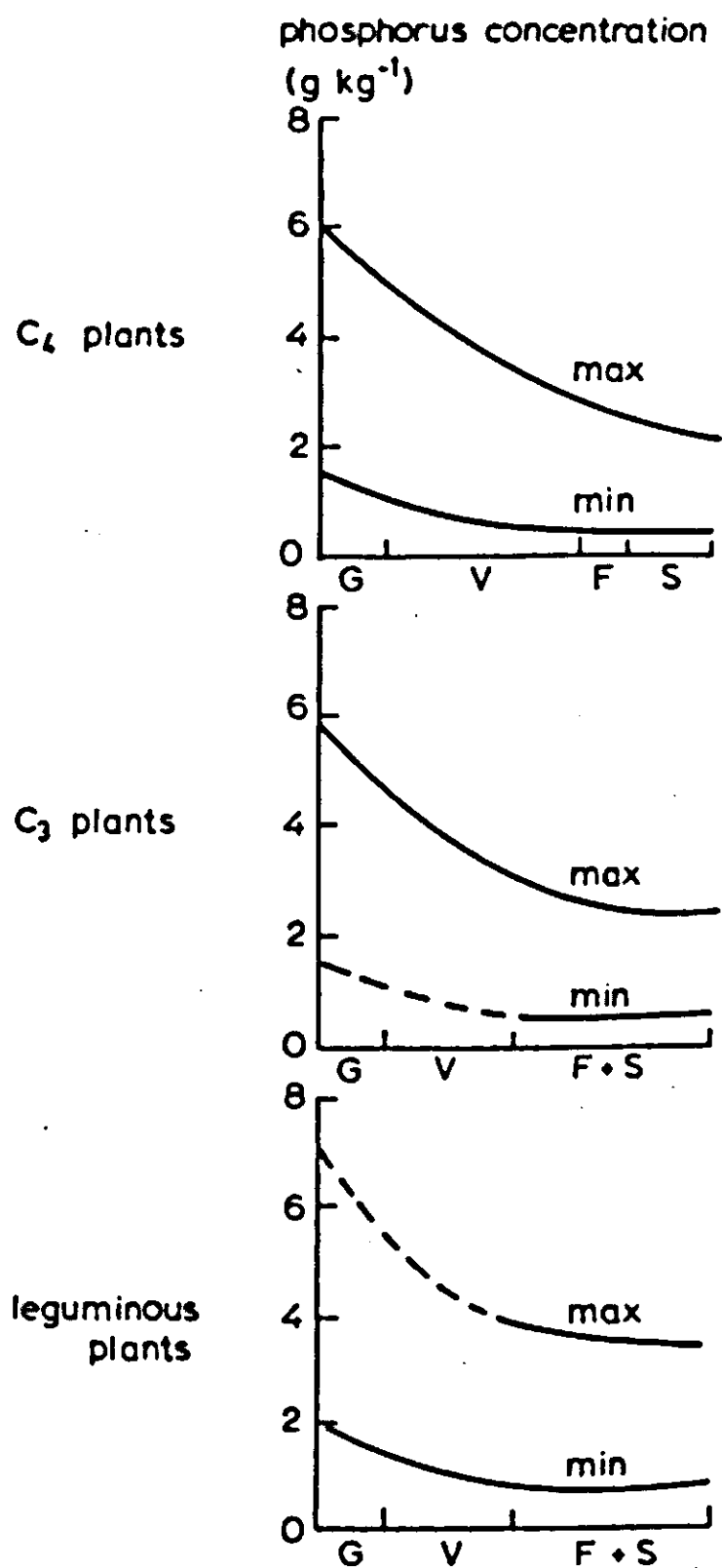
Figure 68. The course of the maximum and the minimum concentration of P in whole plants at different development stages: G stands for germination and early growth, V for vegetative phase, F for flowering and S for seed filling. Broken parts of the lines are based on a few observations only.

The implication of the coupling of N and P concentrations is that at a very low availability of N, P absorption is restricted, and that at a very low availability of P for growth N absorption, or N fixation in the case of legumes, may be restricted. In terms of a simulation model: availability of N and of P are not independent reduction factors between 0 and 1. Their ratio also needs to be considered. It is a question of how far the same ratio applies to all organs, and for the different functions. It is conceivable that N shortage has quite different effects on certain processes than P shortage has.

5.2 Modelling of the behaviour of nitrogen in soil

J.A. van Veen and M.J. Frissel

5.2.1 Introduction

In the last decade numerous mathematical models of the terrestrial nitrogen cycle have been developed. Depending on the ultimate goal, the models differ widely in concept. Moreover models were developed by scientists specialized in different fields, which hindered communication, so that even models with the same goal differed significantly in concept. For this reason a workshop on modelling N in soil-plant systems was organized. During this workshop about 29 nitrogen models and the present 'state of art' of the soil-physical, microbiological and plantphysiological aspects of the fate of N in the soil-plant system were discussed (Frissel & van Veen, 1981). Several classification devices of models of the soil N cycle were proposed. A rough classification is the division into budgeting and dynamic models; budgeting models consist mainly of material balances whereas dynamic models are based on a description of the processes of the system by rate equations, usually in the form of differential equations. Another classification device distinguishes between models which are mainly developed for better scientific understanding, for forecasting and for management purposes (cf. Subsection 1.3.1). A third classification dealt specially with dynamic models of the N cycle, dividing the models into groups depending on whether emphasis was on transport processes, on crop growth or on organic matter transformations.

Subsection 5.2.2 deals with the model developed by the authors, which is a typical representative of the last category (organic matter transformations) since it stresses growth and turnover of the soil microbial biomass and related N and carbon (C) transformations. Furthermore, the present 'state of art' with respect to the soil-physical, chemical and biological aspects of modelling the terrestrial N cycle will be discussed (Subsection 5.2.3). The text of this section is based on papers published elsewhere by van Veen (1977), van Veen et al. (1981) and Frissel & van Veen (1981).

5.2.2 Description of the model

The model, and some general microbiological features

A scheme of the model is shown in Figure 69. The present model does not include a detailed description of N uptake by plants. When the model is used to simulate the fate of N in soil in the presence of crops, the rate of uptake is calculated from the total observed N uptake and it is therefore a driving variable. The transformation processes presented in Figure 69 are described in separate
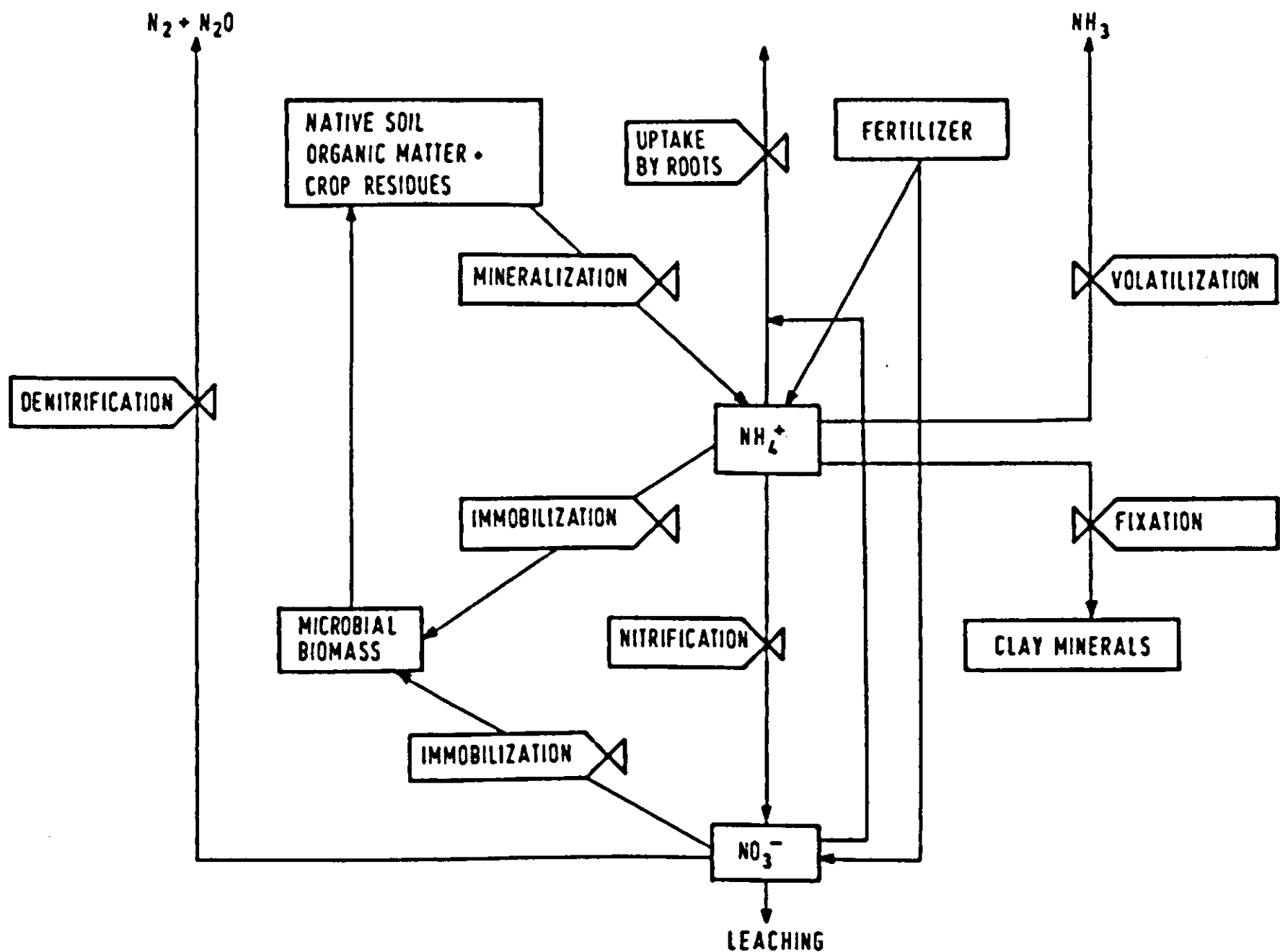
Figure 69. A simplified relational diagram of the N model (van Veen et al., 1981).

submodels. Submodels are: mineralization and immobilization, nitrification, denitrification, volatilization of ammonia, ammonium fixation on clay minerals and leaching. A detailed scheme of the mineralization and immobilization submodel in relation to NO_3^- production and transport is presented in Figure 70. The model is a multilayer model i.e., several layers of soil are distinguished. The equations, described below, are identical for all layers except in case of the first or upper and last or lower layer, for which adapted input and output equations are used. The number of layers, as well as their thickness, depends on the situation under study. Besides the vertical compartmentalization of the total model, in the submodel of denitrification a radial division of a soil volume around an airfilled pore is considered. In this description the number of layers is fixed (10), but their thickness is calculated depending on the relative air volume in the soil.

Growth of micro-organisms is considered to be determined by the concentration of a growth limiting substrate. This relationship is described according to the hyperbolic equation, Monod or Michaelis Menten equation. Thus:

$$GBIOM = GRMAX * BIOM * CX/(KX + CX) \tag{91}$$

where GBIOM is the gross growth rate of microbes, GRMAX the maximum specific growth rate, CX the concentration of the growth limiting substrate X, BIOM the amount of micro-organisms and KX the saturation constant. The

223
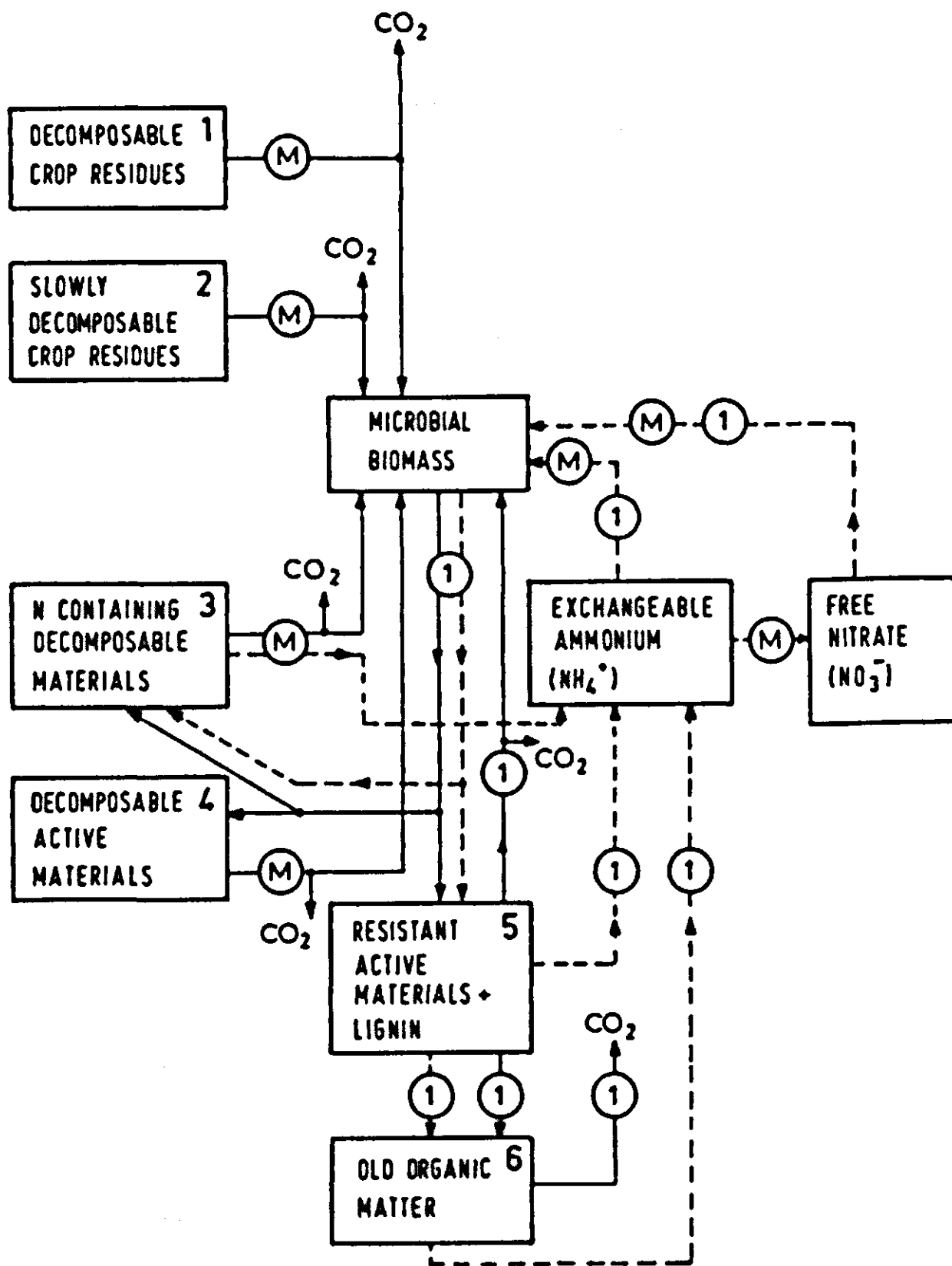
Figure 70. Schematic presentation of the third version of the submodel of mineralization and immobilization (van Veen et al., 1981). Drawn lines represent the flux of carbon, dashed lines represent the flow of nitrogen. Ⓜ stands for Michaelis-Menten kinetics, ① for first order kinetics. The numbers 1-6 of state variables are explained in the text.

consumption rate (= transformation rate) of a substrate, DCX, is linearly related to the gross growth rate GBIOM:

$$DCX = -GBIOM * 1./EFFX \qquad (92)$$

where EFFX is the growth yield (amount of micro-organisms formed per unit of substrate consumed).

The hyperbolic model describes the reactions in which a certain compound is transformed due to catalytic action with a limited 'reach'. This means that the transformation rate not only depends on the amount of the transformed material but also on the amount of transformer, which is not transformed itself. Enzymatic (soil microbiological) reactions are these kind of reactions and are therefore properly described by the hyperbolic model.

Although the hyperbolic model itself is considered to be a correct description of microbial growth and concurrent decomposition of organic matter in soil, it requires data on the maximum specific growth rate and the saturation constant, which cannot or can only very roughly, be determined in soil. Therefore the more simple first-order rate kinetics are often used. The latter model implies that the decomposition rate of an organic component is only dependent on its concentration and that the biological potential to decompose organic matter in soil is not limiting.

Exercise 62

Derive zero and first-order rate equations from the hyperbolic model and discuss the use of zero and first-order rate kinetics to describe microbially mediated transformations.

Nitrifications

Nitrification is described as the result of the activity of only two genera of bacteria, *Nitrosomonas* and *Nitrobacter*. The hyperbolic model is used to describe growth with NH_4^+ and NO_2^- being the growth limiting substrates. The size of the nitrifier population is controlled by the balance between growth and death of the organisms. The latter process is described with first-order rate kinetics.

Mineralization and immobilization

The submodel for immobilization and mineralization has passed three stages during its development. At the first stage the C/N ratio of the organic material was used to control mineralization and immobilization. In a second stage, differences in the decomposability of the several compounds of plant residues were realized and five types of organic compounds were included: (hemi-) cellulose, lignin, sugar, protein and microbial biomass. C/N ratios of the organic matter were no longer used to control the decomposition, but the uptake of C by the growing biomass was determining the decomposition rate. At a third stage the substrates arrangement was revised so that it corresponded better with organic matter distributions as they are used by soil scientists. In this contribution we will deal with the last version only (Figure 70). For the other two versions see Beek & Frissel (1973), van Veen (1977) or Frissel & van Veen (1980).

Mineralization and immobilization are considered to be controlled by the growth and activity of the total microbial biomass in soil. C and N are considered to be the growth limiting substrates, with N being limiting at very low concentrations only (1-2 mg kg^{-1}). To recognize the differences in availability of organic matter compounds as substrates for micro-organisms, both plant residues and soil organic matter are divided into several components.

Crop residue C is split into sugars and other well decomposable carbohydra-

tes (Pool 1, Figure 70) and slowly decomposable material, mostly (hemi-) cellulose (Pool 2). The third pool contains all easily decomposable N containing substances, proteins and aminosugars. The fourth and fifth pool contain microbial debris products and lignins, which thus provide a base for chemical stabilization of organic matter. Those fractions can be considered together as the active fraction, according to Jansson's (1958) nomenclature. The difference between Pool 4 and Pool 5 is based on the consideration that material of Pool 5 consists of organic matter, which is adsorbed on clay minerals or entrapped in soil aggregates, but which is chemically identical to the material in the Pool 4 (Paul & van Veen, 1978). In contrast, the material of Pool 6 is considered to be chemically resistant, i.e. recalcitrant, old organic matter.

When C is used for synthesis of microbial biomass, a corresponding quantity of N (depending on the C/N ratio of the biomass and the substrate) is transferred to the inorganic N pool. But the N flux from the old organic matter (6) to the inorganic N pool is the only one which is not controlled by the soil microbial biomass because of its resistance, and biomass growth is not considered with C of this pool of substrate. The types of the conversion processes in Figure 70 are indicated with ① for processes described by first-order rate kinetics and with Ⓜ for those ones described by the hyperbolic or Monod model.

When using the hyperbolic model, the reaction rates depend on the amount of microbial biomass which is involved in the utilization of a particular substrate, X. Therefore it is assumed that each of the C pools is utilized by a fraction of the total microbial biomass, this fraction being proportional to the ratios of the amount of the particular C compound (CX) to the total amount of C in Pools 1-5 (CT).

The decay rate of the microbial biomass is specific for each type of microorganisms. The types which grow on easily available compounds are assumed to have a fast turnover rate, the types which grow on the resistant fractions turnover slowly. When assuming that the fraction of the biomass, which is involved in the decomposition of compound X, BIOMX, is proportional to the ratio CX/CT, i.e.:

$$BIOMX = CX/CT * BIOM \qquad \text{-(93)}$$

then the decay rate, KBIOMX, will be:

$$KBIOMX = KB * BIOMX \qquad (94)$$

where KB is the decay rate constant. The net growth of the biomass is calculated from the difference between the growth rate and the decay rate.

To obtain the C losses from substrate Pools 1-4 (Figure 70), it must be taken into account that part of each compound is used for biosynthesis and the other part for energy production and related CO_2 production. So the utilization rate of C for biosynthesis, UBIOMX, is equal to the growth rate GBIOMX. The rate of CO_2 production equals:

$$DCO2X = GBIOMX * (1. - EFFX)/EFFX \qquad (95)$$

and the total utilization rate of C is found by summation of UBIOMX and DCO2X. The rate of loss of C from Pools 5 and 6 is calculated according to first-order rate kinetics.

Finally, the N mineralization rate is calculated from the decomposition rate of the N containing components by dividing the C transfer rate by the C/N ratio of the components. The immobilization rate is proportional to the growth rate of microbial biomass (expressed in C equivalents) and is thus calculated by dividing the growth rate of the biomass by the C/N ratio of the biomass.

Exercise 63

Write a computer program to simulate the decomposition of two organic matter components, P and L.

The initial concentration of P, ICP, expressed as a mass fraction of C in soil is 100 μg g^{-1}. P contains nitrogen, its C/N ratio equals 3. Parameters to describe the decomposition of P are: the maximum specific growth rate of microbial biomass on P, GRMAP, equals 0.5 (d^{-1}), the growth yield of biomass on P, EFFP, is 0.6 (g g^{-1}), the saturation constant, KCP is 50 (μg g^{-1} soil) and the death rate of biomass involved in decomposition of P, KBP is 0.3 (d^{-1}).

The initial microbial content, IBIOM also expressed in C is 100 μg g^{-1}soil. The initial inorganic N concentration, INIT, is 100 μg g^{-1} soil and the C/N ratio of the biomass is 8.

L does not contain nitrogen. The important parameters to describe the decomposition of L are: the maximum specific growth rate of the microbial biomass on L, GRMAL, is 0.05 (d^{-1}); the growth yield of biomass on L, EFFL, is 0.1 (g g^{-1}); the saturation constant KCL is 200 (μg g^{-1} soil); the initial concentration, ICL, also expressed in C, is 400 (μg g^{-1} soil); and the death rate of biomass involved in decomposition of L, KBL, is 0.02 (d^{-1}).

Run the program for 15 days, and study the sensitivity of the inorganic N content for an assumed variation in the value of the growth yields.

Denitrification

The submodel of denitrification contains a description of the behaviour of oxygen (O_2) in water-saturated soils and in non-water-logged soils, to determine the occurrence of anaerobic zones in which denitrification is considered to occur. Therefore the number of air-filled pores per soil volume unit is calculated depending on the soil-water content and the pF curve of the soil (see Subsection 4.2.2). Transport of O_2 and NO_3^- from the pores into the surrounding soil is considered as being the result of diffusion due to concentration gradients.

Consumption of O_2, and of NO_3^- in the absence of O_2, is assumed to result from microbial activity, which is calculated in the submodel of mineralization and immobilization.

Ammonia volatilization

Ammonia (NH_3) volatilization is calculated as a function of the following equilibria:

$$NH_4^+ \text{ (exchangeable)} \rightleftharpoons NH_4^+ \text{ (dissolved)} \rightleftharpoons NH_3 \text{ (dissolved)} \rightleftharpoons NH_3 \text{ (gas)} \quad (96)$$

Instantaneous equilibria are assumed, with the equilibrium constants dependent upon temperature. This treatment allows surface soil pH and moisture to be considered. The dynamic step is the calculation of the amount of NH_3 that diffuses from the surface soil into the atmosphere.

Ammonium fixation

Fixation of ammonium ions (NH_4^+) on clay minerals is described by the equilibrium:

$$NH_4^+ \text{ (free)} \rightleftharpoons NH_4^+ \text{ (fixed)} \quad (97)$$

This means that the fixation of NH_4^+ is assumed to be a reversible process between free NH_4^+, i.e. exchangeable and dissolving NH_4^+ and fixed NH_4^+. It should be pointed out, however, that the fixation rate greatly exceeds the rate of release of fixed NH_4^+.

Leaching

Leaching is described by a multicompartment submodel. A typical model suitable for combination with the N conversion equations may consider five soil layers of 20 cm each. It is assumed that NO_3^- is the only N component which migrates, because transport of NH_4^+ is negligible. The simplified transport equation is:

$$TNO3 = DIFN * (NO3(I) - NO3(I+1))/DX + LE * WFU * (NO3(I) + \dots$$
$$NO3(I+1))/2 \quad (98)$$

where TNO3 is the flux of NO_3^- which passes the boundary between the layers I and I+1

NO3(I) is the concentration of NO_3^- in compartment I ($g\ m^{-3}$)
DX   is the distance between centres of compartments I and I+1 (m)
WFU   is the moisture flux ($m^3\ m^{-2}\ s^{-1}$)
LE   is the leaching efficiency factor (−)
DIFN   is the apparent diffusion coefficient ($m^2\ s^{-1}$), computed as:

$$DIFN = TET * TORT * DIFNW + DISP * WFU \quad (99)$$

where TET is the moisture content ($m^3\ m^{-3}$)
TORT is the tortuosity factor (−)
DIFNW is the diffusion coefficient of NO_3^- in water ($m^2\ s^{-1}$)
DSIP is the dispersion distance (m).
(Dispersion results from the random direction of diffusion of NO_3^-; tortuosity accounts for the elongation of the diffusion pathway that results from the heterogeneity of the soil pores filled with water.)

Environmental factors

Effects of environmental factors, such as temperature and moisture on the microbially mediated processes are included by using multiplicative reduction factors. The way in which combined effects of environmental factors are expressed in simulation models has a profound impact on the calculations (Frissel & van Veen, 1978). If the reduction factors for temperature, moisture content, and O_2 pressure are represented by TCOF, WCOF and O2COF, respectively, many possibilities exist for combining them (cf. Subsection 3.3.3). An extreme view is the assumption that all factors act independently, which leads to the multiplication of all factors.

EFFECT = TCOF * WCOF * O2COF   (100)

If the values of the reduction factors (dimensionless) are, 0.8, 0.7 and 0.4, respectively, Equation 100 results in EFFECT = 0.2. Another extreme view is consideration of the minimum value only, giving EFFECT = 0.4. A third possibility is consideration of temperature separately and its multiplication with the minimum value of the other two reduction factors, resulting in EFFECT = 0.3.

In this model the last possibility was chosen. The effect of pH on biological processes was not included. It was assumed that changes of the pH of a soil did not influence bacterial growth and that thus the microbial population was adapted to the pH of a soil.

5.2.3 The 'state of art' on modelling the terrestrial nitrogen cycle

In general, it appears that our mathematical skills exceed our knowledge of the biological system being described and the quality of input data available. Thus, care should be taken when evaluating output from N models based on minimal knowledge and inadequate input data. The 'state of the art' on modelling the terrestrial N cycle will be considered briefly on the level of the individual processes.

Nitrification

Nitrification has been the most intensively examined of all the processes of the nitrogen cycle. Several other simulation models of nitrification in both aquatic and terrestrial systems have been developed (see van Veen et al., 1981). However, not one model includes microbial growth, death, non-steady state conditions, saturation kinetics for N oxidation, diffusional effects on oxidation under static water conditions (which do exist often in soil), and ion-exchange effects on NH_4^+ supply and movement together.

Nitrification is usually modelled as the result of the activity of chemoautotrophic micro-organisms: *Nitrosomonas* for oxidation of NH_4^+ and *Nitrobacter* for oxidation of NO_2^-. Heterotrophic nitrification is not considered explicitly in modelling.

Because only a few species of micro-organisms are involved, the effects of the

principal environmental variables affecting nitrification (temperature, pH, moisture and O_2 status) are well defined. Moreover, the process occurs within a much narrower range as compared to other processes, where a more diverse population of micro-organisms is involved. Thus, modelling of the effect of a particular environmental factor is comparatively easy and excellent fits with reality have been obtained. However, the combined effect of several factors has not yet been well defined. The lack of data and experimental evidence on correct mathematical expressions of the combined effects has appeared to be a very serious limitation to modelling, not only of nitrification, but also of other N cycle processes.

Mineralization and immobilization

As in most of the more comprehensive models of mineralization and immobilization, in this model the exogenous and soil substrates are divided into several components. Although this approach is superior to a description in which soil organic matter is considered to be an entity, it should be pointed out that the possibilities to measure quantity and turnover rate of the several soil organic matter fractions are limited.

The role of soil in protecting organic matter against decomposition and so, in controlling organic matter dynamics, together with tillage effects on this protection, requires further elucidation. Long-term modelling studies indicate that changes in the amount of protected compounds might be instrumental in controlling the decrease of soil organic-matter content of virgin grassland after cultivation (Paul & van Veen, 1978). Models usually treat stable soil N as consisting of several components. Good methods to partition soil N among these components are still lacking, and this probably constitutes one of the most severe single deficiencies in our understanding of soil N dynamics, regardless of the type of model used. This lack of good methodology exists because, in spite of our reasonably good understanding of what causes N to cycle, we do not understand the mechanisms, unique to soil systems, which prevent N from cycling. The presence of considerable quantities of organic compounds, such as sugars and amino acids, in soil among a large abundance of mostly starving micro-organisms which are capable of decomposition of these compounds, continues to be a highly remarkable observation.

Models explicitly including micro-organisms may be of no more value as general predictive tools for a given site with defined management or environment, than those without micro-organisms. (The model PAPRAN, e.g. discussed in the next section, does not consider micro-organisms explicitly.) The value of the larger models lies in a greater requirement to treat (if even superficially for lack of good data) mechanisms of action and control, resulting in greater applicability and flexibility. The range of conditions that can be examined is greater because mechanisms, and not only observations, are modelled with such explanatory models (Subsection 1.1.2). A proper understanding of mechanisms controlling processes is necessary to understand the terrestrial N cycles.

Soil microbial biomass measurements are essential and continue to be a problem. Comparisons between different methods such as plate counting, direct microscopic techniques, and chemical techniques, such as ATP measurements and CO_2 production measurement after fumigation, show that the data obtained are rather inconsistent, with the chemical techniques giving the highest biomass values (Paul & van Veen, 1978). There is a need for methods, which can be conveniently applied, to obtain reliable and comparable biomass values in soil ecosystem studies.

Many parameter values describing microbial processes are based on data from laboratory experiments with continuous cultures in chemostats. The use of these data in soil ecosystem studies has been justified on the basis of the continuous supply of nutrients in growth limiting concentrations in both systems (Veldkamp & Kuenen, 1973). Although this hypothesis seems reasonable, it should be carefully checked, especially since the continuously changing conditions in soil may lead to important differences between the systems. A case in point is the discrepancy between estimates of maintenance respiration rates in soil and in liquid culture.

The description of microbial organic matter transformation, which actually is biomass turnover, is a key point in N simulation models. Sound data are necessary on the rate of uptake, the efficiency of the use of organic compounds for biosynthesis or energy supply, the rate of release from the biomass and the quality of the released products. The first two aspects are quite well described in the literature with respect to uptake from solution, but substrate supply to the solution in soil is still poorly understood. On the quality and quantity of N and C compounds being released from the biomass in soil, no data are available.

The concept of concurrent growth, maintenance and death or debris production of micro-organisms is inadequately defined and most data provide only net growth rates. Death, endogenous metabolism and debris production have traditionally been handled by high maintenance rates. This is unacceptable (van Veen, 1977).

Alternatively, a portion of the population has been considered active with a high maintenance rate, while the remainder is inactive with a low maintenance rate (Hunt, 1977; Frissel & van Veen, 1978). It is generally accepted that the most realistic modelling results are obtained with an explicit treatment of death or decay plus debris production. Further development of either treatment requires more experimental data on the mechanisms controlling the release in soil of C and N from biomass either through death or waste production.

Denitrification

Our submodel of denitrification should be considered to be a first attempt to simulate the complex process of the occurrence of anaerobic sites in soil and subsequent denitrification at these sites. The concept of cylindrical pores filled with water or air, depending on the actual moisture content and the soil pF curve, may be used as was described above, or a more detailed description con-

sidering aggregate sizes and the occurrence of anaerobic zones within aggregates (Leffelaar, 1979; Smith, 1980) may be employed.

Further development of denitrification models and testing on experimental results are seriously hampered by great uncertainties in the reliability of existing methods for measuring denitrification. Newly developed methods for direct measurements, using acetylene blockage of N_2O reduction, are promising. The current interest in N_2O-N_2 ratios in the gases evolved has drawn attention to some of the fundamental problems related to this process in soil.

In addition to limitations to the O_2 supply, questions on the energy supply to denitrifiers in soil, and on the NO_3^- concentration and denitrifier population controlling the overall rate, are of continuing concern. For instance, in describing the effect of NO_3^- concentration on denitrification rate with the hyperbolic model, a 800-fold difference has been observed between values reported in the literature for the saturation constant in aquatic systems and in soil (van Veen, 1977).

Volatilization of NH_3

Significant losses of N from the soil can occur through volatilization of NH_3. These losses occur when high concentrations of urea are placed on the soil surface. The volatilization occurs from shallow soil surface layers (0-5 cm); very little NH_3 volatilizes from deeper soil layers. The diffusion of NH_3 through the soil can be modelled using Fick's diffusion equation. The major problem centres around estimating the diffusion coefficient as a function of soil-water content and soil type. Volatilization of NH_3 from the top soil layers into the atmosphere can be modelled using the diffusion equation. This flux is a function of the boundary layer resistance which is controlled by wind speed and air stability (Freney et al., 1981).

NH_3 volatilization from the soil may not, however, be a loss from the system since NH_3 can be absorbed by the plant canopy (cf. Subsection 5.1.4). Preliminary models for describing volatilization of NH_3 have been developed (e.g. van Veen, 1977; Parton et al., 1981), however these models are not appropriate for field applications.

Ammonium fixation

Soils that have potential for NH_4^+ fixation are rare, but if clay minerals such as vermiculite and illite not saturated with K^+ or NH_4^+ are present they must be included in any model at the research level. In other cases, a suitable parameter in the ion-exchange part of the model will handle NH_4^+, which is temporarily, but strongly, held.

Leaching

The leaching of NO_3^- is entirely controlled by the flow of water through the system. The only uncertainty is that the NO_3^- concentration in a part of the water flowing downward might not be in equilibrium with the NO_3^- concentra-

tion in other, adjacent, parts of the liquid phase. Although this uncertainty is increased because of NO_3^- production by nitrification, this non-equilibrium phenomenon will be equal for all anions. So the leaching of NO_3^- is the only part of the N model which can be derived from data collected for other materials, e.g., water itself and chloride ions. There is a wealth of hydrology literature: there are three-dimensional models, models that consider a stagnant phase and a moving phase with exchange between the two phases, and models that specialize in the spatial distribution of the water flux (e.g. Burns, 1974; Rowse & Stone, 1978; Addescott, 1981). The only problem seems to be selecting the appropriate approach from the many ones available. More details on modelling of water transport in soils and related topics are given in the Sections 4.2 and 4.3.

An interesting observation from a comparison of output of our model with results of an experiment in one of the newly reclaimed Lake IJssel polders is the observation that a considerable portion of the water that flows downward through wide pores and cracks does not contribute, or does so only to a small extent, to the transport of NO_3^-. This phenomenon is described, using the leaching efficiency factor, LE of Equation 98.

5.3 Crop production under semi-arid conditions, as determined by nitrogen and moisture availability

H. van Keulen

5.3.1 Introduction

The sequence of models on plant growth and production presented in this book is such that at each subsequent step more potentially limiting factors are taken into account. This requires extension of the models, to include simulation of the status of the relevant factors, both in the vegetation and in the soil in which it is growing. This requirement very soon leads to the construction of models that become unwieldy by their very size. It is therefore almost a prerequisite that concurrent with the addition of one more limiting factor, the remainder of the model description is simplified (cf. Subsection 1.2.3). That in itself need not be a serious disadvantage, since introduction of the additional factor is sensible only if it is expected to have an appreciable effect on the final result and the other factors consequently become relatively less important. The model presented here is, to my judgement at the limit of what can be handled reasonably. It has basically the same structure as the one in which only water as a limiting factor was considered (Section 4.1 and 4.2). State variables pertaining to the nitrogen (N) balance in soil and plants have been added. Most attention will be paid here to these state variables and the associated processes.

The model is outlined in Subsection 5.3.2 and its principle is repeated in an example (Subsection 5.3.3). A discussion of the performance of the model is presented in the Subsections 5.3.4 and 5.3.5.

5.3.2 The simulation model PAPRAN

A detailed description of the simulation model PAPRAN, whose main elements are illustrated in the simplified relational diagram of Figure 71, is presented elsewhere (Seligman & van Keulen, 1981). Conceptually the model is a soil-water balance model, where plant growth is closely related to the amount of water transpired by the canopy and its N status. The description of N uptake and redistribution in the plant tissue is based on a relatively simple set of demand and supply functions (Seligman et al., 1975); N transformations in the soil are represented by immobilization and mineralization processes, the rates of which are dependent on environmental conditions and on the C/N ratio of the organic material present.

Nitrogen in the soil

Nitrogen transformations in the soil have long been recognized as important processes in connection with the supply of the element to the plants. The com-

234
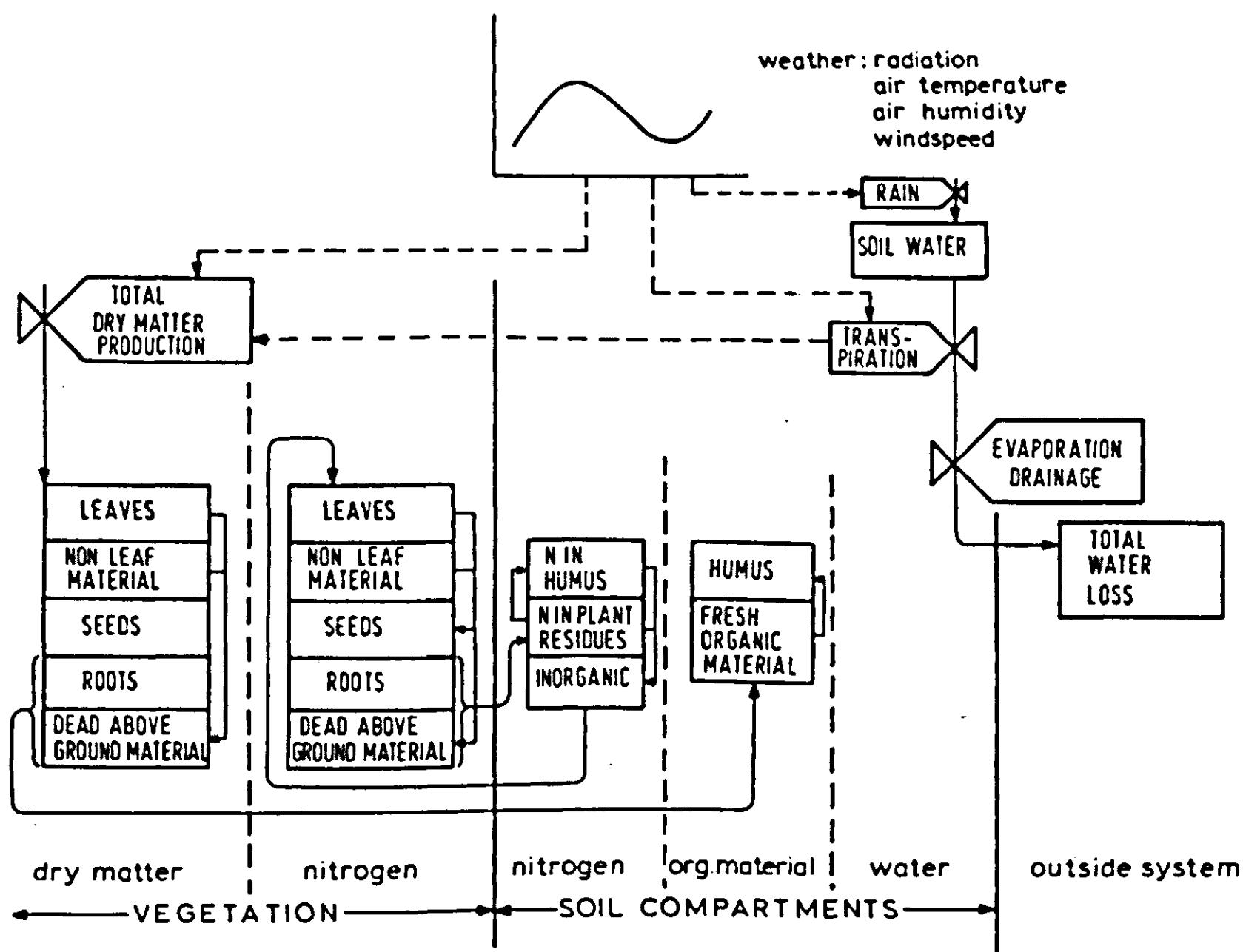
Figure 71. Schematized relational diagram of the simulation model PAPRAN.

plexity of the subject is well reflected in the voluminous literature available, as well as in detailed models of the soil N system that have been developed (Beek & Frissel, 1973; Hagin & Amberger, 1974; van Veen, 1977). Especially van Veen has emphasized that a useful method to treat the complexity is to divide the overall model into submodels that deal with the major processes separately but still influence each other through the relevant state variables. Van Veen's model (Section 5.2) focuses on microbiological processes, and the microbial biomass and its N content are treated as separate state variables. However, because of methodological problems, it is almost impossible to determine the relevant microbial values, and it is also very difficult to determine components of the soil organic matter for field situations. That situation seriously restricts the applicability of these concepts since both initialization and validation must then be based on indirect measurements so that unverifiable detail has been added to the model. Nevertheless, these concepts are theoretically sound, since most of the N transformations in the soil are governed by microbiological activities, so that their application awaits the development of more accurate experimental techniques (Subsection 5.2.3).

The soil N section included in the present model is compatible with the degree of detail and the time resolution of the other parts of the model. In this concept, the total N store in the soil is separated into three states only; inorganic N (in-

cluding NH_4^+, NO_3^- and NO_2^-), N in 'fresh' organic material (including N in plant debris, roots of last year's crop and also N incorporated in the microbial biomass) and N in the 'stable' organic material, which has at least once undergone microbial transformation. This approach necessitates lumping of some of the processes and their associated parameter values:

– immobilization, i.e. the transformation of inorganic N into organic compounds through microbial action, indicates total immobilization of any form of inorganic N by microbial growth. This generalization seems permitted since the microbial population in the soil active in decomposition of organic material is highly diverse and can easily adapt to the available source of inorganic N.

– mineralization from organic N to NH_4^+ and the (possible) transformation into NO_3^- are not distinguished in the model. This simplification is justified by the fact that in the well-aerated soils in semi-arid conditions the rates of nitrification are not normally limited by lack of suitable oxidizing micro-organisms nor by environmental conditions affecting oxidation. The rate-limiting process is generally the decomposition rate of the organic material, so that usually NH_4^+ or NO_2^- do not accumulate in the soil. (Exceptions are however possible as indicated by experimental results obtained in the Sahelian region, where NH_4^+ accumulation was observed, especially after hot-dry periods. This phenomenon could be the result of partial soil sterilization, when soil surface temperatures rise above 50 °C, thus leading to a depletion of the population of nitrifying organisms. Such situations cannot be treated with the present version of the model.)

– incorporation of the microbial biomass in the fresh organic material presents two problems:

1 how to deal with the lag associated with the initial build-up of the microbial population and its subsequent adaptation to various substrates?

2 how to handle the influence of the dying microbial biomass on the composition of the fresh organic material?

The first problem is on the whole not too serious with models of the present type, which simulate crop growth on a seasonal basis. The time coefficient for adaptation of the microbial populations has a value on the order of days, hence initial population size itself will not be the limiting factor for decomposition on a seasonal basis. Major controlling factors are then the available carbon (C) and N as substrates and environmental conditions, particularly temperature and moisture conditions. In the present model the rate of decomposition of the fresh organic matter is reduced when its C/N ratio exceeds 25. The inorganic N present is included in the calculation of the current C/N ratio.

The second point is part of a more general problem, since the overall rate of decomposition depends on the composition of the fresh organic material. This is accounted for in the model by changing the rate constants for decomposition sequentially as more of the originally present material had decomposed. The switch for the various rate constants can be adjusted to allow for different compositions of the added material. Continuous or discrete additions of dead

microbial biomass to the fresh organic material could be treated in the general framework of the model, but they have not been incorporated. This simplification is probably the main reason why the so-called 'flush' of mineralization frequently observed after hot and dry periods, and presumably the result of rapid decomposition of dead microbial biomass, is not reproduced by the current version of the model.

The actual calculation procedure in the model PAPRAN is best explained on the basis of the relational diagram presented in Figure 72. The rate of decomposition of the fresh organic material is based on first-order kinetics (Subsection 5.2.2), the relative rate (RDX) being determined by the component currently decomposing. Since RDX represents the specific decomposition rate under optimum conditions for growth of the micro-organisms, the actual rate of decomposition is also influenced by soil temperature (TS), the moisture status of the soil (WCON) and the overall C/N ratio (CNR) in the profile. The N contained in the material being decomposed is mineralized and added to the pool of inorganic N in the soil. The concurrent build-up of microbial tissue requires nitrogen (NREQ), which is immobilized. The rate of immobilization is directly proportional to the decomposition rate of the organic material, it being assumed that a fixed proportion of the C (EFFBS, the biosynthesis efficiency) is used for
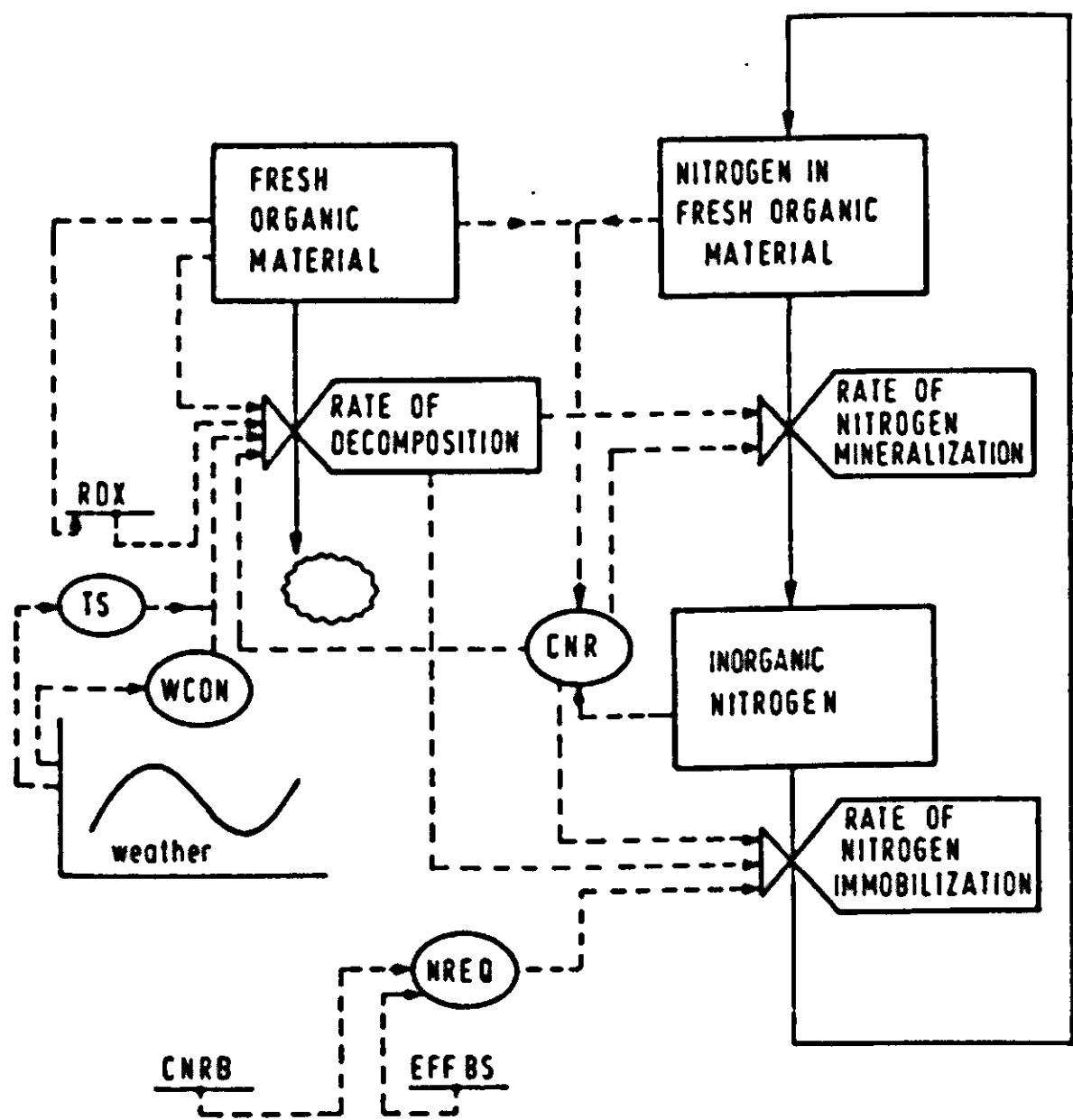
Figure 72. Schematized relational diagram of the PAPRAN module for decomposition of fresh organic material in the soil.

the formation of microbial tissue, the remainder being lost in respiration. The rate of N accretion is furthermore dependent on the C/N ratio of the microbial biomass (CNRB). Whether the result of both processes is net mineralization or net immobilization depends on the intensities of both processes.

Volatilization of ammonia takes place from the top soil layer only, and is treated in a rather rudimentary way in the model. In reality the rate of N loss through volatilization is dependent on the NH_4^+ concentration, on pH and temperature and on environmental conditions governing the rate of exchange with the atmosphere. Since the time coefficients of the chemical and physical processes involved are much smaller than the resolution of the model, volatilization is approximated by an imitating procedure, assuming a constant relative rate of disappearance of NH_4^+ from the top soil compartment.

Adsorption of NH_4^+ to the exchange complex of the soil is not considered, because the NH_4^+ involved is in general a small and fairly constant fraction of the total amount of inorganic N and changes have only a small effect on the seasonal N dynamics. Fixation of NH_4^+ into the clay mineral lattice is neglected as well, as it is not of significance in most soils of interest in the arid region.

Denitrification is disregarded in the present model, because anaerobic conditions are unlikely to occur in the arid zone. The possibility that local anaerobic pockets may develop as a result of oxygen depletion under intensive biological activity or localized water logging is recognized, but since the extent of these phenomena is not clear and as they are extremely complex for a simulation approach, they have not been treated as yet.

Transport of inorganic N over compartment boundaries takes place with movement of soil water (Subsection 5.2.2), that is with infiltration only (Subsection 4.2.3). To account for combined effects of mass flow and diffusion, the concentration of N in the water transported is calculated by 'mixing' the N present in a compartment and that moving over its upper boundary with the water in that compartment and all water transported through it.

Soil organic matter

In each soil layer, two organic components are distinguished, the 'fresh' organic material consisting of roots and other plant residues of the previous year and 'stable' organic material or soil humus.

The rate of decomposition of the fresh organic material is based on first-order kinetics, modified by the influence of moisture, temperature and the C/N ratio of the available substrate. The rate constants applied in the model are: 0.8 d^{-1} for proteins and sugars, 0.05 d^{-1} for cellulose and hemi-cellulose and 0.0095 d^{-1} for lignin. The rate constants change in a stepwise manner, the moments at which the rate constant changes being controlled by the composition of the material added.

The stable organic material, which has a constant C/N ratio of 10, decomposes at a much slower rate, a rate constant of $8 \cdot 10^{-5} d^{-1}$ being assumed. Again this rate may be modified by temperature and moisture conditions, in the same
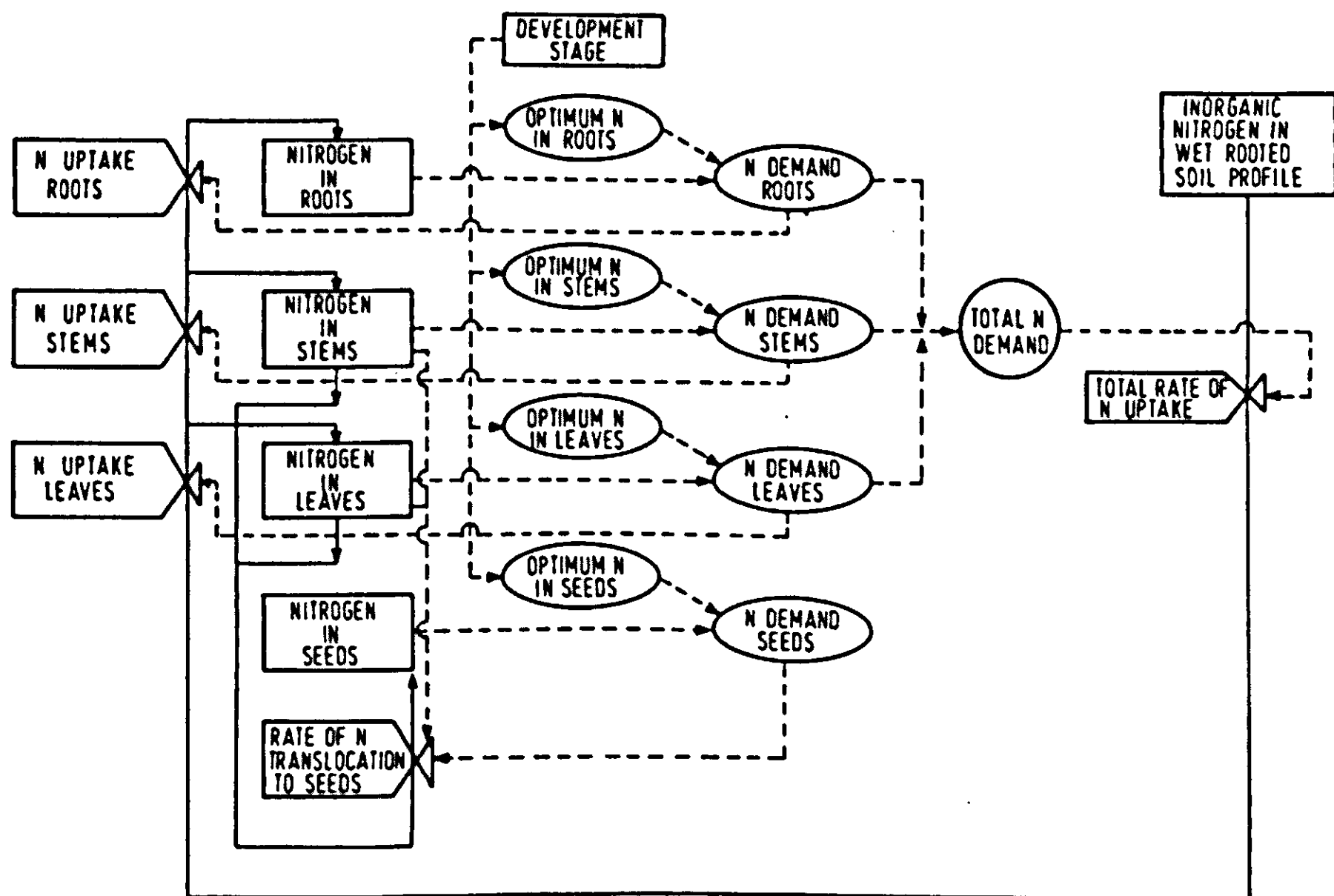
Figure 73. Schematized relational diagram of the PAPRAN module for the nitrogen balance in a natural vegetation.

way as the fresh organic material.

There may also be accretion of stable organic material due to the residual stable compounds originating from the fresh organic material. In the model this is linked to the C/N ratio of the decomposing material. When the C/N ratio is below 25 inorganic N is released, 20% of which is incorporated in the stable fraction. Application of the constant C/N ratio of 10 then also gives the accumulation of C in the humus fraction.

Nitrogen in the vegetation

A simplified relational diagram of this part of the model is given in Figure 73. It is assumed that N is taken up by the plant as NO_3^- and that the root system of the vegetation is dense and active over the full rooted depth. Nitrate is then highly available to the plant either by mass flow with the transpiration stream or by diffusion of the anions along a concentration gradient, created by low NO_3^- concentrations near the root surface (van Keulen et al., 1975), as long as the soil is wet enough. Thus the demand for N can be satisfied within a relatively short time, a time coefficient of 2 days being assumed in the model. The demand for N is created by the difference between the current N content of the plant and a maximum N content. The latter value is different for the various organs of the plant and decreases as the phenological development of the plant proceeds (Figure 74a, cf. Figure 67, Section 5.1). The present version of the model assumes

239
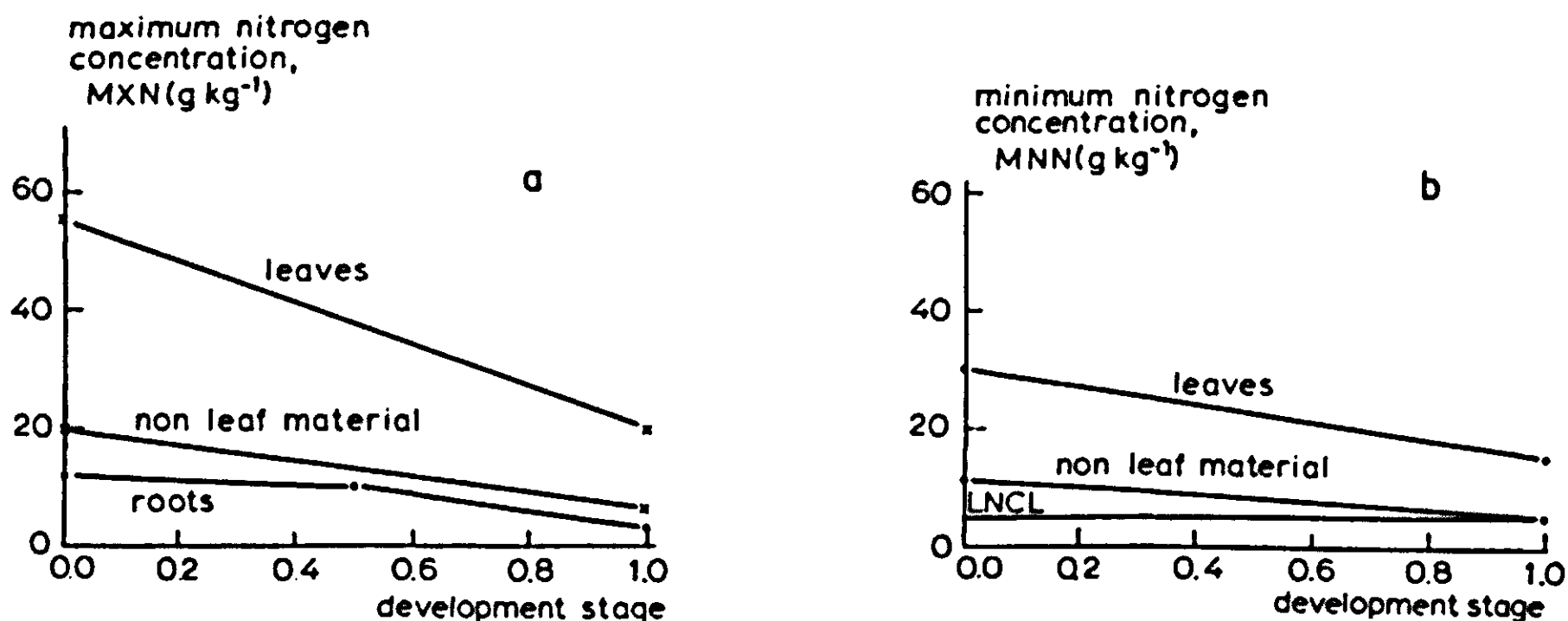
Figure 74. The maximum (a) and minimum (b) nitrogen concentration for various organs of natural grassland vegetation as a function of phenological age (development stage, here defined as being 1.00 at maturity). LNCL is the nitrogen irreversibly incorporated in the leaf tissue.

that under limited supply of N, the actual amount taken up is partitioned among the various vegetative organs (roots, stems and leaves) in proportion to their relative demands (sink-size determined).

The N demand of the seeds is met by translocation from the above-ground vegetative parts. It is withdrawn from leaves and non-leaf material in proportion to the amounts in each of the compartments. As the tissue becomes depleted (below MNN), translocation to the developing seeds is retarded, eventually the demand may not be met and consequently seeds with a lower N concentration are the result. Below an absolute minimum level of non-degradable nitrogenous compounds (LNCL, Figure 74b) redistribution ceases. The definition of the absolute minimum level in PAPRAN corresponds with the minimum concentration of Figure 67, Section 5.1. In reality, part of the N in the seeds may be supplied directly from uptake by the roots. However, with an integration interval of one day the demand will be transferred to the vegetative tissue within a relatively short time and when sufficient N is available in the rooting zone, it will be supplied. When the stock of inorganic N in the soil is exhausted, the vegetative tissue will be depleted of nitrogen, which will lead to impaired functioning of the leaves and accelerated senescence (self-destruction, Subsection 5.1.4. Compare also Subsection 3.4.7 for modelling aspects).

Dying of vegetative tissue also leads to withdrawal of N from the plant. The concentration of the element in the dying tissue depends on the cause of death: if the tissue dies of water shortage or senescence, the dead tissue N concentration equals that of the live tissue; if death occurs from N shortage, the concentration is equal to the unextractable residual concentration, thus imitating the transfer of N from older to younger tissues.

Growth of the vegetation

The total daily dry matter production, unrestricted by N shortage, is calculated in the same way as in the model described earlier (Section 4.1). The influence of the N status of the vegetation is taken into account through a reduced growth rate, when the concentration of N in the leaf tissue (ANCL) drops below a threshold value (MNN, Figure 75), which in itself is a function of the phenological stage of the plants (Figure 74b). The reduction function given is based on a qualitative description of the influence of N shortage on growth, since suitable experimental data to define the instantaneous effect of N level on dry matter production are absent.

The N level of the vegetation also affects the distribution of the dry matter formed. Nitrogen deficiency in the above-ground tissue favours growth of the roots at the expense of the shoot. This description is based on the functional balance principle (Subsection 3.3.6): N shortage hampers growth of the shoot much stronger than that it reduces the rate of CO_2 assimilation, which leads to accumulation of primary photosynthates and hence to a greater availability of carbohydrates to the root system. The actual values of the partitioning function are the results of 'guestimates', as once more experimental data, especially from field situations are extremely scarce. The distribution of dry matter between leaves and non-leaf tissue is also influenced by the N status of the vegetation: when N is limiting growth, a larger fraction is incorporated in non-leaf tissue.

It is obvious from what is presented in this subsection and in Section 5.1 that quantitative descriptions of the influence of N deficiency on processes related to plant growth and production are lacking. That in itself is a surprising conclusion, more than 125 years after the pioneering work of Von Liebig. The finding
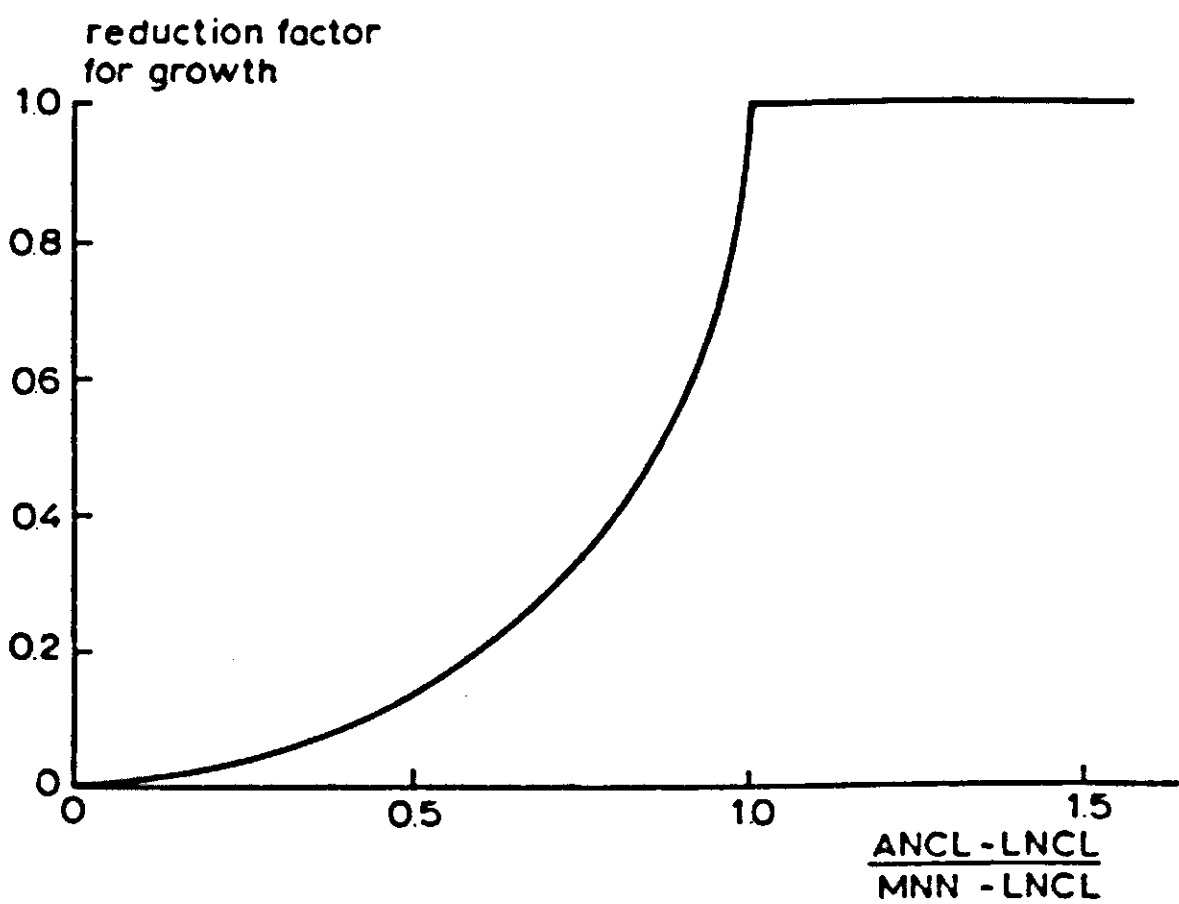
Figure 75. The reduction factor for dry matter accumulation as a function of a normalized nitrogen concentration, computed as: (ANCL-LNCL)/(MNN-LNCL). For abbreviations: see text.
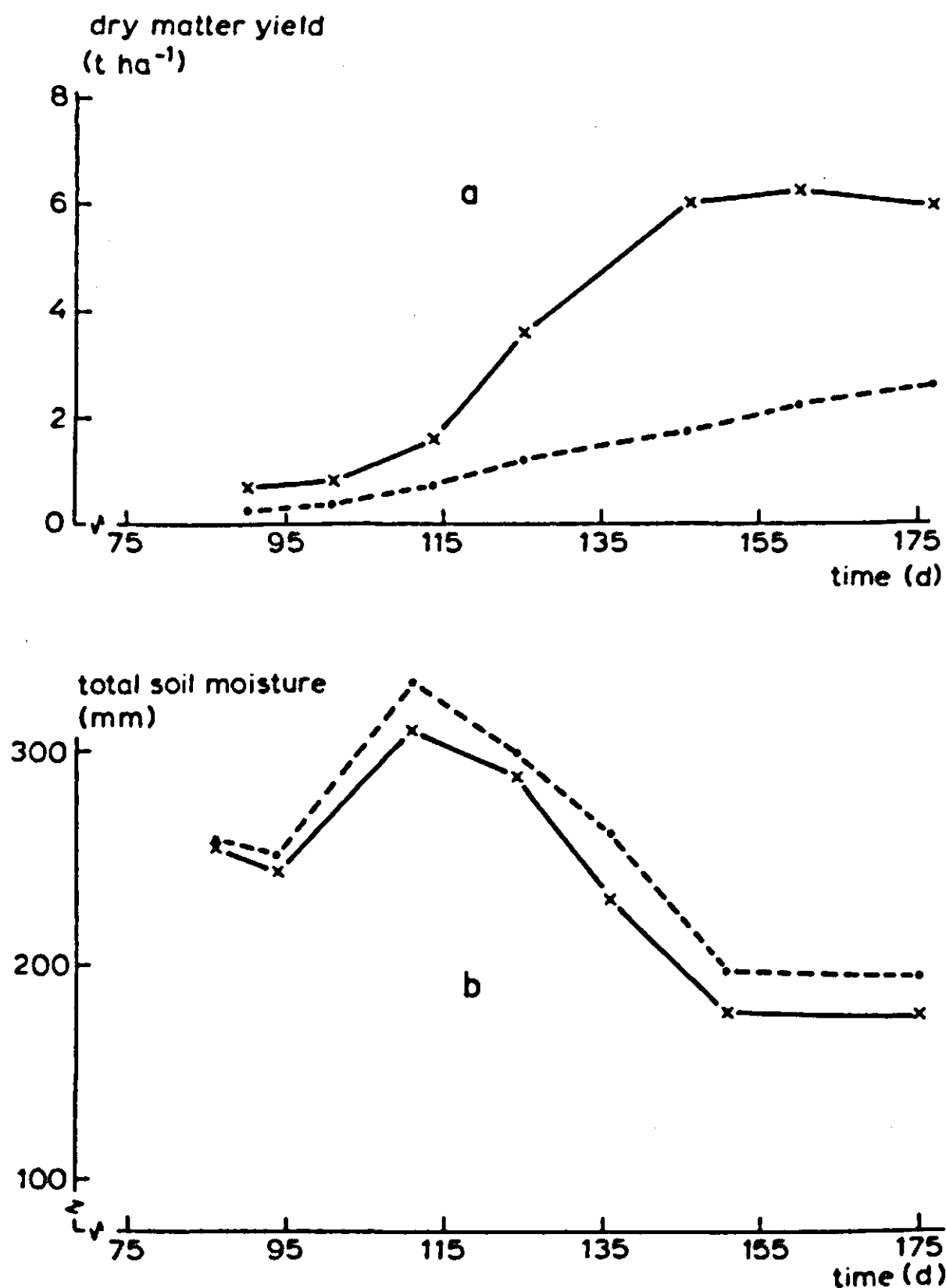
Figure 76. The measured growth curve of a natural vegetation with (x) and without (•) nitrogen fertilizer in Migda, Israel, in 1972/1973 (a), and the time course of total soil moisture in the 0-180 cm layer for both situations (b).

of this gap in knowledge may serve as an argument in favour of systems analysis and model building as useful tools in agricultural research.

Nitrogen nutrition and water use

A basic problem that needs attention is the influence of N deficiency in the vegetation on transpiration. The constancy of the transpiration coefficient, discussed earlier (Section 4.1) was restricted by de Wit (1958) to situations where the 'nutrient status is not too low', whereas Viets (1962) concluded that 'all evidence indicates that water-use efficiency, . . . can be greatly increased if fertilizers increase yield'. The latter conclusion seems to be confirmed by experimental results obtained in the northern Negev desert of Israel (Figure 76), where the soil with the fertilized vegetation, growing substantially faster than the non fertilized soil, loses water at practically the same rate.
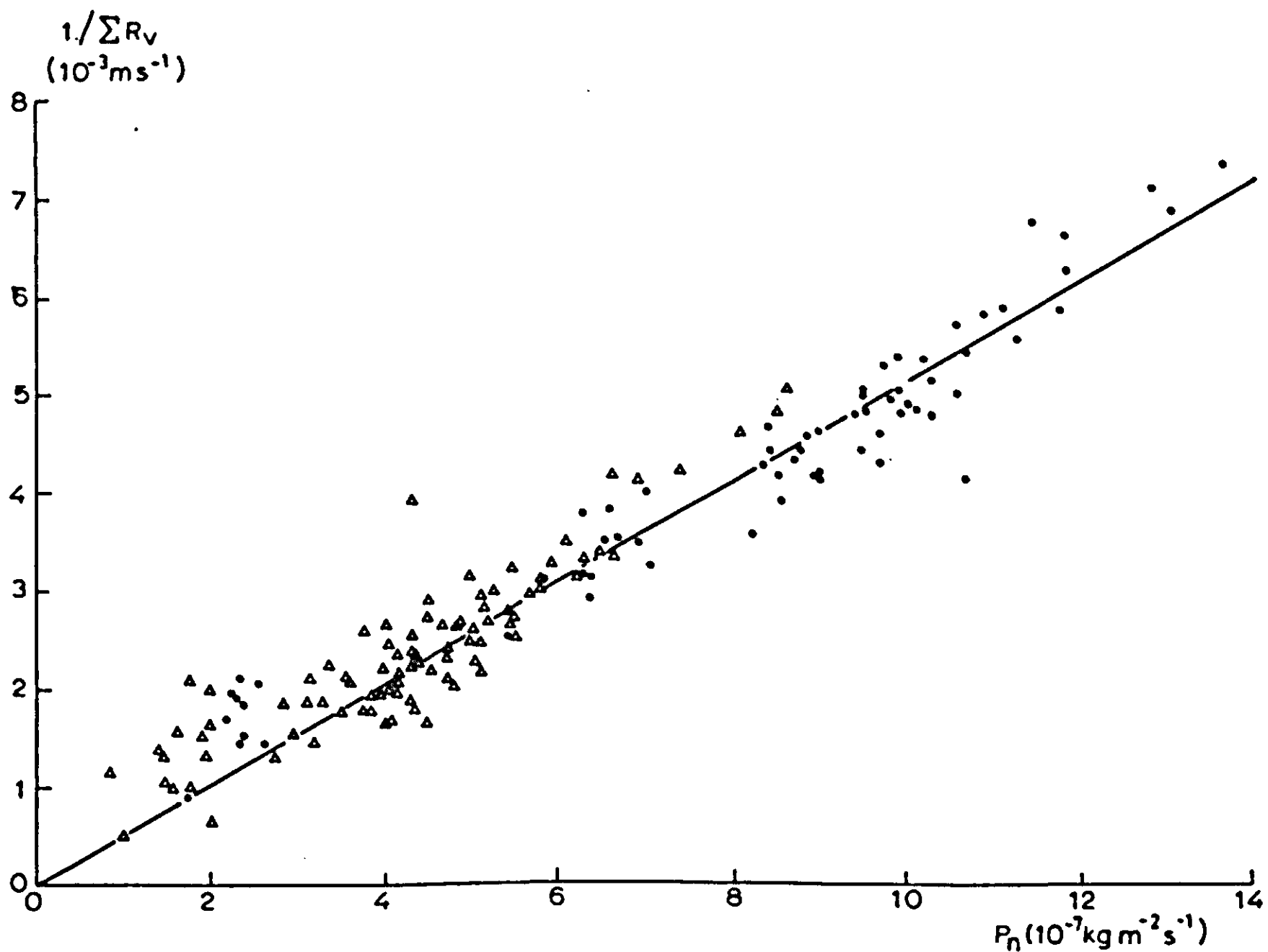
242

Figure 77. The relation between net rate of CO_2 assimilation (P_n) and total conductance for water vapour ($1./\Sigma R_v$) for maize plants grown with ample (•) and limited (△) N supply.

When examining the basic processes of CO_2 assimilation and transpiration, however, the conclusion of a lower water-use efficiency under N deficiency is not so obvious. In Figure 77 the relation between the net rate of CO_2 assimilation (P_n) and total conductance for water vapour exchange ($1./\Sigma R_v$) (Goudriaan & van Laar, 1978) is given for maize under optimal and suboptimal N supply. The data were obtained under controlled conditions on attached individual leaves of plants grown in the greenhouse. In maize, plants with suboptimal N supply exhibit a markedly lower maximum rate of net CO_2 assimilation compared to the plants amply supplied with N, but there is a proportional decrease in conductance for water vapour, hence a virtually constant assimilation/transpiration ratio. A more or less similar behaviour is shown by *Hordeum leporinum* plants, a grass species from the natural vegetation in Israel (Lof, 1976): a drop in N concentration in the dry matter from about 43 to 23 g kg^{-1} is coupled with a decrease in net CO_2 assimilation of about 25%, however again with a proportional decrease in conductance. The behaviour of *Phalaris minor*, another natural grassland species, tends to be slightly different, in that a somewhat more favourable assimilation/transpiration ratio exists for the plants well supplied with N, especially at higher light intensities at which most of the production takes place in the field (Figure 78). These data would thus suggest that,

243
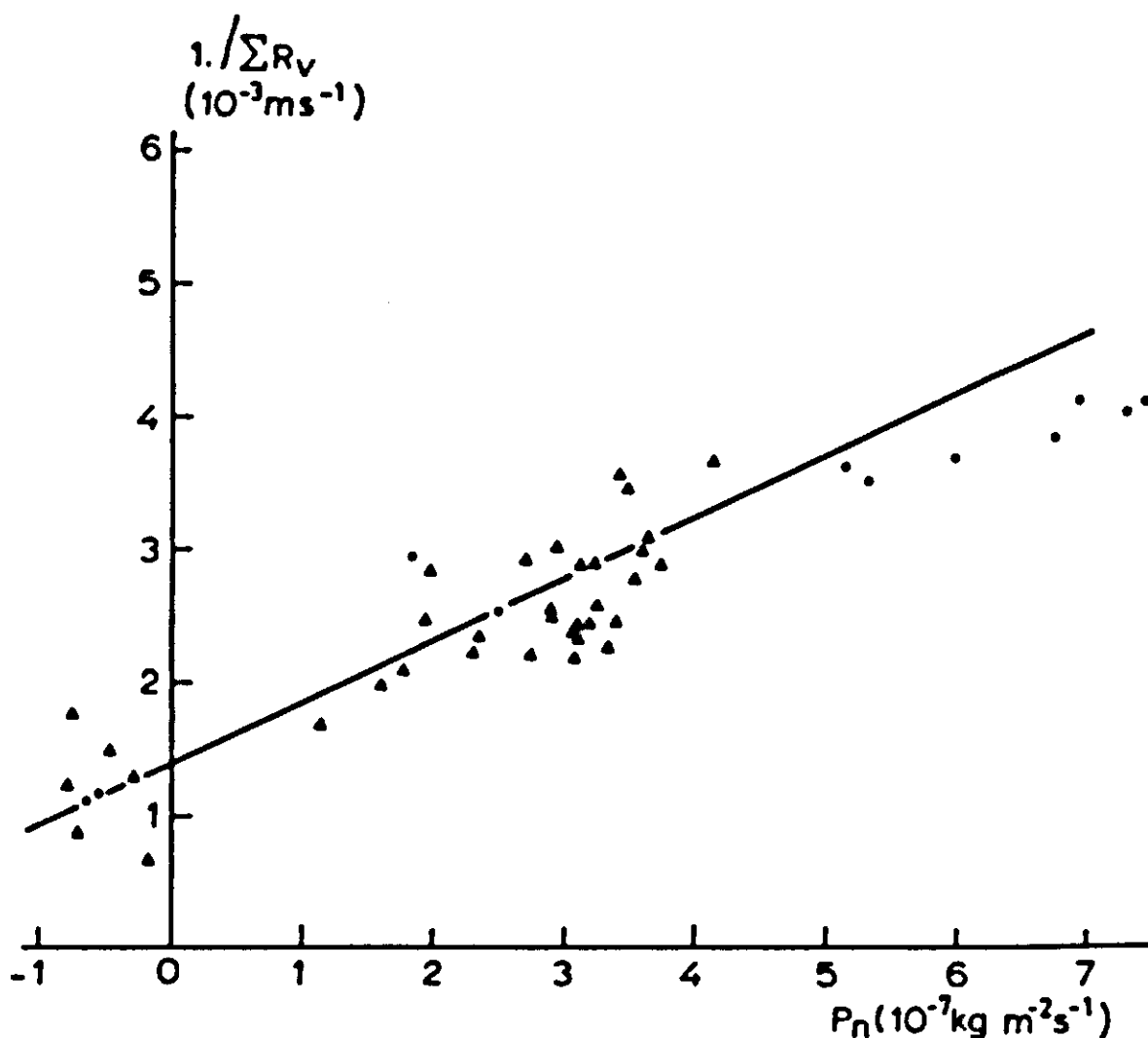
Figure 78. The relation between net rate of CO_2 assimilation (P_n) and total conductance for water vapour $(1./\Sigma R_v)$ for *Phalaris minor* for nitrogen depleted plants (▲) and controls (•).

maybe with the exception of *Phalaris*, no differences in water-use efficiency or at least in transpiration efficiency are to be expected for different nutritional conditions. Overall water-use efficiency may be affected, however, since vegetation low in N exhibits a slower rate of accumulation of dry matter, which combined with a different distribution pattern of the material may lead to prolonged periods in which soil cover is incomplete. During such periods appreciable losses of moisture may occur through direct soil surface evaporation (Subsection 4.2.3). That may result in a much more unfavourable ratio between non-productive and productive water consumption. A more thorough investigation of the processes of assimilation, transpiration and growth under N deficient conditions is necessary, however.

5.3.3 Application in the simplified crop growth model SUCROS

These considerations may be illustrated with the simplified model developed in Sections 3.1 and 4.1. The data specified relate to a cereal crop, in particular. The amount of N in the various plant organs is established in integrals:

ANLV = INTGRL(ANLVI, NUPL−NUPSO* ANLV/(ANLV+ANST))
ANST = INTGRL(ANSTI, NUPST−NUPSO*ANST/(ANLV+ANST))
ANRT = INTGRL(ANRTI, NUPRT)
ANSO = INTGRL(ANSOI, NUPSO)

244

INCON ANLVI = 1.125, ANRTI = 0.28, ANSTI = 0., ANSOI = 0.

referring to the N in leaf (ANLV), stem (ANST), root (ANRT) and storage organs (ANSO) expressed in kg ha^{-1}, respectively. The rate variables for the vegetative organs are calculated from the total N uptake from the soil (TNUPSL, kg ha^{-1} d^{-1}):

NUPL = TNUPSL * NDEML/(NDEML + NDEMST + NDEMRT)
NUPST= TNUPSL * NDEMST/(NDEML + NDEMST + NDEMRT)
NUPRT= TNUPSL * NDEMRT/(NDEML + NDEMST + NDEMRT)

The demand for N of the vegetative organs (kg ha^{-1} d^{-1}) at any particular moment is:

NDEML = (WLV * XNCL – ANLV)/TC
NDEMST = (WST * XNCST – ANST)/TC
NDEMRT = (WRT * XNCRT – ANRT)/TC

TC, the time coefficient (Subsection 2.1.7) for fulfillment of the demand, is set at 2 days.

The maximum levels of N in the vegetative organs (kg kg^{-1}) are defined in dependence on the development stage of the vegetation (cf. Figure 74), in a schematized way:

XNCL   = AFGEN(XNCLT, DVS)
FUNCTION XNCLT = 0., .045, .7, .0275, 2., .02
XNCST = 0.5 * XNCL
XNCRT = 0.5 * XNCST

The total uptake of N is equal to the minimum of the demand of the vegetation or the maximum supply by the soil:

TNUPSL = AMIN1(NDEML + NDEMST + NDEMRT, ANSL/DELT)

The soil N stock, considered for simplicity as one state variable, is represented by an integral:

ANSL   = INTGRL(ANSLI, – TNUPSL)
INCON ANSLI = 50.

The expression 'ANSL/DELT' in the rate equation thus indicates uptake of all available N in one time step.

The initial amount may represent the amount of N available from the unfertilized soil. Alternatively, simulating fertilization in its simplest form, ANSLI may be computed in an INITIAL section of the program by:

ANSLI = ANSLU + FERT * REC

in which ANSLU is the N available from the unfertilized soil, FERT the amount of fertilizer applied, and REC the recovery fraction.

PARAM REC = 0.7

will often be a good first estimate.

Somewhat more detail could also be added by incorporating a net rate of mineralization, but that leads to speculative formulations in this example, geared to the response of the crop to N availability.

The storage organ is treated in a somewhat different way:

NUPSO   = NDEMSO * FNDEF
NDEMSO = (WSO * XNCS − ANSO)/TC
PARAM XNCS = 0.025   (species specific)
FNDEF   = 1. − SQRT (1. − AUX * AUX)
AUX   = (LIMIT(LNCL, MNCL, ANCL) − LNCL)/(MNCL − LNCL)
ANCL   = ANLV/WLV
PARAM LNCL = 0.005, TC = 2.
MNCL   = 0.5 * XNCL

The latter two variables represent the minimum N concentration for unrestricted growth (MNCL) and the irreversibly incorporated N (LNCL) in the leaf tissue. All concentrations of N in dry matter in this example are given in kg kg^{-1}.

The influence of the N concentration on the rate of production is defined by the auxiliary variable AUX as well:

AGTWN = GTW * AUX

or:

AGTWN = AGTW * AUX

when the soil-water balance (Subsection 4.1.3) is also considered. Two alternative formulations can then be proposed for the influence on transpiration (Subsection 5.3.2, N nutrition and water use):

TRANSA = TRANS * AUX

or:

TRANSA = TRANS

In this schematized way, the major influences of availability of N on growth may be simulated.

Exercise 64

Combine the submodel of the amount of N in the various plant organs and its influence on growth of the crop with the summary model SUCROS and study the results. Replace GTW in Lines 107 and 108 (Table 9, Section 3.1) by AGTWN and add AGTWN = GTW * AUX. Simulate, for instance, situations with little and with ample N in the soil initially (PARAM ANSLU = 10., 25.,

50., and 100., respectively) and with various fertilization rates (PARAM FERT = (0., 50., 200.)).

5.3.4 Performance of the model PAPRAN

The performance of the model PAPRAN was studied by analyzing its behaviour under the conditions prevailing in the semi-arid region of the northern Negev desert of Israel, a winter rainfall area (average precipitation 250 mm per year) with a natural vegetation consisting of a mixture of annual plants species, typical of an abandoned cropland vegetation. For more details reference is made to van Keulen (1975). From this area dry matter yields in situations with and without application of nitrogenous fertilizer are available for a number of years.

Due to a lack of field observations, initial conditions were assumed to be identical for all growing seasons. At the onset of the growing season, an amount of 3000 kg ha^{-1} of fresh organic material was assumed to be present in the upper 60 cm of the profile. The average N content of this material is set at 10 g
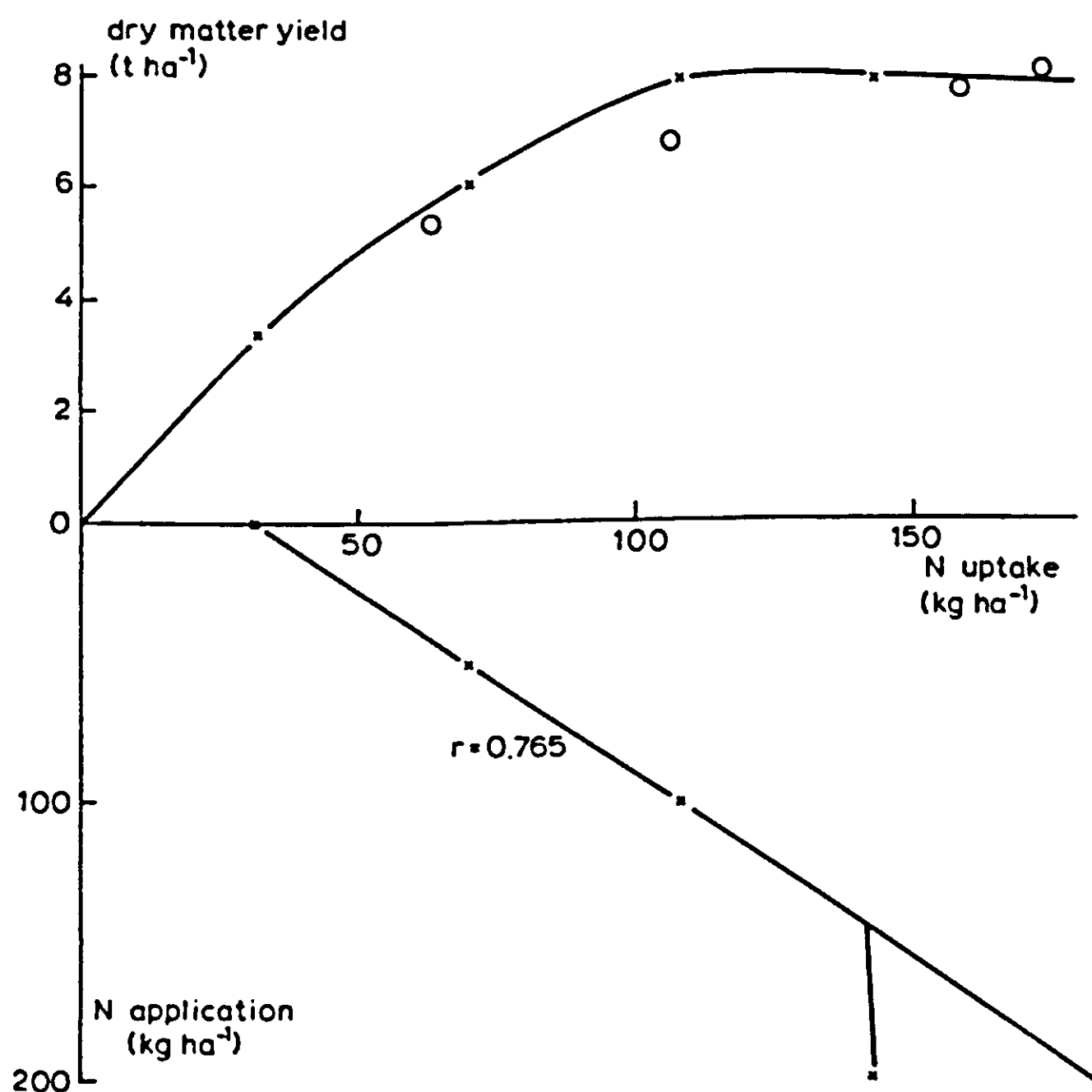
Figure 79. Simulated (x) and measured (o) results of experiments on natural vegetation in the northern Negev in the 1971-1972 growing season. The simulated recovery fraction (r) of fertilizer is indicated.

kg^{-1} (dry matter). When fertilizer was applied in the model, this was assumed to be present at the start of the simulation, in ammoniacal form, evenly distributed in the upper 10 cm of the soil.

Some typical results are presented in Figures 79 and 80, in the form of results of fertilizer trials with experimental data for comparison. This gross output, when inspected in the way introduced in Subsection 5.1.2 with Figure 65 does not show a consistent picture:

– In 1971/1972 the various experimental treatments resulted in the uptake of varying amounts of nitrogen. A 'zero treatment' could not be analyzed in that season since all the experimental fields were disked for uniformity, incorporating into the soil substantial quantities of sheep droppings accumulated from preceding seasons. The simulated yield-uptake curve is situated within the accuracy limits of the measured data points. At the highest application rate, the model predicts a levelling off of the application uptake curve, resulting from 'nitrogen saturation' of the vegetation throughout the growing season. The predicted maximum uptake is in reasonable agreement with the measured value, which was determined at an even higher application rate.

– For 1972/1973 the experimentally determined points of the yield-uptake
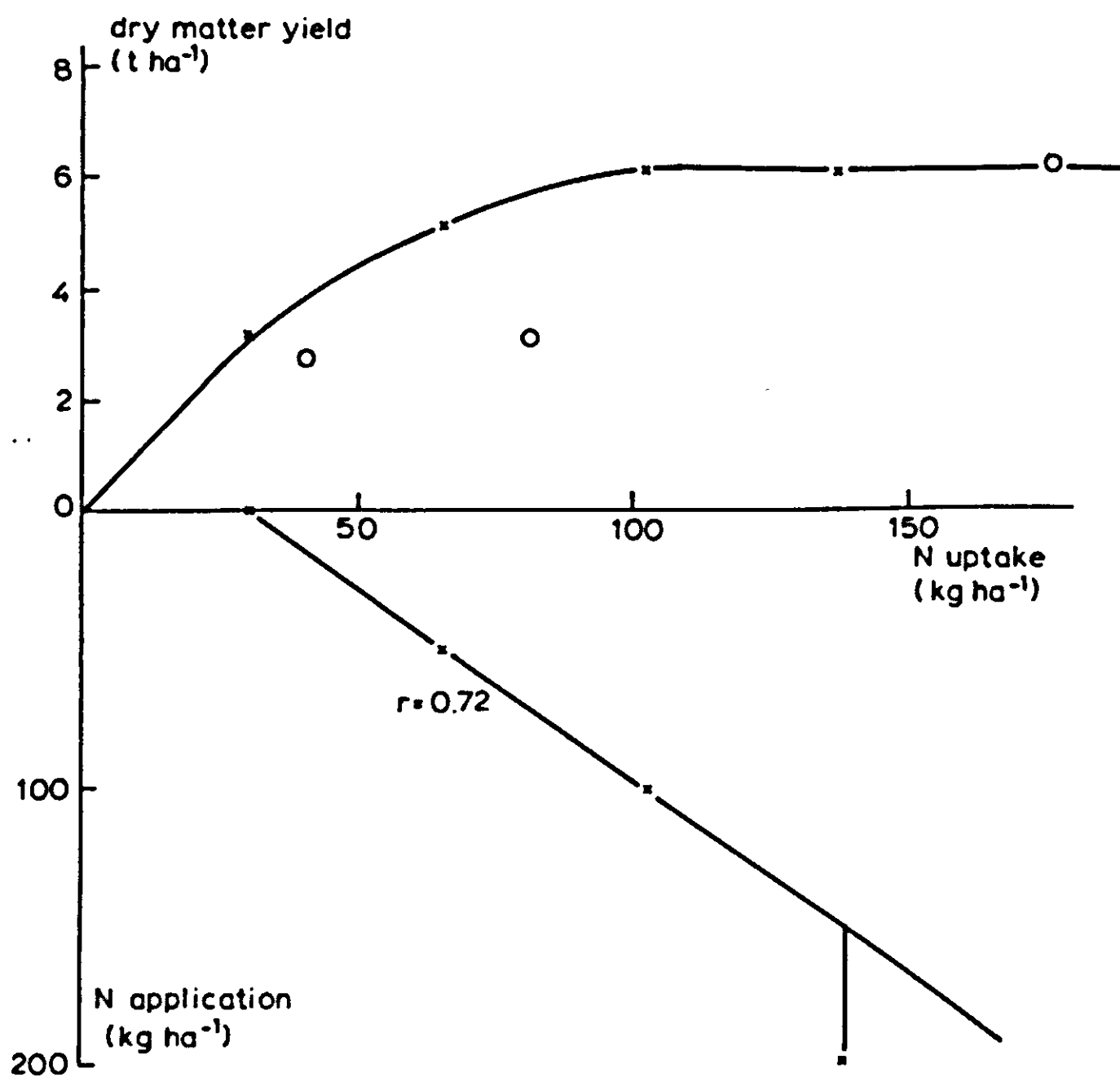
Figure 80. Simulated (x) and measured (o) results of experiments on natural vegetation in the northern Negev in the 1972-1973 growing season. The simulated recovery fraction (r) of fertilizer is indicated.

248

curve deviate considerably from the simulated curve. Part of the explanation could be the relatively high proportion of legumes in the vegetation that season, having inherently a higher N content, even under limiting conditions (Subsection 5.1.3). The measured maximum uptake of the vegetation is about 25% higher than that predicted by the model, which suggests that the maximum concentrations applied in the model may be somewhat low, since total uptake was again dictated by the ability of the vegetation to absorb the element.

5.3.5 Discussion

The gross output of the model as presented in the previous section is probably not the most interesting part of the analysis, since these results were achieved for situations very close to those for which the model was developed (and hence calibrated). At this stage, the behaviour of some particular elements of the model may be more worthwhile looking at.

The fresh organic material, for instance, assumed to be present at the onset of the growing season decomposes almost completely, 5-15% being left at the end of the growing period, depending mainly on moisture conditions. Concurrent with this decomposition there is a slow, but gradual net release of inorganic N from organic material of this quality. When the N concentration of the initially added material is lower, the model predicts net immobilization first, only later followed by net mineralization. The major question in this connection is whether it is possible at all to describe quantitatively the dynamics of the N transformations in the soil and their consequences for the availability of this element to the vegetation, without explicitly simulating the microbial population in the soil. A satisfactory answer to this question is hampered by the inaccuracy of the experimental techniques available for the determination of the various components of the total N store in the soil and by the inherent heterogeneity of the system under field conditions. When the answer to this question is negative, there is a long way to go before the behaviour of such systems can be accurately described in a quantitative way, considering the state of knowledge at the microbiological side (Subsection 5.2.3).

With respect to the effects of N deficiency on the various processes related to plant growth and production, it has already been said that in many cases they had to be estimated based on incomplete and often qualitative information, and more research seems certainly warranted in that field.

In conclusion, it may be stated that PAPRAN provides a useful framework for a systematic investigation of the relative importance of the various processes that play a role in determining crop growth under semi-arid conditions.

6 MODELLING THE INTERACTION OF CROP GROWTH AND DEVELOPMENT OF DISEASES AND PESTS

6.1 Pests, diseases and crop production

R. Rabbinge

6.1.1 Introduction

Knowledge of plant growth, insight into crop and soil management and appropriate agronomic measures have led in practice to production levels that sometimes equal the potential level. In Section 1.2, four different crop production levels are distinguished, depending on availability of growth requirements and abiotic conditions. At all production levels, pests and diseases may depress the attainable yield through different mechanisms. The nature and species of pests and diseases may differ at different yield levels.

In this chapter we deal with crops grown at Production level 1, thus in the case of ample plant nutrients and soil water all the time. To attain these optimal conditions capital investments and large amounts of fossil energy have to be used. Only a very small fraction of this is used for crop protection measures. However, the financial costs of using and applying pesticides are increasing and the environmental side effects of these compounds are becoming a problem. Therefore interest in crop protection systems with a reduced usage of pesticides is increasing, and crop protection is developing more and more into a science for planning and managing the crop pathogen system.

In most studies on pest and disease management, population dynamics of pest and disease organisms are emphasized, but the combination with the growing crop is virtually neglected. This make it impossible to assess the damage properly, and limits the use of these models. To overcome this limitation, it is necessary to link them with crop growth models. The dynamic character of the interrelations between host and parasite requires a dynamic description of the substrate, i.e. the crop, and of the environment of a pathogenic organism.

Only a few combination models exist in which both crop growth and population dynamics of the pest or disease organisms are based on detailed analysis. Such combination models are often of a dualistic nature, containing on the one hand a great number of descriptive elements, and on the other a great deal of detailed knowledge of sub-processes. When too many phenomena observed at the system level are introduced into the model, its behaviour is governed by the descriptive relationships. In those cases the explanatory value of the models is limited and the modelling effort becomes a sophisticated method of curve fitting. Comprehensive models with a satisfactory compromise between completeness of basic data, time needed, for experimental and modelling effort, and reliable output are rare indeed (Section 1.3).

In this section I give some of the basic relations in population dynamics (Subsection 6.1.2), and describe some attempts at their modelling (Subsection 6.1.3).

Then I present two types of combination models: first I discuss summary models (Subsection 6.1.4). These models are designed to produce a shortcut to the objectives of the comprehensive model, without losing the sensitivity of the full analysis (Section 1.3). Models of this type are used to simulate the effect of a pest or a disease on crop growth without further consideration of the nature of damage.

Crop-pathogen interactions are introduced in these models to compute the impact of the perturbations. The simulations give some insight into the relative importance of the nature of crop pathogen interrelations. A complete explanation cannot be given as too many basic relations are neglected. Secondly I discuss an example of a comprehensive model of crop growth and a disease (Subsection 6.1.5). This combination model is used to test hypotheses on the nature of the disease-crop interrelations. The summary model of crop growth (SUCROS, Section 3.1) suffices in cases where the effect of diseases or pests on crop growth is assessed, whereas the complicated BACROS model (de Wit et al., 1978) is used to test some hypotheses on the nature of the disease-crop interrelations. An extrapolation of use of models for crop protection in practice is discussed briefly in Subsection 6.1.6.

6.1.2 Population dynamics of pests or disease causing organisms

When a population grows without constraints, the well known exponential growth curve describes the number of organisms in time (Section 2.1). This curve transforms into a logistic curve when there is a limited supply of food, or when a growth-retarding compound is produced during the growth process. For example yeast growth is inhibited by alcohol, which is produced during bud formation, the multiplication process in yeast (de Wit & Goudriaan, 1978). Mathematically the growth process can be described by

$$dG/dt = RGR \cdot G \cdot (1.0 - RED) \tag{101}$$

in which RGR represents the relative growth rate, and RED expresses a reduction factor. RED may be described by the ratio between actual amount of organisms (yeast cells, G) and the maximum amount (GM):

$$RED = G/GM \tag{102}$$

The amount of yeast cells is found by the analytical solution of the rate equation

$$G = GM/(1.0 + K \cdot \exp(- RGR \cdot t)) \tag{103}$$

Exercise 65

a. Compute K from an initial value of G and its maximum value. What process or ratio is described by this factor?

b. Derive the rate equation (Equation 101) from the analytical formula (Equation 103) by differentiation.

The exponential growth equation is only valid in very few cases of population growth and during short periods. The logistic equation (Equation 103) is appropriate as a description of the growth of population numbers in simple organisms like yeasts.

To distinguish between development and size of organisms is in these cases not necessary. However as soon as more complicated organisms are considered, development and growth should be treated separately, as is the case with many pest and disease organisms. For example in fungi each spore is not immediately ready to produce new spores, but a whole phase of its life cycle has to be passed before sporulation may start (latent period). A young larva of a pest organism is not able to produce offspring but has to become adult before there is any new egg produced. An adult pest organism is only able to produce offspring during a short period, and the same holds for a sporulating lesion (infectious period). To account for this delay in population development van der Plank (1963) developed a rate equation with which the population growth of many disease organisms can be described:

$$dN_t/dt = R(N_{t-p} - N_{t-i-p})(1 - N_t/N_m) \qquad (104)$$

In which N_t is the number of visibly diseased sites at time t; R is the number of lesions per sporulating lesion per day, or relative growth rate; p is the duration (d) of the latent period; i is the duration (d) of the infectious period; N_m is the maximum number of sites which can become infected.

Exercise 66
a. When does this formula transform in the logistic growth equation?
b. What is the maximum number of sites on a field of 0.5 ha, when the minimum size of a lesion is 0.1 mm² and the crop has a LAI of 4?

It is difficult to solve Equation 104 analytically, so numerical methods have to be used. With the numerical integration of the van der Plank equation, dynamic simulation was introduced in botanical epidemiology (Zadoks, 1971; Waggoner et al., 1972). In pest population dynamics, numerical methods were used earlier, but extensive use of numerical simulation models started only recently (Fransz, 1974; Gutierrez et al., 1975; de Wit & Goudriaan, 1978; Rabbinge, 1976).

6.1.3 Simulation models of population dynamics

Models for pest or disease organisms are in fact a quantitative description of their life cycle. For example, take the life cycle of a fungus. The infection cycle starts when a spore reaches the plant and germinates. After a certain period (the incubation period) the infection becomes visible on the plant. (In the formula-
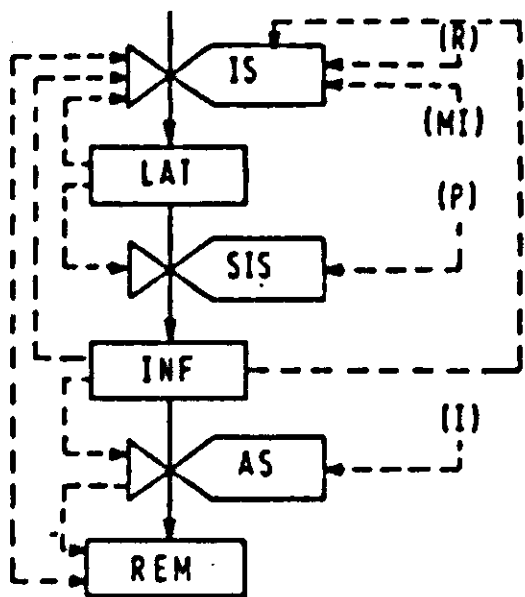
Figure 81. Relational diagram of a summary model of a fungus epidemic.

tion of Equation 104, incubation period and latent period are taken to be identical). The time between infection and time of sporulation by an infected lesion is called the latent period. In many plant fungi the latent period exceeds the incubation period. (In many human diseases the incubation period is larger than the latent period, so that a carrier of the disease is already infectious for other people before the symptoms of the disease are visible.) The newly formed spores are dispersed and may cause new infections on fresh leaf material. The time of sporulation is finite and is called infectious period. In Figure 81 a relational diagram of a fungus epidemic is given. Latent (LAT), infectious (INF) and removed (REM) lesions are distinguished and the rate of decrease and increase of each of these variables is indicated.

Exercise 67

When the incubation period q is not equal to the latent period p, what changes in the rate equation (Equation 104) are then necessary?

Exercise 68

Express the number of latent, infectious and removed lesions with the symbols used in Equation 104.

On basis of the simple relational diagram of Figure 81 a simulation model can be constructed that may answer questions concerning the relative importance of the parameters: relative rate of infection R, the length of the latent period P, the length of the infectious period I and the maximum number of lesions MI. Zadoks (1971) developed such a model and demonstrated the dominating role of the length of the latent period, as shown in Figure 82.
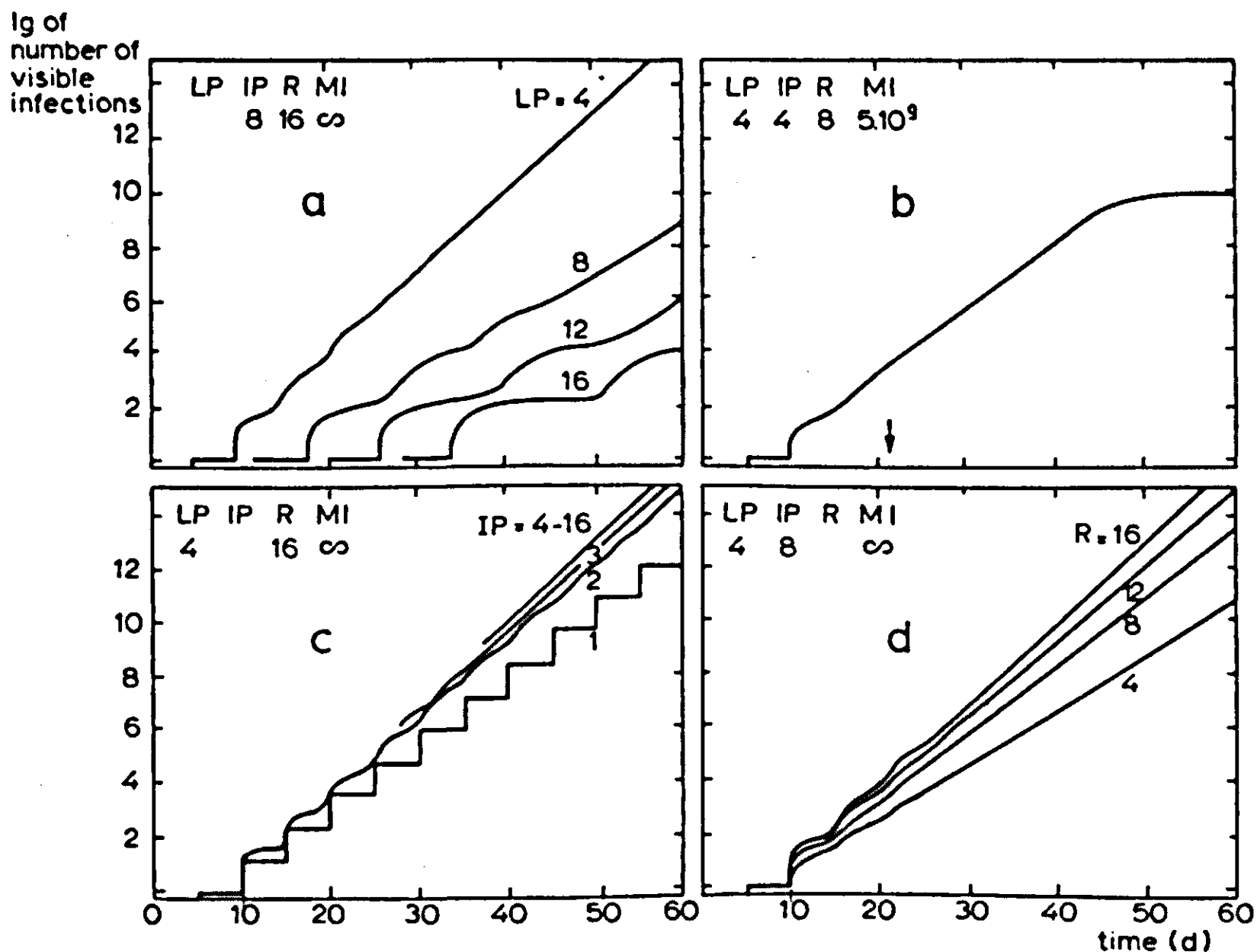
Figure 82. Simulated epidemics. a. The effect of various durations of the latent period (LP). b. The effect of a limited possible number of infections (MI). c. The effect of varying the duration of the infectious period (IP). d. The effect of varying daily multiplication factor (R). Vertical ordinate scale: lg of visible infections. (From: Zadoks, 1971).

Exercise 69
Try to explain the results of Figure 82 by reasoning.

More elaborate population models include other time delays and dispersion in time (Subsection 2.1.8) during development (de Wit & Goudriaan, 1978; Rabbinge, 1976). These models incorporate more or less complicated submodels of the processes and of their relation to climate, crop condition and natural enemies. Processes like lesion growth, spore dispersal and the geographical distribution of disease populations in crops have been studied in this way (Shrum, 1975); Waggoner, 1977; Kampmeijer & Zadoks, 1977; Rijsdijk, 1980). Elaborate models describing parasite and/or predator populations in relation to pest organisms have also been made (Gutierrez et al., 1975; Rabbinge, 1976; Sabelis, 1981). These models incorporate age distribution of the pest organism and dispersion during development. Moreover the complicated predator-prey relations are introduced.

6.1.4 Interactions between plant and disease or pest organisms

In most models of population dynamics the crop is considered as a constant substrate which imposes only limitations when all sites are becoming occupied. Most crop models on the other hand treat pest and/or disease causing organisms as unimportant biotic factors that do not affect the productivity. Combination models are seldom developed, as their architects have to speak two languages, namely that of the agronomist developing crop growth models and that of the plant pathologist developing epidemiological and population dynamical models.

To demonstrate the interactions for some pests and disease-causing organisms, simple pest and disease models, as demonstrated above, are connected to the simplified crop model, SUCROS (Section 3.1). In addition, one example of an interaction between a more elaborate crop model and disease model will be discussed in the next subsection.

Mutilation of leaf mass

To demonstrate the effect of a leaf consumer on crop growth, a simplified simulator of population growth of the cereal leaf beetle has been attached to the simple model of a wheat crop discussed in Section 3.1.

Larvae of cereal leaf beetles *(Lema cyanella)* consume leaf mass at a rate of about $250 \text{ cm}^2 \text{ d}^{-1}$ ($= 1.5$ g dry matter). Only the larvae consume leaves. After growth and development they pupate and later moult into adults that may give rise to another generation. The rate of increase of the numbers of cereal leaf beetle larvae is considered here as an autonomous process, thus it depends on the egg-laying rate of the adult beetles. After hatching, the larvae immediately start feeding. Their effect on crop growth is introduced into the model as a drain on the leaf weight. This rate of decrease of leaf weight is assumed to be proportional to the number of larvae of the beetle, lumping all developmental phases of the larvae together. Consumption of leaf mass by the adults is neglected, and dependency of ageing and reproduction rate on food quality are not considered. The beetle population is introduced in a very simple way by distinguishing four morphological stages: eggs, larvae, pupae and adults. The adult population is assumed to be 50% male, so that after egg-laying only 50% develop into individuals which contribute to the next generation. Reproduction of the adult beetles is diminished when excessively high larval densities are reached; this depends on the ratio number of larvae/weight of leaves. The simulated effect of the growth of the population of beetles on grain growth is shown in Figure 83.

Exercise 70

Develop a simple population model of *Lema cyanella* when the environmental conditions are considered to be constant and the different development stages

weight storage organs
(t ha^{-1})
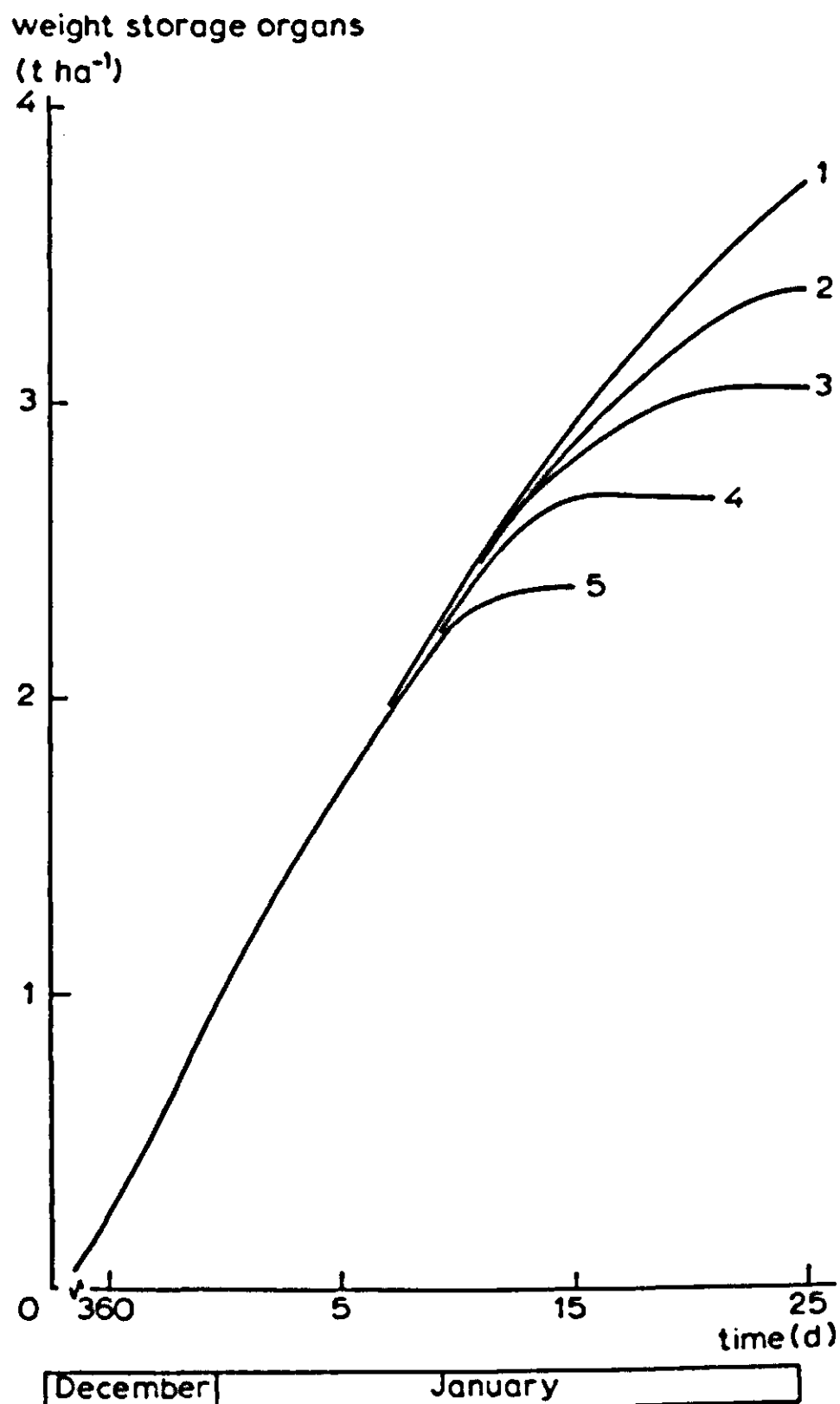
Figure 83. Simulated increase in weight of the storage organs for different levels of cereal leaf beetle attacks (1, no beetles; 2, 3, 4 and 5 starting with 50, 100, 200, 500 adult beetles, respectively at Day 350).

last 5, 10, 4, 20 days for the egg, larval, pupal and adult stages, respectively, and when there are initially 100 adult cereal leaf beetles that produce eggs at a rate of 3 per day. Assume that there is no influence of larval density on the rate of reproduction.

Exercise 71

Link the model of SUCROS and the simple population model and use this combination model to evaluate the effects of different cereal leaf beetle attacks. Assume that the adult cereal leaf beetles enter the crop at Day 350. The simulation should reproduce the results of Figure 83.

Leaf coverage

To demonstrate the effect of a disease that covers the leaves with a thin layer and promotes leaf senescence, the powdery mildew *Erysiphe graminis* is coupled to the simple crop model, SUCROS (Section 3.1). The fungus is simulated with the van der Plank equation (Equation 104). Neither individual spores nor pustules are distinguished; instead, the sites are simulated, i.e. the leaf surface is expressed in terms of potential sites, each site representing the minimum size of one lesion. A field of 1 ha with LAI $= 4$ contains $4 \cdot 10^{11}$ sites.

Only the leaf covering effect of mildew epidemics is introduced in this example; no physiological damage that might occur is considered. This is done by multiplying the gross photosynthetic rate by the ratio between the leaf area not covered and the total leaf area. The simulated effect of a mildew attack on grain growth is shown in Figure 84.

Exercise 72

Construct this combination model and run it for different densities of the disease by setting the initial number of lesions to 10^9, 10^{10}, $2 \cdot 10^{10}$, $5 \cdot 10^{10}$ ha $^{-1}$, the relative infection rate $R = 0.3$, the latent period equals 10 days and the infectious period 4 days. Use the DELAY function, explained in Table 2, Section 2.2, and take $N = 10$ (integer).

It is shown in Figure 84 that when the assumption is made that the fungus is homogeneously distributed in the canopy a considerable loss occurs. However in most cases the fungus grows from the bottom of the canopy towards the top, and it is mainly located in the lower leaf layers. Losses are much lower if this location effect is introduced into the crop model.

Exercise 73

Demonstrate these effects by adapting the combination model and running it for different initial fungus densities.

This combination model is still too simple to be realistic, because many other effects of *E. graminis* are not included. For example, the effect of *E. graminis* on respiration rate and photosynthetic rate are not quantified and introduced in the model. Moreover the use of assimilates by the fungus is not introduced in the model.
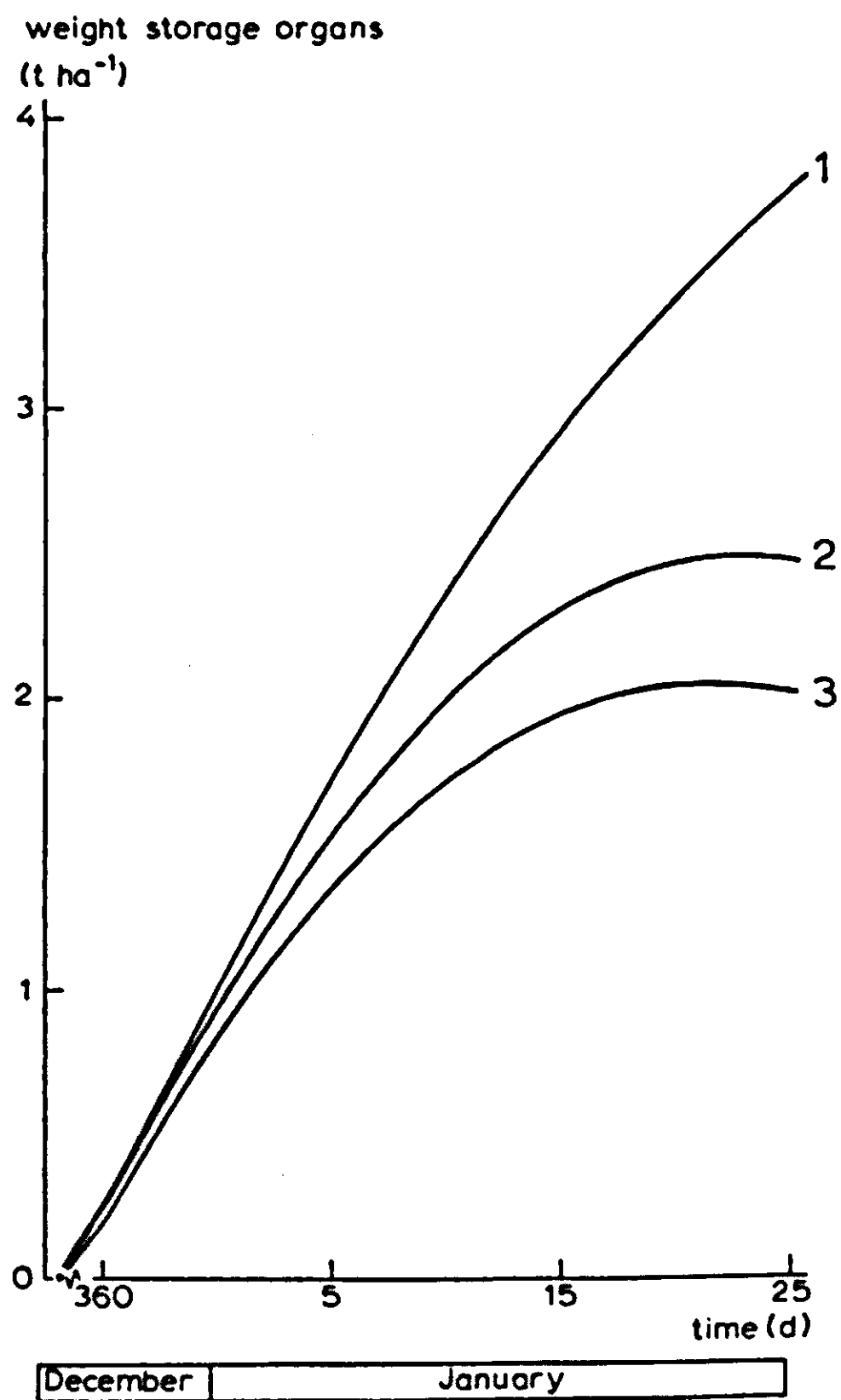
Figure 84. Simulated increase in weight of storage organs under influence of mildew (1: no disease, 2: mildew epidemic reaches a maximum of 67% leaf coverage mainly concentrated in the lower leaf layers, 3: mildew epidemic reaches a maximum of 67% leaf coverage, homogeneously distributed in the canopy).

6.1.5 Stripe rust (Puccinia striiformis) and winter wheat

In an ecophysiological study of crop losses, exemplified in the infection of wheat by leaf rust, van der Wal et al. (1975) demonstrated that leaf rust infection increased the transpiration rate of spring wheat. Similar effects were shown for wheat with stripe rust (F.H. Rijsdijk, unpublished data). The increased transpiration rate may have been due to an increase in leaf conductance or to a shift in shoot-root ratio, a combination of both, or other effects. Simulation studies may help to test the hypothesis that the sporulating pustules of the fungus are just little holes in the leaf cuticle and determine the consequences of such an effect. Summary models of crop growth with simplified relations for water balance and water use are insufficiently detailed to study this problem.

An elaborate and detailed model of assimilation, transpiration and respiration of crop surfaces is needed to test the effect of stripe rust on crop behaviour.

The model BACROS is used to simulate this 'hole making' effect of stripe rust. Within this model, transpiration is computed with a Penman type formula, in which leaf resistance is one of the most important variables (Subsection 3.2.6). Leaf resistance decreases as a result of the many little holes, which leads to an increase in transpiration. Holes in the cuticle can be viewed as non regulating stomata, which in this case are assumed to permit only the diffusion of H_2O.

The diffusion resistance of the holes, parallel to that of the stomata, is introduced by using the calculations for a membrane with cylindrical pores (e.g. Penman & Schofield, 1951; Monteith, 1973). For such a porous membrane made up of n cylindrical pores, length l and diameter d, per unit of surface, the resistance R_m, is normally taken to be:

$$R_m = 4 \cdot l/(d^2 n D) + 2 \cdot 1/(2nDd) \tag{105}$$

in which D is the diffusion coefficient for H_2O, which depends on temperature. The first term of this formula is the diffusion resistance of the tubes proper. The second term is the expression for the diffusional 'end effects' at both sides of the membrane. It represents the diffusion resistance of a semi-infinite space, completely insulated at the free surface with the exception of n independent spots of given constant and uniform concentration. To compute the diffusion resistance of a canopy that contains a large number of these pores, the first part of Equation 105 is small compared to the second one and can be neglected (Stigter & Lammers, 1974).

The number of pores is calculated as follows: when the diameter d of a rust pore (= size of pustule) equals 1.6 mm, the potential number of pores (n), in a canopy with LAI = 5, equals $5 \cdot 10^8 \, cm^2/(\pi \cdot (0.08)^2) = 2.5 \cdot 10^{10} \, ha^{-1}$, or 250 cm^{-2}. When there is a 100% infection of the leaves, about 20% of the leaf area is replaced by pores (Rijsdijk, 1980). D equals 0.2 $cm^2 \, s^{-1}$, so that the diffusion resistance of a surface with these holes amounts to:

$$R = 1/(50 \cdot 0.2 \cdot 0.16) = 0.62 \, s \, cm^{-1}$$

This corresponds with an increase of the conductivity of the canopy of 0.016 m s^{-1}, which indicates that a considerable increase in the transpiration rate is to be expected on basis of this hypothesis. To test this, the assumption was introduced in a computer simulation that a maximum leaf coverage of 20% exists continuously for 30 days. The results of such simulation show that when the other effects of leaf rust on assimilation, etc., are neglected, the total production of dry matter is not much lower, but that there is a shift in shoot-root ratio; the shoot weight is about 10% lower and the root weight is about 20% greater than without rust attack (Figure 85). The transpiration rate of the canopy is on average about twice the normal transpiration rate. These results illustrate the influence of the functional balance (Subsection 3.3.6).
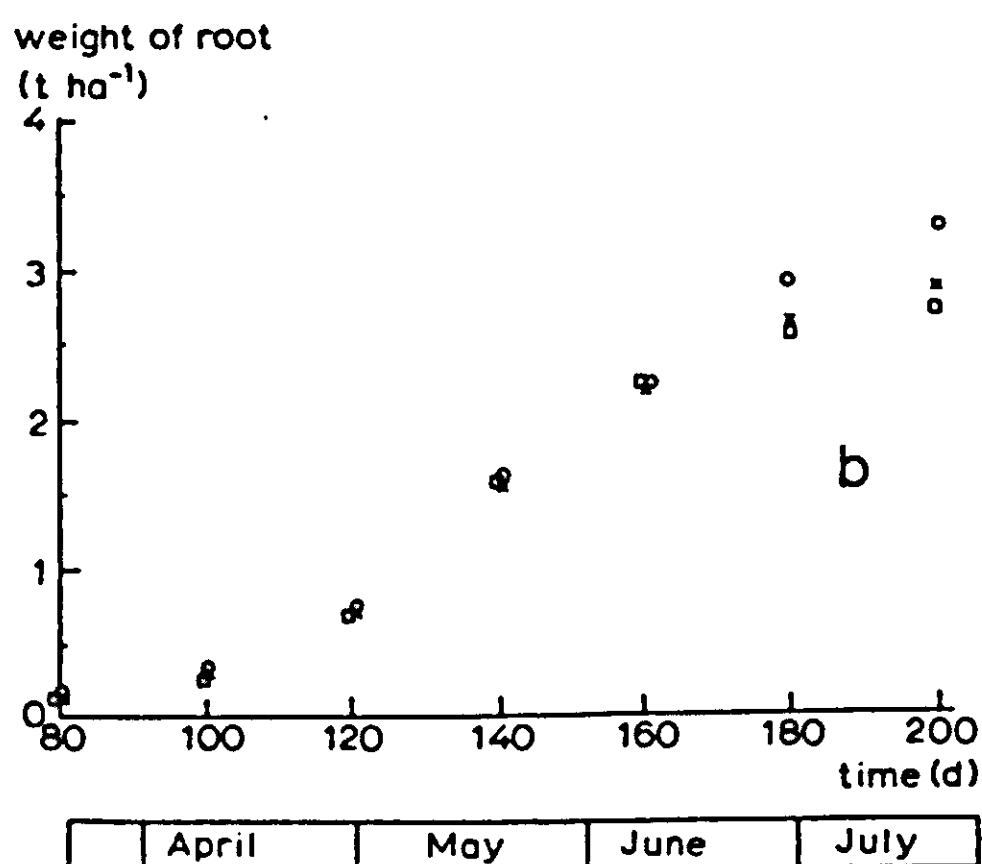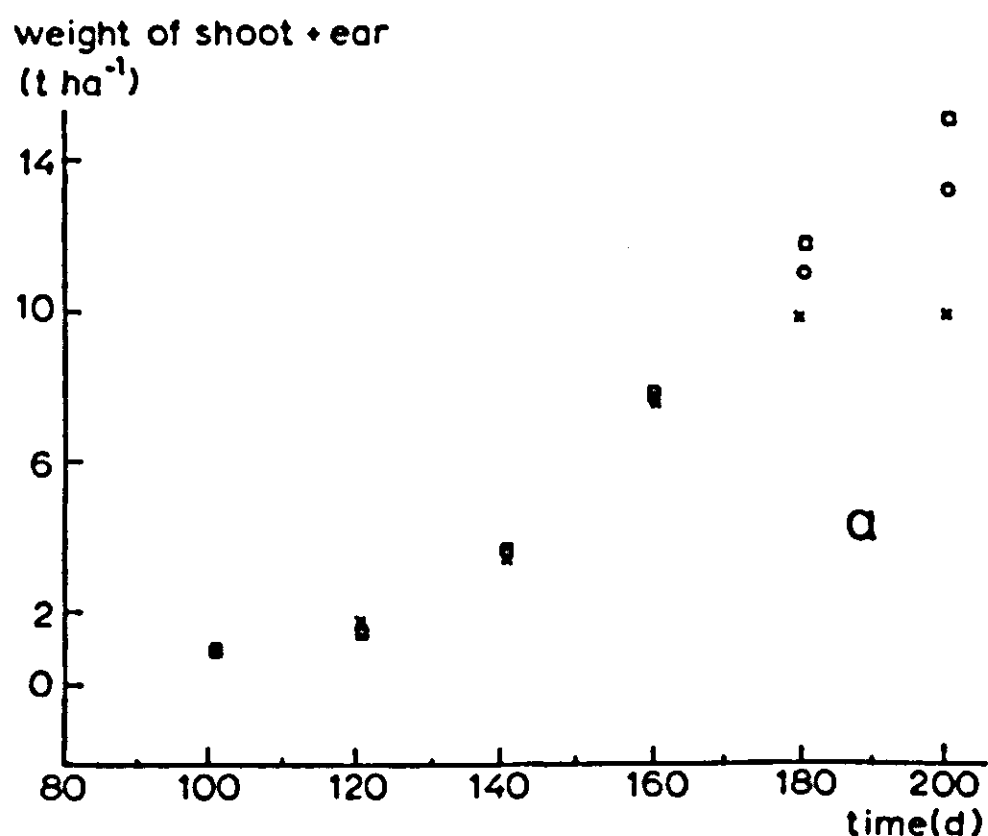
Figure 85. Simulated increase in weight of shoot and ear (a), and weight of root (b) with a comprehensive crop growth simulator. □ = unattacked crop; o = crop infected by a stripe-rust epidemic, maximum leaf coverage of 20%, during a period of 30 days; x = crop infected by strip-rust epidemic, reaching maximum leaf coverage of 100%, i.e. 20% of leaf area replaced by holes, using a realistic simulator of the rust epidemics.

Although these results seem quite logical, they are not in agreement with results obtained from field and container experiments by van der Wal et al. (1975). This is probably because it was unrealistic and incorrect to assume that the decrease in assimilation rate of the canopy and the increase in respiration due to the production of rust material could be neglected. As a next step in hypothesis testing, the decrease of the CO_2 assimilation rate due to absence of photosynthetic activity in the pustules was introduced by multiplying the net CO_2 assimilation rate by the fraction of the total leaf area attacked. As a result, the total amount of above-ground dry matter simulated with the model was

about 25% less in infected than in non-infected control plants, i.e. a yield loss of about 2500 kg ha^{-1}. Again the root weight is higher than in the control. Such figures are 'in the ball park'.

Finally, the crop growth model BACROS was linked to a simulation model of stripe rust epidemics, enabling latent, infectious and removed sites to be distinguished. The results of these calculations (Figure 85) show that a heavy attack of stripe rust causes a considerable decrease in shoot weight and a slight decrease in root weight, a result that is confirmed by field observations. Still the model does not correspond completely with experimental results. Although the total loss in crop yield agrees rather well with the experimental outcome, the relative increase in root weight does not agree completely with some experimental results. This may be due to the incompleteness of the model, e.g. effects on maintenance respiration are neglected, or it may be caused by insufficient understanding of the way hormonal processes interfere with partitioning of carbohydrates. However, in spite of their imperfections, these examples show how an effort is being made to gain a full understanding of various processes that play a role in the crop-pathogen interrelations.

6.1.6 Using a disease crop production model in practice

The latter combination model is used as a research tool that leads to understanding of the effects of a pest or disease organism on its host plant. This insight may lead to better measures. The detailed population dynamic, crop and combination models themselves are seldom used for actual decision-making in crop protection. Their role is to test hypotheses, to gain insight and to pinpoint the most decisive variables for the rate of development of pests and diseases. They are used to compute the range of acceptable disease or pest levels according to the weather and the condition and developmental stage of the plants. These calculations have been made for different diseases and pests in winter wheat and this has resulted in simplified summary models and/or decision rules, which are used to determine whether control measures are needed. In the Netherlands these results are used in a supervised control system called EPIPRE (EPIdemics PREvention) (Rijsdijk et al., 1981). EPIPRE is developed for wheat farmers. It works on a field by field basis and gives specific recommendations for every individual wheat field included. This was done in 1979-1980 by a team of research workers for 1000 fields and based on field information. This information is stored in a data bank and includes data on location, sowing time, cultivar, a few simple physical and chemical soil characteristics, herbicide application and nitrogen (N) fertilization. The information per field is updated whenever additional information is supplied by the farmer on the research team.

This information is used to run the simplified combination or the decision rules models to obtain recommendations that are then sent immediately to the farmers. This EPIPRE supervised control system is now operational in several

European countries and has lead to an improved economic plant protection system with reduced pesticide use and with optimal economic results. This optimal yield may be different from maximum yield as cost-benefit analyses are the basis for the advice.

At present this supervised control system of pests and diseases in winter wheat does not supply information and advice on supervised weed control or N and P fertilization. Reliable simulation models on N in soils and crops (Sections 5.1-5.3) are gradually becoming available, which may be used in future to advise on timing and amount of N added to winter wheat. The same holds for weed control. In this way an integrated crop protection system may be developed in which costs are reduced and economic yields are optimized.

7 ANSWERS TO EXERCISES

Exercise 1
a. Speed or rate
b. $m\,s^{-1}$
c. Speed equals zero

Exercise 2
a. Eighteen litres, which is equal to the area delimited by the rate of flow line and both axes.
b. At $t = 0$ there is no water in the tank; after $t = 30$ the flow stops and the maximum level is reached. The curve lying between these moments can be obtained by dividing the time up into successive time intervals, multiplying the average rate during an interval by the length of the corresponding time interval, and by summing these amounts.
c. Subsitute various values for t into the equation of the amount of water in the tank as function of time; for $t = 30$ the subsitution results in $w = -1.2/60 \cdot 900 + 1.2 \cdot 30$.

Exercise 3
Exponential curve and a straight line, respectively, reaching 44 817 animals after 50 years.

Exercise 4
a. The calculated values do not form a smoothed curve, but a broken one.
b. When the maximum level is reached, i.e. the tank is full. But due to the decreasing rate of inflow it takes a long time before this level is attained.
c. The process is twice as slow.
d. The inflow coefficient, for instance, with dimension T^{-1}.

Exercise 5
a. Overestimated. For instance, 15.5 at time 10 instead of the correct 14.68664.
b. This overestimate is caused by the wrong assumption that the rate is constant during the calculation interval. It could be corrected by making the interval smaller.
c. Results are closer to the analytical solution. At time 10 the content is 15.1.

Exercise 6
a. The rate of change is directly proportional to the difference between actual state and equilibrium state.
b. Negative.
c. $dy/dt = 50 - c \cdot y$. Equilibrium is reached at 1667 kg ha^{-1}. Check this by starting from a level of 1000 and of 3000 kg ha^{-1}.

Exercise 7
a. The time coefficients are: 0.66; 4; 20; 50; 1000.
b. $y_t = 448.17$; 128.4; 105.13; 102.02; 100.1.
c. The percentage of the total increase after one year is $(y_t - y_0)/y_0 \cdot 100 = 348.17$;

7 ANSWERS TO EXERCISES

Exercise 1
a. Speed or rate
b. $m\ s^{-1}$
c. Speed equals zero

Exercise 2
a. Eighteen litres, which is equal to the area delimited by the rate of flow line and both axes.
b. At $t = 0$ there is no water in the tank; after $t = 30$ the flow stops and the maximum level is reached. The curve lying between these moments can be obtained by dividing the time up into successive time intervals, multiplying the average rate during an interval by the length of the corresponding time interval, and by summing these amounts.
c. Subsitute various values for t into the equation of the amount of water in the tank as function of time; for $t = 30$ the subsitution results in $w = -1.2/60 \cdot 900 + 1.2 \cdot 30$.

Exercise 3
Exponential curve and a straight line, respectively, reaching 44 817 animals after 50 years.

Exercise 4
a. The calculated values do not form a smoothed curve, but a broken one.
b. When the maximum level is reached, i.e. the tank is full. But due to the decreasing rate of inflow it takes a long time before this level is attained.
c. The process is twice as slow.
d. The inflow coefficient, for instance, with dimension T^{-1}.

Exercise 5
a. Overestimated. For instance, 15.5 at time 10 instead of the correct 14.68664.
b. This overestimate is caused by the wrong assumption that the rate is constant during the calculation interval. It could be corrected by making the interval smaller.
c. Results are closer to the analytical solution. At time 10 the content is 15.1.

Exercise 6
a. The rate of change is directly proportional to the difference between actual state and equilibrium state.
b. Negative.
c. $dy/dt = 50 - c \cdot y$. Equilibrium is reached at 1667 kg ha^{-1}. Check this by starting from a level of 1000 and of 3000 kg ha^{-1}.

Exercise 7
a. The time coefficients are: 0.66; 4; 20; 50; 1000.
b. $y_t = 448.17;\ 128.4;\ 105.13;\ 102.02;\ 100.1$.
c. The percentage of the total increase after one year is $(y_t - y_0)/y_0 \cdot 100 = 348.17$;

28.4; 5.13; 2.02 and 1.0%. This differs from the relative growth rate and the difference is larger when the relative growth rate is higher.

Exercise 8

a. The rate equation is given by $dw/dt = 1/TC \cdot (16 - w)$. The change during a time interval equal to TC and with constant rate equals $TC \cdot 1/TC \cdot (16 - w)$ or $(16 - w)$. Thus the difference between w and the equilibrium value of 16 is bridged within one interval equal to the time coefficient.

b. In a positive feedback loop, the change is directed away from the equilibrium state, so that the direction of the extrapolation of the tangent must be reversed toward the unstable equilibrium state; the tangent cuts the horizontal equilibrium line a time coefficient interval earlier.

Exercise 9

a. $y_{\Delta t} = 2 \cdot y_0 = y_0 \cdot e^{\Delta t/TC} \rightarrow e^{\Delta t/TC} = 2$. Hence $\Delta t = TC \cdot \ln 2$ or $\Delta t = 0.7 \cdot TC$.

b. The half-life time is the time necessary to reach half the original amount.

Exercise 10

a. The mean residence time is VT time units. There is no difference between both delay elements or boxes, the amounts remain therefore on the average VT/2 time units in every delay element.

b. In a steady state, the amount streaming into and out of both delay elements is the same. Consequently, $R1_t$ and OUT_t equal IN_t. According to the rate equations, the conditions, $IN_t = H1_t/(VT/2)$ and $IN_t = H2_t/(VT/2)$ apply, from which $H1_t = IN_t \cdot VT/2$ and $H2_t = IN_t \cdot VT/2$ follow.

c. $t = 0$ IN   = R1 = OUT = 100 m³ week⁻¹

$$IN = R1 = OUT = 100 \text{ m}^3 \text{ week}^{-1}$$

c. $t = 0$ $IN = R1 = OUT = 100 \text{ m}^3 \text{ week}^{-1}$
            $H1 = H2 = 400 \text{ m}^3$

$t = 2$ $H1 = 400 + 2 \cdot (200 - 100) = 600$
         $H2 = 400 + 2 \cdot (100 - 100) = 400$
         $R1 = 600/4 = 150$
         $OUT = 400/4 = 100$

$t = 4$ $H1 = 600 + 2 \cdot (200 - 150) = 700$
         $H2 = 400 + 2 \cdot (150 - 100) = 500$
         $R1 = 700/4 = 175$
         $OUT = 500/4 = 125$

$t = 6$ $H1 = 700 + 2 \cdot (200 - 175) = 750$
         $H2 = 500 + 2 \cdot (175 - 125) = 600$
         $R1 = 187.5$
         $OUT = 150$

$t = 8$ $H1 = 750 + 2 \cdot (200 - 187.5) = 775$
         $H2 = 600 + 2 \cdot (187.5 - 150) = 675$
         $R1 = 193.75$
         $OUT = 168.75$

$t = 10$ $H1 = 787.5$
         $H2 = 725$
         $R1 = 196.875$
         $OUT = 181.25$

$t = 12$ H1 $= 793.75$
       H2 $= 756.25$
       R1 $= 198.44$
       OUT $= 189.06$

d. The equilibrium is H1 $=$ H2 $= 800\,m^3$
                       IN $=$ R1 $=$ OUT $= 200\,m^3\,week^{-1}$

Exercise 11

A few specific job control commands are required to let your computer execute the job. Ask at your computer centre. CSMP has to be implemented on the computer system, of course.

Exercise 12

a. TWT $=$ INTGRL(TWTI,GTW)
   GTW $=$ (GPHST $-$ MAINT)*CVF
   MAINT $=$ TWT*0.015
   PARAM CVF $=$ 0.7, GPHST $=$ 400.
   INCON TWTI $=$ 1000.

b. Maintenance respiration is related to the amount of dry matter. The higher this amount, the more carbohydrates are used for maintenance respiration, so less carbohydrates will be available for growth. The system has one negative feedback loop, and behaves therefore similar to that of filling a water tank as discussed in Subsection 2.1.4: the amount of dry matter grows to an equilibrium level. The differential equation for growth is:
   $d(TWT)/dt = (GPHST - 0.015 \cdot TWT) \cdot 0.7$
   or, similarly
   $d(TWT)/dt = (GPHST/0.015 - TWT) \cdot 0.7 \cdot 0.015$
   The equilibrium level is found when $d(TWT)/dt = 0$:
   $TWT_{eq} = GPHST/0.015 = 26\,667\ kg\ ha^{-1}$.
   The time coefficient is $1/(0.7 \cdot 0.015) = 95$ d.

c. A second feedback loop (positive) in involved. The time coefficient is changing continuously.

Exercise 13

   GPHOT $=$ DTR*(1.$-$REFL)*(1.$-$EXP($-$0.7*LAI))*EPS*30./44.
   DTR $=$ AFGEN(RADTB,TIME)*1.E10
   FUNCTION RADTB $= \ldots\ldots$ (see question of Exercise 13)
   PARAM REFL $=$ 0.1, EPS $=$ 4.35E$-$9
   TIMER TIME $=$ 60., FINTIM $=$ 210., DELT $=$ 1., PRDEL $=$ 5.

   With other conditions and parameters similar to the program of Subsection 2.2.2, the simulated final total dry matter is $19\,679\ kg\ ha^{-1}$.

Exercise 14

   MAINT $=$ (WSH+WRT)*MC
   MC $=$ AFGEN(MCTB, TEMP)
   FUNCTION MCTB $=$ (10.,0.008), (20.,0.015), (30.,0.030)
   TEMP $=$ AFGEN(TEMPTB, TIME)
   FUNCTION TEMPTB $=$ (60.,10.), (210.,20.)

Adding these equations to the program of Exercise 13 results in a simulated dry matter production of 20 874 kg ha^{-1}.

Exercise 15

The output shows important deviations between the calculated values of the AFGEN and NLFGEN function, especially at the place of a minimum or maximum. In general, profitable use of the NLFGEN is restricted to non-linear data sets without abrupt discontinuities. (Do not forget to add END, STOP and ENDJOB to the program).

Exercise 16

Computational order:

```
LAI    = AMIN1(WSH/500.,5.)
GPHOT  = GPHST*(1.-EXP(-0.7*LAI))
MAINT  = (WSH + WRT)*0.015
GTW    = (GPHOT-MAINT)*CVF
GSH    = 0.7*GTW
WSH    = INTGRL(WSHI, GSH)
GRT    = 0.3*GTW
WRT    = INTGRL(WRTI, GRT)
TWT    = WSH + WRT
```

When the name of a variable is incorrectly spelled, e.g. MAINE instead of MAINT, CSMP sets the undefined variable to zero and reports this at the end of the translation output. Check this.

If a rate variable is written as function of another rate variable, CSMP tells you that such a problem cannot be executed: 'simulation involves an algebraic loop containing the following elements GSH, GTW, MAINT, GTW', and also another loop: GTW, MAINT, GRT, GTW.

Exercise 17

```
LAI            = AMIN1(WSH/RATIO, 5.)
PARAM RATIO = (400., 500., 600.)
PARAM GPHST = 300.
END
PARAM GPHST = 400.
END
PARAM GPHST = 500.
END
STOP
ENDJOB
```

Some results for total dry matter calculated in this program are:

RATIO	GPHST		
	300	400	500
400	11 841	16 053	20 255
500	11 516	15 749	19 960
600	11 148	15 410	19 637

Exercise 18

Note that in the UPDATE, several variable names are written of the kind ZZ1002. These names have been created by the translator to represent the variables that are internal for a certain MACRO invokation. A variable name like GTW is replaced by one ZZ.... name, and by another ZZ.... name in the next MACRO invokation. Also note the changed sequence of the statements. (If you do not receive the UPDATE listing automatically by running the program, contact your computer centre for instructions on how to obtain it).

Exercise 19

At a very low reserve level, RESL is negligible with respect to KRESL, so that CGR is equal to RES . 0.1/ ($\approx$ 0.1), or numerically RES itself. The time coefficient is now equal to one unit of time, in this case to 1 d.

Exercise 20

For TWT = 10 000. the implicit loop gives RESL = 0.0312 and GPHRED = 387.92. With the state variable approach this value for RESL is almost reached at TIME = 6.0 (0.0346), and completely at TIME = 17. For TWT = 2000. the results of the state variable approach are given in Table 4, Section 2.3. With the implicit loop RESL = -0.27597 (!) and GPHRED = 343.66. These results differ very much!

Exercise 21

A possible CSMP program is given in Figure 86. A is the numerical result and AA the analytical result. Results of this program are given in Table 5, Section 2.3.

```
TITLE INTEGRATION METHOD
      A=INTGRL(U.,R)
      R=RU*EXP(RGR*TIME)
INCON RU=1.
PARAM RGR=1.
      AA=(EXP(RGR*FINTIM)-1.)/RGR
      ERR=AA-A
METHOD RECT
TIMER FINTIM=4.,DELT=(1.,0.1,0.01),PRDEL=4.
PRINT A,ERR
END
METHOD TRAPZ
END
METHOD RKSFX
END
STOP
ENDJOB
```

Figure 86. Listing of a CSMP program to integrate a driving force in the form of an exponential function. The difference with the analytic solution is also calculated.

Exercise 22

a. The analytical solution of the integral of TIME with respect to TIME itself is 0.5 . TIME². At the end of the run TIME equals FINTIM, so that the analytical solution AA can be calculated as FINTIM . FINTIM . 0.5. With FINTIM at 0.5 the analytical solution is 0.125. A program to evaluate the numerical solution is given in Figure 87.

Its results for the error can be summarized in the following table:

DELT	METHOD		
	RECT	TRAPZ	RKSFX
0.1	0.025	0	9.31E-10
0.01	0.0025	−1.86E-9	−1.86E-9

Theoretically, the errors for TRAPZ and RKSFX should be zero, because these methods can exactly integrate a linear function. The very small remaining error is due to truncation in number representation. Here TRAPZ is just as good as RKSFX. As expected, RECT shows a linear dependence of the error on DELT.

b. The second problem has as numerical solution AA $= \mathrm{FINTIM}^3/3$. The table of errors is:

DELT	METHOD		
	RECT	TRAPZ	RKSFX
0.1	0.011667	−0.8333E-3	0
0.01	1.2417E-3	−8.3330E-6	−4.656E-10

Only RKSFX can exactly integrate this function, the others show the usual first and second order dependence of the error on DELT.

c. The analytical solution of the integral of the sine wave is 1/PI. The table of errors is:

DELT	METHOD		
	RECT	TRAPZ	RKSFX
0.1	0.0105416	0.0105415	−1.74344E-5
0.01	1.04729E-4	1.04722E-4	−7.45058E-9

```
TITLE INTEGRATION METHODS
TIMER FINTIM=0.5,DELT=(0.1,0.01),PRDEL=0.5
METHOD RECT
       AA=FINTIM*FINTIM*0.5
       R=TIME
       A=INTGRL(0.,R)
       ERR=AA-A
PRINT A,ERR
END
METHOD TRAPZ
END
METHOD RKSFX
END
STOP
ENDJOB
```

Figure 87. Listing of a CSMP program to integrate a driving force in the form of a linear function. The difference with the analytic solution is also calculated.

Rather surprisingly, RECT does just as well as TRAPZ and has even a second order relation of the error with DELT. This peculiar result is due to the symmetry of the sine function in the region of integration. The first order error made in the rising region is compensated by the first order error in the falling region, and the second order error remains the dominating one.

Exercise 23

a. COUNT1 and COUNT2 must be set equal to zero in an initial section. Some results are:

DELT	METHOD					
	RECT		TRAPZ		RKSFX	
	COUNT1	COUNT2	COUNT1	COUNT2	COUNT1	COUNT2
1.	6	5	10	5	18	5
0.1	42	41	82	41	162	41
0.01	402	401	802	401	1602	401

At time 0 the program is executed twice, once with KEEP = 0 and once with KEEP = 1.

b. If we want to make a PROCEDURE we must determine what are input and what are output variables. In this example the output variables are COUNT1 and COUNT2. The only input variable is KEEP, so that we get:
PROCEDURE COUNT1, COUNT2 = COUNT(KEEP)
         COUNT1 = COUNT1 + 1
         COUNT2 = COUNT2 + KEEP
ENDPRO

Exercise 24

The daily photosynthetically active irradiation (DRC) and the daily gross CO_2 assimilation (DGAC) can be calculated with only the Lines 205-233 of Table 9, Section 3.1. It is necessary to specify LAT, LAI, TIME and FOV. Take care that FINTIM and DELT are specified correctly. E.g.:
PARAM LAT = 52., LAI = 5., FOV = 0.
TIMER FINTIM = 173., DELT = 1., TIME = 172.
PRINT DRC, DGAC
Results: DRC = $1.69654 \cdot 10^7$ J m^{-2}
        DGAC = 795.21 kg ha^{-1}

Exercise 25

SLFA determines the value of the LAI and hence influences the rate of CO_2 assimilation and the growth rate of the various organs. A too high value of SLFA leads to too high values for the weights of the organs. There is a positive feedback (Subsection 2.1.6), which implies that the situation gets worse as simulation progresses. For example, with SLFA = 0.002, WSO = 3805 and WLV = 759 kg ha^{-1} at TIME = 390. (Figure 24), but with SLFA = 0.0022 these value are 4319 and 911 kg ha^{-1}, respectively.

Exercise 26

c. These data can be introduced in the model by changing FUNCTION FSHTB, FSTTB and FLVTB. But if no other factors are changed, the results cannot be related to any existent crop.

d. Two examples of a set of values of important species specific parameters are:

	Potato	Soybean
PARAM DVR	0.0208	0.0167
INCON WRTI	60.	100.
INCON WLVI	500.	100.
PARAM SLFA	0.00285	0.0033
PARAM CVFSO	0.81	0.57
FINISH DVS	2.5	2.

The yield (WSO) of soybean is 4750 kg ha^{-1} at Day 55 and of potatoes 10435 kg ha^{-1} at Day 57. WLV is then 1579 and 388 kg ha^{-1}, respectively.

Exercise 27

F_m, F_n, and R_d have the same units. The product εH must also have the unit kg ha^{-1} h^{-1}, so that for ε the numerical value 0.5 must be used. The following table gives the calculated values of F_n for a number of absorbed light intensities (in W m^{-2}).

H	F_n		H	F_n	
	asymptotic exponential	rectangular hyperbola		asymptotic exponential	rectangular hyperbola
0	−4	−4	100	30.698	24.070
10	0.8096	0.6377	200	46.584	35.024
50	16.695	13.977	500	58.713	46.955

This table shows the much slower approach of the maximum rate when the rectangular hyperbola is used.

Exercise 28

For a consistent set of units the net CO_2 assimiliation rate must be expressed in kg m^{-2} s^{-1}, light use efficiency in kg J^{-1}, absorbed light intensity in W m^{-2}. The ratio C/r_x must also be expressed in kg m^{-2} s^{-1}, so that C is best expressed in kg m^{-3} and r_x in s m^{-1}.

Exercise 29

At both low light and low CO_2 the maximum assimilation rate F_{mm} can be considered as infinitely high, so that εH can be omitted from the denominator of Equation 16. Dividing by F_{mm} and multiplication with C then gives

$$F_g = \frac{\varepsilon H C}{\varepsilon H r_x + C}$$

274

so that the Michaelis-Menten constant for CO_2 equals $\varepsilon H r_x$. This structure corresponds to the notion that saturation with CO_2 will occur earlier when the light intensity is lower.

Exercise 30

To reduce Equation 18 to Equation 14 both numerator and denominator must be divided by $(F_{mm}r_x/C + 1)$. We then see that $F_m + R_d$ corresponds with $F_{mm}/(F_{mm}r_x/C + 1)$, so that F_m can be written as

$$F_m = \frac{F_{mm}C/r_x}{F_{mm} + C/r_x} - R_d$$

This expression shows how the net assimilation rate at saturating light intensities depends on the CO_2 concentration at the carboxylation site.

Exercise 31

In Equation 18 F_n must be set to zero, R_d must be brought to the other side, and the expression must be inverted:

$$\frac{1}{\varepsilon H} + \frac{r_x}{C} + \frac{1}{F_{mm}} = \frac{1}{R_d}$$

This equation gives the relation between H and C at the compensation line. The so-called compensation points can be found by letting H approach infinity and solving for C, and vice versa. With the given numbers we find $H_c = 8.1$ W m^{-2} and C_c (usually denoted by Γ) = $9.07 \ 10^{-6}$ kg m^{-3}. To express the CO_2 concentration in cm^3 m^{-3} it must be divided by $1.83 \ 10^{-6}$ so that we find that $\Gamma = 5$ cm^3 m^{-3}. The value $1.83 \ 10^{-6}$ is the weight in kg of 1 cm^3 of pure CO_2 at 1 bar and 20 °C.

Exercise 32

When the leaf area index of a model layer is L_s, it will intercept and also absorb a fraction L_s of the irradiation flux falling on it, and transmit a fraction $(1 - L_s)$. When n such layers are arranged above each other, the overall transmission will be $(1 - L_s)^n$. According to Equation 25 this transmission must be equal to $e^{-K \cdot LAI}$, where LAI = $n \cdot L_s$.

$$K = -\frac{1}{L_s} \ln (1 - L_s)$$

For $L_s = 0.5, 0.1$ and 0.01 we find that K is $1.38, 1.05$ and 1.005, respectively. The smaller L_s, the closer the asymptotic value 1 is approached.

The fraction of light absorbed is $1 - (1 - L_s)^n$, which gives $0.984, 0.958$ and 0.951, respectively, for $L_s = 0.5, 0.1$ and 0.01.

Exercise 33

It stands to reason that the influence of the soil surface decreases exponentially with LAI. The leaf area index (LAI) must be larger than about 4 before the reflection of the soil surface has lost its influence on the total reflectance. Figure 88 shows how ϱ_c depends on σ. For low values of σ, K is approximately equal to $1 - 0.5 \cdot \sigma$, so that ϱ_c is about equal to $0.5 \cdot \sigma/(1 + 1 - 0.5 \cdot \sigma)$. The product $0.5 \cdot \sigma$ may be neglected in the denominator, but not in the numerator where it occurs as the only term, so that ϱ_c can be simplified to $0.25 \cdot \sigma$. Even for a closed canopy, reflectance is then only about half the value of individual leaf reflectance, which is $0.5 \cdot \sigma$. The reason is that most leaves are partially shaded and reflect less than those at the very top.
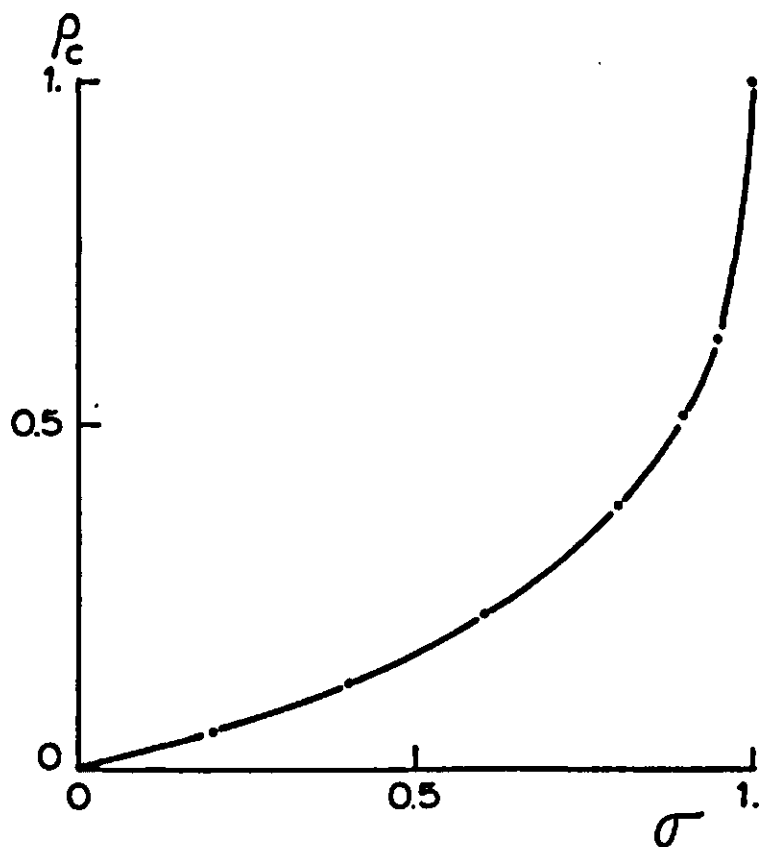
Figure 88. The dependence of the reflection coefficient (ϱ_c) of the closed canopy on the scattering coefficient (σ) of the individual leaves.

Exercise 34

According to Equation 24 the incoming visible irradiation under a clear sky with solar height of 60 degrees is about 470 W m^{-2}. Under an overcast sky it will be about one-fifth of this, and for simplicity we take 100 W m^{-2}. The crop reflection coefficient for visible irradiation ($\sigma = 0.2$) is 0.056, so that the net visible radiation above the canopy is 94.4 W m^{-2}. Equation 26 gives an extinction coefficient of 0.894 for diffuse visible irradiation. That means that each layer with leaf area unity will transmit a fraction $e^{-0.894} = 0.409$, and absorb a fraction 0.591 of the net flux just above it. This gives the following scheme of the partitioning of the visible irradiation:

		net assimilation
incoming	100	
reflected	5.6 −	
net	94.4	
absorbed by Layer 1	55.8 −	13.2
	38.6	
absorbed by Layer 2	22.8 −	5.0
	15.8	
absorbed by Layer 3	9.3 −	0.5
	6.5	
absorbed by Layer 4	3.8 −	−1.5
	2.7	
absorbed by Layer 5	1.6 −	−2.4
absorbed by soil surface	1.1	crop 14.8

To find the net assimilation rate of each layer the asymptotic exponential (Equation 13) can be used as photosynthesis-light response curve. We then find the contributions of the five subsequent layers as given above. Layers 4 and 5 receive so little irradiation that they operate below the compensation point.

276

Exercise 35

In each layer L_s the fraction of sunlit leaf area is equal to the overall fraction of the direct irradiation that reaches that level. Therefore the total sunlit leaf area is the integral of $e^{-K_{dir} \cdot LAI'}$ from top to bottom. From basic calculus this integral appears as $(1. - e^{-K_{dir} \cdot LAI})/K_{dir}$, which approaches $1/K_{dir}$ if LAI is large enough. For horizontal leaves K_{dir} is alway 1, irrespective of solar height. For a spherical leaf angle distribution, which is much more common, K_{dir} equals $0.5/\sin \beta$, so that the sunlit leaf area is equal to $2 \cdot \sin \beta$. Even if all sunlit leaves are saturated with light, assimilation still increases with solar height, just because sunlit leaf area increases.

Exercise 36

When time t_h in Equation 30 is made explicit, it is possible to calculate the moment a certain solar height β' is reached, and also the number of hours that the solar height exceeds β'. This day length is equal to

$$ DLENG = \frac{24}{\pi} \cdot \arccos \frac{(\sin \beta' - \sin \lambda \cdot \sin \delta)}{\cos \lambda \cos \delta} $$

The upper edge of the disk of the sun appears exactly on the horizon when the solar height is $-50'$ (-0.833 degrees), so that β' must be set at -0.833 degrees. The disk radius accounts for $16'$ of arc and the refraction in the atmosphere for $34'$. Because of this correction, day length is longer than expected if sunrise and sunset are assumed

```
TITLE DAILY RADIATION
CONST PI=3.1415927
INITIAL
        RAD=PI/180.
        RISE=SIN(-RAD*0.833)
*       RISE IS THE SINUS OF THE TIME OF SUNRISE
        DEC=-23.45*COS(PI*(DAY+10.173)/182.6)
        SINLD=SIN(RAD*LAT)*SIN(RAD*DEC)
        COSLD=COS(RAD*LAT)*COS(RAD*DEC)
DYNAMIC
        HOUR=TIME
        SNHSS=SINLD+COSLD*COS(2.*PI*(HOUR+12.)/24.)
*       SNHSS IS THE SINUS OF SOLAR HEIGHT

PROCEDURE S,D=RADIA(SNHSS,RISE)
        S=0.
        D=0.
        IF(SNHSS.LE.RISE)GOTO 230
        D=1.
        IF(SNHSS.LE.0.)GOTO 230
        S=2.*640.*SNHSS*EXP(-0.15/SNHSS)
230 CONTINUE
ENDPRO

        DRAD=INTGRL(0.,3600.*S)
        DLENG=INTGRL(0.,D)
TIMER FINTIM=24.,PRDEL=24.
PRINT DRAD,DLENG
PARAM DAY=(15.,46.,74.,105.,135.,166.,196.,227.,258.,288.,319.,349.)
PARAM LAT=0.
END
STOP
ENDJOB

.
```

Figure 89. Listing of a CSMP program to simulate total daily global irradiation and day length.

to occur at zero degrees. At the equator day length is 12 h 07 min instead of exactly 12 h, and at 60 degrees latitude in midsummer, day length is 18 h 53 min instead of 18 h 29 min.

In SUCROS, the day length (DL) is calculated in principle similar to the above equation but in a slighty different formulation (see Section 3.1, Exercise 24).

In a CSMP program the integration routine can be used to find the day length in an alternative fashion. Depending on solar height, the rate of change of the integral DLENG has been set at either zero or unity. A possible program listing is given in Figure 89. In this program the daily total global irradiation is also computed. Daily visible irradiation (DRC) in Section 3.1 is given as a mathematical expression of latitude and time that yields exactly half the value as DRAD in this program if $K_{atm} = 0.1$.

Exercise 37
See Figure 90.

Exercise 38
In the state variable approach the areal heat content of the leaf is integrated by

$$HC = INTGRL(HCI, RN - W - LE)$$

The leaf temperature TL is equal to the heat content (HC) divided by the areal heat capacity. W and LE are calculated with the Equations 43, 44 and 46. After 200 seconds of simulated time, equilibrium is established. The results are then:

	RL				
	0	10	100	1000	10 000
TL	16.778	17.719	20.794	22.928	23.290
W	−193.35	−136.86	47.66	175.68	197.41
LE	393.35	336.86	152.34	24.32	2.59

In the Penman approach first the slope of the saturated vapour pressure curve must be calculated by differentiation of Equation 46:

$$s = \frac{4158.6 \cdot e_s (T_a)}{(T_a + 239.)}$$

Then Equation 37 can be used to calculate the latent heat loss, the energy balance equation to calculate W, and a rearranged form of Equation 43 to calculate the leaf temperature. The results are:

	RL				
	0	10	100	1000	10 000
TL	16.965	17.802	20.799	22.939	23.292
W	−182.12	−131.90	47.95	176.31	197.49
LE	382.12	331.90	152.05	23.69	2.51

```
TITLE NET CO2-ASSIMILATION ,HORIZONTAL LEAVES
CONST PI=3.1415926
PARAM LAT=40.
PARAM LAI=5.,LS=1.
PARAM SCV=0.2
*       SCATTERING COEFFICIENT FOR VISIBLE RADIATION
PARAM DAY=166.
PARAM EFF=0.4,AMAX=30.
PARAM RDARK=3.
INITIAL
       RAD=PI/180.
       DEC=-23.45*COS(PI*(DAY+10.17)/182.6)
       SINLD=SIN(RAD*LAT)*SIN(RAD*DEC)
       COSLD=COS(RAD*LAT)*COS(RAD*DEC)
       SQVI=SQRT(1-SCV)
       REFV=(1.-SQVI)/(1.+SQVI)
*       REFLECTION COEFFICIENT
       KDIR=1.
*       EXTINCTION COEFFICIENT DIRECT LIGHT
       KDIF=KDIR*SQVI
*       EXTINCTION COEFFICIENT DIFFUSE LIGHT (INCLUDES MULTIPLE SCATTERING)
       EDIR=EXP(-KDIR*LS)
       EDIF=EXP(-KDIF*LS)
*       INTERMEDIATE VARIABLES
DYNAMIC
       HOUR=TIME
       SNHSS=SINLD+COSLD*COS(2*PI*(HOUR+12.)/24.)
PROCEDURE FNET,SPAR=ASSIM(SNHSS,EFF,AMAX,RDARK,LAI,LS)
*       FNET AND SPAR ARE TOTAL NET FOTOSYNTHESIS AND VISIBLE RADIATION
       FNET=0.
       SPAR=0.
       LAIC=0.
       IF(SNHSS.LE.0.) GOTO 230
       FRDIR=EXP(-0.2/SNHSS)
*       FRACTION DIRECT LIGHT
       SPAR=640*SNHSS*EXP(-0.15/SNHSS)
       SUNDCL=SPAR*FRDIR
       DIFCL=SPAR*(1.-FRDIR)
       VISDF=(1.-REFV)*DIFCL*(1.-EDIF)
*       ABSORBED FLUX OF INCOMING DIFFUSE LIGHT
       VIST =(1.-REFV)*SUNDCL*(1.-EDIF)
       VISD =(1.-SCV)*SUNDCL*(1.-EDIR)
       SLLA=(1.-EDIR)/(LS*KDIR)
*       FRACTION OF SUNLIT LEAVES
  154  VISDFC=(VISDF+VIST-VISD)/LS
       VISSUN=VISDFC+(1.-SCV)*SUNDCL
       FNSUN= (AMAX+RDARK)*(1.-EXP(-VISSUN*EFF/(AMAX+RDARK)))-RDARK
       FNSUN=FNSUN*SLLA
*       NET FOTOSYNTHESIS SUNLIT LEAVES
       FNSHAD=(AMAX+RDARK)*(1.-EXP(-VISDFC*EFF/(AMAX+RDARK)))-RDARK
       FNSHAD=FNSHAD*(1.-SLLA)
*       NET FOTOSYNTHESIS SHADED LEAVES
       FNL=LS*(FNSHAD+FNSUN)
       FNET=FNET+FNL
       LAIC=LAIC+LS
*       NEXT 5 LINES: UPDATING OF THE VARIABLES FOR CALCULATIONS IN THE
*       NEXT LAYERS
       SLLA=SLLA*EDIR
       VISDF=VISDF*EDIF
       VIST=VIST*EDIF
       VISD=VISD*EDIR
       IF(LAIC.LT.LAI) GOTO 154
       GOTO 231
  230  CONTINUE
       FNET=-LAI*RDARK
  231  CONTINUE
ENDPRO
PRINT FNET,SPAR
METHOD RECT
TIMER FINTIM=24.,PRDEL=1.,DELT=1.
END
STOP
ENDJOB
```

Figure 90. Listing of a CSMP program to simulate net CO_2 assimilation of a canopy with horizontal leaves.

The largest deviation can be observed at leaf resistance 0 and 10. These values correspond to practically wet surfaces. In the normal range of resistance (100-1000) the error of the Penman approach is very small.

Exercise 39

In this situation the implicit loop converges and gives good results, in perfect agreement with those of the state variable method. A possible formulation of the implicit loop is:

TL = IMPL(20., 1.E-4, TL1)
EL = 6.11 * EXP(17.4 * TL/(TL + 239.))
LE = (EL − EA) * RHOCP/(GAMMA * (RL + RB))
W   = RN − LE
TL1 = TA + W * RB/RHOCP

For the halving/doubling method, consult Figure 20, Section 2.3.

Exercise 40

With CO_2 assimilation rate expressed in $kg\,ha^{-1}\,h^{-1}$, resistance in $s\,m^{-1}$ and CO_2 concentration in $cm^3\,m^{-3}$, the assimilation rate must be divided by a conversion coefficient of 66 (at 20 °C) for dimensional consistency. Results are given in Figure 91.

The resistance-light response curve of C_3 and C_4 plants calculated in this way are almost the same. A higher assimilation rate in C_4 plants is accompanied by a lower internal CO_2 concentration, so that resistances do not differ much. ·

Exercise 41

In this exercise the transpiration-assimilation ratio can be broken up in the ratio of the gradients and of the diffusion coefficients of water and CO_2. The difference of water vapour is $e_s(T_l) − e_a$ or $23.4 − 15 = 8.4$ mbar. One cubic metre of air at 20 °C and 1
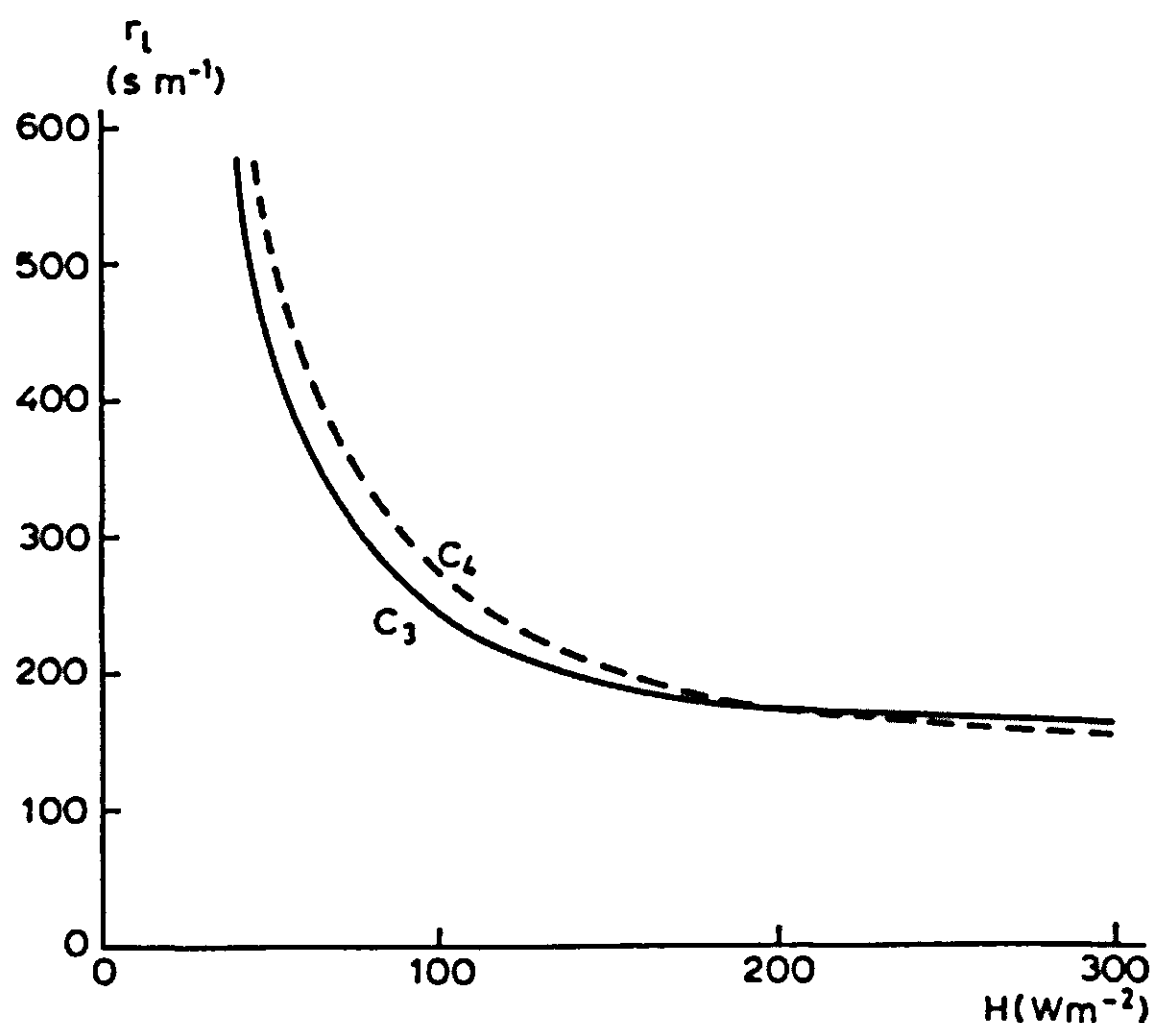
Figure 91. The computed relation of the leaf resistance (r_l) with the absorbed radiation flux (400-700 nm) (H) for C_3 and C_4 type species.

bar weighs 1200 g, so that a similar volume of (supersaturated) water vapour should weigh $1200 \cdot 18/29 = 745$ g. The gradient of 8.4 mbar corresponds to $8.4 \cdot 745 = 6258$ mg m^{-3} of H_2O. There is a gradient of 200 mg m^{-3} of CO_2 across the same pores, so that the gradient ratio is $6258/200 = 31.3$. Because water vapour diffuses 1.6 times faster than CO_2 the transpiration-assimilation ratio in this example is $31.3 \cdot 1.6 = 50$. To compare it to experimental transpiration ratio's it must still be divided by 30/44 for conversion to glucose and divided by 0.7 to allow for growth respiration. We then arrive at almost 100 kilograms of water per kilogram of dry matter as a minimal water requirement.

Exercise 42

The change in DVR with temperature is non-linear and is larger between 20 and 25 °C than between 15 and 20 °C (the increase is 0.0086 d^{-1} and 0.0057 d^{-1}, respectively), so that the fluctuating temperature is effectively higher than its average value.

Exercise 43

a. Change the TIMER statement and FUNCTION DVRDTB into:

    TIMER TIME = (147., 300.)
    FUNCTION DVRDTB = 10., 0.575, 17., 0.575

Results are:

day of sowing	147		300	
type of crop	sensitive	insensitive	sensitive	insensitive
day of maturity	267	263	25	41
WSO (kg ha^{-1})	5602	5439	3805	4478
yield change		-163		$+673$

b. The functions DVRTTB and DVRRTB have to be changed into:

    FUNCTION DVRTTB = 9.,.63,14.,.83,19.,.92,24.,.96,29.,.98,34.,.99
    FUNCTION DVRRTB = 9.,.08,14.,.38,19.,.575,24.,.71,29.,.80,34.,.865

Result: WSO is 3804 kg ha^{-1}, when the crop was sown at Day 300., and 5534 kg ha^{-1} when sown at Day 147. In both cases the yield remains almost unaffected.

Exercise 44

The following changes have to be made in SUCROS:

    WLV   = RWLVI + WLV1 + WLV2 + WLV3 + WLV4 + WLV5
    RWLVI = INTGRL(WLVI, −DLVI)
    WLV1   = INTGRL (0., GLV1−DLV1)
    WLV2   = INTGRL (0., GLV2−DLV2)
    .
    .
    .
    DVLI   = WLVI*RDR
    DLV1   = WVL1*RDR
    .
    .
    .
    GLV1   = INSW(TIME−310.1,INSW(TIME−300.,0.,GLV),0.)

281

GLV2   = INSW(TIME − 320.1,INSW(TIME − 310.1,0.,GLV),0.)
GLV3   = INSW(TIME − 330.1, INSW(TIME − 320.1,0.,GLV),0.)

.

.

.

RWLVI is the remainder of the initial leaf mass; WLV1 is the first age class (leaves formed between Day 300 and 311), WLV2 is the second age class (leaves formed between Day 311 and 321), etc. The small value of 0.1 has been added to the values of time at which the INSW function changes argument to ensure that the growth rate at times 310, 320, etc., is included in the appropriate growth rates. Results are:

Leaf class	Weight at anthesis (Day 358)	Weight at maturity (Day 25)
WLVI	25.000	1.25
WLV1	55.872	21.607
WLV2	161.77	62.561
WLV3	627.80	242.78
WLV4	810.47	313.43
WLV5	281.81	108.98

If only one INSW function is used, it is impossible to program both the start and the end of the growth of an age class. If only the start of an age class is programmed, the first age class contains all the biomass formed, the second age class the biomass formed since Day 311, etc.

Exercise 45

Leaves die after one unit of DVS (or more precisely, 0.98 units in average), so that 25 classes of 0.04 units of DVS contain all live leaves. The program SUCROS (Table 9, Section 3.1) and the BOXCAR (Table 13, Section 3.3) can be combined. Remove Lines 101 and 112-115 from SUCROS and replace Line 301 by

DVS = INTGRL (0., DVR)
DVR = INSW(DVS − 1.,DVRV,DVRR)

Figure 30 (Section 3.3) shows that the Classes 1-10 are empty at DVS = 1.25 because no new leaves have been formed since DVS = 0.85 (see Figure 33a, Section 3.3).

Exercise 46

If the relation of growth rate and reserve level used in the model is too low, the sequence of events is: Proper reserve level → underestimated growth rate → accumulation of reserves → overestimated reserve level → proper growth rate.

Exercise 47

By multiplying the factors, one assumes (implicitly) that they influence different aspects of the process and that their effects are independent. The limiting factor approach implies that a certain minimum ratio must exist between growth factors, as is the case for absorption of nutrients. Subsection 5.1.5 will provide an example of this. See also Subsection 5.2.2.

282

Both possibilities can be distinguished experimentally by measuring the growth rate for structural biomass (see for example Penning de Vries et al., 1979) at 20 and 30 °C, with and without a − 20 bar water stress. Such experiments have not been done yet.

Exercise 48
Results are:

	Leaves	Stems	Roots	Wheat grains
CVF	0.7213	0.6859	0.7213	0.7350
CPF	0.3281	0.3205	0.3147	0.2598

Exercise 49
A carbon balance out of equilibrium proves that one or more things are incorrect. A carbon balance in equilibrium is a strong indication that the assumptions, calculations and programming of its processes are consistent. When, for instance, the CVF value for leaves is, incorrectly, given as 0.62, or when the growth respiration of the roots is neglected, the C balance is no longer in equilibrium. However, when all of the maintenance processes are ignored, the C balance remains correct but the model is wrong. A carbon balance for the model SUCROS consists of the weight of C in total plant material (WCTP), on one hand, and of the C in the net CO_2 assimilation (WC) on the other. Both values must be equal:

```
WCTP = WCL + WCS + WCR + WCO
WCL  = (WLVT − WLVI)*FCL
WCS  = WST*FCS
WCO  = WSO*FCO
WCR  = (WRT − WRTI)*FCR
PARAM FCL = 0.464998, FCS = 0.495746, FCR = 0.468722, FCO = 0.473328
```

FCL, FCS, FCR and FCO are the fractions of C in the weight of the leaves, stems, roots and storage organs, respectively. They are calculated from the composition of the organs given in Exercise 48 and the C content of the various components given in the text. Note that WLVI and WRTI did not grow during the simulation period!

```
WC   = 12./30.*(AA−BB)−12./44.*CC
AA   = INTGRL(0.,GPHOT)
BB   = INTGRL(0.,MAINT)
CC   = INTGRL(0.,GTW*CPF)
RDPF = ABS((WCTP−WC)/(NOT(WCTP)+WCTP))
* ABS TAKES THE ABSOLUTE VALUE OF ITS ARGUMENT
FINISH RDPF = 0.01
CPF  = (FLV*CPFL+FST*CPFST+FSO*CPFSO)*FSH+...
       (1.−FSH)*CPFR
PARAM CPFL = 0.328, CPFST = 0.321, CPFSO = 0.260, CPFR = 0.315
```

CPFL, etc., stand for the CO_2 production factors for leaves, stems, roots and storage organs, respectively. They are calculated with the equation given in the text and the data of Exercise 48.

Exercise 50

Add:

GLMAIN = INTGRL(0., MAINT)
PARAM Q10 = (1.75, 2., 2.5)

Results of the standard program with different Q_{10} values are:

Q_{10}	WSO	GLMAIN
1.75	3756	5591
2	3805	5506
2.5	3886	5366

To change the coefficients for organs, change Line 235 in

MAINTS = WLV*ML + WST*MS + WSO*MO + WRT*MR

and choose different values for the parameters ML, MS, MO and MR. These can be put in reruns. The model appears to be moderately sensitive for alternative assumptions about this process:

ML	MS	MO	MR	WSO	GLMAIN
0.03	0.015	0.01	0.01 (standard)	3805	5506
0.04	0.02	0.015	0.015	2924	6536
0.04	0.015	0.01	0.01	3572	5446
0.03	0.02	0.015	0.015	3464	5879
0.03	0.015	0.015	0.01	3721	5411
0.03	0.015	0.01	0.015	3658	5615
0.025	0.015	0.01	0.01	4112	4925
0.03	0.01*	0.01	0.01	3927	5129

Exercise 51

GGR1 = GDW*GGRC*TFGG
PARAM GGRC = 0.3
TFGG = Q10* *(TEMP/10. - 1.6)
PARAM Q10 = 2.0

where GGR1 is grain growth rate during the lag period ($g \, m^{-2} d^{-1}$), GDW is grain dry weight ($g \, m^{-2}$), GGRC is grain growth rate constant ($g \, g^{-1} \, d^{-1}$), TFGG is temperature factor grain growth (−) and TEMP is mean daily temperature (°C).

Exercise 52

GGR = AMIN1(GGR1,GGR2)

or

GGR = INSW(GGR1 - GGR2,GGR1,GGR2)

GGR is grain growth rate at any time during grain filling ($g \, m^{-2} \, d^{-1}$), GGR1 is grain

growth rate during the lag period (exponential) and GGR2 is grain growth rate during rest of the grain filling period (constant at fixed temperature and adequate carbohydrate supply).

```
GGR1              see Exercise 51.

GGR2       = 25 * TFGG2
TFGG2      = Q102* *(TEMP/10. - 1.6)
PARAM Q102 = 1.5
GDW        = INTGRL(7.5, GGR)
PARAM TEMP = (16.,25.)
METHOD RKSFX
PRINT GDW,GGR,GGR1,GGR2
TIMER FINTIM = 20., DELT = 1., PRDEL = 1.
END
```

Results are:

TEMP = 16., GGR = GGR1 until TIME = 9; GGR = GGR2 from TIME = 9 onwards (= 25.00)

TEMP = 25., GGR = GGR1 until TIME = 4; GGR = GGR2 from TIME = 4 onwards (= 36.01)

Hence, an earlier transition from lag to linear stage with higher temperature. Furthermore: the growth rate is much larger with a higher temperature!

Exercise 53

a. Some results are:

	GPHOTS	30.	25.	30.
Input				
	FNS	0.010	0.010	0.015
GDW (g m^{-2})		507.	452.	694.
NG (g m^{-2})		11.32	11.26	14.43
NHI (g g^{-1})		0.78	0.77	0.82
DHI (g g^{-1})		0.44	0.41	0.52

Reductions due to low availability of nitrogen or carbohydrates occur in the following periods:

Input	Affected process	Affected by N availability (AN)	Affected by C availability (ACH)
GPHOTS = 30.0	rate of photosynthesis	Day 23 →	Day 1-13
FNS = 0.010	growth rate	Day 25-31	Day 32 →
GPHOTS = 25.0	rate of photosynthesis	Day 23 →	—
FNS = 0.010	growth rate	—	Day 24 →
GPHOTS = 30.0	rate of photosynthesis	Day 40 →	Day 1-13
FNS = 0.015	growth rate	Day 42-46	Day 47 →

b. According to the calculation of RED, 0-2 times the standard concentration of protein of 125 mg g^{-1} or in N: 0-42.5 mg g^{-1}.

Exercise 54

a. Next to the statements given in the text, the following additions to SUCROS are necessary:

```
EARN   = INTGRL(0., REARI)
CHAVG  = (GST+GLV)/CVF
CHAGG  = GSO/CVF
DVR    = INSW(DVS-1.,DVRV,DVRR)
```

Furthermore, the rates, defined in the text, have to be multiplied by appropriate INSW functions:

```
RTF with INSW(DVS-0.425,1.,0.)
REARI and RSPLF with: INSW(DVS-0.425,INSW(DVS-0.35,0.,1.),0.)
and RFGF with INSW(DVS-1.05, INSW(DVS-1.,0.,1.),0.)
CHFPE  = CHAVG/(EARN+NOT(EARN))
CHFPSP = CHAGG/(SPNR+NOT(SPNR))
GN     = FGNR/(SPNR+NOT(SPNR))
```

The NOT statement is used to prevent division by zero, see Table 2, Section 2.2.
RTF = AMAX1(0.,(MXNT−ANT)/TCTF*INSW(....)), to prevent the dying off of tillers at the start of the season.
Some results are

```
ANT    = 8.77E+06 tiller ha⁻¹
EARN   = 4.85E+06 ear ha⁻¹
SP     = 1.60       spikelet ear⁻¹
GN     = 0.94       grain spikelet⁻¹
FGNR   = 7.27E+06 grain ha⁻¹
```

b. Replace Line 222 by

PARAM FOV = (0.2,0.8), FOV = INSW(DVS−1.,0.2,0.8) or
FOV = INSW(DVS−1.,0.8,0.2)

Results are:

FOV	0.2	0.8	0.2/0.8	0.8/0.2	
WSO	4580	2161	2646	3186	kg ha⁻¹
ANT	1.02E+07	4.69E+06	1.02E+07	4.69E+06	tiller ha⁻¹
FGNR	8.46E+06	4.24E+06	6.58E+06	5.37E+06	grain ha⁻¹

c. Change the definition of GGR into:
GGR = AMIN1(GGR1, PGR, GRC, GRN)
Some results with GPHOTS = 30., and FNL = 0.010 and 0.015 are GDW = 530 and 707 kg ha^{-1} and NG = 11.32 and 14.63 kg ha^{-1}, respectively. The transition from exponential to linear growth takes place between Day 6 and 7.

Exercise 55

FUNCTION RAINTB = 300., 0., 301.99,0., 302., 15.E4, 302.99, 15.E4, ...
303.,0.,315.99,0., 316., 15.E4, 316.99, 15.E4, 317., 0., etc.

Results are WSO is 1619 kg ha^{-1} and SWAT is 9.62E4 kg ha^{-1} at maturity.

Exercise 56

FUNCTION RAINTB = 300.,0.,306.99,0.,307.,3.57E4,313.99,3.57E4,...
314.,0.,320.99,0.,321.,3.57E4,327.99,3.57E4,328.,0., etc.

Results are WSO is 1819 kg ha^{-1} and SWAT 9.66E4 kg ha^{-1}. Note that the plants don't die in this simple example from stress and that soil evaporation is not considered.

Exercise 57

RARDEF = INSW(RTRDEF−0.4,0.,RTRDEF/10.)
CTRD   = INTGRL(0.,RARDEF−RDRDEF)
CTRDEF = LIMIT(0., 1., CTRD) or: CTRDEF = AMAX1(1., CTRD)

Here the rate of increase of the relative transpiration deficit is not dependent on the cumulative relative transpiration deficit as in the original formulation. Only in the original formulation does biomass remain capable of a little photosynthesis, even after a prolonged stress period. This can be interpreted as an increasing stress resistance or stress tolerance of the remaining plant organs, or, alternatively, as a heterogeneity of the field where some plants have more water available than others.

Exercise 58

a.

		RRNOFF		
P =	12 mm	= 12•0.30•0.64 =	2.30 mm
P =	21 mm	= 21•0.30•1.23 =	7.75 mm
P =	8 mm	= 8•0.30•0.38 =	0.91 mm
P =	53 mm	= 53•0.30•1.64 =	26.08 mm
P =	18 mm	= 18•0.30•1.06 =	5.72 mm

Total rain   112 mm   Total runoff   42.76 mm

b. Average runoff percentage = 100•42.76/112 = 38%
c. Since the runoff is strongly influenced by the factor ROFINT, the shower of 53 mm contributes heavily in the total runoff.

Exercise 59

Layer 1 (0.25 − 0.10)•20 = 3.00 mm
Layer 2 (0.25 − 0.18)•30 = 2.10 mm
Layer 3 (0.25 − 0.12)•40 = 5.20 mm
Layer 4 (0.25 − 0.24)•50 = 0.50 mm

Total   10.80 mm

Exercise 60

Initial situation is the final situation of Example 3, thus:

$\theta1$ = 0.10 − 0.05 = 0.05
$\theta2$ = 0.18 − 0.08 = 0.10
$\theta3$ = 0.12 − 0.03 = 0.09
$\theta4$ = 0.24 − 0.03 = 0.21

VAR1 = (0.05 − 0.02)•exp (−15.0•0.010) = 0.026
VAR2 = (0.10 − 0.02)•exp (−15.0•0.035) = 0.047
VAR3 = (0.09 − 0.02)•exp (−15.0•0.070) = 0.024
VAR4 = (0.21 − 0.02)•exp (−15.0•0.115) = 0.034

SUM1 = 0.026•0.02 = 0.00052
SUM2 = 0.00052 + 0.047•0.03 = 0.00193
SUM3 = 0.00193 + 0.024•0.04 = 0.00289
SUM4 = 0.00289 + 0.034•0.05 = 0.00459

F1 = 0.02•0.026/0.00459 = 0.113
F2 = 0.03•0.047/0.00459 = 0.307
F3 = 0.04•0.024/0.00459 = 0.209
F4 = 0.05•0.034/0.00459 = 0.370

ER1 = 0.113•4.0 = 0.45 mm d^{-1} ($\Delta\theta$ = −0.02)
ER2 = 0.307•4.0 = 1.23 mm d^{-1} ($\Delta\theta$ = −0.04)
ER3 = 0.209•4.0 = 0.84 mm d^{-1} ($\Delta\theta$ = −0.02)
ER4 = 0.370•4.0 = 1.48 mm d^{-1} ($\Delta\theta$ = −0.03)

                         4.00 mm

Exercise 61

$\theta 1$ = 0.29
$\theta 2$ = 0.67
$\theta 3$ = 0.38
$\theta 4$ = (0.24 − 0.04)/(0.25 − 0.04) = 0.95

EDPTF1 = 0.80	TEC1 = 0.30	WRED1 = 0.70
EDPTF2 = 1.00	TEC2 = 0.75	WRED2 = 1.00
EDPTF3 = 0.90	TEC3 = 0.94	WRED3 = 0.85
EDPTF4 = 1.00	TEC4 = 1.00	WRED4 = 1.00

ERLB1 = 0.02•0.80 = 0.016
ERLB2 = 0.016 + (0.03•1.00) = 0.046
ERLB3 = 0.046 + (0.04•0.90) = 0.082
ERLB4 = 0.082 + (0.05•1.00) = 0.132

TRPMM = PTRANS/ERLB4 = 2.5/0.132 = 18.94 mm m^{-1} d^{-1}

TRR1 = 18.94•0.02•0.80•0.30•0.70 = 0.06 mm d^{-1}
TRR2 = 18.94•0.03•1.00•0.75•1.00 = 0.43 mm d^{-1}
TRR3 = 18.94•0.04•0.90•0.94•0.85 = 0.54 mm d^{-1}
TRR4 = 18.94•0.05•1.00•1.00•1.00 = 0.95 mm d^{-1}

                            1.98 mm d^{-1}

TRAN = TRB4 = 1.98 mm d^{-1}

Exercise 62
The hyperbolic model

$$V = -\frac{ds}{dt} = V_{max} \cdot \frac{S}{K_s + S} \qquad (106)$$

can be simplified for two cases:

$S >>> K_s$ in this case Equation 106 can be reformulated

$$-\frac{ds}{dt} = V_{max} \qquad (107)$$

In (soil)biological terms, this means that in presence of large quantities of substrate (S) the biological potential (micro-organisms + enzymes) is the limiting factor in the transformation process. This is a rather rare situation in soil systems. With respect to the terrestrial N cycle, nitrification might follow zeroth-order rate kinetics at high NH_4^+ and NO_3^- concentrations. Also the denitrification rate has been found to be independent on the NO_3^- concentration over a NO_3^- concentration range that is common in many arable soils.

$S <<< K_s$ if, in this case, S is neglected in the denominator Equation 106 can be reduced to:

$$-\frac{ds}{dt} = k_1 S \qquad (108)$$

Such first order models on soil nitrogen transformation processes incorporate several assumptions: (a) the biological potential to transform a certain substrate is not limiting; (b) the substrate pool is initially kinetically homogeneous and remains so; (c) additions of N, if they occur, are proportional to the amount present; (d) there is no upper or lower limit to the quantity of the substrate.

If environmental influences and density dependent effects are ignored, assumption (a) may often be valid. Assumption (b) has been proved to be wrong for soil organic matter by tracer and C-dating studies. Assumption (c) is invalid in highly managed systems, but may hold for accumulation in virgin systems through feedback effects on plant growth, or in cultivated systems when a constant proportion of the plant growth is returned each year and productivity is strongly controlled by soil organic-matter content.

Exercise 63

The program is given in Figure 92. The inorganic N concentration (NIT) is sensitive to the value of EFFP, but the microbial biomass content (BIOM) is sensitive to the value of EFFL. Some values of NIT obtained with this program are:

EFFL	EFFP	
	0.4	0.6
0.05	91.0	72.0
0.10	89.7	72.5
0.20	89.0	73.1

and some results of BIOM are:

EFFL •	EFFP	
	0.4	0.6
0.05	65.5	63.4
0.10	89.0	89.0
0.20	101.0	101.7

Exercise 64

The results are given in Figure 93, which is similar to Figure 79, Section 5.3 and Quadrant b of Figure 65, Section 5.1.

Exercise 65

a. At $t = 0$, we have the initial amount GI, thus:

$$GI = \frac{GM}{1 + K \cdot e^{-RGR \cdot t}} = \frac{GM}{1 + K}$$

so that

$$K = \frac{GM - GI}{GI}$$

```
TITLE DECOMPOSITION AND RELATED GROWTH OF MICROBIAL BIOMASS
MACRO DBX,DCX,GBIOMX=DECC(CX,CT,BIOM,GRMAX,KCX,EFFX,KBX)

        BIOMX=CX/CT*BIOM
        GBIOMX=GRMAX*BIOMX*CX/(KCX+CX)
        CO2X=GBIOMX*(1-EFFX)/EFFX
        DBIOMX=KBX*BIOMX
        DBX=GBIOMX-DBIOMX
        DCX=-(GBIOMX+CO2X)
ENDMAC

PARAM KCP=50., GRMAP=0.5
PARAM EFFP=0.6,KBP=0.3
PARAM KCL=200., GRMAL=0.05
PARAM EFFL=0.1,KBL=0.02
PARAM CN=3., CNB=8.
INCON ICP=100., ICL=400.
INCON IBIOM=100., INIT=100.
        BIOM=INTGRL(IBIOM,DBT)
        CP=INTGRL(ICP,DCP)
        CL=INTGRL(ICL,DCL)
        CT=CP+CL
        DBP,DCP,GBIOMP=DECC(CP,CT,BIOM,GRMAP,KCP,EFFP,KBP)
        DBL,DCL,GBIOML=DECC(CL,CT,BIOM,GRMAL,KCL,EFFL,KBL)
        DBT=DBP+DBL
        RCP=CP/ICP*100.
        RCL=CL/ICL*100.
        NIT=INTGRL(INIT,(-DCP/CN)-(GBIOMP+GBIOML/CNB))
TIMER FINTIM=15., OUTDEL=1., DELT=0.1
METHOD RKSFX
OUTPUT NIT,RCP,RCL,BIOM
END
STOP
ENDJOB
```

Figure 92. Listing of a CSMP program to simulate the decomposition of organic matter and the related growth of the microbial biomass.
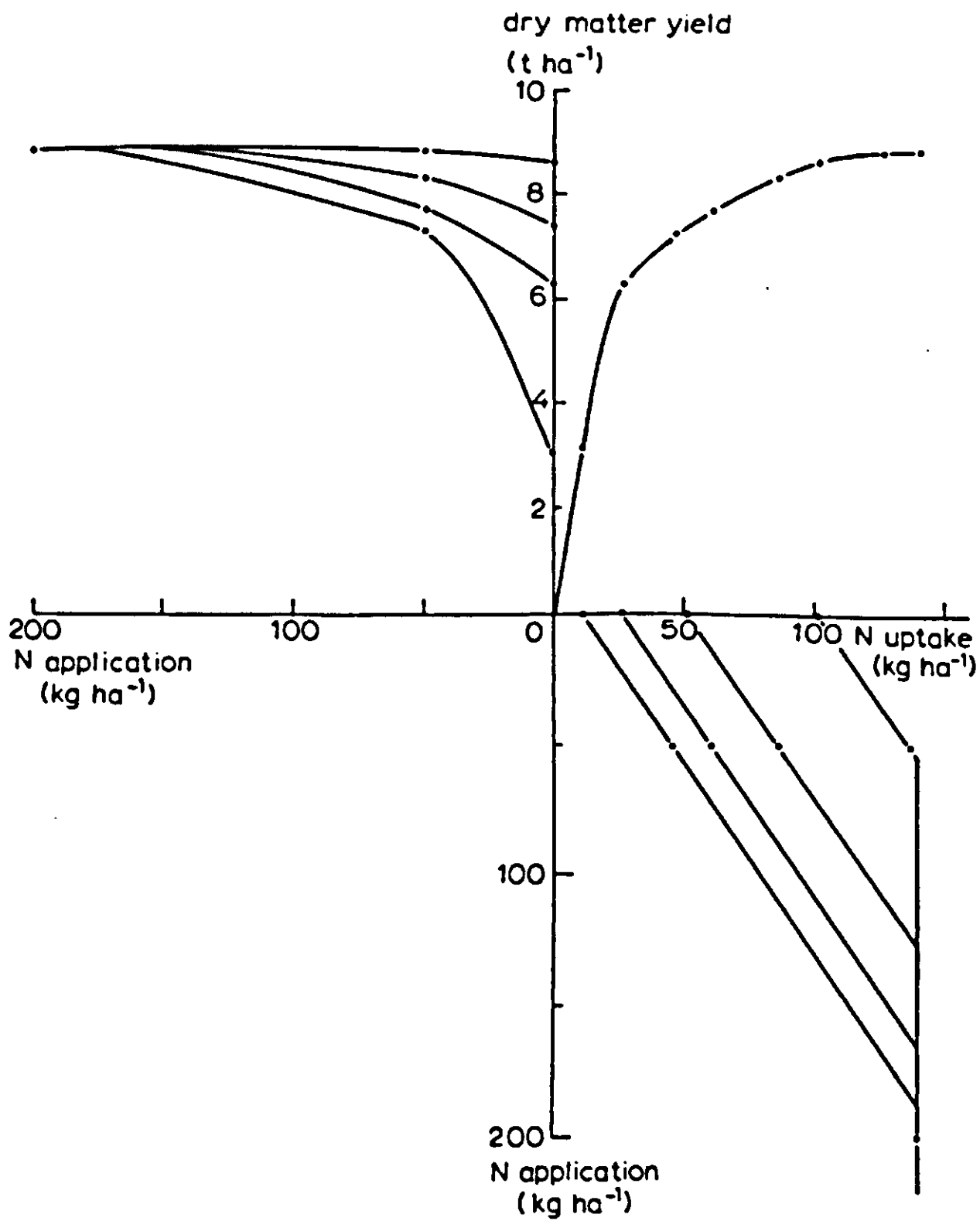
Figure 93. The simulated relations of N application, N uptake and dry matter yield for four different values of N available in the unfertilized soil.

and this ratio expresses the potential relative increase of the population.
b. Differentiation of Equation 103 is as follows:

$$\frac{dG}{dt} = \frac{-GM}{(1 + K \cdot e^{-RGR \cdot t})^2} * (-K \cdot RGR \cdot e^{-RGR \cdot t})$$

Since $G = \dfrac{GM}{1 + K \cdot e^{-RGR \cdot t}}$

this can be rewritten as:

$$\frac{dG}{dt} = G \cdot \frac{K \cdot RGR \cdot e^{-RGR \cdot t}}{1 + K \cdot e^{-RGR \cdot t}}$$

in this formula

$$\frac{K \cdot RGR \cdot e^{-RGR \cdot t}}{1 + K \cdot e^{-RGR \cdot t}} \text{ equals } (1 - \frac{1}{1 + K \cdot e^{-RGR \cdot t}}) \cdot RGR$$

so that

$$\frac{dG}{dt} = G \cdot RGR \cdot (1 - \frac{1}{1 + K \cdot e^{-RGR \cdot t}})$$

and as

$$\frac{GM}{G} = 1 + K \cdot e^{-RGR \cdot t}$$

this gives:

$$\frac{dG}{dt} = G \cdot RGR \cdot (1 - \frac{G}{GM})$$

Exercise 66

a. When the duration of the latent period p approaches zero and of the infectious period i reaches infinity, Equation 104 transforms in:

$$\frac{dN_t}{dt} = R(N_t - 0)(1 - \frac{N_t}{N_m})$$

so that the logistic growth formula is again appropriate.

b. The maximum number of lesions amounts to $20 \cdot 10^{10}$.

Exercise 67

Replace p by q.

Exercise 68

At time t, the number of latent (LAT), infectious (INF) and removed lesions (REM) equal, respectively:

LAT $= N_{t+p} - N_t$
INF $= N_t - N_{t-i}$
REM $= N_{t-i}$

Exercise 69

The relative large effect of a change in the latent period is due to its polycyclic effect. A decrease in the length of the latent period gives a faster repetition of new cycles of infectious periods and thus a multiplicative effect, which is relatively more important than changes in the length of the infectious period.

Exercise 70

See Figure 94.

```
TITLE LEMA CYANELLA POPULATIONS
INCON IEGG=0.,ILARV=0.,IPUP=0.,IADUL=100.
        EGG=INTGRL(IEGG,REPR-EGG*PUSE)
        LARV=INTGRL(ILARV,EGG*PUSE-LARV*PUSL)
        PUP=INTGRL(IPUP,LARV*PUSL-PUP*PUSP)
        ADUL=INTGRL(IADUL,PUP*PUSP-ADUL*PUSA)
*  NUMBER OF ORGANISMS PER HA IN EACH OF 4 DEVELOPMENT PHASES
*  ORGANISMS GO INTO THE NEXT PHASE WHEN THE DEVELOPMENT STAGE REACHES 1
        TOTAL=ADUL+PUP+LARV

        PUSE=INSW(DSE-1.,0.,1./DELT)
        PUSL=INSW(DSL-1.,0.,1./DELT)
        PUSP=INSW(DSP-1.,0.,1./DELT)
        PUSA=INSW(DSA-1.,0.,1./DELT)

        DSE=INTGRL(0.,1./RESE-DSE*PUSE)
        DSL=INTGRL(0.,1./RESL-DSL*PUSL)
        DSP=INTGRL(0.,1./RESP-DSP*PUSP)
        DSA=INTGRL(0.,1./RESA-DSA*PUSA)
*  DEVELPMENT STAGE OF EACH OF THE 4 LIFE FORMS
PARAM RESE=5., RESL=10., RESP=4., RESA=20.
        REPR=SR*ADUL*FERT
PARAM FERT=3., SR=0.5
METHOD RECT
PRINT EGG, LARV,PUP,ADUL,TOTAL
OUTPUT TOTAL
TIMER FINTIM=50., DELT=.25, OUTDEL=2., PRDEL=2.
END
STOP
ENDJOB
```

Figure 94. Listing of a CSMP program to simulate the population growth of the cereal leaf beetle *(Lema cyanella)*.

Exercise 71

Combine the program of Figure 94 with SUCROS and introduce the following changed statements for the connection of the population model and the crop model:

WLV   = INTGRL(WLVI, GLV − DLV − LARV * 1.5E − 3)
ADUL = INTGRL(0.,PUSH * IADUL/DELT + PUP * PUSP − ADUL * PUSA)
PUSH = IMPULS(350., 1000.)

Some results of this combination model are presented in Figure 83 of Section 6.1. IADUL amounts to 50., 100., 200. and 500., respectively. The density of the various development stages of the beetle (number per hectare) on the last day that there are still green leaves available are

	IADUL			
	50	100	200	500
DAY	388	388	384	378
EGG	251062	502124	0	332280
LARV	19170	38340	76680	108180
PUP	0	0	176184	0
ADUL	44046	88092	0	42600

Exercise 72

The fungus population dynamics can be simulated with:

LESI	= AMIN1 (LESIM,INTGRL(0.,RLESI + ILESI * PUSI/DELT))
PUSI	= IMPULS (350., 1000.)
RLESI	= R * LESII * (1. − LESI/LESIM)
LESII	= LESIP − LESIF
LESIM	= LAI * 1.E11
LESIP	= DELAY (10, P, LESI)
LESIF	= DELAY (10, IP, LESI)
PARAM P	= 6., I = 4., ILESI = (1.E9, 1.E10, 2.E10, 5.E10), R = 0.3
IP	= I + P

RLESI is the rate of increase of the number of lesions, LESI. It is calculated with the quantity of lesions that are infectious, thus the number of lesions at time t-p minus that at time t-p-i, i.e. LESIP and LESIF, respectively. The maximum number of lesions is calculated from the LAI and the maximum number per LAI of 1. To define an upper limit for LESI the AMIN1 function is introduced.

The coupling of this simple population dynamical model to SUCROS is achieved by way of the following statements:

LAIC	= LESI/1.E11
GPHOTR	= GPHOT * (1. − LAIC/LAI)

GPHOTR is to be used in Line 106 to calculate GTW. Some results of this combination model and the one of Exercise 73 are given in Figure 84, Section 6.1

Exercise 73

The assumption that a disease affects the photosynthesis of the canopy from the bottom leaves upwards or from the top leaves downwards can be programmed easily with SUCROS. In both cases, the computation of canopy photosynthesis is to be repeated twice: once for the full leaf area index, and once for the leaf area index of the upper part of the canopy (unaffected in the first case, affected in the second). The difference between both rates of photosynthesis, the contribution of the lower leaves, is what is lost in the first case, and is all that is left in the second. Of course this is valid for the gross photosynthesis only.

The first case can be more simplified by computing the photosynthesis of the upper, unaffected leaves only. For instance by:

TLAI	= WLV * SLFA
LAI	= TLAI * (1. − LESI/TLAI * 1.E11)

In that case:

LESIM = TLAI * 1.E11

Some results of this version of the combination model are presented in Figure 84, Section 6.1

294

8 REFERENCES

Aase, J.K., 1978. Relationship between leaf area and dry matter in winter wheat. Agron. J. 70: 563-565.

Addescott, T.M., 1981. Leaching of nitrate in structured soils. In: Simulation of nitrogen behaviour of soil-plant systems. Eds. M.J. Frissel & J.A. van Veen. Pudoc, Wageningen, 245-253.

Angus, J.F., D.H. Mackenzie, R. Morton & C.A. Schafer, 1981. Phasic development in field crops. II. Thermal and photoperiodic responses of spring wheat. Field Crops Res., 4, 269-283.

Arkin, G.F., C.L. Wiegand & H. Huddleston, 1979. The future role of a crop model in large area yield estimating. Proc. Crop Model Workshop, Columbia, MO, Oct. 3-5, 1977, U.S. Dept. of Commerce, NOAA, Environmental Data and Information Service.

Arya, L.M., 1973. Water flow in soil in presence of soybean root sinks. Thesis Univ. of Minnesota, Minneapolis Bull. 60, 163 pp.

Baker, C.H. & R.B. Curry, 1976. Structure of agricultural simulations: a philosophic view. Agric. Systems, 1, 201-218.

Beek, J., 1979. Phosphate retention by soil in relation to waste disposal. Ph.D. thesis, Agricultural University, Wageningen, 162 pp.

Beek, J. & M.J. Frissel, 1973. Simulation of nitrogen behaviour in soils. Simulation Monographs. Pudoc, Wageningen, 76 pp.

Belmans, C., J.G. Wesseling & R.A. Feddes, 1981. Simulation model of the water balance of a cropped soil providing different types of boundary conditions (SWATRE). Nota ICW 1257, Wageningen, 61 pp.

Bierhuizen, J.F. & R.O. Slatyer, 1965. Effect of atmospheric concentration of water vapour and CO_2 in determining transpiration - photosynthesis relationships of cotton leaves. Agric. Meteor. 2: 259-270.

Björkman, O., H.A. Mooney & J. Ehleringer, 1975. Photosynthetic responses of plants from habitats with contrasting thermal environments. Carnegie Institution Year Book 1975, 743-759.

Breman, H., A.M. Cisse, M.A. Djiteye & W.Th. Elberse, 1979. Pasture dynamics and forage availability in the Sahel. Israel J. of Bot. Vol(28): 227-251.

Briggs, L.J. & H.L. Shantz, 1913. The water requirements of plants. I. Investigations in the Great Plains in 1910 and 1911. U.S. Dept. Agr. Bur. of Plant Ind. Bull. 284.

Brockington, N.R., 1979. Computer modelling in agriculture. Oxford Univ. Press, Oxford, 154 pp.

Brocklehurst, P.A., 1979. Control of grain morphogenesis in wheat and its relation to grain yield. In: Crop Physiology and cereal breeding. Eds. J.H.J. Spiertz & Th. Kramer. Proc. EUCARPIA - workshop, 1978, Pudoc, Wageningen, 41-44.

Brouwer, R., 1963. Some aspects of the equilibrium between overground and underground plant parts. Jaarboek Instituut voor Biologisch en Scheikundig onderzoek (IBS), 31-39.

Brouwer, R. & C.T. de Wit, 1968. A simulation model of plant growth with special attention to root growth and its consequences. Proc. 15th Easter School Agric. Sci., Univ.

of Nottingham, 224-242.

Burns, I.G., 1974. A model for predicting the redistribution of salt, applied to fallow soils after excess rainfall or evaporation. J. Soil Sci. 25: 165-178.

Bykov, O.D., V.A. Koshkin & J. Čatský, 1981. Carbon dioxide compensation concentration of C_3 and C_4 plants: dependence on temperature. Photosynthetica 15(1): 114-121.

Challa, H., 1976. An analysis of the diurnal course of growth, carbon dioxide exchange and carbohydrate reserve content of cucumber. Agric. Res. Rep. 861, Pudoc, Wageningen, 88 pp.

Cole, C.V., G.S. Innis & J.W.B. Steward, 1977. Simulation of phosphorus cycling in semi arid grasslands. Ecology, 58, 1-15.

Dayan, E., H. van Keulen & A. Dovrat, 1981. Tiller dynamics and growth of Rhodes grass after defoliation: a model named TILDYN. Agro - ecosystems (7) 2: 101-112.

Dijkshoorn, W. & J.E.M. Lampe, 1980. A plant test for sufficiency of phosphorus based on the phosphorus - nitrogen interaction in sunflower nutrition. Neth. J. Agric. Sci. 28, 135-146.

Doss, B.D., D.A. Ashley, O.L. Bennett, R.M. Patterson & L.E. Ensminger, 1964. Yield, nitrogen content and water use of Sart Sorghum. Agron. J. 56: 589-592.

Downton, W.J.S., 1975. The occurrence of C_4 photosynthesis among plants. Photosynthetica 9, 96-105.

Egmond, F. van, 1975. The ionic balance of the sugar-beet plant. Agric. Res. Rep. 832, Pudoc, Wageningen, 70 pp.

English, S.D. 1976. Light interception, photosynthesis and development of sunflower. Ph.D. thesis, Univ. of New England, Armidale, N.S.W. Australia.

Ennik, G.C., M. Gillet & L. Sibma, 1980. Effect of high nitrogen supply on sward deterioration and root mass. In: The role of nitrogen in intensive grassland production. Eds. W.H. Prins & G.H. Arnold. Proc. Int. Symp. Eur. Grassl. Fed., Wageningen, 67-76.

Farquhar, G.D., E.-D. Schulze & M. Kuppers, 1980. Responses to humidity by stomata of Nicotiana glauca L. and Corylus avellana L. are consistent with the optimization of carbon dioxide uptake with respect to water loss. Austr. J. Plant Physiol., 7, 315-327.

Feddes, R.A., P.J. Kowalik & H. Zaradny, 1978. Simulation of field water use and crop yield. Simulation Monographs. Pudoc, Wageningen, 189 pp.

Ferrari, Th.J., 1978. Elements of systems-dynamics simulation. Pudoc, Wageningen, 86 pp.

Fisher, R.A., 1982. Wheat. Proc. Symp. 'Potential productivity of field crops under different environments', IRRI, Los Banos, Philippines (in press).

Freney, J.R., J.R. Simpson & O.T. Denmead, 1981. Ammonia volatilization. In: Terrestrial nitrogen cycles. Eds. F.E. Clark & T. Rosswall. Ecol. Bull. 33: 291-302.

Fransz, H.G., 1974. The functional response to prey density in an acarine system. Simulation Monographs. Pudoc, Wageningen, 143 pp.

Frissel, M.J. & J.A. van Veen, 1978. Critique of computer simulation modelling for nitrogen in irrigated croplands. In: Nitrogen in the environment: Vol. 1. Nitrogen behaviour in field soils. Eds. D.R. Nielsen & J.G. MacDonald. New York - San Francisco - London: Academic Press, 145-162.

Frissel, M.J. & J.A. van Veen, 1980. Soil nitrogen transformations in relation to leaching. In: Soil nitrogen as fertilizer or pollutant. Proc. Research Coord. Meeting. IAEA/ FAO/GSF, Piracicaba, Brasil, 1978, 61-75.

Frissel, M.J. & J.A. van Veen (Eds.), 1981. Simulation of nitrogen behaviour of soil-

plant systems. Pudoc, Wageningen, 277 pp.

Forrester, J.W., 1961. Industrial Dynamics. Massachusetts Institute of Technology Press, Cambridge, Mass., U.S.A.

Gale, M.D., 1979. Genetic variation for hormonal activity and yield. In: Crop physiology and cereal breeding. Eds. J.H.J. Spiertz & Th. Kramer. Proc. EUCARPIA-workshop, 1978, Pudoc, Wageningen, 29-34.

Gallagher, N., 1979. Ear development: processes and prospects. In: Crop physiology and cereal breeding. Eds. J.H.J. Spiertz & Th. Kramer, Proc. EUCARPIA-workshop, 1978, Pudoc, Wageningen, 3-9.

Goudriaan, J., 1973. Dispersion in simulation models of population growth and salt movement in the soil. Neth. J. Agric. Sci. 21: 269-281.

Goudriaan, J., 1977. Crop micrometeorology: a simulation study. Simulation Monographs. Pudoc, Wageningen, 249 pp.

Goudriaan, J. & H.H. van Laar, 1978. Calculation of daily totals of the gross CO_2 assimilation of leaf canopies. Neth. J. Agric. Sci. 26: 373-382.

Goudriaan, J. & H.H. van Laar, 1978. Relations between leaf resistance, CO_2-concentration and CO_2-assimilation in maize, beans, lalang grass and sunflower. Photosynthetica 12 (3): 241-249.

Goudriaan, J. & H. van Keulen, 1979. The direct and indirect effects of nitrogen shortage on photosynthesis and transpiration in maize and sunflower. Neth. J. Agric. Sci. 27, 227-234.

Gutierrez, A.P., L.A. Falcan, W. Loew, P.A. Leipzig & R. van de Bosch, 1975. An analysis of cotton production in California: a model of Acala cotton and the effect of defoliators on its yield. Environmental Entomology, 4, 125-136.

Hagin, J. & A. Amberger, 1974. Contribution of fertilizers and manures to the N- and P-load of waters. A computer simulation. Final Rep. to the Deutsche Forschungs Gemeinschaft, Technion Haifa and Techn. Univ. München.

Hanks, R.J., A. Klute & E. Bresler, 1969a. A numeric method for estimating infiltration, redistribution, drainage and evaporation of water from soil. Water Resour. Res. 5: 1064-1069.

Hanks, R.J., H.R. Gardner & R.L. Florian, 1969b. Plant - growth - evapotranspiration relations for several crops in the Central Great Plains. Agron. J. 61: 30-34.

Haverkamp, R., M. Vauclin, J. Touma, P.J. Wieringa & G. Vachaud, 1977. A comparison of numerical simulation models for one-dimensional infiltration into layered soils. Soil Sci. Soc. Am. J. 41 (2): 285-294.

Hesketh, J.D., C.D. Elmore & J.W. Jones, 1980. Predicting flowering and subsequent leaf expansion. In: Predicting photosynthesis for ecosystem models. Eds. J.D. Hesketh & J.W. Jones. CRC Press Inc., Boca Raton, Florida, USA, Vol. 2, 123-131.

Hillel, D., 1977. Computer simulation of soil-water dynamics; a compendium of recent work. IDRC, Ottawa, 214 pp.

Hodges, T. & P.C. Doraiswany, 1979. Crop phenology literature review for corn, soybean, wheat, barley, sorghum, rice, cotton and sunflower. Lockheed Electronics Company, Inc., Houston, Texas, USA, Technical Report no.: LEC-13722, 90 pp.

Hoogland, J.C., C. Belmans & R.A. Feddes, 1981. Root water uptake model depending on soil water pressure head and maximum extraction rate. 3rd Int. Symp. on Water Supply and Irrig. in the open and under protect. cultiv. March 1-7, 1981, Wageningen.

Horie, T., C.T. de Wit, J. Goudriaan & J. Bensink, 1979. A formal template for the development of cucumber in its vegetative stage. I, II and III, Proc. Kon. Ned. Acad.

van Wet., Series C, 82(4), 433-479.

Hunt, H.W., 1977. A simulation model for decomposition in grassland. Ecology 58: 469-484.

IBM, 1975. Continuous System Modeling Program III (CSMP III), Program Reference Manual. IBM SH19-7001-3. Techn. Publ. Dept., White Plains, USA, 206 pp.

Innis, G.S., 1978. Grassland Simulation Model. Springer Verlag, New York.

Janssen, B.H., 1972. The significance of the fallow year in the dry farming system of the Great Konya Basin, Turkey, Neth. J. Agric. Sci. 20: 247-260.

Janssen, J.G.M., 1974. Simulation of germination of winter annuals in relation to microclimate and microdistribution. Oecologia (Berl.), 14, 197-228.

Jansson, S.L., 1958. Tracer studies on nitrogen transformations in soil with special attention to mineralization - immobilization relationships. Kungl. Lantbrukshogskolans Annaler 24: 101-361.

Jones, J.W. & J.D. Hesketh, 1980. Predicting leaf expansion. In: Predicting photosynthesis for ecosystem models. Eds. J.D. Hesketh & J.W. Jones. CRC Press Inc., Boca Raton, Florida, Vol. 2, 85-122.

Jonker, J.J., 1958. Root studies and subsoiling in the North-Eastern polder. Ph.D. thesis, Agric. Univ., Wageningen, Tjeenk Willink N.V., Zwolle, 164 pp. (Dutch, with English summary).

Kampmeijer, P. & J.C. Zadoks, 1977. EPIMUL, a simulator of foci and epidemics in mixtures, multilines and mosaics of resistant and susceptible plants. Simulation Monographs. Pudoc, Wageningen, 50 pp.

Keulen, H. van, 1975. Simulation of water use and herbage growth in arid regions. Simulation Monographs. Pudoc, Wageningen, 184 pp.

Keulen, H. van, 1976. A calculation method for potential rice production. Contr. Centr. Res. Inst. Bogor, No. 21: 26 pp.

Keulen, H. van, 1976. Evaluation of models. In: Critical evaluation of systems analysis in ecosystems research and management. Eds. G.W. Arnold & C.T. de Wit. Simulation Monographs. Pudoc, Wageningen, 22-29.

Keulen, H. van & C.G.E.M. van Beek, 1971. Water movement in layered soils; A simulation model. Neth. J. Agric. Sci. 19: 138-153.

Keulen, H. van, N.G. Seligman & J. Goudriaan, 1975. Availability of anions in the growth medium to roots of an actively growing plant. Neth. J. Agric. Sci. 23: 131-138.

Keulen, H. van, N.G. Seligman & R.W. Benjamin, 1981. Simulation of water use and herbage growth in arid regions - a re-evaluation of the model 'ARID CROP'. Agricultural Systems 6, 159-193.

Keulen, H. van & H.D.J. van Heemst, 1982. Crop response to nutrient availability. Agric. Res. Rep. 916, Pudoc, Wageningen (in press).

Khan, M.A. & S. Tsunoda, 1970. Evolutionary trends in leaf photosynthesis and related leaf characteristics among cultivated wheat species and its wild relatives. Japan J. Breed. 20(3): 133-140.

Krul, J.M., F.W.T. Penning de Vries, L. Stroosnijder & F. van der Pol, 1982. Le phosphore dans le sol et son accessibilité aux plantes. In: La productivité des pâturages Sahéliens. Eds. F.W.T. Penning de Vries & M.A. Djiteye. Agr. Res. Rep. 918, Pudoc, Wageningen, 246-263.

Ku, M.S.B., M.R. Schmitt & G.E. Edwards, 1979. Quantitative determination of RuBP carboxylase - oxygenase protein in leaves of several C_3 and C_4 plants. J. exp. Bot., 30(114), 89-98.

Laar, H.H. van, J. Goudriaan & F.W.T. Penning de Vries, 1983. Improvement of the model BACROS. Simulation Reports CABO/Dept. Theor. Prod. Ecology, Agric. Univ., Wageningen, (in prep.).

Laing, W.A., W.L. Ogren & R.H. Hageman, 1974. Regulation of soybean net photosynthetic CO_2 - fixation by the interaction of CO_2, O_2 and ribulose 1,5 - diphosphate carboxylase. Plant Phys. 54, 678-685.

Lanczos, C., 1967. Applied Analysis. Prentice-Hall Mathematics Series, Sir Isaac Pitman & Sons, Ltd., London, 539 pp.

Lawlor, D.W. & J.G. Pearlman, 1981. Compartmental modelling of photorespiration and carbon metabolism of water stressed leaves. Plant, Cell and Environment 4, 37-52.

Leffelaar, P.A., 1979. Simulation of partial anaerobiosis in a model soil in respect to denitrification. Soil Sci. 128: 110-120.

Lof, H., 1976. Water use efficiency and competition between arid zone annuals, especially the grasses Phalaris minor and Hordeum murinum. Versl. Landbouwk. Onderz. (Agr. Res. Rep.) 853, Pudoc, Wageningen, 109 pp.

Loomis, R.S., R. Rabbinge & E. Ng, 1979. Explanatory models in crop physiology. Ann. Rev. Plant Physiology, 30, 339-367.

Loon, L. van & H. Wösten, 1979. A model to simulate evaporation of bare soils in arid regions. Internal Rep. No. 10, Dept. of Theoretical Production Ecology, Agric. Univ., Wageningen, 96 pp.

Louwerse, W., 1980. Effects of CO_2 concentration and irradiance on the stomatal behaviour of maize, barley and sunflower plants in the field. Plant, Cell and Environment 3, 391-398.

Louwerse, W. & J.W. Eikhoudt, 1975. A mobile laboratory for measuring photosynthesis, respiration and transpiration of field crops. Photosynthetica 9, 31-34.

Lugg, D.G. & T.R. Sinclair, 1981. Seasonal changes in photosynthesis of field - grown soybean leaflets. 2. Relation to nitrogen content. Photosynthetica, 15(1), 138-144.

Makkink, G.F. & H.D.J. van Heemst, 1975. Simulation of the water balance of arable land and pastures. Simulation Monographs. Pudoc, Wageningen, 77 pp.

McCree, K.J., 1974. Equations for the rate of dark respiration of white clover and grain sorghum as functions of dry weight, photosynthetic rate and temperature. Crop Sci. 14(4), 509-514.

Meyer, G.E., R.B. Curry, J.G. Streeter & H.J. Mederski, 1979. SOYMOD/OARDC, a dynamic simulator of soybean growth, development and seed yield, I. Res. Bull. 1113, Ohio Agric. Res. Devel. Center, Wooster, Ohio, USA.

Minchin, F.R., R.J. Summerfield, P. Hadley, E.H. Roberts & S. Rawsthorne, 1981. Carbon and nitrogen nutrition of nodulated roots of grain legumes. Plant, Cell and Environment, 4, 5-26.

Moldau, H. & A. Karolin, 1977. Effect of the reserve pool on the relationship between respiration and photosynthesis. Photosynthetica 11, 38-47.

Moldau, H. & J. Sôber, 1981. Growth rate-reserve content relationship as influenced by irradiance, CO_2 concentration, and temperature. Photosynthesis Research 1: 217-231.

Monteith, J.L., 1973. Principles of environmental physics. Edward Arnold, London, 241 pp.

Paul, E.A. & J.A. van Veen, 1978. The use of tracers to determine the dynamic nature of organic matter. Trans. 11th Intern. Congr. Soil Sci., Edmonton, 3: 61-102.

Parton, W.J., W.D. Gould, F.J. Adamsen, S. Torbit & R.G. Woodmansee, 1981. NH_3 volatilization model. In: Simulation of nitrogen behaviour of soil-plant systems. Eds.

M.J. Frissel & J.A. van Veen, Pudoc, Wageningen, 233-244.

Patterson, D.T., 1980. Light and temperature adaptation. In: Predicting photosynthesis for ecosystem models. Eds. J.D. Hesketh & J.W. Jones. CRC Press Inc., Boca Raton, Florida, USA, Vol. 2, 205-235.

Peat, W.E., 1970. Relationships between photosynthesis and light intensity in the tomato. Ann. Bot. 34, 319-328.

Penman, H.L., 1948. Natural evaporation from water, bare soil and grass. Proc. Roy. Soc. A., 193: 120-146.

Penman, H.L. & R.K. Schofield, 1951. Some physical aspects of assimilation and transpiration. Soc. for Exp. Biol. Symposia, V, 119-129.

Penning de Vries, F.W.T., 1975. The use of assimilates in higher plants. In: Photosynthesis and productivity in different environments. Ed. J.P. Cooper. Cambridge Univ. Press, 459-480.

Penning de Vries, F.W.T., 1975. The cost of maintenance processes in plant cells. Ann. Bot. 39: 77-92.

Penning de Vries, F.W.T., 1977. Evaluation of simulation models in agriculture and biology: conclusions of a workshop. Agric. Systems, 2: 99-107.

Penning de Vries, F.W.T., 1981. Simulation models of growth of crops, particularly under nutrient stress. In: Physiological aspects of crop productivity. Eds. A. von Peter & H. Künzli. Proc. 15th Colloq. Int. Potash Institute, Bern (1980), 213-226.

Penning de Vries, F.W.T., 1982a. Le potentiel physiologique des pâturages et des cultures agricoles. In: La productivité des pâturages Sahéliens. Eds. F.W.T. Penning de Vries & M.A. Djiteye. Agr. Res. Rep. 918, Pudoc, Wageningen, 87-98.

Penning de Vries, F.W.T., 1982b. Modeling growth and production. In: New Encyclopedia of plant physiology, Springer Verlag, Berlin-Heidelberg, Chapter B17 (in press).

Penning de Vries, F.W.T., A.H.M. Brunsting & H.H. van Laar, 1974. Products, requirements and efficiency of biosynthesis: a quantitative approach. J. theor. Biol. 45: 339-377.

Penning de Vries, F.W.T., J.M. Witlage & D.J. Kremer, 1979. Rates of respiration and of increase in structural dry matter in young wheat, ryegrass and maize plants in relation to temperature, to water stress and to their sugar content. Ann. Bot., 44, 591-609.

Penning de Vries, F.W.T., & M.A. Djiteye (Eds.), 1982. La productivité des pâturages Sahéliens. Agr. Res. Rep. 918, Pudoc, Wageningen, 525 pp.

Penning de Vries, F.W.T., & H. van Keulen, 1982. La production actuelle et l'action de l'azote et du phosphore. In: La productivité des pâturages Sahéliens. Eds. F.W.T. Penning de Vries & M.A. Djiteye. Agr. Res. Rep. 918, Pudoc, Wageningen 196-226.

Penning de Vries, F.W.T., H.H. van Laar & M.C.M. Chardon, 1982. Bio-energetics of growth of seeds, fruits and storage organs. Proc. Symp. 'Potential productivity of field crops under different environments', IRRI, Los Banos, Philippines (in press).

Pheloung, P. & C.J. Brady, 1979. Soluble and fraction 1 protein of C_3 and C_4 grasses. J. Sci. Food Agric., 30, 246-250.

Plank, J.E. van der, 1963. Plant diseases. Epidemics and control. Academic Press, New York, N.Y., 210 pp.

Rabbinge, R., 1976. Biological control of fruit-tree red spider mite. Simulation Monographs. Pudoc, Wageningen, 228 pp.

Raghavendra, A.S. & V.S.R. Das, 1978. The occurrence of C_4 photosynthesis: A supplementary list of C_4 plants reported during late 1974 - mid 1977. Photosynthetica 12, 200-208.

300

Rawson, H.M. & G. Hofstra, 1969. Translocation and remobilization of C-14 assimilated at different stages by each leaf of the wheat plant. Aust. J. Biol. Sci. 22: 321-331.

Rawson, H.M. & A.K. Bagga, 1979. Influence of temperature between floral initiation and flag leaf emergence on grain number in wheat. Aust J. Plant Physiol. 6, 391-400.

Rees, A.R. & J.H.M. Thornley, 1973. A simulation of tulip growth in the field. Ann. Bot. 37, 121-131.

Ridder, N. de, 1979. Fotoperiodiciteit in de Sahel. Int. Report, Dept. Theor. Prod. Ecology, Agric. Univ., Wageningen, (Dutch) 27 pp.

Rietveld, J.J., 1978. Soil non wettability and its relevance as a contributing factor to surface runoff on sandy dune soils in Mali. Report of project 'Production Primaire au Sahel', Dept. of Theor. Production Ecology, Agric. Univ., Wageningen, 179 pp.

Rijsdijk, F.H., 1980. Systems analysis at the cross roads of plant pathology and crop physiology. Zeitschrift für Pflanzenkrankheiten und Pflanzenschutz, 87(7), 404-408.

Rijsdijk, F.H., R. Rabbinge & J.C. Zadoks, 1981. A system approach to supervised control of pests and diseases of wheat in the Netherlands. Proc. IX th Int. Congr. of Plant Pathology, Washington, 1979, (in press).

Ross, J., 1981. The radiation regime and architecture of plant stands. Dr. W. Junk Publishers, The Hague, The Netherlands, 391 pp.

Rowse, H.R. & D.A. Stone, 1978. Simulation of the water distribution in soil. I. Measurement of soil hydraulic properties and the model for an uncropped soil. Plant & Soil 49: 517-531.

Sabelis, M.W., 1981. Biological control of two-spotted spider mites using phytoseiid predators. Agric. Res. Rep. 910, Pudoc, Wageningen, 242 pp.

Sager, J.C. & W. Giger Jr, 1980. Re-evaluation of published data on the relative photosynthetic efficiency of intermittent and continuous light. Agric. Meteorology, 22, 289-302.

Sar, D. van der, N. de Ridder, H. Breman & F.W.T. Penning de Vries, 1983. Photoperiodism and draught in Sahelian pastures (in prep.).

Scheid, F., 1968. Numerical analysis. Schaum's outline series. McGraw-Hill Book Company, New York, 422 pp.

Seligman, N.G. & H. van Keulen, 1981. PAPRAN: A simulation model of annual pasture production limited by rainfall and nitrogen. In: Simulation of nitrogen behaviour of soil-plant systems. Eds. M.J. Frissel & J.A. van Veen, Pudoc, Wageningen, 192-220.

Seligman, N.G., H. van Keulen & J. Goudriaan, 1975. An elementary model of nitrogen uptake and redistribution by annual species. Oecologia (Berl.) 21: 243-261.

Shaykewich, G.F. & L. Stroosnijder, 1977. The concept of matrix flux potential applied to simulation of evaporation from soil. Neth. J. Agric. Sci. 25: 63-82.

Shrum, R., 1975. Simulation of wheat stripe rust (Puccinia striiformis West.) using EPIDEMIC, a flexible plant disease simulator. Pennsylvania State Univ., College of Agric. Exp. Station Progress Rep., Pennsylvania State University, No. 371.

Sinclair, T.R. & C.T. de Wit, 1976. Analysis of the carbon and nitrogen limitations to soybean yield. Agronomy Journal 68: 319-324.

Smith, K.A., 1980. A model of the extent of anaerobic zones in aggregated soils, and its potential application to estimates of denitrification. J. Soil Sci. 31: 263-277.

Spiertz, J.H.J., 1977. The influence of temperature and light intensity on grain growth in relation to the carbohydrate and nitrogen economy of the wheat plant. Neth. J. Agric. Sci. 25: 182-197.

Spiertz, J.H.J., 1980. Grain production of wheat in relation to nitrogen, weather and diseases. In: Opportunities for increasing crop yields. Eds. R.G. Hurd, P.V. Biscoe & C. Dennis. Proc. Ass. Appl. Biol., Reading, 17-21 Sept. 1979, 97-114.

Stewart, J.I., R.M. Hagen, W.O. Pruitt, R.J. Hanks, J.P. Riley, R.E. Danielsen, W.T. Franklin & E.B. Jackson, 1977. Optimizing crop production through control of water and salinity levels in the soil. Utah Water Research Lab., Utah State Univ., Logan, Pub. No. PRWG 151-1, 191 pp.

Stigter, C.J. & B. Lammers, 1974. Leaf diffusion resistance to water vapour and its direct measurement. III. Results regarding the improved diffusion porometer in growth rooms and fields of Indian corn (Zea mays). Mededelingen Landbouwhogeschool, Wageningen, 21, 1-76.

Stoy, V., 1965. Photosynthesis, respiration and carbohydrate accumulation in spring wheat in relation to yield. Physiol. Plant. Supplementum 4, 125 pp.

Stroosnijder, L., 1976. Infiltratie en herverdeling van water in grond (Infiltration and redistribution of water in soils). Versl. Landbouwk. Onderz. (Agric. Res. Rep.) 847, Pudoc, Wageningen, 213 pp.

Stroosnijder, L., 1978. Résultats des expériences d'évaporation du sol. Report of project 'Production Primaire au Sahel', Dept. of Theor. Prod. Ecology, Agric. Univ., Wageningen.

Stroosnijder, L. & D. Koné, 1982. Le bilan d'eau du sol. In: La productivité des pâturages Sahéliens. Eds. F.W.T. Penning de Vries & M.A. Djiteye. Agr. Res. Rep. 918, Pudoc, Wageningen, 133-165.

Tadmor, N.H., M. Evenari & L. Shanan, 1972. Primary production of pasture plants as function of water use. In: Eco-physiological foundation of ecosystems productivity in arid zone. Int. Symposium, USSR Academy of Sciences. Publishing house 'NAUKA', Leningrad Branch, Leningrad, 151-157.

Tanner, C.B. & T.R. Sinclair, 1982. Efficient water use in crop production: research or re-search. In: Limitations to efficient water use in crop production. Eds. H.M. Taylor, W.A. Jordan & T.R. Sinclair. A.S.A. Monograph Series. Publ. by Am. Soc. of Agron., Madison, Wi., U.S.A. (in press).

Turner, N.C. & P.J. Kramer, 1980. Adaptation of plants to water and high temperature stress. John Wiley and Sons, New York, 482 pp.

Ungar, E.D. & H. van Keulen, 1982. The simulation model ARID CROP in Fortran. Simulation Reports. Centre for Agrobiological Research/Theoretical Production Ecology, Agric. Univ., Wageningen, No. 1, 39 pp.

Vauclin, M., R. Haverkamp & G. Vachaud, 1979. Resolution numerique d'une equation de diffusion non lineaire. Presses universitaires de Grenoble, 183 pp.

Veen, J.A. van, 1977. The behaviour of nitrogen in soil. A computer simulation model. Ph.D. thesis, Free University, Amsterdam, 164 pp.

Veen, J.A. van, W.B. McGill, H.W. Hunt, M.J. Frissel & C.V. Cole, 1981. Simulation models of the terrestrial nitrogen cycle. In: Nitrogen cycling in terrestrial ecosystems. Processes, ecosystem strategies, and management impacts. Eds. F.E. Clark & T. Rosswall. Ecol. Bull. (Stockholm) 33, (in press).

Veldkamp, H. & J.G. Kuenen, 1973. The chemostat as a model system for ecological studies. In: Modern Methods in the Study of Microbial Ecology. Ed. T. Rosswall. Bull. Ecol. Res. Comm. (Stockholm) 17: 347-355.

Viets, F.G. Jr., 1962. Fertilizers and the efficient use of water. Adv. Agron. 14: 223-264.

Vos, J., 1981. Effects of temperature and nitrogen supply on post-floral growth of wheat;

measurements and simulations. Agric. Res. Rep. 911, Pudoc, Wageningen, 164 pp.

Vos, N.M. de, 1975. Field photosynthesis of winter wheat during the grain-filling phase under highly fertile conditions. Proc. of the Sec. Int. Winter Wheat Conf. Zagreb, Yugoslavia, 251-255.

Wal, A.F. van de, H. Smeitink & G.C. Maan, 1975. A crop physiological approach to crop losses exemplified in the system wheat, leaf rust and glume blotch. 3. Effects of soil water potential on development, growth, transpiration, symptoms and spore production of leaf rust infected wheat. Neth. J. of Plant Pathology, 81, 1-13.

Waggoner, P.E., 1977. Simulation of modelling of plant physiological processes to predict crop yields. In: Environmental Effects on Crop Physiology. Eds. J.J. Landsberg & C.V. Cutting. Academic Press, New York, 351-363.

Waggoner, P.E., J.G. Horsfall & R.J. Lukens, 1972. EPIMAY, a simulator of southern corn leaf blight. Bulletin of the Connecticut Agric. Exp. Station, New Haven, Connecticut, No. 729.

Warrick, A.W., G.J. Mullen & D.R. Nielsen, 1977. Scaling field - measured soil hydraulic properties using a similar media concept. Water Resour. Res., 13(2), 355-362.

Wetselaar, R. & G.D. Farquhar, 1980. Nitrogen losses from tops of plants. Academic Press, Adv. Agron. 33, 263-305.

Wit, C.T. de, 1958. Transpiration and crop yields. Versl. Landbouwk. Onderz. (Agr. Res. Rep.) 64.6, Pudoc, Wageningen, 88 pp.

Wit, C.T. de, 1965. Photosynthesis of leaf canopies. Agr. Res. Rep. 663, Pudoc, Wageningen, 57 pp.

Wit, C.T. de & H. van Keulen, 1972. Simulation of transport processes in soils. Simulation Monographs. Pudoc, Wageningen, 108 pp.

Wit, C.T. de, R. Brouwer & F.W.T. Penning de Vries, 1970. The simulation of photosynthetic systems. In: Prediction and measurement of photosynthetic productivity. Proc. IBP/PP technical meeting. Trebon, 1969. Ed. I. Šetlik. Pudoc, Wageningen, 47-50.

Wit, C.T. de et al., 1978. Simulation of assimilation, respiration and transpiration of crops. Simulation Monographs. Pudoc, Wageningen, 140 pp.

Wit, C.T. de & J. Goudriaan, 1978. Simulation of ecological processes. Simulation Monographs. Pudoc, Wageningen, 167 pp.

Wit, C.T. de & J.M. Krul, 1982. La production actuelle dans une situation d'équilibre. In: La productivité des pâturages Sahéliens. Eds. F.W.T. Penning de Vries & M.A. Djiteye. Agr. Res. Rep. 918, Pudoc, Wageningen, 275-283.

Wit, C.T. & F.W.T. Penning de Vries, 1982. L'analyse des systèmes de production primaire. In: La productivité des pâturages Sahéliens. Eds. F.W.T. Penning de Vries & M.A. Djiteye. Agr. Res. Rep. 918, Pudoc, Wageningen, 20-23.

Wong, S.C., I.R. Cowan & G.D. Farquhar, 1979. Stomatal conductance correlates with photosynthetic capacity. Nature, Vol. 282, 424-426.

Wright, M.J., 1977. Plant adaptation to mineral stress in problem soils. Proc. Workshop Cornell Univ. Agric. Exp. Station, Cornell Univ., Ithaca, New York.

Yanuka, M., Y. Leshem & A. Dovrat, 1981. Forage corn response to several trickle irrigation and fertilization regimes. Contribution from the Hebrew Univ. of Jerusalem, Faculty of Agriculture, P.O. Box 12, Rehovot, Israel (in press).

Zadoks, J.C., 1971. Systems analysis and the dynamics of epidemics. Phytopathology, 61, 600-610.

INDEX

C.T. de Wit and H. van Keulen. Simulation of transport processes in soils (2nd ed., revised). 1975. 109 pp. ISBN 90-220-0591-7.

J. Beek and M.J. Frissel. Simulation of nitrogen behaviour in soils. 1973. 76 pp. ISBN 90-220-0440-6.

H.G. Fransz. The functional response to prey density in an acarine system. 1974. 149 pp. ISBN 90-220-0509-7.

M.J. Frissel and P. Reiniger. Simulation of accumulation and leaching in soils. 1974. 124 pp. ISBN 90-220-0530-5.

H. van Keulen. Simulation of water use and herbage growth in arid regions. 1975. 184 pp. ISBN 90-220-0557-7.

G.F. Makkink and H.D.J. van Heemst. Simulation of the water balance of arable land and pastures. 1975. 87 pp. ISBN 90-220-0566-6.

G.W. Arnold and C.T. de Wit (Eds). Critical evaluation of systems analysis in ecosystems research and management. 1976. 114 pp. ISBN 90-220-0593-3.

J. van den Bos and R. Rabbinge. Simulation of the fluctuations of the grey larch bud moth. 1976. 91 pp. ISBN 90-220-0589-5.

R. Rabbinge. Biological control of fruit-tree red spider mite. 1976. 234 pp. ISBN 90-220-0590-8.

J. Goudriaan. Crop micrometeorology: a simulation study. 1977. 257 pp. ISBN 90-220-0614-X.

E. van Elderen. Heuristic strategy for scheduling farm operations. 1977. 233 pp. ISBN 90-220-0612-3.

P. Kampmeijer and J.C. Zadoks. EPIMUL, a simulator of foci and epidemics in mixtures of resistant and susceptible plants, mosaics and multilines. 1977. 56 pp. ISBN 90-220-0636-0.

T. Kozai, J. Goudriaan and M. Kimura. Light transmission and photosynthesis in greenhouses. 1978. 105 pp. ISBN 90-220-0646-8.

K.R. Christian et al. Simulation of grazing systems. 1978. 121 pp. ISBN 90-220-0645-X.

C.T. de Wit and J. Goudriaan. Simulation of ecological processes. (2nd ed. revised and extended). 1978. 183 pp. ISBN 90-220-0652-2. (Published by Pudoc outside USA, Canada and Latin America)

C.T. de Wit et al. Simulation of assimilation, respiration and transpiration of crops. 1978. 148 pp. ISBN 90-220-00601-8. (Published by Pudoc outside USA, Canada and Latin America)

R.A. Feddes, P.J. Kowalik and H. Zaradny. Simulation of field water use and crop yield. 1978. 195 pp. ISBN 90-220-0676-X. (Published by Pudoc outside USA, Canada and Latin America)

S.M. Welch and B.A. Croft. The design of biological monitoring systems for pest management. 1979. 84 pp. ISBN 90-220-0687-5. (Published by Pudoc outside USA, Canada and Latin America)

N.D. Barlow & A.F.G. Dixon. Simulation of lime aphid population dynamics. 1980. 171 pp. ISBN 90-220-0706-5.